

Design, synthesis, and biological activity
of nature-derived herbicides

Dissertation

zur Erlangung des
Doktorgrades der Naturwissenschaften (Dr. rer. nat.)

der

Naturwissenschaftlichen Fakultät II
Chemie, Physik und Mathematik

der Martin-Luther-Universität
Halle-Wittenberg

vorgelegt von

Herrn Tristan Fuchs

This dissertation has been developed from November 2018 to December 2022 under the supervision of Prof. Dr. Ludger A. Wessjohann at the Department of Bioorganic Chemistry of the Leibniz Institute of Plant Biochemistry (IPB) in cooperation with the Martin Luther University Halle-Wittenberg.

1st Reviewer: Prof. Dr. Ludger A. Wessjohann

2nd Reviewer: Prof. Dr. Jürgen Scherkenbeck

Date of public defense: 03.07.2025

*„Das Leben ist wie Fahrrad fahren. Man muss sich vorwärts bewegen,
um das Gleichgewicht nicht zu verlieren.“*

Albert Einstein

Design, synthesis, and biological activity of nature-derived herbicides

Table of contents

Acknowledgements	II
List of abbreviations	III
Zusammenfassung.....	1
Summary	2
1 Introduction	4
2 Total synthesis and biological studies of tentoxin and derivatives	16
3 Synthesis and biological evaluation of niacin derivatives as a new class of nature-inspired herbicides	88
4 Synthesis and biological evaluation of 4-hydroxy-2-pyrones and 3-phenylcoumarins as potential antimycotics and herbicides.....	130
Appendix.....	VI
Curriculum vitae	CXXXIX
Eidesstattliche Erklärung	CXL

Acknowledgements

This dissertation journey was both challenging and rewarding. I would like to acknowledge the valuable assistance and support of those who helped me along the way. In the following, I would like to express my gratitude to all those who have contributed to this work.

First of all, I would like to express my deepest gratitude to my supervisor, Professor Ludger A. Wessjohann, for his guidance and support throughout this journey. His profound expertise and insightful feedback as well as the freedom he allowed me in my research have been invaluable to the successful completion of this dissertation.

Besides this, I would like to thank Professor Bernhard Westermann for his very constructive input for this dissertation and intriguing discussions about chemistry and life. Also for his interesting Friday seminars and the proofreading of this thesis.

An important part of this work was the characterization of the substances produced and the determination of their biological activity. I received valuable support from many scientists and technical assistants, whom I would like to thank as follows:

I would like to thank Katharina Wolf for her work as a lab technician in C116. Moreover Dr. Annegret Laub and Elana Kysil for their support with mass spectroscopy. For the recording of countless NMR spectra, I would like to thank Dr. Andrea Porzel, Gudrun Hahn and Dr. Hidayat Hussain. I would also like to thank Hidayat for his kind company as a lab neighbour and for the helpful chemical advice he gave me from his deep knowledge. In addition, I would like to thank Martina Brode for her support with the antifungal assays and Anja Ehrlich for introducing me to the exciting world of HPLC and Marvin Hempel for his support with the instruments. Dr. Robert Rennert and Martina Lerbs deserve my thanks for their help with the cell assays. Finally, a very special thanks goes to Mariia Khamdan, not only for the countless Lemnitas that she has looked after so well, but also for the mutual support with the smaller and larger problems of our theses.

Dr. Martin Dippe and Svitlana Manoilenko are thanked for collaborating on the 2-pyrone project. I would also like to thank Anna Reineke for her support in the laboratory. A special thanks also goes to Evelyn Funke for help with the modelling.

I would also like to thank the entire NWC working group for the pleasant working atmosphere and many enjoyable hours both inside and outside the laboratory. I will always remember the uncountable birthday celebrations, barbecues and parties as well as the fun breaks to play ping pong or foosball. Many thanks to every one of you!

Finally, I would like to thank my family for their constant support throughout this journey. Their understanding and belief in me have been very helpful. I deeply appreciate their patience and support during the completion of this dissertation. Especially my dear Mar for the indispensable love, support and patience, but also for the valuable help in designing the graphics of this thesis.

List of abbreviations

3-SBzl	3-Benzylthio
3LC	3-Letter-code
4CR	Four-component reaction
4-DMAP	<i>N,N</i> -Dimethylpyridin-4-amine
AA	Amino acid
Ac ₂ O	Acetic acid anhydride
ACN	Acetonitrile
Ala	Alanine
Asp	Aspartic acid
aq	Aqueous
B.C.	Before Christ
Boc	<i>tert</i> -Butoxycarbonyl
Bzl	Benzoyl group
Cbz	Benzoyloxy carbonyl group
CV	Crystal violet
d	Doublet
DBU	Diazabicycloundecene
DCC	<i>N,N'</i> -Dicyclohexylcarbodiimide
DCVC	Dry column vacuum chromatography
DCM	Dichloro methane
DDQ	2,3-Dichloro-5,6-dicyano-1,4-benzoquinone
DIC	<i>N,N'</i> -Diisopropylcarbodiimide
DIPEA	<i>N,N</i> -Diisopropylethylamine
DPPA	Diphenylphosphoryl azide
DME	Dimethoxyethane
DMEDA	1,2-Dimethylethylenediamine
DMF	Dimethylformamide
DMI	1,3-Dimethyl-2-imidazolidinone
DMP	<i>Dess-Martin</i> periodinane
DMPU	<i>N,N'</i> -Dimethylpropyleneurea
DMSO	Dimethyl sulfoxide
EDC	1-Ethyl-3-(3-dimethylaminopropyl)carbodiimide
EDTA	Ethylenediaminetetraacetic acid
ESI	Electron spray ionization
EtOAc	Ethyl acetate
eq	Equivalent
FA	Formic acid
FDA	Food and drug administration
FRAC	Fungicide resistance action committee
FTMS	Fourier transform mass spectrometry
GBVI	Generalized born/volume integral
Gly	Glycine

HATU	1,2,3-Triazolo[4,5-b]pyridinium 3-oxid hexafluoro phosphate
HIV	Human immunodeficiency virus
HPPD	4-Hydroxyphenylpyruvate dioxygenase
HMDS	Hexamethyldisilazane
HOBt	1-Hydroxybenzotriazole
HPLC	High performance liquid chromatography
HR-MS	High-resolution mass spectroscopy
HCT	Human colon cancer cell line
<i>i</i> Bu	Isobutyl
IPB	Leibniz institute for plant biochemistry
irr	Irradiation
<i>J</i>	Coupling constant
Leu	Leucine
LDA	Lithium diisopropylamide
LiHMDS	Lithium hexamethyldisilazide
<i>m</i>	Multiplet
<i>m/z</i>	Mass-to-charge ratio
<i>M</i>	Molar
MeOH	Methanol
MOA	Mode of action
MS	Molecular sieve
MTBE	Methyl <i>tert</i> -butyl ether
MTT	3-(4,5-Dimethylthiazol-2-yl)-2,5-diphenyltetrazolium bromide
MW	Molecular weight
NMR	Nuclear magnetic resonance
NP	Natural product
NPD	Natural product derivative
NPM	Natural product mimetic
NPSE	Natural product synthetic equivalent
<i>o</i>	<i>ortho</i>
<i>p</i>	<i>para</i>
<i>p</i>	Quintet
PEG	Polyethylene glycol
Phe	Phenylalanine
<i>q</i>	Quartet
quant	Quantitative
ROS	Reactive oxygen species
RP	Reverse phase
rt	Room temperature
<i>s</i>	Singlet
sat	Saturated
SPPS	Solid phase peptide synthesis
SYN	Synthetic molecule
<i>t</i>	Triplet

^t Bu	<i>tert</i> -Butyl
t _R	Retention time
T3P	Propanephosphonic acid anhydride
TEA	Triethyl amine
TFA	Trifluoroacetic acid
THF	Tetrahydrofuran
Thr	Threonine
TLC	Thin layer chromatography
TMEDA	<i>N,N,N',N'</i> -Tetramethylethane-1,2-diamine
TMG	1,1,3,3-Tetramethylguanidine
TMS	Tetramethylsilane
TMSCl	Chlorotrimethylsilane
TOF	Time of flight
TTX	Tentoxin
Tyr	Tyrosine
UV	Ultraviolet
w/w	Weight for weight
μw	Microwave
ΔAA	Dehydroamino acid

Zusammenfassung

Naturstoffe aus Pflanzen, Pilzen oder Mikroorganismen sind wertvolle Quellen bei der Entwicklung von neuen Wirkstoffen für Pharmazeutika, Biozide oder Pflanzenschutzmittel. Hierfür können sie entweder direkt oder durch gezielte Veränderung der chemischen Struktur als Naturstoff-abgeleitete Wirkstoffe oder Mimetika eingesetzt werden. Durch ihre strukturelle Vielfalt und biologischen Herkunft können sich neue Wirkmechanismen eröffnen. In dieser Arbeit wird die Entwicklung von neuen Syntheserouten für biologisch aktive Naturstoffe sowie Naturstoff-abgeleitete Herbizide präsentiert, deren biologische Aktivität untersucht und so Rückschlüsse auf die Struktur-Wirkungsbeziehung gezogen.

Im Kapitel 1 dieser Arbeit wird ein allgemeiner Überblick über die historische Entwicklung von Herbiziden sowie ihrer aktuellen weltweiten Verwendung präsentiert. Darüber hinaus werden die Herausforderungen, die sich aus einer exzessiven Nutzung synthetischer Herbizide ergeben, ausführlich dargestellt. Ein vielversprechender Lösungsansatz wird in der Erforschung und Verwendung von herbiziden Naturstoffen identifiziert und eingehend erläutert.

Im Kapitel 2 wird eine neue Totalsynthese für den herbizid wirkenden Naturstoff Tentoxin vorgestellt. Die Syntheseroute wurde mit dem Ziel entwickelt, eine Derivatisierung von Tentoxin an der Dehydroamino-säure zu ermöglichen, um deren Einfluss auf die biologische Aktivität zu untersuchen und diese zu erhöhen. Der Derivatisierungsschritt wurde in den späten Abschnitt der Totalsynthese integriert, wodurch eine effiziente Herstellung einer Vielzahl von Derivaten ermöglicht wird. Die Totalsynthese führte zur erfolgreichen Herstellung von Tentoxin in sieben Schritten mit einer Ausbeute von 33 %. Darüber hinaus wurden 14 Derivate erfolgreich synthetisiert. Zusätzlich wurden fünf weitere Derivate mithilfe einer Literatursynthese dargestellt, was deren Versatilität unterstreicht. Sämtliche hergestellten Substanzen wurden eingehend auf ihre biologische Aktivität hin untersucht, wodurch neue Erkenntnisse zur Struktur-Wirkungsbeziehung von Tentoxin gewonnen werden konnten.

Im Kapitel 3 wird eine neue Klasse von Herbiziden vorgestellt, welche sich durch niedrig mikromolare Aktivitäten *in vivo* und einfache Synthesen auszeichnet. Ausgehend von 6-Decyloxy-nicotinsäure, für welche die herbizide Aktivität erstmals gefunden wurde, konnte eine Bibliothek von 54 Substanzen mit unterschiedlichen Seitenketten, Funktionalitäten und Substitutionsmustern hergestellt werden. Untersuchungen zur herbiziden Wirkung konnten die vielversprechenden biologischen Aktivitäten von Vertretern dieser Substanzklasse zeigen und geben wichtige Rückschlüsse auf relevante Strukturelemente für diese.

Im Kapitel 4 wird die Synthese einer Substanzbibliothek von substituierten Pyronen und Phenylkumarinen beschrieben. Insgesamt konnten 20 Pyrone und 7 Phenylkumarine hergestellt und auf ihre biologische Aktivität untersucht werden. Hierbei wurde auch die erste Totalsynthese des antifungischen Naturstoffes Fistupyrone erzielt. Die Untersuchung der biologischen Aktivität zeigte, dass einige der hergestellten Substanzen gegen verschiedene phytopathogene Pilze wirken. Des Weiteren konnte bei 9 Substanzen eine moderate herbizide Aktivität festgestellt werden.

Summary

Natural products from plants, fungi or microorganisms are valuable sources for the development of new active ingredients for pharmaceuticals, biocides, or plant protectants. They can be used directly or through targeted chemical structure modification as natural product-derived active ingredients or mimetics. Their structural diversity and biological origin can open up new mechanisms of action. This thesis describes the development of new synthesis routes for biologically active natural products and natural product-derived herbicides, examines their biological activity, and thus draws conclusions about their structure-activity relationships.

Chapter 1 of this thesis presents a general overview of the historical development of herbicides and their current global use. In addition, the challenges arising from the excessive use of synthetic herbicides are presented in detail. A promising solution is identified in the development and use of herbicidal natural products which is explained in detail.

Chapter 2 presents a new total synthesis for the herbicidal natural product tentoxin. The synthesis route was developed with the aim of enabling a derivatization of tentoxin at the dehydroamino acid in order to investigate its influence on the biological activity and to enhance it. The derivatization step was integrated into the late stage of the total synthesis, enabling efficient production of a variety of derivatives. The total synthesis led to the successful synthesis of tentoxin in seven steps with a yield of 33 %. In addition, 14 derivatives were successfully prepared. Furthermore, the synthesis of five additional derivatives is presented using a literature synthesis, thus emphasizing its versatility. The biological activity of all substances was examined in detail, providing new insights into the structure-activity relationship of tentoxin.

Chapter 3 presents a new class of herbicides, characterized by low micromolar activities *in vivo* and very straightforward syntheses. Starting from 6-decyloxy nicotinic acid, the accidentally discovered herbicidal activity which triggered this research, a library of 54 substances with different side-chains, functionalities and substitution patterns was prepared. Studies of their herbicidal activity have confirmed the excellent herbicidal potential of this substance class and provide valuable first insights into a structure-activity-relationship.

Chapter 4 describes the synthesis of a substance library of substituted pyrones and phenylcoumarins. A total of 20 pyrones and 7 phenylcoumarins were synthesized and tested for their biological activity. The first total synthesis of the antifungal natural product fistupyrone was achieved. The investigation of the biological activity showed that some of these substances are effective against various phytopathogenic fungi. Furthermore, 9 substances were found to have moderate herbicidal activity.

Chapter 1

Introduction

History of weed control

Weed control, the practice of managing unwanted plants that compete with cultivated crops, has been a part of agriculture since the rise of the beginning of plant cultivation following the Neolithic revolution.^{1,2} According to current research, it started around 21.000 B.C. on the shore of the Sea of Galilee, Israel together with the first cultivation of wild wheat and barley, among others.³ As described by *Zimdahl*, the history of weed control can be divided into three main eras.⁴

The manual era

The first era, also called the “blood, sweat, and tears era”, was when the earliest forms of weed control were used. Ancient farmers used manual, labour-intensive methods, to uproot or bury weeds typically using hand tools, such as hoes and ploughs, thus limiting the area and productivity of early agriculture. Furthermore, crop rotation and fallow (or shmita) were performed to lower weed pressure as well as to avoid the depletion of nutrients in the soil.⁵⁻⁷

The mechanical era

The second stage of development is the mechanical era. It is estimated to date back to the second millennium B.C. and is the result of the domestication of oxen, horses, and camels, which made it possible to pull larger ploughs with less effort. However, the golden age of these techniques began with the (re)invention of these tools by Jethro Tull in 1701. The English agriculturist, who invented the horse-drawn seed drill and hoe, paved the way to the second agricultural revolution.^{8,9} These inventions not only facilitated the labour but also enabled precise sowing and ploughing, thus improving mechanical weed control.



Figure 1: Painting of farmers using hand tools and a plough. Theban Tomb TT52, Sheikh Abd el-Qurna, Egypt. Circa 1400 B.C.¹

The chemical era

The most recent era began in the 20th century with the introduction of synthetic chemicals. The first achievements in weed control were made in the century before with inorganic compounds and acids, but the breakthrough came with the use of synthetic organic chemicals as herbicides. The first successful synthetic herbicide, 2,4-dichlorophenoxyacetic acid (2,4-D), was developed during World War II, starting a new era in weed control, as synthetic herbicides offered more precision and effectiveness compared to mechanical weed control. The development of chemical herbicides can be divided as follows:

1850s – 1920s: The first reports of herbicidal effects of inorganic salts such as iron(II) and copper(II) sulfate, as well as various acids (acetic acid, sulfuric acid, and nitric acid) and petroleum products, have been published.

1920s – 1950s: The beginning of the use of organic substances. With dinitro-*ortho*-cresol (Sinox, 1925) and 2,4-D (1940s), the first synthetic herbicides were commercialized.^{10,11}

1950s - 1960s: The introduction and extended use of selective herbicides allowed for the control of specific (usually broadleaf) weeds without harming crops, thus revolutionizing agriculture.¹²

1970s - 1980s: Glyphosate (Monsanto, 1974) was introduced in 1974 to the market, becoming the most widely used herbicide globally until today due to its broad-spectrum effectiveness.^{13,14}

1980s - 2000s: Herbicide-resistant crops (usually glyphosate-resistant) which are genetically modified were developed, allowing farmers to apply herbicides without damaging their crops.¹⁵

2000s - Present: Continued research and development is leading to the creation of more environmentally friendly and selective herbicides, addressing the rise of resistant weeds and concerns about environmental and human health.

Today's situation of herbicides

The global use of plant protectants in agriculture has increased continuously since the development of synthetic products and has recently peaked at a global consumption of 3.53 million tons (2021; Germany: 16.1 kilotons). Among them, herbicides contribute almost half (49 %, 1.73 million tons) of the applied products and are therefore the agricultural products with the highest relevance.^{16,17} The largest consumption comes from countries that use herbicide-resistant plants on a large scale (mainly the USA and Brazil). In many developing countries, the use per cultivated area is much lower due to a lack of financial resources and low wages, so more manual methods are used up to today. The increase in herbicide use has slowed over the past 10 years, with no peak in sight despite restrictions and bans on various substances in this timeframe.

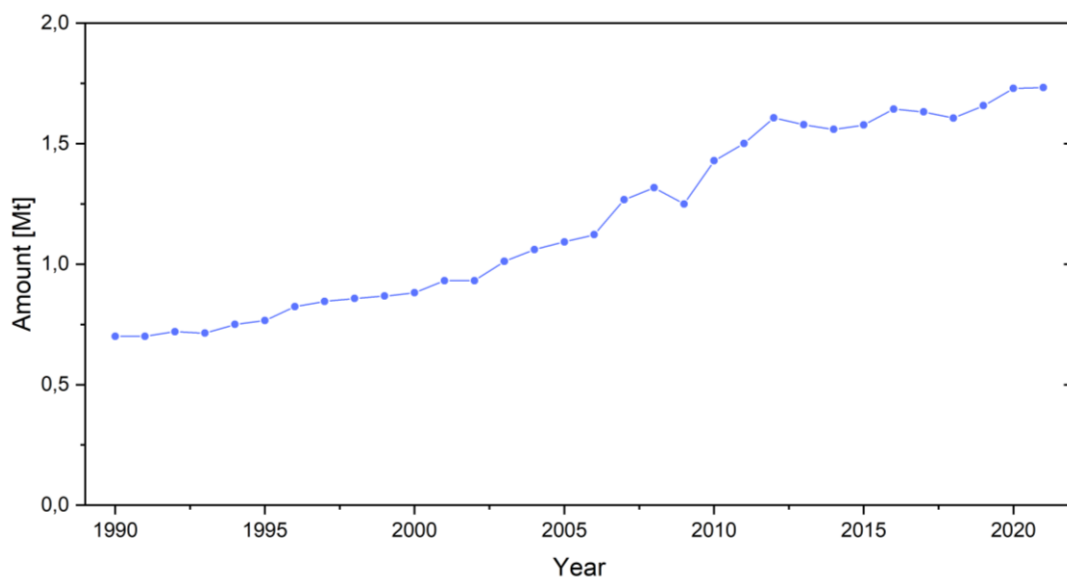


Figure 2: Amount of applied herbicides worldwide from 1990 to 2021.

The synthetic herbicides currently used are usually small molecules (< 500 MW) that selectively target processes in plants. These targets can be divided into 3 groups as defined by *Dayan*:¹⁸

- 1) Herbicides that target biochemical pathways and physiological processes involved with photosynthesis
- 2) Herbicides that inhibit the formation of biological building blocks (i.e., sugars, amino acids and fatty acids) or their assembly into macromolecules
- 3) Herbicides with other modes of action

Based on this, commercial herbicides with a total of 34 different MOAs are currently used according to the herbicide resistance action committee (HRAC).¹⁹

Problems with overuse of synthetic herbicides

While synthetic herbicides have greatly improved weed control and crop yields, they have also raised environmental and health concerns.²⁰ With their large-scale use, which is also limited to comparatively few active ingredients, various problems have emerged in the past and present. Especially at the beginning of the chemical era, toxic agents led to a range of health problems, from rashes to death. The use of new active ingredients has minimized this to a large extent, and current health problems can usually be traced back to misuse. Other problems include the risk of groundwater contamination due to a too-slow breakdown in the environment. Indirectly, excessive use of herbicides can also lead to increased insect mortality through a lowering of biodiversity which restricts the food sources for some insects as well as other animals.

The greatest problem for conventional agriculture due to the use of synthetic herbicides is, however, the development of herbicide-resistant plants.²¹ It is defined by the HRAC as “the natural ability of a weed biotype to survive an application of a herbicide that would normally kill it.”¹⁹ Herbicide resistance develops as a result of too frequent and one-sided use of herbicides to control weeds. The emergence of resistance usually begins with individual plants with lower sensitivity to herbicides that occur in any natural population. Repeated applications of herbicides with the same mechanism of action result in selection pressure. Sensitive plants are decimated, and the proportion of resistant plants increases. The survival and reproduction of appropriately adapted (resistant) individual plants is thus favoured. The first resistant crops were discovered in 1957, and the acreage where they were found increased sharply in the 1960s.^{22,23} With the introduction of glyphosate and herbicide-resistant crops, the development was temporarily halted, just to reemerge and increase until today. The larger number of applications per crop cycle has increased and fewer changes in herbicides and crop rotation are made.^{24,25} This evolution has resulted in the development of resistant weeds for at least 21 of the 34 MOAs used in commercial herbicides today. These include all major herbicide modes of action.²⁶ In addition, in the golden era of herbicide research in the 1970s and 1980s, a new MOA was discovered and commercialized on average every 3 - 4 years. However, since the last discovery of a new MOA in 1982, only one more has been discovered to date.²⁷ Currently, it seems as if herbicide research has been paused. One reason for this may be the ever-increasing development costs of an estimated >250 million USD per new active ingredient, together with expanding demands such as high effectiveness and selectivity combined with rapid degradation in the environment and low production costs.

Use of natural products for the development of new plant protectants

"All the pests that out of earth arise, the earth itself the antidote supplies"

Lithica poem, ca. 400 B.C.²⁸

One approach to solve many of the mentioned problems with current synthetic plant protectants and especially the discovery of new MOAs in pesticide research could be the search for new bioactive natural products (NPs). Their development and state of research will be summarised in this chapter.

Natural products are chemical substances, which are produced by a living organism.²⁹ They are found in nature as primary (basic) or secondary metabolites and have been used in medicine since the dawn of human history. But NPs have also been used as pesticides, at least since the time of settlement. Initially, plant extracts were used for this purpose, but with the advent of industrial chemistry in the 19th century the research into active substances has increased. This has led to some of the first synthetic pesticides based on natural substances (i.e. parathion, allethrin I, rotenone).

NPs could serve as a valuable source of agrochemicals since they are designed from the interactions of an organism with its ecological surroundings. The producing organism has coevolved alongside the target organism, developing these natural products as tools for attack or defence against other species. Being of natural origin, the NPs usually have a shorter half-life in the environment which reduces their impact on the environment. Furthermore, they often have complex chemical structures or possess unusual structural elements, which are not included in the standard preparation of derivative libraries during the (non-bioguided) search for new active compounds and can therefore extend the search to unexplored chemical space and be a valuable source of novel bioactivities.

Many natural substances have been investigated in the past for use as plant protectants, but except for insecticides and fungicides, only with moderate success due to various disadvantages.³⁰ As mentioned before, NPs often have complex structures which are interesting from a chemical point of view, but these often have several stereocenters, which complicates efficient synthesis and upscaling. Furthermore, their physicochemical properties are often not ideal for use as agrochemicals. Their short half-life, for example, is indeed good for the environment, but limits their use and efficiency in crop protection. Another common misconception is that all natural products are "safe" for humans because they derive from nature. This can be contradicted by the mere fact that many of the most toxic substances known are natural substances (i.e. maitotoxin, batrachotoxin or botulinum toxin).^{31,32}

The agrochemicals used today can be divided into 5 different groups according to their origin, as proposed by Sparks and Duke.^{33,34} The first two groups are natural products and derivatives of natural products (NPDs), which are synthetically modified natural products. Both groups account for 2 % of the agrochemicals used today. The third group are the so-called natural product mimics (NPMs). These are structurally highly modified substances with the aim of simplifying the synthesis route and/or improving the physicochemical properties whilst keeping the biological activity. This substance class accounts for 14 % of agrochemicals. In contrast to this are the last two substance classes, which both include chemicals which were discovered through non-NP-related synthetic products and screening.

The largest group, with a share of 44 %, are the synthetic molecules (SYNs), which have no relation to natural substances and their MOAs. The second group, the so-called natural product synthetic equivalents (NPSEs), are substances found by synthesis for which an NP exists as a model but did not serve as such.

In summary, it can be said that more than half of the agrochemicals used today are based on MOAs that are also served by natural products (as far as known today). This, together with the mentioned beneficial properties, underlines the high importance of NP research for the development of new and more sustainable agrochemicals.

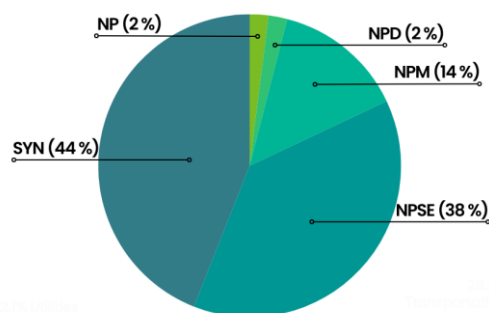


Figure 3: Distribution of the various categories of origin of substances used in the agrochemical market.^{26,27} Abbreviations: NP – natural product, NPD – natural product derivative, NPM – natural product mimetic, NPSE – natural product synthetic equivalent, SYN – synthetic molecule.

Natural products as herbicides

All that is stated above for agrochemicals also applies in particular to herbicides, as these account for around half of all agrochemicals applied. Compared to insecticides, where NPMs are already used on a larger scale, there are comparatively few conventional herbicides which are NPs, NPDs or NPMs.³⁵ However, given the currently uncertain future and the poor reputation in the public and political opinion on conventional synthetic herbicides, and in particular on the most widely used herbicide glyphosate, many users are looking for alternatives. For example, Deutsche Bahn, the largest single consumer of glyphosate in Germany with 65.4 tons (Roundup, in 2018), has decided to abandon the use of glyphosate completely and has found an alternative in the NP pelargonic acid, alongside other methods.³⁶ A brief overview of some commercial herbicides derived from natural products is given in the following.

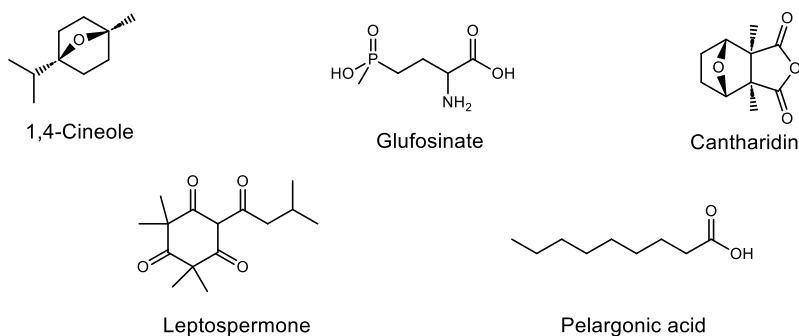


Figure 4: Structures of several herbicidal natural products which are either commercialized or inspired commercial herbicides.

The aforementioned pelargonic acid belongs to the class of herbicidal fatty acids which are found in many plants, especially in the form of esters in plants of the genus *Pelargonium*. Pelargonic acid can be used in agriculture as a postharvest sanitizer, blossom thinner, and broad-spectrum herbicide due to its diverse biological activities.^{37–39} The class of herbicidal fatty acids have been used for many decades in agriculture.⁴⁰ They act through a disruption of the plant cuticle which leads to intercalation of the acid, followed by light-driven peroxidase activity that causes the necrosis of plant tissue a few hours after application. The herbicidal activity depends strongly on

the length of the aliphatic chain with the best results being found for C₈ to C₁₁ chain lengths (see Chapter 3 for similar results).

The commercially most successful natural product herbicide is glufosinate, also known as phosphinothricin, which is a unique amino acid and derivative of glutamate.⁴¹ It forms part of the also herbicidal NP bialaphos, a tripeptide consisting of glufosinate and two alanine units.^{42,43} Both NPs can be found in several *Streptomyces* species and act as broad-spectrum herbicides. The latter one is a protoxin and is metabolized in the plant to phosphinothricin. It acts via inhibition of glutamine synthetase which hinders the production of glutamine but more importantly, stops ammonia detoxification, leading to an accumulation of ammonia and the following cell death.^{44–46}

Another intriguing natural substance is leptospermone, which has led to the development of the so-called triketone herbicides. The biologist Reed Gray first noted its herbicidal effect, and noticed reduced weed growth under bottle brush plants (*Callistemon citrinus*).^{30,47} By extracting soil samples, he found that the already known NP leptospermone was responsible for bleaching of plant tissue and therefore the lack of weeds. An investigation of the MOA showed that the triketones act via inhibition of 4-hydroxyphenylpyruvate dioxygenase (HPPD), an enzyme responsible for the catabolism of the amino acid tyrosine.^{48,49} The blockage of this enzyme leads to an increase of ROS species in the plant as well as a reduction of carotenoid synthesis, which protects the photosystem. Those two effects ultimately lead to the destruction of chlorophyll and the photosystem and by this to a bleaching and the death of the plant. By modification and simplification of the structure, a whole family of herbicidal compounds was produced from which several were commercialized, such as mesotrione.⁵⁰

Furthermore, several essential oils or plant parts with herbicidal activity have been identified and commercialized. For many of them, the active ingredient or mechanism of action has not been clarified yet. Examples include citrus oil, cinnamon oil, clove oil and pine oil.^{51,52} As plant parts, for example, cinnamon bark or corn gluten are used.⁵³ A major disadvantage of using these products is the high quantity of product to be applied, which is often more than a hundred times that of a synthetic herbicide.⁵⁴ Together with the often higher costs, they have so far not proven to be very practicable for mass application in agriculture.

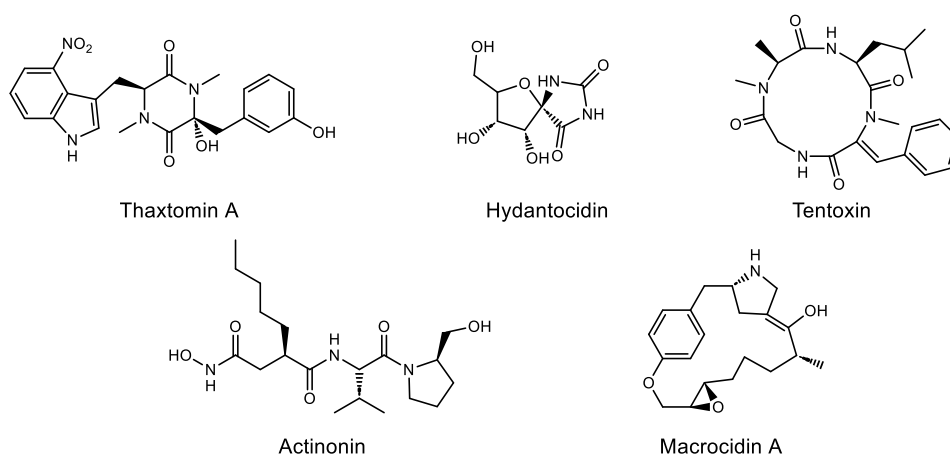


Figure 5: Structures of several herbicidal natural products which are not commercialized.^{55–59}

In addition to the commercialized herbicides already mentioned, there is a large number of further natural products with a reported herbicidal effect. Many of these act via MOAs different from those utilized by commercial herbicides (see Figure 5 for examples). A good source for these can be plant pathogens and soil microbes.³⁰ The advantage of using microbe-derived NPs lies in the possibility of producing them through large-scale fermentation of the host.⁶⁰ This avoids the problem of complicated synthesis of the usually complex molecules.

Outlook

As shown in this chapter, crop protection has a long history and has undergone rapid development in the last century. The use of synthetic herbicides, together with the use of fertilizers, has led to a sharp increase in crop yields per acre and minimized the impact of crop failures. At the same time, the widespread and excessive use of these herbicides has had a negative impact on agriculture and the environment. A loss of biodiversity, the entry of pesticides into the groundwater and a worrying increase in the occurrence of herbicide-resistant weeds are the biggest problems and are driving the demand for new technologies. Many alternative methods such as organic farming, agroforestry or intercropping have been (re)discovered in recent decades. They can sometimes be a good alternative, but today they only account for a very small proportion of the cultivated area and usually have lower yields. Additionally, a ban on all agrochemicals is also not advisable, as the complete ban in Sri Lanka has shown.^{61,62} Here, yields fell sharply and led to a famine, followed by a withdrawal of the ban.

A better alternative is a controlled and combined use of herbicides together with other weed control methods in the concept of integrated pest management. This can minimize the disadvantages of each individual practice and at the same time secure agricultural yields in the long term. The continuous search for new herbicides with novel mechanisms of action is also crucial. In particular, natural products and mimetics can be an important part of the solution due to their aforementioned advantages.

References

- (1) Bellwood, P. *First Farmers: the Origins of Agricultural Societies*; Malden Blackwell, Oxford, **2005**.
- (2) Bocquet-Appel, J.-P. *Science* (New York) **2011**, 333, 560–561.
- (3) Snir, A.; Nadel, D.; Groman-Yaroslavski, I.; Melamed, Y.; Sternberg, M.; Bar-Yosef, O.; Weiss, E. *PLoS One* **2015**, 10, e0131422.
- (4) Zimdahl, R. L. *A history of weed science in the United States*; Elsevier, London, **2010**.
- (5) Krantz, D. *Religions* **2016**, 7, 100.
- (6) White, K. D. *Agric. Hist.* **1970**, 1970, 281–290.
- (7) Li, M.; Guo, J.; Ren, T.; Luo, G.; Shen, Q.; Lu, J.; Guo, S.; Ling, N. *Agric. Ecosyst. Environ.* **2021**, 319, 107550.
- (8) Sayre, L. B. *Phys. Chem. Earth (2002)* **2010**, 35, 851–859.
- (9) Tull, J. *The horse-hoeing husbandry*; Printed by A. Rhames, for R. Gunne, G. Risk, G. Ewing, W. Smith, & Smith and Bruce, Booksellers, Dublin, **1733**.
- (10) Hayes, W. J.; Laws, E. R., Eds. *Handbook of pesticide toxicology*; Academic Press, San Diego, **1991**.
- (11) Pokorny, R. J. *Am. Chem. Soc.* **1941**, 63, 1768.
- (12) Cudney, D. W. *CEPPC* **1996**, 2007.
- (13) Dill, G. M.; Sammons, R. D.; Feng, P. C. C.; Kohn, F.; Kretzmer, K.; Mehrsheikh, A.; Bleeke, M.; Honegger, J. L.; Farmer, D.; Wright, D.; Haupfear, E. A. Glyphosate: Discovery, Development, Applications, and Properties. In *Glyphosate resistance in crops and weeds. History, development, and management*; Nandula, V. K., Ed.; Wiley: Hoboken, **2010**, 1–33.
- (14) Duke, S. O.; Powles, S. B. *Pest Manag. Sci.* **2008**, 64, 319–325.
- (15) Green, J. M.; Owen, M. D. K. *J. Agric. Food Chem.* **2011**, 59, 5819–5829.
- (16) FAOSTAT. faostat.fao.org, July 14, **2023**.
- (17) Sharma, A.; Kumar, V.; Shahzad, B.; Tanveer, M.; Sidhu, G. P. S.; Handa, N.; Kohli, S. K.; Yadav, P.; Bali, A. S.; Parihar, R. D.; Dar, O. I.; Singh, K.; Jasrotia, S.; Bakshi, P.; Ramakrishnan, M.; Kumar, S.; Bhardwaj, R.; Thukral, A. K. *SN Appl. Sci.* **2019**, 1–16.
- (18) Dayan, F. E. *Plants* **2019**, 8, 341.
- (19) Herbicide Resistance Action Committee (HRAC). <https://www.hracglobal.com> July 14, **2023**.
- (20) MacLaren, C.; Storkey, J.; Menegat, A.; Metcalfe, H.; Dehnen-Schmutz, K. *Agron. Sustainable Dev.* **2020**, 40, 1–29.
- (21) Peterson, M. A.; Collavo, A.; Ovejero, R.; Shivrain, V.; Walsh, M. J. *Pest Management Science* **2018**, 74, 2246–2259.
- (22) Harper, J. L. *Proceedings of the Third British Weed Control Conference* **1956**.
- (23) Hilton, H. W. *Hawaiian Sugar Planters Association Annual Report* **1957**, 1957.
- (24) Shaner, D. L. *Weed Science* **2014**, 62, 427–431.
- (25) Green, J. M. *Weed Science* **2009**, 57, 108–117.
- (26) Délye, C.; Jasieniuk, M.; Le Corre, V. *Trends Genet.* **2013**, 29, 649–658.
- (27) Gerwick, B. C. *Thirty years of herbicide discovery: surveying the past and contemplating the future*; Chapters VII–IX in *Agrow Report. (Silver Jubilee Edition)*., London, 2010.
- (28) Hawqal, I. *Orpheus, peri lithon*: poema Orpheo a quibusdam adscriptum, 1st ed.; Payne, White, and Elmsly, London, **1781**.

- (29) The Free Dictionary. "Natural product". <https://thefreedictionary.com/Natural+product> July 11, **2023**.
- (30) Duke, S. O.; Dayan, F. E.; Romagni J.; Rimando. *Weed Res.* **2000**, 40, 99–111.
- (31) Daly, J.; Witkop, B. *Clin. Toxicol.* **1971**, 4, 331–342.
- (32) Botana, L. M., Ed. *Seafood and freshwater toxins: Pharmacology, physiology, and detection*, 3rd ed.; Taylor & Francis, Boca Raton, **2014**.
- (33) Sparks, T. C.; Duke, S. O. *J. Agric. Food Chem.* **2021**, 69, 8324–8346.
- (34) Sparks, T. C.; Hahn, D. R.; Garizi, N. V. *Pest Manag. Sci.* **2017**, 73, 700–715.
- (35) Dayan, F. E.; Duke, S. O. *Plant Physiol.* **2014**, 166, 1090–1105.
- (36) *DB besiegelt Glyphosat-Ausstieg ab 2023*
(https://www.deutschebahn.com/de/presse/pressestart_zentrales_uebersicht/DB-besiegelt-Glyphosat-Ausstieg-ab-2023--10414622), Berlin, June 19, **2023**.
- (37) Fallahi, E. *Horttech* **1997**, 7, 395–399.
- (38) Dev Kumar, G.; Mis Solval, K.; Mishra, A.; Macarisin, D. *Sci Rep* **2020**, 10, 10287.
- (39) Loddo, D.; Jagarapu, K. K.; Strati, E.; Trespidi, G.; Nikolić, N.; Masin, R.; Berti, A.; Otto, S. *Agronomy (Basel)* **2023**, 13, 1511.
- (40) Ciriminna, R.; Fidalgo, A.; Ilharco, L. M.; Pagliaro, M. *Biofuel. Bioprod. Biorefin.* **2019**, 13, 1476–1482.
- (41) Hoerlein, G. Glufosinate (Phosphinothricin), A Natural Amino Acid with Unexpected Herbicidal Properties. In *Reviews of Environmental Contamination and Toxicology. Continuation of Residue Reviews*; Ware, G. W., Ed.; Reviews of Environmental Contamination and Toxicology 138; Springer: New York, **1994**, 73–145.
- (42) Thompson, C. J.; Seto, H. *Biotechnol.* **1995**, 28, 197–222.
- (43) Copping, L. G.; Duke, S. O. *Pest Manag. Sci.* **2007**, 63, 524–554.
- (44) Takano, H. K.; Dayan, F. E. *Pest Manag. Sci.* **2020**, 76, 3911–3925.
- (45) Takano, H. K.; Beffa, R.; Preston, C.; Westra, P.; Dayan, F. E. *Planta* **2019**, 249, 1837–1849.
- (46) Tachibana, K. *J. Pestic. Sci.* **1986**, 11, 33–37.
- (47) Knudsen, C. G.; Lee, D. L.; Michaely, W. J.; Chin, H.-L.; Nguyen, N. H.; Rusay, R. J.; Cromartie, T. H.; Gray, R.; Lake, B. H.; Fraser, T. E. M.; Cartwright, D. Discovery of the triketone class of HPPD inhibiting herbicides and their relationship to naturally occurring β -triketones. In *Allelopathy in Ecological Agriculture and Forestry*; Springer, Dordrecht, **2000**, 101–111.
- (48) van Almsick, A. *Outlook Pest Man* **2009**, 20, 27–30.
- (49) Moran, G. R. *Arch. Biochem. Biophys.* **2005**, 433, 117–128.
- (50) Mitchell, G.; Bartlett, D. W.; Fraser, T. E.; Hawkes, T. R.; Holt, D. C.; Townson, J. K.; Wichert, R. A. *Pest Manag. Sci.* **2001**, 57, 120–128.
- (51) Tworowski, T. *Weed Sci.* **2002**, 50, 425–431.
- (52) Chang, Y.; Harmon, P. F.; Treadwell, D. D.; Carrillo, D.; Sarkhosh, A.; Brecht, J. K. *Front. Nutr.* **2021**, 8, 805138.
- (53) Korres, N. E.; Burgos, N. R.; Duke, S. O. *Weed control: Sustainability, hazards and risks in cropping systems worldwide*; CRC Press, Boca Raton, **2019**.
- (54) Young, S. *West Central Research and Extension Center, North Platte* **2004**.
- (55) King, R. R.; Lawrence, C. H.; Gray, J. A. *J. Agric. Food Chem.* **2001**, 49, 2298–2301.
- (56) Haruyama, H.; Takayama, T.; Kinoshita, T.; Kondo, M.; Nakajima, M.; Haneishi, T. *J. Chem. Soc. Perkin 1* **1991**, 1637.
- (57) Arntzen, C. J. *BBA* **1972**, 283, 539–542.

- (58) Hou, C.-X.; Williams, M. Actinonin-Induced Inhibition of Plant Peptide Deformylase: A Paradigm for the Design of Novel Broad-Spectrum Herbicides. In *Natural products for pest management*; Rimando, A. M.; Duke, S. O., Eds.; ACS symposium series 927; American Chemical Society: Washington, DC, **2006**, 243–254.
- (59) Graupner, P. R.; Carr, A.; Clancy, E.; Gilbert, J.; Bailey, K. L.; Derby, J.-A.; Gerwick, B. C. *J. Nat. Prod.* **2003**, 66, 1558–1561.
- (60) Rodrigo Klaic; Raquel C. Kuhn; Edson L. Foletto; Valéria Dal Prá; Rodrigo J. S. Jacques; Jerson V. C. Guedes; Helen Treichel; Altemir J. Mossi; Débora Oliveira; J. Vladimir Oliveira; Sérgio L. Jahn; Marcio A. Mazutti. An overview regarding bioherbicide and their production methods by fermentation. In *Fungal Biomolecules*; John Wiley & Sons, Ltd, **2015**, 183–199.
- (61) Ghose, D., Draga, E. Fernandes, A. *Fertilizer Import Bans, Agricultural Exports, and Welfare*; The World Bank, **2023**.
- (62) Jayasiri, M. M. J. G. C. N.; Ingold, K.; Weerahewa, J.; Dayawansa, N. D. K.; Yadav, S. *Environ Dev Sustain* **2024**, 1–20.

Chapter 2

Total synthesis and biological studies of tentoxin and derivatives

Abstract

A new total synthesis for the natural product tentoxin was developed, starting from commercially available phosphonate **7** in seven steps with an overall yield of 33 %. The key step of the synthesis is a *Horner-Wadsworth-Emmons* (HWE) olefination to the dehydroamino acid moiety. This step also allows a late-stage derivatization by exchange of the aldehyde building block and therefore a rapid synthesis of derivatives. In total, 14 derivatives were synthesized using this new approach as well as 5 derivatives using an already established synthesis route. A docking study was performed *in silico* for a rational selection of derivatives. All compounds were tested *in vivo* for their herbicidal activity using the *Lemna minor* toxicity bioassay. For the first time, derivatives were found to have a higher activity compared to the natural product. Compound **5e**, which has a *para*-methylation at the aromatic core, was found to show the highest growth inhibition activity.

Introduction

The natural product tentoxin (TTX) is a cyclic tetrapeptide with the sequence cyclo(*N*-Me-L-Ala-L-Leu-*N*-Me Δ Phe^Z-Gly). It is produced by various phytopathogenic fungi of the *Alternaria* genus

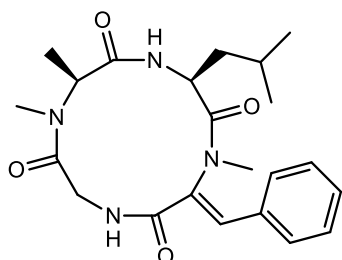


Figure 6: Structure of tentoxin.

and was first found in *Alternaria alternata* (Fr.) Keissl. (Fr.) in 1965 by Templeton and coworkers.¹ They investigated diseased cotton seedlings with diminished stands and found TTX to be the active metabolite that caused the demise of the seedlings. Furthermore, they discovered that TTX is produced by other *Alternaria* species such as *Alternaria solani* or *Alternaria raphani*. In 2012, TTX was also isolated from the fungus *Phoma* sp., derived from the giant jellyfish *Nemopilema nomurai*.²

In the following, many studies have been conducted to decipher its biological activity. It was found that TTX is a non-specific phytotoxin which can lead to chlorosis in higher plants.³ Initial studies suggested that the toxin only affects dicotyledons, with the exception of tomatoes and members of the Cruciferae. However, it was later found that there are numerous deviations from this general rule and even plants of the same plant family are affected differently by the toxin.⁴ Several potential targets have been identified in the search for the MOA of TTX. The main cause for its biological activity has been found to be the binding of TTX to the F1-ATPase, which results in a reduction of ATPase activity and photophosphorylation.⁵⁻⁸ This leads to the blocking of ATP synthesis in the chloroplasts of sensitive species. Interestingly, the effect of tentoxin on the ATPase activity changes with its concentration. At low concentrations, the F1-ATPase activity is inhibited, and the treated plant shows chlorosis. At higher concentrations of tentoxin, the ATPase activity seems to be stimulated, whereas the photophosphorylation is still inhibited.⁹ This leads to the assumption of two different binding sides with different affinities to tentoxin.¹⁰ Furthermore, a variety of secondary targets were found, for example, TTX can also block K⁺ uptake from roots as well as promote its translocation.^{11,12}



Figure 7: Location of tentoxin in the crystal structure of the chloroplast F1-ATPase, schematic representation of the molecular structure of a single chloroplast $\alpha\beta$ -pair with the proposed TTX-binding.

Tentoxin synthesis methods

The peptide sequence of TTX was first assigned in 1974 by Meyer and coworkers as cyclo(*N*-Me-L-Ala-L-Leu-*N*-Me Δ Phe^Z-Gly).¹³ The peculiarity of its structure is first of all that it is a 12-membered macrocycle, belonging to the class of cyclic tetrapeptides. These compounds have a strained ring system and are usually unstable as most cyclotri- and tetrapeptides are prone to transannular reactions, forming e.g. diketopiperazines. NMR studies showed that TTX is especially rigid and stable.¹⁴ One reason for this is that two of the four amino acids are *N*-methylated. However, the rigidity is even stronger influenced by another structural element of TTX, the dehydroamino acid (Δ AA) (*Z*)-*N*-methyl didehydrophenylalanine (*N*-Me Δ Phe^Z).

Δ AAs can be found in various cyclic peptides with interesting biological activities, usually, they are the active site and part of the mechanism of action (MOA), often acting as irreversible electrophilic Michael acceptor. Biological active examples are tuberactinomycins (antibiotic), syringopeptins (phytotoxic) or vitilevuamide (cytotoxic towards HCT 116), wherein the Δ AAs were shown to affect their biological activities as well as physicochemical properties.^{15–20} Furthermore, Δ AAs can lead to an improvement in resistance to degradation.²¹ The influence of the Δ AA on the activity of tentoxin was also confirmed by testing dihydrotentoxin, which does not induce chlorosis in plants.^{22–24}

The synthesis of Δ AAs can be carried out using four principally different reaction mechanisms. The most widely used approach in the literature is via a β -elimination of functionalised amino acids, such as cysteine, serine, or threonine (**A**).²⁵ The latest approach features the late-stage installation of Δ AAs by *N*-chlorination of the peptide bond, followed by a subsequent β -elimination (**B**).²⁶ Furthermore, *Horner-Wadsworth-Emmons* (HWE) olefination can be used to synthesize the Δ AAs starting from various phosphonates (**C**).^{27,28} Another approach achieves the synthesis of Δ AAs by coupling two peptide fragments at the α -carbon (**D**).^{29,30}

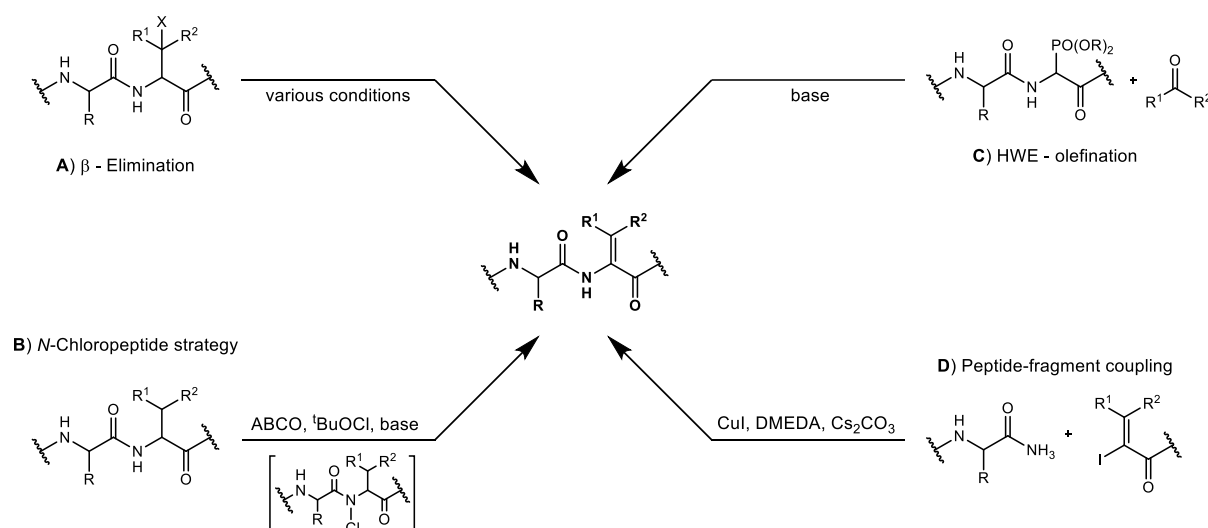
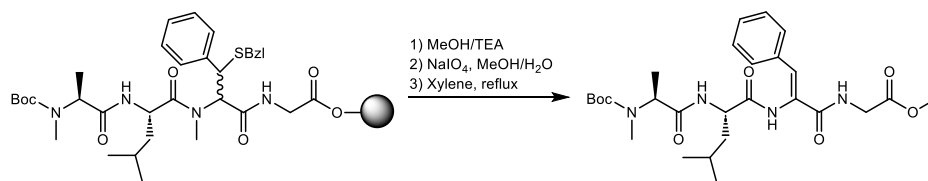


Figure 8: Different synthesis strategies towards Δ AAs.

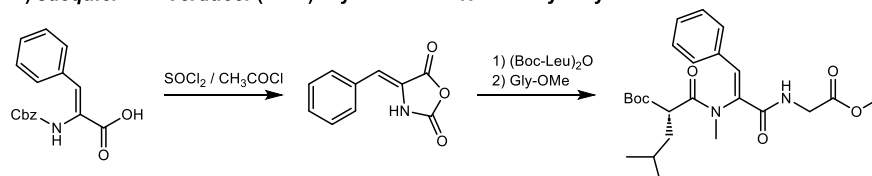
The difficulty of the total synthesis of tentoxin arises mainly from the introduction of Δ Phe in its (*Z*) configuration, selective methylation of Ala and Δ Phe^{*Z*}, and a racemization-free macrocyclization. Until today, seven total syntheses of TTX have been published, all of which perform the cyclization at the same peptide bond and therefore use the same linear precursor tetrapeptide (compound **4a**, *N*-Me-L-Ala-L-Leu-*N*-Me Δ Phe^{*Z*}-Gly).^{31–37}

The first total synthesis of tentoxin was achieved in 1974 by *Rich* and *Mathiapparanam*.³¹ They approached the total synthesis via solid phase peptide synthesis (SPPS), reaching the linear precursor Boc-*N*-Me-L-Ala-L-Leu-Phe(3-SBzl)-Gly-OMe. After cleaving from the resin, the nonmethylated 3-benzylthiophenylalanine was converted into *N*-Me Δ Phe^{*Z*} by first oxidation to the corresponding sulfoxide which subsequently undergoes a thermolytic dehydrosulfenylation at 140 °C. The mixture of isomers resulting from this β -elimination was separated by column chromatography. Selective *N*-methylation of Δ Phe^{*Z*} gave the linear tetrapeptide (Boc-*N*-Me-L-Ala-L-Leu-*N*-Me Δ Phe^{*Z*}-Gly-OMe), which after deprotection, activation and cyclization gave the desired natural product TTX.

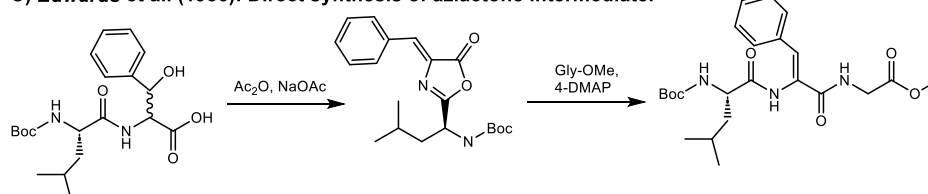
A) Rich et al. (1977): β -Elimination to install the Δ Phe^Z in tetrapeptid backbone via semi-solid phase synthesis.



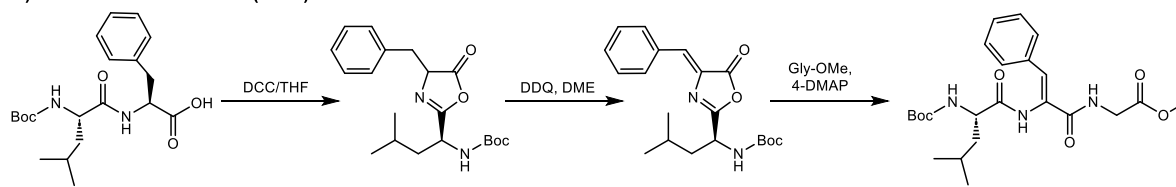
B) Jacquier and Verducci (1984): Synthesis via *N*-carboxyanhydride.



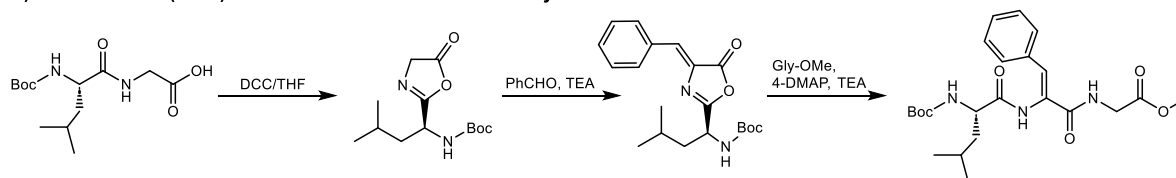
C) Edwards et al. (1986): Direct synthesis of azlactone intermediate.



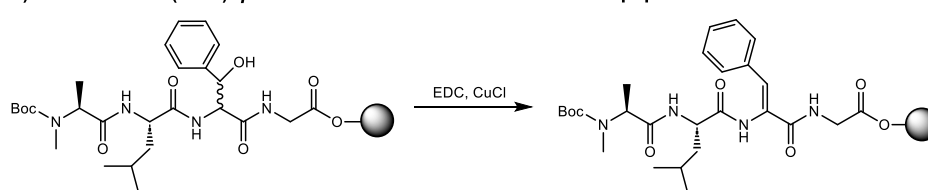
D) Cavelier and Verducci (1995): Installation of Δ Phe via azlactone intermediate.



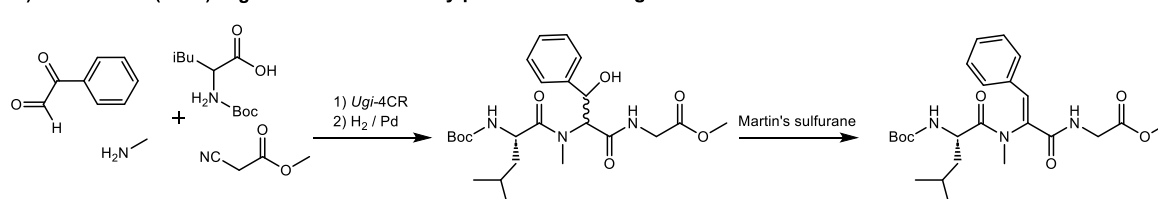
E) Loiseau et al. (2002): Installation of Δ Phe via Erlenmeyer aldolization reaction.



F) Jiménez et al. (2003): β -Elimination to install the Δ Phe in tetrapeptid backbone via SPPS.



G) Neves et al. (2015): *Ugi*-reaction followed by β -elimination using Martin's sulfuran.



Scheme 1: Overview of the different synthesis methods of Δ Phe^Z within the seven different total syntheses of tentoxin.

Jacquier and Verducci achieved the next total synthesis of tentoxin in 1984. They initially also attempted a route via SPPS by direct coupling of *N*-Boc- Δ Phe^Z-OH to a glycine preloaded resin. However, the subsequent Boc deprotection always led to hydrolysis.³² Therefore, they developed

a method in solution phase based on the preparation of the *N*-carboxyanhydride of Cbz-protected $\Delta\text{Phe}^Z\text{-OH}$, which could then be coupled without difficulty. Afterwards, they followed the procedures of *Rich* et al. towards TTX, achieving an overall yield of 16 %.

Later on, *Edwards* and coworkers established a synthesis route starting from phenyl serine via an azlactone intermediate, which readily reacted with Gly-OMe to the linear precursor.³³ *Cavelier* and *Verducci* improved this approach by starting from phenyl alanine, hence making the route ready for the synthesis of derivatives by replacement of the used amino acid.^{9,34} *Loiseau* et al. came to the same intermediate but used an *Erlenmeyer* aldolization to set up the azlactone intermediate.³⁵

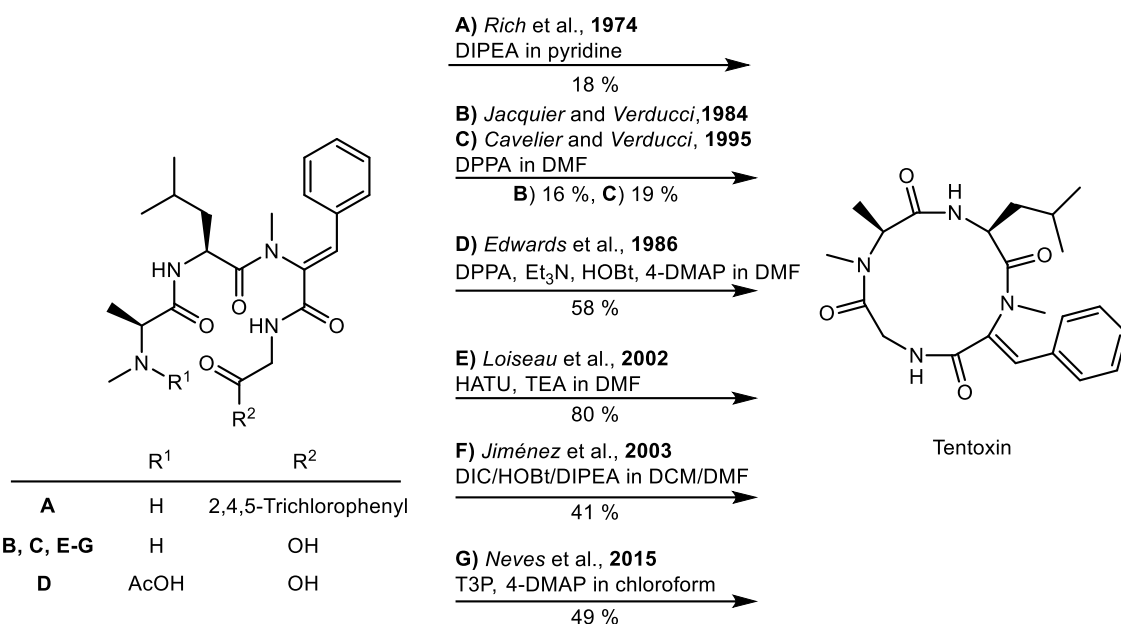
The two most recent total synthesis used again the β -elimination approach. *Jiménez* et al. developed a new route towards TTX using SPPS and performed all steps besides the macrocyclization on resin.³⁶ They introduced phenyl serine in the peptide sequence which converts via dehydration / β -elimination to ΔPhe^Z using CuCl and EDC. *Neves*, on the other hand, used the *Ugi*-4CR to synthesize a linear tripeptide containing *N*-methylated phenyl serine after hydrogenation.³⁷ This amino acid could then be converted to *N*-Me ΔPhe^Z using Martin's sulfurane.^{38,39}

The last and also complicated step is the macrocyclization of the linear tetrapeptide. Due to the four peptide bonds within tentoxin, four peptide linkage sites are theoretically possible, which would require one of the following linear precursors:

- A) $\text{R}^1\text{-N-Me-L-Ala-L-Leu-N-Me}\Delta\text{Phe}^Z\text{-Gly-R}^2$
- B) $\text{R}^1\text{-Gly-N-Me-L-Ala-L-Leu-N-Me}\Delta\text{Phe}^Z\text{-R}^2$
- C) $\text{R}^1\text{-L-Leu-N-Me}\Delta\text{Phe}^Z\text{-Gly-N-Me-L-Ala-R}^2$
- D) $\text{R}^1\text{-N-Me}\Delta\text{Phe}^Z\text{-Gly-N-Me-L-Ala-L-Leu-R}^2$

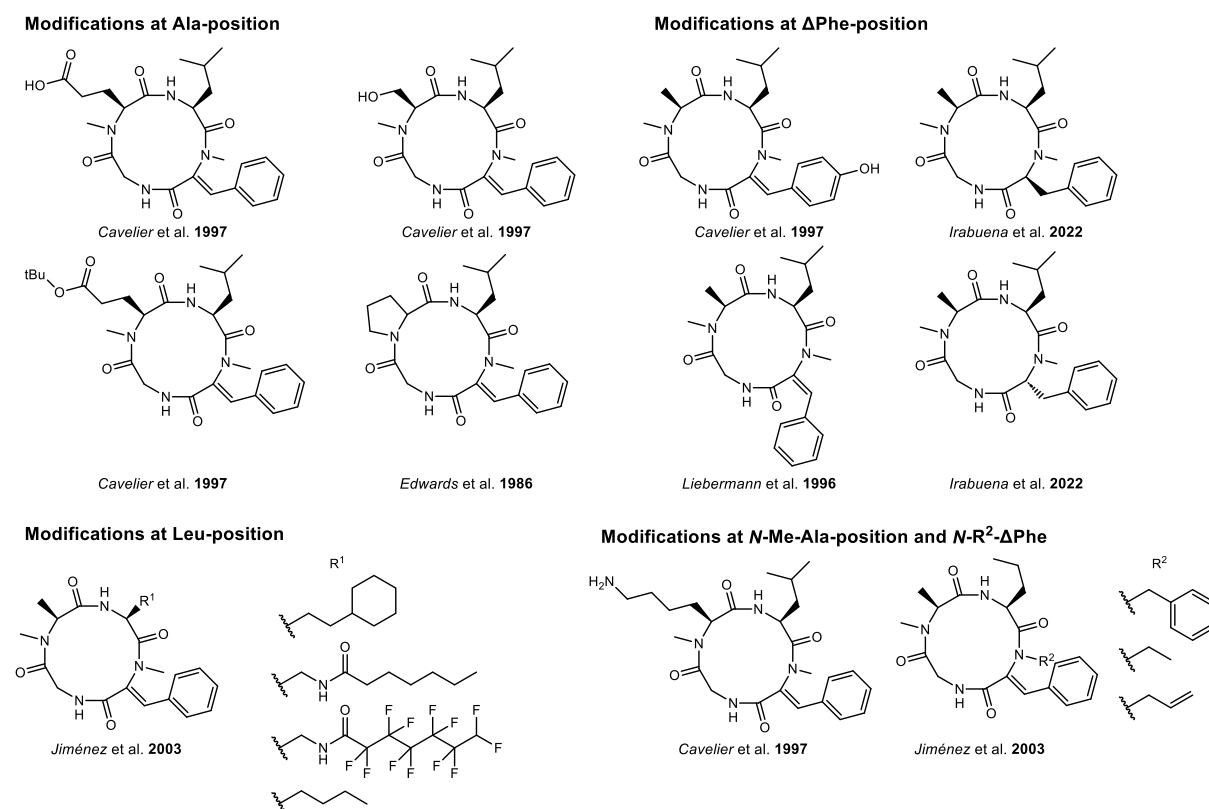
However, the choice of the best precursor is limited by several factors. ΔAAs have low nucleophilicity due to their enamine functionality, making macrocyclization of **B** and **D** difficult. With tetrapeptide **C**, on the other hand, the risk of epimerization during macrocyclization is very high. For this reason, all total syntheses to date have been based on the linear tetrapeptide **A** (see Scheme 2). Here, no epimerization can be expected due to the terminal glycine which also serves as a sufficiently reactive C-terminal.

As shown in Scheme 2, a total of six different cyclization conditions have been used in the literature. Yields ranging from 16 % to 80 % were obtained, the highest by *Loiseau* et al. using HATU and TEA in DMF. *Neves* et al., on the other hand, screened different reagents and could not reproduce the high yields described before. In their studies, the use of propanephosphonic acid anhydride (T3P) together with 4-DMAP and TEA in chloroform proved to be the most promising method, yielding 49 %.



Scheme 2: Overview of the different cyclization conditions and yields (as given in literature) of the seven different total syntheses of tentoxin.

Derivatization of tentoxin



Scheme 3: Overview of all tentoxin derivatives described in the literature to date.⁴⁰

Based on these total syntheses, several derivatives of TTX have already been prepared (see Scheme 3). The authors' aim was either to determine the structure-activity relationship (i.e. *Cavelier et al.*) or to demonstrate the possibilities of their synthesis (i.e. *Jimenez et al.*) without testing the

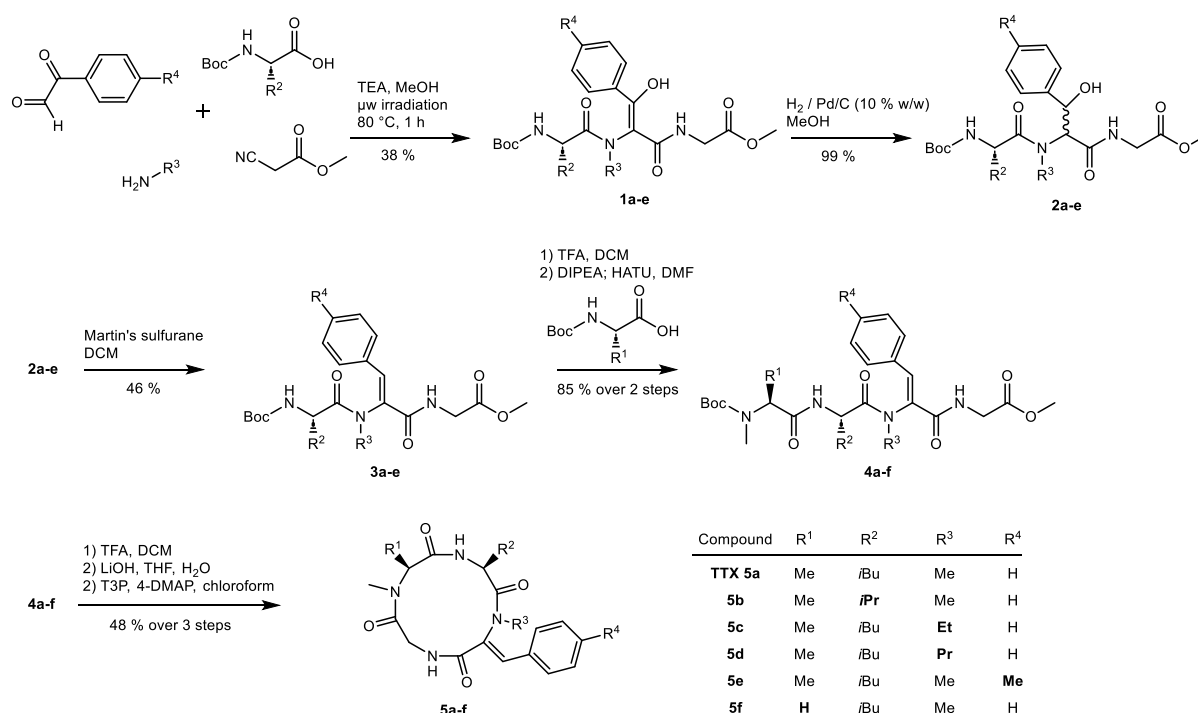
biological activity of the new compounds. Most of the derivatizations focus on the change of the amino acid side-chains, with the only change of the aromatic core being made by *Cavelier* and *Verducci*, who replaced it with *N*-Me- Δ Tyr^z.

None of the synthesized derivatives could increase the activity of TTX, only the *N*-Me-Ser and *N*-Me- Δ Tyr^z substituted analogues were found to have similar activities as the natural product.⁹ This shows great potential for further investigation of the promising natural product tentoxin with the aim of understanding its structure-activity relationship further and also finding derivatives that outperform the biological activity of TTX.

Results and discussion

Synthesis of tentoxin derivatives based on the *Ugi-4CR* approach by Neves et al.

To elucidate the structure-activity relationship of the herbicidal activity of tentoxin and to potentially improve its activity, the synthesis of new derivatives is crucial. The synthetic method developed by Neves et al. based on an *Ugi-4CR* allows relatively simple derivatization of all side-chains of TTX.³⁷ Therefore, a modified synthetic route based on the findings of Neves et al., developed at the Leibniz Institute of Plant Biochemistry (Halle, Germany) was initially used.



Scheme 4: Synthesis route for the synthesis of tentoxin **5a** and derivatives **5b-f**. Yields given for the synthesis of **5a**.

The synthesis route starts with a microwave assisted *Ugi-4CR* reaction.⁴¹ Here, the corresponding amine first reacts with phenylglyoxal, which forms the imine. Then, the amino acid and isonitrile are added to the reaction, from which the tetrapeptide **1a** is formed. Through this reaction, a direct formation of the (β -OH)- Δ Phe is achieved. This can be converted by subsequent hydrogenation and dehydration (β -elimination) exclusively to Δ Phe². The β -elimination can be achieved in good yields using Martin's sulfurane, a hypervalent organosulfur compound. The next step is the addition of the last AA, which can be linked after Boc-deprotection using standard peptide coupling conditions (HATU, *Hünig's* base). The last step after deprotection of the C- and N-terminus is the macrocyclization. Here, propanephosphonic acid anhydride (T3P) and 4-DMAP were used. The reaction was carried out in chloroform at a concentration of 0.005 M to avoid di- and oligomerization. Using this protocol, tentoxin was obtained in eight steps in a total yield of 7 %.

Using the *Ugi-4CR*, an easy derivatization is possible by changing the components of the reaction.⁴² As shown in Scheme 4, four different derivatives **5b-e** were prepared this way. The only limitation is the availability of substrates, i.e., only few phenyl glyoxal derivatives and isonitriles are commercially available. By changing the different substrates, the side-chains of the amino acids Gly, Leu and *N*-Me Δ Phe² can be modified as well as the alkylation on the nitrogen of *N*-Me Δ Phe². In the fifth step, further modification is possible by replacing *N*-MeAla with another amino acid

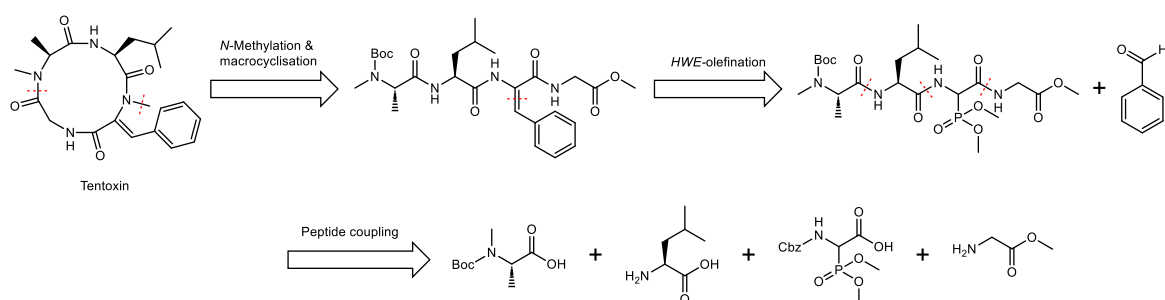
used for the preparation of **5f**. Synthesis of the five derivatives demonstrated that this method can be used for practical derivatization of tentoxin. Furthermore, bioassays which were subsequently carried out have already provided important insights into the need for further derivatives.

Development of a new synthesis method for TTX

The synthesis method developed by Neves et al. offers the possibility of synthesizing a wide variety of derivatives by modifying the starting materials. However, the method also has two shortcomings: first, the modification is usually introduced in the first step - the *Ugi* reaction - which means that the following seven reaction steps have to be carried out individually for each new derivative. Second, there is a dependence on the availability of the starting materials, which limits the number of possible derivatives. Especially the modification of the aromatic moiety is cumbersome since there are very few substituted phenylglyoxal derivatives commercially available. However, since the *N*-Me Δ Phe^z is the most special feature of TTX and is of outstanding importance for its activity, and since the activity might be increased with the help of its modification, as it will be shown in this chapter, a special focus is required on this moiety.

Synthesis plan

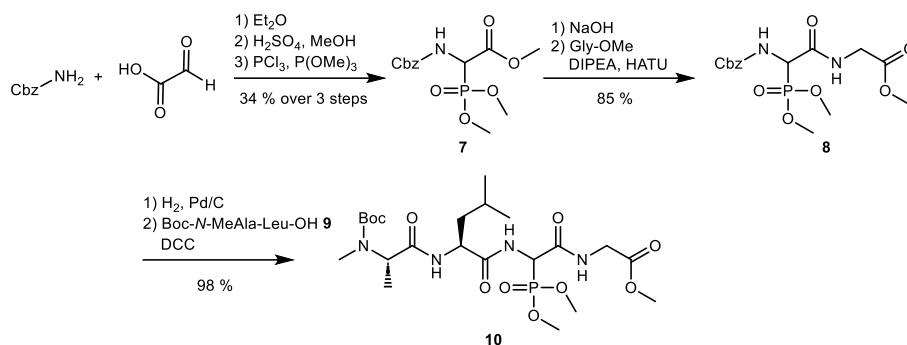
The aim of this chapter is to develop a new total synthesis for tentoxin with the possibility of a selective modification of the aromatic moiety. The derivatization should ideally take place as late as possible in the total synthesis. The retrosynthetic analysis, shown in Scheme 5, highlights the key steps of the new approach. The main point of the synthesis is the synthesis of the dehydroamino acid by means of an HWE-olefination reaction. This allows the tetrapeptide phosphonate to be coupled with various aldehydes or ketones. The subsequent methylation and macrocyclization can be performed following established methods from other total syntheses. The setup of the phosphonate can be done by peptide coupling of commercially available amino acids. From thereon, a further late stage derivatization is possible.



Scheme 5: Retrosynthetic approach to TTX.

Synthesis of the precursor **10** for the HWE-olefination

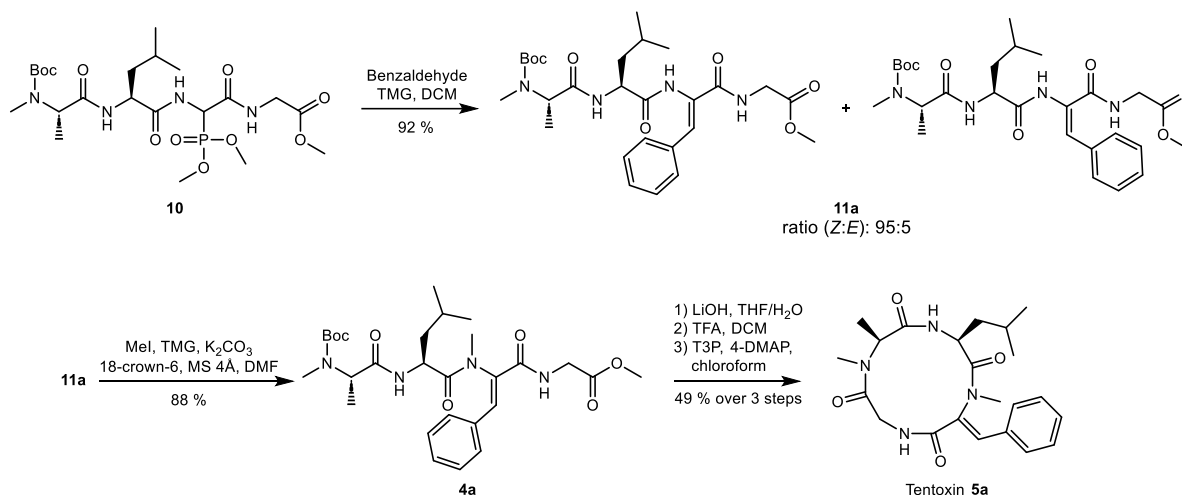
As shown in Scheme 6, the synthesis of the precursor **10** for the HWE-olefination starts with the coupling of glyoxal and benzyl carbamate. The resulting intermediate **6** reacts subsequently with phosphorus trichloride, followed by trimethyl phosphite, giving the corresponding phosphonate **7** via a *Arbuzov* reaction. Subsequently, **7** is linked by peptide coupling to glycine methyl ester to give dipeptide **8**. Next, the Cbz protecting group is cleaved off by hydrogenation, and dipeptide **9** Boc-*N*-Me-L-Ala-L-Leu-OH, which was synthesized before, is attached. This gives the linear tetrapeptide **10**, used for the following coupling.



Scheme 6: Synthesis of the precursor **10** for the HWE-olefination.

Synthesis of Tentoxin via HWE-olefination

In the second part of the total synthesis of tentoxin, ΔPhe^Z is generated using the *Horner-Wadsworth-Emmons* olefination from the previously prepared phosphonate **10** with benzaldehyde (see Scheme 7).^{43–46} Under mild reaction conditions, it yields the desired linear tetrapeptide **11a** in excellent yield together with the (*E*)-isomer, the ratio being 95:5 (*Z*:*E*). The isomers are easily separated by column chromatography.



Scheme 7: Synthesis of tentoxin starting from phosphonate **10**.

Subsequently, selective *N*-methylation of ΔPhe^Z provides the linear tentoxin **4a**, which is also the intermediate from the total synthesis described before. The methylation is carried out by an excess of methyl iodide with the aid of potassium carbonate and 18-crown-6. Under these conditions, only the ΔAA is selectively methylated. A strict exclusion of water is important for the reaction, for which molecular sieve was also added to the reaction mixture. Finally, the linear tetrapeptide **4a** gets deprotected and cyclized using T3P and 4-DMAP as described before.

In summary, it was possible to obtain tentoxin starting from commercially available phosphonate **7** in eight steps with an overall yield of 33 %. The synthesis product agrees in all spectroscopic data with the literature values of the natural product and the products of the other total syntheses.^{1,37}

Docking study of derivatives of TTX in the chloroplast ATPase

To achieve a more targeted synthesis of derivatives, an *in silico* docking study was performed. The aim of this study was to elucidate the energetic relationship between the amino acids of the ATPase and the TTX derivatives with the purpose of achieving an increased interaction, from which a higher activity *in vivo* should follow. In this study, various tentoxin derivatives, modified at the Δ AA were docked into an enzyme model based on the crystal structure of native spinach chloroplast F1-ATPase, complexed with TTX.⁴⁷ The docked structures are phenyl-modified tentoxins. Since the aromatic moieties interact with the lipophilic part of the pocket belonging mostly to the α -subunit, mainly nonpolar side-chains were selected i.e., aryl chains or ether chains, among others.

The study showed that especially substitutions in *meta*- and *para*-positions on the aromatic core led to increased interactions. In total, 79 preselected structures were docked, of which 14 derivatives were chosen to be synthesized. They either showed stronger interaction with the ATPase than tentoxin or were of interest for comparison. In Scheme 8, some examples of the chosen modifications can be seen. Comparing the interaction energies of the derivatives with substitution in *para*-position, it was found that the strongest interaction was achieved with the derivative possessing a C₃-chain. If another aliphatic side-chain was added in *meta*-position, the calculated interaction energy could be further increased. These calculations provided a rational starting point for the following derivatizations.

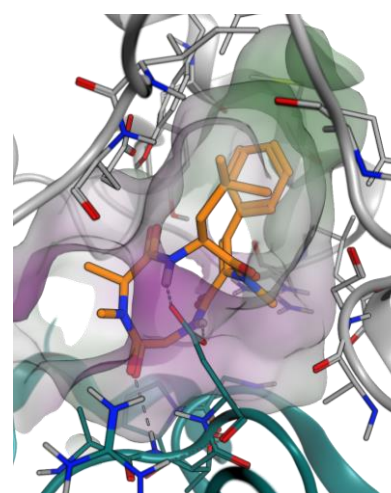
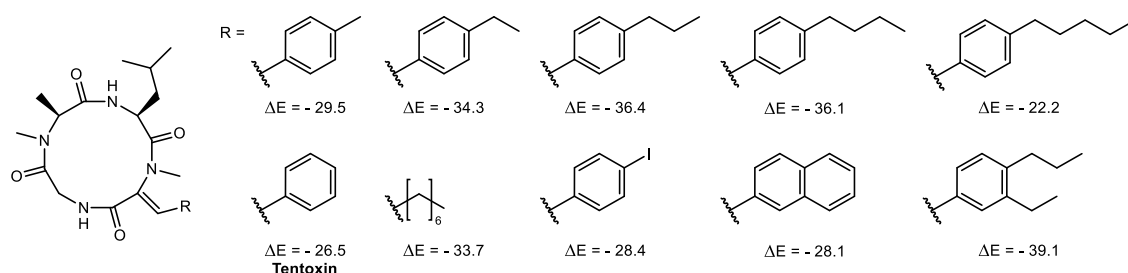
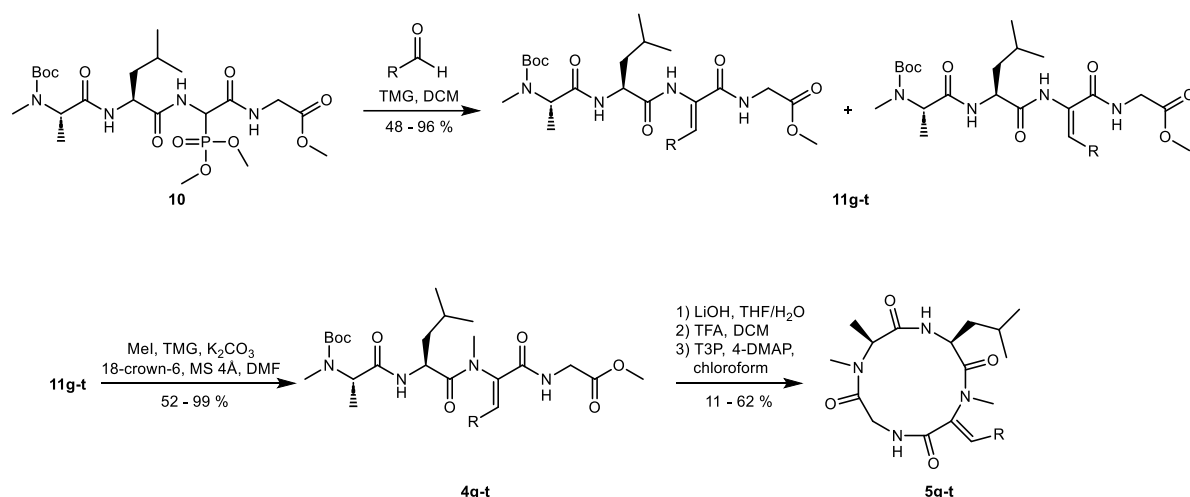


Figure 9: Docking of tentoxin (orange) in the alpha (grey) and beta (cyan) subunit of the ATPase. Green: lipophile, purple: hydrophile, white: neutral.



Scheme 8: Calculated interaction energies of exemplary structures with a modified aromatic ring. Units in kcal * mol⁻¹.

Synthesis of TTX derivatives by late-stage modification



Scheme 9: Synthesis of tentoxin derivatives **5g-t** starting from phosphonate **10**.

The main advantage of the new synthesis method is the possibility to introduce different side-chains at the ΔAA . This is done by exchanging the aldehyde in the HWE-olefination step (see Scheme 9). Furthermore, this reaction yields predominantly the desired (*Z*)-isomer, which, at least for the natural product, is responsible for the biological activity.⁴⁸

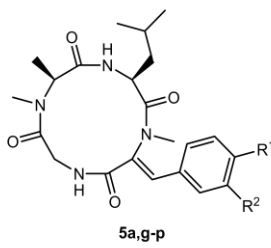
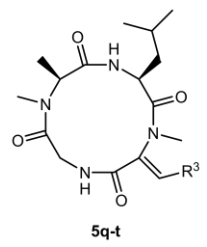
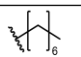
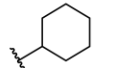
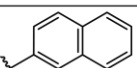
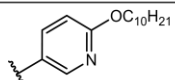
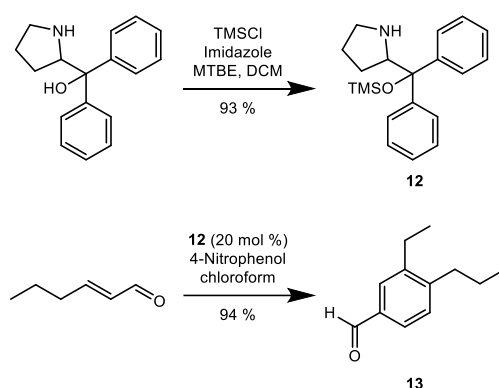
	#	R ¹	R ²	<i>Z/E</i> ratio	Yield HWE	Yield methylation	Yield cyclization
	5a	H	H	95:5	92 %	88 %	49 %
	5g	ethyl	H	96:4	79 %	91 %	49 %
	5h	<i>n</i> -propyl	H	96:4	65 %	89 %	27 %
	5i	<i>i</i> -propyl	H	95:5	60 %	99 %	12 %
	5j	<i>n</i> -butyl	H	94:6	64 %	96 %	27 %
	5k	<i>n</i> -propyl	ethyl	98:2	74 %	91 %	27 %
	5l	F	H	95:5	87 %	73 %	30 %
	5m	Cl	H	90:10	82 %	90 %	44 %
	5n	Br	H	94:6	90 %	88 %	36 %
	5o	I	H	94:6	91 %	81 %	62 %
	5p	Cl	Cl	92:8	96 %	90 %	60 %
	#	R ³		<i>Z/E</i> ratio	Yield HWE	Yield methylation	Yield cyclization
	5q			95:5	66 %	95 %	17 %
	5r			86:14	48 %	52 %	11 %
	5s			95:5	86 %	91 %	37 %
	5t			97:3	88 %	97 %	11 %

Figure 10: Tentoxin derivatives **5a** and **5g-t** with reaction results.

Studies have shown that the corresponding (*E*)-isomer does not stimulate chlorosis in plants in the investigated species and concentration range. The reaction allows the usage of a variety of different moieties, i.e., aliphatic and aromatic aldehydes as well as ketones.

Using this protocol, tentoxin **5a** and 14 derivatives **5g-t** were synthesized in moderate to excellent yields. For this purpose, the aromatic core was modified by attaching different substituents. Various aliphatic chains were added in the *para*-position (**5g-j**) as well as halogens (**5l-o**). Furthermore, the *meta/para* dichlorinated **5p** was prepared. The derivative **5k**, which has two alkyl side-chains (*m*-ethyl-*p*-propyl), revealed the highest interaction with the ATPase *in silico* and thus was synthesized. For its organocatalytic synthesis, aldehyde **13** and the required organocatalyst **12** had to be prepared (see Scheme 10).^{49,50}



Scheme 10: Synthesis of organocatalyst **12** and aldehyde **13**.

In addition to the derivatives possessing substituted phenyl moieties, four derivatives (**5q-t**) were prepared in which the phenylic side-chain of the Δ AA was replaced. The first two were prepared by implementing alkyl side-chains: substance **5q** with a linear, aliphatic C_7 -chain and substance **5r** with a cyclohexyl ring. Furthermore, derivative **5s** was prepared, containing 2-naphthalene as a side-chain.

The last derivative is a so-called chimera, a combination of two potential herbicides from different classes. Chimeric molecules find application in drug design, where combining distinct molecular fragments can lead to novel compounds with combined or improved biological activities or enhanced reactivity in chemical reactions.^{51,52} Here, the substance class of tentoxins was combined with a substituted nicotinic acid. To do so, the chlorosis-inducing 6-(decyloxy)nicotinic acid (see chapter 3) was first reduced to the corresponding aldehyde, which also showed good herbicidal activity. This could subsequently be coupled with the phosphonate **10**, resulting in the chimera **5t**.

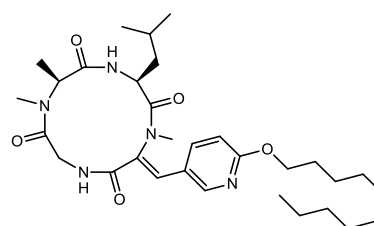


Figure 11: Structure of chimera **5t**.

Biological evaluation

Herbicidal activity

Lemna minor bioassay

Lemna minor, commonly known as duckweed, is a fast-growing, small vascular plant which belongs to the family Araceae. The plant is used in toxicology and phytoeffector studies due to the capability of the test plant to accumulate chemicals from water.^{53–55} It has various physiological properties that make it an advantageous test organism, such as small size and vegetative reproduction - making all test plants clones - and a high multiplication rate. Furthermore, it has a flat leaf surface, which allows the observation of plant growth by measuring the leaf surface area.⁵⁶ The growth rate of *Lemna minor* usually correlates with the concentration of chlorophyll and carotenoid, which allows to analyse and generalise the effect of different chemical compounds on the tested plants.⁵⁷



Figure 12: Cultivation of *Lemna minor*.

To determine the herbicidal activity of the synthesized TTX and its derivatives, all compounds were tested *in vivo* for their growth inhibition activity on *Lemna minor*. The *Lemna minor* bioassay is used in toxicology and phytoeffector studies due to the capability of the test plant to accumulate chemicals from water.^{53–55} The plants are usually exposed to toxins, which are added to their growth media, for up to seven days. Subsequently, the growth inhibition is estimated by comparing the final and initial plant size.⁵⁸

To study the herbicidal activity of different tentoxins, an adapted version of the bioassay developed by Geissler and Wessjohann was used.⁵⁸ In brief, tentoxin and all derivatives were tested in five concentrations ranging from 50 μM to 0.01 μM in absence and presence of polyethylene glycol 6000 (PEG) supplemented to *Steinberg* medium.⁵⁹ The addition of PEG is used to mimic osmotic stress conditions as found under drought, frost or saline conditions.⁶⁰ The plants were incubated for 24 hours after which the medium was exchanged to fresh toxin- and PEG-free *Steinberg* medium. After 96 hours, the plant leaf sizes were determined to calculate the growth inhibition. All tests were performed in triplicates.

Results

As previously described, TTX and all 19 derivatives were tested for growth inhibition activity using the mentioned bioassay at concentrations ranging from 50 μM to 0.01 μM . None of the compounds showed significant activity below 1 μM , therefore only the three highest concentrations are displayed in Figure 13.

Tentoxin itself shows a strong growth inhibition of 73 % at a concentration of 50 μM and a weaker inhibition (26 %) at a concentration of 10 μM under normal conditions (*Steinberg* medium). If the stress-inducing medium (*Steinberg* medium with PEG) is used, an activity of only 45 % can be detected at the highest tested concentration. Using a concentration of 1 μM , no activity could be detected for the natural product, regardless of the medium.

By comparing the results of TTX with the newly synthesized derivatives, it was demonstrated, for the first time, that phenyl-modified derivatives with a higher activity compared to the natural product (see Figure 13) could be synthesized. Until now, any changes to the structure of TTX only led to a decrease in activity in literature.⁶¹

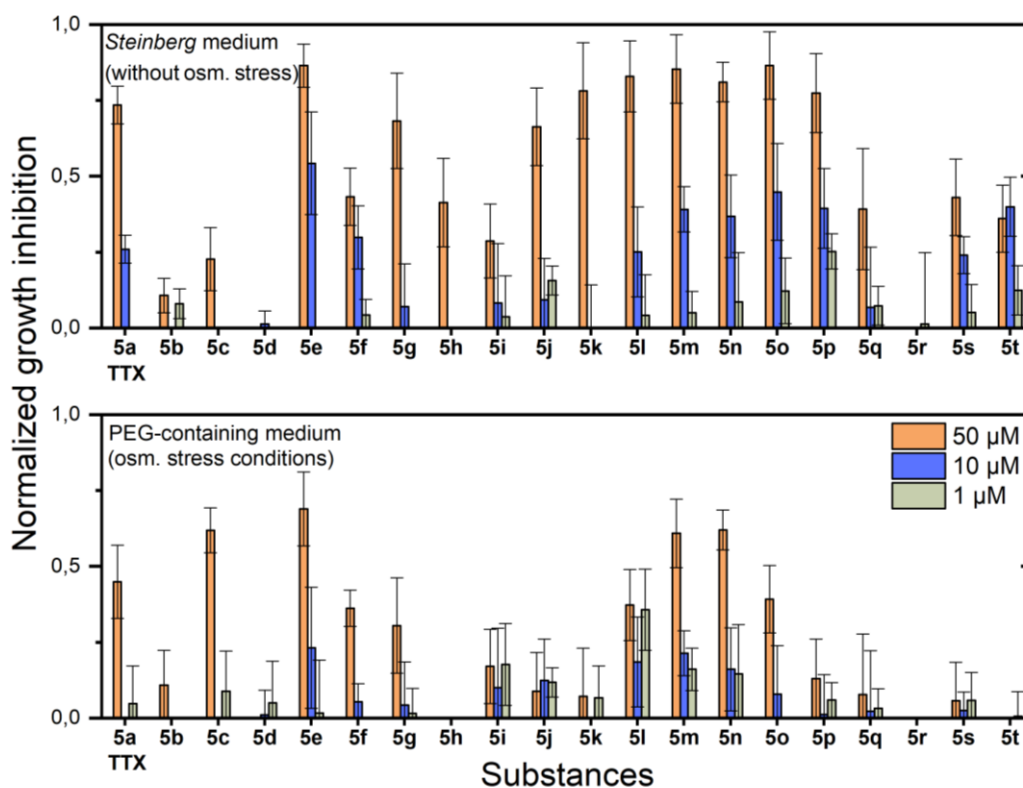


Figure 13: Normalized growth inhibition of *Lemna minor* treated with different concentrations of tentoxin (5a) and derivatives (5b-t). Top: plants being tested in Steinberg medium, Bottom: plants being tested in PEG-containing medium (to trigger osmotic stress). Only concentrations of 50, 10 and 1 μM are shown.

When comparing the activities of the derivatives with the natural product, various trends can be observed. First, all changes in the structure of TTX, which did not take place at ΔPhe^Z , led to a reduction of the activity (substances 5b-d, 5f). Among them, 5b and 5d in particular lose their activity almost completely. In derivative 5b, leucine was replaced with valine, and in derivative 5d, $N\text{-Me-}\Delta\text{Phe}^Z$ was replaced with $N\text{-Pr-}\Delta\text{Phe}^Z$. In contrast, the exchange at the same position to $N\text{-Et-}\Delta\text{Phe}^Z$ (substance 5c) led to an increase in activity under stress conditions. Under normal conditions, only a low activity is detectable. Finally, the amino acid $N\text{-Me-Ala}$ was replaced by $N\text{-Me-Gly}$ (substance 5f), which led to a slight decrease in activity.

Further, the derivatives with alkyl substitutions at the phenyl ring (5e, 5g-k) will be compared. Out of these derivatives, 5e, which is methyl-substituted in *para*-position, shows the highest activity, and exceeds that of TTX under normal as well as stress conditions. In contrast, the derivatives with *n*- and *iso*-propyl substituents (5h and 5i) show a lower growth-inhibition activity. When the size of substituents is further increased (5j and 5k), the activity increases slightly as well but does not reach that of the natural product.

The next group of derivatives can be summarized as those possessing one or two halogen substituents (**5l-p**). They all show very similar activities as tentoxin and even exceed it at low concentrations. The best activity in *Steinberg* medium showed the derivative with iodine substituents (**5o**), whereas in stress medium the derivatives **5m** and **5n** with chlorine and bromine substitution.

In the last group of derivatives (**5q-t**), in which the side group of Δ AA was completely replaced, no growth inhibitory activity was detected under stress conditions. Under normal conditions, however, at least **5q**, **5s** and **5t** show similar moderate activities.

Comparison with the modelling results

The comparison of *in vivo* and *in silico* activity results is difficult. Some compounds are less active than TTX at high concentrations but more than TTX at low concentrations, or activities differ between normal and stress conditions. Also, Steinberg medium contains nutrients which make the plants partially independent from photosynthesis. However, some trends can still be observed.

Comparing the derivatives with alkyl substitution on the phenyl ring, it was shown, that the highest *in vivo* activity can be achieved by methyl substitution (**5e**), whereas in the model, stronger interactions could be achieved by more and longer side-chains (for example derivative **5k**). First of all, it must be mentioned that the model is not based on *Lemna minor* ATPase so that slight variation may apply. Another reason could be that although the higher substituted molecule may bind more strongly in the receptor, the transport may be hindered due to its physicochemical characteristics. Halogenation of the same positions (**5l-p**), on the other hand, always led to a gain in activity under normal growth conditions, although this was predicted for **5o** only. This derivative was also found to be the most active one of the halogen series, so that the qualitative comparison between the derivatives can be useful.

Table 1: Comparison of modelling and bioassay results for compounds **5a-t**. ΔE_{theo} : calculated binding energies, GI_{normal} : growth inhibition at 50 μM in *Steinberg* medium, GI_{stress} : growth inhibition at 50 μM in stress-inducing medium. Yellow: TTX; green: higher activity than TTX; red: lower activity than TTX. ΔE_{theo} in [kcal/mol].

#	5a	5b	5c	5d	5e	5f	5g	5h	5i	5j
ΔE_{theo}	- 26.53	- 19.81	- 16.23	- 27.11	- 29.52	- 27.00	- 34.30	- 36.43	- 33.83	- 36.08
GI_{normal}	73 %	11 %	23 %	0 %	86 %	43 %	68 %	41 %	29 %	66 %
GI_{stress}	45 %	11 %	62 %	0 %	69 %	36 %	30 %	0 %	17 %	9 %

#	5k	5l	5m	5n	5o	5p	5q	5r	5s	5t
ΔE_{theo}	- 39.08	- 19.97	- 23.39	- 20.32	- 28.39	- 24.88	- 33.71	- 29.22	- 28.09	- 8.01
GI_{normal}	78 %	83 %	85 %	81 %	87 %	77 %	39 %	0 %	43 %	36 %
GI_{stress}	7 %	37 %	61 %	62 %	39 %	13 %	8 %	0 %	6 %	0 %

Moderate activity at 50 μ M and 10 μ M was detected for chimera **5t** under normal conditions. The calculated activity, however, was by far the lowest. Here it could be hypothesized that the activity does not originate from one part (most likely only from the nicotinic moiety) and the unusually bulky rest is inhibiting what is left in activity.

In summary, the modelling results could not be completely confirmed in the whole plant bioassay. This is unsurprising as no direct protein-TTX-derivative interaction is measured with uptake and metabolism influencing the molecules on the way to the target. However, some general qualitative trends could be derived from the model. For example, nonpolar substitutions on the aromatic ring can lead to a gain in activity and within the halogens the best atom was predicted correctly.

Conclusion

The synthesis of the natural product tentoxin and 19 derivatives is presented. For this purpose, it was shown that the total synthesis described by Neves is suitable for the modification of tentoxin. Five derivatives (**5b-f**) were prepared using this approach, which possess modifications at different sites of the molecule.

Furthermore, a new total synthesis of tentoxin was introduced, which allows a late-stage modification in the synthesis route. The main feature of the total synthesis is the installation of the Δ AA using a *Horner-Wadsworth-Emmons* olefination, which reacts the previously prepared tetrapeptide phosphonate **10** with various aldehydes. This allows a simple and efficient synthesis of tentoxin derivatives by exchanging the aldehyde used in the reaction. It opens up the possibility of introducing almost any modifications to the Δ AA. Another advantage of this synthesis is that it almost exclusively produces the required Z-isomer.

With the aid of this new total synthesis, it was possible to produce the natural product tentoxin **5a** starting from commercially available phosphonate **7** in seven steps with an overall yield of 33 %. Furthermore, 14 derivatives **5g-t** could be prepared using the new route, doubling the number of known TTX derivatives. The prepared derivatives were selected with the help of a previously performed computer modelling *in silico*, selecting structures which showed a particularly high binding affinity to the native spinach chloroplast F1-ATPase. The subsequent bioassays *in vivo* determined the biological activity of the derivatives in comparison to tentoxin. They showed that for the first time, tentoxin derivatives were found which have a higher activity than the natural product. Derivatives **5e** and **5o** showed the strongest activity under normal conditions, inhibiting growth by 86 % and 87 %, respectively, at a concentration of 50 μ M. Under stress-induced conditions, **5e** again showed the highest inhibition of 69 % at 50 μ M.

Experimental part

General information

Column chromatography was carried out using Merck silica gel 60 (40 – 63 μm) from Merck (Darmstadt, Germany). For analytic thin layer chromatography, Merck TLC silica gel 60 F₂₅₄ aluminium sheets from Merck (Darmstadt, Germany) were used. Compounds were visualised by UV-quenching using UV light (254 / 366 nm) or by spraying the TLC plates with cerium(IV)-molybdophosphoric acid stain followed by heating in a hot air stream.

All solvents were purchased from Merck (Darmstadt, Germany) and were distilled prior to use. Deuterated solvents for NMR spectroscopy were purchased from Deutero (Kastellaun, Germany). Commercially available starting material for chemical synthesis was purchased from Sigma Aldrich (St. Louis, USA), Roth (Karlsruhe, Germany), Carbolution (Sankt Ingbert, Germany), Alfa Aesar (Haverhill, USA) and abcr chemicals (Karlsruhe, Germany). Microwave reactions were performed in a 5 ml microwave vial using a Biotage Initiator+ synthesis microwave (Uppsala, Sweden) at the specified temperature with automatically adjusted wattage (0 – 400 W from magnetron at 2.45 GHz).

NMR spectra were recorded using a 400 MHz Agilent DD2 400 NMR spectrometer (Santa Clara, USA) or a 500 MHz Bruker Avance Neo NMR spectrometer (Billerica, USA) or a 600 MHz Agilent VNMRs 600 NMR spectrometer (Santa Clara, USA) at 25 °C. The chemical shifts of the ¹H NMR spectra are referenced on the signal of the internal standard tetramethylsilane. Chemical shifts of the ¹³C NMR spectra are referenced on the solvent residual signals. Data analysis was carried out with MestreNova (14.1.2-25024, Mestrelab Research, Santiago de Compostela, Spain).

The positive and negative ion high resolution mass spectra were either obtained from a Thermofisher Scientific Orbitrap Elite mass spectrometer (Karlsruhe, Germany) equipped with a HESI electrospray ion source (spray voltage 4.0 kV; capillary temperature 275 °C, source heater temperature 40 °C; FTMS resolution 60.000, nitrogen sheath gas) or from an ABSciex TripleTOF 6600 Hybrid Quadrupole-TOF Mass Spectrometer (Framingham, USA) equipped with a DuoSpray Ion Source (spray voltage 5.5 kV; source temperature 450 °C; nitrogen sheath gas).

Analytical RP18 HPLC was carried out with an Agilent 1260/1290 system (Santa Clara, USA) equipped with a quaternary pump and a diode array detector VL+ using a Poroshell 120 C18ec column (length: 50 mm, internal diameter: 4.6 mm, pore size: 100 Å, particle size 2.7 μm , Agilent). For the separation, the mobile phases were H₂O (A; bidistilled, Millipore) and CH₃CN (B; gradient grade, LiChrosolv, Merck) with formic acid (0.1 %, Merck) and a gradient system was used (0 – 15 min, 5 – 100 % B (5 min); flow rate 0.8 mL/min). Automated peak-based/time-based fractionation was carried out using UV detection.

In silico substrate docking studies

The *in silico* analysis of various synthesized and theoretical derivatives was performed using the crystal structure of native spinach chloroplast F1-ATPase complexed with TTX (PDB-Code: 1KMH).⁴⁷ The structure was loaded into the Molecular Operating Environment software platform (MOE; version 2022.02), where all further steps were carried out via integrated software tools.⁶² For all relevant steps, the Amber10:EHT forcefield together with the born solvation model was applied.^{63–}

⁶⁵ Missing charges and protons were added and termini capped with the Structure Preparation

command. The covalently bound TTX molecule was removed for the docking, and all backbone atoms were fixed. An initial docking of TTX in its binding site was carried out, to define a noncovalent binding pose as reference for the related derivatives. Initially, 50 poses were generated with the Triangle Matcher placement method and scored with Affinity dG. A refinement was carried out with the Induced Fit placement method and poses were reevaluated with the GBVI/WSA dG score, after which the best ten poses were saved. As a result, a pose closely resembling the covalent binding depicted in 1KMH was generated, forming multiple hydrogen bonds with two residues of the beta subunit of F1-ATPase.⁶⁶ The hydrogen bonds between the secondary amino groups of TTX and Asp83 contribute majorly to the specific binding and were therefore ensured during docking by applying a pharmacophore filter. The respective nitrogen atoms were used as centres of two essential 1.2 Å Don-features. Subsequently, all derivatives were docked as described before under application of this pharmacophore. The resulting docking poses were checked for the formation of hydrogen bonds, for which in most cases a minimum of two (with Asp83) but quite often also three H-bonds (additional bond between the backbone nitrogen of Thr82 and carbonyl oxygen of TTX) were possible. The interaction energies (in kcal/mol) of the respective ligand-receptor complexes were read out and summed up with the Protein Contacts tool.

Phytotoxicity test (herbicidal activity)

The compounds were tested for their toxicity by inhibiting the growth of duckweed (*Lemna minor*) in 24-well microtiter plates in a serial dilution, ranging from 100 to 0.01 µM, keeping DMSO at 0.1 %. DMSO in water (0.1 % (v/v)) was also used as a negative control, while 100 µM of 2,4-dichlorophenoxyacetic acid was used as a positive control. The screening procedures took place under sterile conditions (laminar airflow cabinet).

Experimental procedure using normal medium: First, 2 µl of the negative control (100 % DMSO) and of the substances in the concentration (10 µM, 100 µM, 1 mM, 10 mM, 50 mM, and 100 mM) were added to the plate. After that, each well of a 24-well microtiter plate was loaded with 2 ml of Steinberg medium so that the final compound concentrations in a plate comprised 0.01, 0.1, 1, 10, 50 and 100 µM.⁵⁹ Using an inoculation loop, one duckweed with three leaves from the preculture was transferred in each vial of the microtiter plate. The plates were incubated in the phytocabinet at 24 °C and 100 µmolm⁻²s⁻¹ continuous light for 96 hours. To evaluate the frond surfaces, a photo of the plate was taken using the LemnaTec scan analyzer on the first day (t = 0 h), second day (t = 24 h) and fourth day (t = 96 h). Before the second measuring point, the stress medium was exchanged for fresh Steinberg medium. All experiments were carried out in triplicates.

Experimental procedure using drought-stress inducing medium: First, 2 µl of the negative control (100 % DMSO) and of the substances in the appropriate concentration (10 µM, 100 µM, 1 mM, 10 mM, 50 mM, and 100 mM) were added to the plate. After that, each well of a 24-well microtiter plate was loaded with 2 ml of stress medium (Steinberg medium + polyethylene glycol 6000) so that the final concentrations of compound in a plate comprised 0.01 µM, 0.1 µM, 1 µM, 10 µM, 50 µM and 100 µM. Using an inoculation loop, one duckweed with three leaves from the preculture was transferred in each vial of the microtiter plate. The plates were incubated in the phytocabinet at 24 °C and 100 µmolm⁻²s⁻¹ continuous light for 96 hours. To evaluate the frond surfaces, a photo of the plate was taken using the LemnaTec scan analyzer on the first day (t = 0 h), second day (t = 24 h) and fourth day (t = 96 h).

Before the second measuring point, the stress medium was exchanged for fresh Steinberg medium (without PEG 6000). All experiments were carried out in triplicates.

The photos are later exported in PNG format and processed with Image *J* to calculate the leaf area. To calculate the specific growth rate μ of the duckweeds, the leaf area A is first logarithmized and then the difference between the measuring points is determined. These values are normalized in R by negative control (growth factor = 1) and processed in Excel for further comparison.

$$\log(A_p) = \mu \cdot t + A_{p_0}$$

ED₅₀ values (effective dose required for 50 % inhibition of growth) were calculated using OriginPro 2020 dose-response analysis function. Here the raw data is fitted with a sigmoidal fit, which was then used to calculate the concentrations at 50 % inhibition.

Steinberg medium: Steinberg medium was prepared by mixing five stock solutions in water: stock solution 1 (KNO₃, KH₂PO₄, K₂HPO₄), stock solution 2 (MgSO₄ x H₂O), stock solution 3 (Ca(NO₃)₂ x 4 H₂O), stock solution 4 (H₃BO₃, ZnSO₄ x 7H₂O, Na₂MoO₄ x 2 H₂O, MnCl₂ x 4 H₂O), stock solution 5 (FeCl₃ x 6 H₂O), EDTA. Stock solutions 1 - 3 were added in proportion of 20 mL per 1 L of final medium while stock solutions 4 and 5 – 1 mL per 1 L of final medium. The pH of the Steinberg medium was adjusted to 5.5 using aqueous sodium hydroxide solution (1 M) and aqueous hydrochloric acid (1 M) solution. Afterwards, the medium was autoclaved.

Stress medium: First, 150.4 mg of PEG 6000 was added to 700 mL of water. Then, five stock solutions used for the Steinberg medium preparation were added to the PEG solution in the same proportions. The pH was adjusted to 5.5 using aqueous sodium hydroxide solution (1 M) and aqueous hydrochloric acid (1 M) solution and the final volume was adjusted to 1 L. The medium was sterilized by filtration through 0.2 μ m filters and stored under the laminar flow hood.

Syntheses

General methods

General synthesis method I – Microwave-assisted *Ugi* reaction

A solution of amine (5 mmol), glyoxal hydrate (5 mmol) and triethylamine (0.69 mL, 5 mmol) in methanol (15 mL) was heated to 80 °C for 10 minutes using a synthesis microwave. Subsequently, Boc-protected amino acid (4 mmol) and methyl 2-isocyanoacetate (4 mmol) were added and the mixture was heated again to 80 °C for 60 minutes, after which the solvent was removed under reduced pressure. The residue was dissolved in ethyl acetate (50 mL) and was washed using aqueous hydrochloric acid (2 M, 2x 25 mL), sat. aq. NaHCO₃ solution (2x 25 mL) and brine (25 mL). The organic phase was dried over Na₂SO₄, filtered, and evaporated to dryness. Purification was done by column chromatography.

General synthesis method II – Hydrogenation

To a stirred solution of the tripeptide (1 eq) in dry methanol (50 mL) was added palladium on carbon (10 % w/w, 0.1 eq). The suspension was stirred overnight under hydrogen atmosphere (1 atm), after which it was filtered through Celite. The filtrate was evaporated to dryness and used in the next step without further purification.

General synthesis method III – Dehydration

A mixture of hydrogenated tripeptide (1 eq) and Martin's sulfurane (1.5 eq) in dry dichloromethane (20 mL) was stirred overnight under nitrogen atmosphere. After removal of the solvent, the residue was purified by column chromatography.

General synthesis method IV – Peptide coupling

A solution of the tripeptide (1 eq) in dichloromethane (12 mL) and trifluoroacetic acid (3 mL) was stirred for 5 hours, after which the solvent was removed. Subsequently, toluene (50 mL) was added, and the solvent was removed again in vacuo. This procedure was repeated three times to remove remaining trifluoroacetic acid. The residue was dissolved in DMF (10 mL) and Boc-protected amino acid (1.2 eq), DIPEA (3 eq) and HATU (1.2 eq) were added. After stirring overnight, the mixture was poured into water (80 mL) and extracted using ethyl acetate (3x 50 mL). The combined organic phases were washed using aqueous hydrochloric acid (2 M, 2x 25 mL), sat. aq. NaHCO₃ solution (2x 25 mL) and brine (25 mL). The organic phase was dried over Na₂SO₄, filtered, and evaporated to dryness. Purification was done by column chromatography.

General synthesis method V – Macrocyclization

To a solution of the linear tetrapeptide (1 eq) in a mixture of THF and water (3:1, 10 mL) at 0 °C was added lithium hydroxide hydrate (4 eq). The mixture was stirred at room temperature until all starting material was consumed (followed by TLC). Subsequently, the solution was acidified to pH ~ 2 - 3 using aqueous hydrochloric acid (1 M). Brine (10 mL) was added, and the aqueous phase was extracted using ethyl acetate (3x 25 mL). The combined organic layers were dried over Na₂SO₄, filtered, and evaporated to dryness.

The residue was dissolved in dichloromethane (12 mL) and trifluoroacetic acid (3 mL) was added. The mixture was stirred for 3 hours, after which the solvent was removed in vacuo. Subsequently, toluene (50 mL) was added, and the solvent was removed again in vacuo. This procedure was repeated three times to remove remaining trifluoroacetic acid.

The so obtained deprotected peptide was dissolved in dry chloroform (0.005 mmol / mL) and 4-DMAP (10 eq) and T3P (50 % w/w in EtOAc, 4 eq) were added. The mixture was stirred at room temperature for 72 hours, after which the solvent was removed in vacuo. The residue was redissolved in ethyl acetate (30 mL) and washed using water (20 mL), aqueous hydrochloric acid (0.5 M, 20 mL), sat. aq. NaHSO₄ solution (20 mL) and brine (20 mL). The organic phase was dried over Na₂SO₄, filtered, and evaporated to dryness. Purification was done by column chromatography (pure EtOAc).

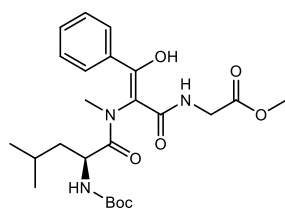
General synthesis method VI – Horner-Wadsworth-Emmons coupling

A solution of phosphonate **10** (1 eq) and TMG (3 eq) in dry DCM (8 mL) was stirred for 15 minutes, after which the aldehyde (3 eq) was added. Stirring was continued for 72 h, followed by addition of sat. aq. NaHCO₃ solution (20 mL). The mixture was extracted using DCM (3x 25 mL), the combined organic phases were dried over Na₂SO₄, filtered, and evaporated to dryness. Purification was done by column chromatography.

General synthesis method VII – N-Methylation

Tetrapeptide (1 eq) was dissolved in dry DMF (5 mL) over molecular sieve (4 Å). Pre-dried K₂CO₃ (8 eq), 18-crown-6 (0.1 eq) and methyl iodide (15 eq) were added. The mixture was stirred for 18 hours and was subsequently filtered. After adding ethyl acetate (50 mL) to the filtrate, it was washed with water (20 mL), aqueous hydrochloric acid (20 mL, 0.5 M), aqueous NaHCO₃ solution (20 mL, 10 %) and brine (20 mL), then dried over Na₂SO₄, filtered, and evaporated to dryness.

Methyl (*S,E*)-(2-(2-((*tert*-butoxycarbonyl)amino)-*N*,4-dimethylpentanamido)-3-hydroxy-3-phenylacryloyl)glycinate (**1a**)

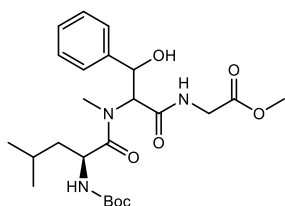


According to general method I, methyl amine hydrochloride (332 mg, 5 mmol), phenylglyoxal hydrate (0.76 g, 5 mmol), Boc-*L*-leucin (1.0 g, 4 mmol) and methyl 2-isocyanoacetate (0.36 mL, 4 mmol) were used. Purification was done by column chromatography (DCM / EtOAc 8:2), giving compound **1a** as a yellow oil (0.73 g, 1.52 mmol, 38 %).

¹H NMR (400 MHz, CDCl₃) δ 15.11 and 14.23 (2s, 1H), 7.62 – 7.05 (m, 7H), 4.90 - 4.84 (m, 1H), 4.34 – 3.97 (m, 2H), 3.79 – 3.66 (m, 3H), 3.17, 3.16 and 3.10 (3s, 3H), 1.47 – 1.29 (m, 12H), 0.90 (t, *J* = 7.0 Hz, 3H), 0.81 – 0.68 (m, 3H).

¹³C NMR (101 MHz, CDCl₃) δ 175.33, 175.03, 174.30, 170.81, 170.13, 169.64, 169.36, 168.94, 156.94, 156.55, 139.96, 139.58, 139.20, 128.91, 128.72, 128.28, 128.06, 127.24, 127.13, 126.13, 125.48, 80.75, 80.13, 63.73, 60.87, 52.26, 52.19, 49.38, 48.49, 47.52, 41.20, 41.04, 40.98, 40.53, 38.55, 33.66, 31.95, 28.26, 28.19, 24.53, 24.09, 24.05, 23.25, 23.11, 22.91, 22.09, 21.60, 20.55.

Methyl (2-((*S*)-2-((*tert*-butoxycarbonyl)amino)-*N*,4-dimethylpentanamido)-3-hydroxy-3-phenylpropanoyl)glycinate (mixture of diastereomers) (**2a**)

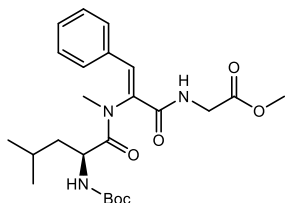


According to general method II, tripeptide **1a** (0.60 g, 1.26 mmol) and palladium on carbon (10 % w/w, 60 mg) were used, giving compound **2a** as a light yellow oil (0.60 g, 1.25 mmol, 99 %).

^1H NMR (400 MHz, CDCl_3) δ 7.51 – 7.15 (m, 6H), 5.74 – 5.35 (m, 1H), 5.08 – 4.79 (m, 1H), 4.33 – 4.14 (m, 1H), 4.13 – 3.92 (m, 1H), 3.91 – 3.80 (m, 1H), 3.75 (s, 3H), 3.71 (d, $J = 3.2$ Hz, 1H), 3.19 – 3.14 (m, 3H), 3.10 (s, 1H), 1.42 (s, 3H), 1.38 (s, 9H), 0.94 – 0.69 (m, 6H).

^{13}C NMR (101 MHz, CDCl_3) δ 175.32, 175.03, 174.29, 170.82, 170.21, 169.66, 169.36, 169.18, 156.94, 156.55, 156.13, 139.96, 139.58, 139.20, 128.91, 128.28, 128.06, 127.24, 127.13, 126.13, 125.48, 80.76, 80.13, 73.54, 72.83, 72.17, 71.93, 63.73, 60.87, 52.26, 49.38, 48.49, 47.52, 41.04, 40.97, 40.52, 33.66, 31.94, 28.26, 28.19, 24.10, 24.06, 23.25, 23.12, 22.91, 22.09, 21.60, 20.55.

Methyl (*S,Z*)-(2-(2-((*tert*-butoxycarbonyl)amino)-*N*,4-dimethylpentanamido)-3-phenylacryloyl)glycinate (**3a**)

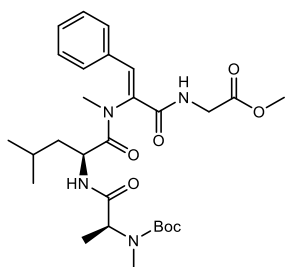


According to general method III, tripeptide **2a** (500 mg, 1.04 mmol) and Martin's sulfurane (1.05 g, 1.56 mmol) were used. Purification was done by column chromatography (DCM / MeOH 99:1 – 90:10), giving compound **3a** (221.4 mg, 0.48 mmol, 46 %) as a yellow oil.

^1H NMR (400 MHz, CDCl_3) δ 8.36 (t, $J = 5.8$ Hz, 1H), 7.71 (s, 1H), 7.44 – 7.34 (m, 5H), 4.85 – 4.78 (m, 1H), 4.22 – 4.04 (m, 3H), 3.71 (s, 3H), 3.21 (s, 3H), 1.42 (d, $J = 6.8$ Hz, 1H), 1.37 (s, 9H), 1.24 (t, $J = 7.2$ Hz, 1H), 1.14 (s, 1H), 0.58 (d, $J = 6.5$ Hz, 3H), 0.54 (d, $J = 6.6$ Hz, 3H).

^{13}C NMR (101 MHz, CDCl_3) δ 172.72, 169.98, 164.93, 156.27, 135.66, 132.30, 132.02, 130.54, 130.41, 129.27, 80.26, 52.12, 51.40, 41.81, 39.06, 34.46, 29.12, 28.21 (3C), 24.57, 23.18 (2C), 20.42.

Methyl ((Z)-2-((S)-2-((S)-2-((*tert*-butoxycarbonyl)(methyl)amino)propanamido)-*N*,4-dimethylpentanamido)-3-phenylacryloyl)glycinate (**4a**)

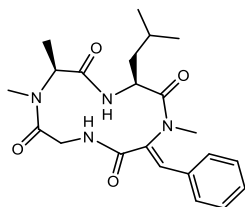


According to general method IV, compound **3a** (57 mg, 0.13 mmol), Boc-*N*-methyl-*L*-alanine (30.2 mg, 0.15 mmol), DIPEA (65.3 μ L, 0.37 mmol) and HATU (57 mg, 0.15 mmol) were used. Purification was done by column chromatography (DCM / EtOAc, 99:1 – 80:20), giving compound **4a** (57.3 mg, 0.11 mmol, 85 %) as a yellow oil.

^1H NMR (500 MHz, CDCl_3) δ 8.54 (s, 1H), 7.73 (s, 1H), 7.42 (d, J = 3.2 Hz, 5H), 7.36 (d, J = 3.2 Hz, 1H), 4.67 (s, 1H), 4.33 (dt, J = 10.7, 3.6 Hz, 1H), 4.13 (q, J = 6.8 Hz, 2H), 3.72 (s, 3H), 3.22 (s, 3H), 2.70 (s, 3H), 1.51 – 1.39 (m, 9H), 1.33 – 1.23 (m, 6H), 0.57 (t, J = 6.4 Hz, 6H).

^{13}C NMR (126 MHz, CDCl_3) δ 172.24, 171.56, 169.99, 165.03, 156.26, 135.74, 132.25, 132.04, 130.58, 130.41 (2C), 129.28 (2C), 80.66, 53.83, 52.02, 50.95, 41.83, 38.67, 34.39, 29.61, 28.33 (3C), 24.72, 23.12 (2C), 14.17.

(3*S*,6*S*)-12-((*Z*)-Benzylidene)-3-isobutyl-1,6,7-trimethyl-1,4,7,10-tetraazacyclododecane-2,5,8,11-tetraone (Tentoxin (**5a**))



According to general method V, compound **4a** (40 mg, 0.07 mmol), lithium hydroxide hydrate (12.2 mg, 0.29 mmol), 4-DMAP (89.2 mg, 0.73 mmol) and T3P (50 % w/w in EtOAc, 178.8 μ L, 0.3 mmol) were used, giving tentoxin **5a** (15.2 mg, 0.04 mmol, 48 %) as a white solid. A sample was purified by semipreparative RP-HPLC for biological assays and characterization.

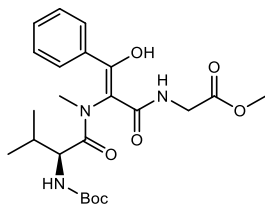
t_R = 11.05 min (5 % ACN (0 min) > 100 % ACN (15 min) > 100 % ACN (20 min))

HR-MS m/z 413.2201 (calculated for $\text{C}_{22}\text{H}_{29}\text{N}_4\text{O}_4$: 413.2189)

^1H NMR (500 MHz, CDCl_3) δ 7.97 (s, 1H), 7.76 (s, 1H), 7.45 – 7.37 (m, 5H), 7.12 (s, 1H), 5.19 (t, J = 13.1 Hz, 1H), 4.36 (s, 1H), 4.17 (s, 1H), 3.59 (d, J = 15.2 Hz, 1H), 3.19 (s, 3H), 2.81 (s, 3H), 1.88 – 1.61 (m, 2H), 1.53 (d, J = 7.1 Hz, 3H), 1.38 – 1.17 (m, 1H), 0.64 (d, J = 6.5 Hz, 3H), 0.52 (d, J = 6.5 Hz, 3H).

^{13}C NMR (126 MHz, CDCl_3) δ 171.67, 171.43, 170.03, 164.54, 136.71, 131.95, 130.80 (2C), 129.75 (2C), 129.42 (2C), 56.70, 49.53, 44.45, 40.51, 35.29, 30.18, 24.59, 22.28, 22.11, 15.56.

Methyl (*S,E*)-(2-(2-((*tert*-butoxycarbonyl)amino)-*N*,3-dimethylbutanamido)-3-hydroxy-3-phenylacryloyl)glycinate (**1b**)

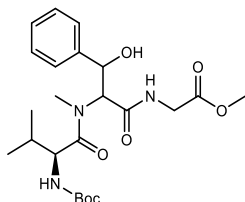


According to general method I, methyl amine hydrochloride (332 mg, 5 mmol), phenylglyoxal hydrate (0.76 g, 5 mmol), Boc-*L*-valine (869.0 mg, 4 mmol) and methyl 2-isocyanoacetate (0.36 mL, 4 mmol) were used. Purification was done by column chromatography (DCM / EtOAc 8:2), giving compound **1b** as a yellow oil (0.76 g, 1.6 mmol, 41 %).

^1H NMR (400 MHz, CDCl_3) δ 15.12, 14.68 and 14.23 (3s, 1H), 7.97 – 7.30 (m, 6H), 5.20 – 5.10 (m, 1H), 4.83 (d, J = 6.6 Hz, 1H), 4.12 (t, J = 6.1 Hz, 2H), 3.76 and 3.74 (2s, 3H), 3.28 and 3.20 (2s, 3H), 1.69 – 1.43 (m, 1H), 1.41 and 1.38 (2s, 9H), 0.97 – 0.57 (m, 6H).

^{13}C NMR (101 MHz, CDCl_3) δ 175.02, 174.69, 171.37, 169.96, 169.82, 169.74, 167.76, 166.70, 157.41, 156.17, 133.70, 133.60, 133.06, 132.82, 131.02, 130.73, 130.23, 129.94, 128.69, 128.60, 128.18, 128.07, 127.80, 127.33, 80.51, 80.01, 52.25, 52.17, 50.34, 49.62, 41.25, 41.17, 40.91, 40.83, 38.87, 37.32, 28.26 (3C), 28.16 (3C), 24.33 (2C), 23.16 (2C).

Methyl (2-((*S*)-2-((*tert*-butoxycarbonyl)amino)-*N*,3-dimethylbutanamido)-3-hydroxy-3-phenylpropanoyl)glycinate (mixture of diastereomers) (**2b**)

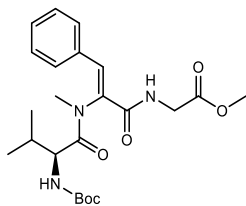


According to general method II, tripeptide **6** (0.60 g, 1.29 mmol) and palladium on carbon (10 % w/w, 60 mg) were used, giving compound **2b** as a light yellow oil (0.60 g, 1.28 mmol, 99 %).

^1H NMR (400 MHz, CDCl_3) δ 7.51 – 7.15 (m, 6H), 6.73 (s, 1H), 5.75 – 5.64 (m, 1H), 5.45 – 5.10 (m, 1H), 4.97 (d, J = 7.5 Hz, 1H), 4.32 – 3.80 (m, 3H), 3.74 and 3.71 (2s, 3H), 3.22 and 3.17 (2s, 3H), 1.92 – 1.63 (m, 1H), 1.42 and 1.38 (2s, 9H), 0.88 (d, J = 6.7 Hz, 3H), 0.68 (d, J = 6.7 Hz, 3H).

^{13}C NMR (101 MHz, CDCl_3) δ 174.38, 170.82, 169.65, 169.61, 156.85, 156.09, 139.83, 139.30, 128.70, 128.31, 128.22 (2C), 127.79, 127.28, 126.95, 126.27, 125.54 (2C), 80.17, 79.96, 72.22, 71.70, 64.24, 61.03, 55.72, 55.57, 52.31, 52.25, 52.19, 41.07 (2C), 41.00, 33.92, 30.63, 30.19, 29.61, 28.31 (3C), 28.27 (3C), 19.42, 18.42, 18.13, 17.55.

Methyl (S,Z)-2-(2-((*tert*-butoxycarbonyl)amino)-*N*,3-dimethylbutanamido)-3-phenylacryloyl)-glycinate (**3b**)

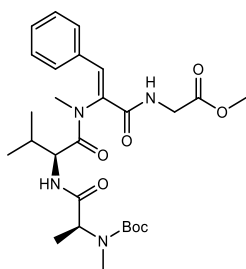


According to general method III, tripeptide **2b** (515 mg, 1.11 mmol) and Martin's sulfurane (1.12 g, 1.7 mmol) were used. Purification was done by column chromatography (DCM / MeOH 99:1 – 90:10), giving compound **3b** (193.7 mg, 0.43 mmol, 39 %) as a yellow oil.

^1H NMR (400 MHz, CDCl_3) δ 7.75 (s, 1H), 7.52 – 7.29 (m, 5H), 6.44 (s, 1H), 5.18 – 4.86 (m, 2H), 4.17 – 3.94 (m, 2H), 3.81 – 3.69 (m, 3H), 3.23 – 3.18 (m, 3H), 2.20 (dq, J = 13.4, 6.8 Hz, 1H), 1.45 (s, 9H), 0.98 (d, J = 6.8 Hz, 3H), 0.93 (d, J = 6.9 Hz, 3H).

^{13}C NMR (101 MHz, CDCl_3) δ 172.07, 171.82, 170.08, 170.04, 164.58, 135.64, 131.84, 130.63, 130.42, 130.08, 129.19, 128.97, 128.65, 80.12, 57.53, 52.37, 41.10, 34.39, 30.71, 28.29 (3C), 19.23.

Methyl ((Z)-2-((S)-2-((S)-2-((*tert*-butoxycarbonyl)(methyl)amino)propanamido)-*N*,3-dimethyl-but-anamido)-3-phenylacryloyl)glycinate (**4b**)

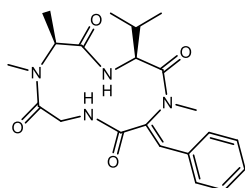


According to general method IV, compound **3b** (70 mg, 0.15 mmol), Boc-*N*-methyl-*L*-alanine (30 mg, 0.15 mmol), DIPEA (65.6 μL , 0.37 mmol) and HATU (58 mg, 0.15 mmol) were used. Purification was done by column chromatography (DCM / EtOAc, 99:1 – 80:20), giving compound **4b** (63.8 mg, 0.12 mmol, 79 %) as a yellow oil.

^1H NMR (400 MHz, CDCl_3) δ 8.10 (s, 1H), 7.75 (s, 1H), 7.48 – 7.33 (m, 6H), 4.69 (s, 1H), 4.33 – 3.93 (m, 2H), 3.73 (s, 3H), 3.19 (s, 3H), 2.80 (s, 3H), 1.57 (s, 9H), 1.48 (d, J = 5.9 Hz, 3H), 1.40 – 1.22 (m, 2H), 0.79 – 0.69 (m, 6H).

^{13}C NMR (101 MHz, CDCl_3) δ 172.66, 171.16, 170.83, 170.05, 164.74, 135.81, 132.16, 131.77, 130.68, 130.43 (2C), 129.22 (2C), 80.69, 56.31, 52.37, 52.08, 42.48, 34.34, 30.03, 28.33 (3C), 27.66, 21.04, 19.29, 15.95

(3*S*,6*S*)-12-((*Z*)-Benzylidene)-3-isopropyl-1,6,7-trimethyl-1,4,7,10-tetraazacyclododecane-2,5,8,11-tetraone (**5b**)



According to general method V, compound **4b** (55 mg, 0.1 mmol), lithium hydroxide hydrate (16.8 mg, 0.4 mmol), 4-DMAP (122.2 mg, 1.0 mmol) and T3P (50 % w/w in EtOAc, 235.7 μ L, 0.4 mmol) were used, giving derivative **5b** (18.5 mg, 0.05 mmol, 46 %) as a white solid. A sample was purified by semipreparative RP-HPLC for biological assays and characterization.

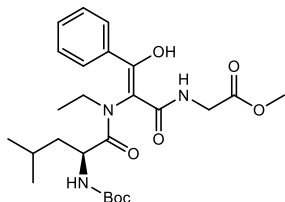
HR-MS m/z 399.2031 (calculated for $C_{21}H_{27}N_4O_4$: 399.2027)

t_R = 10.31 min (5 % ACN (0 min) > 100 % ACN (15 min) > 100 % ACN (20 min))

1H NMR (500 MHz, $CDCl_3$) δ 8.27 (s, 1H), 7.77 (s, 1H), 7.43 – 7.40 (m, 5H), 7.18 (s, 1H), 5.22 (s, 1H), 4.44 (s, 1H), 4.04 (s, 1H), 3.56 (d, J = 15.3 Hz, 1H), 3.17 (s, 3H), 2.80 (s, 2H), 2.08 – 1.88 (m, 2H), 1.56 (d, J = 7.0 Hz, 3H), 0.74 (d, J = 6.8 Hz, 3H), 0.59 (d, J = 6.6 Hz, 3H).

^{13}C NMR (126 MHz, $CDCl_3$) δ 172.33, 171.16, 169.82, 164.35, 137.28, 132.06, 130.71, 130.41, 129.80 (2C), 129.33 (2C), 57.47, 55.84, 44.41, 35.24, 30.23, 29.20, 19.98, 18.06, 15.61.

Methyl (*S,E*)-(2-(2-((*tert*-butoxycarbonyl)amino)-*N*-ethyl-4-methylpentanamido)-3-hydroxy-3-phenylacryloyl)glycinate (**1c**)

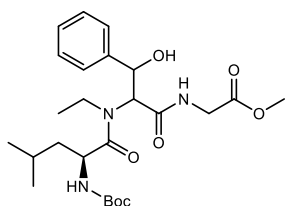


According to general method I, ethyl amine (327 μ L, 5 mmol), phenylglyoxal hydrate (0.76 g, 5 mmol), Boc-*L*-leucine (0.93 g, 4 mmol) and methyl 2-isocyanoacetate (0.36 mL, 4 mmol) were used. Purification was done by column chromatography (DCM / EtOAc 8:2), giving compound **1c** as a yellow oil (0.64 g, 1.3 mmol, 33 %).

1H NMR (400 MHz, $CDCl_3$) δ 15.40, 14.81 and 14.51 (3s, 1H), 8.34 – 7.30 (m, 6H), 5.05 – 4.74 (m, 1H), 4.47 – 4.07 (m, 3H), 3.76 and 3.74 (2s, 3H), 3.07 – 2.82 (m, 2H), 1.80 – 1.62 (m, 3H), 1.57 (s, 9H), 1.44 – 1.23 (m, 9H).

^{13}C NMR (101 MHz, $CDCl_3$) δ 178.52, 172.26, 171.56 (2C), 170.01 (2C), 165.04, 160.45, 158.67, 158.27, 137.61, 135.74, 132.27, 132.05, 130.59 (2C), 130.42 (2C), 130.1, 129.29 (2C), 128.66, 120.23, 120.18, 80.77, 80.71, 52.33, 52.03, 51.40, 50.96, 41.84, 41.13, 38.68, 38.53, 34.66, 34.40, 28.33 (3C), 28.28 (3C), 24.73, 24.66, 23.13 (2C), 20.34 (2C), 13.26, 13.08.

Methyl (2-((*S*)-2-((*tert*-butoxycarbonyl)amino)-*N*-ethyl-4-methylpentanamido)-3-hydroxy-3-phenylpropanoyl)glycinate (mixture of diastereomers) (**2c**)

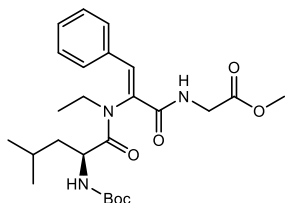


According to general method II, tripeptide **1c** (0.50 g, 1.02 mmol) and palladium on carbon (10 % w/w, 50 mg) were used, giving compound **2c** as a light yellow oil (0.51 g, 1.02 mmol, quant).

^1H NMR (400 MHz, CDCl_3) δ 7.56 – 7.20 (m, 6H), 5.68 – 5.47 (m, 1H), 5.34 – 5.06 (m, 1H), 5.04 – 4.82 (m, 1H), 4.42 – 3.79 (m, 4H), 3.75 and 3.74 (2s, 3H), 3.28 – 3.01 (m, 1H), 2.97 – 2.82 (m, 1H), 1.76 – 1.60 (m, 3H), 1.43 and 1.41 (2s, 9H), 1.16 and 1.10 (2t, $J = 7.2$ Hz, 3H), 0.97 – 0.79 (m, 6H).

^{13}C NMR (101 MHz, CDCl_3) δ 176.40, 176.15, 169.88, 169.63, 169.30, 168.20, 156.60, 156.16, 139.74, 139.60, 128.80, 128.51, 128.27 (2C), 128.16 (2C), 127.59, 127.37, 125.83, 125.73, 80.39, 80.02, 72.96, 72.17, 63.77, 62.62, 52.26, 52.15, 50.07, 49.47, 41.31, 41.28, 41.18, 41.01, 40.68, 40.08, 28.29 (3C), 28.26 (3C), 24.58, 24.54, 23.32 (2C), 21.18 (2C), 13.24, 13.01.

Methyl (*S,Z*)-(2-(2-((*tert*-butoxycarbonyl)amino)-*N*-ethyl-4-methylpentanamido)-3-phenylacryloyl)-glycinate (**3c**)

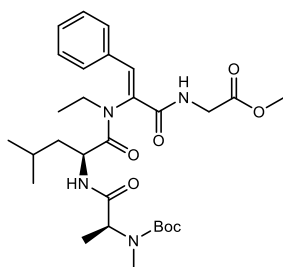


According to general method III, tripeptide **2c** (430 mg, 0.87 mmol) and Martin's sulfurane (0.88 g, 1.31 mmol) were used. Purification was done by column chromatography (DCM / MeOH 99:1 – 90:10), giving the desired product **3c** (211.0 mg, 0.44 mmol, 51 %) as a yellow oil.

^1H NMR (400 MHz, CDCl_3) δ 8.45 (t, $J = 5.8$ Hz, 1H), 7.70 – 7.32 (m, 6H), 5.22 – 5.09 (m, 1H), 4.82 – 4.75 (m, 1H), 4.19 – 4.01 (m, 2H), 3.71 (s, 3H), 3.12 – 2.90 (m, 2H), 1.75 – 1.42 (m, 3H), 1.38 (s, 9H), 1.21 – 1.14 (m, 3H), 0.59 (d, $J = 6.5$ Hz, 3H), 0.56 (d, $J = 6.6$ Hz, 3H).

^{13}C NMR (101 MHz, CDCl_3) δ 172.67, 169.96, 165.55, 156.32, 135.74, 132.28, 131.89, 130.55 (2C), 130.40, 129.16 (2C), 80.29, 52.17, 51.00, 41.86, 39.16, 34.46, 28.20 (3C), 24.57, 21.18 (2C), 13.42.

Methyl (S,Z)-(2-(2-((*tert*-butoxycarbonyl)amino)-*N*-ethyl-4-methylpentanamido)-3-phenylacryloyl)-glycinate (**4c**)

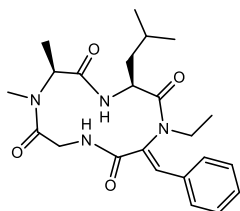


According to general method IV, compound **3c** (75 mg, 0.16 mmol), Boc-*N*-methyl-*L*-alanine (38.5 mg, 0.19 mmol), DIPEA (82.4 μ L, 0.47 mmol) and HATU (71.9 mg, 0.19 mmol) were used. Purification was done by column chromatography (DCM / EtOAc, 99:1 – 80:20), giving compound **4c** (71.5 mg, 0.13 mmol, 82 %) as a yellow oil.

^1H NMR (400 MHz, CDCl_3) δ 8.63 (s, 1H), 7.76 (s, 1H), 7.47 – 7.33 (m, 6H), 4.68 (s, 1H), 4.39 – 4.30 (m, 1H), 4.27 – 4.10 (m, 2H), 3.72 (s, 3H), 3.40 – 3.27 (m, 2H), 2.70 (s, 3H), 1.78 – 1.54 (m, 3H), 1.51 – 1.39 (m, 9H), 1.33 – 1.18 (m, 6H), 0.59 (t, J = 6.8 Hz, 6H).

^{13}C NMR (101 MHz, CDCl_3) δ 172.38, 171.48, 169.99, 165.88, 157.10, 135.79, 132.20, 131.72, 130.62 (2C), 130.41, 129.24 (2C), 80.71, 52.54, 51.89, 50.83, 41.90, 38.73, 34.40, 29.68, 28.31 (3C), 24.78, 23.15 (2C), 14.18, 13.09.

(3*S*,6*S*)-12-((*Z*)-Benzylidene)-1-ethyl-3-isobutyl-6,7-dimethyl-1,4,7,10-tetraazacyclododecane-2,5,8,11-tetraone (**5c**)



According to general method V, compound **4c** (40 mg, 0.07 mmol), lithium hydroxide hydrate (12.3 mg, 0.29 mmol), 4-DMAP (89.4 mg, 0.7 mmol) and T3P (50 % w/w in EtOAc, 174.2 μ L, 0.29 mmol) were used, giving compound **5c** (11.6 mg, 0.03 mmol, 37 %) as a white solid. A sample was purified by semipreparative RP-HPLC for biological assays and characterization.

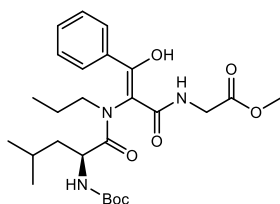
HR-MS m/z 427.2353 (calculated for $\text{C}_{23}\text{H}_{32}\text{N}_4\text{O}_4$: 427.2351)

t_R = 11.65 min (5 % ACN (0 min) > 100 % ACN (15 min) > 100 % ACN (20 min))

^1H NMR (500 MHz, CDCl_3) δ 8.08 (s, 1H), 7.86 (s, 1H), 7.51 – 7.38 (m, 6H), 7.17 (s, 1H), 5.19 (dd, J = 15.2, 10.4 Hz, 1H), 4.39 (d, J = 7.7 Hz, 1H), 4.28 (s, 1H), 3.82 (dq, J = 14.7, 7.4 Hz, 1H), 3.64 – 3.54 (m, 2H), 2.79 (s, 3H), 1.79 – 1.65 (m, 1H), 1.54 (d, J = 7.0 Hz, 3H), 1.40 – 1.30 (m, J = 7.5, 6.8 Hz, 1H), 1.22 (t, J = 7.4 Hz, 3H), 0.63 (d, J = 6.5 Hz, 3H), 0.56 (d, J = 6.6 Hz, 3H).

^{13}C NMR (126 MHz, CDCl_3) δ 171.89, 171.63, 169.62, 165.25, 137.87, 132.04, 130.88, 130.02 (2C), 129.25 (2C), 128.68, 57.03, 49.88, 44.55, 43.79, 41.11, 30.18, 24.53, 22.36, 22.23, 15.43, 12.34.

Methyl (*S,E*)-(2-(2-((*tert*-butoxycarbonyl)amino)-4-methyl-*N*-propylpentanamido)-3-hydroxy-3-phenylacryloyl)glycinate (**1d**)

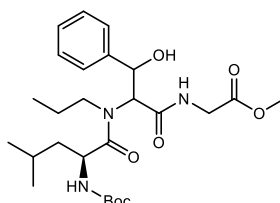


According to general method I, propyl amine (410 μ L, 5 mmol), phenylglyoxal hydrate (0.76 g, 5 mmol), Boc-*L*-leucine (0.93 g, 4 mmol) and methyl 2-isocyanoacetate (0.36 mL, 4 mmol) were used. Purification was done by column chromatography (DCM / EtOAc 8:2), giving compound **1d** as a yellow oil (0.75 g, 1.48 mmol, 37 %).

^1H NMR (400 MHz, CDCl_3) δ 15.43 and 14.50 (2s, 1H), 7.72 (dd, $J = 7.7, 2.2$ Hz, 1H), 7.58 – 7.30 (m, 5H), 5.08 – 4.70 (m, 1H), 4.46 – 3.98 (m, 3H), 3.86 – 3.68 (m, 4H), 3.19 – 2.62 (m, 2H), 1.78 – 1.52 (m, 4H), 1.41 (s, 9H), 1.01 – 0.61 (m, 9H).

^{13}C NMR (101 MHz, CDCl_3) δ 174.85, 174.42, 172.40, 169.94, 169.73, 167.53, 157.53, 156.71, 134.06, 132.90, 131.03, 130.39, 128.68, 128.63, 128.38, 128.09, 128.00, 127.59, 107.98, 107.24, 80.52, 80.18, 60.38 (2C), 53.53, 53.49, 52.16, 52.14, 51.36, 50.22, 41.32, 41.11, 39.23, 39.12, 28.34 (3C), 28.18 (3C), 24.61, 24.52, 23.46 (2C), 23.30 (2C), 21.29, 20.96, 20.90, 20.47, 11.55, 11.28.

Methyl (2-((*S*)-2-((*tert*-butoxycarbonyl)amino)-4-methyl-*N*-propylpentanamido)-3-hydroxy-3-phenylpropanoyl)glycinate (mixture of diastereomers) (**2d**)

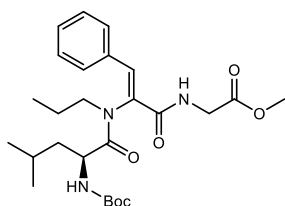


According to general method II, tripeptide **1d** (0.60 g, 1.19 mmol) and palladium on carbon (10 % w/w, 60 mg) were used, giving compound **2d** as a light yellow oil (0.59 g, 1.17 mmol, 98 %).

^1H NMR (400 MHz, CDCl_3) δ 7.59 – 7.18 (m, 6H), 5.70 – 5.49 (m, 1H), 5.06 – 4.81 (m, 2H), 4.40 – 3.81 (m, 4H), 3.74 (2s, 3H), 3.67 – 3.49 (m, 1H), 3.18 – 2.66 (m, 1H), 1.78 – 1.53 (m, 5H), 1.42 (2s, 9H), 0.98 – 0.77 (m, 9H).

^{13}C NMR (101 MHz, CDCl_3) δ 176.38, 176.19, 170.67, 169.84, 169.60, 168.21, 156.58, 154.07, 140.99, 139.59, 128.83, 128.78, 128.28, 128.17 (2C), 127.61, 127.40 (2C), 125.85, 125.75, 80.34, 79.98, 73.01, 72.15, 53.80, 52.25, 52.13, 50.72, 50.12, 49.57, 41.33, 41.18, 41.05, 40.73, 28.29 (6C), 24.54 (2C), 24.46, 24.25, 23.33 (2C), 22.00, 21.38, 21.23, 21.06, 11.21, 11.05.

Methyl (2-((*S*)-2-((*tert*-butoxycarbonyl)amino)-4-methyl-*N*-propylpentanamido)-3-hydroxy-3-phenylpropanoyl)glycinate (**3d**)

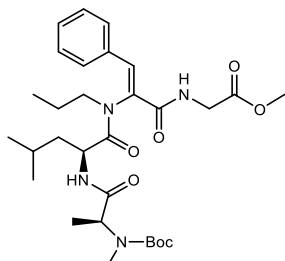


According to general method III, tripeptide **2d** (500 mg, 0.99 mmol) and Martin's sulfurane (0.99 g, 1.48 mmol) were used. Purification was done by column chromatography (DCM / MeOH 99:1 – 90:10), giving the desired product **3d** (218.1 mg, 0.45 mmol, 45 %) as a yellow oil.

^1H NMR (400 MHz, CDCl_3) δ 8.60 (t, J = 5.8 Hz, 1H), 7.49 – 7.37 (m, 5H), 7.35 (s, 1H), 5.30 (s, 1H), 4.80 (d, J = 6.4 Hz, 1H), 4.27 – 4.08 (m, 2H), 3.73 (s, 3H), 2.91 (ddd, J = 13.1, 10.6, 5.1 Hz, 2H), 1.79 – 1.41 (m, 5H), 1.40 (s, 9H), 0.90 (t, J = 7.3 Hz, 3H), 0.62 (d, J = 6.5 Hz, 3H), 0.58 (d, J = 6.6 Hz, 3H).

^{13}C NMR (101 MHz, CDCl_3) δ 172.64, 169.95, 165.72, 156.61, 135.78, 132.23, 131.60, 130.66 (2C), 130.56, 129.18 (2C), 80.31, 52.19, 52.04, 50.89, 41.94, 39.28, 28.19 (3C), 24.70, 23.24 (2C), 21.08, 11.54.

Methyl (2-((*S*)-2-((*tert*-butoxycarbonyl)amino)-4-methyl-*N*-propylpentanamido)-3-hydroxy-3-phenylpropanoyl)glycinate (**4d**)

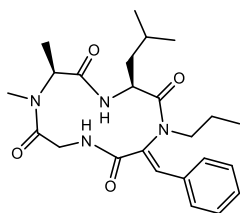


According to general method IV, compound **3d** (100 mg, 0.20 mmol), Boc-*N*-methyl-*L*-alanine (49.8 mg, 0.25 mmol), DIPEA (106.8 μL , 0.61 mmol) and HATU (93.2 mg, 0.25 mmol) were used. Purification was done by column chromatography (DCM / EtOAc, 99:1 – 80:20), giving compound **4d** (96.6 mg, 0.17 mmol, 82 %) as a yellow oil.

^1H NMR (400 MHz, CDCl_3) δ 8.73 (s, 1H), 7.79 (s, 1H), 7.49 – 7.37 (m, 5H), 7.34 (s, 1H), 4.69 (s, 1H), 4.38 – 4.30 (m, 1H), 4.27 – 4.00 (m, 2H), 3.71 (s, 3H), 2.99 – 2.86 (m, 2H), 2.70 (s, 3H), 1.79 – 1.60 (m, 5H), 1.50 – 1.43 (m, 7H), 1.26 (t, J = 7.3 Hz, 5H), 0.88 (t, J = 7.4 Hz, 3H), 0.60 (t, J = 7.2 Hz, 6H).

^{13}C NMR (101 MHz, CDCl_3) δ 172.42, 171.41, 169.98, 166.73, 157.87, 135.88, 132.16, 131.46, 130.68 (2C), 130.63, 129.20 (2C), 80.79, 55.09, 51.95, 51.74, 50.75, 41.94, 38.91, 29.68, 28.28 (3C), 24.85, 23.17 (2C), 21.10, 14.18, 11.52.

(3S,6S)-12-((Z)-Benzylidene)-3-isobutyl-6,7-dimethyl-1-propyl-1,4,7,10-tetraazacyclododecane-2,5,8,11-tetraone (**5d**)



According to general method V, compound **4d** (45 mg, 0.08 mmol), lithium hydroxide hydrate (16.3 mg, 0.39 mmol), 4-DMAP (50.5 mg, 0.45 mmol) and T3P (50 % w/w in EtOAc, 178.8 μ L, 0.3 mmol) were used, giving the TTX derivative **5d** (13.1 mg, 0.03 mmol, 37 %) as a white solid. A sample was purified by semipreparative RP-HPLC for biological assays and characterization.

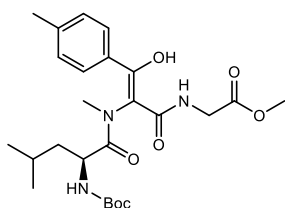
HR-MS m/z 441.2495 (calculated for $C_{24}H_{33}N_4O_4$: 441.2507)

t_R = 12.37 min (5 % ACN (0 min) > 100 % ACN (15 min) > 100 % ACN (20 min))

1H NMR (500 MHz, $CDCl_3$) δ 8.11 (s, 1H), 7.82 (s, 1H), 7.48 (dq, J = 7.1, 4.1, 3.4 Hz, 2H), 7.41 (h, J = 2.1 Hz, 3H), 7.16 (s, 1H), 5.19 (dd, J = 15.2, 10.5 Hz, 1H), 4.38 (d, J = 7.5 Hz, 1H), 4.28 (s, 1H), 3.64 (td, J = 12.7, 5.2 Hz, 1H), 3.58 (d, J = 15.2 Hz, 1H), 3.42 (td, J = 12.7, 4.6 Hz, 1H), 2.79 (s, 3H), 1.76 – 1.67 (m, 3H), 1.54 (d, J = 7.0 Hz, 3H), 1.43 – 1.17 (m, 2H), 0.90 (t, J = 7.3 Hz, 3H), 0.63 (d, J = 6.5 Hz, 3H), 0.56 (d, J = 6.6 Hz, 3H).

^{13}C NMR (126 MHz, $CDCl_3$) δ 171.85, 171.59, 169.57, 165.21, 137.47, 132.02, 130.88, 130.67, 130.08 (2C), 129.24 (2C), 57.02, 51.35, 49.82, 44.52, 41.15, 30.15, 24.53, 22.39, 22.22, 20.59, 15.41, 11.59.

Methyl (*S,E*)-(2-(2-((*tert*-butoxycarbonyl)amino)-*N*,4-dimethylpentanamido)-3-hydroxy-3-(*p*-tolyl)acryloyl)glycinate (**1e**)



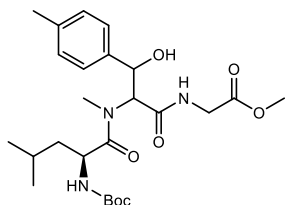
According to general method I, methyl amine hydrochloride (332 mg, 5 mmol), *p*-methyl phenylglyoxal (0.74 g, 5 mmol), Boc-*L*-leucine (0.93 g, 4 mmol) and methyl 2-isocyanoacetate (0.36 mL, 4 mmol) were used. Purification was done by column chromatography (DCM / EtOAc 8:2), giving compound **1e** as a yellow oil (0.83 g, 1.7 mmol, 42 %).

1H NMR (400 MHz, $CDCl_3$) δ 15.10, 14.66, 14.23 (3s, 1H), 7.88 – 7.06 (m, 5H), 5.15 – 4.50 (m, 1H), 4.39 – 4.02 (m, 1H), 3.78 – 3.72 (m, 5H), 3.17 (s, 3H), 2.38 (s, 3H), 1.70 – 1.44 (m, 3H), 1.48 – 1.35 (m, 9H), 0.98 – 0.81 (m, 3H), 0.76 – 0.60 (m, 3H).

^{13}C NMR (101 MHz, $CDCl_3$) δ 174.86, 174.71, 174.23, 171.50, 170.11, 170.04, 169.81, 167.86, 156.23, 155.80, 141.59, 140.48, 132.71, 130.74, 129.95, 129.44, 129.43, 129.40, 129.36, 128.78,

128.45, 127.88, 127.48, 127.37, 80.55, 80.03, 52.21, 52.18, 50.44, 49.69, 41.42, 41.29, 41.21, 41.14, 38.98, 37.07, 28.30 (3C), 28.20 (3C), 24.71, 24.44, 23.30, 23.21 (2C), 21.37 (2C), 20.47.

Methyl (2-((*S*)-2-((*tert*-butoxycarbonyl)amino)-*N*,4-dimethylpentanamido)-3-hydroxy-3-(*p*-tolyl)propanoyl)glycinate (mixture of diastereomers) (**2e**)

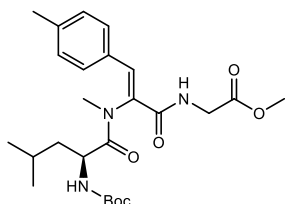


According to general method II, tripeptide **1e** (0.65 g, 1.36 mmol) and palladium on carbon (10 % w/w, 65 mg) were used, giving compound **2e** as a light yellow oil (0.65 g, 1.36 mmol, quant.).

^1H NMR (400 MHz, CDCl_3) δ 7.32 – 7.07 (m, 5H), 5.70 – 5.55 (m, 1H), 5.10 – 4.75 (m, 2H), 4.38 – 4.15 (m, 1H), 4.08 – 3.81 (m, 3H), 3.78 – 3.68 (m, 3H), 3.16 (s, 3H), 2.37 – 2.28 (m, 3H), 1.47 – 1.33 (m, 12H), 0.75 (t, J = 6.2 Hz, 6H).

^{13}C NMR (101 MHz, CDCl_3) δ 174.98, 174.24, 170.88, 170.35, 169.63, 169.38, 156.95, 156.50, 137.91, 136.73, 136.52, 136.16, 129.63, 129.00, 128.76 (2C), 127.01, 126.05, 125.39 (2C), 80.76, 80.10, 73.61, 72.08, 63.65, 60.91, 52.27, 52.19, 49.39, 48.50, 41.13, 41.04, 40.69, 38.45, 33.67, 32.08, 28.27 (3C), 28.20 (3C), 24.11, 24.02, 23.16 (2C), 22.96 (2C), 21.12, 21.07.

Methyl (*S,Z*)-(2-(2-((*tert*-butoxycarbonyl)amino)-*N*,4-dimethylpentanamido)-3-(*p*-tolyl)acryloyl)glycinate (**3e**)

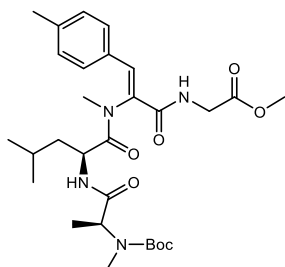


According to general method III, tripeptide **2e** (550 mg, 1.11 mmol) and Martin's sulfurane (1.12 g, 1.7 mmol) were used. Purification was done by column chromatography (DCM / MeOH 99:1 – 90:10), giving **3e** (211.2 mg, 0.44 mmol, 40 %) as a yellow oil.

^1H NMR (500 MHz, CDCl_3) δ 8.30 (t, J = 6.0 Hz, 1H), 7.34 – 7.15 (m, 4H), 6.60 (s, 1H), 5.30 (s, 1H), 4.88 – 4.73 (m, 1H), 4.05 (d, J = 5.3 Hz, 2H), 3.76 (s, 3H), 3.20 (s, 3H), 2.38 (s, 3H), 1.76 – 1.57 (m, 3H), 1.45 (s, 9H), 0.61 (d, J = 6.5 Hz, 3H), 0.58 (d, J = 6.7 Hz, 3H).

^{13}C NMR (126 MHz, CDCl_3) δ 172.74, 170.10, 165.04, 156.28, 141.13, 135.72, 131.07, 130.49, 129.98, 129.83, 129.51, 126.52, 80.23, 52.36, 51.46, 41.83, 41.14, 34.30, 28.29 (3C), 24.72, 23.21, 22.94, 21.46.

Methyl ((Z)-2-((S)-2-((S)-2-((tert-butoxycarbonyl)(methyl)amino)propanamido)-N,4-dimethylpentanamido)-3-(*p*-tolyl)acryloyl)glycinate (**4e**)

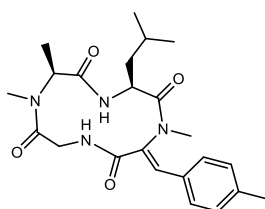


According to general method IV, compound **3e** (100 mg, 0.21 mmol), Boc-*N*-methyl-*L*-alanine (51.3 mg, 0.25 mmol), DIPEA (110.3 μ L, 0.63 mmol) and HATU (79.9 mg, 0.25 mmol) were used. Purification was done by column chromatography (DCM / EtOAc, 99:1 – 80:20), giving compound **4e** (103.7 mg, 0.18 mmol, 88 %) as a yellow oil.

^1H NMR (500 MHz, CDCl_3) δ 8.49 (s, 1H), 7.70 (s, 1H), 7.34 – 7.29 (m, 2H), 7.22 (d, J = 8.0 Hz, 2H), 6.71 (s, 1H), 4.65 (s, 1H), 4.12 (q, J = 7.2 Hz, 1H), 4.02 (d, J = 5.4 Hz, 2H), 3.75 (s, 3H), 3.20 (s, 3H), 2.79 (s, 3H), 2.36 (s, 3H), 1.63 (s, 3H), 1.48 (s, 9H), 1.26 (dd, J = 7.6, 6.7 Hz, 3H), 0.92 (dd, J = 16.1, 6.4 Hz, 6H).

^{13}C NMR (126 MHz, CDCl_3) δ 172.23, 171.98, 170.05, 165.17, 156.29, 135.22, 131.05, 130.49, 130.00, 129.45, 126.09, 80.83, 52.34, 52.00, 51.40, 41.83, 41.14, 34.24, 30.17, 28.32 (3C), 28.28, 24.66, 23.15, 21.46, 21.04, 14.18.

(3*S*,6*S*)-3-Isobutyl-1,6,7-trimethyl-12-((*Z*)-4-methylbenzylidene)-1,4,7,10-tetraazacyclododecane-2,5,8,11-tetraone (**5e**)



According to general method V, compound **4e** (60 mg, 0.11 mmol), lithium hydroxide hydrate (18.0 mg, 0.43 mmol), 4-DMAP (130.7 mg, 1.1 mmol) and T3P (50 % w/w in EtOAc, 191.1 μ L, 0.32 mmol) were used, giving TTX derivative **5e** (16.0 mg, 0.04 mmol, 35 %) as a white solid. A sample was purified by semipreparative RP-HPLC for biological assays and characterization.

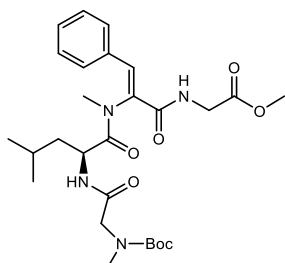
HR-MS m/z 427.2337 (calculated for $\text{C}_{23}\text{H}_{32}\text{N}_4\text{O}_4$: 427.2351)

t_R = 11.74 min (5 % ACN (0 min) > 100 % ACN (15 min) > 100 % ACN (20 min))

^1H NMR (400 MHz, CDCl_3) δ 8.17 (s, 1H), 7.81 (s, 1H), 7.53 – 7.45 (m, 2H), 7.43 – 7.37 (m, 2H), 7.19 (s, 1H), 5.20 (dd, J = 15.2, 10.4 Hz, 1H), 4.39 (q, J = 6.9 Hz, 1H), 4.33 – 4.19 (m, 1H), 3.65 (dt, J = 12.8, 6.3 Hz, 1H), 3.58 (d, J = 15.1 Hz, 1H), 3.42 (td, J = 12.6, 4.9 Hz, 1H), 2.78 (s, 3H), 1.78 – 1.66 (m, 1H), 1.54 (d, J = 7.0 Hz, 3H), 1.40 – 1.16 (m, 3H), 0.90 (t, J = 7.3 Hz, 3H), 0.63 (d, J = 6.5 Hz, 3H), 0.56 (d, J = 6.6 Hz, 3H).

^{13}C NMR (101 MHz, CDCl_3) δ 171.86, 171.51, 169.53, 165.27, 137.45 (2C), 132.04, 130.85, 130.07 (2C), 129.22 (2C), 57.03, 51.37, 49.84, 44.54, 41.17, 30.15, 24.52, 22.39, 22.21, 20.59, 15.40.

Methyl (*S,Z*)-(2-(2-(2-((*tert*-butoxycarbonyl)(methyl)amino)acetamido)-*N*,4-dimethylpentan-amido)-3-phenylacryloyl)glycinate (**4f**)

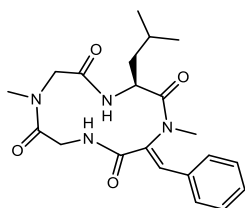


According to general method IV, compound **3a** (40 mg, 0.09 mmol), Boc-*N*-methyl-*L*-glycine (19.7 mg, 0.10 mmol), DIPEA (45.3 μL , 0.26 mmol) and HATU (39.5 mg, 0.10 mmol) were used. Purification was done by column chromatography (DCM / EtOAc, 99:1 – 80:20), giving compound **4f** (41.5 mg, 0.08 mmol, 90 %) as a yellow oil.

^1H NMR (400 MHz, CDCl_3) δ 8.73 (s, 1H), 7.73 (s, 1H), 7.48 – 7.30 (m, 5H), 6.57 – 6.35 (m, 1H), 4.32 (d, J = 10.9 Hz, 1H), 4.22 – 3.94 (m, 2H), 3.85 – 3.74 (m, 2H), 3.71 (s, 4H), 3.21 (s, 3H), 2.70 (s, 3H), 2.25 – 2.11 (m, 1H), 1.78 – 1.45 (m, 2H), 1.44 (s, 9H), 0.96 (d, J = 6.5 Hz, 3H), 0.85 (d, J = 6.7 Hz, 2H).

^{13}C NMR (126 MHz, CDCl_3) δ 171.65, 171.15, 170.05, 170.03, 165.17, 156.50, 141.20, 135.81, 131.06, 130.49, 130.20, 130.00, 129.45, 126.51, 80.83, 52.35, 52.00, 51.40, 41.84, 41.14, 34.24, 30.17, 28.33 (2C), 24.66, 23.15.

(*S,Z*)-12-Benzylidene-3-isobutyl-1,7-dimethyl-1,4,7,10-tetraazacyclododecane-2,5,8,11-tetra-one (**5f**)



According to general method V, compound **4f** (25 mg, 0.05 mmol), lithium hydroxide hydrate (7.9 mg, 0.18 mmol), 4-DMAP (57.3 mg, 1.8 mmol) and T3P (50 % w/w in EtOAc, 111.8 μL , 0.19 mmol) were used, giving TTX derivative **5f** (10.0 mg, 0.03 mmol, 53 %) as a white solid. A sample was purified by semipreparative RP-HPLC for biological assays and characterization.

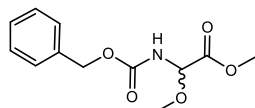
HR-MS m/z 399.2028 (calculated for $\text{C}_{21}\text{H}_{27}\text{N}_4\text{O}_4$: 399.2027)

t_R = 10.18 min (5 % ACN (0 min) > 100 % ACN (15 min) > 100 % ACN (20 min))

^1H NMR (500 MHz, CDCl_3) δ 8.12 (s, 1H), 7.79 (s, 1H), 7.43 (d, J = 9.1 Hz, 6H), 5.36 – 5.08 (m, 1H), 4.48 – 4.29 (m, 2H), 3.71 – 3.58 (m, 1H), 3.21 (s, 3H), 2.97 – 2.93 (m, 3H), 1.79 – 1.57 (m, 3H), 1.43 – 1.23 (m, 1H), 0.66 – 0.61 (m, 3H), 0.54 (s, 3H).

^{13}C NMR (126 MHz, CDCl_3) δ 172.41, 169.93, 169.33, 164.72, 137.33, 136.81, 131.95, 130.81, 129.75 (2C), 129.43 (2C), 54.19, 48.67, 44.22, 41.07, 35.41, 30.93, 24.50, 22.27 (2C).

Methyl 2-(((benzyloxy)carbonyl)amino)-2-methoxyacetate (**6**)



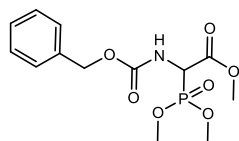
Benzyl carbamate (15.0 g, 107.8 mmol, 1 eq) and glyoxylic acid (10.0 g, 135.1 mmol, 1.25 eq) were suspended in diethyl ether (150 mL) and stirred overnight. After removing the solvent under reduced pressure, the residue was redissolved in methanol (150 mL) and sulfuric acid (3.3 mL, 61.5 mmol, 0.6 eq) was added. The mixture was stirred for four days after which it was neutralized using Na_2CO_3 and extracted using ethyl acetate (3 x 100 mL). The combined organic layers were dried over Na_2SO_4 , filtered, and evaporated to dryness, giving product **6** as a colourless oil (11.1 g, 43.6 mmol, 41 %).

HR-MS m/z 254.1027 (calculated for $\text{C}_{12}\text{H}_{16}\text{NO}_5$: 254.1023)

^1H NMR (400 MHz, CDCl_3) δ 7.40 – 7.29 (m, 5H), 5.86 (d, J = 9.6 Hz, 1H), 5.36 (d, J = 9.5 Hz, 1H), 5.15 (s, 2H), 3.81 (s, 3H), 3.46 (s, 3H).

^{13}C NMR (101 MHz, CDCl_3) δ 167.97, 155.66, 135.75, 128.60 (2C), 128.39, 128.20 (2C), 80.65, 67.44, 56.29, 52.93.

Methyl 2-(((benzyloxy)carbonyl)amino)-2-(dimethoxyphosphoryl)acetate (**7**)



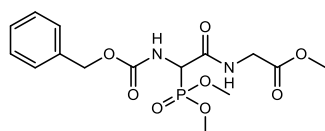
To a solution of **6** (7.05 g, 27.9 mmol, 1 eq) in toluene (40 mL) under N_2 atmosphere, PCl_3 (2.89 mL, 33.0 mmol, 1.2 eq) was slowly added. The solution was stirred for three hours at 100 °C after which $\text{P}(\text{OMe})_3$ (3.93 mL, 33.3 mmol, 1.2 eq) was added, followed by stirring at 100 °C for three hours after which the solvent was removed under reduced pressure. The residue was redissolved in EtOAc (50 mL), and the solution was washed with sat. aq. NaHCO_3 solution (30 mL). The water phase was reextracted with EtOAc (3x 30 mL). The combined organic layers were dried over Na_2SO_4 , filtered, and evaporated to dryness. *n*-Hexane (50 mL) was added to the residue, resulting in a white precipitate which was separated via filtration. The residue was washed with cold *n*-hexane, giving product **7** (7.7 g, 23.2 mmol, 83 %) as a white solid. The crude product was used without further purification.

HR-MS m/z 332.0904 (calculated for $\text{C}_{13}\text{H}_{19}\text{NO}_7\text{P}$: 332.0894)

^1H NMR (400 MHz, CDCl_3) δ 7.39 – 7.29 (m, 5H), 5.69 (d, J = 8.8 Hz, 1H), 5.14 (d, J = 3.6 Hz, 1H), 4.96 (d, J = 9.2 Hz, 1H), 4.91 (d, J = 9.2 Hz, 1H), 3.83 (s, 3H), 3.80 (s, 3H), 3.77 (s, 3H).

^{13}C NMR (101 MHz, CDCl_3) δ 167.16, 155.60 (d, J = 7.6 Hz), 135.82, 128.52 (2C), 128.30, 128.11 (2C), 67.62, 54.12 (d, J = 6.5 Hz), 54.00 (d, J = 6.8 Hz), 53.32, 52.06 (d, J = 148.2 Hz).

Methyl (2-(((benzyloxy)carbonyl)amino)-2-(dimethoxyphosphoryl)acetyl)glycinate (**8**)



To a solution of **7** (5.8 g, 17.5 mmol, 1 eq) in methanol (36 mL) under N_2 atmosphere, aq. NaOH solution (1 M, 18 mL, 18.0 mmol) was added dropwise. The mixture was stirred for two hours after which the methanol was removed under reduced pressure. The remaining suspension was filtered, and the filtrate acidified to pH ~ 2 using aq. sulfuric acid (1 M) and extracted with ethyl acetate (2x 30 mL). The combined organic phases were washed with brine (30 mL), dried over Na_2SO_4 , filtered, and evaporated to dryness. The crude intermediate (5.33 g, 96 %) and glycine hydrochloride (2.06 g, 18.5 mmol, 1.1 eq) were suspended in DMF / DCM (40 mL, 1:1). After cooling the mixture to 0 °C, DIPEA (8.58 mL, 50.43 mmol, 3 eq) and HATU (7.67 g, 20.2 mmol, 1.2 eq) were added. After 10 min, the cooling bath was removed, and the mixture was stirred overnight at room temperature after which water (100 mL) was added to mixture. The organic phase was separated, and the aqueous phase extracted with EtOAc (3x 50 mL). The combined organic phases were washed using aq. hydrochloric acid (0.5 M, 50 mL), sat. aq. NaHCO_3 solution (50 mL) and brine (50 mL). The organic phase was dried over Na_2SO_4 , filtered, and evaporated to dryness. The crude product was purified by dry column vacuum chromatography (DCVC) (EtOAc : *n*-hexane 0:1 - 1:1 (5 % gradient), 1:1-1:0 (3.3 % gradient) with fraction volume of 40 mL), giving **8** as a light red solid (5.53 g, 85 %).

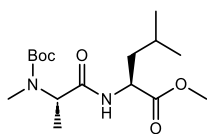
HR-MS m/z 387.0963 (calculated for $\text{C}_{15}\text{H}_{20}\text{N}_2\text{O}_8\text{P}$: 387.0963)

^1H NMR (400 MHz, CDCl_3) δ 7.52 (t, J = 5.4 Hz, 1H), 7.39 – 7.30 (m, 4H), 5.93 (d, J = 8.7 Hz, 1H), 5.13 (d, J = 3.6 Hz, 2H), 4.97 (dd, J = 20.5, 8.6 Hz, 1H), 4.27 (d, J = 7.6 Hz, 1H), 4.06 (t, J = 4.9 Hz, 2H), 3.85 (dd, J = 8.4, 6.1 Hz, 3H), 3.79 (d, J = 10.9 Hz, 3H), 3.74 (s, 3H).

^{13}C NMR (101 MHz, CDCl_3) δ 169.47, 165.08 (d, J = 4.3 Hz), 157.00, 155.91 (d, J = 4.3 Hz), 135.88, 128.46 (2C), 128.20, 128.00 (2C), 67.48, 54.29 (d, J = 6.0 Hz), 53.92 (d, J = 7.0 Hz), 52.27, 41.83 (d, J = 43.5 Hz).

^{31}P NMR (162 MHz, CDCl_3) δ 20.54.

Methyl *N*-(*tert*-butoxycarbonyl)-*N*-methyl-*L*-alanyl-*L*-leucinate (**9**)



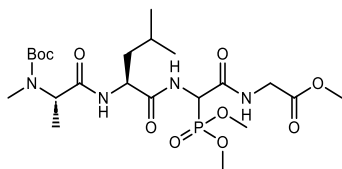
L-Leucine hydrochloride (5.52 g, 27.14 mmol) and Boc-*N*(Me)-Ala-OH (5.55 g, 27.15 mmol) were dissolved in DCM / DMF (120 mL, 11:1) and cooled to 0 °C. DIPEA (9.39 mL, 54.3 mmol) and HATU (12.39 g, 32.58 mmol) were added and the mixture stirred overnight at rt. Water (150 mL) was added, the organic phase separated, and the aqueous phase extracted with EtOAc (3x 50 mL). The combined organic phases were washed using aq. hydrochloric acid (50 mL, 0.5 M), sat. aq. NaHCO₃ solution (50 mL) and brine (50 mL), then dried over Na₂SO₄, filtered, and evaporated to dryness, giving **9** (7.3 g, 22.1 mmol, 81 %) as a white solid.

HR-MS *m/z* 331.2230 (calculated for C₁₆H₃₁N₂O₅: 331.2227)

¹H NMR (400 MHz, CDCl₃) δ 6.47 (s, 1H), 4.69 (s, 1H), 4.59 (td, *J* = 8.5, 4.5 Hz, 1H), 3.73 (s, 3H), 2.77 (s, 3H), 1.72 – 1.50 (m, 3H), 1.49 (s, 9H), 1.34 (d, *J* = 7.1 Hz, 3H), 0.92 (d, *J* = 5.9 Hz, 6H).

¹³C NMR (101 MHz, CDCl₃) δ 173.13, 171.25, 156.03, 80.63, 53.33, 52.20, 50.56, 41.49, 29.76, 28.32 (3C), 24.80, 22.79, 21.72, 13.46.

Methyl (2-((*S*)-2-((*S*)-2-((*tert*-butoxycarbonyl)(methyl)amino)propanamido)-4-methylpentan-amido)-2-(dimethoxyphosphoryl)acetyl)glycinate (**10**)



A solution of dipeptide **9** (7.3 g, 22.1 mmol) and lithium hydroxide hydrate (2.76 g, 66.3 mmol) in THF/H₂O (120 mL, 2:1) was stirred overnight at room temperature. The solution was acidified to pH ~ 2 - 3 using sat. aq. NaHCO₃ solution. Water (50 mL) was added, and the aqueous phase was extracted using ethyl acetate (3x 50 mL). The combined organic layers were dried over Na₂SO₄, filtered, and evaporated to dryness, giving hydrolysed dipeptide **10** (6.8 g, 2.2 mmol, 98 %) as a white solid which was used in the following step without further purification.

To a stirred solution of **8** (1.36 g, 3.5 mmol) in dry methanol (30 mL) was added palladium on carbon (10 % w/w, 68 mg). The suspension was stirred overnight under a hydrogen atmosphere (1 atm), after which it was filtered through Celite. The filtrate was evaporated to dryness and redissolved in DCM (20 mL) and cooled to - 10 °C. Hydrolysed dipeptide (1.1 g, 3.5 mmol) in DCM (20 mL), then DCC (0.8 g, 3.85 mmol) were added. The solution was allowed to warm to room temperature and stirred for five hours, after which it was filtered. The filtrate was washed using aqueous NaHSO₄ solution (30 mL, 1 M), sat. aq. NaHCO₃ solution (30 mL) and brine (30 mL), then dried over Na₂SO₄, filtered, and evaporated to dryness. Purification was done by column chromatography on silica gel (*n*-hexane / EtOAc 5:5 – 0:1), giving peptide **10** (1.9 g, 3.4 mmol, 98 %) as a white solid.

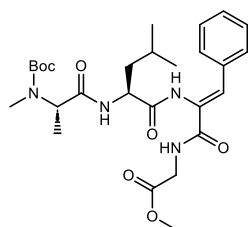
HR-MS m/z 551.2493 (calculated for $C_{22}H_{40}N_4O_{10}P$: 551.2488)

1H NMR (600 MHz, $CDCl_3$) δ 7.50 (q, J = 5.5, 5.0 Hz, 1H), 7.40 (q, J = 5.6, 4.7 Hz, 1H), 7.14 (s, 1H), 5.19 (ddd, J = 20.8, 8.5, 4.3 Hz, 1H), 4.70 (s, 1H), 4.46 (p, J = 6.4 Hz, 1H), 4.06 (dd, J = 7.5, 5.7 Hz, 2H), 3.87 – 3.79 (m, 6H), 3.74 (d, J = 2.8 Hz, 3H), 2.78 (s, 3H), 1.72 – 1.52 (m, 3H), 1.48 (d, J = 3.9 Hz, 9H), 1.33 (dd, J = 7.2, 3.8 Hz, 3H), 0.93 (d, J = 6.3 Hz, 3H), 0.91 (d, J = 6.1 Hz, 3H).

^{13}C NMR (151 MHz, $CDCl_3$) δ 172.05, 171.76 (d, J = 3.9 Hz), 169.50, 164.85, 156.40, 80.73, 54.45 (t, J = 6.3 Hz), 53.84 (t, J = 6.3 Hz), 53.33, 52.33 (d, J = 5.1 Hz), 51.83 (d, J = 12.8 Hz), 49.68 (dd, J = 148.6, 21.4 Hz), 41.54, 40.38, 29.87, 28.29 (3C), 24.62 (d, J = 8.0 Hz), 22.94 (d, J = 18.0 Hz), 21.56, 13.36.

^{31}P NMR (162 MHz, $CDCl_3$) δ 20.30.

Methyl ((*Z*)-2-((*S*)-2-((*S*)-2-((*tert*-butoxycarbonyl)(methyl)amino)propanamido)-4-methylpentan-amido)-3-phenylacryloyl)glycinate (**11a**)



According to general method VI, tetrapeptide **10** (250 mg, 0.45 mmol), TMG (170.3 μ L, 1.36 mmol) and benzaldehyde (141.5 μ L, 1.35 mmol) were used. Purification was done by column chromatography on silica gel (*n*-hexane / EtOAc 6:4 – 3:7), giving compound **11a** (209.2 mg, 0.39 mmol, 87 %) and the corresponding (*E*)-isomer (11.6 mg, 0.02 mmol, 4.8 %) as white solids.

(*Z*)-Isomer

1H NMR (600 MHz, $CDCl_3$) δ 7.99 (s, 1H), 7.44 (s, 1H), 7.44 – 7.31 (m, 4H), 7.35 (d, 1H), 7.33 – 7.29 (m, 1H), 6.73 (s, 1H), 4.52 (q, J = 7.2 Hz, 1H), 4.33 (dd, J = 9.7, 5.4 Hz, 1H), 4.12 (q, J = 6.8 Hz, 2H), 3.75 (s, 3H), 2.79 (s, 3H), 1.75 (td, J = 8.2, 3.5 Hz, 1H), 1.63 (tt, J = 12.4, 7.2 Hz, 2H), 1.43 (s, 9H), 1.32 (d, J = 7.1 Hz, 3H), 0.96 (d, J = 6.3 Hz, 3H), 0.90 (d, J = 6.2 Hz, 3H).

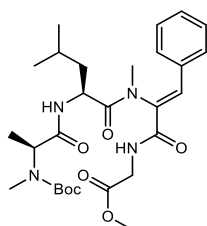
^{13}C NMR (151 MHz, $CDCl_3$) δ 172.01, 170.68, 169.03, 163.95, 156.57, 134.47, 129.37, 128.88, 128.82 (2C), 128.56, 128.15, 121.31, 80.78, 53.51, 52.55, 52.31, 41.68, 40.56, 30.04, 28.32 (3C), 24.74, 23.04, 21.48, 13.45.

(*E*)-Isomer (side product)

1H NMR (600 MHz, $CDCl_3$) δ 8.55 (s, 1H), 8.03 (s, 1H), 7.34 (dd, J = 27.5, 7.3 Hz, 5H), 6.69 (s, 1H), 6.17 (t, J = 5.2 Hz, 1H), 4.72 (s, 1H), 4.51 (td, J = 8.6, 4.8 Hz, 1H), 3.91 (d, J = 5.2 Hz, 2H), 3.66 (s, 3H), 2.80 (s, 3H), 1.78 – 1.72 (m, 1H), 1.67 – 1.55 (m, 2H), 1.48 (s, 9H), 1.37 (d, J = 7.1 Hz, 3H), 0.94 (dd, J = 18.9, 6.6 Hz, 6H).

^{13}C NMR (151 MHz, $CDCl_3$) δ 175.92, 174.06, 173.83, 173.12, 167.69, 136.27, 134.90, 132.07 (2C), 131.71, 131.15 (2C), 129.98, 83.69, 57.08, 55.57, 54.90, 44.33, 42.08, 33.57, 30.91 (3C), 27.37, 25.62, 23.69, 16.83.

Methyl ((*Z*)-2-((*S*)-2-((*S*)-2-((*tert*-butoxycarbonyl)(methyl)amino)propanamido)-*N*,4-dimethylpentanamido)-3-phenylacryloyl)glycinate (**4a**)

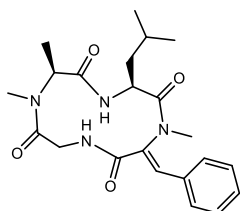


According to general method VII, tetrapeptide **11a** (64 mg, 0.12 mmol), K₂CO₃ (132.5 mg, 0.96 mmol), 18-crown-6 (3.2 mg, 0.012 mmol) and methyl iodide (0.12 mL, 1.85 mmol) were used, giving **4a** (57.7 mg, 0.11 mmol, 88 %) as a white solid.

¹H NMR (500 MHz, CDCl₃) δ 8.54 (d, *J* = 6.1 Hz, 1H), 7.73 (s, 1H), 7.42 (d, *J* = 3.3 Hz, 5H), 7.36 (d, *J* = 3.4 Hz, 1H), 4.67 (s, 1H), 4.39 – 4.28 (m, 1H), 4.13 (p, *J* = 6.8 Hz, 2H), 3.72 (s, 3H), 3.22 (s, 3H), 2.70 (s, 3H), 2.05 (s, 1H), 1.69 (s, 2H), 1.45 (s, 9H), 1.27 (d, *J* = 7.2 Hz, 3H), 0.57 (t, *J* = 6.4 Hz, 6H).

¹³C NMR (126 MHz, CDCl₃) δ 172.23, 171.54, 169.98, 165.02, 162.52, 135.72, 132.24, 132.02, 130.57, 130.39 (2C), 129.27 (2C), 80.67, 60.37, 52.01, 50.94, 41.83, 38.66, 36.46, 34.39, 28.26 (3C), 24.72, 23.12, 20.33, 14.28.

(3*S*,6*S*)-12-((*Z*)-Benzylidene)-3-isobutyl-1,6,7-trimethyl-1,4,7,10-tetraazacyclododecane-2,5,8,11-tetraone (Tentoxin, (**5a**))



According to general method V, compound **4a** (77 mg, 0.07 mmol), lithium hydroxide hydrate (31.5 mg, 0.75 mmol), 4-DMAP (97.6 mg, 0.87 mmol) and T3P (50 % w/w in EtOAc, 346 μL, 0.58 mmol) were used, giving tentoxin **5a** (18.4 mg, 0.04 mmol, 49 %) as a white solid. A sample was purified by semipreparative RP-HPLC for biological assays and characterization.

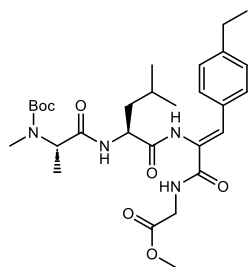
HR-MS *m/z* 413.2189 (calculated for C₂₂H₂₉N₄O₄: 413.2194).

*t*_R = 11.03 min (5 % ACN (0 min) > 100 % ACN (15 min) > 100 % ACN (20 min))

¹H NMR (500 MHz, CDCl₃) δ 7.97 (s, 1H), 7.76 (s, 1H), 7.41 – 7.35 (m, 5H), 7.09 (s, 1H), 5.19 (t, *J* = 13.1 Hz, 1H), 4.36 (s, 1H), 3.59 (d, *J* = 15.2 Hz, 1H), 3.19 (s, 3H), 2.81 (s, 3H), 1.73 – 1.63 (m, 2H), 1.53 (d, *J* = 7.1 Hz, 3H), 1.37 – 1.20 (m, 1H), 0.64 (d, *J* = 6.5 Hz, 3H), 0.52 (d, *J* = 6.4 Hz, 3H).

¹³C NMR (126 MHz, CDCl₃) δ 171.75, 171.54, 170.11, 164.52, 136.90, 131.93, 130.79 (2C), 129.73 (2C), 129.41 (2C), 56.93, 49.58, 44.46, 40.60, 35.35, 30.18, 24.60, 22.28, 22.11, 15.55.

Methyl ((Z)-2-((S)-2-((S)-2-((*tert*-butoxycarbonyl)(methyl)amino)propanamido)-4-methylpentan-
amido)-3-phenylacryloyl)glycinate (**11g**)



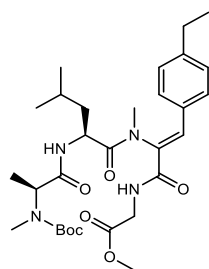
According to general method VI, tetrapeptide **10** (150 mg, 0.27 mmol), TMG (84.9 μ L, 0.68 mmol) and *p*-ethyl benzaldehyde (72.5 μ L, 0.54 mmol) were used. Purification was done by column chromatography on silica gel (*n*-hexane / EtOAc 6:4 – 4:6), giving **11g** (114 mg, 0.2 mmol, 75 %) and the corresponding (*E*)-isomer (5 mg, 0.089 mmol, 3.3 %) as white solids.

HR-MS m/z 559.3138 (calculated for $C_{29}H_{43}N_4O_7$: 559.3137)

1H NMR (400 MHz, $CDCl_3$) δ 7.85 (s, 1H), 7.44 – 7.13 (m, 6H), 6.70 (s, 1H), 4.52 (q, J = 7.0 Hz, 1H), 4.34 (dd, J = 9.5, 5.6 Hz, 1H), 4.12 (dd, J = 13.7, 6.5 Hz, 2H), 3.74 (s, 3H), 2.81 (d, J = 7.7 Hz, 3H), 2.64 (q, J = 7.6 Hz, 2H), 1.81 (s, 1H), 1.80 – 1.56 (m, 3H), 1.43 (s, 9H), 1.34 (t, J = 9.0 Hz, 2H), 1.24 (dt, J = 11.5, 7.4 Hz, 3H), 1.03 – 0.81 (m, 6H).

^{13}C NMR (101 MHz, $CDCl_3$) δ 173.20, 171.31, 170.45 (2C), 165.10, 145.58, 132.20, 130.91, 129.55 (2C), 128.05 (2C), 126.47, 81.01, 60.36, 52.88, 52.21, 41.67, 39.45, 30.89, 28.70, 28.25 (3C), 24.72, 22.97, 21.46, 15.26, 13.22.

Methyl ((Z)-2-((S)-2-((S)-2-((*tert*-butoxycarbonyl)(methyl)amino)propanamido)-*N*,4-dimethyl-
pentanamido)-3-(4-ethylphenyl)acryloyl) (**4g**)



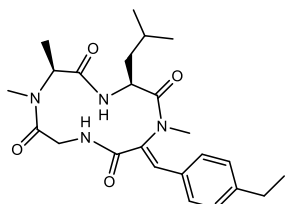
According to general method VII, tetrapeptide **11g** (100 mg, 0.18 mmol), K_2CO_3 (246 mg, 1.78 mmol), 18-crown-6 (4.8 mg, 0.02 mmol) and methyl iodide (166.5 μ L, 2.68 mmol) were used, giving **4g** (93 mg, 0.16 mmol, 91 %) as a white solid.

HR-MS m/z 573.3296 (calculated for $C_{30}H_{45}N_4O_7$: 573.3294)

1H NMR (500 MHz, $CDCl_3$) δ 8.49 (t, J = 6.1 Hz, 1H), 7.71 (s, 1H), 7.38 – 7.17 (m, 5H), 4.67 (s, 1H), 4.37 – 4.30 (m, 1H), 4.22 – 4.07 (m, 2H), 3.72 (s, 3H), 3.21 (s, 3H), 2.74 – 2.59 (m, 5H), 1.67 (s, 2H), 1.51 – 1.37 (m, 10H), 1.33 – 1.19 (m, 6H), 0.57 (dd, J = 6.8, 4.7 Hz, 6H).

^{13}C NMR (126 MHz, CDCl_3) δ 172.20, 171.64, 170.05, 165.19, 147.47, 135.81, 131.13, 130.56 (2C), 130.31, 129.69, 128.80 (2C), 80.67, 52.00, 50.92, 41.83, 38.68, 34.33, 29.67, 28.78, 28.33, 28.27 (3C), 24.74, 23.13, 20.33, 15.27, 13.24.

(3S,6S)-12-((Z)-4-Ethylbenzylidene)-3-isobutyl-1,6,7-trimethyl-1,4,7,10-tetraazacyclododecane-2,5,8,11-tetraone (**5g**)



According to general method V, compound **4g** (85 mg, 0.15 mmol), lithium hydroxide hydrate (31 mg, 0.74 mmol), 4-DMAP (99 mg, 0.88 mmol) and T3P (50 % w/w in EtOAc, 176 μL , 0.61 mmol) were used, giving **5g** (32.3 mg, 0.07 mmol, 49 %) as a white solid. A sample was purified by semipreparative RP-HPLC for biological assays and characterization.

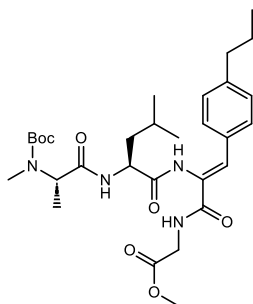
t_{R} = 10.29 min (5 % ACN (0 min) > 100 % ACN (15 min) > 100 % ACN (20 min))

HR-MS m/z 441.2515 (calculated for $\text{C}_{24}\text{H}_{33}\text{N}_4\text{O}_4$: 441.2507)

^1H NMR (400 MHz, CDCl_3) δ 8.09 (s, 1H), 7.72 (s, 1H), 7.32 (d, J = 8.2 Hz, 2H), 7.24 (d, J = 8.2 Hz, 2H), 7.19 (s, 1H), 5.25 – 5.13 (m, 1H), 4.38 (d, J = 5.8 Hz, 1H), 3.64 (d, J = 6.1 Hz, 1H), 3.18 (s, 3H), 2.81 (s, 3H), 2.66 (q, J = 7.6 Hz, 2H), 1.70 (dt, J = 13.1, 6.4 Hz, 1H), 1.54 (d, J = 7.0 Hz, 3H), 1.36 – 1.29 (m, 1H), 1.26 (s, J = 4.0 Hz, 2H), 1.22 (t, J = 7.6 Hz, 3H), 0.57 (dd, J = 49.3, 6.3 Hz, 6H).

^{13}C NMR (101 MHz, CDCl_3) δ 171.77, 171.50, 169.85, 164.79, 147.70, 136.84, 129.92 (2C), 129.34, 128.94 (2C), 122.30, 70.55, 56.88, 49.53, 40.74, 35.23, 30.20, 29.67, 28.78, 22.33, 22.08, 17.23, 5.54.

Methyl ((Z)-2-((S)-2-((S)-2-((tert-butoxycarbonyl)(methyl)amino)propanamido)-4-methylpentan-amido)-3-(4-propylphenyl)acryloyl)glycinate (**11h**)



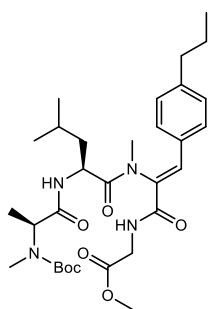
According to general method VI, tetrapeptide **10** (150 mg, 0.27 mmol), TMG (84.9 μL , 0.68 mmol) and *p*-propyl benzaldehyde (79.6 μL , 0.54 mmol) were used. Purification was done by column chromatography on silica gel (*n*-hexane / EtOAc 6:4 – 3:7), giving **11h** (96.0 mg, 0.17 mmol, 62 %) and the corresponding (Z)-isomer (4.5 mg, 0.01 mmol, 2.9 %) as white solids.

HR-MS m/z 573.3297 (calculated for $C_{30}H_{45}N_4O_7$: 573.3294)

1H NMR (400 MHz, $CDCl_3$) δ 7.81 (s, 1H), 7.42 (s, 1H), 7.34 (d, J = 8.0 Hz, 2H), 7.24 (s, 1H), 7.15 (d, J = 8.0 Hz, 2H), 6.69 (s, 1H), 4.52 (q, J = 7.0 Hz, 1H), 4.38 – 4.27 (m, J = 9.5, 5.5 Hz, 1H), 4.11 (d, J = 5.5 Hz, 2H), 3.74 (s, 3H), 2.81 (s, 3H), 2.61 – 2.54 (m, 2H), 1.76 (s, 1H), 1.71 – 1.55 (m, 4H), 1.43 (s, 9H), 1.33 (d, J = 7.1 Hz, 3H), 0.99 – 0.85 (m, 9H).

^{13}C NMR (101 MHz, $CDCl_3$) δ 173.23, 171.29, 170.43, 165.08, 156.58, 144.11, 132.25, 130.94, 129.48 (2C), 128.67 (2C), 126.46, 81.04, 54.46, 52.91, 52.21, 41.69, 39.49, 37.86, 30.91, 28.26 (3C), 24.73, 24.29, 22.98, 21.46, 13.79, 13.21.

Methyl ((Z)-2-((S)-2-((S)-2-((*tert*-butoxycarbonyl)(methyl)amino)propanamido)-*N*,4-dimethylpentanamido)-3-(4-propylphenyl)acryloyl)glycinate (**4h**)



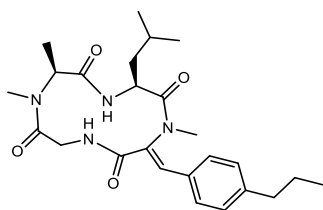
According to general method VII, tetrapeptide **11h** (86 mg, 0.15 mmol), K_2CO_3 (207.4 mg, 1.5 mmol), 18-crown-6 (4.8 mg, 0.02 mmol) and methyl iodide (139.7 μ L, 2.24 mmol) were used, giving **4h** (78.6 mg, 0.13 mmol, 89 %) as a white solid.

HR-MS m/z 587.3432 (calculated for $C_{31}H_{47}N_4O_7$: 587.3445)

1H NMR (400 MHz, $CDCl_3$) δ 8.50 (t, J = 6.0 Hz, 1H), 7.71 (s, 1H), 7.33 (d, J = 8.1 Hz, 2H), 7.22 (d, J = 8.1 Hz, 2H), 6.46 (s, 2H), 4.66 (s, 1H), 4.33 (ddd, J = 11.5, 5.0, 2.3 Hz, 1H), 4.14 (dd, J = 6.0, 4.4 Hz, 2H), 3.71 (s, 3H), 3.21 (s, 3H), 2.69 (s, 3H), 2.64 – 2.57 (m, 2H), 1.72 – 1.46 (m, 4H), 1.45 (s, 9H), 1.26 (d, J = 7.0 Hz, 3H), 0.92 (t, J = 7.3 Hz, 3H), 0.57 (t, J = 5.9 Hz, 6H).

^{13}C NMR (101 MHz, $CDCl_3$) δ 172.19, 171.62, 170.04, 165.19, 156.19, 145.91, 135.83, 131.14, 130.45 (2C), 129.73, 129.41 (2C), 80.68, 51.99, 50.92, 41.82, 38.67, 37.82, 34.35, 29.67, 28.27 (3C), 24.73, 24.20, 23.12, 20.32, 13.64, 13.26.

(3*S*,6*S*)-3-Isobutyl-1,6,7-trimethyl-12-((*Z*)-4-propylbenzylidene)-1,4,7,10-tetraazacyclododecane-2,5,8,11-tetraone (**5h**)



According to general method V, compound **4h** (68.6 mg, 0.12 mmol), lithium hydroxide hydrate (24.4 mg, 0.58 mmol), 4-DMAP (131.3 mg, 1.17 mmol), T3P (50 % w/w in EtOAc, 148.9 μ L,

0.47 mmol) and DCM (24 mL) were used, giving **5h** (14.9 mg, 0.03 mmol, 27 %) as a white solid. A sample was purified by semipreparative RP-HPLC for biological assays and characterization.

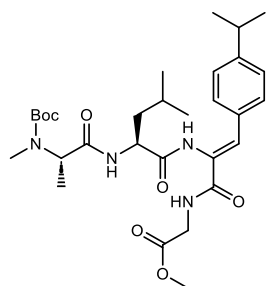
HR-MS m/z 455.2667 (calculated for $C_{25}H_{35}N_4O_4$: 455.2664)

t_R = 11.11 min (5 % ACN (0 min) > 100 % ACN (15 min) > 100 % ACN (20 min))

1H NMR (400 MHz, $CDCl_3$) δ 8.08 (s, 1H), 7.72 (s, 1H), 7.31 (d, J = 8.3 Hz, 2H), 7.22 (d, J = 8.1 Hz, 2H), 5.24 – 5.13 (m, 1H), 4.38 (d, J = 8.4 Hz, 1H), 4.17 (m, 2H), 3.58 (d, J = 15.1 Hz, 1H), 3.18 (s, 3H), 2.81 (s, 3H), 2.59 (t, J = 7.6 Hz, 2H), 1.75 – 1.57 (m, 3H), 1.54 (d, J = 7.0 Hz, 3H), 1.38 – 1.23 (m, 2H), 0.92 (t, J = 7.3 Hz, 3H), 0.63 (d, J = 6.5 Hz, 3H), 0.52 (d, J = 6.5 Hz, 3H).

^{13}C NMR (101 MHz, $CDCl_3$) δ 171.71, 171.54, 169.95, 164.77, 146.19, 136.86, 129.84 (3C), 129.56 (2C), 129.36, 56.86, 49.60, 44.50, 40.76, 37.85, 35.23, 30.20, 24.61, 24.20, 22.32, 22.12, 15.55, 13.67.

Methyl ((Z)-2-((S)-2-((S)-2-((tert-butoxycarbonyl)(methyl)amino)propanamido)-4-methylpentan-amido)-3-(4-isopropylphenyl)acryloyl)glycinate (**11i**)



According to general method VI, tetrapeptide **10** (150 mg, 0.27 mmol), TMG (84.9 μ L, 0.68 mmol) and *p*-isopropylbenzaldehyde (81.9 μ L, 0.54 mmol) were used. Purification was done by column chromatography on silica gel (*n*-hexane / EtOAc 6:4 – 3:7), giving **11i** (88.0 mg, 0.15 mmol, 57 %) and the corresponding (*E*)-isomer (4.5 mg, 0.01 mmol, 2.9 %) as white solids.

(*Z*)-Isomer

HR-MS m/z 573.3298 (calculated for $C_{30}H_{45}N_4O_7$: 573.3294)

1H NMR (500 MHz, $CDCl_3$) δ 7.78 (s, 1H), 7.43 (s, 1H), 7.37 (d, J = 7.9 Hz, 2H), 7.27 (s, 1H), 7.21 (d, J = 8.2 Hz, 2H), 6.71 (s, 1H), 4.53 (q, J = 7.2 Hz, 1H), 4.33 (dd, J = 10.1, 5.5 Hz, 1H), 4.19 – 4.05 (m, 2H), 3.76 (s, 3H), 2.90 (p, J = 6.9 Hz, 1H), 2.81 (s, 3H), 1.82 – 1.59 (m, 3H), 1.43 (s, 9H), 1.34 (d, J = 7.1 Hz, 3H), 1.29 – 1.21 (m, 6H), 0.98 (d, J = 6.1 Hz, 3H), 0.91 (d, J = 6.1 Hz, 3H).

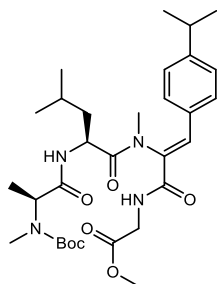
^{13}C NMR (126 MHz, $CDCl_3$) δ 173.30, 171.24, 170.44, 165.02, 156.38, 150.20, 132.16, 131.06, 129.57 (2C), 126.69 (2C), 126.50, 81.11, 54.45, 52.96, 52.25, 41.69, 39.33, 33.99, 30.94, 28.27 (3C), 24.74, 23.76 (2C), 22.98, 21.47, 13.17.

(*E*)-Isomer (side product)

1H NMR (400 MHz, $CDCl_3$) δ 8.49 (s, 1H), 8.00 (s, 1H), 7.29 – 7.17 (m, 4H), 6.64 (s, 1H), 6.23 (t, J = 5.3 Hz, 1H), 4.69 (s, 1H), 4.50 (td, J = 8.9, 5.1 Hz, 1H), 3.91 (d, J = 5.2 Hz, 2H), 3.66 (s, 3H), 2.91 (p, J = 6.9 Hz, 1H), 2.80 (s, 3H), 1.68 – 1.53 (m, 3H), 1.48 (s, 9H), 1.37 (d, J = 7.2 Hz, 3H), 1.25 (d, J = 6.9 Hz, 6H), 0.94 (dd, J = 11.9, 6.2 Hz, 6H).

^{13}C NMR (101 MHz, CDCl_3) δ 171.94, 170.60, 169.05, 164.10, 155.54, 149.10, 131.78, 128.85 (2C), 128.11, 126.98 (2C), 121.71, 80.81, 53.79, 52.56, 52.23, 41.68, 41.08, 33.88, 30.07, 28.34 (3C), 24.75, 23.81 (2C), 23.04, 21.54, 13.56.

Methyl ((Z)-2-((S)-2-((S)-2-((*tert*-butoxycarbonyl)(methyl)amino)propanamido)-*N*,4-dimethylpentanamido)-3-(4-isopropylphenyl)acryloyl)glycinate (**4i**)



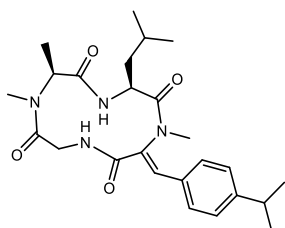
According to general method VII, tetrapeptide **11i** (80 mg, 0.14 mmol), K_2CO_3 (192 mg, 1.39 mmol), 18-crown-6 (4.8 mg, 0.02 mmol) and methyl iodide (130 μL , 2.09 mmol) were used, giving **4i** (81.0 mg, 0.14 mmol, 99 %) as a white solid.

HR-MS m/z 587.3444 (calculated for $\text{C}_{31}\text{H}_{47}\text{N}_4\text{O}_7$: 587.3450)

^1H NMR (500 MHz, CDCl_3) δ 8.49 (t, J = 6.1 Hz, 1H), 7.71 (s, 1H), 7.35 (d, J = 8.4 Hz, 2H), 7.28 (d, J = 8.4 Hz, 2H), 6.48 (s, 1H), 4.66 (s, 1H), 4.36 – 4.29 (m, 1H), 4.16 – 4.08 (m, 2H), 3.72 (s, 3H), 3.22 (s, 3H), 2.92 (dt, J = 13.5, 6.8 Hz, 1H), 2.69 (s, 3H), 1.55 (d, J = 75.1 Hz, 3H), 1.45 (s, 9H), 1.25 (dtd, J = 12.8, 6.4, 4.4 Hz, 9H), 0.56 (t, J = 6.6 Hz, 6H).

^{13}C NMR (126 MHz, CDCl_3) δ 172.18, 171.63, 170.06, 165.21, 156.55, 152.04, 135.78, 131.21, 130.56 (2C), 129.86, 127.37 (2C), 80.67, 52.52, 52.01, 50.85, 41.83, 38.66, 34.42, 34.07, 29.68, 28.28 (3C), 24.70, 23.69, 23.65, 23.11, 20.31, 13.26.

(3*S*,6*S*)-3-Isobutyl-12-((Z)-4-isopropylbenzylidene)-1,6,7-trimethyl-1,4,7,10-tetraazacyclodecane-2,5,8,11-tetraone (**5i**)



According to general method V, compound **4i** (75 mg, 0.13 mmol), lithium hydroxide hydrate (29.4 mg, 0.7 mmol), 4-DMAP (116.7 mg, 1.04 mmol), T3P (50 % w/w in EtOAc, 124.0 μL , 0.73 mmol) and DCM (26 mL) were used, giving **5i** (7.2 mg, 0.02 mmol, 12 %) as a white solid. A sample was purified by semipreparative RP-HPLC for biological assays and characterization.

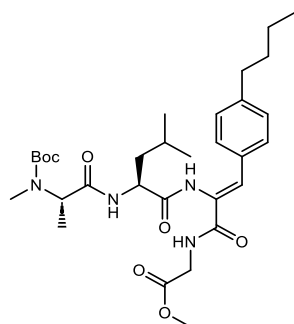
HR-MS m/z 455.2667 (calculated for $\text{C}_{25}\text{H}_{35}\text{N}_4\text{O}_4$: 455.2664)

t_R = 10.97 min (5 % ACN (0 min) > 100 % ACN (15 min) > 100 % ACN (20 min))

^1H NMR (500 MHz, CDCl_3) δ 7.99 (s, 1H), 7.73 (s, 1H), 7.33 – 7.21 (m, 5H), 5.18 (t, J = 13.1 Hz, 1H), 4.36 (s, 1H), 3.58 (d, J = 15.2 Hz, 1H), 3.18 (s, 3H), 2.91 (p, J = 7.0 Hz, 1H), 2.81 (s, 3H), 1.75 – 1.66 (m, 2H), 1.53 (d, J = 7.0 Hz, 3H), 1.28 (d, J = 26.2 Hz, 3H), 1.24 (s, 3H), 1.23 (s, 3H), 0.63 (d, J = 6.4 Hz, 3H), 0.50 (d, J = 6.6 Hz, 3H).

^{13}C NMR (126 MHz, CDCl_3) δ 171.56, 170.28, 164.72, 152.30, 136.87, 129.97 (3C), 129.49, 127.54 (2C), 56.80, 49.63, 44.47, 40.73, 35.29, 34.10, 30.18, 29.69, 24.64, 23.64, 22.38, 22.05, 15.55.

Methyl ((Z)-2-((S)-2-((S)-2-((*tert*-butoxycarbonyl)(methyl)amino)propanamido)-4-methylpentan-amido)-3-(4-butylphenyl)acryloyl)glycinate (**11j**)



According to general method VI, tetrapeptide **10** (150 mg, 0.27 mmol), TMG (84.9 μL , 0.68 mmol) and *p*-butyl benzaldehyde (90.5 μL , 0.54 mmol) were used. Purification was done by column chromatography on silica gel (*n*-hexane / EtOAc 6:4 – 3:7), giving **11j** (96.0 mg, 0.16 mmol, 60 %) and the corresponding (*E*)-isomer (6 mg, 0.01 mmol, 3.7 %) as white solids.

HR-MS m/z 587.3445 (calculated for $\text{C}_{31}\text{H}_{47}\text{N}_4\text{O}_7$: 587.3450)

(*Z*)-Isomer

^1H NMR (500 MHz, $(\text{CD}_3)_2\text{SO}$) δ 9.59 (s, 1H), 8.22 (t, J = 5.9 Hz, 1H), 8.14 – 8.01 (m, 1H), 7.48 (d, J = 8.0 Hz, 2H), 7.22 (s, 1H), 7.18 (d, J = 8.0 Hz, 2H), 4.63 – 4.35 (m, 1H), 4.31 (s, 1H), 3.99 – 3.81 (m, 2H), 3.64 (s, 3H), 3.32 (s, 3H), 2.75 (s, 2H), 2.58 (t, J = 7.6 Hz, 2H), 1.64 (s, 1H), 1.59 – 1.50 (m, 4H), 1.38 (s, 9H), 1.34 – 1.26 (m, 3H), 1.23 (d, J = 6.8 Hz, 3H), 0.93 (d, J = 6.4 Hz, 3H), 0.89 (t, J = 7.4 Hz, 3H).

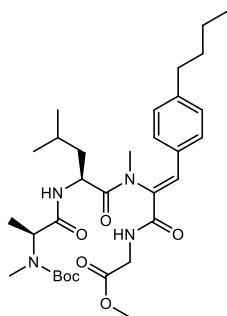
^{13}C NMR (126 MHz, $(\text{CD}_3)_2\text{SO}$) δ 172.49, 172.00, 170.11, 164.98, 154.96, 143.43, 131.15, 130.14, 129.63 (2C), 128.30 (2C), 127.82, 79.01, 53.08, 51.86, 51.67, 41.21, 38.22, 34.56, 32.90, 30.19, 27.97 (3C), 24.03, 22.92, 21.64, 21.53, 14.28, 13.72.

(*E*)-Isomer (side product)

^1H NMR (500 MHz, CDCl_3) δ 8.49 (s, 1H), 8.02 (s, 1H), 7.23 (d, J = 7.9 Hz, 2H), 7.17 (d, J = 8.2 Hz, 2H), 6.65 (s, 1H), 6.22 (t, J = 5.2 Hz, 1H), 4.70 (s, 1H), 4.55 – 4.46 (m, 1H), 3.91 (d, J = 5.3 Hz, 2H), 3.66 (s, 3H), 2.80 (s, 3H), 2.61 (t, J = 7.6 Hz, 2H), 1.78 – 1.54 (m, 5H), 1.48 (s, 9H), 1.43 (s, 3H), 1.40 – 1.24 (m, 6H), 0.94 (dt, J = 14.6, 9.5 Hz, 5H).

^{13}C NMR (126 MHz, CDCl_3) δ 171.89, 170.60, 170.40, 169.06, 164.09, 156.55, 131.64, 129.47, 128.97 (2C), 128.77 (2C), 121.69, 80.82, 52.95, 52.56, 52.24, 41.66, 40.68, 35.38, 33.41, 30.04, 28.34 (3C), 24.75, 23.04, 22.28, 21.52, 13.94, 13.75.

Methyl ((Z)-2-((S)-2-((S)-2-((*tert*-butoxycarbonyl)(methyl)amino)propanamido)-*N*,4-dimethylpentanamido)-3-(4-butylphenyl)acryloyl)glycinate (**4j**)



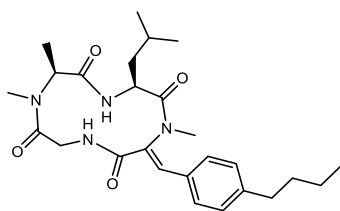
According to general method VII, tetrapeptide **11j** (90 mg, 0.15 mmol), K₂CO₃ (207.3 mg, 1.5 mmol), 18-crown-6 (4.8 mg, 0.02 mmol) and methyl iodide (142 μ L, 2.29 mmol) were used, giving **4j** (87.0 mg, 0.14 mmol, 96 %) as a white solid.

HR-MS *m/z* 601.3610 (calculated for C₃₂H₄₉N₄O₇: 601.3607)

¹H NMR (400 MHz, CDCl₃) δ 8.50 (s, 1H), 7.71 (s, 1H), 7.33 (d, *J* = 8.2 Hz, 2H), 7.22 (d, *J* = 8.1 Hz, 2H), 6.67 – 6.10 (m, 2H), 4.66 (s, 1H), 4.37 – 4.28 (m, 1H), 4.18 – 4.09 (m, 2H), 3.71 (s, 3H), 3.21 (s, 4H), 2.69 (s, 3H), 2.63 (t, *J* = 7.6 Hz, 2H), 1.67 – 1.53 (m, 3H), 1.45 (s, 9H), 1.38 – 1.22 (m, 5H), 0.91 (t, *J* = 7.3 Hz, 3H), 0.57 (dd, *J* = 6.7, 4.9 Hz, 6H).

¹³C NMR (101 MHz, CDCl₃) δ 172.20, 171.61, 170.04, 165.20, 156.22, 146.16, 135.83, 131.13, 130.47 (2C), 129.69, 129.37 (2C), 80.68, 53.26, 51.99, 50.92, 41.83, 38.68, 35.48, 34.35, 33.23, 29.69, 28.27 (3C), 24.73, 23.11, 22.18, 20.32, 13.85, 13.26.

(3*S*,6*S*)-12-((*Z*)-4-Butylbenzylidene)-3-isobutyl-1,6,7-trimethyl-1,4,7,10-tetraazacyclododecane-2,5,8,11-tetraone (**5j**)



According to general method V, compound **4j** (78 mg, 0.13 mmol), lithium hydroxide hydrate (27.1 mg, 0.65 mmol), 4-DMAP (144.7 mg, 1.29 mmol), T3P (50 % w/w in EtOAc, 153.7 μ L, 0.52 mmol) and DCM (26 mL) were used, giving **5j** (15.8 mg, 0.034 mmol, 27 %) as a white solid. A sample was purified by semipreparative RP-HPLC for biological assays and characterization.

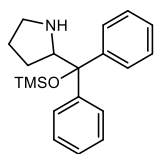
HR-MS *m/z* 469.2810 (calculated for C₂₆H₃₇N₄O₄: 469.2820)

*t*_R = 11.95 min (5 % ACN (0 min) > 100 % ACN (15 min) > 100 % ACN (20 min))

¹H NMR (400 MHz, CDCl₃) δ 8.10 (s, 1H), 7.71 (s, 1H), 7.31 (d, *J* = 8.3 Hz, 2H), 7.22 (d, *J* = 8.1 Hz, 2H), 5.19 (t, *J* = 12.9 Hz, 1H), 4.38 (d, *J* = 7.5 Hz, 1H), 4.17 (s, 1H), 3.57 (d, *J* = 15.1 Hz, 1H), 3.18 (s, 3H), 2.81 (s, 3H), 2.62 (t, *J* = 7.7 Hz, 2H), 1.69 (dt, *J* = 13.8, 6.8 Hz, 1H), 1.63 – 1.51 (m, 5H), 1.31 (qd, *J* = 13.2, 11.4, 5.6 Hz, 4H), 0.92 (t, *J* = 7.3 Hz, 3H), 0.63 (d, *J* = 6.5 Hz, 3H), 0.52 (d, *J* = 6.5 Hz, 3H).

^{13}C NMR (101 MHz, CDCl_3) δ 171.72, 171.53, 169.96, 164.79, 146.42, 136.87, 129.85 (3C), 129.51 (2C), 129.31, 56.90, 49.59, 44.51, 40.79, 35.50, 35.23, 33.22, 30.21, 24.61, 22.32, 22.20, 22.11, 15.55, 13.85.

2-(Diphenyl(trimethylsilyl)oxy)methylpyrrolidine (**12**)



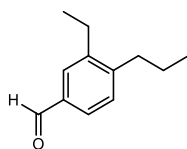
To a stirred solution of (*S*)-diphenylprolinol (1 g, 3.95 mmol) in DCM (10 mL) at 0 °C was added imidazole (0.81 g, 11.9 mmol) and subsequently trimethylsilyl chloride (1.25 mL, 9.9 mmol). The mixture was stirred overnight at room temperature, after which MTBE (100 mL) was added. After filtration, the filtrate was washed with water (25 mL) and brine (2x 25 mL), dried over Na_2SO_4 , filtered, and evaporated to dryness, yielding **12** (1.2 g, 3.68 mmol, 93 %) as a light orange liquid.

HR-MS m/z 326.1935 (calculated for $\text{C}_{20}\text{H}_{28}\text{NOSi}$: 326.0953)

^1H NMR (500 MHz, CDCl_3) δ 7.45 (dt, J = 6.5, 1.4 Hz, 2H), 7.35 (dt, J = 6.2, 1.4 Hz, 2H), 7.31 – 7.20 (m, 5H), 7.24 – 7.17 (m, 1H), 4.05 (t, J = 7.4 Hz, 1H), 2.90 – 2.82 (m, 1H), 2.82 – 2.74 (m, 1H), 1.94 (s, 1H), 1.64 – 1.52 (m, 3H), 1.42 – 1.32 (m, 1H), -0.10 (s, 9H).

^{13}C NMR (126 MHz, CDCl_3) δ 146.67, 145.66, 128.40 (2C), 127.61 (2C), 127.55 (2C), 127.54 (2C), 126.92, 126.74, 83.12, 65.40, 47.12, 27.47, 25.01, 2.15.

3-Ethyl-4-propylbenzaldehyde (**13**)

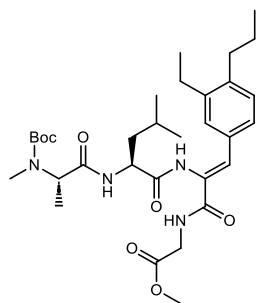


To a solution of *trans*-hex-2-enal (0.28 mL, 2.4 mmol) in chloroform (3 mL), *p*-nitrophenol (83.5 mg, 0.6 mmol) and catalyst **12** (78 mg, 0.24 mmol) was added. The mixture was stirred overnight at room temperature until no starting material was detectable (reaction followed by TLC). The solvent was removed under reduced pressure and the crude product purified by column chromatography (*n*-hexane / EtOAc 8:2 – 2:8), giving **13** (198.8 mg, 1.12 mmol, 94 %) as a colourless oil.

^1H NMR (400 MHz, CDCl_3) δ 9.96 (s, 1H), 7.69 (d, J = 1.8 Hz, 1H), 7.63 (dd, J = 7.8, 1.8 Hz, 1H), 7.30 (d, J = 7.8 Hz, 1H), 2.77 – 2.62 (m, 4H), 1.71 – 1.57 (m, 2H), 1.43 – 1.24 (m, 3H), 1.00 (t, J = 7.3 Hz, 3H).

^{13}C NMR (101 MHz, CDCl_3) δ 192.36, 147.90, 142.79, 134.63, 129.76, 129.47, 127.49, 34.97, 25.31, 23.90, 14.97, 14.15.

Methyl ((Z)-2-((S)-2-((S)-2-((tert-butoxycarbonyl)(methyl)amino)propanamido)-4-methylpentan-amido)-3-(3-ethyl-4-propylphenyl)acryloyl)glycinate (**11k**)



According to general method VI, tetrapeptide **10** (150 mg, 0.27 mmol), TMG (84.9 μ L, 0.68 mmol) and aldehyde **13** (95.2 mg, 0.54 mmol) were used. Purification was done by column chromatography on silica gel (*n*-hexane / EtOAc 8:2 – 3:7), giving **11k** (117 mg, 0.19 mmol, 72 %) and the corresponding (*E*)-isomer (3.0 mg, 0.005 mmol, 1.8 %) as white solids.

HR-MS *m/z* 601.3613 (calculated for C₃₂H₄₉N₄O₇: 601.3607)

(*Z*)-Isomer

¹H NMR (400 MHz, CDCl₃) δ 7.75 (s, 1H), 7.40 (s, 1H), 7.22 (d, *J* = 5.5 Hz, 3H), 7.11 (d, *J* = 8.4 Hz, 1H), 6.69 (s, 1H), 4.52 (q, *J* = 7.1 Hz, 1H), 4.33 (dd, *J* = 9.7, 5.2 Hz, 1H), 4.11 (dd, *J* = 4.9, 2.7 Hz, 2H), 3.74 (s, 3H), 2.82 – 2.77 (m, 3H), 2.61 (dt, *J* = 15.9, 7.7 Hz, 4H), 1.78 (ddd, *J* = 13.7, 9.7, 4.0 Hz, 1H), 1.67 (dd, *J* = 11.3, 5.6 Hz, 2H), 1.59 (dt, *J* = 14.9, 7.4 Hz, 2H), 1.43 (s, 9H), 1.33 (d, *J* = 7.1 Hz, 3H), 1.20 (t, *J* = 7.6 Hz, 3H), 1.01 – 0.94 (m, 6H), 0.91 (d, *J* = 6.1 Hz, 3H).

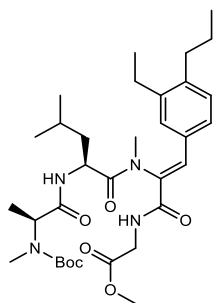
¹³C NMR (101 MHz, CDCl₃) δ 173.21, 171.31, 170.44, 165.09, 156.30, 142.13, 141.79, 132.47, 131.13, 129.96, 129.33, 126.71, 126.22, 81.00, 54.41, 52.93, 52.21, 41.68, 39.51, 34.58, 30.92, 28.25 (3C), 25.48, 24.73, 24.05, 23.05, 21.34, 15.36, 14.19, 13.17.

(*E*)-Isomer (side product)

¹H NMR (500 MHz, CDCl₃) δ 8.50 (s, 1H), 8.04 (s, 1H), 7.16 – 7.06 (m, 3H), 6.65 (s, 1H), 6.27 (t, *J* = 5.3 Hz, 1H), 4.71 (s, 1H), 4.54 – 4.46 (m, 1H), 3.90 (d, *J* = 5.3 Hz, 2H), 3.65 (s, 3H), 2.80 (s, 3H), 2.67 – 2.55 (m, 4H), 1.80 – 1.71 (m, 1H), 1.67 – 1.55 (m, 4H), 1.48 (s, 9H), 1.37 (d, *J* = 7.1 Hz, 3H), 1.18 (t, *J* = 7.6 Hz, 3H), 1.01 – 0.90 (m, 9H).

¹³C NMR (126 MHz, CDCl₃) δ 171.87, 170.56, 169.00, 164.14, 156.48, 142.62, 140.49, 131.92, 129.69, 128.83, 127.83, 126.09, 122.00, 80.76, 53.63, 52.58, 52.22, 41.65, 40.82, 34.47, 30.02, 28.34 (3C), 25.36, 24.75, 24.05, 23.04, 21.58, 15.27, 14.13, 13.47.

Methyl ((Z)-2-((S)-2-((S)-2-((*tert*-butoxycarbonyl)(methyl)amino)propanamido)-*N*,4-dimethylpentanamido)-3-(3-ethyl-4-propylphenyl)acryloyl)glycinate (**4k**)



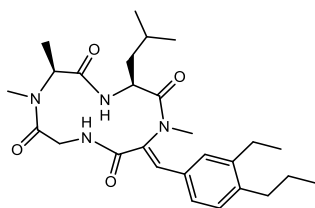
According to general method VII, tetrapeptide **11k** (107 mg, 0.18 mmol), K₂CO₃ (246 mg, 1.78 mmol), 18-crown-6 (4.8 mg, 0.02 mmol) and methyl iodide (166.2 μ L, 2.67 mmol) were used, giving **4k** (100.0 mg, 0.16 mmol, 91 %) as a white solid.

HR-MS m/z 615.3767 (calculated for C₃₃H₅₁N₄O₇: 615.3763)

¹H NMR (500 MHz, CDCl₃) δ 8.46 (d, J = 6.1 Hz, 1H), 7.69 (s, 1H), 7.23 (s, 1H), 7.18 (d, J = 1.2 Hz, 2H), 6.47 (s, 1H), 4.66 (s, 1H), 4.37 – 4.30 (m, 1H), 4.22 – 4.07 (m, 2H), 3.71 (s, 3H), 3.21 (s, 3H), 2.69 (s, 3H), 2.68 – 2.54 (m, 4H), 1.68 – 1.47 (m, 5H), 1.45 (s, 9H), 1.26 (d, J = 7.2 Hz, 3H), 1.20 (t, J = 7.6 Hz, 3H), 0.97 (t, J = 7.4 Hz, 3H), 0.56 (t, J = 6.5 Hz, 6H).

¹³C NMR (126 MHz, CDCl₃) δ 172.14, 171.63, 170.08, 165.26, 156.27, 143.57, 142.76, 136.06, 130.97, 130.59, 130.07, 129.93, 127.78, 80.63, 52.60, 51.99, 50.86, 41.81, 38.68, 34.61, 34.39, 29.68, 28.27 (3C), 25.34, 24.70, 23.93, 23.13, 20.29, 15.13, 14.06, 13.28.

(3*S*,6*S*)-12-((*Z*)-3-Ethyl-4-propylbenzylidene)-3-isobutyl-1,6,7-trimethyl-1,4,7,10-tetraazacyclodecane-2,5,8,11-tetraone (**5k**)



According to general method V, compound **4k** (90 mg, 0.15 mmol), lithium hydroxide hydrate (30.6 mg, 0.73 mmol), 4-DMAP (163.8 mg, 1.46 mmol), T3P (50 % w/w in EtOAc, 217.5 μ L, 0.73 mmol) and DCM (30 mL) were used, giving **5k** (19 mg, 0.04 mmol, 27 %) as a white solid. A sample was purified by semipreparative RP-HPLC for biological assays and characterization.

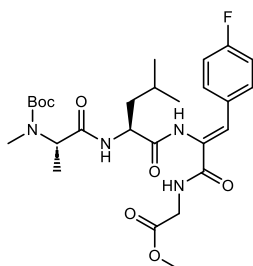
HR-MS m/z 483.2977 (calculated for C₂₇H₃₉N₄O₄: 483.2977)

t_R = 12.34 min (5 % ACN (0 min) > 100 % ACN (15 min) > 100 % ACN (20 min))

¹H NMR (400 MHz, CDCl₃) δ 7.70 (s, 1H), 7.25 (s, 1H), 7.22 (d, J = 1.7 Hz, 1H), 7.22 – 7.12 (m, 2H), 5.19 (t, J = 12.9 Hz, 1H), 4.38 (d, J = 7.5 Hz, 1H), 4.28 – 4.05 (m, 1H), 3.57 (d, J = 15.1 Hz, 1H), 3.19 (s, 3H), 2.81 (s, 3H), 2.69 – 2.55 (m, 4H), 1.68 (td, J = 16.1, 14.8, 8.0 Hz, 1H), 1.64 – 1.57 (m, 1H), 1.61 – 1.54 (m, 1H), 1.54 (d, J = 7.0 Hz, 3H), 1.39 – 1.29 (m, 2H), 1.21 (t, J = 7.5 Hz, 4H), 0.97 (t, J = 7.3 Hz, 3H), 0.63 (d, J = 6.5 Hz, 3H), 0.51 (d, J = 6.5 Hz, 3H).

^{13}C NMR (101 MHz, CDCl_3) δ 171.68, 171.58, 170.10, 164.83, 143.89, 142.97, 137.08, 130.22, 129.99, 129.77, 129.59, 127.23, 56.78, 49.62, 44.48, 40.89, 35.23, 34.63, 30.21, 25.40, 24.62, 23.93, 22.37, 22.08, 15.57, 15.09, 14.09.

Methyl ((Z)-2-((S)-2-((S)-2-((tert-butoxycarbonyl)(methyl)amino)propanamido)-4-methylpentan-amido)-3-(4-fluorophenyl)acryloyl)glycinate (**11I**)



According to general method VI, tetrapeptide **10** (150 mg, 0.27 mmol), TMG (84.9 μL , 0.68 mmol) and *p*-fluorobenzaldehyde (56.8 μL , 0.54 mmol) were used. Purification was done by column chromatography on silica gel (*n*-hexane / EtOAc 6:4 – 3:7), giving **11I** (122 mg, 0.22 mmol, 82 %) and the corresponding (*E*)-isomer (7 mg, 0.01 mmol, 4.7 %) as white solids.

(*Z*)-Isomer

HR-MS m/z 549.2729 (calculated for $\text{C}_{27}\text{H}_{38}\text{FN}_4\text{O}_7$: 549.2730)

^1H NMR (400 MHz, CDCl_3) δ 8.03 (s, 1H), 7.46 (d, J = 8.4 Hz, 2H), 7.35 (s, 1H), 7.31 (d, J = 5.1 Hz, 1H), 7.30 – 7.26 (m, 2H), 6.67 (s, 1H), 4.46 (q, J = 7.1 Hz, 1H), 4.33 – 4.25 (m, 1H), 4.10 (d, J = 5.3 Hz, 2H), 3.74 (s, 3H), 2.81 (s, 3H), 1.78 – 1.69 (m, 1H), 1.68 – 1.54 (m, 2H), 1.41 (s, 9H), 1.34 (t, J = 8.2 Hz, 3H), 0.96 (d, J = 6.2 Hz, 3H), 0.90 (d, J = 6.1 Hz, 3H).

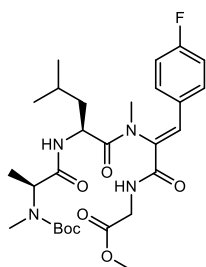
^{13}C NMR (101 MHz, CDCl_3) δ 173.36, 171.27, 170.36, 164.82, 156.23, 132.58, 131.69 (2C), 130.93, 130.86 (2C), 127.81, 123.19, 81.12, 54.88, 52.97, 52.26, 41.67, 39.33, 31.21, 28.24 (3C), 24.75, 22.96, 21.38, 13.22.

(*E*)-Isomer (side product)

^1H NMR (400 MHz, CDCl_3) δ 8.49 (s, 1H), 7.79 (s, 1H), 7.48 (d, J = 8.4 Hz, 2H), 7.20 (d, J = 8.3 Hz, 2H), 6.65 (s, 1H), 6.17 (s, 1H), 4.67 (s, 1H), 4.52 – 4.43 (m, 1H), 3.95 (d, J = 5.3 Hz, 2H), 3.69 (s, 3H), 2.80 (s, J = 8.0 Hz, 3H), 1.74 (dt, J = 15.2, 5.0 Hz, 1H), 1.65 – 1.54 (m, 2H), 1.48 (s, J = 5.1 Hz, 9H), 1.36 (t, J = 7.5 Hz, 3H), 0.93 (dd, J = 14.3, 6.2 Hz, 6H).

^{13}C NMR (101 MHz, CDCl_3) δ 172.18, 170.77, 169.02, 163.99, 156.50, 133.35, 131.97 (2C), 130.55 (2C), 129.36, 122.27, 119.83, 80.89, 53.74, 52.53, 52.41, 41.64, 40.40, 30.19, 28.32 (3C), 24.73, 23.03, 21.51, 13.45.

Methyl ((Z)-2-((S)-2-((S)-2-((*tert*-butoxycarbonyl)(methyl)amino)propanamido)-*N*,4-dimethylpentanamido)-3-(4-fluorophenyl)acryloyl)glycinate (**4I**)



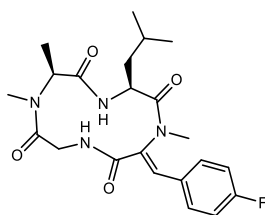
According to general method VII, tetrapeptide **11I** (112.0 mg, 0.20 mmol), K₂CO₃ (280.0 mg, 2.03 mmol), 18-crown-6 (4.8 mg, 0.02 mmol) and methyl iodide (190.0 μ L, 3.05 mmol) were used, giving **4I** (84 mg, 0.15 mmol, 73 %) as a white solid.

HR-MS *m/z* 563.2880 (calculated for C₂₈H₄₀FN₄O₇: 563.2887)

¹H NMR (400 MHz, CDCl₃) δ 8.56 (t, *J* = 5.6 Hz, 1H), 7.67 (s, 1H), 7.56 (d, *J* = 8.5 Hz, 2H), 7.28 (d, *J* = 8.5 Hz, 2H), 6.63 (s, 1H), 4.66 (s, 1H), 4.31 (dd, *J* = 11.2, 2.5 Hz, 1H), 4.13 (dt, *J* = 11.1, 6.1 Hz, 2H), 3.72 (s, *J* = 5.1 Hz, 3H), 3.18 (s, *J* = 6.1 Hz, 3H), 2.70 (s, 3H), 1.66 (s, 2H), 1.47 (s, *J* = 4.5 Hz, 1H), 1.45 (s, *J* = 15.0 Hz, 9H), 1.26 (d, *J* = 7.1 Hz, 3H), 0.61 (t, *J* = 6.9 Hz, 6H).

¹³C NMR (126 MHz, CDCl₃) δ 172.33, 171.50, 169.91, 164.76, 156.27, 134.37, 132.65, 132.60 (2C), 131.70 (2C), 131.12, 125.08, 80.45, 60.38, 52.04, 51.03, 41.84, 38.85, 34.25, 29.69, 28.27 (3C), 24.79, 23.20, 20.44, 13.20.

(3*S*,6*S*)-12-((*Z*)-4-Fluorobenzylidene)-3-isobutyl-1,6,7-trimethyl-1,4,7,10-tetraazacyclododecane-2,5,8,11-tetraone (**5I**)



According to general method V, compound **4I** (75 mg, 0.13 mmol), lithium hydroxide hydrate (28.0 mg, 0.7 mmol), 4-DMAP (89.5 mg, 0.80 mmol), T3P (50 % w/w in EtOAc, 158.5 μ L, 0.53 mmol) and DCM (27 mL) were used, giving **5I** (17 mg, 0.04 mmol, 30 %) as a white solid. A sample was purified by semipreparative RP-HPLC for biological assays and characterization.

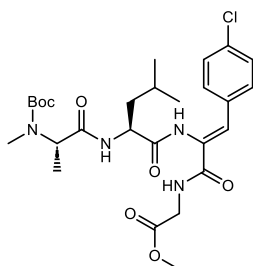
HR-MS *m/z* 431.2105 (calculated for C₂₂H₂₈FN₄O₄: 431.2100)

*t*_R = 9.15 min (5 % ACN (0 min) > 100 % ACN (15 min) > 100 % ACN (20 min))

¹H NMR (500 MHz, CDCl₃) δ 8.02 (s, 1H), 7.70 (s, 1H), 7.56 (d, *J* = 8.4 Hz, 2H), 7.25 (d, *J* = 8.3 Hz, 2H), 7.05 (s, 1H), 5.24 – 5.12 (m, 1H), 4.34 (s, 1H), 3.59 (d, *J* = 15.2 Hz, 1H), 3.16 (s, 3H), 2.80 (s, 3H), 1.53 (d, *J* = 7.1 Hz, 3H), 1.33 – 1.28 (m, 2H), 1.26 (s, 2H), 0.67 (d, 6.5 Hz, 3H), 0.56 (d, *J* = 5.6 Hz, 3H).

^{13}C NMR (126 MHz, CDCl_3) δ 172.83, 171.72, 171.35, 169.85, 164.46, 135.60, 132.70 (2C), 131.04 (2C), 130.88, 125.30, 56.93, 49.20, 44.48, 40.73, 30.18, 29.69, 24.66, 22.28, 22.11, 15.54.

Methyl ((Z)-2-((S)-2-((S)-2-((*tert*-butoxycarbonyl)(methyl)amino)propanamido)-4-methylpentan-amido)-3-(4-chlorophenyl)acryloyl)glycinate (**11m**)



According to general method VI, tetrapeptide **10** (150 mg, 0.27 mmol), TMG (84.9 μL , 0.68 mmol) and *p*-chlorobenzaldehyde (75.9 μL , 0.54 mmol) were used. Purification was done by column chromatography on silica gel (*n*-hexane / EtOAc 6:4 – 3:7), giving **11m** (113 mg, 0.20 mmol, 74 %) and the corresponding (*E*)-isomer (12 mg, 0.02 mmol, 7.8 %) as white solids.

(*Z*)-Isomer

HR-MS m/z 565.2439 (calculated for $\text{C}_{27}\text{H}_{38}\text{ClN}_4\text{O}_7$: 565.2435)

^1H NMR (600 MHz, CDCl_3) δ 8.49 (s, 1H), 7.83 (s, 1H), 7.33 (d, J = 8.4 Hz, 2H), 7.27 (d, J = 8.1 Hz, 2H), 6.66 (s, 1H), 6.16 (s, 1H), 4.69 (d, J = 6.9 Hz, 1H), 4.52 – 4.44 (m, 1H), 3.95 (dd, J = 5.2, 1.5 Hz, 2H), 3.69 (d, J = 5.4 Hz, 3H), 2.80 (s, 3H), 1.75 (ddd, J = 13.6, 8.4, 4.9 Hz, 1H), 1.63 – 1.56 (m, 2H), 1.47 (d, J = 7.5 Hz, 9H), 1.37 (d, J = 7.1 Hz, 3H), 0.95 (d, J = 6.2 Hz, 3H), 0.92 (d, J = 6.2 Hz, 3H).

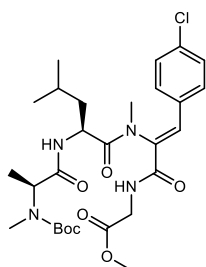
^{13}C NMR (151 MHz, CDCl_3) δ 172.20, 170.73, 169.00, 163.95, 156.56, 134.08, 132.86, 130.67, 130.27 (2C), 129.02 (2C), 119.83, 80.83, 53.61, 52.52, 52.39, 41.63, 40.31, 30.16, 28.32 (3C), 24.72, 23.03, 21.40, 13.28.

(*E*)-Isomer (side product)

^1H NMR (600 MHz, CDCl_3) δ 8.07 (s, 1H), 7.38 (s, 1H), 7.35 (d, J = 8.5 Hz, 2H), 7.33 (s, 1H), 7.30 (d, J = 8.5 Hz, 2H), 6.69 (s, 1H), 4.47 (q, J = 7.1 Hz, 1H), 4.33 – 4.27 (m, 1H), 4.10 (d, J = 3.4 Hz, 2H), 3.75 (s, 3H), 2.81 (s, 3H), 1.79 – 1.71 (m, 1H), 1.67 – 1.57 (m, 2H), 1.42 (s, 9H), 1.33 (d, J = 7.1 Hz, 3H), 0.97 (d, J = 6.2 Hz, 3H), 0.95 (d, J = 6.1 Hz, 3H).

^{13}C NMR (126 MHz, CDCl_3) δ 173.37, 171.38, 170.47, 164.91, 156.55, 134.89, 132.13, 131.01, 130.68 (2C), 128.73 (2C), 127.67, 81.11, 54.81, 52.98, 52.27, 41.66, 39.34, 31.17, 28.24 (3C), 24.75, 22.96, 21.39, 13.24.

Methyl ((Z)-2-((S)-2-((S)-2-((*tert*-butoxycarbonyl)(methyl)amino)propanamido)-*N*,4-dimethylpentanamido)-3-(4-chlorophenyl)acryloyl)glycinate (**4m**)



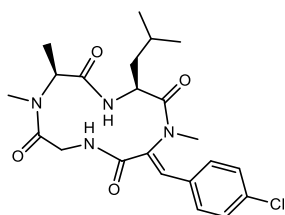
According to general method VII, tetrapeptide **11m** (100.0 mg, 0.18 mmol), K₂CO₃ (242.0 mg, 1.75 mmol), 18-crown-6 (4.8 mg, 0.02 mmol) and methyl iodide (164.4 μ L, 2.64 mmol) were used, giving **4m** (91 mg, 0.16 mmol, 90 %) as a white solid.

HR-MS *m/z* 579.2593 (calculated for C₂₈H₄₀ClN₄O₇: 579.2591)

¹H NMR (500 MHz, CDCl₃) δ 8.56 (t, *J* = 6.0 Hz, 1H), 7.41 (d, *J* = 8.7 Hz, 2H), 7.36 (d, *J* = 8.8 Hz, 2H), 7.34 – 7.28 (m, 1H), 6.56 (s, 1H), 4.67 (s, 1H), 4.32 (ddd, *J* = 11.4, 5.1, 2.4 Hz, 1H), 4.13 (qd, *J* = 17.5, 6.0 Hz, 2H), 3.72 (s, 3H), 3.19 (s, 3H), 2.70 (s, 3H), 1.69 (s, 3H), 1.45 (s, 9H), 1.27 (d, *J* = 7.2 Hz, 3H), 0.64 – 0.58 (m, 6H).

¹³C NMR (126 MHz, CDCl₃) δ 172.34, 171.56, 169.93, 164.76, 162.58, 156.50, 136.68, 134.32, 132.48, 131.55 (2C), 130.70, 129.61 (2C), 80.75, 52.57, 52.04, 51.02, 41.84, 38.84, 34.26, 29.67, 28.27 (3C), 23.19, 20.43, 13.22.

(3*S*,6*S*)-12-((*Z*)-4-Chlorobenzylidene)-3-isobutyl-1,6,7-trimethyl-1,4,7,10-tetraazacyclododecane-2,5,8,11-tetraone (**5m**)



According to general method V, compound **4m** (80.0 mg, 0.14 mmol), lithium hydroxide hydrate (29 mg, 0.7 mmol), 4-DMAP (86.2 mg, 0.77 mmol), T3P (50 % w/w in EtOAc, 153 μ L, 0.51 mmol) and DCM (28 mL) were used, giving **5m** (25.6 mg, 0.06 mmol, 44 %) as a white solid. A sample was purified by semipreparative RP-HPLC for biological assays and characterization.

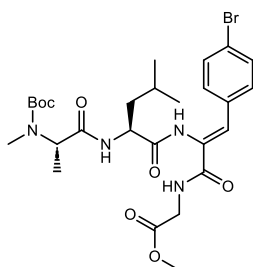
HR-MS *m/z* 447.1810 (calculated for C₂₂H₂₈ClN₄O₄: 447.1805)

*t*_R = 9.89 min (5 % ACN (0 min) > 100 % ACN (15 min) > 100 % ACN (20 min))

¹H NMR (400 MHz, CDCl₃) δ 8.03 (s, 1H), 7.71 (s, 1H), 7.44 – 7.28 (m, 4H), 7.07 (s, 1H), 5.29 – 5.09 (m, 1H), 4.39 – 4.02 (m, 2H), 3.70 – 3.47 (m, 1H), 3.17 (s, 3H), 2.78 (s, 3H), 1.53 (d, *J* = 7.1 Hz, 3H), 1.33 – 1.20 (m, 3H), 0.67 (d, *J* = 6.5 Hz, 3H), 0.56 (d, *J* = 6.1 Hz, 3H).

¹³C NMR (126 MHz, CDCl₃) δ 171.70, 171.37, 169.83, 164.44, 136.90, 135.50, 131.17, 130.90 (2C), 130.44, 129.72 (2C), 56.89, 49.57, 44.49, 40.58, 35.32, 30.19, 24.65, 22.26, 22.12, 15.54.

Methyl ((Z)-3-(4-bromophenyl)-2-((S)-2-((S)-2-((*tert*-butoxycarbonyl)(methyl)amino)propanamido)-4-methylpentanamido)acryloyl)glycinate (**11n**)



According to general method VI, tetrapeptide **10** (150 mg, 0.27 mmol), TMG (84.9 μ L, 0.68 mmol) and *p*-bromobenzaldehyde (99.9 μ L, 0.54 mmol) were used. Purification was done by column chromatography on silica gel (*n*-hexane / EtOAc 6:4 – 3:7), giving **11n** (140 mg, 0.23 mmol, 85 %) and the corresponding (*E*)-isomer (9 mg, 0.01 mmol, 5.5 %) as white solids.

(*Z*)-Isomer

HR-MS *m/z* 609.1924 (calculated for $C_{27}H_{38}BrN_4O_7$: 609.1929)

^1H NMR (400 MHz, CDCl_3) δ 7.95 (s, 1H), 7.42 (t, *J* = 6.9 Hz, 4H), 7.32 – 7.27 (m, 1H), 7.03 (t, *J* = 8.6 Hz, 2H), 6.67 (s, 1H), 4.48 (q, *J* = 7.1 Hz, 1H), 4.35 – 4.25 (m, 1H), 4.15 – 4.06 (m, *J* = 12.0, 5.1 Hz, 2H), 3.75 (s, 3H), 2.81 (s, 3H), 1.82 – 1.73 (m, 1H), 1.69 – 1.56 (m, 2H), 1.42 (s, 9H), 1.34 (d, *J* = 7.1 Hz, 3H), 0.97 (d, *J* = 6.2 Hz, 3H), 0.91 (d, *J* = 6.2 Hz, 3H).

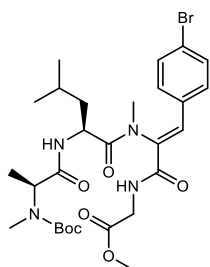
^{13}C NMR (101 MHz, CDCl_3) δ 173.37, 171.16, 170.43, 164.93, 164.10, 161.61, 156.31, 131.41, 131.33, 129.76, 126.92, 115.70, 115.48, 81.13, 54.85, 53.00, 52.26, 41.67, 39.38, 31.16, 28.24 (3C), 24.76, 22.96, 21.39, 13.23.

(*E*)-Isomer (side product)

^1H NMR (400 MHz, CDCl_3) δ 8.49 (s, 1H), 7.88 (s, 1H), 7.31 (dd, *J* = 8.5, 5.5 Hz, 2H), 7.06 (t, *J* = 8.6 Hz, 2H), 6.64 (s, 1H), 6.19 – 6.13 (m, 1H), 4.68 (s, 1H), 4.49 (dd, *J* = 11.2, 6.1 Hz, 1H), 3.94 (d, *J* = 5.2 Hz, 2H), 3.68 (s, 3H), 2.80 (s, 3H), 1.81 – 1.70 (m, 1H), 1.69 – 1.60 (m, 2H), 1.48 (s, 9H), 1.37 (d, *J* = 7.1 Hz, 3H), 0.95 (d, *J* = 6.2 Hz, 3H), 0.92 (d, *J* = 6.1 Hz, 3H).

^{13}C NMR (101 MHz, CDCl_3) δ 172.11, 170.75, 169.07, 163.97, 163.76, 161.28, 156.44, 130.80, 130.72, 129.77, 120.33, 116.04, 115.82, 80.86, 53.59, 52.55, 52.36, 41.63, 40.48, 30.15, 28.33 (3C), 24.74, 23.04, 21.51, 13.45.

Methyl ((Z)-3-(4-bromophenyl)-2-((S)-2-((S)-2-((*tert*-butoxycarbonyl)(methyl)amino)propanamido)-*N*,4-dimethylpentanamido)acryloyl)glycinate (**4n**)



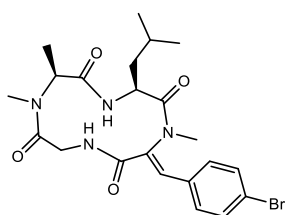
According to general method VII, tetrapeptide **11n** (112 mg, 0.2 mmol), K₂CO₃ (280.0 mg, 2.03 mmol), 18-crown-6 (4.8 mg, 0.02 mmol) and methyl iodide (190.0 μ L, 3.05 mmol) were used, giving **4n** (110 mg, 0.18 mmol, 88 %) as a white solid.

HR-MS *m/z* 623.2074 (calculated for C₂₈H₄₀BrN₄O₇: 623.2086)

¹H NMR (500 MHz, CDCl₃) δ 8.55 (t, *J* = 6.0 Hz, 1H), 7.70 (s, 1H), 7.43 (dd, *J* = 8.7, 5.5 Hz, 2H), 7.13 (t, *J* = 8.6 Hz, 2H), 6.55 (s, 1H), 4.67 (s, 1H), 4.33 (ddd, *J* = 11.4, 5.2, 2.4 Hz, 1H), 4.24 – 4.06 (m, 2H), 3.72 (s, 3H), 3.20 (s, 3H), 2.70 (s, 3H), 1.68 (s, 2H), 1.45 (s, 9H), 1.36 – 1.29 (m, 1H), 1.27 (d, *J* = 7.2 Hz, 3H), 0.60 (dd, *J* = 6.6, 3.9 Hz, 6H).

¹³C NMR (126 MHz, CDCl₃) δ 172.33, 171.63, 169.96, 164.91, 162.69, 156.51, 134.41, 132.54, 132.47, 131.66, 128.55, 116.63, 116.46, 80.73, 52.85, 52.03, 51.00, 41.84, 38.79, 34.23, 29.67, 28.27 (3C), 24.76, 23.20, 20.40, 13.20.

(3*S*,6*S*)-12-((*Z*)-4-Bromobenzylidene)-3-isobutyl-1,6,7-trimethyl-1,4,7,10-tetraazacyclododecane-2,5,8,11-tetraone (**5n**)



According to general method V, compound **4n** (100.0 mg, 0.16 mmol), lithium hydroxide hydrate (23.5 mg, 0.80 mmol), 4-DMAP (101.7 mg, 0.91 mmol), T3P (50 % w/w in EtOAc, 180.0 μ L, 0.60 mmol) and DCM (31 mL) were used, giving **5n** (28.2 mg, 0.06 mmol, 36 %) as a white solid. A sample was purified by semipreparative RP-HPLC for biological assays and characterization.

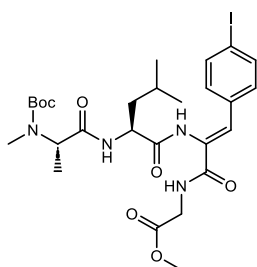
HR-MS *m/z* 491.1304 (calculated for C₂₂H₂₈BrN₄O₄: 491.1299)

t_R = 10.08 min (5 % ACN (0 min) > 100 % ACN (15 min) > 100 % ACN (20 min))

¹H NMR (400 MHz, CDCl₃) δ 8.05 (s, 1H), 7.72 (s, 1H), 7.41 (dd, *J* = 8.4, 5.4 Hz, 2H), 7.12 (t, *J* = 8.5 Hz, 3H), 5.26 – 5.11 (m, 1H), 4.36 (s, 1H), 3.64 (d, *J* = 5.9 Hz, 2H), 3.17 (s, 3H), 2.81 (s, 3H), 1.53 (d, *J* = 7.0 Hz, 3H), 1.35 – 1.11 (m, 3H), 0.66 (d, *J* = 6.4 Hz, 3H), 0.56 (d, *J* = 6.0 Hz, 3H).

¹³C NMR (126 MHz, CDCl₃) δ 171.47, 169.90, 164.89, 162.87, 135.55, 131.94, 131.87, 130.34, 128.24, 116.75, 116.58, 56.98, 49.50, 44.49, 40.81, 35.26, 30.18, 24.62, 22.26, 22.12, 15.53.

Methyl ((Z)-2-((S)-2-((S)-2-((*tert*-butoxycarbonyl)(methyl)amino)propanamido)-4-methylpentan-
amido)-3-(4-iodophenyl)acryloyl)glycinate (**11o**)



According to general method VI, tetrapeptide **10** (150 mg, 0.27 mmol), TMG (84.9 μ L, 0.68 mmol) and *p*-iodobenzaldehyde (125.3 μ L, 0.54 mmol) were used. Purification was done by column chromatography on silica gel (*n*-hexane / EtOAc 6:4 – 3:7), giving **11o** (146 mg, 0.22 mmol, 82 %) and the corresponding (*E*)-isomer (12 mg, 0.02 mmol, 6.7 %) as white solids.

HR-MS m/z 657.1789 (calculated for $C_{27}H_{38}IN_4O_7$: 657.1791)

(*Z*)-Isomer

1H NMR (400 MHz, $CDCl_3$) δ 8.02 (s, 1H), 7.67 (d, J = 8.3 Hz, 2H), 7.37 – 7.27 (m, 2H), 7.14 (d, J = 8.3 Hz, 2H), 6.67 (s, 1H), 4.46 (q, J = 7.1 Hz, 1H), 4.33 – 4.25 (m, 1H), 4.11 (d, J = 7.0 Hz, 2H), 3.75 (s, 3H), 2.80 (s, 3H), 1.76 – 1.70 (m, 1H), 1.67 – 1.56 (m, 2H), 1.42 (s, 9H), 1.34 (d, J = 7.1 Hz, 3H), 0.97 (d, J = 6.1 Hz, 3H), 0.90 (d, J = 6.1 Hz, 3H).

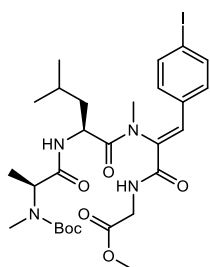
^{13}C NMR (101 MHz, $CDCl_3$) δ 173.35, 171.23, 170.36, 164.81, 156.46, 137.66 (2C), 133.15, 130.94 (3C), 127.92, 95.11, 81.12, 54.90, 52.97, 52.26, 41.67, 39.32, 31.22, 28.25 (3C), 24.75, 22.97, 21.44, 13.27.

(*E*)-Isomer (side product)

1H NMR (400 MHz, $CDCl_3$) δ 8.49 (s, 1H), 7.77 (s, 1H), 7.68 (d, J = 8.3 Hz, 2H), 7.07 (d, J = 8.3 Hz, 2H), 6.64 (s, 1H), 6.18 (s, 1H), 4.67 (s, 1H), 4.53 – 4.43 (m, 1H), 3.95 (d, J = 5.3 Hz, 2H), 3.70 (s, 3H), 2.80 (s, 3H), 1.72 – 1.55 (m, 3H), 1.48 (s, 9H), 1.36 (d, J = 7.1 Hz, 3H), 0.95 (d, J = 6.2 Hz, 3H), 0.91 (d, J = 6.1 Hz, 3H).

^{13}C NMR (101 MHz, $CDCl_3$) δ 172.17, 170.76, 169.01, 164.00, 156.33, 137.90 (2C), 133.94, 130.69 (2C), 129.37, 119.88, 93.88, 80.86, 53.40, 52.53, 52.44, 41.64, 40.42, 30.19, 28.32 (3C), 24.73, 23.03, 21.52, 13.44.

Methyl ((Z)-2-((S)-2-((S)-2-((*tert*-butoxycarbonyl)(methyl)amino)propanamido)-*N*,4-dimethylpentanamido)-3-(4-iodophenyl)acryloyl)glycinate (**4o**)



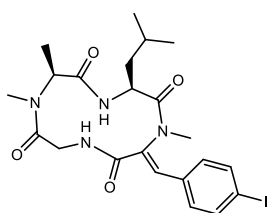
According to general method VII, tetrapeptide **11o** (135.0 mg, 0.21 mmol), K₂CO₃ (283.3 mg, 2.05 mmol), 18-crown-6 (4.8 mg, 0.02 mmol) and methyl iodide (191.0 μ L, 3.08 mmol) were used, giving **4o** (115 mg, 0.17 mmol, 81 %) as a white solid.

HR-MS *m/z* 671.1958 (calculated for C₂₈H₄₀IN₄O₇: 671.1947)

¹H NMR (500 MHz, CDCl₃) δ 8.55 (t, *J* = 5.9 Hz, 1H), 7.77 (d, *J* = 8.3 Hz, 2H), 7.64 (s, 1H), 7.14 (d, *J* = 8.5 Hz, 2H), 6.55 (s, 1H), 4.66 (s, 1H), 4.31 (ddd, *J* = 11.6, 5.0, 2.4 Hz, 1H), 4.21 – 4.06 (m, 2H), 3.72 (s, 3H), 3.18 (s, 3H), 2.70 (s, 3H), 1.75 – 1.29 (m, 3H), 1.45 (s, 9H), 1.26 (d, *J* = 7.4 Hz, 3H), 0.63 (d, *J* = 6.6 Hz, 3H), 0.60 (d, *J* = 6.6 Hz, 3H).

¹³C NMR (126 MHz, CDCl₃) δ 172.33, 171.49, 169.91, 164.75, 156.50, 138.57 (2C), 134.53, 132.81, 131.68 (2C), 131.64, 97.16, 80.73, 55.33, 52.04, 51.00, 41.83, 38.85, 34.25, 29.68, 28.27 (3C), 24.78, 23.19, 20.43, 13.24.

(3*S*,6*S*)-12-((*Z*)-4-Iodobenzylidene)-3-isobutyl-1,6,7-trimethyl-1,4,7,10-tetraazacyclododecane-2,5,8,11-tetraone (**5o**)



According to general method V, compound **4o** (103.0 mg, 0.15 mmol), lithium hydroxide hydrate (31.5 mg, 0.75 mmol), 4-DMAP (102.3 mg, 0.91 mmol), T3P (50 % w/w in EtOAc, 181.1 μ L, 0.61 mmol) and DCM (30 mL) were used, giving **5o** (50 mg, 0.09 mmol, 62 %) as a white solid. A sample was purified by semipreparative RP-HPLC for biological assays and characterization.

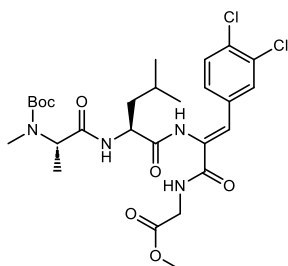
HR-MS *m/z* 539.1168 (calculated for C₂₂H₂₈IN₄O₄: 539.1161)

*t*_R = 10.36 min (5 % ACN (0 min) > 100 % ACN (15 min) > 100 % ACN (20 min))

¹H NMR (400 MHz, CDCl₃) δ 8.16 (s, 1H), 7.77 (d, *J* = 8.4 Hz, 2H), 7.66 (s, 1H), 7.14 (d, *J* = 14.6 Hz, 1H), 7.11 (d, *J* = 8.5 Hz, 2H), 5.23 – 5.12 (m, 1H), 4.34 (s, 1H), 3.56 (d, *J* = 15.1 Hz, 1H), 3.15 (s, 3H), 2.79 (s, *J* = 18.1 Hz, 3H), 1.73 – 1.62 (m, 1H), 1.53 (d, *J* = 7.1 Hz, 3H), 1.37 – 1.27 (m, 1H), 1.26 (s, 2H), 0.67 (d, *J* = 6.5 Hz, 3H), 0.55 (d, *J* = 5.9 Hz, 3H).

^{13}C NMR (101 MHz, CDCl_3) δ 171.65, 171.24, 164.34, 157.86, 138.64 (2C), 135.63, 131.87, 131.42, 130.97 (2C), 97.34, 56.92, 49.54, 44.42, 40.69, 35.30, 30.17, 24.66, 22.26, 22.08, 15.52.

Methyl ((Z)-2-((S)-2-((S)-2-((*tert*-butoxycarbonyl)(methyl)amino)propanamido)-4-methylpentan-
amido)-3-(3,4-dichlorophenyl)acryloyl)glycinate (**11p**)



According to general method VI, tetrapeptide **10** (150 mg, 0.27 mmol), TMG (84.9 μL , 0.68 mmol) and 3,4-dichloro benzaldehyde (94.5 μL , 0.54 mmol) were used. Purification was done by column chromatography on silica gel (*n*-hexane / EtOAc 6:4 – 3:7), giving **11p** (144 mg, 0.24 mmol, 89 %) and the corresponding (*E*)-isomer (12 mg, 0.02 mmol, 7.4 %) as white solids.

(*Z*)-Isomer

HR-MS m/z 599.2045 (calculated for $\text{C}_{27}\text{H}_{37}\text{Cl}_2\text{N}_4\text{O}_7$: 599.2039)

^1H NMR (400 MHz, CDCl_3) δ 8.09 (s, 1H), 7.54 (d, J = 1.8 Hz, 1H), 7.45 (t, J = 5.1 Hz, 1H), 7.40 (d, J = 6.3 Hz, 1H), 7.38 (s, 1H), 7.23 (dd, J = 8.3, 1.7 Hz, 1H), 6.66 (s, 1H), 4.45 (dd, J = 14.0, 7.0 Hz, 1H), 4.30 – 4.22 (m, 1H), 4.13 – 4.06 (m, J = 9.1, 5.2 Hz, 2H), 3.75 (s, 3H), 2.81 (s, 3H), 1.81 – 1.72 (m, 1H), 1.69 – 1.58 (m, 2H), 1.42 (s, 9H), 1.34 (d, J = 7.1 Hz, 3H), 0.98 (d, J = 6.2 Hz, 3H), 0.92 (d, J = 6.2 Hz, 3H).

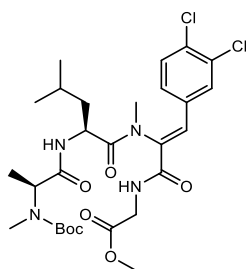
^{13}C NMR (101 MHz, CDCl_3) δ 173.57, 171.22, 170.31, 164.55, 156.59, 133.81, 132.91, 132.59, 130.50, 130.47, 130.10, 128.96, 128.38, 81.18, 55.07, 53.28, 52.26, 41.67, 39.39, 31.39, 28.23 (3C), 24.84, 23.00, 21.32, 13.24.

(*E*)-Isomer (side product)

^1H NMR (500 MHz, CDCl_3) δ 8.51 (s, 1H), 7.68 (s, 1H), 7.41 (d, J = 8.6 Hz, 2H), 7.18 (dd, J = 8.4, 2.1 Hz, 1H), 6.66 (s, 1H), 6.21 (s, 1H), 4.66 (s, 1H), 4.51 – 4.43 (m, 1H), 3.98 (dd, J = 5.2, 2.7 Hz, 2H), 3.70 (s, 3H), 2.80 (s, 3H), 1.76 – 1.56 (m, 3H), 1.48 (s, 9H), 1.37 (d, J = 7.3 Hz, 3H), 0.95 (d, J = 6.1 Hz, 3H), 0.91 (d, J = 6.0 Hz, 3H).

^{13}C NMR (126 MHz, CDCl_3) δ 172.32, 170.84, 169.03, 163.82, 156.59, 134.48, 130.68, 130.62 (2C), 130.34, 128.24 (2C), 118.28, 80.91, 53.80, 52.63, 52.49, 41.63, 40.76, 30.26, 28.32 (3C), 24.72, 23.03, 21.87, 13.75.

Methyl ((Z)-2-((S)-2-((S)-2-((*tert*-butoxycarbonyl)(methyl)amino)propanamido)-*N*,4-dimethylpentanamido)-3-(3,4-dichlorophenyl)acryloyl)glycinate (**4p**)



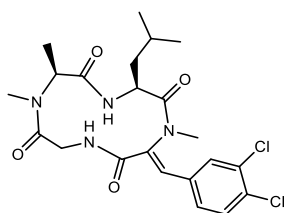
According to general method VII, tetrapeptide **11p** (130.0 mg, 0.22 mmol), K₂CO₃ (298.5 mg, 2.16 mmol), 18-crown-6 (4.8 mg, 0.02 mmol) and methyl iodide (201.8 μ L, 3.24 mmol) were used, giving **4p** (120 mg, 0.20 mmol, 90 %) as a white solid.

HR-MS *m/z* 613.2190 (calculated for C₂₈H₃₉Cl₂N₄O₇: 613.2201)

¹H NMR (500 MHz, CDCl₃) δ 8.55 (t, *J* = 5.9 Hz, 1H), 7.63 (s, 1H), 7.53 – 7.49 (m, 1H), 7.52 – 7.42 (m, 1H), 7.28 – 7.17 (m, 1H), 6.58 (s, 1H), 4.66 (s, 1H), 4.31 (ddd, *J* = 11.4, 5.3, 2.5 Hz, 1H), 4.21 – 4.06 (m, 2H), 3.72 (s, 3H), 3.18 (s, 3H), 2.70 (s, 3H), 1.70 – 1.30 (m, 3H), 1.46 (s, 9H), 1.27 (d, *J* = 7.3 Hz, 3H), 0.64 (dd, *J* = 8.8, 6.5 Hz, 6H).

¹³C NMR (126 MHz, CDCl₃) δ 172.37, 171.44, 169.86, 164.42, 156.50, 134.70, 133.73, 133.64, 133.01, 132.43, 132.23, 131.31, 128.43, 80.77, 53.23, 52.07, 51.02, 41.84, 38.89, 34.41, 29.67, 28.33 (3C), 24.83, 23.20, 20.50, 13.30.

(3*S*,6*S*)-12-((*Z*)-3,4-Dichlorobenzylidene)-3-isobutyl-1,6,7-trimethyl-1,4,7,10-tetraazacyclododecane-2,5,8,11-tetraone (**5p**)



According to general method V, compound **4p** (108 mg, 0.18 mmol), lithium hydroxide hydrate (37.7 mg, 0.9 mmol), 4-DMAP (113.1 mg, 1.01 mmol), T3P (50 % w/w in EtOAc, 200 μ L, 0.67 mmol) and DCM (36 mL) were used, giving **5p** (52 mg, 0.11 mmol, 60 %) as a white solid. A sample was purified by semipreparative RP-HPLC for biological assays and characterization.

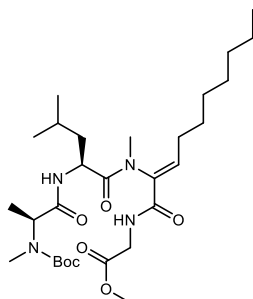
HR-MS *m/z* 481.1417 (calculated for C₂₂H₂₇Cl₂N₄O₄: 481.1415)

t_R = 10.71 min (5 % ACN (0 min) > 100 % ACN (15 min) > 100 % ACN (20 min))

¹H NMR (400 MHz, CDCl₃) δ 7.95 (s, 1H), 7.66 (s, 1H), 7.50 (t, *J* = 5.2 Hz, 2H), 7.20 (dd, *J* = 8.5, 2.0 Hz, 1H), 7.00 (s, 1H), 5.22 – 5.11 (m, 1H), 4.33 (s, 1H), 3.59 (d, *J* = 15.1 Hz, 1H), 3.16 (s, 3H), 2.81 (s, 3H), 1.53 (d, *J* = 7.1 Hz, 3H), 1.26 (s, 4H), 0.70 (d, *J* = 6.5 Hz, 3H), 0.58 (d, *J* = 6.2 Hz, 3H).

^{13}C NMR (126 MHz, CDCl_3) δ 171.56, 171.22, 169.91, 163.91, 134.92, 134.23, 133.84, 132.11, 131.94, 131.71, 131.36, 127.95, 56.81, 49.44, 44.47, 40.66, 30.18, 29.68, 24.68, 22.33, 21.98, 15.54.

Methyl ((Z)-2-((S)-2-((S)-2-((tert-butoxycarbonyl)(methyl)amino)propanamido)-4-methylpentan-amido)dec-2-enoyl)glycinate (**11q**)



According to general method VI, tetrapeptide **10** (150 mg, 0.27 mmol), TMG (84.9 μL , 0.68 mmol) and octanal (84.2 μL , 0.54 mmol) were used. Purification was done by column chromatography on silica gel (*n*-hexane / EtOAc 6:4 – 2:8), giving **11q** (93.0 mg, 0.17 mmol, 62 %) and the corresponding (*E*)-isomer (5.4 mg, 0.01 mmol, 3.6 %) as white solids.

(*Z*)-Isomer

HR-MS m/z 553.3615 (calculated for $\text{C}_{28}\text{H}_{49}\text{N}_4\text{O}_7$: 553.3607)

^1H NMR (500 MHz, CDCl_3) δ 7.60 (s, 1H), 7.09 (t, J = 5.4 Hz, 1H), 6.78 – 6.31 (m, 2H), 4.56 (q, J = 7.3 Hz, 1H), 4.29 (dd, J = 9.5, 5.6 Hz, 1H), 4.06 (d, J = 5.4 Hz, 2H), 3.74 (s, 3H), 2.81 (s, 3H), 2.07 (qd, J = 9.6, 8.6, 2.4 Hz, 2H), 1.78 (ddd, J = 13.5, 8.1, 5.7 Hz, 2H), 1.47 (s, 9H), 1.46 – 1.39 (m, 2H), 1.34 (d, J = 7.2 Hz, 3H), 1.32 – 1.24 (m, 9H), 0.98 (d, J = 6.3 Hz, 3H), 0.93 (d, J = 6.3 Hz, 3H), 0.87 (t, J = 6.7 Hz, 3H).

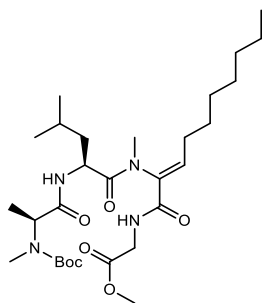
^{13}C NMR (126 MHz, CDCl_3) δ 173.39, 170.81, 170.58, 164.72, 156.75, 137.76, 127.35, 81.08, 54.55, 52.96, 52.24, 41.48, 39.62, 31.75, 30.83, 29.41, 29.05, 28.30 (3C), 28.16, 27.90, 24.82, 22.90, 22.63, 21.63, 14.08, 13.29.

(*E*)-Isomer (side product)

^1H NMR (400 MHz, CDCl_3) δ 7.88 (s, 1H), 6.74 (s, 1H), 6.56 (s, 1H), 6.29 (s, 1H), 4.59 (d, J = 7.7 Hz, 1H), 4.35 (ddd, J = 9.1, 7.1, 5.1 Hz, 1H), 4.10 (d, J = 5.3 Hz, 2H), 3.76 (s, 3H), 2.80 (s, 3H), 2.49 (q, J = 7.5 Hz, 2H), 1.73 (dt, J = 13.2, 3.8 Hz, 2H), 1.66 – 1.53 (m, 2H), 1.47 (s, 9H), 1.51 – 1.40 (m, 2H), 1.35 (d, J = 7.1 Hz, 3H), 1.35 – 1.22 (m, 7H), 0.99 – 0.83 (m, 9H).

^{13}C NMR (101 MHz, CDCl_3) δ 172.52, 170.88, 170.13, 164.58, 156.44, 132.44, 127.51, 80.91, 54.05, 52.44, 52.34, 41.37, 40.09, 31.74, 30.54, 29.64, 29.22, 29.08, 28.32 (3C), 27.99, 24.72, 23.00, 22.62, 21.56, 14.07, 13.40.

Methyl ((*Z*)-2-((*S*)-2-((*S*)-2-((*tert*-butoxycarbonyl)(methyl)amino)propanamido)-*N*,4-dimethylpentanamido)dec-2-enoyl)glycinate (**4q**)



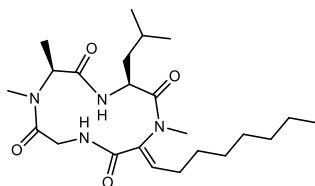
According to general method VII, tetrapeptide **11q** (89.0 mg, 0.16 mmol), K₂CO₃ (221.1 mg, 1.60 mmol), 18-crown-6 (4.8 mg, 0.02 mmol) and methyl iodide (149.8 μ L, 2.4 mmol) were used, giving **4q** (86.0 mg, 0.15 mmol, 95 %) as a white solid.

HR-MS *m/z* 567.3761 (calculated for C₂₉H₅₁N₄O₇: 567.3763)

¹H NMR (500 MHz, CDCl₃) δ 8.25 (s, 1H), 7.01 (t, *J* = 7.7 Hz, 1H), 6.58 (s, 1H), 4.69 – 4.66 (m, 1H), 4.33 – 4.25 (m, 1H), 4.19 – 3.97 (m, 2H), 3.69 (s, 3H), 3.07 (s, 3H), 2.88 (s, 3H), 2.22 – 2.02 (m, 2H), 1.74 – 1.57 (m, 3H), 1.47 (s, 9H), 1.36 – 1.22 (m, 13H), 1.01 – 0.78 (m, 9H).

¹³C NMR (126 MHz, CDCl₃) δ 172.19, 171.89, 169.98, 163.92, 156.31, 141.63, 134.25, 80.68, 53.02, 51.96, 50.67, 41.62, 39.67, 31.73, 31.65, 29.56, 29.04, 28.47, 28.29 (3C), 28.25, 24.91, 23.52, 22.61, 22.55, 20.67, 14.02, 13.27.

(3*S*,6*S*,*Z*)-3-Isobutyl-1,6,7-trimethyl-12-octylidene-1,4,7,10-tetraazacyclododecane-2,5,8,11-tetraone (**5q**)



According to general method V, compound **4q** (78.0 mg, 0.14 mmol), lithium hydroxide hydrate (28.2 mg, 0.69 mmol), 4-DMAP (145.9 mg, 1.3 mmol), T3P (50 % w/w in EtOAc, 155 μ L, 0.52 mmol) and DCM (28 mL) were used, giving **5q** (10.2 mg, 0.02 mmol, 17 %) as a white solid. A sample was purified by semipreparative RP-HPLC for biological assays and characterization.

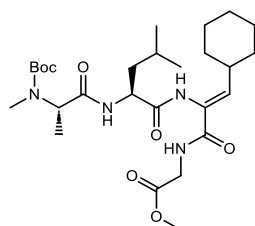
HR-MS *m/z* 435.2981 (calculated for C₂₃H₃₉N₄O₄: 435.2977)

*t*_R = 11.95 min (5 % ACN (0 min) > 100 % ACN (15 min) > 100 % ACN (20 min))

¹H NMR (500 MHz, CDCl₃) δ 7.88 (s, 1H), 7.10 (s, 1H), 7.01 (s, 1H), 5.10 (d, *J* = 13.1 Hz, 1H), 4.34 (s, 2H), 3.48 (d, *J* = 15.2 Hz, 1H), 3.01 (s, 3H), 2.80 (s, 3H), 2.09 (q, *J* = 8.2 Hz, 2H), 1.81 (ddd, *J* = 13.9, 8.1, 5.8 Hz, 1H), 1.60 – 1.47 (m, 5H), 1.36 – 1.20 (m, 10H), 0.94 – 0.84 (m, 9H).

¹³C NMR (126 MHz, CDCl₃) δ 173.78, 172.03, 169.79, 163.60, 142.60, 133.23, 56.85, 49.46, 44.15, 41.21, 36.20, 31.63, 30.14, 29.57, 29.02, 28.04, 27.78, 24.64, 23.08, 22.58, 22.24, 15.53, 14.03.

Methyl ((Z)-2-((S)-2-((S)-2-((*tert*-butoxycarbonyl)(methyl)amino)propanamido)-4-methylpentan-amido)-3-cyclohexylacryloyl)glycinate (**11r**)



According to general method VI, tetrapeptide **10** (150 mg, 0.27 mmol), TMG (84.9 μ L, 0.68 mmol) and cyclohexyl methanal (65.1 μ L, 0.54 mmol) were used. Purification was done by column chromatography on silica gel (*n*-hexane / EtOAc 6:4 – 3:7), giving **11r** (60.0 mg, 0.11 mmol, 41 %) and the corresponding (*E*)-isomer (10.0 mg, 0.02 mmol, 6.9 %) as white solids.

(*Z*)-Isomer

HR-MS m/z 537.3304 (calculated for $C_{27}H_{45}N_4O_7$: 537.3294)

^1H NMR (400 MHz, $(\text{CD}_3)_2\text{SO}$) δ 9.20 (s, 1H), 8.04 (t, J = 5.8 Hz, 1H), 7.99 (s, 1H), 6.28 (d, J = 9.8 Hz, 1H), 4.62 – 4.34 (m, 1H), 4.27 (s, 1H), 3.93 – 3.75 (m, 2H), 3.62 (s, 3H), 2.74 (s, 3H), 2.25 – 2.13 (m, 1H), 1.72 – 1.47 (m, 7H), 1.38 (s, 9H), 1.23 (d, J = 6.6 Hz, 3H), 1.20 – 1.12 (m, 4H), 1.12 – 1.03 (m, 2H), 0.94 (d, J = 6.3 Hz, 3H), 0.89 (d, J = 5.9 Hz, 3H).

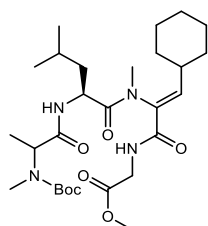
^{13}C NMR (101 MHz, $(\text{CD}_3)_2\text{SO}$) δ 172.35, 171.78, 170.11, 164.43, 154.87, 139.77, 127.57, 78.89, 53.87, 51.89, 51.61, 40.99, 39.76, 36.10, 31.23, 30.08, 27.97 (3C), 25.33, 25.14, 24.16, 22.64, 22.09, 15.17, 14.51, 14.05.

(*E*)-Isomer (side product)

^1H NMR (500 MHz, CDCl_3) δ 7.88 (s, 1H), 6.79 (s, 1H), 6.58 (s, 1H), 6.03 (s, 1H), 4.57 (d, J = 7.7 Hz, 1H), 4.34 (ddd, J = 9.3, 7.1, 4.8 Hz, 1H), 4.16 – 4.08 (m, 2H), 3.77 (s, 3H), 2.90 – 2.82 (m, 1H), 2.80 (s, 3H), 1.79 – 1.68 (m, 6H), 1.66 – 1.54 (m, 2H), 1.47 (s, 9H), 1.38 – 1.24 (m, 5H), 1.21 – 1.08 (m, 3H), 0.94 (d, J = 6.3 Hz, 3H), 0.90 (d, J = 6.1 Hz, 3H).

^{13}C NMR (126 MHz, CDCl_3) δ 172.59, 170.91, 170.19, 164.67, 156.55, 137.69, 126.24, 80.92, 54.32, 52.36 (2C), 41.37, 40.01, 36.71, 33.13 (2C), 30.64, 28.32 (3C), 25.80, 25.43 (2C), 24.71, 23.01, 21.51, 13.39.

Methyl ((Z)-2-((S)-2-((S)-2-((*tert*-butoxycarbonyl)(methyl)amino)propanamido)-*N*,4-dimethylpentanamido)-3-cyclohexylacryloyl)glycinate (**4r**)



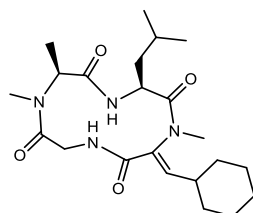
According to general method VII, tetrapeptide **11r** (60.0 mg, 0.11 mmol), K₂CO₃ (152.0 mg, 1.1 mmol), 18-crown-6 (4.8 mg, 0.02 mmol) and methyl iodide (102.7 μ L, 1.65 mmol) were used, giving **4r** (31.7 mg, 0.06 mmol, 52 %) as a white solid.

HR-MS m/z 551.3457 (calculated for C₂₈H₄₇N₄O₇: 551.3450)

¹H NMR (500 MHz, CDCl₃) δ 8.22 (s, 1H), 6.87 (d, J = 11.1 Hz, 1H), 6.42 (s, 1H), 4.66 (s, 1H), 4.34 – 4.28 (m, 1H), 4.19 – 4.10 (m, 2H), 3.69 (s, 3H), 3.10 (s, 3H), 2.70 (s, 3H), 1.80 – 1.58 (m, 8H), 1.47 (s, 9H), 1.39 – 1.16 (m, 9H), 0.90 (d, J = 6.3 Hz, 3H), 0.83 (d, J = 6.1 Hz, 3H).

¹³C NMR (126 MHz, CDCl₃) δ 172.11, 171.93, 170.04, 164.14, 156.34, 146.20, 132.45, 80.70, 52.64, 51.97, 50.43, 41.69, 39.47, 37.39, 36.94, 31.99, 31.79, 29.68, 28.30 (3C), 25.60, 25.34, 24.82, 23.48, 23.42, 20.47, 13.33.

(3*S*,6*S*,*Z*)-12-(Cyclohexylmethylene)-3-isobutyl-1,6,7-trimethyl-1,4,7,10-tetraazacyclododecane-2,5,8,11-tetraone (**5r**)



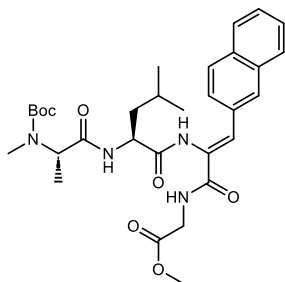
According to general method V, compound **4r** (24.7 mg, 0.05 mmol), lithium hydroxide hydrate (9.4 mg, 0.22 mmol), 4-DMAP (50.2 mg, 0.45 mmol), T3P (50 % w/w in EtOAc, 53.3 μ L, 0.18 mmol) and DCM (9 mL) were used, giving **5r** (2.0 mg, 0.005 mmol, 10.6 %) as a white solid. A sample was purified by semipreparative RP-HPLC for biological assays and characterization.

HR-MS m/z 419.2667 (calculated for C₂₂H₃₅N₄O₄: 419.2664)

t_R = 10.01 min (5 % ACN (0 min) > 100 % ACN (15 min) > 100 % ACN (20 min))

¹H NMR (400 MHz, CDCl₃) δ 7.48 (d, J = 34.8 Hz, 1H), 6.84 (s, 1H), 5.35 (s, 1H), 5.09 (s, 1H), 4.44 – 4.20 (m, 2H), 3.79 – 3.32 (m, 1H), 3.04 (s, 3H), 2.84 (s, 3H), 2.15 – 1.96 (m, 1H), 2.00 – 1.53 (m, 9H), 1.50 (d, J = 7.1 Hz, 3H), 1.24 (d, J = 10.6 Hz, 4H), 0.94 – 0.84 (m, 6H).

Methyl ((Z)-2-((S)-2-((S)-2-((tert-butoxycarbonyl)(methyl)amino)propanamido)-4-methylpentan-amido)-3-(naphthalen-2-yl)acryloyl)glycinate (**11s**)



According to general method VI, tetrapeptide **10** (150 mg, 0.27 mmol), TMG (84.9 μ L, 0.68 mmol) and 2-naphthaldehyde (84.3 mg, 0.54 mmol) were used. Purification was done by column chromatography on silica gel (*n*-hexane / EtOAc 6:4 – 1:9), giving **11s** (129 mg, 0.22 mmol, 82 %) and the corresponding (*E*)-isomer (6.2 mg, 0.01 mmol, 4.0 %) as white solids.

(*Z*)-Isomer

HR-MS *m/z* 581.2976 (calculated for C₃₁H₄₁N₄O₇: 581.2981)

¹H NMR (400 MHz, CDCl₃) δ 8.03 (s, 1H), 7.88 (s, 1H), 7.84 – 7.72 (m, 3H), 7.57 (s, 1H), 7.54 – 7.43 (m, 2H), 7.35 (t, *J* = 5.5 Hz, 2H), 6.69 (s, 1H), 4.48 (q, *J* = 7.0 Hz, 1H), 4.38 – 4.30 (m, 1H), 4.15 – 4.09 (m, 2H), 3.74 (s, 3H), 2.78 (s, 3H), 1.80 – 1.73 (m, *J* = 10.2, 4.8 Hz, 1H), 1.69 – 1.59 (m, 2H), 1.40 (s, 9H), 1.28 (d, *J* = 5.1 Hz, 3H), 0.95 (d, *J* = 6.2 Hz, 3H), 0.88 (d, *J* = 6.2 Hz, 3H).

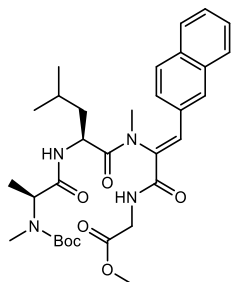
¹³C NMR (101 MHz, CDCl₃) δ 173.27, 171.52, 170.46, 165.08, 156.43, 133.33, 133.10, 132.22, 131.12, 129.60, 128.40, 128.04, 127.57, 127.44, 126.88, 126.37, 126.24, 81.01, 54.58, 52.99, 52.23, 41.70, 39.55, 30.97, 28.22 (3C), 24.74, 23.01, 21.34, 13.20.

(*E*)-Isomer (side product)

¹H NMR (400 MHz, CDCl₃) δ 8.57 (s, 1H), 8.13 (s, 1H), 7.86 – 7.76 (m, 4H), 7.48 (dt, *J* = 6.8, 3.4 Hz, 2H), 7.42 (dd, *J* = 8.5, 1.6 Hz, 1H), 6.68 (s, 1H), 6.23 (t, *J* = 5.4 Hz, 1H), 4.70 (s, 1H), 4.53 (td, *J* = 8.9, 5.0 Hz, 1H), 3.89 (d, *J* = 5.4 Hz, 2H), 3.48 (s, 3H), 2.81 (s, 3H), 1.84 – 1.57 (m, 3H), 1.49 (s, 9H), 1.38 (d, *J* = 7.2 Hz, 3H), 0.97 (d, *J* = 6.1 Hz, 3H), 0.94 (d, *J* = 6.0 Hz, 3H).

¹³C NMR (101 MHz, CDCl₃) δ 172.03, 170.74, 168.80, 164.18, 156.50, 133.33, 132.79, 131.91, 128.91, 128.52, 128.21, 128.12, 127.67, 126.59, 126.54, 126.51, 121.24, 80.83, 53.75, 52.58, 52.14, 41.67, 40.61, 30.12, 28.34 (3C), 24.76, 23.05, 21.56, 13.47.

Methyl ((Z)-2-((S)-2-((S)-2-((*tert*-butoxycarbonyl)(methyl)amino)propanamido)-*N*,4-dimethylpentanamido)-3-(naphthalen-2-yl)acryloyl)glycinate (**4s**)



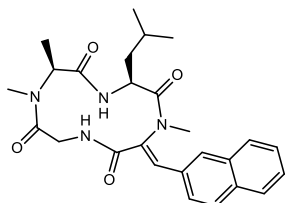
According to general method VII, tetrapeptide **11s** (115.0 mg, 0.20 mmol), K₂CO₃ (273.0 mg, 1.97 mmol), 18-crown-6 (4.8 mg, 0.02 mmol) and methyl iodide (184.0 μ L, 2.96 mmol) were used, giving **4s** (107 mg, 0.18 mmol, 91 %) as a white solid.

HR-MS *m/z* 595.3126 (calculated for C₃₂H₄₃N₄O₇: 595.3137)

¹H NMR (500 MHz, CDCl₃) δ 8.55 (t, *J* = 6.0 Hz, 1H), 7.94 (d, *J* = 1.9 Hz, 1H), 7.90 (s, 1H), 7.89 – 7.83 (m, 2H), 7.86 – 7.77 (m, 1H), 7.59 – 7.46 (m, 3H), 6.53 (s, 1H), 4.68 (s, 1H), 4.39 (ddd, *J* = 11.4, 5.2, 2.5 Hz, 1H), 4.25 – 4.08 (m, 2H), 3.73 (s, 3H), 3.27 (s, 3H), 2.70 (s, 3H), 2.04 (s, 1H), 1.73 (s, 1H), 1.52 – 1.46 (m, 1H), 1.45 (s, 9H), 1.33 – 1.23 (m, 3H), 0.55 (d, *J* = 6.6 Hz, 3H), 0.43 (d, *J* = 6.6 Hz, 3H).

¹³C NMR (126 MHz, CDCl₃) δ 172.26, 171.74, 170.02, 162.55, 156.55, 135.89, 133.90, 133.17, 132.39, 132.00, 129.74, 129.15, 128.79, 127.84, 127.63, 126.89, 125.47, 80.73, 52.51, 52.02, 51.05, 41.87, 38.71, 34.62, 29.46, 28.30 (3C), 24.77, 23.01, 20.35, 13.27.

(3*S*,6*S*,*Z*)-3-Isobutyl-1,6,7-trimethyl-12-(naphthalen-2-ylmethylene)-1,4,7,10-tetraazacyclododecane-2,5,8,11-tetraone (**5s**)



According to general method V, compound **4s** (95.0 mg, 0.16 mmol), lithium hydroxide hydrate (33.0 mg, 0.8 mmol), 4-DMAP (87.5 mg, 0.78 mmol), T3P (50 % w/w in EtOAc, 155 μ L, 0.52 mmol) and DCM (32 mL) were used, giving **5s** (27.5 mg, 0.06 mmol, 37 %) as a white solid. A sample was purified by semipreparative RP-HPLC for biological assays and characterization.

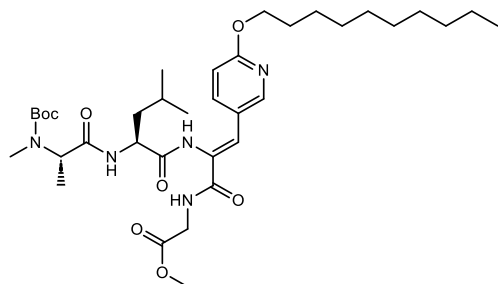
HR-MS *m/z* 463.2350 (calculated for C₂₆H₃₁N₄O₄: 463.2351)

*t*_R = 10.18 min (5 % ACN (0 min) > 100 % ACN (15 min) > 100 % ACN (20 min))

¹H NMR (400 MHz, CDCl₃) δ 8.10 (s, 1H), 7.97 (s, 1H), 7.92 (s, 1H), 7.90 – 7.79 (m, 3H), 7.54 (tt, *J* = 6.9, 5.5 Hz, 2H), 7.42 (dd, *J* = 8.7, 1.4 Hz, 1H), 7.26 (s, 1H), 5.28 – 5.16 (m, 1H), 4.41 (d, *J* = 5.1 Hz, 1H), 3.64 (d, *J* = 5.5 Hz, 1H), 3.27 (s, 3H), 2.90 – 2.74 (m, 3H), 1.55 (d, *J* = 7.1 Hz, 3H), 1.40 – 1.29 (m, 2H), 1.24 (s, 2H), 0.54 (d, *J* = 6.3 Hz, 3H), 0.37 (d, *J* = 6.2 Hz, 3H).

^{13}C NMR (101 MHz, CDCl_3) δ 171.64, 170.03, 164.63, 159.11, 136.92, 134.05, 133.27, 131.86, 130.81, 129.40, 129.28, 128.84, 127.85, 127.58, 126.89, 124.81, 70.46, 56.90, 49.66, 44.54, 40.61, 35.53, 30.22, 24.56, 22.06, 15.59.

Methyl ((Z)-2-((S)-2-((S)-2-((tert-butoxycarbonyl)(methyl)amino)propanamido)-4-methylpentan-amido)-3-(6-(decyloxy)pyridin-3-yl)acryloyl)glycinate (**11t**)



According to general method VI, tetrapeptide **10** (150 mg, 0.27 mmol), TMG (84.9 μL , 0.68 mmol) and 6-(decyloxy)nicotinaldehyde (142.2 mg, 0.54 mmol) were used. Purification was done by column chromatography on silica gel (*n*-hexane / EtOAc 6:4 – 3:7), giving **11t** (159.0 mg, 0.23 mmol, 85 %) and the corresponding (*E*)-isomer (5.0 mg, 0.007 mmol, 2.7 %) as white solids.

HR-MS m/z 688.4290 (calculated for $\text{C}_{36}\text{H}_{58}\text{N}_5\text{O}_8$: 688.4291)

(*Z*)-Isomer

^1H NMR (400 MHz, $(\text{CD}_3)_2\text{SO}$) δ 8.31 (d, J = 2.4 Hz, 1H), 8.24 (t, J = 5.9 Hz, 1H), 8.06 (d, J = 34.0 Hz, 1H), 7.90 (dd, J = 8.8, 2.5 Hz, 1H), 7.21 (s, 1H), 6.76 (d, J = 8.7 Hz, 1H), 4.58 (s, 1H), 4.26 (t, J = 6.6 Hz, 2H), 4.01 – 3.78 (m, 2H), 3.64 (s, 1H), 3.32 (s, 3H), 2.75 (s, 3H), 1.70 (p, J = 6.7 Hz, 2H), 1.63 – 1.48 (m, 1H), 1.38 (s, 12H), 1.33 – 1.21 (m, 18H), 0.93 (d, J = 6.2 Hz, 3H), 0.90 – 0.81 (m, 6H).

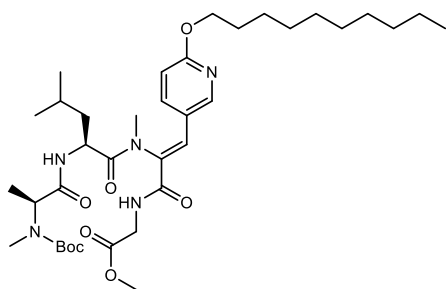
^{13}C NMR (101 MHz, $(\text{CD}_3)_2\text{SO}$) δ 171.88, 170.11, 164.83, 163.17, 155.41, 154.34, 148.67, 139.30, 127.91, 126.93, 123.36, 110.28, 78.92, 65.65, 53.22, 51.85, 51.69, 41.22, 31.26, 30.25, 28.96, 28.91, 28.72, 28.65, 28.39, 27.97 (3C), 25.46, 24.04, 22.94, 22.06, 21.47, 15.27, 13.93.

(*E*)-Isomer (side product)

^1H NMR (500 MHz, $(\text{CD}_3)_2\text{SO}$) δ 9.71 (s, 1H), 8.56 (t, J = 5.8 Hz, 1H), 8.06 (d, J = 2.5 Hz, 1H), 7.73 (dd, J = 8.8, 2.5 Hz, 1H), 6.74 (s, 1H), 6.68 (d, J = 8.7 Hz, 1H), 4.40 (s, 2H), 4.22 (t, J = 6.6 Hz, 2H), 3.82 (d, J = 5.8 Hz, 2H), 3.64 (s, 3H), 2.75 (s, 3H), 1.68 (p, J = 6.8 Hz, 2H), 1.58 – 1.45 (m, 1H), 1.38 (s, 10H), 1.26 (q, J = 9.5, 6.3 Hz, 19H), 0.92 – 0.82 (m, 9H).

^{13}C NMR (126 MHz, $(\text{CD}_3)_2\text{SO}$) δ 171.14, 169.81, 164.84, 162.23, 155.00, 154.80, 146.77, 138.45, 131.16, 123.89, 114.68, 109.89, 78.89, 69.77, 65.39, 53.45, 51.68, 51.22, 41.08, 31.26, 30.11, 28.97, 28.92, 28.76, 28.66, 28.47, 27.98 (3C), 25.51, 24.12, 23.18, 22.07, 21.25, 15.48, 13.94.

Methyl ((Z)-2-((S)-2-((S)-2-((*tert*-butoxycarbonyl)(methyl)amino)propanamido)-*N*,4-dimethylpentanamido)-3-(6-(decyloxy)pyridin-3-yl)acryloyl)glycinate (**4t**)



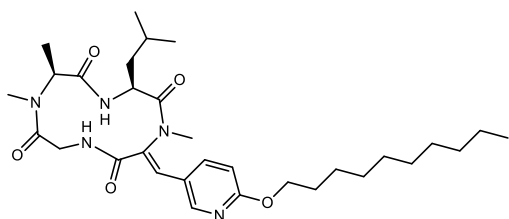
According to general method VII, tetrapeptide **11t** (145 mg, 0.20 mmol), K₂CO₃ (276.4 mg, 2.00 mmol), 18-crown-6 (4.8 mg, 0.02 mmol) and methyl iodide (196 μ L, 3.15 mmol) were used, giving **4t** (143 mg, 0.20 μ mol, 97 %) as a white solid.

HR-MS *m/z* 702.4445 (calculated for C₃₇H₆₀N₅O₈: 702.4447)

¹H NMR (500 MHz, DMSO) δ 8.64 (t, *J* = 5.9 Hz, 1H), 8.21 (d, *J* = 2.4 Hz, 1H), 7.60 (dd, *J* = 8.8, 2.4 Hz, 1H), 7.51 (s, 1H), 6.79 (d, *J* = 8.8 Hz, 1H), 4.65 (d, *J* = 11.0 Hz, 1H), 4.31 – 4.20 (m, 2H), 3.95 (d, *J* = 5.8 Hz, 2H), 3.65 (s, 3H), 2.98 (s, 3H), 2.46 (s, 3H), 1.77 – 1.63 (m, 4H), 1.41 – 1.11 (m, 29H), 0.93 – 0.67 (m, 9H).

¹³C NMR (126 MHz, DMSO) δ 172.76, 170.06, 164.09, 163.91, 155.05, 149.83, 138.96, 132.00, 131.55, 130.65, 122.23, 111.02, 78.87, 65.86, 53.03, 51.80, 48.39, 46.74, 41.47, 33.89, 31.32, 29.03, 29.00, 28.97, 28.76, 28.72, 28.41, 27.99, 25.52, 25.46, 23.71, 23.36, 22.69, 22.13, 20.99, 15.53, 13.99.

(3*S*,6*S*,*Z*)-12-((6-(Decyloxy)pyridin-3-yl)methylene)-3-isobutyl-1,6,7-trimethyl-1,4,7,10-tetraazacyclododecane-2,5,8,11-tetraone (**5t**)



According to general method V, compound **4t** (140 mg, 0.20 mmol), lithium hydroxide hydrate (41.7 mg, 0.99 mmol), 4-DMAP (223.3 mg, 1.99 mmol), T3P (50 % w/w in EtOAc, 273 μ L, 0.80 mmol) and DCM (40 mL) were used, giving **5t** (11.6 mg, 0.02 mmol, 10 %) as a white solid. A sample was purified by semipreparative RP-HPLC for biological assays and characterization.

*t*_R = 16.54 min (5 % ACN (0 min) > 100 % ACN (15 min) > 100 % ACN (20 min))

HR-MS *m/z* 570.3663 (calculated for C₃₁H₄₈N₅O₅: 570.3661)

¹H NMR (400 MHz, CDCl₃) δ 8.28 (d, *J* = 2.5 Hz, 1H), 7.98 (s, 1H), 7.70 (s, 1H), 7.53 (dd, *J* = 8.9, 2.6 Hz, 1H), 7.23 – 7.11 (m, 1H), 6.75 (d, *J* = 8.8 Hz, 1H), 5.18 (t, *J* = 13.0 Hz, 1H), 4.33 (t, *J* = 6.7 Hz, 3H), 4.22 – 4.03 (m, 1H), 3.58 (d, *J* = 15.1 Hz, 1H), 3.16 (s, 3H), 2.82 (s, 3H), 1.80 – 1.69 (m, 3H), 1.53 (d,

$J = 7.1$ Hz, 3H), 1.45 – 1.20 (m, 15H), 0.88 (t, $J = 6.8$ Hz, 4H), 0.71 (d, $J = 6.4$ Hz, 3H), 0.59 (d, $J = 6.5$ Hz, 3H).

^{13}C NMR (101 MHz, CDCl_3) δ 171.58, 170.02, 165.24, 164.34, 150.90, 137.54, 133.62, 129.83, 121.19, 112.09, 66.80, 56.90, 49.61, 44.45, 41.09, 35.12, 31.87, 30.19, 29.55, 29.54, 29.35, 29.29, 28.88, 25.95, 24.64, 22.65, 22.40, 22.12, 15.57, 14.09.

References

- (1) Fulton, N. D., Bollenbacher, K., Templeton, G. E. *Phytopathology* **1965**, 49–51.
- (2) La Kim, E.; Li, J. L.; Xiao, B.; Hong, J.; Yoo, E. S.; Yoon, W. D.; Jung, J. H. *Chem. Pharm. Bull.* **2012**, 60, 1590–1593.
- (3) Templeton, G. E., Grable C. I., Fulton N. D., Bollenbacher K. *Phytopathology* **1967**, 516–518.
- (4) Durbin, R. D. *Phytopathology* **1977**, 77, 602.
- (5) Dahse, I.; Pezennec, S.; Girault, G.; Berger, G.; André, F.; Liebermann, B. *J. Plant Physiol.* **1994**, 143, 615–620.
- (6) Steele, J. A.; Uchytel, T. F.; Durbin, R. D.; Bhatnagar, P.; Rich, D. H. *PNAS* **1976**, 73, 2245–2248.
- (7) Arntzen, C. J. *BBA* **1972**, 283, 539–542.
- (8) Hu, N.; Mills, D. A.; Huchzermeyer, B.; Richter, M. L. *J. Biol. Chem.* **1993**, 268, 8536–8540.
- (9) Cavelier, F.; Enjalbal, C.; Santolini, J.; Haraux, F.; Sigalat, C.; Verducci, J.; André, F. *Lett. Pept. Sci.* **1997**, 4, 283–288.
- (10) Tucker, W. C.; Du, Z.; Hein, R.; Gromet-Elhanan, Z.; Richter, M. L. *Biochemistry* **2001**, 40, 7542–7548.
- (11) Klotz, M. G. *Physiol. Plant.* **1988**, 74, 575–582.
- (12) Klotz, M. G.; Erdei, L. *Physiol. Plant.* **1988**, 72, 298–304.
- (13) Meyer, W. L.; Kuyper, L. F.; Lewis, R. B.; Templeton, G. E.; Woodhead, S. H. *Biochem. Biophys. Res. Com.* **1974**, 56, 234–240.
- (14) Pinet, E.; Neumann, J. M.; Dahse, I.; Girault, G.; André, F. *Biopolymers* **1995**, 36, 135–152.
- (15) Siodlak, D. *Amino Acids* **2015**, 47, 1–17.
- (16) Hamada, Y.; Shioiri, T. *Chem. Rev.* **2005**, 105, 4441–4482.
- (17) Edler, M. C.; Fernandez, A. M.; Lassota, P.; Ireland, C. M.; Barrows, L. R. *Biochem. Pharmacol.* **2002**, 63, 707–715.
- (18) Ballio, A.; Barra, D.; Bossa, F.; Collina, A.; Grgurina, I.; Marino, G.; Moneti, G.; Paci, M.; Pucci, P.; Segre, A. *FEBS letters* **1991**, 291, 109–112.
- (19) Matsuda, S.; Koyasu, S. *Immunopharmacology* **2000**, 47, 119–125.
- (20) Yokoi, K.; Nagaoka, K.; Nakashima, T. *Chem. Pharm. Bull.* **1986**, 34, 4554–4561.
- (21) Bonauer, C.; Walenzyk, T.; König, B. *Synthesis* **2006**, 2006, 1–20.
- (22) Beltzig, R.; Klotz, M. G.; Müller, E.; Liebermann, B. *Biochem. Physiol. Pflanz.* **1984**, 179, 707–709.
- (23) Liebermann, B.; Ihn, W.; Baumann, E.; Tresselt, D. *Phytochemistry* **1988**, 27, 357–359.
- (24) Liebermann, B.; Ihn, W. *J. Basic Microbiol.* **1988**, 28, 63–70.
- (25) Rich, D. H.; Tam, J. P. *J. Org. Chem.* **1977**, 42, 3815–3820.
- (26) Nanjo, T.; Oshita, T.; Matsumoto, A.; Takemoto, Y. *Chemistry* **2022**, 28, e202201120.
- (27) Schmidt, U.; Lieberknecht, A.; Wild, J. *Synthesis* **1984**, 1984, 53–60.
- (28) Schmidt, U.; Griesser, H.; Leitenberger, V.; Lieberknecht, A.; Mangold, R.; Meyer, R.; Riedl, B. *Synthesis* **1992**, 1992, 487–490.
- (29) Itoh, H.; Miura, K.; Kamiya, K.; Yamashita, T.; Inoue, M. *Angew. Chem. Int. Ed. Engl.* **2020**, 59, 4564–4571.
- (30) Kuranaga, T.; Sesoko, Y.; Sakata, K.; Maeda, N.; Hayata, A.; Inoue, M. *J. Am. Chem. Soc.* **2013**, 135, 5467–5474.
- (31) Rich, D. H.; Mathiaramanam, P. *Tetrahedron Lett.* **1974**, 15, 4037–4040.
- (32) Jacquier, R.; Verducci, J. *Tetrahedron Lett.* **1984**, 25, 2775–2778.

- (33) Edwards, J. V.; Lax, A. R.; Lillehoj, E. B.; Boudreaux, G. J. *Int. J. Pept. Protein Res.* **1986**, 28, 603–612.
- (34) Cavelier, F.; Verducci, J. *ChemInform* **1995**, 26, 4425–4428.
- (35) Loiseau, N.; Cavelier, F.; Noel, J.-P.; Gomis, J.-M. *J. Pept. Sci.* **2002**, 8, 335–346.
- (36) Jiménez, J. C.; Chavarría, B.; López-Macià, A.; Royo, M.; Giralt, E.; Albericio, F. *Org. Lett.* **2003**, 5, 2115–2118.
- (37) Neves Filho, R. A. W. *Total synthesis of natural products with Ugi reactions*; Universitäts- und Landesbibliothek Sachsen-Anhalt, **2015**.
- (38) Pooppanal, S. *Synlett* **2009**, 850–851.
- (39) Martin J. C., Arhart R. J., Franz J. A., Perozzi E. F., Kaplan L. J. *Org. Synth.* **1977**, 57, 22.
- (40) Irabuena, C.; Posada, L.; Rey, L.; Scarone, L.; Davyt, D.; Villalba, J.; Serra, G. *Molecules* **2022**, 27.
- (41) Ugi, I. *Angew. Chem. Int. Ed. Engl.* **1962**, 1, 8–21.
- (42) Wessjohann, L. A.; Rivera, D. G.; Vercillo, O. E. *Chem. Rev.* **2009**, 109, 796–814.
- (43) Horner, L.; Hoffmann, H.; Wippel, H. G. *Ber.* **1958**, 91, 61–63.
- (44) Wadsworth, W. S.; Emmons, W. D. *J. Am. Chem. Soc.* **1961**, 83, 1733–1738.
- (45) Wadsworth, W. S. Synthetic Applications of Phosphoryl-Stabilized Anions. In *Organic Reactions*, **1977**, 73–253.
- (46) Saavedra, C. J.; Hernández, D.; Boto, A. *Chemistry* **2018**, 24, 599–607.
- (47) Groth, G. *PNAS* **2002**, 99, 3464–3468.
- (48) Liebermann, B.; Ellinger, R.; Pinet, E. *Phytochemistry* **1996**, 42, 1537–1540.
- (49) Murar, C. E.; Harmand, T. J.; Bode, J. W. *Bioorg. Med. Chem.* **2017**, 25, 4996–5001.
- (50) Song, X.; Zhang, X.; Zhang, S.; Li, H.; Wang, W. *Chem. Eur. J.* **2012**, 18, 9770–9774.
- (51) Borsari, C.; Trader, D. J.; Tait, A.; Costi, M. P. *J. Med. Chem.* **2020**, 63, 1908–1928.
- (52) Lautenslager, G. T.; Simpson, L. L. Chimeric Molecules Constructed with Endogenous Substances. In *Advances in Molecular and Cell Biology : Homing Mechanisms and Cellular Targeting*; Bittar, E. E.; Zetter, B. R., Eds.; Elsevier, **1994**, 233–262.
- (53) OECD. *Test No. 221: Lemna sp. Growth Inhibition Test*; OECD Publishing, Paris, **2006**.
- (54) Blaise, C.; Féraud, J.-F. *Small-scale Freshwater Toxicity Investigations: Toxicity Test Methods*; Springer, Dordrecht, **2005**.
- (55) Ekperusi, A. O.; Sikoki, F. D.; Nwachukwu, E. O. *Chemosphere* **2019**, 223, 285–309.
- (56) Schubert, R.; Hilbig, W.; Klotz, S. *Bestimmungsbuch der Pflanzengesellschaften Deutschlands*, 2. Auflage; Spektrum Akademie Verlag, Heidelberg, **2010**.
- (57) Artetxe, U.; García-Plazaola, J. I.; Hernández, A.; Becerril, J. M. *Plant Physiol. Biochem.* **2002**, 40, 859–863.
- (58) Geissler, T.; Wessjohann, L. A. *J. Plant Growth Regul.* **2011**, 30, 504–511.
- (59) *Cold Spring Harb. Protoc.* **2021**, 2021, pdb.rec107177.
- (60) Lentz, B. R. *Eur. Biophys. J.* **2007**, 36, 315–326.
- (61) Cavelier, F.; Verducci, J.; André, F.; Haraux, F.; Sigalat, C.; Traris, M.; Vey, A. *Pestic. Sci.* **1998**, 52, 81–89.
- (62) *Chemical Computing Group ULC. Molecular Operating Environment (MOE), 2022.02.* **2022**.
- (63) Onufriev, A. V.; Case, D. A. *Annu. Rev. Biophys.* **2019**, 48, 275–296.
- (64) Ponder, J.; Case, D. A. *Adv. Protein Chem.* **2003**, 2003, 27–85.
- (65) Hoffmann, R. *Chem. Phys.* **1963**, 39, 1397–1412.
- (66) Yang, J.-H.; Williams, D.; Kandiah, E.; Fromme, P.; Chiu, P.-L. *Commun. Biol.* **2020**, 3, 482.

Chapter 3

Synthesis and biological evaluation of niacin derivatives as a new class of nature-inspired herbicides

Abstract

6-Alkoxy-modified nicotinic acids were found to possess excellent herbicidal activities. A total of 54 derivatives with different side-chains, functional groups and substitution patterns were prepared, mostly by a microwave-assisted condensation. All compounds were tested *in vivo* towards their growth inhibition activity against *Lemna minor*, in which 6-(*n*-octyloxy) niacin (**7**) showed the lowest ED₅₀ value of 2.3 μ M. Also, derivatives of picolinic acid and isonicotinic acid were found to possess promising herbicidal activities. Furthermore, several substances were found to have moderate antifungal activities against *Septoria tritici*, *Botrytis cinerea* and *Phytophthora infestans*.

Introduction

Heterocyclic compounds are widespread in nature. Prominent members are alkaloids, which are basic, nitrogen-containing cyclic natural products. Alkaloids are known for their wide range of biological activities and have often provided the template for various bioactive compounds including many marketed pharmaceuticals. For example, of all the small-molecule drugs approved by the FDA in 2014, 59 % contained a nitrogen heterocycle.^{1,2} Pyridine-based substances are also known for their diverse range of activities. In nature, they have significant roles in various biological processes, from acting as vitamins or coenzymes to controlling the metabolism or defence mechanisms and signalling in living organisms. Furthermore, many synthetic bioactive compounds contain pyridine derivatives as core components.³ These may be synthesized based on or inspired by naturally occurring compounds or designed to target specific biological processes. Often the pyridine ring was used to replace benzene to produce bioisosteres with improved properties like water solubility.⁴ This is because molecules containing the pyridine moiety usually have a basic character, are more polar (hydrophobic constants: pyridine log P = 0.65 vs benzene log P = 2.13), hydrophilic, and electron-deficient which can lead to better bioactivities and lower toxicities (but also can have the opposite effect), all tuneable by pH.

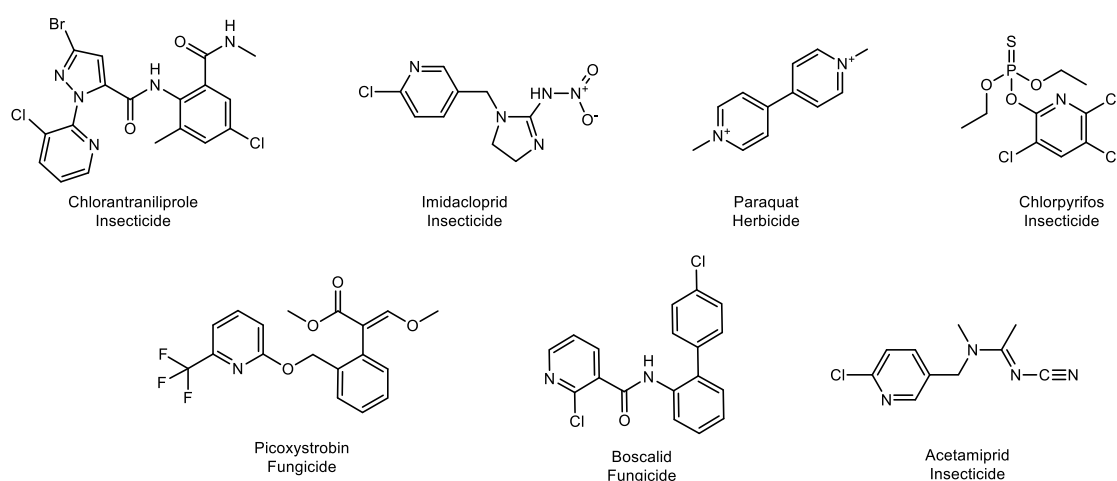


Figure 14: The top seven pyridine-based commercial pesticides (as of 2019).

Agrochemicals, which contain the pyridine moiety in their structure, also account for a large proportion of all pesticides.⁵ As such, seven of these substances were among the top 45 pesticides used worldwide, with total sales of 5 billion USD and a market share of around 10 % in 2019. Also, two of these substances are among the top 10, which are: chlorantraniliprole (insecticide, #2, 1.8 billion USD) and imidacloprid (insecticide, #8, 0.9 billion USD).⁶ The only pyridine-containing herbicide in this list is paraquat, one of the oldest synthetic herbicides and still the seventh best-selling herbicide in 2019 despite bans in numerous countries due to its high toxicity to warm-blooded animals. Paraquat was found as early as 1958 when the biological activity of quaternary ammonium salts was studied.⁷

Substitution of pyridine leads to a variety of other interesting substance classes. Among these are the group of pyridinecarboxylic acids, which are picolinic acid (2-pyridinecarboxylic acid), niacin (3-pyridinecarboxylic acid) and isonicotinic acid (4-pyridinecarboxylic acid).

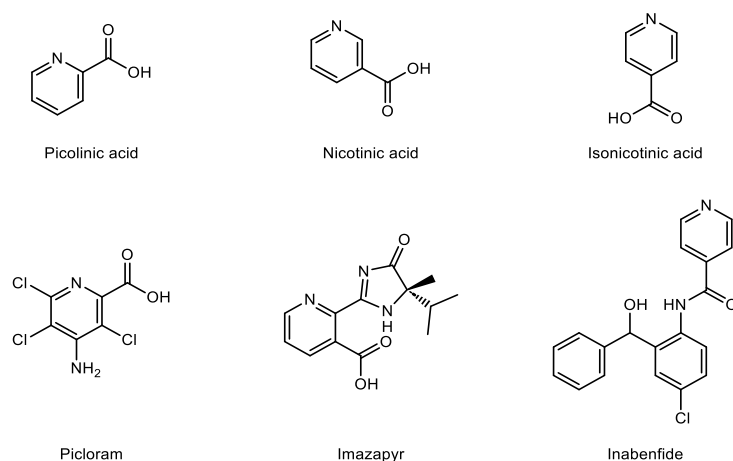


Figure 15: Pyridinecarboxylic acids and commercial herbicides containing their structural element.

Niacin, also known as nicotinic acid, has the greatest biological importance of these three compounds. It is a vitamer and forms together with nicotinamide and nicotinamide riboside vitamin B₃ which is essential for human life and the crucial energy and redox metabolite couples $\text{NAD}^+/\text{NADH}^+$ and $\text{NADP}^+/\text{NADPH}^+$. It is also found in plants, particularly in cereal grains where it is bound to sugar molecules as glycoside.⁸ In medicine, niacin is used as a drug to treat or prevent pellagra, which is caused by a deficiency of vitamin B3.⁹

For the development of agrochemicals, it also serves as an important structural element in many active ingredients. These include the herbicides imazapyr (see Figure 15) and thiazopyr, which are mentioned here exemplarily. Currently, niacin triketones, which act as inhibitors of 4-hydroxyphenylpyruvate dioxygenase (HDDP), are also being developed in research.^{10,11} In contrast, 4-alkyl- and alkyloxy-substituted niacin derivatives have not yet been described as pesticides.

Results and discussion

A library of compounds was synthesised to investigate the herbicidal activity of niacin derivatives, starting with 6-decyloxy niacin (**9**) from which a herbicidal activity was initially observed as part of a drought tolerance enhancer screening. The synthesis of this compound could be easily achieved with 6-chloro niacin and 1-decanol using a nucleophilic aromatic substitution (S_NAr).¹² Optimizations were performed using different temperatures, solvents, bases, stoichiometries and microwave irradiation (see Table 3).

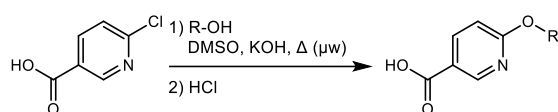


Figure 16: Synthesis of different niacin derivatives.

6-Chloro niacin was chosen as substrate since it already contains the pyridine core as well as the carboxyl group and allows easy functionalization at the 6-position which facilitates the rapid synthesis of various derivatives.

Table 3: Reaction screening for the synthesis of **9**.

#	Temp [°C]	Base	Solvent	Time [h]	μw irr.	Yield (%)
I	reflux	KOH 5 eq	DMSO	12	No	83
II	80	KOH 5 eq	DMSO	1	Yes	37
III	100	KOH 5 eq	DMSO	1	Yes	80
IV	120	KOH 5 eq	DMSO	0.5	Yes	93
V	140	KOH 5 eq	DMSO	0.5	Yes	93
VI	120	KOH 5 eq	Toluene	0.5	Yes	56
VII	120	KOH 5 eq	none	0.5	Yes	-
VIII	120	-	DMSO	0.5	Yes	-
IX	120	NaH	DMSO	12	No	87

These optimizations revealed that increased yields can be achieved using two equivalents of alcohol and five equivalents of potassium hydroxide as base for the ether synthesis. By performing the coupling in a microwave oven (details see experimental part), the reaction time can be reduced to as short as 30 minutes at 120 °C while increasing the conversion rate. Acidifying the reaction mixture in water led to the precipitation of the desired product as pure hydrochloride without further purification.

Table 2: Synthesis of various niacin derivatives with modified side-chain.

#	C-6 side chain	Yield [%]
1		69
2		68
3		84
4		88
5		56
6		84
7		87
8		91
9		84
10		91
11		78
12		67
13		72
14		66
15		54
16		70
17		85
18		83
19		55
20		68
21		77
22		80
23		56

Modifications of the alkoxy side-chain

These optimized reaction conditions were used for the synthesis of different derivatives by altering the C-6 side-chain. Depending on the lengths and properties of the side-chain, an additional extraction and purification step had to be performed since more polar molecules did not precipitate after acidification.

The side-chains varied from C₁ to C₁₆ aliphatic chains as well as acyclic branched and unsaturated, or cyclic substituents (see Table 2). Furthermore, derivatives with polyethylene glycol (**19** and **23**), and ω -hydroxylated side-chains (**22**) were synthesized to increase the hydrophilicity of the molecules whilst keeping the chain length similar. This could improve its viability as agrochemicals and its biotic breakdown and also give hints on the importance of membrane permeation. All substances were synthesized using the reaction conditions optimized for the C₁₀ side-chain established before. Noteworthy is the synthesis of substance **17**, which was intended to yield the derivative with a terminal triple bond by reaction of the substrate with 5-hexyn-1-ol. During the synthesis, a shift of the terminal triple bond was observed.

Further modifications of the side-chain

In the next step, the side-chain was further modified. For this purpose, the heteroatom of the alcohol was exchanged. The thiol ether **24** was easily prepared using the corresponding octanethiol as coupling partner.

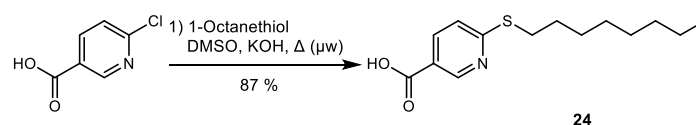


Figure 17: Synthesis of thiol derivative **24**.

Subsequently, the oxygen atom was exchanged with nitrogen. For this purpose, the methyl ester of 6-chloro niacin was used as starting material to avoid side reactions with the free acid. The coupling itself was carried out as a *Buchwald-Hartwig* amination using palladium(II) acetate and XPhos as catalysts.¹³ The subsequently obtained ester was further saponified with the aid of lithium hydroxide.

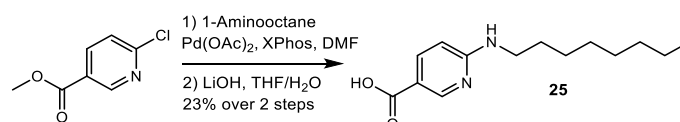


Figure 18: Synthesis of the aminated derivative **25**.

Furthermore, derivatives **26** – **29**, possessing carbon-only side-chains, were prepared. Various C-C coupling reactions were tried to produce the desired derivative **29**, yet most of them failed due to lack of reactivity or complexity of the product mixture. However, with the aid of a *Sonogashira* coupling, the interesting alkyne derivative **26** could be produced first, which was then converted to the desired alkyl derivative **28** by hydrogenation.¹⁴ The final saponification of the ester group led to the two nicotinic acids **27** and **29**.

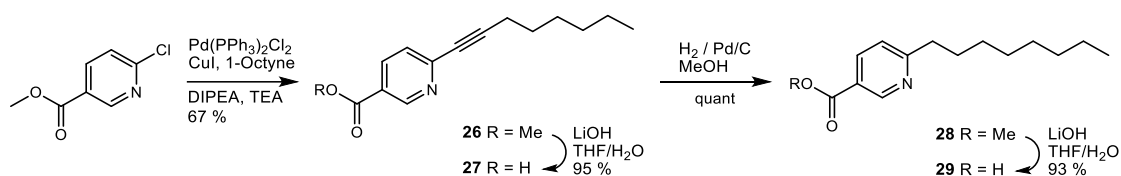


Figure 19: Synthesis of derivatives **26** - **29**.

Finally, different aryl side-chains were coupled to the substrate. By coupling methyl 6-chloro nicotinate with toluene, the corresponding methyl ester **30** could first be produced, which was converted into acid **31** by saponification (see Figure 20).

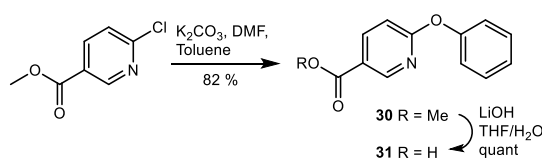


Figure 20: Synthesis of diaryl-derivatives **30** and **31**.

The last coupling product is dimer **32** which can be prepared by coupling two molecules of 6-chloronicotinic acid. Here, the method of *Bamfield* et al. was used, which describes a palladium-catalysed C-C coupling under strongly basic conditions (see Figure 21).^{15,16}

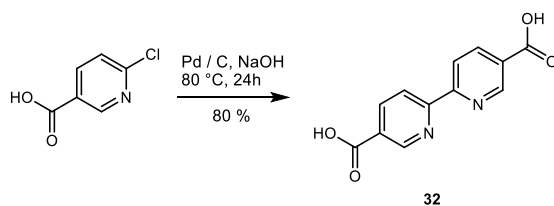


Figure 21: Synthesis of the bipyridyl dimer **32**.

Modification of the functional group

Many commercial herbicides are known to possess a carboxylic acid moiety (i.e. 2,4-dichlorophenoxyacetic acid) and even contain a substituted pyridine ring with an attached carboxylic acid.¹⁷ Examples of this are aminopyralid, imazapyr, picloram among others. But apart from the carboxylic acid and halogenations, not many other functional groups are used in commercial herbicides, which contain a pyridine moiety. To gain more knowledge about the importance of the carboxylic acid function for the herbicidal activity, another series of derivatives was synthesized by altering this functionality (see Figure 22). The easiest approach to a wide range of functionalities are acyl chlorides. Niacin derivative **9** which already possesses a decyloxy side-chain was chosen as substrate for further modifications. The acid chloride **9-Cl** could be prepared by reacting **9** with oxalyl chloride or thionyl chloride which was subsequently reacted with various reagents (see Figure 22).

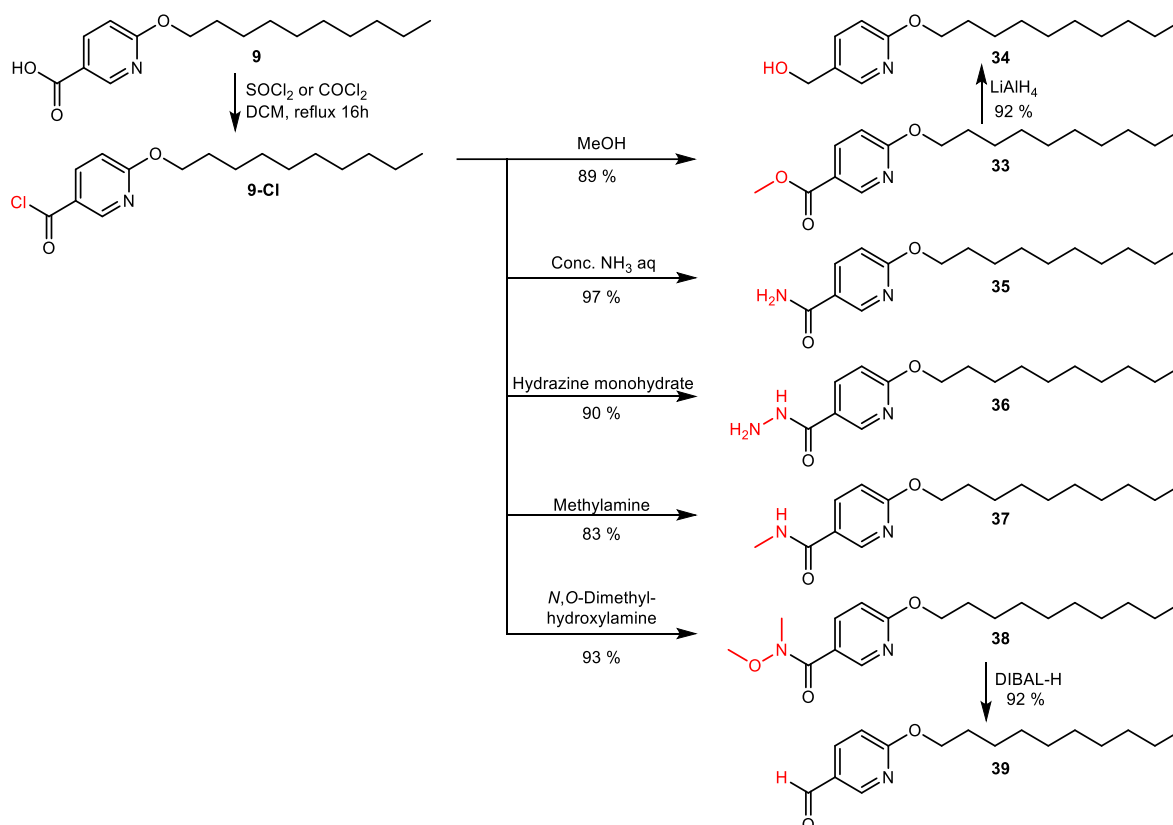


Figure 22: Modification of the carboxylic group.

First, the acid chloride **9-Cl** was reacted with methanol, which gave the methyl ester **33**. The ester could then be reduced to the corresponding nicotinyl alcohol **34** in 92 % yield using lithium aluminium hydride. The corresponding nicotinamide **35** could be obtained by adding the acid chloride to an aqueous ammonia solution. The corresponding hydrazide **36** was obtained by treatment of the acid chloride in a methanolic solution of hydrazine monohydrate with microwave radiation at 110 °C for one hour. The methyl amide **37** could be synthesised using a methyl amine solution. The penultimate derivative is the *Weinreb* amide **38** of the corresponding acid, which was prepared using *N,O*-dimethylhydroxylamine.¹⁸ This amide can serve as a facile starting material for the synthesis of further derivatives such as ketones or the corresponding aldehyde **39**.

Synthesis of bioisosteres of the carboxylic acid

The carboxylic acid group is a valuable component in designing new herbicides, but it can also have negative effects such as instability, toxicity, and difficulty crossing cell membranes.¹⁹ To overcome these issues while still utilizing the benefits of the carboxylic acid group, drug designers often explore similar chemical structures with comparable bioactivity, known as bioisosteres.²⁰ There are various options for carboxylic acid isosteres, but it is difficult to predict the outcome of this substitution strategy since it depends on the specific context.²¹ In the following, the synthesis of three bioisosteres that replace the carboxylic acid with a nitro, tetrazole or triketo group is described.

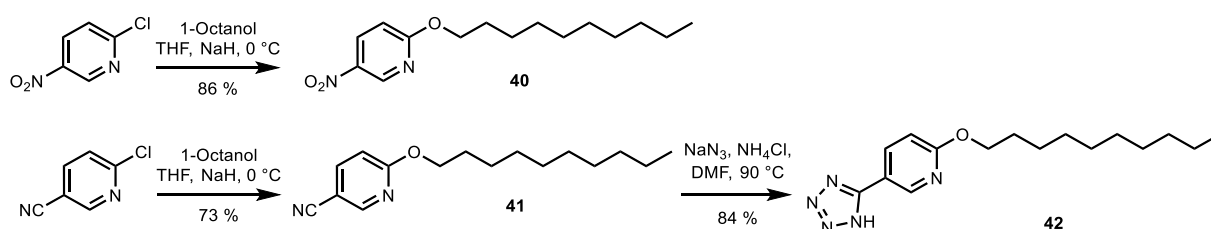


Figure 23: Synthesis of the nitro, cyano and tetrazole derivatives **40** - **42**.

The 6-ether modified derivative **40** was prepared by using 6-chloro-3-nitropyridine. The nitro group facilitates the coupling with octanol, which could be performed even at 0 °C in high yield. For the preparation of the tetrazole derivative **42**, 2-chloro-5-cyanopyridine was used first, which was reacted analogously with octanol in the presence of sodium hydride to give **41**. Subsequently, the cyano group was converted into the desired tetrazole derivative **42** with the aid of sodium azide.

Synthesis of potential 4-hydroxyphenylpyruvate dioxygenase inhibitor **44**

In the literature, niacin derivatives with modified carboxylic acid moieties are known to act as inhibitors of 4-hydroxyphenylpyruvate dioxygenase.^{11,22,23} These belong to the herbicide subgroup of so-called triketones, in which the acid group is replaced by a triketone, which significantly influences the inhibitory activity. To check for combinatory effects between the triketone functionality with the activity of the new alkyloxy niacin derivatives, the chimera **44** was synthesized (see Figure 24).

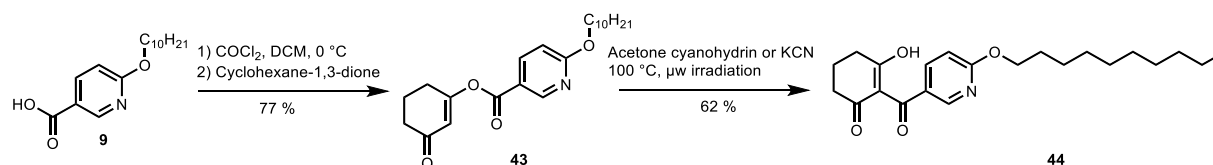


Figure 24: Synthesis of the niacin triketone derivative **44**.

The starting point of the synthesis is 4-decyloxy niacin **9**, which was first activated with oxalyl chloride and then coupled to cyclohexane-1,3-dione. The resulting intermediate **43** could then be rearranged to the desired triketone **44** via a *Fries*-rearrangement catalysed by cyanide. This reaction is described to run at room temperature normally. But in our hands no conversion could be observed, and a thermal activation in combination with microwave irradiation was necessary. The cyanide source for this reaction can be catalytic potassium cyanide or acetone cyanohydrin.

Modification of the aromatic core

Until now, only the influence of alkyloxy side-chains attached to niacin in *para*-position to the carboxylic acid was investigated. By altering the position of the two substituents at the pyridine ring, 10 different molecules are conceivable. From this, eight regioisomers using different substituted pyridine carboxylic acids were synthesized (see Table 4).

Since the preliminary biological assays had shown that compound **7** with an octyloxy side-chain had the highest activity, the regioisomers were also synthesized with the same C₈ side-chain.

The synthesis itself was performed as described before by using the microwave approach for the nucleophilic aromatic substitution. The variety of resulting regioisomers was only limited by commercial availability and affordability of the necessary substrates. Additionally, compounds **52** and **53** were synthesized in the same manner. **52** possesses a pyrimidine core whereas **53** has a further chloro substituent which does not substitute under this reaction conditions. For comparison reason, the benzoic acid derivative **54** was synthesised as well.

Table 4: Structures of derivatives with modified aromatic core.

#	Structure	Yield [%]
7		94
45		82
46		85
47		88
48		77
49		80
50		83
51		71
52		67
53		33
54		72

Biological activity

Herbicidal activity

To investigate the biological activity of the synthesized niacin derivatives, the compounds were tested in several bioassays. The most promising test is the herbicidal activity assay, which was conducted *in vivo* on duckweed (*Lemna minor*). Duckweed is a widely used test organism for toxicity testing because it has favourable physiological characteristics (fast growth, small size, flat leaf surface and vegetative propagation).²⁴ For this purpose, plants were grown in medium and then exposed to different concentrations of the compounds (100 μM - 0.01 μM) for 4 days. Then, to determine the growth inhibition, the size of the leaf surfaces was compared with the initial size. After the initial screening, all compounds were tested again which showed a growth inhibition higher than 50 % at 10 μM . Those were tested in a second dilution series (10 μM , 8 μM , 6 μM , 4 μM , 2 μM) to determine the ED_{50} value. In general, this assay is used to study growth-inhibiting properties. When testing the niacin derivatives, not only was the growth inhibited but, in most cases, the plants showed complete chlorosis and were deceased.

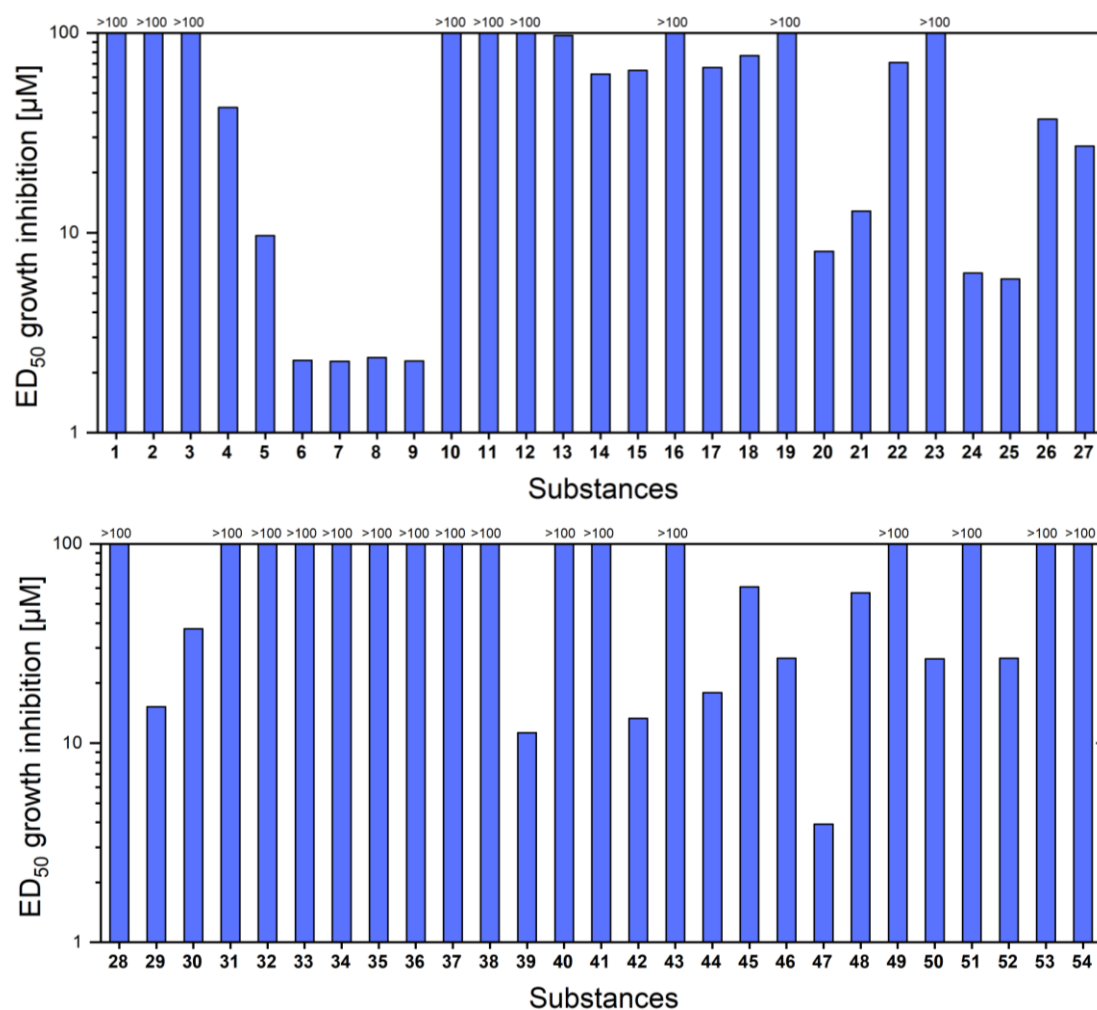


Figure 25: ED_{50} growth inhibition of substances 1 - 54.

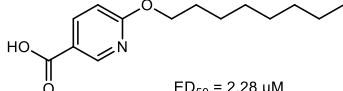
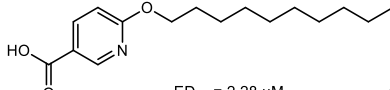
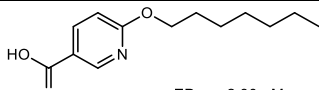
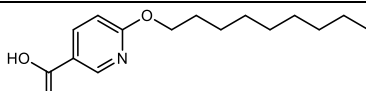
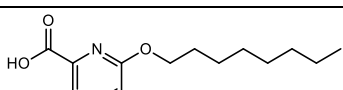
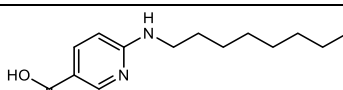
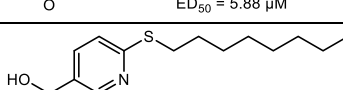
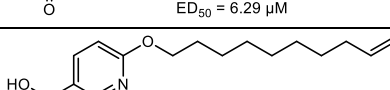
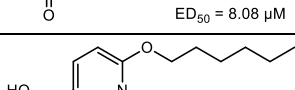
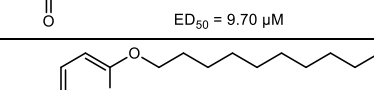
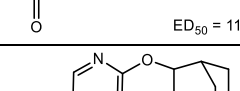
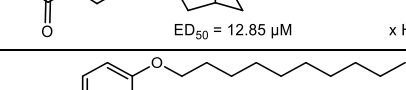
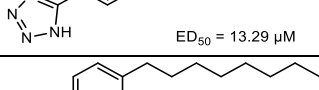
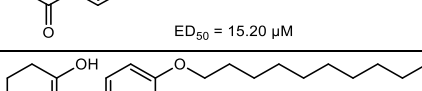
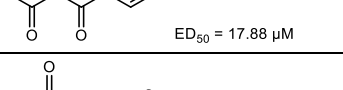
The most active compounds are those niacin derivatives with a side-chain length from C₇ to C₁₀, possessing all a nearly indistinguishable ED₅₀ value of 2.3 – 2.4 µM. The most active of those is the C₈ derivative (ED₅₀ = 2.28 µM).

A shorter side-chain leads to a decreased activity, already the C₆ niacin only possesses an ED₅₀ of 9.7 µM, the C₅ niacin of 42.4 µM and the C₄ derivative lost all herbicidal activity within the tested concentration rate (ED₅₀ > 100 µM). A longer side-chain leads to a similar effect, already the C₁₂ derivative does not show any growth inhibition. The activity furthermore does not reoccur at the doubled lengths (C₁₆ side-chain) which was reported before for other substrates due to folding of the chain. A further elongation of the side-chain leads to a very low polarity which results in a very poor solubility in the test medium and the necessity of additives to even test the compounds. Since no further activity was expected, this particular test series was concluded at C₁₆.

Interestingly, the branching of the side-chain also drastically affects the activity, which shows that not only the molecular weight and polarity are the main factors. The branched C₈ derivative **18** shows only an ED₅₀ value of 76.8 µM (compared to 2.3 µM with linear side-chain). Substituting the C₁₀ side-chain (ED₅₀ = 2.3 µM) with adamantane lowers the value to 12.9 µM. A similar but less strong effect can be observed by changing the linear C₅ (ED₅₀ = 42.4 µM) to a terminal isopropyl (ED₅₀ = 62.1 µM). In contrast, only the branched butyl showed an activity, albeit low, with an ED₅₀ value of 97.0 µM.

Introducing unsaturation also lowers the activity. The derivative **20** with a terminal double bond on the C₁₀ side-chain still strongly inhibits growth (ED₅₀ = 8.1 µM), which is much weaker than the saturated derivative (ED₅₀ = 2.3 µM). Also, a triple bond in derivative **17** (ED₅₀ = 67.0 µM) leads to a strong decrease in activity compared to the corresponding saturated derivative (ED₅₀ = 9.7 µM).

Table 5: Structures and ED₅₀ values of the most active compounds.

7		ED ₅₀ = 2.28 µM	x HCl
9		ED ₅₀ = 2.28 µM	x HCl
6		ED ₅₀ = 2.30 µM	x HCl
8		ED ₅₀ = 2.38 µM	x HCl
47		ED ₅₀ = 3.92 µM	x HCl
25		ED ₅₀ = 5.88 µM	
24		ED ₅₀ = 6.29 µM	
37		ED ₅₀ = 8.08 µM	
5		ED ₅₀ = 9.70 µM	x HCl
39		ED ₅₀ = 11.28 µM	
21		ED ₅₀ = 12.85 µM	x HCl
42		ED ₅₀ = 13.29 µM	
29		ED ₅₀ = 15.20 µM	
44		ED ₅₀ = 17.88 µM	
50		ED ₅₀ = 26.48 µM	

Furthermore, it should be noted that introducing polyethylene glycol side-chains (**19** and **23**) led to a complete loss of activity in the measured range. Replacement of the heteroatom in the side-chain also leads to a decrease in activity, starting with nitrogen **25** ($ED_{50} = 5.9 \mu\text{M}$), to sulphur **24** ($ED_{50} = 6.3 \mu\text{M}$) and a complete carbon chain **29** ($ED_{50} = 15.2 \mu\text{M}$). The latter again shows that an unsaturation as with derivative **27** ($ED_{50} = 27.2 \mu\text{M}$) results in a further lowering of the activity.

Modifying the carboxyl group leads in most cases to a complete loss of herbicidal activity. This underlines the great importance of this functional group in the structure-activity relationship. The exceptions are the following three tested derivatives with a C_8 side-chain. The highest activity was measured for aldehyde **39** ($ED_{50} = 11.3 \mu\text{M}$), which is though not ideal for storage and reactivity reasons. This is directly followed by tetrazole **42** ($ED_{50} = 13.3 \mu\text{M}$). The triketone derivative **44** ($ED_{50} = 17.9 \mu\text{M}$) also still has good activity against *Lemna minor*. Noteworthy is that the methyl ester **33** did not show any activity, whereas the two methyl esters **27** ($ED_{50} = 37.1 \mu\text{M}$) and **30** ($ED_{50} = 37.4 \mu\text{M}$) both showed moderate activities. The latter possessing a phenyloxy side-chain is even more active than its saponified counterpart **31** ($ED_{50} > 100 \mu\text{M}$).

Altering the substitution pattern on the pyridine core also drastically changes the observed herbicidal activities. 6-Substituted nicotinic acid **9** ($ED_{50} = 2.28 \mu\text{M}$) showed the highest activity and also 2-substituted picolinic acid **47** ($ED_{50} = 3.9 \mu\text{M}$) is of high activity. For nicotinic acid derivatives, the activity decreases when the side-chain is attached at the 4-position (**49**, $ED_{50} = 26.5 \mu\text{M}$) and even further at the 2-position (**48**, $ED_{50} = 56.8 \mu\text{M}$). Of the isonicotinic acid derivatives, only compound **46** showed moderate activity ($ED_{50} = 26.6 \mu\text{M}$), similar to pyrimidine **52** ($ED_{50} = 26.6 \mu\text{M}$). Substituted benzoic acid **54** showed no activity ($ED_{50} > 100 \mu\text{M}$).

Antifungal activity

The synthesized compounds **1** – **54** were tested towards their antiphytopathogenic activity against the plant pathogenic fungi *Botrytis cinerea* and *Septoria tritici* and the oomycete *Phytophthora infestans*. Most of the tested compounds showed a strong antiphytopathogenic activity at a high concentration of $125 \mu\text{M}$, especially against *Botrytis cinerea*. When lowering the concentration to $42 \mu\text{M}$ and $14 \mu\text{M}$, only a few compounds still possessed an activity. Compound **28** was identified as the most active substance against *Septoria tritici*, with an inhibition of 94 % at a concentration of $14 \mu\text{M}$.

The substances with the strongest herbicidal activity (see Table 5) are only antimycotic at much higher concentrations. This is advantageous for potential application in the agricultural sector, as the substances are therefore expected not to be harmful to mycorrhiza in the soil. Some compounds like **50** have a good starting activity as fungicide/antioomycotic, but for that purpose, their low herbicidal activity would have to be reduced further.

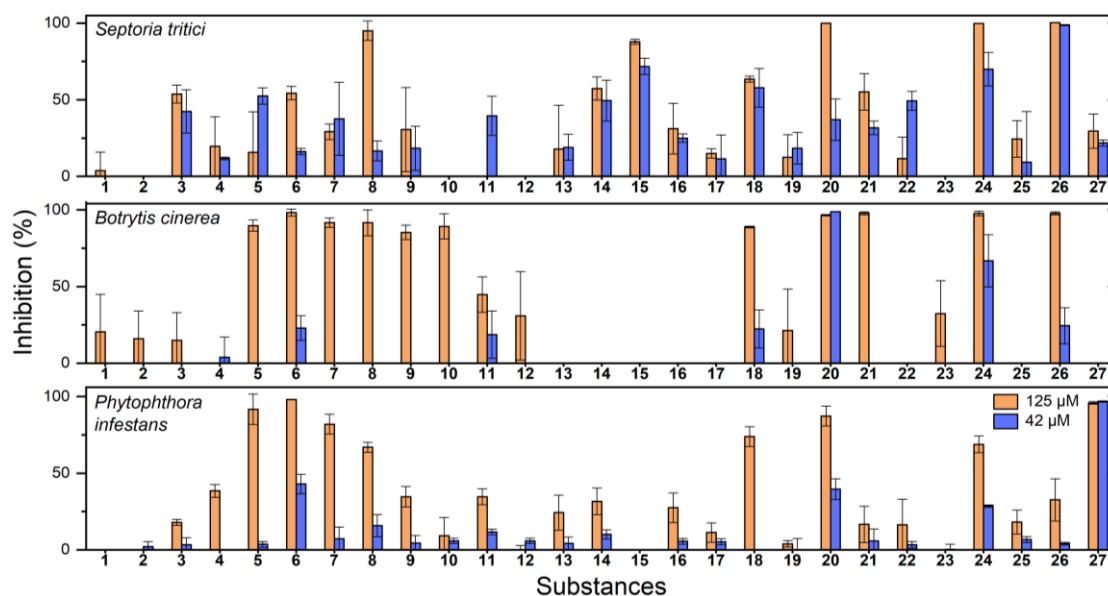


Figure 26: Inhibition of growth for compounds **1 - 27** against *Septoria tritici* (top), *Botrytis cinerea* (middle) and *Phytophthora infestans* (bottom) at different concentrations.

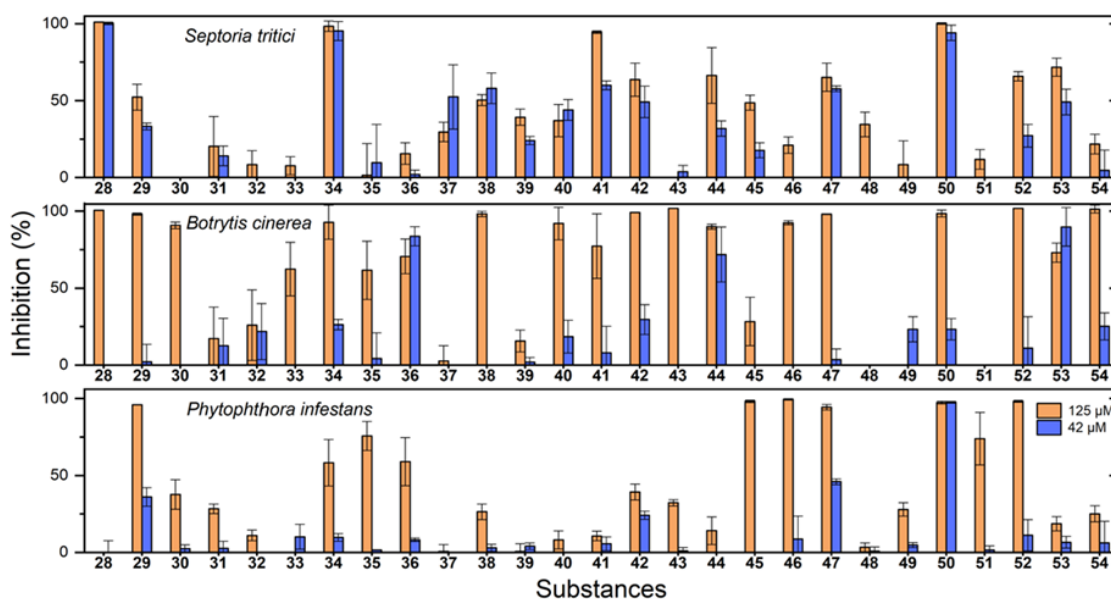


Figure 27: Inhibition of growth for compounds **28 - 54** against *Septoria tritici* (top), *Botrytis cinerea* (middle) and *Phytophthora infestans* (bottom) at different concentrations.

Cytotoxic activity

Anti-proliferative and cytotoxic effects of compounds **1 - 54** were investigated by performing colorimetric MTT (3-(4,5-dimethylthiazol-2-yl)-2,5-diphenyltetrazolium bromide) and CV (crystal violet)-based cell viability assays respectively (see Appendix for data). None of the compounds showed significant differences to the negative control.

Conclusion

In this chapter, a new class of natural product-based herbicides was introduced. A total of 54 derivatives containing a pyridine core with different side-chains, functional groups and substitution patterns were prepared. The first variants were derived from 6-decyloxy nicotinic acid for which herbicidal activity was found initially. For this purpose, the synthesis conditions for this substance were optimized for yield and time, so that the best conditions were subsequently used for the synthesis of the majority of the derivatives.

For derivatization, the decyloxy side-chain was replaced by other non-polar alkoxy groups. Linear alkoxy groups with a carbon chain length ranging from C₇ to C₁₀ gave the best herbicidal activities of all derivatives, ranging from ED₅₀ = 2.3 – 2.4 µM. Changing the heteroatom or addition aryl groups did not improve the activity. However, replacement by sulphur, nitrogen or methylene did not affect much the activity. In the third step, the importance of the carboxylic acid group itself was investigated. For this purpose, ten derivatives were synthesized. The best herbicidal activity was found for the carboxylic acid derivatives, with very good activities observed for the tetrazole and triketone surrogates. The substitution pattern on the pyridine ring was changed in the last step. For this purpose, niacin, picolinic acid and isonicotinic acid derivatives with regioisomeric positioning of the octyloxy side-chain were prepared. Here, the original substitution pattern of 6-octyloxy niacin showed the best results, but 6-octyloxy picolinic acid also has very strong herbicidal activity. In addition to the investigation of herbicidal activity, the antifungal and cytotoxic activity of all synthesized compounds was tested.

None of the derivatives had a cytotoxic effect on the cell lines tested. Some showed moderate antifungal activity activities against *Septoria tritici*, *Botrytis cinerea* and anti-oomycotic properties against *Phytophthora infestans*, but this does not coincide with the herbicidal strength, leaving the choice of derivatives with both activities or – mostly – herbicidals, which do not alter fungal health.

Experimental part

General information

The materials used, analytical methods, and bioassays are described in detail in Chapter 2. Any additions or modifications are outlined below.

Antiphytopathogenic activity

The compounds were evaluated in 96-well microtiter plate assays against the phytopathogenic ascomycetous fungi *Botrytis cinerea* Pers. and *Septoria tritici* Desm. as well as the oomycete *Phytophthora infestans* (Mont.) de Bary according to the monitoring methods approved by the fungicide resistance action committee (FRAC) with minor modifications as described by Otto et al.²⁵ Compounds were evaluated in a serial dilution at concentrations of 125 µM, 41.7 µM, 13.9 µM, 4.6 µM and 1.5 µM. The solvent DMSO was used as negative control (max. concentration 2.5 %), while epoxiconazole and pyraclostrobin served as positive control (100 % inhibition at 125 µM). Seven days after inoculation, the pathogen growth was evaluated by measuring of the optical density (OD) at $\lambda = 405$ nm using a TecanSpark microplate reader (5 measurements per well using multiple reads). Each experiment was conducted in triplicates.

Phytotoxicity test (herbicidal activity)

The compounds were tested for their plant toxicity by inhibiting the growth of duckweed (*Lemna minor*) in 24-well microtiter plates in a serial dilution, ranging from 0.01 to 100 µM. 0.1 % (v/v) DMSO in water was used as a negative control, while 100 µM of 2,4-dichlorophenoxyacetic acid was used as a positive control.²⁴ The screening procedures took place under sterile conditions (laminar airflow cabinet).

First, 2 µl of the negative control (100 % DMSO) and of the substances in the appropriate concentration (10 µM, 100 µM, 1 mM, 10 mM, 50 mM, and 100 mM) were added to the plate. After that, each well of a 24-well microtiter plate was loaded with 2 ml of Steinberg medium so that the final concentrations of compound in a plate comprised 0.01 µM, 0.1 µM, 1 µM, 10 µM, 50 µM and 100 µM.²⁶ Using an inoculation loop, in each vial of the microtiter plate one duckweed was transferred with 3 leaves from the preculture. The plates were incubated in the phytocabinet at 24 °C and 100 µmol m⁻² s⁻¹ continuous light for 96 hours. To evaluate the frond surfaces, a photo of the plate was taken using the LemnaTec scan analyzer on the first day (t = 0 h), second day (t = 24 h) and fourth day (t = 96 h). All experiments were carried out in triplicates.

The photos were later exported in PNG format and processed with Image J to calculate the leaf area A. For the calculation of the specific growth rate μ of the duckweeds, the leaf area was first logarithmized and then the difference between the measuring points was determined. These values are then normalized in R by negative control (growth factor = 1) and processed in Excel for further comparison.

$$\log(A_p) = \mu \cdot t + A_{p_0}$$

ED₅₀ values (effective dose required for 50 % inhibition of growth) were calculated using OriginPro 2020 dose-response analysis function. Here the raw data was fitted with a sigmoidal fit, which was then used to calculate the concentrations at 50 % inhibition.

Cytotoxic activity—in vitro cell viability assays

Anti-proliferative and cytotoxic effects of the compounds were investigated by performing colorimetric MTT (3-(4,5-dimethylthiazol-2-yl)-2,5-diphenyltetrazolium bromide) and CV (crystal violet)-based cell viability assays (Sigma-Aldrich, Taufkirchen, Germany), respectively. The cell handling and assay techniques followed the method *Khan et al.* described.²⁷ For this purpose, cells were seeded in low densities in 96-well plates (6000 cells/100 μ L/well for both PC3 and MDA-MB-468; 4000 cells/100 μ L/well for MDA-MB-231; and 12,000 cells/100 μ L/well for SK-N-MC) using the cell culture media. The cells were allowed to adhere for 24 h, followed by the 48 h compound treatment. Based on 20 mM DMSO stock solutions, the compounds were diluted in standard growth media to reach final concentrations of 10 and 0.1 μ M for cell treatment. For control measures, cells were treated in parallel with 100 μ M digitonin (positive control, for data normalization set to 0 % cell viability). Each data point was determined in technical quadruplicates and two independent biological replicates. As soon as the 48 h incubation was finished, cell viability was measured. For the MTT assay, cells were washed once with phosphate-buffered saline, followed by incubation with MTT working solution (0.5 mg/mL MTT in culture medium) for 1 h under standard growth conditions. After discarding the MTT solution, DMSO was added to dissolve the formed formazan, followed by measuring formazan absorbance at 570 nm, and additionally at the reference/background wavelength of 670 nm, by using a SpectraMax M5 multi-well plate reader (Molecular Devices, San Jose, USA).

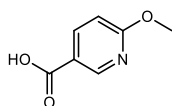
For the CV assay, cells were washed once with phosphate-buffered saline and fixed with 4 % paraformaldehyde for 20 min at room temperature. After discarding the paraformaldehyde solution, the cells were left to dry for 10 min and then stained with 1 % crystal violet solution for 15 min at rt. The cells were washed with water and were dried overnight at rt. Afterwards, acetic acid (33 % in aqua bidest) was added to the stained cells and absorbance was measured at 570 nm and 670 nm (reference wavelength) using a SpectraMax M5 multi-well plate reader (Molecular Devices, San Jose, USA). For data analyses, GraphPad Prism version 8.0.2 and Microsoft Excel 2013 were used.

Syntheses

General synthesis method – Nucleophilic aromatic substitution (ether coupling)

6-Chloropyridine-3-carboxylic acid (1 eq) and potassium hydroxide (5 eq) were suspended in DMSO (3 ml) in a microwave vial. To the suspension was added the selected alcohol (2 eq). The capped vial was heated to 120 °C for 30 minutes using a synthesis microwave oven. After cooling, the residue was poured into an ice bath (100 ml), which then was acidified to pH ~ 2 - 3 using aqueous hydrochloric acid (2 M), leading to the precipitation of the desired product as hydrochloride. The precipitate was filtered off and evaporated to dryness. If no precipitate formed, the aqueous phase was extracted using ethyl acetate (3x 50 mL) and the combined organic phases were dried over Na₂SO₄, filtered, and evaporated to dryness.

6-Methoxynicotinic acid (**1**)



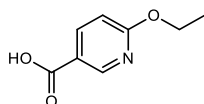
According to general method, methanol (42.9 μ L, 1 mmol), 6-chloropyridine-3-carboxylic acid (79 mg, 0.5 mmol) and potassium hydroxide (140.3 mg, 2.5 mmol) were used. Purification was done by column chromatography (*n*-hexane / ethyl acetate + 0.1 % FA), giving derivative **1** (52.8 mg, 0.34 mmol, 69 %) as a white amorphous solid:

HR-MS m/z 154.0497 (calculated for $C_7H_8NO_3$: 154.0499)

1H NMR (400 MHz, $(CD_3)_2SO$) δ 13.02 (s, 1H), 8.73 (d, J = 2.3 Hz, 1H), 8.14 (dd, J = 8.7, 2.4 Hz, 1H), 6.91 (d, J = 8.7 Hz, 1H), 3.93 (s, 3H).

^{13}C NMR (101 MHz, $(CD_3)_2SO$) δ 166.14, 166.10, 149.45, 139.84, 120.35, 110.51, 53.81.

6-Ethoxynicotinic acid (**2**)



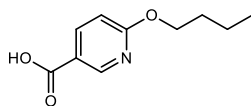
According to general method, ethanol (58.4 μ L, 1 mmol), 6-chloropyridine-3-carboxylic acid (79 mg, 0.5 mmol) and potassium hydroxide (140.3 mg, 2.5 mmol) were used. Purification was done by column chromatography (*n*-hexane / ethyl acetate + 0.1 % FA), giving product **2** (56.6 mg, 0.34 mmol, 68 %) as a white amorphous solid:

HR-MS m/z 168.0654 (calculated for $C_8H_{10}NO_3$: 168.0655)

1H NMR (400 MHz, $(CD_3)_2SO$) δ 13.01 (s, 1H), 8.71 (d, J = 2.4 Hz, 1H), 8.13 (dd, J = 8.7, 2.4 Hz, 1H), 6.87 (d, J = 8.7 Hz, 1H), 4.38 (q, J = 7.0 Hz, 2H), 1.34 (t, J = 7.0 Hz, 3H).

^{13}C NMR (101 MHz, $(CD_3)_2SO$) δ 166.12, 165.83, 149.48, 139.82, 120.16, 110.58, 62.05, 14.36.

6-Butoxynicotinic acid (**3**)



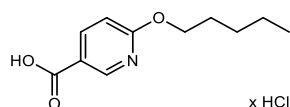
According to general method, 1-butanol (91.5 μ L, 1 mmol), 6-chloropyridine-3-carboxylic acid (79 mg, 0.5 mmol) and potassium hydroxide (140.3 mg, 2.5 mmol) were used. Purification was done by column chromatography (*n*-hexane / ethyl acetate + 0.1 % FA), giving product **3** (66.4 mg, 0.34 mmol, 84 %) as a white amorphous solid:

HR-MS m/z 196.0967 (calculated for $C_{10}H_{14}NO_3$: 196.0968)

^1H NMR (400 MHz, $(\text{CD}_3)_2\text{SO}$) δ 13.00 (s, 1H), 8.71 (d, $J = 2.3$ Hz, 1H), 8.13 (dd, $J = 8.7, 2.4$ Hz, 1H), 6.88 (d, $J = 8.7$ Hz, 1H), 4.33 (t, $J = 6.6$ Hz, 2H), 1.71 (p, $J = 6.8$ Hz, 2H), 1.42 (h, $J = 7.4$ Hz, 2H), 0.93 (t, $J = 7.4$ Hz, 3H).

^{13}C NMR (101 MHz, $(\text{CD}_3)_2\text{SO}$) δ 166.09, 165.98, 149.46, 139.82, 120.13, 110.56, 65.92, 30.40, 18.67, 13.64.

6-(Pentyloxy)nicotinic acid (**4**)



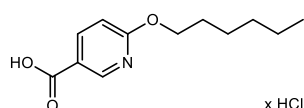
According to general method, 1-pentanol (108.3 μL , 1 mmol), 6-chloropyridine-3-carboxylic acid (79 mg, 0.5 mmol) and potassium hydroxide (140.3 mg, 2.5 mmol) were used, giving product **4** (108.1 mg, 0.44 mmol, 88 %) as a white amorphous solid:

HR-MS m/z 210.1124 (calculated for $\text{C}_{11}\text{H}_{16}\text{NO}_3$: 210.1125)

^1H NMR (600 MHz, $(\text{CD}_3)_2\text{SO}$) δ 13.01 (s, 1H), 8.71 (dd, $J = 2.4, 0.8$ Hz, 1H), 8.13 (dd, $J = 8.7, 2.4$ Hz, 1H), 6.88 (dd, $J = 8.7, 0.8$ Hz, 1H), 4.32 (t, $J = 6.7$ Hz, 2H), 1.76 – 1.69 (m, 2H), 1.42 – 1.29 (m, 4H), 0.89 (t, $J = 7.1$ Hz, 3H).

^{13}C NMR (151 MHz, $(\text{CD}_3)_2\text{SO}$) δ 166.11, 165.99, 149.47, 139.82, 120.14, 110.56, 66.21, 28.04, 27.62, 21.86, 13.86.

6-(Hexyloxy)nicotinic acid (**5**)



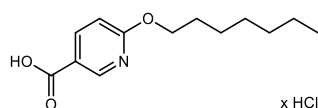
According to general method, 1-hexanol (125.5 μL , 1 mmol), 6-chloropyridine-3-carboxylic acid (79 mg, 0.5 mmol) and potassium hydroxide (140.3 mg, 2.5 mmol) were used, giving product **5** (73 mg, 0.28 mmol, 56 %) as a white amorphous solid:

HR-MS m/z 224.1279 (calculated for $\text{C}_{12}\text{H}_{18}\text{NO}_3$: 224.1281)

^1H NMR (400 MHz, $(\text{CD}_3)_2\text{SO}$) δ 13.01 (s, 1H), 8.70 (d, $J = 2.4$ Hz, 1H), 8.12 (dd, $J = 8.6, 2.4$ Hz, 1H), 6.88 (d, $J = 8.7$ Hz, 1H), 4.32 (t, $J = 6.7$ Hz, 2H), 1.72 (p, $J = 6.8$ Hz, 2H), 1.45 – 1.35 (m, 2H), 1.31 (dh, $J = 7.3, 3.3$ Hz, 4H), 0.87 (t, $J = 7.3$ Hz, 3H).

^{13}C NMR (101 MHz, $(\text{CD}_3)_2\text{SO}$) δ 166.10, 165.98, 149.46, 139.82, 120.13, 110.56, 66.22, 30.95, 28.30, 25.09, 22.01, 13.86.

6-(Heptyloxy)nicotinic acid (**6**)



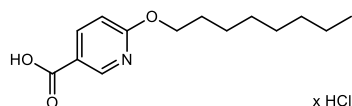
According to general method, 1-heptanol (108.3 μ L, 1 mmol), 6-chloropyridine-3-carboxylic acid (79 mg, 0.5 mmol) and potassium hydroxide (140.3 mg, 2.5 mmol) were used, giving product **6** (115 mg, 0.42 mmol, 84 %) as a white amorphous solid:

HR-MS m/z 238.1236 (calculated for $C_{13}H_{20}NO_3$: 238.1426)

1H NMR (400 MHz, $(CD_3)_2SO$) δ 12.85 (s, 1H), 8.71 (d, J = 2.4 Hz, 1H), 8.13 (dd, J = 8.6, 2.4 Hz, 1H), 6.87 (d, J = 8.7 Hz, 1H), 4.32 (t, J = 6.7 Hz, 2H), 1.72 (p, J = 6.8 Hz, 2H), 1.37 (dt, J = 13.1, 7.3 Hz, 2H), 1.34 – 1.21 (m, 6H), 0.86 (t, J = 6.6 Hz, 3H).

^{13}C NMR (101 MHz, $(CD_3)_2SO$) δ 166.10, 165.98, 149.46, 139.80, 120.13, 110.54, 66.20, 31.18, 28.40, 28.34, 25.40, 22.01, 13.89.

6-(Octyloxy)nicotinic acid (**7**)



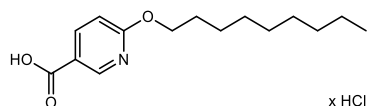
According to general method, 1-octanol (156.9 μ L, 1 mmol), 6-chloropyridine-3-carboxylic acid (79 mg, 0.5 mmol) and potassium hydroxide (140.3 mg, 2.5 mmol) were used, giving product **7** (125.2 mg, 0.44 mmol, 87 %) as a white amorphous solid:

HR-MS m/z 252.1593 (calculated for $C_{14}H_{22}NO_3$: 252.1594)

1H NMR (400 MHz, $(CD_3)_2SO$) δ 13.00 (s, 1H), 8.71 (d, J = 2.4 Hz, 1H), 8.13 (dd, J = 8.6, 2.4 Hz, 1H), 6.87 (d, J = 8.7 Hz, 1H), 4.32 (t, J = 6.6 Hz, 2H), 1.71 (p, J = 6.9 Hz, 2H), 1.44 – 1.34 (m, 2H), 1.34 – 1.19 (m, 8H), 0.86 (t, J = 6.5 Hz, 3H).

^{13}C NMR (101 MHz, $(CD_3)_2SO$) δ 166.09, 165.98, 149.46, 139.81, 120.13, 110.55, 66.20, 31.19, 28.69, 28.60, 28.33, 25.42, 22.04, 13.90.

6-(Nonyloxy)nicotinic acid (**8**)



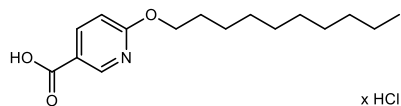
According to general method, 1-nonanol (174.4 μ L, 1 mmol), 6-chloropyridine-3-carboxylic acid (79 mg, 0.5 mmol) and potassium hydroxide (140.3 mg, 2.5 mmol) were used, giving product **8** (137.3 mg, 0.46 mmol, 91 %) as a white amorphous solid:

HR-MS m/z 266.1749 (calculated for $C_{15}H_{24}NO_3$: 266.1751)

^1H NMR (400 MHz, $(\text{CD}_3)_2\text{SO}$) δ 13.00 (s, 1H), 8.71 (d, J = 2.4 Hz, 1H), 8.13 (dd, J = 8.7, 2.4 Hz, 1H), 6.87 (d, J = 8.7 Hz, 1H), 4.32 (t, J = 6.6 Hz, 2H), 1.71 (p, J = 6.9 Hz, 2H), 1.43 – 1.34 (m, 2H), 1.34 – 1.22 (m, 10H), 0.85 (t, J = 6.6 Hz, 3H).

^{13}C NMR (101 MHz, $(\text{CD}_3)_2\text{SO}$) δ 166.09, 165.98, 149.45, 139.80, 120.13, 110.54, 66.19, 31.24, 28.90, 28.73, 28.61, 28.33, 25.41, 22.06, 13.91.

6-(Decyloxy)nicotinic acid (**9**)



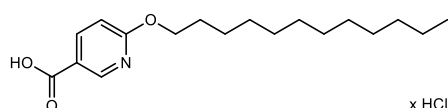
According to general method, 1-decanol (190.7 μL , 1 mmol), 6-chloropyridine-3-carboxylic acid (79 mg, 0.5 mmol) and potassium hydroxide (140.3 mg, 2.5 mmol) were used, giving product **9** (133 mg, 0.42 mmol, 84.2 %) as a white amorphous solid:

HR-MS m/z 280.1903 (calculated for $\text{C}_{16}\text{H}_{26}\text{NO}_3$: 280.1907)

^1H NMR (400 MHz, $(\text{CD}_3)_2\text{SO}$) δ 13.00 (s, 1H), 8.70 (s, 1H), 8.12 (d, J = 8.6 Hz, 1H), 6.87 (d, J = 8.7 Hz, 1H), 4.32 (t, J = 6.7 Hz, 2H), 1.71 (p, J = 6.9 Hz, 2H), 1.42-1.34 (m, 2H), 1.34-1.17 (m, 12H), 0.90-0.81 (m, 3H).

^{13}C NMR (101 MHz, $(\text{CD}_3)_2\text{SO}$) δ 166.08, 165.97, 149.44, 139.80, 120.12, 110.54, 66.18, 31.24, 28.92, 28.88, 28.68, 28.63, 28.30, 25.38, 22.05, 13.90.

6-(Dodecyloxy)nicotinic acid (**10**)



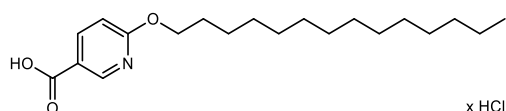
According to general method, 1-dodecanol (224 μL , 1 mmol), 6-chloropyridine-3-carboxylic acid (79 mg, 0.5 mmol) and potassium hydroxide (140.3 mg, 2.5 mmol) were used, giving product **10** (158.2 mg, 0.46 mmol, 91 %) as a white amorphous solid:

HR-MS m/z 308.2217 (calculated for $\text{C}_{18}\text{H}_{30}\text{NO}_3$: 308.2220)

^1H NMR (400 MHz, $(\text{CD}_3)_2\text{SO}$) δ 13.00 (s, 1H), 8.70 (d, J = 2.4 Hz, 1H), 8.12 (dd, J = 8.7, 2.4 Hz, 1H), 6.87 (d, J = 8.7 Hz, 1H), 4.31 (t, J = 6.6 Hz, 2H), 1.71 (p, J = 6.8 Hz, 2H), 1.43 – 1.17 (m, 18H), 0.85 (t, J = 6.7 Hz, 3H).

^{13}C NMR (101 MHz, $(\text{CD}_3)_2\text{SO}$) δ 166.09, 165.97, 149.45, 139.79, 120.13, 110.53, 66.17, 31.27, 29.00, 28.97, 28.93, 28.92, 28.70, 28.68, 28.31, 25.39, 22.07, 13.90.

6-(Tetradecyloxy)nicotinic acid (**11**)



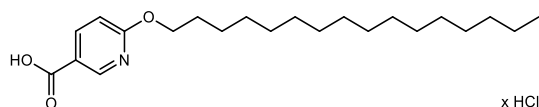
According to general method, 1-tetradecanol (260 μ L, 1 mmol), 6-chloropyridine-3-carboxylic acid (79 mg, 0.5 mmol) and potassium hydroxide (140.3 mg, 2.5 mmol) were used, giving product **11** (145.1 mg, 0.39 mmol, 78 %) as a white amorphous solid:

HR-MS m/z 336.2529 (calculated for $C_{20}H_{34}NO_3$: 336.2533)

1H NMR (400 MHz, $(CD_3)_2SO$) δ 13.01 (s, 1H), 8.70 (d, J = 2.3 Hz, 1H), 8.12 (dd, J = 8.7, 2.4 Hz, 1H), 6.87 (d, J = 8.7 Hz, 1H), 4.31 (t, J = 6.6 Hz, 2H), 1.71 (p, J = 6.8 Hz, 2H), 1.42 – 1.33 (m, 2H), 1.33 – 1.21 (m, 20H), 0.85 (t, J = 6.6 Hz, 3H).

^{13}C NMR (101 MHz, $(CD_3)_2SO$) δ 166.09, 165.97, 149.45, 139.81, 120.15, 110.54, 66.18, 31.26, 29.01, 28.98, 28.97, 28.96, 28.90, 28.90, 28.68, 28.67, 28.30, 25.38, 22.06, 13.92.

6-(Hexadecyloxy)nicotinic acid (**12**)

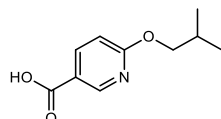


According to general method, 1-hexadecanol (299 μ L, 1 mmol), 6-chloropyridine-3-carboxylic acid (79 mg, 0.5 mmol) and potassium hydroxide (140.3 mg, 2.5 mmol) were used, giving product **12** (136.1 mg, 0.34 mmol, 67 %) as a white amorphous solid:

1H NMR (400 MHz, $(CD_3)_2SO$) δ 12.90 (s, 1H), 8.70 (d, J = 2.5 Hz, 1H), 8.12 (dd, J = 8.6, 2.5 Hz, 1H), 6.85 (d, J = 8.5 Hz, 1H), 4.32 (t, J = 6.7 Hz, 2H), 1.71 (p, J = 6.9 Hz, 2H), 1.42 – 1.34 (m, 2H), 1.34 – 1.13 (m, 24H), 0.85 (t, J = 6.6 Hz, 3H).

^{13}C NMR (101 MHz, $(CD_3)_2SO$) δ 165.92, 165.88, 149.31, 139.65, 139.63, 120.08, 110.37, 110.35, 66.06, 31.12, 28.85, 28.84, 28.82, 28.80, 28.75, 28.53, 28.51, 28.20, 25.26, 21.90, 13.72, 13.71.

6-(Isobutyloxy)nicotinic acid (**13**)



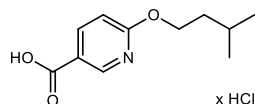
According to general method, isobutanol (92.7 μ L, 1 mmol), 6-chloropyridine-3-carboxylic acid (79 mg, 0.5 mmol) and potassium hydroxide (140.3 mg, 2.5 mmol) were used. Purification was done by column chromatography (*n*-hexane / ethyl acetate + 0.1 % FA), giving product **13** (70.3 mg, 0.36 mmol, 72 %) as a white amorphous solid:

HR-MS m/z 196.0967 (calculated for $C_{10}H_{14}NO_3$: 196.0968)

^1H NMR (500 MHz, $(\text{CD}_3)_2\text{SO}$) δ 13.01 (s, 1H), 8.70 (d, J = 2.3 Hz, 1H), 8.13 (dd, J = 8.7, 2.4 Hz, 1H), 6.90 (d, J = 8.6 Hz, 1H), 4.11 (d, J = 6.7 Hz, 2H), 2.04 (dq, J = 13.4, 6.7 Hz, 1H), 0.97 (d, J = 6.7 Hz, 6H).

^{13}C NMR (126 MHz, $(\text{CD}_3)_2\text{SO}$) δ 166.10, 166.08, 149.44, 139.86, 120.17, 110.54, 72.25, 27.36, 18.96 (2C).

6-(Isopentyloxy)nicotinic acid (**14**)



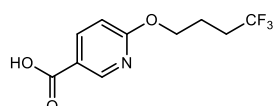
According to general method, isoamyl alcohol (109 μL , 1 mmol), 6-chloropyridine-3-carboxylic acid (79 mg, 0.5 mmol) and potassium hydroxide (140.3 mg, 2.5 mmol) were used, giving product **14** (81.1 mg, 0.33 mmol, 66 %) as a white amorphous solid:

HR-MS m/z 210.1123 (calculated for $\text{C}_{11}\text{H}_{16}\text{NO}_3$: 210.1125)

^1H NMR (400 MHz, $(\text{CD}_3)_2\text{SO}$) δ 13.01 (s, 1H), 8.71 (d, J = 2.5 Hz, 1H), 8.13 (dd, J = 8.8, 2.5 Hz, 1H), 6.87 (d, J = 8.5 Hz, 1H), 4.36 (t, J = 6.8 Hz, 2H), 1.88 – 1.68 (m, 1H), 1.62 (q, J = 6.8 Hz, 2H), 0.99 – 0.86 (m, 6H).

^{13}C NMR (101 MHz, $(\text{CD}_3)_2\text{SO}$) δ 166.09, 165.94, 149.46, 139.81, 120.14, 110.57, 64.66, 37.08, 24.58, 22.37, 22.36.

6-(4,4,4-Trifluorobutoxy)nicotinic acid (**15**)



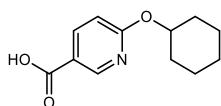
According to general method, 4,4,4-trifluoro-1-butanol (128 mg, 1 mmol), 6-chloropyridine-3-carboxylic acid (79 mg, 0.5 mmol) and potassium hydroxide (140.3 mg, 2.5 mmol) were used. Purification was done by column chromatography (*n*-hexane / ethyl acetate + 0.1 % FA), giving product **15** (67.3 mg, 0.27 mmol, 54 %) as a white amorphous solid:

HR-MS m/z 250.0691 (calculated for $\text{C}_{10}\text{H}_{11}\text{F}_3\text{NO}_3$: 250.0686)

^1H NMR (400 MHz, $(\text{CD}_3)_2\text{SO}$) δ 13.05 (s, 1H), 8.72 (d, J = 2.3 Hz, 1H), 8.15 (dd, J = 8.7, 2.4 Hz, 1H), 6.92 (d, J = 8.6 Hz, 1H), 4.39 (t, J = 6.4 Hz, 2H), 2.51 – 2.34 (m, 2H), 2.02 – 1.91 (m, 2H).

^{13}C NMR (101 MHz, $(\text{CD}_3)_2\text{SO}$) δ 166.05, 165.62, 149.39, 139.96, 127.58 (q, J = 276.1 Hz), 120.48, 110.66, 64.57, 29.47 (q, J = 28.1 Hz), 21.33 (q, J = 3.0 Hz).

6-(Cyclohexyloxy)nicotinic acid (**16**)



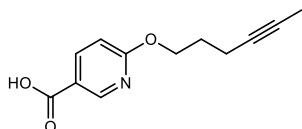
According to general method, cyclohexanol (104 μ L, 1 mmol), 6-chloropyridine-3-carboxylic acid (79 mg, 0.5 mmol) and potassium hydroxide (140.3 mg, 2.5 mmol) were used. Purification was done by column chromatography (*n*-hexane / ethyl acetate + 0.1 % FA), giving derivative **16** (77.4 mg, 0.35 mmol, 70 %) as a white amorphous solid:

HR-MS m/z 222.1123 (calculated for $C_{12}H_{16}NO_3$: 222.1125)

1H NMR (400 MHz, $(CD_3)_2SO$) δ 12.97 (s, 1H), 8.72 – 8.67 (m, 1H), 8.13 – 8.08 (m, 1H), 6.85 – 6.81 (m, 1H), 5.10 – 5.06 (m, 1H), 1.98 – 1.94 (m, 2H), 1.75 – 1.70 (m, 2H), 1.61 – 1.14 (m, 6H).

^{13}C NMR (101 MHz, $(CD_3)_2SO$) δ 166.09, 165.42, 149.45, 139.88, 119.88, 111.00, 73.44, 31.23 (2C), 25.00, 23.37 (2C).

6-(Hex-4-ynyloxy)nicotinic acid (**17**)



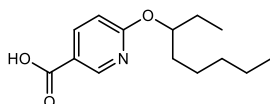
According to general method, 5-hexin-1-ol (110.3 μ L, 1 mmol), 6-chloropyridine-3-carboxylic acid (79 mg, 0.5 mmol) and potassium hydroxide (140.3 mg, 2.5 mmol) were used. Purification was done by column chromatography (*n*-hexane / ethyl acetate + 0.1 % FA), giving derivative **17** (93.3 mg, 0.43 mmol, 85 %) as a white amorphous solid:

HR-MS m/z 220.0967 (calculated for $C_{12}H_{14}NO_3$: 220.0968)

1H NMR (400 MHz, $(CD_3)_2SO$) δ 13.02 (s, 1H), 8.71 (d, J = 2.4 Hz, 1H), 8.14 (dd, J = 8.6, 2.5 Hz, 1H), 6.89 (d, J = 8.7 Hz, 1H), 4.37 (t, J = 6.4 Hz, 2H), 2.27 (td, J = 6.9, 3.1 Hz, 2H), 1.87 (p, J = 6.7 Hz, 2H), 1.76 – 1.70 (m, 3H).

^{13}C NMR (101 MHz, $(CD_3)_2SO$) δ 166.08, 165.83, 149.45, 139.87, 120.28, 110.62, 78.32, 76.23, 65.07, 27.86, 14.82, 3.07.

6-(1-Ethyl-hexyloxy)nicotinic acid (**18**)



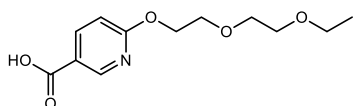
According to general method, octan-3-ol (158.8 μ L, 1 mmol), 6-chloropyridine-3-carboxylic acid (79 mg, 0.5 mmol) and potassium hydroxide (140.3 mg, 2.5 mmol) were used. Purification was done by column chromatography (*n*-hexane/ ethyl acetate + 0.1 % FA), giving product **18** (104.3 mg, 0.42 mmol, 83 %) as a white amorphous solid:

HR-MS m/z 252.1592 (calculated for $C_{14}H_{22}NO_3$: 252.1594)

1H NMR (400 MHz, $(CD_3)_2SO$) δ 12.97 (s, 1H), 8.69 (d, J = 2.4 Hz, 1H), 8.11 (dd, J = 8.7, 2.4 Hz, 1H), 6.84 (d, J = 8.6 Hz, 1H), 5.21 (p, J = 6.1 Hz, 1H), 1.73 – 1.55 (m, 4H), 1.40 – 1.14 (m, 6H), 0.91 – 0.79 (m, 6H).

^{13}C NMR (101 MHz, $(CD_3)_2SO$) δ 166.23, 166.09, 149.40, 139.91, 119.87, 110.85, 76.22, 32.75, 31.16, 26.19, 24.38, 21.95, 13.81, 9.36.

6-(2-(2-Ethoxyethoxy)ethoxy)nicotinic acid (**19**)



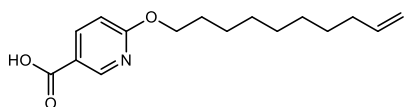
According to general method, diethylene glycol monoethyl ether (136 μ L, 1 mmol), 6-chloropyridine-3-carboxylic acid (79 mg, 0.5 mmol) and potassium hydroxide (140.3 mg, 2.5 mmol) were used. Purification was done by column chromatography (*n*-hexane / ethyl acetate + 0.1 % FA), giving product **19** (71.5 mg, 0.28 mmol, 55 %) as a white amorphous solid:

HR-MS m/z 256.1177 (calculated for $C_{12}H_{18}NO_5$: 256.1179)

1H NMR (400 MHz, $CDCl_3$) δ 9.52 (s, 1H), 8.87 (d, J = 2.4 Hz, 1H), 8.18 (dd, J = 8.7, 2.4 Hz, 1H), 6.83 (d, J = 8.7 Hz, 1H), 4.58 (d, J = 4.6 Hz, 2H), 3.89 (d, J = 4.6 Hz, 2H), 3.73 (dd, J = 5.9, 3.6 Hz, 2H), 3.64 (dd, J = 5.9, 3.6 Hz, 2H), 3.55 (q, J = 7.0 Hz, 2H), 1.22 (t, J = 7.0 Hz, 3H).

^{13}C NMR (101 MHz, $CDCl_3$) δ 170.28, 166.83, 150.74, 139.97, 118.92, 111.15, 70.70, 69.79, 69.47, 66.71, 65.97, 15.07.

6-(Dec-9-enyloxy)nicotinic acid (**20**)



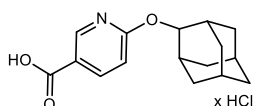
According to general method, 9-decenol (184.5 μ L, 1 mmol), 6-chloropyridine-3-carboxylic acid (79 mg, 0.5 mmol) and potassium hydroxide (140.3 mg, 2.5 mmol) were used. Purification was done by column chromatography (*n*-hexane / ethyl acetate + 0.1 % FA), giving product **20** (94.3 mg, 0.34 mmol, 68 %) as a white amorphous solid:

HR-MS m/z 278.1745 (calculated for $C_{16}H_{24}NO_3$: 278.1751)

1H NMR (400 MHz, $(CD_3)_2SO$) δ 13.00 (s, 1H), 8.70 (d, J = 2.3 Hz, 1H), 8.12 (dd, J = 8.7, 2.4 Hz, 1H), 6.87 (d, J = 8.7 Hz, 1H), 5.79 (ddt, J = 16.9, 10.1, 6.6 Hz, 1H), 5.04 – 4.89 (m, 2H), 4.32 (t, J = 6.6 Hz, 2H), 2.00 (q, J = 6.9 Hz, 2H), 1.71 (p, J = 6.8 Hz, 2H), 1.43 – 1.21 (m, 10H).

^{13}C NMR (101 MHz, $(CD_3)_2SO$) δ 166.09, 165.97, 149.45, 139.81, 138.78, 120.12, 114.59, 110.55, 66.19, 33.13, 28.74, 28.66, 28.40, 28.31, 28.21, 25.39.

6-(((1r,3r,5r,7r)-Adamantan-2-yl)oxy)nicotinic acid (**21**)



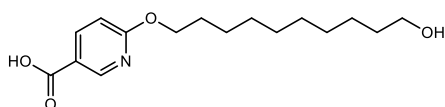
According to general method, 2-adamantanol (152.2 mg, 1 mmol), 6-chloropyridine-3-carboxylic acid (79 mg, 0.5 mmol) and potassium hydroxide (140.3 mg, 2.5 mmol) were used, giving derivative **21** (119.3 mg, 0.39 mmol, 77 %) as a white amorphous solid:

HR-MS m/z 274.1444 (calculated for $C_{16}H_{20}NO_3$: 274.1443)

1H NMR (400 MHz, $(CD_3)_2SO$) δ 12.98 (s, 1H), 8.69 (s, 1H), 8.13 (d, J = 8.6 Hz, 1H), 6.89 (d, J = 8.6 Hz, 1H), 5.22 (s, 1H), 2.14 – 1.99 (m, 4H), 1.89 – 1.69 (m, 8H), 1.54 (d, J = 12.3 Hz, 2H).

^{13}C NMR (101 MHz, $(CD_3)_2SO$) δ 166.10, 165.44, 149.48, 139.91, 119.92, 111.12, 77.45, 36.83, 35.70 (2C), 31.16 (2C), 31.03 (2C), 26.64, 26.50.

6-((10-Hydroxydecyl)oxy)nicotinic acid (**22**)



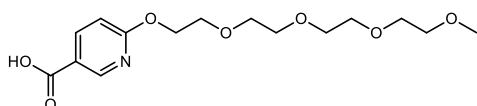
According to general method, 1,10-decanediol (174 mg, 1 mmol), 6-chloropyridine-3-carboxylic acid (79 mg, 0.5 mmol) and potassium hydroxide (140.3 mg, 2.5 mmol) were used. Purification was done by column chromatography (*n*-hexane / ethyl acetate + 0.1 % FA), giving product **22** (118.2 mg, 0.4 mmol, 80 %) as a white amorphous solid:

HR-MS m/z 296.1851 (calculated for $C_{16}H_{26}NO_4$: 296.1856)

1H NMR (400 MHz, $(CD_3)_2SO$) δ 13.00 (s, 1H), 8.70 (d, J = 2.4 Hz, 1H), 8.12 (dd, J = 8.7, 2.5 Hz, 1H), 6.87 (d, J = 8.7 Hz, 1H), 4.31 (t, J = 6.6 Hz, 2H), 3.37 (t, J = 6.5 Hz, 2H), 1.71 (p, J = 6.9 Hz, 2H), 1.43 – 1.35 (m, 4H), 1.34 – 1.20 (m, 11H).

^{13}C NMR (101 MHz, $(CD_3)_2SO$) δ 166.08, 165.98, 149.45, 139.82, 120.13, 110.56, 66.21, 60.68, 32.51, 28.99, 28.91, 28.90, 28.72, 28.32, 25.46, 25.41.

6-((2,5,8,11-Tetraoxatridecan-13-yl)oxy)nicotinic acid (**23**)



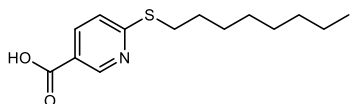
According to general method, tetraethyleneglycol monomethyl ether (195 μ L, 1 mmol), 6-chloropyridine-3-carboxylic acid (79 mg, 0.5 mmol) and potassium hydroxide (140.3 mg, 2.5 mmol) were used. Purification was done by column chromatography (*n*-hexane / ethyl acetate + 0.1 % FA), giving product **23** (92.2 mg, 0.28 mmol, 56 %) as a white amorphous solid:

HR-MS m/z 330.1546 (calculated for $C_{15}H_{24}NO_7$: 330.1553)

^1H NMR (400 MHz, $(\text{CD}_3)_2\text{SO}$) δ 13.06 (s, 1H), 8.71 (d, J = 2.3 Hz, 1H), 8.14 (dd, J = 8.7, 2.4 Hz, 1H), 6.92 (d, J = 8.7 Hz, 1H), 4.48 – 4.42 (m, 2H), 3.79 – 3.72 (m, 2H), 3.60 – 3.46 (m, 10H), 3.46 – 3.38 (m, 2H), 3.23 (s, 3H).

^{13}C NMR (101 MHz, $(\text{CD}_3)_2\text{SO}$) δ 166.07, 165.71, 149.34, 139.93, 120.44, 110.66, 71.23, 69.83, 69.78, 69.74, 69.73, 69.54, 68.55, 65.57, 58.00.

6-(Octylthio)nicotinic acid (**24**)



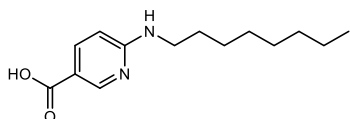
According to general method, 1-octanthiol (173.5 μL , 1 mmol), 6-chloropyridine-3-carboxylic acid (79 mg, 0.5 mmol) and potassium hydroxide (140.3 mg, 2.5 mmol) were used. Purification was done by column chromatography (*n*-hexane / ethyl acetate 8:2 – 5:5 + 0.1 % FA), giving product **24** (76.2 mg, 0.29 mmol, 57 %) as a white amorphous solid:

HR-MS m/z 268.1362 (calculated for $\text{C}_{14}\text{H}_{22}\text{NO}_2\text{S}$: 268.1371)

^1H NMR (400 MHz, $(\text{CD}_3)_2\text{SO}$) δ 13.32 (s, 1H), 8.88 (d, J = 2.1 Hz, 1H), 8.03 (dd, J = 8.4, 2.3 Hz, 1H), 7.38 (d, J = 8.4 Hz, 1H), 3.17 (t, J = 7.3 Hz, 2H), 1.63 (dq, J = 13.8, 6.9 Hz, 2H), 1.45 – 1.35 (m, 2H), 1.32 – 1.21 (m, 8H), 0.86 (t, J = 7.0 Hz, 3H).

^{13}C NMR (101 MHz, $(\text{CD}_3)_2\text{SO}$) δ 166.20, 163.86, 150.19, 136.71, 122.69, 121.14, 31.18, 29.21, 28.66, 28.53, 28.46, 28.17, 22.04, 13.91.

6-(Octylamino)nicotinic acid (**25**)



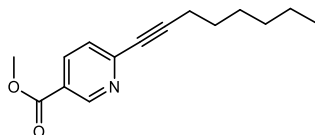
To a solution of 6-chloronicotinic acid methyl ester (100 mg, 0.58 mmol) in anhydrous DMF (7 mL) was added 1-amino-octane (0.5 mL, 3.0 mmol), $\text{Pd}(\text{OAc})_2$ (2 mol%, 2.7 mg, 0.012 mmol) and XPhos (2 mol%, 5.7 mg, 0.012 mmol). The solution was stirred for 72 h at rt, after which it was filtrated through a Celite pad. Purification of the intermediate was done by column chromatography (*n*-hexane / ethyl acetate). The intermediate (methyl 6-(octylamino)nicotinate) was dissolved in a mixture of THF and water (3:1, 10 mL) and was cooled to 0 $^\circ\text{C}$. To this solution, lithium hydroxide (25 mg, 0.6 mmol) was added, and the mixture was stirred overnight at room temperature, after which it was acidified to pH ~ 2 - 3 using aqueous hydrochloric acid (2 M). The aqueous phase was extracted using ethyl acetate (3x 25 mL) and the combined organic phases were dried over Na_2SO_4 , filtered, and evaporated to dryness, giving product **25** (23.6 mg, 0.1 mmol, 23 % over 2 steps) as a colourless oil.

HR-MS m/z 251.1752 (calculated for $\text{C}_{14}\text{H}_{23}\text{N}_2\text{O}_2$: 251.1754)

^1H NMR (500 MHz, $(\text{CD}_3)_2\text{SO}$) δ 12.29 (s, 1H), 8.52 (d, J = 2.2 Hz, 1H), 7.76 (dd, J = 8.8, 2.4 Hz, 1H), 7.28 (t, J = 5.5 Hz, 1H), 6.45 (d, J = 8.8 Hz, 1H), 3.31 – 3.24 (m, 2H), 1.51 (p, J = 7.0 Hz, 2H), 1.35 – 1.23 (m, 10H), 0.85 (t, J = 6.8 Hz, 3H).

^{13}C NMR (126 MHz, $(\text{CD}_3)_2\text{SO}$) δ 166.87, 160.94, 151.01, 137.07, 113.66, 107.22, 40.57, 31.22, 28.81, 28.77, 28.66, 26.51, 22.06, 13.93.

Methyl 6-(oct-1-yn-1-yl)nicotinate (**26**)



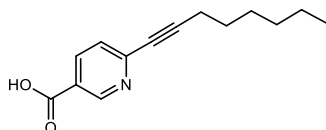
6-(Chloromethyl)nicotinic acid (0.86 g, 5 mmol), $\text{Pd}(\text{PPh}_3)_2\text{Cl}_2$ (105 mg, 0.15 mmol) and copper iodide (57 mg, 0.3 mmol) were suspended in DIPEA (0.87 mL, 5 mmol) and TEA (10 mL), after which octin (1.1 mL, 7.5 mmol) was added. The mixture was stirred for 12 hours at 80 °C, after which a saturated ammonia chloride solution (10 mL) was added. The aqueous phase was extracted using *n*-hexane (3x 20 mL), and the combined organic phases were washed using brine (20 mL), dried over Na_2SO_4 , filtered, and evaporated to dryness. Purification was done by column chromatography (*n*-hexane / ethyl acetate 10:0 - 8:2), giving product **26** (0.83 g, 3.4 mmol, 67 %) as a colourless oil:

HR-MS m/z 246.1496 (calculated for $\text{C}_{15}\text{H}_{20}\text{NO}_2$: 246.1489)

^1H NMR (400 MHz, CDCl_3) δ 9.13 (d, J = 1.4 Hz, 1H), 8.21 (dd, J = 8.2, 2.2 Hz, 1H), 7.43 (dd, J = 8.3, 0.9 Hz, 1H), 3.95 (s, 3H), 2.47 (t, J = 7.2 Hz, 2H), 1.65 (p, J = 7.2 Hz, 2H), 1.52 – 1.40 (m, 2H), 1.40 – 1.25 (m, 4H), 0.90 (t, J = 6.8 Hz, 3H).

^{13}C NMR (101 MHz, CDCl_3) δ 165.41, 150.88, 147.60, 137.01, 126.23, 124.09, 94.80, 80.20, 52.37, 31.27, 28.62, 28.15, 22.47, 19.44, 14.00.

6-(Oct-1-ynyl)nicotinic acid (**27**)



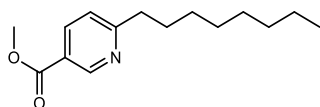
To a solution of methyl 6-(oct-1-yn-1-yl)nicotinate (200 mg, 0.81 mmol) in THF / water (2:1, 10 mL) was added lithium hydroxide hydrate (200 mg, 5.0 mmol) at 0 °C. The solution was stirred overnight at room temperature, after which it was acidified to pH ~ 2 - 3 using aqueous hydrochloric acid (2 M). The aqueous phase was extracted using ethyl acetate (3x 25 mL) and the combined organic phases were dried over Na_2SO_4 , filtered, and evaporated to dryness, giving derivative **27** (178 mg, 0.77 mmol, 95 %) as a colourless oil.

HR-MS m/z 232.1340 (calculated for $\text{C}_{14}\text{H}_{18}\text{NO}_2$: 232.1332)

^1H NMR (400 MHz, $(\text{CD}_3)_2\text{SO}$) δ 13.44 (s, 1H), 8.99 (d, J = 2.2 Hz, 1H), 8.22 (dd, J = 8.2, 2.2 Hz, 1H), 7.56 (d, J = 8.1 Hz, 1H), 2.49 (d, J = 7.1 Hz, 2H), 1.57 (p, J = 7.1 Hz, 2H), 1.48 – 1.37 (m, 2H), 1.36 – 1.24 (m, 4H), 0.88 (t, J = 7.0 Hz, 3H).

^{13}C NMR (101 MHz, $(\text{CD}_3)_2\text{SO}$) δ 165.80, 150.46, 146.33, 137.31, 126.57, 125.06, 93.88, 80.47, 30.70, 27.96, 27.68, 21.98, 18.51, 13.89.

Methyl 6-octylnicotinate (**28**)



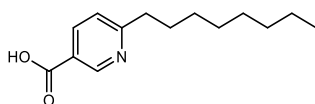
To a solution of **27** (400 mg, 1.63 mmol) in dry methanol (20 mL) was added palladium (10 % on carbon, 400 mg). The reaction vessel was evacuated and filled with hydrogen (3x), and the suspension was stirred overnight at room temperature, after which it was filtered using celite. The filtrate was concentrated in vacuo, giving product **28** (405 mg, 1.63 mmol, quant.) as a colourless oil.

HR-MS m/z 250.1806 (calculated for $\text{C}_{15}\text{H}_{24}\text{NO}_2$: 250.1807)

^1H NMR (400 MHz, CDCl_3) δ 9.12 (d, J = 2.2 Hz, 1H), 8.18 (dd, J = 8.1, 2.2 Hz, 1H), 7.22 (d, J = 8.1 Hz, 1H), 3.94 (s, 3H), 2.88 – 2.80 (m, 2H), 1.73 (p, J = 7.2 Hz, 2H), 1.39 – 1.23 (m, 10H), 0.87 (t, J = 6.6 Hz, 3H).

^{13}C NMR (101 MHz, CDCl_3) δ 167.26, 166.01, 150.52, 137.28, 123.40, 122.29, 52.20, 38.59, 31.81, 29.64, 29.38, 29.34, 29.17, 22.62, 14.06.

6-Octylnicotinic acid (**29**)



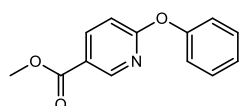
To a solution of methyl 6-octylnicotinate (100 mg, 0.4 mmol) in THF (3 mL) was dropwise added a sodium hydroxide solution (1 M, 0.45 mL) at 0 °C. The solution was stirred overnight at room temperature, after which water (10 mL) was added and it was acidified to pH ~ 2 - 3 using aqueous hydrochloric acid (2 M). The aqueous phase was extracted using ethyl acetate (3x 15 mL) and the combined organic phases were dried over Na_2SO_4 , filtered, and evaporated to dryness, giving derivative **29** (87.5 mg, 0.37 mmol, 93 %) as a white solid.

HR-MS m/z 236.1655 (calculated for $\text{C}_{14}\text{H}_{22}\text{NO}_2$: 236.1645)

^1H NMR (400 MHz, $(\text{CD}_3)_2\text{SO}$) δ 13.16 (s, 1H), 8.97 (d, J = 2.3 Hz, 1H), 8.15 (dd, J = 8.1, 2.2 Hz, 1H), 7.38 (d, J = 8.1 Hz, 1H), 2.79 (t, J = 7.6 Hz, 2H), 1.68 (p, J = 7.0 Hz, 2H), 1.32 – 1.21 (m, 10H), 0.85 (t, J = 6.7 Hz, 3H).

^{13}C NMR (101 MHz, $(\text{CD}_3)_2\text{SO}$) δ 166.35, 166.27, 149.84, 137.13, 124.00, 122.53, 37.47, 31.21, 28.85, 28.75, 28.62, 28.56, 22.04, 13.91.

Methyl 6-phenoxy nicotinate (**30**)



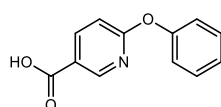
Methyl 6-chloropyridine-3-carboxylate (250 mg, 1.45 mmol) and phenol (137 mg, 1.45 mmol) were dissolved in dry DMF (10 mL). Potassium carbonate (302 mg, 2.18 mmol) was added, and the mixture was stirred overnight at 80 °C, after which water (100 mL) was added. The aqueous phase was extracted using ethyl acetate (3x 100 mL), and the combined organic phases were washed with sat. aq. NaHCO₃ solution (2x 100 mL) and brine solution (100 mL). Purification was done by column chromatography (*n*-hexane / ethyl acetate 9:1 – 7:3), giving product **30** (270 mg, 1.2 mmol, 82 %) as a white amorphous solid:

HR-MS *m/z* 230.0809 (calculated for C₁₃H₁₂NO₃: 230.0812)

¹H NMR (400 MHz, (CD₃)₂SO) δ 8.69 (d, *J* = 2.4 Hz, 1H), 8.31 (dd, *J* = 8.7, 2.4 Hz, 1H), 7.51 – 7.41 (m, 2H), 7.27 (t, *J* = 7.4 Hz, 1H), 7.19 (d, *J* = 8.5 Hz, 2H), 7.13 (d, *J* = 8.6 Hz, 1H), 3.86 (s, 3H).

¹³C NMR (101 MHz, (CD₃)₂SO) δ 165.87, 164.75, 153.00, 149.42, 140.83, 129.83 (2C), 125.26, 121.53 (2C), 120.94, 111.14, 52.19.

6-Phenoxy nicotinic acid (**31**)



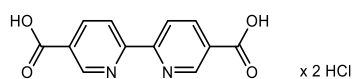
Compound **30** (130 mg, 0.6 mmol) was dissolved in a mixture of THF and methanol (3:1, 8 mL), which was cooled to 0 °C. An ice-cooled solution of lithium hydroxide (2 M, 2 mL) was slowly added, and the mixture was stirred overnight at room temperature, after which it was acidified to pH ~ 2 - 3 using aqueous hydrochloric acid (2 M). The aqueous phase was extracted using ethyl acetate (3x 25 mL) and the combined organic phases were dried over Na₂SO₄, filtered, and evaporated to dryness, giving product **31** (122 mg, 0.6 mmol, quant.) as a white amorphous solid.

HR-MS *m/z* 216.0651 (calculated for C₁₂H₁₀NO₃: 216.0655)

¹H NMR (400 MHz, (CD₃)₂SO) δ 13.21 (s, 1H), 8.67 (d, *J* = 2.3 Hz, 1H), 8.29 (dd, *J* = 8.6, 2.4 Hz, 1H), 7.51 – 7.41 (m, 2H), 7.31 – 7.23 (m, 1H), 7.23 – 7.16 (m, 2H), 7.11 (d, *J* = 8.6 Hz, 1H).

¹³C NMR (101 MHz, (CD₃)₂SO) δ 165.80, 165.69, 153.12, 149.55, 141.00, 129.81 (2C), 125.17, 121.97 (2C), 121.53, 110.98.

[2,2'-Bipyridine]-5,5'-dicarboxylic acid (**32**)



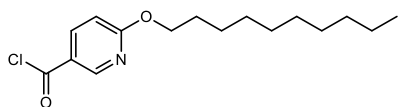
To a solution of chloropyridine-3-carboxylic acid (300 mg, 1.9 mmol) and powdered sodium hydroxide (168 mg, 4.2 mmol) in methanol (50 mL) was added palladium (10 % w/w on charcoal, 60 mg). The resulting suspension was stirred for 24 h at 80 °C, after which it was passed through a celite pad. The filtrate was acidified to pH ~ 2 using aqueous hydrochloric acid (2 M), forming a white precipitate. The precipitate was filtered off and evaporated to dryness, giving product **32** (482 mg, 1.52 mmol, 80 %) as a white amorphous solid.

HR-MS m/z 245.0554 (calculated for $C_{12}H_9N_2O_4$: 245.0557)

1H NMR (400 MHz, $(CD_3)_2SO$) δ 13.57 (s, 2H), 9.20 (dd, J = 2.2, 0.9 Hz, 2H), 8.57 (dd, J = 8.3, 0.9 Hz, 2H), 8.45 (dd, J = 8.3, 2.1 Hz, 2H).

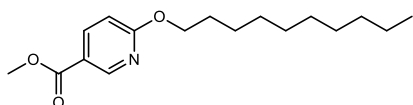
^{13}C NMR (101 MHz, $(CD_3)_2SO$) δ 165.98 (2C), 157.29 (2C), 150.29 (2C), 138.43 (2C), 127.20 (2C), 121.07 (2C).

6-(Decyloxy)nicotinoyl chloride (**9-Cl**)



A suspension of 6-(decyloxy)nicotinic acid (1 g, 3.2 mmol) in thionyl chloride (5 mL) was refluxed for 3 hours. The mixture was concentrated in vacuo, giving 6-(decyloxy)nicotinoyl chloride (0.95 g, 3.2 mmol, quant.) as a white amorphous solid which was used in the following reactions without further purification.

Methyl 6-(decyloxy)nicotinate (**33**)



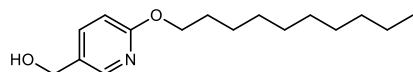
To a stirred solution of **9-Cl** (235 mg, 0.79 mmol) in anhydrous methanol (5 mL) under nitrogen atmosphere was added dropwise anhydrous triethylamine (118.5 μ L, 0.85 mmol). The solution was stirred at rt for 3 h after which it was quenched by addition of sat. aq. $NaHCO_3$ solution (10 mL). The aqueous phase was extracted using DCM (3x 15 mL), the combined organic phases were washed with brine (10 mL), dried over Na_2SO_4 , filtered, and evaporated to dryness. The residue was purified by column chromatography (n -hexane / ethyl acetate 95:5), giving product **33** (206.3 mg, 0.70 mmol, 89 %) as a white amorphous solid:

HR-MS m/z 294.2060 (calculated for $C_{17}H_{28}NO_3$: 294.2064)

^1H NMR (400 MHz, $(\text{CD}_3)_2\text{SO}$) δ 8.73 (d, J = 2.4 Hz, 1H), 8.15 (dd, J = 8.7, 2.4 Hz, 1H), 6.90 (d, J = 8.8 Hz, 1H), 4.32 (t, J = 6.6 Hz, 2H), 3.84 (s, 3H), 1.71 (d, J = 7.4 Hz, 2H), 1.44 – 1.33 (m, 2H), 1.33 – 1.18 (m, 12H), 0.89 – 0.81 (m, 3H).

^{13}C NMR (101 MHz, $(\text{CD}_3)_2\text{SO}$) δ 166.16, 165.03, 149.35, 139.61, 119.15, 110.76, 66.31, 52.00, 31.24, 28.92, 28.88, 28.68, 28.64, 28.28, 25.37, 22.05, 13.91.

6-(Decyloxy)pyridin-3-yl)methanol (**34**)



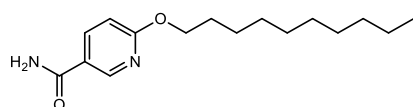
LiAlH_4 (20 mg, 0.53 mmol) was dissolved in dry THF (5 mL) under N_2 atmosphere and cooled down to 0°C . To this, a solution of **33** (20 mg, 0.07 mmol) in dry THF (5 mL) was added slowly and the mixture was stirred for 15 minutes at 0°C and subsequently 2 hours at rt. The reaction mixture was carefully quenched by addition of water and was extracted using ethyl acetate (3x 20 mL). The combined organic phases were washed with brine (50 mL), dried over Na_2SO_4 , filtered, and evaporated to dryness. Purification was done by column chromatography (*n*-hexane / ethyl acetate 8:2), giving product **34** (17 mg, 0.06 mmol, 92 %) as a colourless oil:

HR-MS m/z 266.2111 (calculated for $\text{C}_{16}\text{H}_{28}\text{NO}_2$: 266.2111)

^1H NMR (400 MHz, $(\text{CD}_3)_2\text{SO}$) δ 8.05 (d, J = 2.4 Hz, 1H), 7.62 (dd, J = 8.4, 2.4 Hz, 1H), 6.74 (d, J = 8.4 Hz, 1H), 5.13 (s, 1H), 4.41 (s, 2H), 4.21 (t, J = 6.6 Hz, 2H), 1.74 – 1.62 (m, 2H), 1.43 – 1.34 (m, 2H), 1.37 – 1.21 (m, 12H), 0.89 – 0.81 (m, 3H).

^{13}C NMR (101 MHz, $(\text{CD}_3)_2\text{SO}$) δ 162.54, 145.04, 138.34, 130.45, 110.10, 65.23, 60.22, 31.25, 28.96, 28.91, 28.76, 28.65, 28.48, 25.50, 22.06, 13.92.

6-(Decyloxy)nicotinamide (**35**)



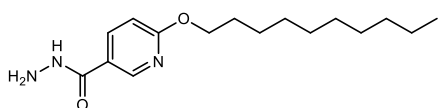
6-(Decyloxy)nicotinoyl chloride (50 mg, 0.17 mmol) was slowly added to a cooled ammonia solution (25 % w/w). The resulting precipitate was filtered off and dried in vacuo. Purification was done by column chromatography (dichloromethane / methanol 100:0 – 95:5), giving product **35** (45.3 mg, 0.16 mmol, 97 %) as a white amorphous solid:

HR-MS m/z 279.2063 (calculated for $\text{C}_{16}\text{H}_{27}\text{N}_2\text{O}_2$: 279.2067)

^1H NMR (400 MHz, $(\text{CD}_3)_2\text{SO}$) δ 8.66 (d, J = 2.4 Hz, 1H), 8.11 (dd, J = 8.7, 2.5 Hz, 1H), 7.95 (s, 1H), 7.37 (s, 1H), 6.84 (d, J = 8.7 Hz, 1H), 4.29 (t, J = 6.6 Hz, 2H), 1.71 (p, J = 6.8 Hz, 2H), 1.42 – 1.34 (m, 2H), 1.37 – 1.21 (m, 12H), 0.85 (t, J = 6.7 Hz, 3H).

^{13}C NMR (101 MHz, $(\text{CD}_3)_2\text{SO}$) δ 166.12, 165.01, 147.29, 138.34, 123.26, 110.01, 65.90, 31.25, 28.95, 28.90, 28.72, 28.65, 28.37, 25.44, 22.06, 13.92.

6-(Decyloxy)nicotinohydrazide (**36**)



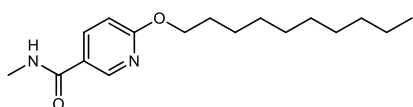
To a solution of **9-Cl** (35 mg, 0.12 mmol) in methanol (5 mL) was added hydrazine monohydrate (49 μ L, 1 mmol). The solution was heated for 3 hours to 110 °C using a synthesis microwave. After cooling and evaporation of the solvent, the residue was purified by column chromatography (*n*-hexane / ethyl acetate), giving product **36** (31.7 mg, 0.11 mmol, 90 %) as a white amorphous solid:

HR-MS m/z 294.2060 (calculated for $C_{16}H_{28}N_3O_2$: 294.2064)

1H NMR (400 MHz, $(CD_3)_2SO$) δ 9.74 (s, 1H), 8.60 (d, J = 2.4 Hz, 1H), 8.07 (dd, J = 8.6, 2.5 Hz, 1H), 6.84 (d, J = 8.6 Hz, 1H), 4.47 (s, 2H), 4.28 (t, J = 6.6 Hz, 2H), 1.70 (p, J = 6.8 Hz, 2H), 1.42 – 1.34 (m, 2H), 1.37 – 1.22 (m, 12H), 0.85 (t, J = 6.7 Hz, 3H).

^{13}C NMR (101 MHz, $(CD_3)_2SO$) δ 164.88, 164.26, 146.52, 137.78, 122.41, 110.18, 65.90, 31.25, 28.95, 28.90, 28.72, 28.65, 28.36, 25.44, 22.06, 13.92.

Methyl 6-(decyloxy)nicotinoate (**37**)



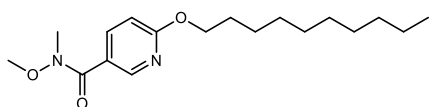
6-(Decyloxy)nicotinoyl chloride (**9-Cl**, 50 mg, 0.17 mmol) and methyl amine (1 mL, 33 % in EtOH) were each dissolved in dry dichloromethane (5 mL). The first solution was added dropwise to the second and the resulting mixture was stirred for 2 hours at room temperature, after which the solvent was removed in vacuo. Purification was done by column chromatography (*n*-hexane / ethyl acetate 5:5), giving product **37** (40.3 mg, 0.14 mmol, 83 %) as a white amorphous solid.

HR-MS m/z 293.2220 (calculated for $C_{17}H_{29}N_2O_2$: 293.2224)

1H NMR (400 MHz, $(CD_3)_2SO$) δ 8.61 (d, J = 2.4 Hz, 1H), 8.41 (q, J = 4.7 Hz, 1H), 8.08 (dd, J = 8.7, 2.5 Hz, 1H), 6.84 (d, J = 8.7 Hz, 1H), 4.28 (t, J = 6.6 Hz, 2H), 2.77 (d, J = 4.4 Hz, 3H), 1.70 (p, J = 6.8 Hz, 2H), 1.42 – 1.30 (m, 2H), 1.33 – 1.22 (m, 12H), 0.85 (t, J = 6.6 Hz, 3H).

^{13}C NMR (101 MHz, $(CD_3)_2SO$) δ 164.86, 164.84, 146.71, 137.93, 123.56, 110.07, 65.90, 31.25, 28.94, 28.90, 28.72, 28.65, 28.37, 26.04, 25.44, 22.06, 13.92.

6-(Decyloxy)-*N*-methoxy-*N*-methylnicotinamide (**38**)



A solution of 6-chloronicotinoyl chloride (56.5 mg, 0.19 mmol) and *N,O*-dimethylhydroxylamine hydrochloride (29.3 mg, 0.3 mmol) in dichloromethane (20 mL) was cooled down to 0 °C. Triethylamine (55.7 μ L, 0.4 mmol) was added, after which the solution was allowed to warm to

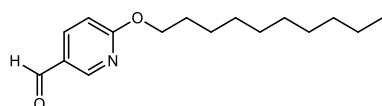
room temperature and was stirred overnight. The reaction was quenched by addition of sat. aq. NaHCO_3 solution (50 mL), the phases were separated, and the aqueous phase was extracted using dichloromethane (3x 50 mL). The combined organic phases were washed with brine (50 mL), dried over Na_2SO_4 , filtered, and evaporated to dryness. Purification was done by column chromatography (*n*-hexane / ethyl acetate 7:3 – 3:7), giving product **38** (58.7 mg, 0.18 mmol, 93 %) as a white amorphous solid:

HR-MS m/z 323.2324 (calculated for $\text{C}_{18}\text{H}_{31}\text{N}_2\text{O}_3$: 323.2329)

^1H NMR (400 MHz, CDCl_3) δ 8.63 (d, J = 1.8 Hz, 1H), 7.99 (dd, J = 8.7, 2.4 Hz, 1H), 6.73 (dd, J = 8.7, 0.7 Hz, 1H), 4.33 (t, J = 6.7 Hz, 2H), 3.58 (s, 3H), 3.37 (s, 3H), 1.84 – 1.72 (m, 2H), 1.50 – 1.39 (m, 2H), 1.38–1.23 (m, 12H), 0.88 (t, J = 6.8 Hz, 3H).

^{13}C NMR (101 MHz, CDCl_3) δ 167.43, 165.32, 148.34, 139.37, 122.53, 110.28, 66.63, 61.04, 33.38, 31.88, 29.56, 29.54, 29.37, 29.30, 28.96, 26.00, 22.66, 14.10.

6-(Decyloxy)nicotinaldehyde (**39**)

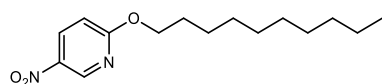


To a cooled solution (-15 °C) of Weinreb amide **38** (167 mg, 0.52 mmol) in dry toluene (20 mL) was added a solution of DIBAL-H (1 M in toluene, 0.54 mL, 0.54 mmol). The mixture was stirred for 10 minutes, after which the reaction was quenched by addition of ethyl acetate (53 μL). A semi-saturated aq. solution of tartaric acid was added (30 mL) and the mixture was shaken vigorously, after which the organic phase was separated and the aqueous phase reextracted using toluene (20 mL). The combined organic phases were dried over Na_2SO_4 , filtered, and evaporated to dryness, giving product **39** (126 mg, 0.48 mmol, 92 %) as a colourless oil.

^1H NMR (400 MHz, CDCl_3) δ 9.94 (s, 1H), 8.61 (d, J = 2.3 Hz, 1H), 8.05 (dd, J = 8.7, 2.4 Hz, 1H), 6.82 (d, J = 8.6 Hz, 1H), 4.40 (t, J = 6.7 Hz, 2H), 1.85 – 1.72 (m, 2H), 1.50 – 1.40 (m, 2H), 1.40 – 1.21 (m, 12H), 0.88 (t, J = 6.9 Hz, 3H).

^{13}C NMR (101 MHz, CDCl_3) δ 189.48, 167.66, 152.96, 137.34, 126.45, 112.16, 67.24, 31.87, 29.54, 29.53, 29.32, 29.29, 28.84, 25.94, 22.66, 14.09.

2-(Decyloxy)-5-nitropyridine (**40**)



To a solution of 2-chloro-5-nitropyridine (0.5 g, 3.2 mmol) and 1-decanol (0.6 mL, 3.2 mmol) in dry THF (20 mL) was added sodium hydride (60 %, 140 mg, 5.8 mmol) at 0 °C. After stirring for 30 min, the reaction was quenched by addition of water (30 mL). The solution was extracted using ethyl acetate (3x 30 mL) and the combined organic phases were washed with brine (2x 30 mL), dried over Na_2SO_4 , filtered, and evaporated to dryness. Purification was done by column

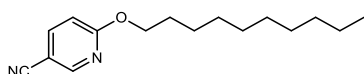
chromatography (*n*-hexane / ethyl acetate 9:1), giving product **40** (0.77 g, 2.8 mmol, 86 %) as a colourless oil:

HR-MS *m/z* 281.1873 (calculated for C₁₅H₂₅N₂O₃: 281.1860)

¹H NMR (400 MHz, CDCl₃) δ 9.06 (d, *J* = 2.8 Hz, 1H), 8.34 (dd, *J* = 9.1, 2.8 Hz, 1H), 6.80 (d, *J* = 9.1 Hz, 1H), 4.41 (t, *J* = 6.7 Hz, 2H), 1.79 (p, *J* = 6.9 Hz, 2H), 1.50 – 1.38 (m, 2H), 1.38 – 1.22 (m, 12H), 0.88 (t, *J* = 6.7 Hz, 3H).

¹³C NMR (101 MHz, CDCl₃) δ 167.33, 144.89, 139.23, 133.77, 111.27, 67.87, 31.87, 29.52, 19.51, 29.30, 29.29, 28.75, 25.90, 22.66, 14.09.

6-(Decyloxy)nicotinonitrile (**41**)



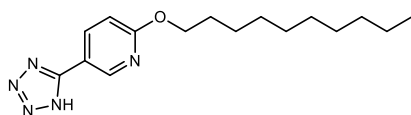
To a solution of 2-chloro-5-cyanopyridine (1 g, 6.3 mmol) and 1-decanol (1.2 mL, 6.3 mmol) in dry THF (20 mL) was added sodium hydride (60 %, 280 mg, 11.6 mmol) at 0 °C. After stirring for 30 min, the reaction was quenched by addition of water (30 mL). The solution was extracted using ethyl acetate (3x 30 mL) and the combined organic phases were washed with brine (2x 30 mL), dried over Na₂SO₄, filtered, and evaporated to dryness. Purification was done by column chromatography (*n*-hexane / ethyl acetate 9:1), giving product **41** (1.21 g, 4.6 mmol, 73 %) as a colourless oil:

HR-MS *m/z* 261.1957 (calculated for C₁₆H₂₅N₂O: 261.1961)

¹H NMR (400 MHz, CDCl₃) δ 8.47 (d, *J* = 2.4 Hz, 1H), 7.76 (dd, *J* = 8.7, 2.3 Hz, 1H), 6.79 (d, *J* = 8.7 Hz, 1H), 4.35 (t, *J* = 6.7 Hz, 2H), 1.77 (p, *J* = 6.9 Hz, 2H), 1.49 – 1.38 (m, 2H), 1.38 – 1.25 (m, 12H), 0.88 (t, *J* = 6.6 Hz, 3H).

¹³C NMR (101 MHz, CDCl₃) δ 165.94, 151.97, 140.78, 117.35, 111.87, 102.05, 67.22, 31.85, 29.51, 29.50, 29.28, 29.27, 28.72, 25.89, 22.64, 14.07.

2-(Decyloxy)-5-(1*H*-tetrazol-5-yl)pyridine (**42**)



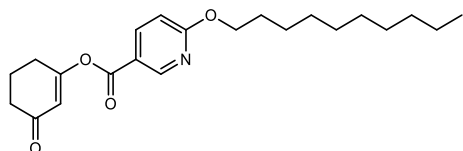
A solution of compound **41** (0.5 g, 1.9 mmol), sodium azide (0.37 g, 5.8 mmol) and ammonium chloride (0.31 g, 5.8 mmol) in dry DMF (20 mL) was stirred for 18 hours at 90 °C. Water (30 mL) was added to the solution, which was acidified to pH ~ 2 - 3 using aqueous hydrochloric acid (1 M) and the aqueous phase was subsequently extracted using ethyl acetate (3x 30 mL). The combined organic phases were washed with brine (30 mL), dried over Na₂SO₄, filtered, and evaporated to dryness. The resulting solid was recrystallized from ethanol at - 20 °C, giving product **42** (256 mg, 1.6 mmol, 84 %) as a white solid:

HR-MS *m/z* 304.2128 (calculated for C₁₆H₂₆N₅O: 304.2132)

^1H NMR (400 MHz, $(\text{CD}_3)_2\text{SO}$) δ 16.84 (s, 1H), 8.81 (d, J = 2.4 Hz, 1H), 8.27 (dd, J = 8.7, 2.4 Hz, 1H), 7.02 (d, J = 8.7 Hz, 1H), 4.33 (t, J = 6.6 Hz, 2H), 1.73 (p, J = 6.9 Hz, 2H), 1.46 – 1.34 (m, 2H), 1.33 – 1.20 (m, 12H), 0.85 (t, J = 6.7 Hz, 3H).

^{13}C NMR (101 MHz, $(\text{CD}_3)_2\text{SO}$) δ 165.36, 153.84, 146.41, 137.96, 114.64, 111.91, 66.57, 31.73, 29.43, 29.39, 29.21, 29.14, 28.81, 25.91, 22.53, 14.35.

3-Oxocyclohex-1-en-1-yl 6-(decyloxy)nicotinate (**43**)



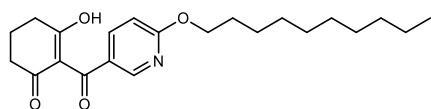
6-(Decyloxy)nicotinic acid (110 mg, 0.35 mmol) and oxalyl chloride (1.6 mL) were dissolved in dry DCM (10 mL + 0.1 % DMF) at 0 °C and stirred for 5 hours, after which the solvent was removed in vacuo, giving crude 6-(decyloxy)nicotinoyl chloride. Triethylamine (98 μL , 0.7 mmol) and cyclohexane-1,3-dione (39 mg, 0.35 mmol) were dissolved in dry DCM (10 mL), to which the acid chloride in dry DCM (10 mL) was dropwise added at 0 °C. The mixture was stirred at this temperature for 30 minutes, after which water (40 mL) was added followed by another stirring period of 30 minutes. After separation of the phases, the organic phase was washed using sat. aq. NaHCO_3 solution (2x 40 mL), brine (40 mL), dried over Na_2SO_4 , filtered, and evaporated to dryness. Purification was done by column chromatography (*n*-hexane / ethyl acetate 9:1 – 8:2), giving derivative **43** (100 mg, 0.27 mmol, 77 %) as a colourless oil:

HR-MS m/z 374.2321 (calculated for $\text{C}_{22}\text{H}_{32}\text{NO}_4$: 374.2326)

^1H NMR (400 MHz, CDCl_3) δ 8.87 (d, J = 2.4 Hz, 1H), 8.16 (dd, J = 8.7, 2.5 Hz, 1H), 6.79 (d, J = 8.8 Hz, 1H), 6.05 (d, J = 1.4 Hz, 1H), 4.38 (t, J = 6.7 Hz, 2H), 2.67 (td, J = 6.2, 1.3 Hz, 2H), 2.46 (dd, J = 7.4, 6.0 Hz, 2H), 2.13 (p, J = 6.4 Hz, 2H), 1.79 (q, J = 7.4 Hz, 2H), 1.50 – 1.39 (m, 2H), 1.38 – 1.23 (m, 12H), 0.88 (t, J = 7.0 Hz, 3H).

^{13}C NMR (101 MHz, CDCl_3) δ 199.38, 169.84, 167.46, 162.10, 151.07, 139.79, 117.88, 117.87, 111.21, 67.18, 36.78, 31.87, 29.54, 29.53, 29.33, 29.29, 28.84, 28.46, 25.94, 22.66, 21.33, 14.09.

2-(6-(Decyloxy)nicotinoyl)-3-hydroxycyclohex-2-en-1-one (**44**)



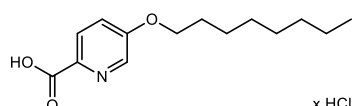
Compound **43** (75 mg, 0.2 mmol), triethylamine (84 μL , 0.6 mmol) and dried potassium cyanide (1.3 mg, 0.02 mmol) were dissolved in dry acetonitrile (3 mL) in a microwave vial and heated to 100 °C for 1 hour using a synthesis microwave. The suspension was cooled down to room temperature, diluted with ethyl acetate (30 mL) and was washed using aqueous hydrochloric acid (1 M, 2x 30 mL) and brine (30 mL), dried over Na_2SO_4 , filtered, and evaporated to dryness. Purification was done by column chromatography (*n*-hexane / ethyl acetate 9:1 – 6:4), giving product **44** (46.3 mg, 0.12 mmol, 62 %) as a white solid:

HR-MS m/z 374.2322 (calculated for $C_{22}H_{32}NO_4$: 374.2326)

1H NMR (400 MHz, $CDCl_3$) δ 17.00 (s, 1H), 8.42 (d, $J = 2.4$ Hz, 1H), 7.76 (dd, $J = 8.7, 2.4$ Hz, 1H), 6.70 (d, $J = 8.7$ Hz, 1H), 4.35 (t, $J = 6.7$ Hz, 2H), 2.78 – 2.70 (m, 2H), 2.55 – 2.47 (m, 2H), 2.07 (p, $J = 6.4$ Hz, 2H), 1.78 (p, $J = 7.6$ Hz, 2H), 1.49 – 1.38 (m, 2H), 1.37 – 1.25 (m, 12H), 0.88 (t, $J = 7.3$ Hz, 3H).

^{13}C NMR (101 MHz, $CDCl_3$) δ 196.24, 195.69, 194.41, 166.30, 149.15, 139.23, 126.80, 112.98, 109.80, 66.84, 38.11, 32.43, 31.86, 29.54, 29.52, 29.33, 29.28, 28.90, 25.97, 22.65, 19.01, 14.08.

5-(Octyloxy)picolinic acid (**45**)



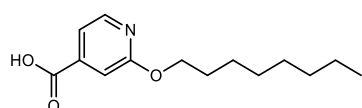
According to general method, 1-octanol (156.9 μ L, 1 mmol), 5-chloropyridine-2-carboxylic acid (79 mg, 0.5 mmol) and potassium hydroxide (140.3 mg, 2.5 mmol) were used. Purification was done by column chromatography (*n*-hexane / ethyl acetate + 0.1 % FA), giving derivative **45** (103.0 mg, 0.41 mmol, 82 %) as a white amorphous solid:

HR-MS m/z 252.1591 (calculated for $C_{14}H_{22}NO_3$: 252.1594)

1H NMR (400 MHz, $(CD_3)_2SO$) δ 12.85 (s, 1H), 8.30 (dd, $J = 4.9, 2.0$ Hz, 1H), 8.06 (dd, $J = 7.4, 2.0$ Hz, 1H), 7.04 (dd, $J = 7.4, 4.9$ Hz, 1H), 4.32 (t, $J = 6.6$ Hz, 2H), 1.70 (p, $J = 6.7$ Hz, 2H), 1.40 (td, $J = 9.3, 8.5, 4.3$ Hz, 2H), 1.35 – 1.22 (m, 8H), 0.85 (t, $J = 7.5$ Hz, 3H).

^{13}C NMR (101 MHz, $(CD_3)_2SO$) δ 166.18, 161.10, 150.05, 140.54, 116.46, 115.25, 65.77, 31.17, 28.65, 28.63, 28.36, 25.41, 22.05, 13.92.

2-(Octyloxy)isonicotinic acid (**46**)



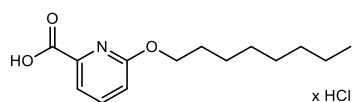
According to general method, 1-octanol (156.9 μ L, 1 mmol), 2-chloro-4-pyridinecarboxylic acid (79 mg, 0.5 mmol) and potassium hydroxide (140.3 mg, 2.5 mmol) were used. Purification was done by column chromatography (*n*-hexane / ethyl acetate 8:2 – 7:3 + 0.1 % FA), giving derivative **46** (106.8 mg, 0.43 mmol, 85 %) as a white amorphous solid:

HR-MS m/z 252.1592 (calculated for $C_{14}H_{22}NO_3$: 252.1594)

1H NMR (400 MHz, $(CD_3)_2SO$) δ 13.62 (s, 1H), 8.31 (d, $J = 5.2$ Hz, 1H), 7.36 (dd, $J = 5.2, 1.4$ Hz, 1H), 7.15 (t, $J = 1.0$ Hz, 1H), 4.28 (t, $J = 6.6$ Hz, 2H), 1.71 (d, $J = 6.8$ Hz, 2H), 1.45 – 1.32 (m, 2H), 1.32 – 1.22 (m, 8H), 0.86 (t, $J = 7.2$ Hz, 3H).

^{13}C NMR (101 MHz, $(CD_3)_2SO$) δ 165.83, 164.05, 147.96, 141.36, 115.68, 110.23, 65.90, 31.19, 28.69, 28.60, 28.34, 25.44, 22.04, 13.90.

6-(Octyloxy)picolinic acid (**47**)



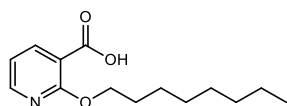
According to general method, 1-octanol (156.9 μ L, 1 mmol), 6-chloropyridine-2-carboxylic acid (79 mg, 0.5 mmol) and potassium hydroxide (140.3 mg, 2.5 mmol) were used, giving product **47** (126.6 mg, 0.44 mmol, 88 %) as a white amorphous solid:

HR-MS m/z 252.1592 (calculated for C₁₄H₂₂NO₃: 252.1594)

¹H NMR (400 MHz, (CD₃)₂SO) δ 13.01 (s, 1H), 7.84 (dd, J = 8.3, 7.2 Hz, 1H), 7.64 (d, J = 7.2 Hz, 1H), 7.02 (d, J = 8.2 Hz, 1H), 4.30 (t, J = 6.6 Hz, 2H), 1.72 (p, J = 6.8 Hz, 2H), 1.46 – 1.35 (m, 2H), 1.33 – 1.19 (m, 8H), 0.86 (t, J = 7.2 Hz, 3H).

¹³C NMR (101 MHz, (CD₃)₂SO) δ 165.83, 163.00, 145.86, 139.92, 118.15, 114.70, 65.63, 31.20, 28.71, 28.63, 28.38, 25.50, 22.05, 13.91.

2-(Octyloxy)nicotinic acid (**48**)



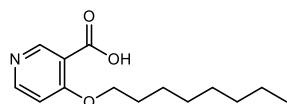
According to general method, 1-octanol (156.9 μ L, 1 mmol), 2-chloropyridine-3-carboxylic acid (79 mg, 0.5 mmol) and potassium hydroxide (140.3 mg, 2.5 mmol) were used. Purification was done by column chromatography (*n*-hexane / ethyl acetate 8:2 + 0.1 % FA), giving compound **48** (96.8 mg, 0.39 mmol, 77 %) as a white amorphous solid:

HR-MS m/z 252.1590 (calculated for C₁₄H₂₂NO₃: 252.1594)

¹H NMR (400 MHz, (CD₃)₂SO) δ 12.85 (s, 1H), 8.30 (dd, J = 4.9, 2.0 Hz, 1H), 8.07 (dd, J = 7.5, 2.0 Hz, 1H), 7.04 (dd, J = 7.4, 4.9 Hz, 1H), 4.32 (t, J = 6.6 Hz, 2H), 1.76 – 1.64 (m, 2H), 1.47 – 1.36 (m, 2H), 1.36 – 1.22 (m, 8H), 0.86 (t, J = 6.8 Hz, 3H).

¹³C NMR (101 MHz, (CD₃)₂SO) δ 166.18, 161.11, 150.06, 140.55, 116.46, 115.22, 65.77, 31.17, 28.65, 28.63, 28.35, 25.41, 22.05, 13.92.

4-(Octyloxy)nicotinic acid (**49**)



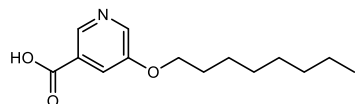
According to general method, 1-octanol (156.9 μ L, 1 mmol), 4-chloropyridine-3-carboxylic acid (79 mg, 0.5 mmol) and potassium hydroxide (140.3 mg, 2.5 mmol) were used. Purification was done by column chromatography (*n*-hexane / ethyl acetate 8:2 + 0.1 % FA), giving product **49** (100.5 mg, 0.4 mmol, 80 %) as a white amorphous solid:

HR-MS m/z 252.1591 (calculated for C₁₄H₂₂NO₃: 252.1594)

^1H NMR (400 MHz, $(\text{CD}_3)_2\text{SO}$) δ 13.01 (s, 1H), 8.66 (s, 1H), 8.50 (d, $J = 5.9$ Hz, 1H), 7.14 (d, $J = 5.9$ Hz, 1H), 4.11 (t, $J = 6.4$ Hz, 2H), 1.72 (q, $J = 7.0$ Hz, 2H), 1.43 (p, $J = 6.8$ Hz, 2H), 1.36 – 1.20 (m, 8H), 0.86 (t, $J = 7.0$ Hz, 3H).

^{13}C NMR (101 MHz, $(\text{CD}_3)_2\text{SO}$) δ 166.01, 163.27, 153.55, 151.33, 117.91, 108.60, 68.23, 31.17, 28.63, 28.57, 28.20, 25.23, 22.06, 13.92.

5-(Octyloxy)nicotinic acid (**50**)



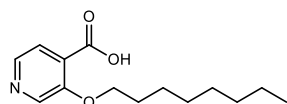
According to general method, 1-octanol (156.9 μL , 1 mmol), 5-chloropyridine-3-carboxylic acid (79 mg, 0.5 mmol) and potassium hydroxide (140.3 mg, 2.5 mmol) were used. Purification was done by column chromatography (*n*-hexane / ethyl acetate 8:2 + 0.1 % FA), giving product **50** (105.6 mg, 0.42 mmol, 83 %) as a white amorphous solid:

HR-MS m/z 252.1592 (calculated for $\text{C}_{14}\text{H}_{22}\text{NO}_3$: 252.1594)

^1H NMR (400 MHz, $(\text{CD}_3)_2\text{SO}$) δ 13.45 (s, 1H), 8.66 (d, $J = 1.6$ Hz, 1H), 8.49 (d, $J = 2.9$ Hz, 1H), 7.72 (dd, $J = 3.0, 1.7$ Hz, 1H), 4.10 (t, $J = 6.5$ Hz, 2H), 1.73 (q, $J = 7.5$ Hz, 2H), 1.42 (dd, $J = 10.6, 5.0$ Hz, 2H), 1.37 – 1.23 (m, 8H), 0.86 (t, $J = 6.9$ Hz, 3H).

^{13}C NMR (101 MHz, $(\text{CD}_3)_2\text{SO}$) δ 166.19, 154.68, 142.10, 142.05, 127.20, 120.44, 68.16, 31.20, 28.65, 28.61, 28.43, 25.33, 22.05, 13.92.

3-(Octyloxy)isonicotinic acid (**51**)



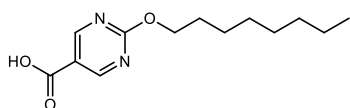
According to general method, 1-octanol (156.9 μL , 1 mmol), 3-chloropyridine-4-carboxylic acid (79 mg, 0.5 mmol) and potassium hydroxide (140.3 mg, 2.5 mmol) were used. Purification was done by column chromatography (*n*-hexane / ethyl acetate 8:2 – 7:3 + 0.1 % FA), giving product **51** (90.5 mg, 0.36 mmol, 71 %) as a white amorphous solid:

HR-MS m/z 252.1593 (calculated for $\text{C}_{14}\text{H}_{22}\text{NO}_3$: 252.1594)

^1H NMR (400 MHz, $(\text{CD}_3)_2\text{SO}$) δ 13.30 (s, 1H), 8.51 (s, 1H), 8.26 (d, $J = 4.8$ Hz, 1H), 7.48 (d, $J = 4.7$ Hz, 1H), 4.15 (t, $J = 6.4$ Hz, 2H), 1.71 (q, $J = 7.0$ Hz, 2H), 1.48 – 1.36 (m, 2H), 1.36 – 1.22 (m, 8H), 0.86 (t, $J = 7.1$ Hz, 3H).

^{13}C NMR (101 MHz, $(\text{CD}_3)_2\text{SO}$) δ 166.31, 151.76, 141.91, 136.79, 128.97, 122.71, 69.00, 31.18, 28.64, 28.63, 28.60, 25.23, 22.06, 13.92.

2-(Octyloxy)pyrimidine-5-carboxylic acid (**52**)



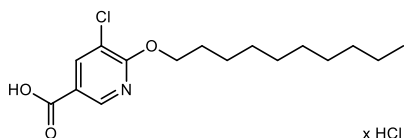
According to general method, 1-octanol (156.9 μ L, 1 mmol), 2-chloropyrimidine-5-carboxylic acid (79 mg, 0.5 mmol) and potassium hydroxide (140.3 mg, 2.5 mmol) were used. Purification was done by column chromatography (*n*-hexane / ethyl acetate 7:3 + 0.1 % FA), giving product **52** (84.5 mg, 0.34 mmol, 67 %) as a white amorphous solid:

HR-MS m/z 253.1545 (calculated for $C_{13}H_{21}N_2O_3$: 253.1545)

1H NMR (400 MHz, $(CD_3)_2SO$) δ 13.43 (s, 1H), 9.00 (s, 2H), 4.38 (t, J = 6.6 Hz, 2H), 1.74 (q, J = 7.5 Hz, 2H), 1.46 – 1.35 (m, 2H), 1.27 (dt, J = 14.8, 5.7 Hz, 8H), 0.86 (t, J = 7.5 Hz, 3H).

^{13}C NMR (101 MHz, $(CD_3)_2SO$) δ 166.42, 164.77, 161.03, 161.02, 118.90, 67.89, 31.17, 28.63, 28.58, 28.13, 25.32, 22.04, 13.91.

5-Chloro-6-(decyloxy)nicotinic acid (**53**)



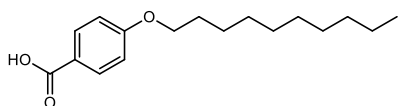
According to general method, 1-decanol (0.19 mL, 1 mmol), 5,6-dichloropyridine-3-carboxylic acid (95 mg, 0.5 mmol) and potassium hydroxide (140.3 mg, 2.5 mmol) were used, giving product **53** (57.8 mg, 0.17 mmol, 33 %) as a white amorphous solid:

HR-MS m/z 314.1523 (calculated for $C_{16}H_{25}NO_3Cl$: 314.1517)

1H NMR (400 MHz, $(CD_3)_2SO$) δ 13.32 (s, 1H), 8.66 – 8.61 (m, 1H), 8.23 – 8.18 (m, 1H), 4.41 (t, J = 6.6 Hz, 2H), 1.75 (p, J = 6.7 Hz, 2H), 1.46 – 1.36 (m, 2H), 1.26 (d, J = 17.4 Hz, 12H), 0.85 (t, J = 6.4 Hz, 3H).

^{13}C NMR (101 MHz, $(CD_3)_2SO$) δ 165.07, 160.97, 147.14, 138.78, 121.36, 116.98, 67.46, 31.25, 28.89, 28.85, 28.63, 28.59, 28.11, 25.30, 22.06, 13.91.

4-(Decyloxy)benzoic acid (**54**)



To potassium hydroxide (1.7 g, 30 mmol) in ethanol (25 mL) was added 4-hydroxybenzoic acid (1.4 g, 10 mmol) and dropwise 1-bromodecane (2.1 mL, 10 mmol). The solution was refluxed for 6 hours after which it was acidified to pH ~ 2 - 3, forming a white precipitate which was filtered off and washed with water. Recrystallization from toluene gave product **54** (2.0 g, 7.2 mmol, 72 %) as white crystals:

HR-MS m/z 279.1960 (calculated for $C_{17}H_{27}O_3$: 279.1955)

1H NMR (400 MHz, $CDCl_3$) δ 11.92 (s, 1H), 8.05 (d, J = 8.8 Hz, 2H), 6.93 (d, J = 8.8 Hz, 2H), 4.02 (t, J = 6.6 Hz, 2H), 1.80 (p, J = 6.8 Hz, 2H), 1.52 – 1.40 (m, 2H), 1.39 – 1.23 (m, 12H), 0.88 (t, J = 6.7 Hz, 3H).

^{13}C NMR (101 MHz, $CDCl_3$) δ 172.02, 163.70, 132.32 (2C), 121.37, 114.18 (2C), 68.28, 31.88, 29.54, 29.54, 29.35, 29.30, 29.08, 25.97, 22.67, 14.10.

References

- (1) Barber, D. M. *J. Agric. Food. Chem.* **2022**, 70, 11075–11090.
- (2) Vitaku, E.; Smith, D. T.; Njardarson, J. T. *J. Med. Chem.* **2014**, 57, 10257–10274.
- (3) Brody, F.; Ruby, P. R. Synthetic and Natural Sources of the Pyridine Ring. In *Pyridine and its derivatives. Part one*; Klingsberg, E., Ed.; The chemistry of heterocyclic compounds v. 14, pt. 1; Interscience: New York, **1960**, 99–589.
- (4) Lima, L. M.; Barreiro, E. J. *Curr. Med. Chem.* **2005**, 12, 23–49.
- (5) Zakharychev, V. V.; Kuzenkov, A. V.; Martsynkevich, A. M. *Chem. Heterocycl. Compd.* **2020**, 56, 1491–1516.
- (6) Food and Agriculture Organization of the United Nations. Database Collection of the Food and Agriculture Organization of the United Nations, <http://www.fao.org/faostat/en/#data> (FAOSTAT, **2023**).
- (7) Darter, I. E.; Wright, N. *International Journal of Pest Management: Part C* **1963**, 9, 203–206.
- (8) Çatak, J. *JAST* **2019**, 61, 138–146.
- (9) Hegyi, J.; Schwartz, R. A.; Hegyi, V. *Int. J. Dermatol.* **2004**, 43, 1–5.
- (10) Fu, Y.; Zhang, S.-Q.; Liu, Y.-X.; Wang, J.-Y.; Gao, S.; Zhao, L.-X.; Ye, F. *Ind. Crops Prod.* **2019**, 137, 566–575.
- (11) Wang, D.-W.; Lin, H.-Y.; Cao, R.-J.; Chen, T.; Wu, F.-X.; Hao, G.-F.; Chen, Q.; Yang, W.-C.; Yang, G.-F. *J. Agric. Food. Chem.* **2015**, 63, 5587–5596.
- (12) Williamson, A. *Lond. Edinb. Dublin philos. mag. j. sci.* **1850**, 37, 350–356.
- (13) Paul, F.; Patt, J.; Hartwig, J. F. *J. Am. Chem. Soc.* **1994**, 116, 5969–5970.
- (14) Sonogashira, K.; Tohda, Y.; Hagihara, N. *Tetrahedron Lett.* **1975**, 16, 4467–4470.
- (15) Geissler, H.; Gross, P. Method for the catalytic production of substituted dipyrindyl derivatives. US6500956 (B1), 12/31/**2002**.
- (16) Bamfield, P.; Quan, P. M. *Synthesis* **1978**, 1978, 537–538.
- (17) Cai, H.; Gan, X.; Jin, Z.; Hao, G. *J. Agric. Food. Chem.* **2023**, 71, 9973–9993.
- (18) Hsieh, S.-Y.; Tang, Y.; Crotti, S.; Stone, E. A.; Miller, S. J. *J. Am. Chem. Soc.* **2019**, 141, 18624–18629.
- (19) Pajouhesh, H.; Lenz, G. R. *NeuroRx* **2005**, 2, 541–553.
- (20) Barber, D. M. *J. Agric. Food. Chem.* **2022**, 70, 11075–11090.
- (21) Ballatore, C.; Huryn, D. M.; Smith, A. B. *ChemMedChem* **2013**, 8, 385–395.
- (22) Knudsen, C. G.; Lee, D. L.; Michaely, W. J.; Chin, H.-L.; Nguyen, N. H.; Rusay, R. J.; Cromartie, T. H.; Gray, R.; Lake, B. H.; Fraser, T. E. M.; Cartwright, D. Discovery of the triketone class of HPPD inhibiting herbicides and their relationship to naturally occurring β -triketones. In *Allelopathy in Ecological Agriculture and Forestry*; Springer, Dordrecht, **2000**, 101–111.
- (23) Narwal, S. S.; Hoagland, R. E.; Dilday, R. H.; Reigosa, M. J., Eds. *Allelopathy in Ecological Agriculture and Forestry*; Springer Netherlands, Dordrecht, **2000**.
- (24) Geissler, T.; Wessjohann, L. A. *J. Plant Growth Regul.* **2011**, 30, 504–511.
- (25) Otto, A. Chemical and biological studies on bioactive secondary metabolites from fungal source, Universitäts- und Landesbibliothek Sachsen-Anhalt; Martin-Luther Universität, **2017**.
- (26) Michel, B. E.; Kaufmann, M. R. *Plant Physiol.* **1973**, 51, 914–916.
- (27) Khan, M. F.; Nasr, F. A.; Noman, O. M.; Alyhya, N. A.; Ali, I.; Saoud, M.; Rennert, R.; Dube, M.; Hussain, W.; Green, I. R.; Basudan, O. A. M.; Ullah, R.; Anazi, S. H.; Hussain, H. *Molecules* **2020**, 25, 4160.

Chapter 4

Synthesis and biological evaluation of 4-hydroxy-2-pyrones and 3-phenylcoumarins as potential antimycotics and herbicides

Abstract

6-Alkylated 4-hydroxy-2-pyrones and substituted 3-phenylcoumarins were found to possess antiphytopathogenic and herbicidal activities. A library of seven phenylcoumarins and twenty pyrone derivatives was prepared. This includes the first reported synthesis of the natural product fistupyrone **15**. All compounds were tested *in vivo* towards their anti-phytopathogenic activity against the plant pathogenic fungi *Botrytis cinerea* and *Septoria tritici* and the oomycete *Phytophthora infestans*. Compound **23** showed the lowest ED₅₀ of 7.2 ± 1.7 μ M against *Botrytis cinerea*. Furthermore, their growth inhibition activity against *Lemna minor* was investigated. Several substances were found to have moderate herbicidal activity of which compound **8** showed the highest growth inhibition of 61 % at a concentration of 50 μ M. It was found that the herbicidal and antiphytopathogenic properties are separated by structure and the required concentrations, making a safe development of either of the properties possible.

Introduction

Phytopathogenic organisms are responsible for major crop losses in the past and present, causing great famines and economic losses.^{1,2} Every year, 9 to 15 percent of the world's food production is destroyed by these pests.³ Among those, plant pathogenic fungi are probably the most diverse group, having a wide range of lifestyles and infest various hosts.² The ascomycetous fungi *Botrytis cinerea* and *Septoria tritici* as well as the oomycete *Phytophthora infestans* play a major role by attacking important crops such as potatoes, wheat, grapes, and strawberries, among others.^{4–6} They are able to rapidly attack new hosts and develop resistance to applied pesticides due to their genetic diversity.¹ Therefore, it is important to continuously develop new active substances in order to find new modes of action to prevent future setbacks.

Similar resistance effects can be observed with all widely used herbicides, whereby resistance was already found for all major herbicide modes of action.⁷ Furthermore, some of those herbicides are additionally facing a ban or their registration is not being renewed in various countries.⁸ Hence, a constant search for new active ingredients and modes of action is indispensable to supply an ever-growing world population.⁹

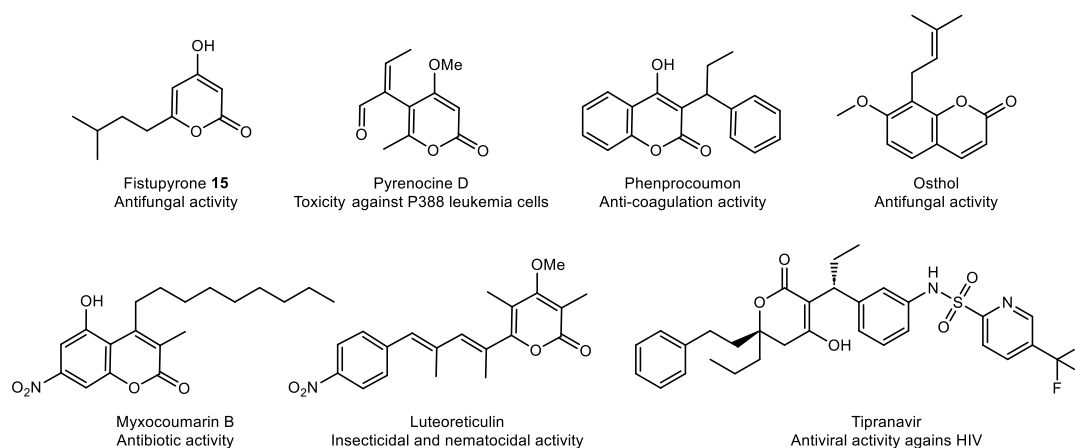


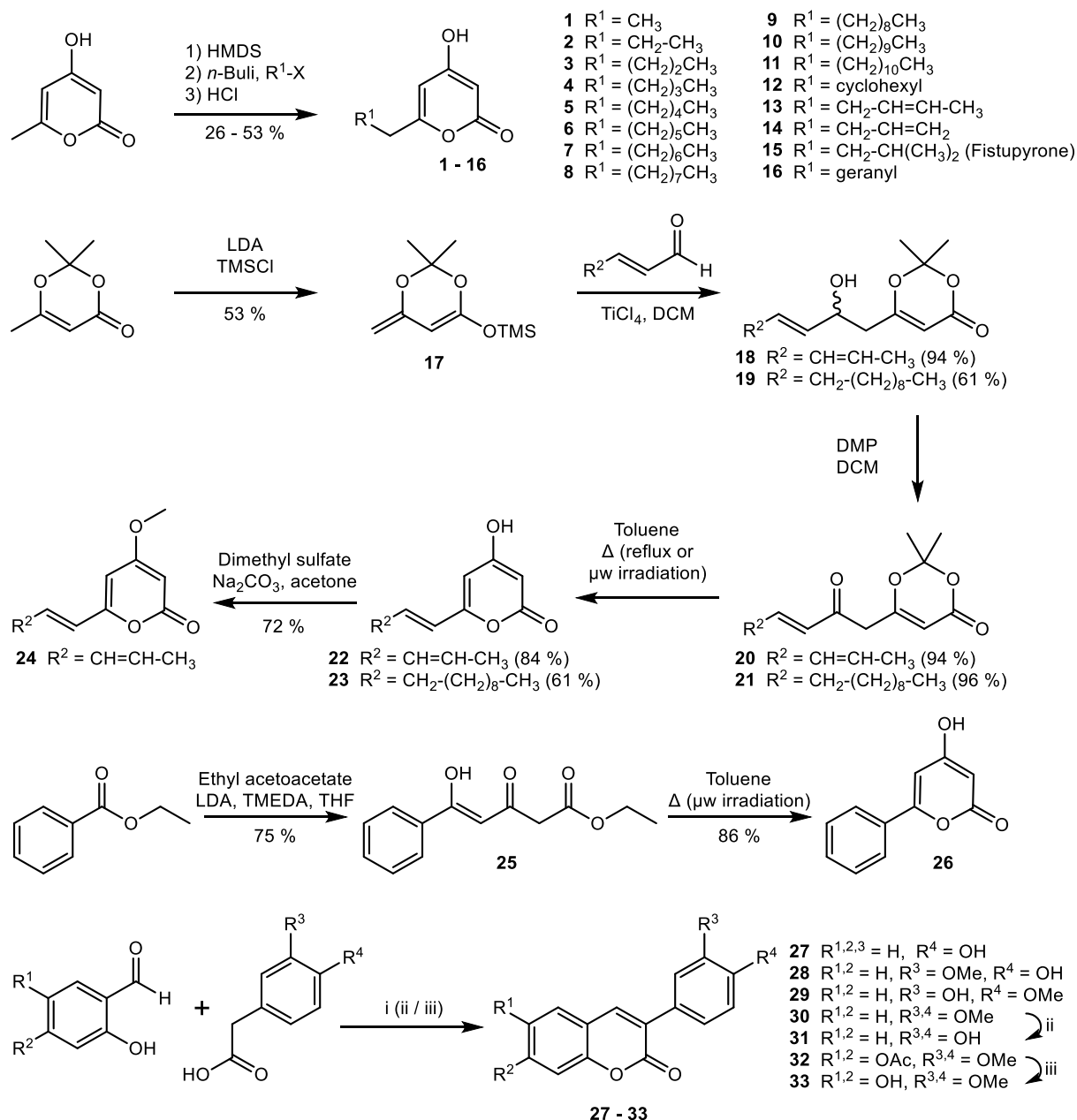
Figure 28: Structures of biologically active molecules containing the 2-pyrone moiety.^{10–16}

Natural products are and will be part of a solution to this problem. Because biologically active NPs can act through novel MOAs that differ from those used in commercial herbicides (currently 23 different MOAs for commercial fungicides and 34 different MOAs for commercial herbicides).^{17,18} Pyrones and coumarins are two groups of natural substances that have been in the focus of research for a long time. Many novel substances with intriguing biological activities have been found and are likely to be found in the future.^{19–21}

An example of a natural substance from this group with interesting biological activity is fistupyrone **15**, which was first described by Igarashi et al. in 2000. It was isolated from the strain *Streptomyces* sp. TP-A0569, which itself was isolated from the onion *Allium fistulosum*.²² In the analysis of biological activity, it was found that fistupyrone inhibited the *in vivo* infection of chinese cabbage seedling by *A. brassicola* without inhibiting mycelial growth.

Results and discussion

In this chapter, the synthesis and biological activity of twenty 4-hydroxy-2-pyrones and seven 3-phenylcoumarins is described. The reaction conditions and characterization data of the synthesized compounds can be found in the experimental section.



Scheme 11: Synthesis of 2-pyrones **1 - 16**, **22 - 24** & **26** and 3-phenylcoumarins **27 – 33**; reagents and conditions: X = Cl or Br or I, i) carbonyldiimidazol, diazabicycloundecene, then aqueous hydrochloric acid (for **32**: KOAc + Ac₂O, then NaHCO₃); ii) boron tribromide; iii) LiOH.

The aliphatic 2-pyrones **1 - 16** were synthesized using an improved two-step procedure from *McLaughlin* et al.^{23,24} Usually, this reaction can be achieved without in-situ protection of the hydroxyl group by using hexamethylphosphoramide as a reagent.²⁵ Attempts to avoid this highly toxic chemical and substitute it with DMPU or DMI were unsuccessful. Therefore, another synthesis route was found in which the 4-hydroxy-6-methyl-2H-pyran-2-one, which served as the starting material, was first protected using hexamethyldisilazane (HMDS).

HMDS acts as solvent and protecting agent for the hydroxyl group *in situ*. The silylated intermediate was then treated with *n*-butyl lithium to form the corresponding anion, which then underwent an electrophilic addition reaction with the added halocarbon. During the acidic workup, the protection group was removed. Using this method, a total of 16 pyrones were synthesized (see Scheme 11).

One of these substances is the natural product fistupyrone **15**, for which the first known total synthesis was achieved. All obtained spectral data are in accordance with the data published for the natural product.²²

The synthesis of 4-hydroxy-6-pentadienyl-2-pyrone **22** was first attempted following the procedure of *Ma* et al. in which the authors describe a two-step synthesis with 1.4 % overall yield.²⁶ Unfortunately, the described cyclization could not be reproduced successfully, instead giving a mixture of compounds, from which the desired pyrone **22** could not be isolated. Therefore, a new strategy starting from sorbic aldehyde (see Scheme 1) was developed.²⁷ After coupling to dioxinone, the obtained ketodioxinone **18** appeared to be more stable and easier to cyclize than the acyclic derivative. The final cyclization could then be achieved either by heating under reflux or μ w irradiation, giving the desired pyrone **22** in 31 % yield. Using the same procedure, the more hydrophilic pyrone **23** was synthesized. Additionally, pyrone **24** was prepared by methylation with dimethyl sulphate. The interest in compound **24** originates from its growth inhibitory activity described in the literature.^{20,28}

The synthesis of 4-hydroxy-6-phenyl-2-pyrone **26** was achieved using an improved two-step protocol from *Douglas* and co-workers.²⁹ The *Claisen* condensation of benzoic acid ethyl ether and ethyl acetoacetate was achieved using LDA and TMEDA.³⁰ Cyclizing intermediate **25** could be accelerated by performing the reaction in a microwave oven at 140 °C in toluene, using one equivalent of DBU as a promoter.

Furthermore, five known and two new coumarins **27** - **33** were synthesized and tested for their antimycotic and herbicidal activity. The synthesis of these coumarins could be achieved as previously reported by *Roussaki* et al.³¹ They describe a straightforward intermolecular condensation reaction between various benzaldehydes and phenylacetic acids at mild conditions, leading to differently substituted 3-phenylcoumarins. Following this procedure, the synthesis of a variety of compounds with different substitutions at both aromatic rings and therefore large variation of the polarity was achieved. Deprotection of the acetyl respectively methoxy groups gave access to two more derivatives **31** and **33**.

Biological activity

Anti-phytopathogenic activity

In the past, it has been shown that pyrones and coumarins can possess strong antimycotic activities.^{32–34} Therefore, the synthesized compounds were tested for their anti-phytopathogenic activities against *Botrytis cinerea* and *Septoria tritici* and the oomycete *Phytophthora infestans*. The commercial antifungal agents epoxiconazole and terbinafine served as positive controls.

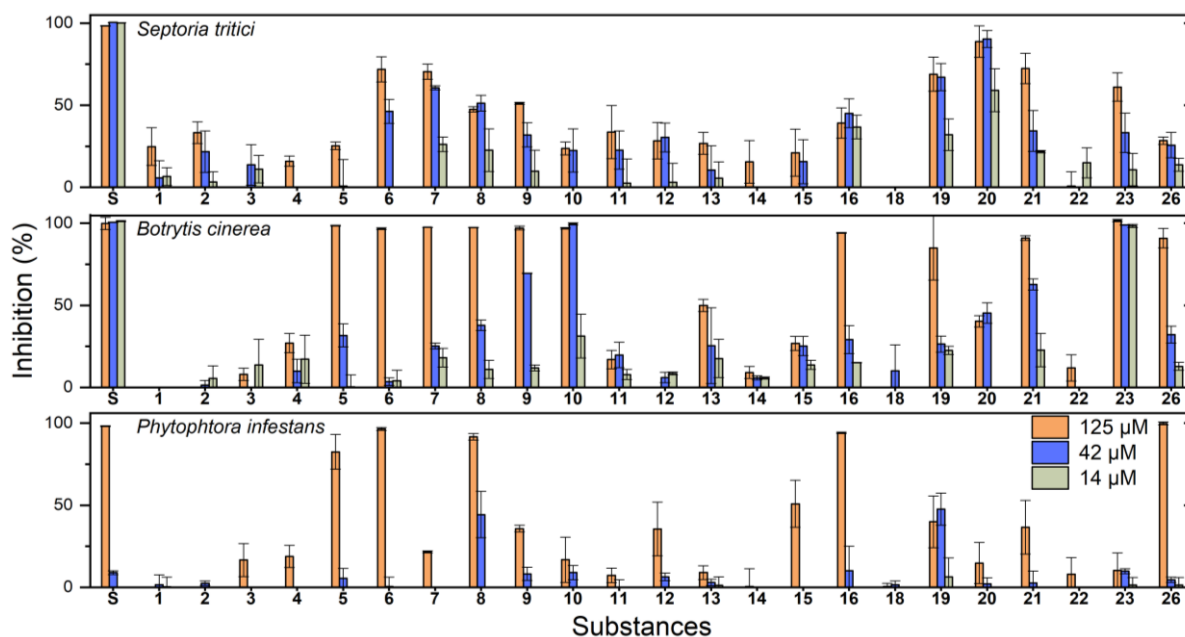


Figure 29: Inhibition of growth for compounds **1** - **23** and **26** against *Septoria tritici* (top), *Botrytis cinerea* (middle) and *Phytophthora infestans* (bottom) at different concentrations. **S**: positive control (epoxiconazole for *Septoria tritici* and *Botrytis cinerea*, terbinafine for *Phytophthora infestans*).

From the selection of 2-pyrones, compound **23**, which has a dodecenyl side-chain, showed the highest inhibition effects on *B. cinerea* with an ED_{50} of 7.2 μM. The same substance, on the other hand, had very little activity against *P. infestans*. The most active against this oomycete was substance **8**, which has a nonyl side-chain. Interestingly, the most active substance against *S. tritici* is compound **20**, the precursor for pyrone **22**.

The natural product fistupyrene **15** only showed a 50 % inhibition at the highest measured concentration of 125 μM against *P. infestans*, which is in accordance with the findings of Furumai et. al. They showed that it acts as a spore germination inhibitor without a strong fungicidal activity.²²

Coumarin *per se* only showed a minimal inhibitory effect against the tested organisms. Diversification by addition of a phenyl group and modification of both aromatic rings could increase the antifungal activity.

All 3-phenylcoumarins showed moderate activity against *B. cinerea* except compound **32**. In contrast, only compounds **27** and **31**, which both have a hydroxyl group at position R⁴, had a significant inhibitory effect against *P. infestans*. Interestingly, compound **28** did not show any effect. These results demonstrate the importance of the substitution pattern and polarity of the substances for their biological activity.

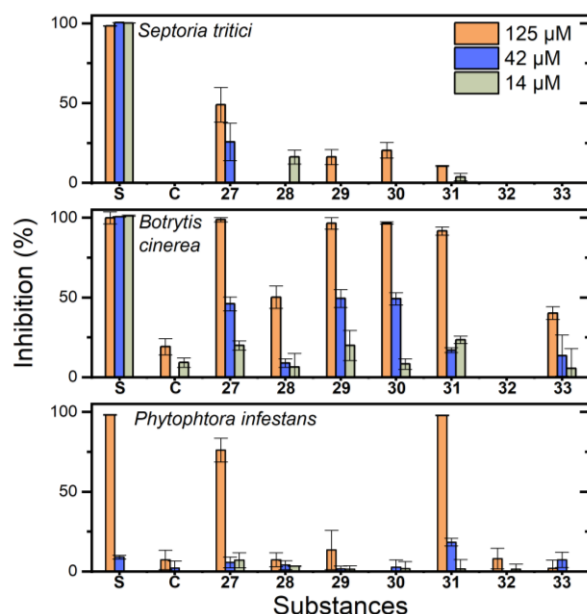


Figure 30: Inhibition of growth of *Septoria tritici* (top), *Botrytis cinerea* (middle) and *Phytophthora infestans* (bottom) by compounds **27**–**33** at different concentrations. **S**: positive control (epoxiconazole for *Septoria tritici* and *Botrytis cinerea*, terbinafine for *Phytophthora infestans*), **C**: Coumarin.

Table 6: ED₅₀ values of the most active compounds against the indicated organisms.

Compound	Organism	ED ₅₀ [μM]
7	<i>S. tritici</i>	26.1 ± 1.2
8	<i>P. infestans</i>	43.8 ± 3.1
9	<i>B. cinerea</i>	25.9 ± 1.7
10	<i>B. cinerea</i>	26.1 ± 8.2
20	<i>S. tritici</i>	10.7 ± 0.8
21	<i>B. cinerea</i>	31.7 ± 0.8
23	<i>B. cinerea</i>	7.2 ± 1.7
26	<i>P. infestans</i>	49.0 ± 1.8
28	<i>B. cinerea</i>	41.4 ± 3.6
30	<i>B. cinerea</i>	28.6 ± 4.1
31	<i>B. cinerea</i>	30.2 ± 6.2

Herbicidal activity

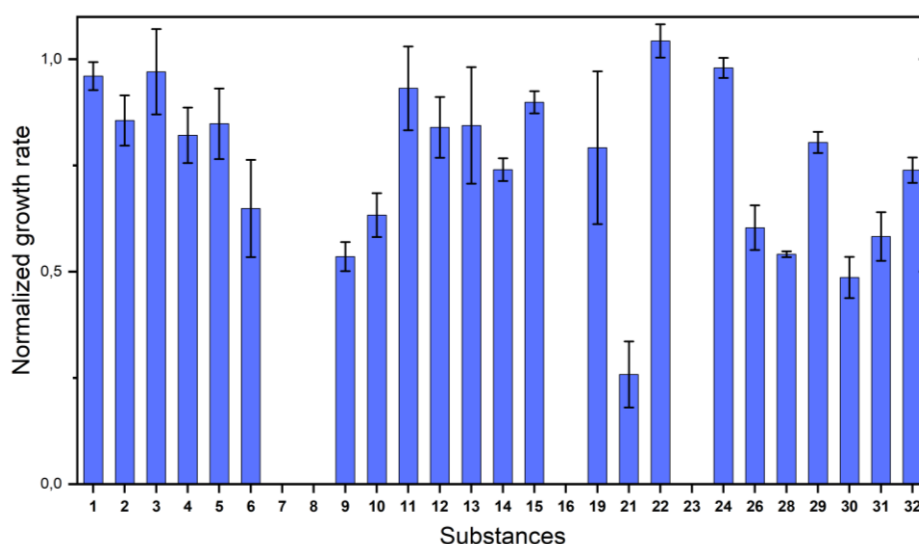


Figure 31: Growth rate of *Lemna minor* after an incubation time of 96 hours in Steinberg medium containing 100 μM of the indicated compound. No growth detected for compounds **7**, **8**, **16** and **23**.

Several molecules containing the pyrone moiety are known in the literature to have herbicidal activity.^{35–37} On one hand this is negative for application as a fungicide, on the other hand, it opens new possibilities as herbicide. Inspired by this, the compounds were tested for their herbicidal

activity using the *Lemna minor* toxicity test (see Chapter 2 for details). In an initial screening, all substances were tested in triplicates at a concentration of 100 μM . Hereby, nine substances showed a growth inhibition higher than 40 % after 96 hours, with four of them inhibiting the growth completely (see Figure 31). These nine compounds were then tested in a dilution concentration series, ranging from 100 μM to 0.01 μM . It is worth mentioning that the herbicidal effect of substance **24** described in the literature was not observed in our assay and at the concentrations used.²⁰

In the dilution assay, it was found that pyrone **8**, the derivative with a nonyl side-chain, showed the highest growth inhibition. The plant growth was inhibited by 61 % at a concentration of 50 μM , followed by pyrone **7**, its derivative with a side-chain shorter by one methylene group with an inhibition of 56 % at the same concentration. The coumarin with the highest herbicidal activity is compound **31** with an inhibition of 50 % at 100 μM . None of the tested compounds showed significant activity at 10 μM or lower concentrations.

Table 7: Growth inhibition of the most active compounds.

Compound	Growth inhibition	
	100 μM	50 μM
8	100 %	61 %
7	100 %	56 %
23	100 %	50 %
31	50 %	45 %
9	44 %	40 %
28	47 %	34 %
16	100 %	29 %
21	74 %	25 %
6	83 %	5 %

Conclusion

In this chapter, the synthesis of twenty 6-alkylated 4-hydroxy-2-pyrones and seven phenylcoumarins is described. Pyrones **1** – **16** were prepared via a two-step one-pot reaction in good yields. Among them, the natural product fistupyrone **15**, which is known for its fungicidal activity, was synthesized for the first time. For derivatives **22** and **23**, which possess an α,β -unsaturated side-chain, another pathway via ketodioxinone intermediates featuring a thermal rearrangement was found to be most practical. Furthermore, five known and two new coumarins **27** - **33** were synthesized through an intermolecular condensation reaction of 2-hydroxyacetophenones and 2-hydroxybenzaldehyde and subsequent deprotection.

All compounds were tested towards their anti-phytopathogenic activity against the plant pathogenic fungi *Botrytis cinerea* and *Septoria tritici* and the oomycete *Phytophthora infestans*. The most active compound against *Botrytis cinerea* was pyrone **23**, which showed an ED₅₀ of 7.2 μ M. Against *Phytophthora infestans*, pyrone **8** proved to be the most active one with an ED₅₀ of 43.8 μ M. Surprisingly, the ketodioxinone intermediate **20**, which was prepared for the synthesis of pyrone **23** showed the highest antifungal activity against *Septoria tritici* with an ED₅₀ of 10.7 μ M. Finally, the herbicidal activity of the synthesized compounds was also investigated using the *Lemna minor* toxicity test. Four substances (**7**, **8**, **16** and **23**) were found to completely inhibit plant growth at a concentration of 100 μ M and led to chlorosis of all plants. Lowering the concentration to 50 μ M, compound **8** showed the highest growth-inhibition of 61 %.

These results provide initial insights into the structure-activity relationship of the substance classes. The herbicidal and antipathogenic properties are partly separated by structure and required concentrations, allowing further development of both properties. Substances with a selective fungicidal activity have also been found, further studies of this would be very promising. Testing of the intermediates has also shown that ketodioxinone **20**, for example, has a high activity against *Septoria tritici*. Further investigations of this substance class should be carried out based on this finding.

Experimental part

General information

The materials used, analytical methods, and bioassays are described in detail in Chapters 2 and 3. Any additions or modifications are outlined below.

Phytotoxicity test (herbicidal activity)

The compounds were tested for their toxicity in 24-well microtiter plates in a first screening at 100 μ M. From these, the substances inhibiting the growth of duckweed (*Lemna minor*) more than 40 % were picked and tested in a serial dilution, according to the protocols described in Chapter 3.

Syntheses

General synthesis methods

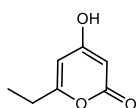
General synthesis method I – Synthesis of pyran-2-ones

4-Hydroxy-6-methyl-2*H*-pyran-2-one (1 eq) was suspended in hexamethyldisilazane (5 mL) and heated to 80 °C for 30 minutes. Subsequently, the solvent was removed under reduced pressure and dry THF (10 mL) was added to the residue. After cooling to - 78 °C, *n*-butyllithium (2.5 M in *n*-hexane, 3 eq) was added. The mixture was stirred for one hour before adding the required alkyl halide (2 eq). After stirring the reaction mixture overnight at rt, the reaction was quenched using aqueous hydrochloric acid (6 M, 5 mL). The organic layer was separated, and its solvent evaporated. The residue was dissolved in EtOAc (50 mL), washed with brine (2x 50 mL), dried over Na₂SO₄, filtered, and evaporated to dryness. Purification was done by column chromatography on silica gel.

General synthesis method II – Synthesis of phenylcoumarins

Phenylacetic acid (1 eq) was dissolved in dichloromethane (10 mL), carbonyldiimidazol (1.2 eq) was added and the mixture was stirred for one hour. In dichloromethane (10 mL) dissolved 2-hydroxybenzaldehyde (1 eq) and diazabicycloundecene (1 eq) were added dropwise and the mixture was stirred for 3 hours. Subsequently, it was acetified to pH ~ 2 using aqueous hydrochloric acid (2 M). The mixture was stirred for another 20 minutes, after which the organic layer was separated, dried over Na₂SO₄, filtered, and evaporated to dryness. Purification was carried out by column chromatography on silica gel.

6-Ethyl-4-hydroxy-2H-pyran-2-one (**1**)



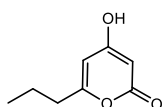
According to general synthesis method I, 4-hydroxy-6-methyl-2H-pyran-2-one (100 mg, 0.8 mmol), *n*-butyllithium (2.5 M in *n*-hexane, 1 mL, 2.5 mmol) and methyl iodide (0.10 mL, 1.6 mmol) were used. Purification was done by column chromatography on silica gel (*n*-hexane/EtOAc, 6:4), yielding product **1** (57.7 mg, 0.41 mmol, 52 %) as a white solid:

HR-MS m/z 139.0404 (calculated for $C_7H_8O_3$: 139.0401)

1H NMR (500 MHz, $CDCl_3$) δ 6.00 (d, $J = 2.0$ Hz, 1H), 5.59 (d, $J = 2.1$ Hz, 1H), 2.53 (q, $J = 7.5$ Hz, 2H), 1.22 (t, $J = 7.5$ Hz, 3H).

^{13}C NMR (126 MHz, $CDCl_3$) δ 172.77, 168.43, 168.31, 100.54, 89.77, 26.85, 10.79.

4-Hydroxy-6-propyl-2H-pyran-2-one (**2**)



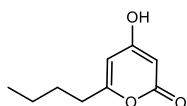
According to general synthesis method I, 4-hydroxy-6-methyl-2H-pyran-2-one (100 mg, 0.8 mmol), *n*-butyllithium (2.5 M in *n*-hexane, 1 mL, 2.5 mmol) and ethyl iodide (0.10 mL, 1.6 mmol) were used. Purification was done by column chromatography on silica gel (*n*-hexane/EtOAc, 6:4), yielding derivative **2** (53.8 mg, 0.35 mmol, 44 %) as a white solid:

HR-MS m/z 153.0561 (calculated for $C_8H_9O_3$: 153.0557)

1H NMR (500 MHz, $CDCl_3$) δ 5.99 (d, $J = 1.9$ Hz, 1H), 5.58 (d, $J = 2.1$ Hz, 1H), 2.46 (t, $J = 7.5$ Hz, 2H), 1.68 (h, $J = 7.4$ Hz, 2H), 0.96 (t, $J = 7.4$ Hz, 3H).

^{13}C NMR (126 MHz, $CDCl_3$) δ 172.67, 168.33, 167.10, 101.49, 89.80, 35.50, 20.05, 13.41.

6-Butyl-4-hydroxy-2H-pyran-2-one (**3**)



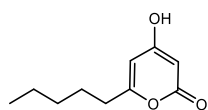
According to general synthesis method I, 4-hydroxy-6-methyl-2H-pyran-2-one (100 mg, 0.8 mmol), *n*-butyllithium (2.5 M in *n*-hexane, 1 mL, 2.5 mmol) and propyl iodide (0.18 mL, 1.6 mmol) were used. Purification was done by column chromatography on silica gel (*n*-hexane/EtOAc, 7:3), yielding product **3** (59.9 mg, 0.36 mmol, 45 %) as a white solid:

HR-MS m/z 167.0717 (calculated for $C_9H_{11}O_3$: 167.0714)

1H NMR (400 MHz, $CDCl_3$) δ 5.97 (d, $J = 2.0$ Hz, 1H), 5.57 (d, $J = 2.1$ Hz, 1H), 2.48 (t, $J = 7.6$ Hz, 2H), 1.62 (p, $J = 7.6$ Hz, 2H), 1.36 (h, $J = 7.3$ Hz, 2H), 0.92 (t, $J = 7.3$ Hz, 3H).

^{13}C NMR (101 MHz, CDCl_3) δ 172.54, 168.14, 167.35, 101.26, 89.81, 33.34, 28.70, 22.02, 13.65.

4-Hydroxy-6-pentyl-2H-pyran-2-one (**4**)



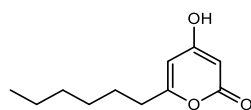
According to general synthesis method I, 4-hydroxy-6-methyl-2H-pyran-2-one (100 mg, 0.8 mmol), *n*-butyllithium (2.5 M in *n*-hexane, 1 mL, 2.5 mmol) and butyl iodide (0.18 mL, 1.6 mmol) were used. Purification was done by column chromatography on silica gel (*n*-hexane/EtOAc, 7:3), yielding product **4** (73.7 mg, 0.40 mmol, 45 %) as a white solid:

HR-MS m/z 181.0875 (calculated for $\text{C}_{10}\text{H}_{13}\text{O}_3$: 181.0870)

^1H NMR (400 MHz, CDCl_3) δ 10.59 (s, 1H), 5.98 (d, J = 2.0 Hz, 1H), 5.58 (d, J = 2.1 Hz, 1H), 2.47 (t, J = 7.6 Hz, 2H), 1.73 – 1.56 (m, 2H), 1.36 – 1.23 (m, 3H), 0.94 – 0.82 (m, 3H).

^{13}C NMR (101 MHz, CDCl_3) δ 172.55, 168.25, 167.41, 101.26, 89.78, 33.61, 31.04, 26.34, 22.26, 13.85.

6-Hexyl-4-hydroxy-2H-pyran-2-one (**5**)



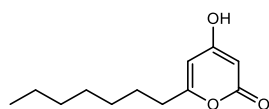
According to general synthesis method I, 4-hydroxy-6-methyl-2H-pyran-2-one (100 mg, 0.8 mmol), *n*-butyllithium (2.5 M in *n*-hexane, 1 mL, 2.5 mmol) and pentyl iodide (0.21 mL, 1.6 mmol) were used. Purification was done by column chromatography on silica gel (*n*-hexane/EtOAc, 7:3), yielding product **5** (81.2 mg, 0.41 mmol, 52 %) as a white solid:

HR-MS m/z 197.1176 (calculated for $\text{C}_{11}\text{H}_{17}\text{O}_3$: 197.1172)

^1H NMR (400 MHz, CDCl_3) δ 11.16 (s, 1H), 6.00 (d, J = 2.0 Hz, 1H), 5.59 (d, J = 2.1 Hz, 1H), 2.48 (t, J = 7.6 Hz, 2H), 1.68 – 1.59 (m, 2H), 1.40 – 1.23 (m, 6H), 0.92 – 0.85 (m, 3H).

^{13}C NMR (101 MHz, CDCl_3) δ 172.67, 168.38, 167.41, 101.32, 89.76, 33.64, 31.37, 28.58, 26.62, 22.43, 13.99.

6-Heptyl-4-hydroxy-2H-pyran-2-one (**6**)



According to general synthesis method I, 4-hydroxy-6-methyl-2H-pyran-2-one (100 mg, 0.8 mmol), *n*-butyllithium (2.5 M in *n*-hexane, 1 mL, 2.5 mmol) and 1-bromohexane (0.25 mL, 1.6 mmol) were

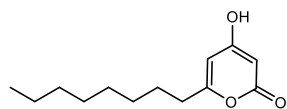
used. Purification was done by column chromatography on silica gel (*n*-hexane/EtOAc, 7:3), yielding product **6** (67.7 mg, 0.32 mmol, 40 %) as a white solid:

HR-MS m/z 211.1333 (calculated for $C_{12}H_{19}O_3$: 211.1329)

1H NMR (400 MHz, $CDCl_3$) δ 10.20 (s, 1H), 5.96 (d, J = 1.8 Hz, 1H), 5.57 (d, J = 2.1 Hz, 1H), 2.47 (t, J = 7.6 Hz, 2H), 1.69 – 1.58 (m, 2H), 1.36 – 1.21 (m, 8H), 0.89 (q, J = 6.7 Hz, 3H).

^{13}C NMR (101 MHz, $CDCl_3$) δ 172.47, 168.17, 167.48, 101.21, 89.81, 33.66, 31.61, 29.69, 28.88, 26.67, 22.58, 14.03.

4-Hydroxy-6-octyl-2H-pyran-2-one (**7**)



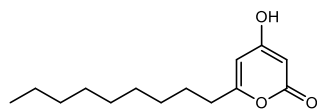
According to general synthesis method I, 4-hydroxy-6-methyl-2H-pyran-2-one (100 mg, 0.8 mmol), *n*-butyllithium (2.5 M in *n*-hexane, 1 mL, 2.5 mmol) and 1-bromoheptane (0.20 mL, 1.6 mmol) were used. Purification was done by column chromatography on silica gel (*n*-hexane/EtOAc, 7:3), yielding product **7** (78.9 mg, 0.35 mmol, 44 %) as a white solid:

HR-MS m/z 223.1355 (calculated for $C_{13}H_{19}O_3$: 223.1334)

1H NMR (400 MHz, $CDCl_3$) δ 11.23 (s, 1H), 6.00 (s, 1H), 5.59 (s, 1H), 2.47 (t, J = 7.7 Hz, 2H), 1.63 (p, J = 7.1 Hz, 2H), 1.37 – 1.17 (m, 10H), 0.88 (t, J = 6.6 Hz, 3H).

^{13}C NMR (101 MHz, $CDCl_3$) δ 172.72, 168.42, 167.39, 101.33, 89.76, 33.64, 31.77, 29.17, 29.08, 28.93, 26.66, 22.61, 14.05.

4-Hydroxy-6-nonyl-2H-pyran-2-one (**8**)



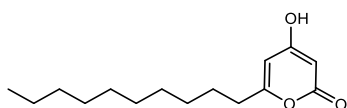
According to general synthesis method I, 4-hydroxy-6-methyl-2H-pyran-2-one (100 mg, 0.8 mmol), *n*-butyllithium (2.5 M in *n*-hexane, 1 mL, 2.5 mmol) and 1-bromooctane (0.21 mL, 1.6 mmol) were used. Purification was done by column chromatography on silica gel (*n*-hexane/EtOAc, 8:2), yielding product **8** (43.0 mg, 0.18 mmol, 23 %) as a white solid:

HR-MS m/z 239.1645 (calculated for $C_{14}H_{23}O_3$: 239.1642)

1H NMR (400 MHz, $CDCl_3$) δ 10.20 (s, 1H), 5.94 (d, J = 2.0 Hz, 1H), 5.55 (d, J = 2.1 Hz, 1H), 2.47 (t, J = 7.6 Hz, 2H), 1.71 – 1.56 (m, 2H), 1.38 – 1.18 (m, 12H), 0.88 (t, J = 6.8 Hz, 3H).

^{13}C NMR (101 MHz, $CDCl_3$) δ 172.58, 168.27, 167.44, 101.27, 89.79, 33.66, 31.83, 29.39, 29.24, 29.22, 28.94, 26.67, 22.65, 14.08.

6-Decyl-4-hydroxy-2H-pyran-2-one (**9**)



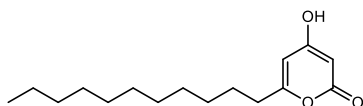
According to general synthesis method I, 4-hydroxy-6-methyl-2H-pyran-2-one (100 mg, 0.8 mmol), *n*-butyllithium (2.5 M in *n*-hexane, 1 mL, 2.5 mmol) and 1-bromononane (0.30 mL, 1.6 mmol) were used. Purification was done by column chromatography on silica gel (*n*-hexane/EtOAc, 8:2), yielding derivative **9** (74.9 mg, 0.30 mmol, 38 %) as a white solid:

HR-MS m/z 251.1655 (calculated for $C_{15}H_{23}O_3$: 251.1653)

1H NMR (400 MHz, $CDCl_3$) δ 11.02 (s, 1H), 5.98 (d, J = 2.0 Hz, 1H), 5.58 (d, J = 2.1 Hz, 1H), 2.47 (t, J = 7.7 Hz, 2H), 1.63 (p, J = 7.5 Hz, 2H), 1.35 – 1.22 (m, 14H), 0.88 (t, J = 6.9 Hz, 3H).

^{13}C NMR (101 MHz, $CDCl_3$) δ 172.67, 168.32, 167.43, 101.31, 89.77, 33.66, 31.87, 29.54, 29.44, 29.28, 29.23, 28.95, 26.67, 22.66, 14.09.

4-Hydroxy-6-undecyl-2H-pyran-2-one (**10**)



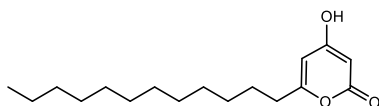
According to general synthesis method I, 4-hydroxy-6-methyl-2H-pyran-2-one (100 mg, 0.8 mmol), *n*-butyllithium (2.5 M in *n*-hexane, 1 mL, 2.5 mmol) and 1-bromodecane (0.30 mL, 1.6 mmol) were used. Purification was done by column chromatography on silica gel (*n*-hexane/EtOAc, 8:2), yielding pyrone **10** (80.9 mg, 0.30 mmol, 38 %) as a white solid:

HR-MS m/z 267.1961 (calculated for $C_{16}H_{27}O_3$: 267.1955)

1H NMR (500 MHz, $CDCl_3$) δ 9.89 (s, 1H), 5.94 (d, J = 2.0 Hz, 1H), 5.54 (d, J = 2.1 Hz, 1H), 2.47 (t, J = 7.7 Hz, 2H), 1.72 – 1.55 (m, 2H), 1.37 – 1.22 (m, 16H), 0.88 (t, J = 6.8 Hz, 3H).

^{13}C NMR (126 MHz, $CDCl_3$) δ 171.71, 167.57, 167.49, 100.78, 89.97, 33.71, 31.90, 29.59, 29.59, 29.44, 29.32, 29.23, 28.94, 26.67, 22.68, 14.11.

6-Dodecyl-4-hydroxy-2H-pyran-2-one (**11**)



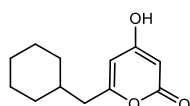
According to general synthesis method I, 4-hydroxy-6-methyl-2H-pyran-2-one (100 mg, 0.8 mmol), *n*-butyllithium (2.5 M in *n*-hexane, 1 mL, 2.5 mmol) and 1-bromoundecane (0.35 mL, 1.6 mmol) were used. Purification was done by column chromatography on silica gel (*n*-hexane/EtOAc, 8:2), yielding **11** (114.2 mg, 0.41 mmol, 52 %) as a white solid:

HR-MS m/z 279.1975 (calculated for $C_{17}H_{27}O_3$: 279.1960)

^1H NMR (400 MHz, CDCl_3) δ 10.89 (s, 1H), 5.97 (s, 1H), 5.57 (s, 1H), 2.47 (t, J = 7.6 Hz, 2H), 1.63 (p, J = 7.2 Hz, 2H), 1.38 – 1.18 (m, 18H), 0.88 (t, J = 6.7 Hz, 3H).

^{13}C NMR (101 MHz, CDCl_3) 172.51, 168.17, 167.45, 101.22, 89.80, 33.67, 31.91, 29.64, 29.62, 29.59, 29.45, 29.34, 29.24, 28.96, 26.68, 22.68, 14.10.

6-(Cyclohexylmethyl)-4-hydroxy-2H-pyran-2-one (**12**)



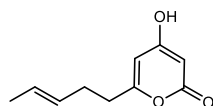
According to general synthesis method I, 4-hydroxy-6-methyl-2H-pyran-2-one (100 mg, 0.8 mmol), *n*-butyllithium (2.5 M in *n*-hexane, 1 mL, 2.5 mmol) and iodocyclohexane (0.21 mL, 1.6 mmol) were used. Purification was done by column chromatography on silica gel (*n*-hexane/EtOAc, 8:2), yielding product **12** (79.7 mg, 0.30 mmol, 45 %) as a white solid:

HR-MS m/z 207.1035 (calculated for $\text{C}_{12}\text{H}_{15}\text{O}_3$: 207.1027)

^1H NMR (400 MHz, CDCl_3) δ 11.01 (s, 1H), 5.97 (d, J = 2.0 Hz, 1H), 5.57 (d, J = 2.2 Hz, 1H), 2.35 (d, J = 6.8 Hz, 2H), 1.79 – 1.61 (m, 6H), 1.35 – 1.06 (m, 3H), 1.03 – 0.82 (m, 2H).

^{13}C NMR (101 MHz, CDCl_3) δ 172.54, 168.39, 166.28, 102.42, 89.75, 41.54, 36.05, 32.90 (2C), 26.14, 25.95 (2C).

(*E*)-4-Hydroxy-6-(pent-3-en-1-yl)-2H-pyran-2-one (**13**)



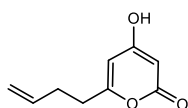
According to general synthesis method I, 4-hydroxy-6-methyl-2H-pyran-2-one (100 mg, 0.8 mmol), *n*-butyllithium (2.5 M in *n*-hexane, 1 mL, 2.5 mmol) and crotyl chloride (0.16 mL, 1.6 mmol) were used. Purification was done by column chromatography on silica gel (*n*-hexane/EtOAc, 7:3), yielding product **13** (52.8 mg, 0.29 mmol, 37 %) as a white solid:

HR-MS m/z 179.0717 (calculated for $\text{C}_{10}\text{H}_{11}\text{O}_3$: 179.0714)

^1H NMR (400 MHz, CDCl_3) δ 5.96 (d, J = 2.1 Hz, 1H), 5.56 (d, J = 2.1 Hz, 1H), 5.53 – 5.32 (m, 2H), 2.52 (t, J = 7.6 Hz, 2H), 2.36 – 2.27 (m, 2H), 1.63 (dd, J = 6.2, 1.5 Hz, 3H).

^{13}C NMR (101 MHz, CDCl_3) δ 172.45, 168.08, 166.60, 128.41, 127.02, 101.54, 89.87, 33.69, 29.54, 17.85.

6-(But-3-en-1-yl)-4-hydroxy-2H-pyran-2-one (**14**)



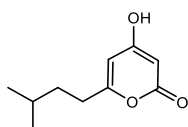
According to general synthesis method I, 4-hydroxy-6-methyl-2H-pyran-2-one (100 mg, 0.8 mmol), *n*-butyllithium (2.5 M in *n*-hexane, 1 mL, 2.5 mmol) and allyl iodide (0.15 mL, 1.6 mmol) were used. Purification was done by column chromatography on silica gel (*n*-hexane/EtOAc, 7:3), yielding product **14** (57.7 mg, 0.41 mmol, 52 %) as a white solid:

HR-MS *m/z* 165.0560 (calculated for C₉H₉O₃: 165.0557)

¹H NMR (400 MHz, CDCl₃) δ 6.00 (s, 1H), 5.78 (m, 1H), 5.58 (s, 1H), 5.13 – 4.94 (m, 2H), 2.58 (t, *J* = 7.5 Hz, 2H), 2.40 (q, *J* = 7.2 Hz, 2H).

¹³C NMR (101 MHz, CDCl₃) δ 172.64, 168.22, 166.18, 135.84, 116.35, 101.78, 89.92, 32.95, 30.52.

4-Hydroxy-6-isopentyl-2H-pyran-2-one (Fistupyrone (**15**))



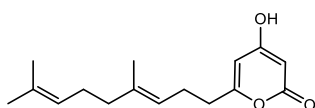
According to general synthesis method I, 4-hydroxy-6-methyl-2H-pyran-2-one (100 mg, 0.8 mmol), *n*-butyllithium (2.5 M in *n*-hexane, 1 mL, 2.5 mmol) and isobutyl iodide (0.18 mL, 1.6 mmol) were used. Purification was done first by column chromatography on silica gel (*n*-hexane/EtOAc, 8:2), then HPLC (reversed phase, H₂O / CH₃CN, 3:7 – 0:10), yielding fistupyrone (37.5 mg, 0.21 mmol, 26 %) as a white solid:

HR-MS *m/z* 181.0875 (calculated for C₁₀H₁₃O₃: 181.0870)

¹H NMR (400 MHz, CDCl₃) δ 6.00 (s, 1H), 5.58 (s, 1H), 2.49 (t, *J* = 7.9 Hz, 2H), 1.65 – 1.48 (m, 3H), 0.92 (d, *J* = 6.3 Hz, 6H);

¹³C NMR (101 MHz, CDCl₃) δ 172.67, 168.36, 167.65, 101.20, 89.74, 35.56, 31.64, 27.52, 22.21 (2C).

(*E*)-6-(4,8-Dimethylnona-3,7-dien-1-yl)-4-hydroxy-2H-pyran-2-one (**16**)



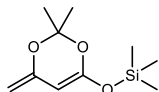
According to general synthesis method I, 4-hydroxy-6-methyl-2H-pyran-2-one (100 mg, 0.8 mmol), *n*-butyllithium (2.5 M in *n*-hexane, 1 mL, 2.5 mmol) and 1-bromo-3,7-dimethyl-2,6-octadien (0.32 mL, 1.6 mmol) were used. Purification was done by column chromatography on silica gel (*n*-hexane/EtOAc, 8:2), yielding **16** (74.9 mg, 0.30 mmol, 38 %) as a white solid:

HR-MS *m/z* 261.1515 (calculated for C₁₆H₂₁O₃: 261.1496)

^1H NMR (400 MHz, CDCl_3) δ 10.88 (s, 1H), 5.98 (d, J = 2.0 Hz, 1H), 5.59 (d, J = 2.0 Hz, 1H), 5.15 – 4.99 (m, 2H), 2.51 (t, J = 7.4 Hz, 2H), 2.34 (q, J = 7.4 Hz, 2H), 2.10 – 1.92 (m, 4H), 1.67 (s, 3H), 1.59 (s, 6H).

^{13}C NMR (101 MHz, CDCl_3) δ 172.36, 168.01, 166.79, 137.46, 131.52, 124.04, 121.49, 101.42, 89.85, 39.59, 33.81, 26.58, 25.66, 25.12, 17.67, 16.00.

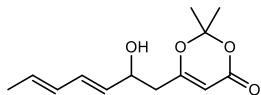
((2,2-Dimethyl-4-methylene-4H-1,3-dioxin-6-yl)oxy)trimethylsilane (**17**)



A solution of LDA (2 M, 13.5 mL, 27 mmol) in THF (50 mL) was cooled to $-78\text{ }^\circ\text{C}$, after which 2,2,6-trimethyl-4H-1,3-dioxin-4-one (3.2 mL, 24.5 mmol) was added slowly. After stirring at $-78\text{ }^\circ\text{C}$ for one hour, freshly distilled trimethylsilyl chloride (3.7 mL, 29.5 mmol) was added dropwise and the mixture was allowed to slowly reach room temperature. Subsequently, the precipitate was filtered off, rinsed with *n*-hexane and the combined organic phases evaporated to dryness. The crude product was purified by vacuum distillation ($p \leq 1\text{ mbar}$, $T \leq 50\text{ }^\circ\text{C}$), giving **17** (2.8 g, 13 mmol, 53 %) as a colourless liquid:

^1H NMR (400 MHz, CDCl_3) δ 4.65 (s, 1H), 4.07 (d, J = 1.0 Hz, 1H), 3.88 (d, J = 0.9 Hz, 1H), 1.55 (s, 6H), 0.27 (s, 9H).

(*E*)-6-(2-Hydroxytetradec-3-en-1-yl)-2,2-dimethyl-4H-1,3-dioxin-4-one (**18**)



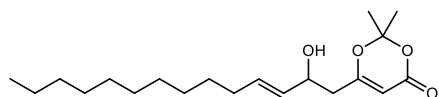
(*E,E*)-2,4-Hexadienal (103.9 μL , 0.94 mmol) was dissolved in dry dichloromethane (20 mL) under nitrogen atmosphere and was cooled down to $-78\text{ }^\circ\text{C}$. Titanium tetrachloride (1 M in DCM, 0.94 mL, 0.94 mmol) and **17** (200 mg, 0.94 mmol) were dropwise added and the solution was stirred for 90 minutes before sat. aq. NaHCO_3 solution (10 mL) was added. After separation of the phases the aqueous phase was extracted using dichloromethane (2x 10 mL). The combined organic phases were dried over Na_2SO_4 , filtered, and evaporated to dryness. Purification was done by column chromatography on silica gel (*n*-hexane/EtOAc, 9:1 – 5:5), yielding product **18** (210 mg, 0.88 mmol, 94 %) as a colourless oil:

HR-MS m/z 239.1275 (calculated for $\text{C}_{13}\text{H}_{19}\text{O}_4$: 239.1283)

^1H NMR (400 MHz, CDCl_3) δ 6.31 – 6.17 (m, 1H), 6.11 – 5.94 (m, 1H), 5.86 – 5.68 (m, 1H), 5.55 (dd, J = 15.3, 6.9 Hz, 1H), 5.40 – 5.25 (m, 1H), 4.43 (q, J = 6.8 Hz, 1H), 2.81 (d, J = 4.9 Hz, 1H), 2.46 (t, J = 6.6 Hz, 2H), 1.77 (dd, J = 6.7, 1.5 Hz, 3H), 1.72 – 1.63 (m, 6H).

^{13}C NMR (101 MHz, CDCl_3) δ 168.34, 161.07, 132.11, 131.40, 130.71, 130.17, 106.63, 95.26, 69.57, 41.49, 25.32, 24.86, 18.10.

(*E*)-6-(2-Hydroxytetradec-3-en-1-yl)-2,2-dimethyl-4*H*-1,3-dioxin-4-one (**19**)



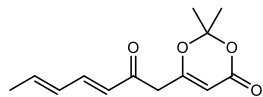
2-Tridecenal (2 g, 10.2 mmol) was dissolved in dry dichloromethane (50 mL) under nitrogen atmosphere and was cooled down to -78 °C. Titanium tetrachloride (1 M in DCM, 10.2 mL, 10.2 mmol) and **27** (2.2 g, 10.2 mmol) were dropwise added and the solution was stirred for 90 minutes before sat. aq. NaHCO₃ solution (25 mL) was added. After separation of the phases the aqueous phase was extracted using dichloromethane (2x 25 mL). The combined organic phases were dried over Na₂SO₄, filtered, and evaporated to dryness. Purification was done by column chromatography on silica gel (*n*-hexane/EtOAc, 9:1 – 5:5), yielding product **19** (2.09 g, 6.2 mmol, 61 %) as a colourless oil:

HR-MS *m/z* 339.2535 (calculated for C₂₀H₃₅O₄: 339.2530)

¹H NMR (400 MHz, CDCl₃) δ 5.73 (dt, *J* = 15.4, 6.7 Hz, 1H), 5.48 (ddt, *J* = 15.4, 7.0, 1.5 Hz, 1H), 5.32 (s, 1H), 4.37 (qd, *J* = 7.2, 3.7 Hz, 1H), 2.51 – 2.36 (m, 2H), 2.08 – 1.98 (m, 2H), 1.69 (d, *J* = 4.2 Hz, 6H), 1.44 – 1.16 (m, 16H), 0.88 (t, *J* = 6.7 Hz, 3H).

¹³C NMR (101 MHz, CDCl₃) δ 168.51, 161.04, 133.79, 130.91, 106.57, 95.22, 69.85, 41.58, 32.07, 31.88, 29.59, 29.56, 29.43, 29.30, 29.14, 28.97, 25.33, 24.85, 22.66, 14.09.

2,2-Dimethyl-6-((3*E*,5*E*)-2-oxohepta-3,5-dien-1-yl)-4*H*-1,3-dioxin-4-one (**20**)

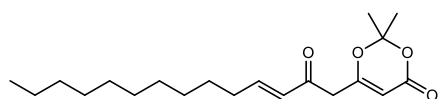


To **18** (0.18 g, 0.74 mmol) in dry dichloromethane (15 mL) was added *Dess-Martin* periodinane (0.41 g, 0.96 mmol). After stirring for two hours, the solution was diluted with diethyl ether (25 mL) and quenched by adding sat. aq. NaHCO₃ solution (10 mL, containing 5 % thiosulfate). After stirring for another 20 min, the phases were separated, the organic phase was dried over Na₂SO₄, filtered, and evaporated to dryness. Purification was done by column chromatography on silica gel (*n*-hexane/EtOAc, 8:2 – 6:4), yielding product **20** (105 mg, 0.71 mmol, 94 %) as a colourless oil:

¹H NMR (400 MHz, CDCl₃) δ 7.19 (dd, *J* = 15.4, 10.0 Hz, 1H), 6.35–6.19 (m, 2H), 6.10 (d, *J* = 15.4 Hz, 1H), 5.37 (s, 1H), 3.46 (s, 2H), 1.90 (d, *J* = 6.1 Hz, 3H), 1.70 (s, 6H).

¹³C NMR (101 MHz, CDCl₃) δ 192.60, 165.09, 160.76, 145.20, 142.62, 129.90, 126.03, 107.15, 96.58, 45.19, 24.98 (2C), 18.93.

(*E*)-2,2-Dimethyl-6-(2-oxotetradec-3-en-1-yl)-4*H*-1,3-dioxin-4-one (**21**)



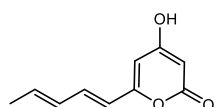
To **19** (0.5 g, 1.48 mmol) in dry dichloromethane (25 mL) was added *Dess-Martin* periodinane (0.81 g, 1.92 mmol). After stirring for two hours, the solution was diluted with diethyl ether (25 mL) and quenched by adding sat. aq. NaHCO₃ solution (10 mL, containing 5 % thiosulfate). After stirring for another 20 min, the phases were separated, the organic phase was dried over Na₂SO₄, filtered, and evaporated to dryness. Purification was done by column chromatography on silica gel (*n*-hexane/EtOAc, 9:1 – 6:4), yielding product **21** (478 mg, 1.42 mmol, 96 %) as a colourless oil:

HR-MS *m/z* 337.2378 (calculated for C₂₀H₃₃O₄: 337.2373)

¹H NMR (400 MHz, CDCl₃) δ 6.92 (dt, *J* = 15.8, 6.9 Hz, 1H), 6.13 (dt, *J* = 15.9, 1.5 Hz, 1H), 5.36 (s, 1H), 3.46 (s, 2H), 2.25 (qd, *J* = 7.1, 1.5 Hz, 2H), 1.71 (s, 6H), 1.47 (p, *J* = 7.2 Hz, 2H), 1.36 – 1.24 (m, 14H), 0.92 – 0.84 (m, 3H).

¹³C NMR (101 MHz, CDCl₃) δ 192.52, 165.09, 160.79, 150.47, 129.11, 107.14, 96.59, 44.63, 32.57, 31.83, 29.51, 29.45, 29.30, 29.24, 29.13, 27.91, 24.95 (2C), 22.62, 14.05.

4-Hydroxy-6-((1*E*,3*E*)-penta-1,3-dien-1-yl)-2*H*-pyran-2-one (**22**)



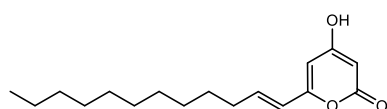
Compound **20** (50 mg, 0.21 mmol) was dissolved in dry toluene (2 mL) and stirred under reflux for 30 minutes. During heating, a pale-yellow precipitate formed, which was filtered off after cooling and was washed with toluene (2x 10 mL), giving derivative **22** (31.4 mg, 0.17 mmol, 84 %) as a pale yellow solid:

HR-MS *m/z* 177.0562 (calculated for C₁₀H₉O₃: 177.0557)

¹H NMR (400 MHz, (CD₃)₂SO) δ 11.96 – 11.22 (m, 1H), 6.92 (dd, *J* = 15.4, 10.5 Hz, 1H), 6.30 – 6.17 (m, 2H), 6.13 (dd, *J* = 15.1, 6.7 Hz, 1H), 6.08 (d, *J* = 2.1 Hz, 1H), 5.27 (d, *J* = 2.0 Hz, 1H), 1.82 (d, *J* = 6.6 Hz, 3H).

¹³C NMR (101 MHz, (CD₃)₂SO) δ 170.14, 162.87, 159.28, 136.38, 135.04, 130.51, 120.63, 100.82, 89.52, 18.38.

(*E*)-6-(Dodec-1-en-1-yl)-4-hydroxy-2*H*-pyran-2-one (**23**)



Compound **21** (50 mg, 0.15 mmol) was dissolved in dry toluene (2 mL) and stirred under reflux for 30 minutes after which the solvent was distilled off. Purification was done by column

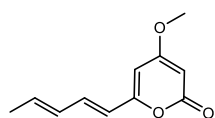
chromatography on silica gel (*n*-hexane/EtOAc, 7:3 + 0.1 % formic acid), yielding pyrone **23** (35.6 mg, 0.13 mmol, 86 %) as a white solid:

HR-MS *m/z* 279.1960 (calculated for C₁₇H₂₇O₃: 279.1966)

¹H NMR (400 MHz, (CD₃)₂SO) δ 11.64 (s, 1H), 6.49 (dt, *J* = 15.6, 7.1 Hz, 1H), 6.16 (d, *J* = 15.9 Hz, 1H), 6.03 (d, *J* = 2.1 Hz, 1H), 5.27 (d, *J* = 2.1 Hz, 1H), 2.19 (q, *J* = 6.9 Hz, 2H), 1.41 (p, *J* = 7.1 Hz, 2H), 1.32 – 1.18 (m, 14H), 0.89 – 0.81 (m, 3H).

¹³C NMR (101 MHz, (CD₃)₂SO) δ 170.31, 162.95, 158.94, 138.49, 122.08, 99.96, 89.40, 31.93, 31.28, 28.97, 28.95, 28.80, 28.68, 28.58, 28.01, 22.08, 13.92.

4-Methoxy-6-((1*E*,3*E*)-penta-1,3-dien-1-yl)-2*H*-pyran-2-one (**24**)

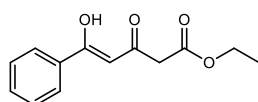


To a solution of **22** (15 mg, 0.08 mmol) in acetone (10 mL) was added flame-dried sodium carbonate (10 mg, 0.09 mmol) and dimethyl sulfate (8 μL, 0.08 mmol). The mixture was refluxed overnight, after which water (15 mL) and ethyl acetate (15 mL) was added. The organic phase was separated, and the aqueous phase extracted using ethyl acetate (2x 15 mL). The combined organic phases were dried over Na₂SO₄, filtered, and concentrated under reduced pressure. Purification was done by column chromatography (DCM / EE 0:1 – 1:0), yielding product **24** (10 mg, 0.06 mmol, 72 %) as a colourless oil:

¹H NMR (400 MHz, CDCl₃) δ 7.10 (dd, *J* = 15.3, 10.6 Hz, 1H), 6.23 – 6.12 (m, 1H), 6.12 – 5.98 (m, 1H), 5.92 (d, *J* = 15.3 Hz, 1H), 5.80 (d, *J* = 2.2 Hz, 1H), 5.44 (d, *J* = 2.2 Hz, 1H), 3.80 (d, *J* = 0.9 Hz, 3H), 1.85 (d, *J* = 6.7 Hz, 3H).

¹³C NMR (101 MHz, CDCl₃) δ 171.16, 164.16, 159.06, 136.96, 136.57, 130.41, 119.61, 100.27, 88.32, 55.82, 18.65.

Ethyl (Z)-5-hydroxy-3-oxo-5-phenylpent-4-enoate (**25**)



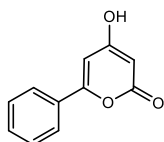
To a solution of TMEDA (0.6 mL, 4 mmol) and LDA (2 M in THF, 5 mL, 10 mmol) in dry THF (30 mL) was added dropwise a solution of ethyl acetoacetate (0.63 mL, 5 mmol) and ethyl benzoate (0.72 mL, 5 mmol) in dry THF (10 mL) at 0 °C. The reaction mixture was warmed to rt and stirred overnight. Aqueous hydrochloric acid (6 M, 5 mL) was added, the organic layer separated, dried over Na₂SO₄, filtered, and evaporated to dryness. Purification was done by column chromatography on silica gel (*n*-hexane/EtOAc, 9:1), yielding **25** (0.87 g, 3.8 mmol, 75 %) as a yellow oil:

HR-MS *m/z* 235.0977 (calculated for C₁₃H₁₅O₄: 235.0965).

^1H NMR (500 MHz, CDCl_3) δ 15.78 (s, 1H), 7.90 – 7.86 (m, 2H), 7.57 – 7.52 (m, 1H), 7.46 (t, J = 7.6 Hz, 2H), 6.30 (s, 1H), 4.23 (q, J = 7.1 Hz, 2H), 3.48 (s, 2H), 1.30 (t, J = 7.2 Hz, 3H).

^{13}C NMR (126 MHz, CDCl_3) δ 189.25, 182.60, 167.55, 134.10, 132.63, 128.68 (2C), 127.10 (2C), 96.71, 61.52, 45.94, 14.11.

4-Hydroxy-6-phenyl-2H-pyran-2-one (**26**)



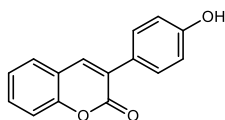
Compound **25** (20 mg, 0.08 mmol) and DBU (0.085 mmol) were dissolved in dry toluene (2 mL) and heated in a microwave oven to 140 °C for 5 minutes. Subsequently, the mixture was cooled down to room temperature and the solvent was distilled off. Purification was done by column chromatography on silica gel (n-hexane/EtOAc, 6:4 - 8:2), yielding product **26** (12 mg, 0.06 mmol, 76 %) as a white solid:

HR-MS m/z 187.0405 (calculated for $\text{C}_{11}\text{H}_7\text{O}_3$: 187.0401).

^1H NMR (400 MHz, $(\text{CD}_3)_2\text{SO}$) δ 11.85 (s, 1H), 7.85 (m, 2H), 7.60 – 7.43 (m, 3H), 6.76 (d, J = 2.0 Hz, 1H), 5.40 (d, J = 1.9 Hz, 1H).

^{13}C NMR (101 MHz, $(\text{CD}_3)_2\text{SO}$) δ 170.49, 162.97, 160.01, 131.01, 130.91, 129.03 (2C), 125.42 (2C), 98.34, 89.57.

3-(4-Hydroxyphenyl)-2H-chromen-2-one (**27**)



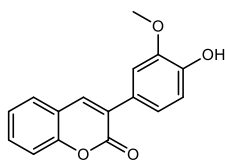
According to general synthesis method II, 4-hydroxyphenylacetic acid (1 g, 6.6 mmol) and 2-hydroxybenzaldehyde (803 mg, 6.6 mmol) were used. Purification was done by HPLC (reversed phase, ACN/ H_2O 7:3 - 1:0), yielding product **27** (456 mg, 1.91 mmol, 29 %) as a light yellow solid:

HR-MS m/z 239.0701 (calculated for $\text{C}_{15}\text{H}_{11}\text{O}_3$: 239.0708).

^1H NMR (400 MHz, $(\text{CD}_3)_2\text{CO}$) δ 8.63 (s, 1H), 8.04 (s, 1H), 7.73 (d, J = 7.8 Hz, 1H), 7.68 (d, J = 8.2 Hz, 2H), 7.58 (t, J = 7.8 Hz, 1H), 7.39 – 7.31 (m, 2H), 6.93 (d, J = 8.8 Hz, 2H).

^{13}C NMR (101 MHz, $(\text{CD}_3)_2\text{CO}$) δ 160.69, 158.87, 154.17, 138.99, 131.75, 130.84 (2C), 129.01, 128.44, 127.16, 125.18, 120.93, 116.65, 115.86 (2C).

3-(4-Hydroxy-3-methoxyphenyl)-2H-chromen-2-one (**28**)



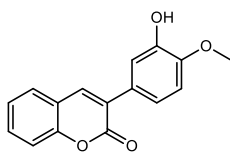
According to general synthesis method II, 4-hydroxy-3-methoxyphenylacetic acid (1 g, 5.5 mmol) and 2-hydroxybenzaldehyde (670 mg, 5.5 mmol) were used. Purification was done by HPLC (reversed phase, ACN/H₂O 7:3 - 1:0), yielding only 17.3 mg of product **28** (17.3 mg, 0.06 mmol, 1.2 %) as a light yellow solid due to solvation problems during purification:

HR-MS m/z 291.0625 (calculated for C₁₆H₁₂O₄Na: 291.0628).

¹H NMR (400 MHz, (CD₃)₂CO) δ 8.09 (s, 1H), 7.91 (br s, 1H), 7.72 (dd, J = 8.0, 1.6 Hz, 1H), 7.64 – 7.55 (m, 1H), 7.46 (d, J = 2.1 Hz, 1H), 7.35 (ddd, J = 7.3, 6.3, 1.1 Hz, 2H), 7.31 (dd, J = 8.3, 2.1 Hz, 1H), 6.91 (d, J = 8.2 Hz, 1H), 3.91 (s, 3H).

¹³C NMR (101 MHz, (CD₃)₂CO) δ 160.64, 154.16, 148.29, 147.95, 139.23, 131.80, 129.03, 128.44, 127.47, 125.20, 122.68, 120.91, 116.65, 115.60, 113.15, 56.36.

3-(3-Hydroxy-4-methoxyphenyl)-2H-chromen-2-one (**29**)



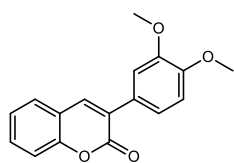
According to general synthesis method II, 3-hydroxy-4-methoxyphenylacetic acid (1 g, 5.5 mmol) and 2-hydroxybenzaldehyde (670 mg, 5.5 mmol) were used. Purification was done by HPLC (reversed phase, ACN/H₂O 7:3 - 1:0), yielding **29** (541 mg, 2.01 mmol, 37 %) as a light yellow solid:

HR-MS m/z 291.0625 (calculated for C₁₆H₁₂O₄Na: 291.0628);

¹H NMR (400 MHz, (CD₃)₂CO) δ 8.05 (s, 1H), 7.74 (dd, J = 7.9, 1.6 Hz, 1H), 7.59 (ddd, J = 8.4, 7.4, 1.6 Hz, 1H), 7.38 – 7.35 (m, 1H), 7.34 (d, J = 2.2 Hz, 2H), 7.29 (dd, J = 8.4, 2.3 Hz, 1H), 7.02 (d, J = 8.4 Hz, 1H), 3.90 (s, 3H).

¹³C NMR (101 MHz, (CD₃)₂CO) δ 160.52, 154.20, 148.97, 147.01, 139.48, 131.86, 129.10, 128.85, 128.25, 125.17, 121.07, 120.85, 116.63, 116.29, 112.00, 56.26.

3-(3,4-Dimethoxyphenyl)-2H-chromen-2-one (**30**)



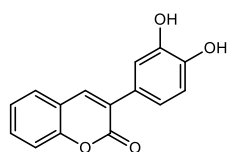
According to general synthesis method II, 3,4-dimethoxyphenylacetic acid (0.76 g, 3.8 mmol) and 2-hydroxybenzaldehyde (467 mg, 3.8 mmol) were used. Purification was done by column chromatography on silica gel (*n*-hexane/EtOAc, 7:3), yielding **30** (615 mg, 2.2 mmol, 57 %) as a yellowish solid:

HR-MS *m/z* 283.0964 (calculated for C₁₇H₁₅O₄: 283.0970).

¹H NMR (400 MHz, CDCl₃) δ 7.78 (s, 1H), 7.57 – 7.48 (m, 2H), 7.39 – 7.25 (m, 4H), 6.94 (d, *J* = 8.3 Hz, 1H), 3.95 (s, 3H), 3.93 (s, 3H).

¹³C NMR (101 MHz, CDCl₃) δ 160.68, 153.26, 149.71, 148.68, 138.68, 131.06, 127.87, 127.68, 127.38, 124.41, 121.22, 119.74, 116.35, 111.78, 110.98, 56.00, 55.93.

3-(3,4-Dihydroxyphenyl)-2H-chromen-2-one (**31**)



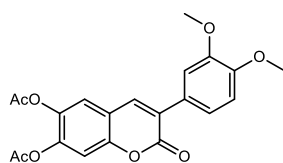
To a cooled (0 °C) solution of **30** (500 mg, 1.77 mmol) in dichloromethane (12 mL) was added boron tribromide (1 M in *n*-hexane, 8.3 mL, 8.3 mmol) and the resulting solution was stirred for one hour at 0 °C. After being warmed to room temperature, it was stirred for another 3 hours before being poured into ice water. The precipitate was dissolved adding methanol and the aqueous phase was extracted using dichloromethane (3x 20 mL). The combined organic layers were dried over Na₂SO₄, filtered, and evaporated to dryness. Purification was done by HPLC (reversed phase, MeOH/H₂O 7:3 + 0.1 % FA), yielding derivative **31** (414.0 mg, 1.63 mmol, 92 %) as white crystals:

HR-MS *m/z* 253.0508 (calculated for C₁₅H₉O₄: 253.0506).

¹H NMR (400 MHz, CD₃OD) δ 7.94 (s, 1H), 7.65 (dd, *J* = 7.7, 1.6 Hz, 1H), 7.55 (ddd, *J* = 8.7, 7.3, 1.6 Hz, 1H), 7.37 – 7.29 (m, 2H), 7.23 (d, *J* = 2.2 Hz, 1H), 7.09 (dd, *J* = 8.2, 2.2 Hz, 1H), 6.83 (d, *J* = 8.3 Hz, 1H).

¹³C NMR (101 MHz, CD₃OD) δ 162.59, 154.40, 147.48, 146.08, 140.05, 132.17, 129.24, 128.96, 127.74, 125.73, 121.56, 121.39, 116.96, 116.88, 116.18.

6,7-Diacetoxy-3-(3,4-dimethoxyphenyl)-2*H*-chromen-2-one (**32**)



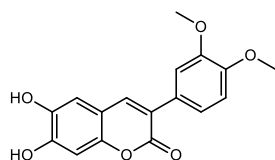
3,4-Dimethoxyphenylacetic acid (1.27 g, 6.5 mmol), 2,4,5-trihydroxybenzaldehyde (1 g, 6.5 mmol) and potassium acetate (1.12 g, 11.4 mmol) were suspended in acetic anhydride (10 mL) and the mixture was stirred under reflux for 3 hours. Subsequently it was neutralized using sodium hydrogen carbonate. The mixture was extracted using ethyl acetate (3x 30 mL) after which the organic layer was separated, dried over Na₂SO₄, filtered, and evaporated to dryness. Purification was done by HPLC (reversed phase, ACN/H₂O 7:3 - 1:0), yielding **32** (0.66 g, 1.7 mmol, 26 %) as a light yellow solid:

HR-MS *m/z* 399.1970 (calculated for C₂₁H₁₉O₈: 399.1074).

¹H NMR (400 MHz, (CD₃)₂CO) δ 8.09 (s, 1H), 7.60 (s, 1H), 7.43 (d, *J* = 2.0 Hz, 1H), 7.39 (dd, *J* = 8.3, 2.2 Hz, 1H), 7.32 (s, 1H), 7.03 (d, *J* = 8.4 Hz, 1H), 3.86 (d, *J* = 0.9 Hz, 6H), 2.33 (s, 3H), 2.31 (s, 3H).

¹³C NMR (101 MHz, (CD₃)₂CO) δ 168.80, 168.40, 160.18, 151.72, 151.16, 149.93, 145.44, 140.05, 138.54, 128.31, 128.22, 122.78, 122.37, 118.82, 113.44, 112.30, 112.15, 56.21, 56.09, 20.50, 20.41.

6,7-Dihydroxy-3-(3,4-dimethoxyphenyl)-2*H*-chromen-2-one (**33**)



Compound **32** (142 mg, 0.36 mmol) was dissolved in THF (10 mL) and water (5 mL) after which lithium hydroxide hydrate (76 mg, 1.8 mmol) was added to the solution which was stirred for 3 hours. Subsequently it was acetified to pH ~ 2 using aqueous hydrochloric acid (3 M). The mixture was extracted using ethyl acetate (3x 30 mL). The combined organic phases were dried over Na₂SO₄, filtered, and evaporated to dryness. Purification was done by HPLC (reversed phase, ACN/H₂O 7:3 - 1:0), yielding **33** (39.2 mg, 0.12 mmol, 35 %) as a yellow solid:

HR-MS *m/z* 313.0716 (calculated for C₁₇H₁₃O₆: 313.0716).

¹H NMR (400 MHz, (CD₃)₂CO) δ 8.66 (br s, 2H), 7.95 (s, 1H), 7.40 (d, *J* = 2.0 Hz, 1H), 7.34 (dd, *J* = 8.4, 2.0 Hz, 1H), 7.12 (s, 1H), 7.00 (d, *J* = 8.4 Hz, 1H), 6.83 (s, 1H), 3.85 (s, 3H), 3.85 (s, 3H).

¹³C NMR (101 MHz, (CD₃)₂CO) δ 161.17, 150.53, 150.17, 149.85, 149.48, 143.37, 139.98, 129.18, 124.43, 121.95, 113.39, 113.35, 112.98, 112.31, 103.08, 56.18, 56.08.

References

- (1) Doehlemann, G.; Ökmen, B.; Zhu, W.; Sharon, A. *Microbiol. Spectr.* **2017**, 5.
- (2) Börner, H.; Schlüter, K.; Aumann, J., Eds. *Pflanzenkrankheiten und Pflanzenschutz*; Springer-Lehrbuch, 8. Aufl.; Springer, Berlin, Heidelberg, **2009**.
- (3) Savary, S.; Willocquet, L.; Pethybridge, S. J.; Esker, P.; McRoberts, N.; Nelson, A. *Nat. Ecol. Evol.* **2019**, 3, 430–439.
- (4) Elad, Y.; Shtienberg, D. *Integr. Pest Manage. Rev.* **1995**, 1, 15–29.
- (5) Fones, H.; Gurr, S. *Fungal Genet. Biol.* **2015**, 79, 3–7.
- (6) Akino, S.; Takemoto, D.; Hosaka, K. *J. Gen. Plant Pathol.* **2014**, 80, 24–37.
- (7) Délye, C.; Jasieniuk, M.; Le Corre, V. *Trends Genet.* **2013**, 29, 649–658.
- (8) Marambe, B.; Herath, S. *Weed Sci.* **2020**, 68, 246–252.
- (9) Gerland, P.; Raftery, A. E.; Sevcíková, H.; Li, N.; Gu, D.; Spoorenberg, T.; Alkema, L.; Fosdick, B. K.; Chunn, J.; Lalic, N.; Bay, G.; Buettner, T.; Heilig, G. K.; Wilmoth, J. *Science* **2014**, 346, 234–237.
- (10) Verotta, L.; Lovaglio, E.; Vidari, G.; Finzi, P. V.; Neri, M. G.; Raimondi, A.; Parapini, S.; Taramelli, D.; Riva, A.; Bombardelli, E. *Phytochemistry* **2004**, 65, 2867–2879.
- (11) Müller, J. I.; Kusserow, K.; Hertrampf, G.; Pavic, A.; Nikodinovic-Runic, J.; Gulder, T. A. M. *Org. Biomol. Chem.* **2019**, 17, 1966–1969.
- (12) Hausteine, K. O. *Semin. Thromb. Hemost.* **1999**, 25, 5–11.
- (13) Hussain, H.; Ahmed, I.; Schulz, B.; Draeger, S.; Krohn, K. *Fitoterapia* **2012**, 83, 523–526.
- (14) Koyama, Y.; Fukakusa, Y.; Kyomura, N.; Yamagishi, S.; Arai, T. *Tetrahedron Lett.* **1969**, 355–358.
- (15) Sparace, S. A.; Reeleder, R. D.; Khanizadeh, S. *Can. J. Microbiol.* **1987**, 33, 327–330.
- (16) Zhang, Z.-R.; Leung, W. N.; Cheung, H. Y.; Chan, C. W. *Evid. Based Complement. Alternat. Med.* **2015**, 919616.
- (17) Fungicide resistance action committee (FRAC). <https://www.frac.info>, June 12, **2023**.
- (18) Herbicide Resistance Action Committee (HRAC). <https://www.hracglobal.com>, June 12, **2023**.
- (19) Bhat, Z. S.; Rather, M. A.; Maqbool, M.; Lah, H. U.; Yousuf, S. K.; Ahmad, Z. *Biomed. Pharmacother.* **2017**, 91, 265–277.
- (20) Fujita, T.; Nishimura, H.; Kaburagi, K.; Mizutani, J. *Phytochemistry* **1994**, 36, 23–27.
- (21) Araniti, F.; Mancuso, R.; Lupini, A.; Giofrè, S. V.; Sunseri, F.; Gabriele, B.; Abenavoli, M. R. *Molecules* **2015**, 20, 17883–17902.
- (22) Igarashi, Y.; Ogawa, M.; Sato, Y.; Saito, N.; Yoshida, R.; Kunoh, H.; Onaka, H.; Furumai, T. *J. Antibiot.* **2000**, 53, 1117–1122.
- (23) McLaughlin, M. J.; Hsung, R. P.; Cole, K. P.; Hahn, J. M.; Wang, J. *Org. Lett.* **2002**, 4, 2017–2020.
- (24) Zhang, X.; McLaughlin, M.; Muñoz, R.; Hsung, R.; Wang, J.; Swiderski, J. *Synthesis* **2007**, 2007, 749–753.
- (25) Groutas, W. C.; Huang, T. L.; Stanga, M. A.; Brubaker, M. J.; Moi, M. K. *J. Heterocycl. Chem.* **1985**, 22, 433–435.
- (26) Ma, S. M.; Li, J. W.-H.; Choi, J. W.; Zhou, H.; Lee, K. K. M.; Moorthie, V. A.; Xie, X.; Kealey, J. T.; Da Silva, N. A.; Vederas, J. C.; Tang, Y. *Science* **2009**, 326, 589–592.

- (27) Brandenburg, C. A.; Castro, C. A.; Blacutt, A. A.; Costa, E. A.; Brinton, K. C.; Corral, D. W.; Drozd, C. L.; Roper, M. C.; Rolshausen, P. E.; Maloney, K. N.; Lockner, J. W. *J. Nat. Prod.* **2020**, *83*, 1810–1816.
- (28) Hansen, C. A.; Frost, J. W. *J. Am. Chem. Soc.* **2002**, *124*, 5926–5927.
- (29) Douglas, C. J.; Sklenicka, H. M.; Shen, H. C.; Mathias, D. S.; Degen, S. J.; Golding, G. M.; Morgan, C. D.; Shih, R. A.; Mueller, K. L.; Scurer, L. M.; Johnson, E. W.; Hsung, R. P. *Tetrahedron* **1999**, *55*, 13683–13696.
- (30) Rogez-Florent, T.; Meignan, S.; Foulon, C.; Six, P.; Gros, A.; Bal-Mahieu, C.; Supuran, C. T.; Scozzafava, A.; Frédérick, R.; Masereel, B.; Depreux, P.; Lansiaux, A.; Goossens, J.-F.; Gluszok, S.; Goossens, L. *Bioorg. Med. Chem.* **2013**, *21*, 1451–1464.
- (31) Roussaki, M.; Kontogiorgis, C. A.; Hadjipavlou-Litina, D.; Hamilakis, S.; Detsi, A. *Bioorg. Med. Chem. Lett.* **2010**, *20*, 3889–3892.
- (32) Chattapadhyay, T. K.; Dureja, P. *J. Agric. Food Chem.* **2006**, *54*, 2129–2133.
- (33) Montagner, C.; Souza, S. M. de; Groposo, C.; Delle Monache, F.; Smânia, E. F. A.; Smânia, A. *Z. Naturforsch. C* **2008**, *63*, 21–28.
- (34) Pan, S.; Bhattacharyya, A. *J. Plant Dis. Prot.* **1983**, *90*, 265–268.
- (35) Li, F.; Ye, Z.; Huang, Z.; Chen, X.; Sun, W.; Gao, W.; Zhang, S.; Cao, F.; Wang, J.; Hu, Z.; Zhang, Y. *Bioorg. Chem.* **2021**, *117*, 105452.
- (36) Marsico, G.; Ciccone, M. S.; Masi, M.; Freda, F.; Cristofaro, M.; Evidente, A.; Superchi, S.; Scafato, P. *Molecules* **2019**, *24*, 3193.
- (37) Andolfi, A.; Boari, A.; Evidente, M.; Cimmino, A.; Vurro, M.; Ash, G.; Evidente, A. *J. Nat. Prod.* **2015**, *78*, 623–629.

Appendix

GGX204_CARBON_01
GGX204/CDCl₃

200 190 180 170 160 150 140 130 120 110 100 90 80 70 60 50 40 30 20 10 0

f1 (ppm)

VII

GGX588.11.fid
GGX588/CDCl₃/1H
Fuchs 20221101_10
Proton_IPB CDCl₃ /opt/nmrdata/2020/GGX walkup 14

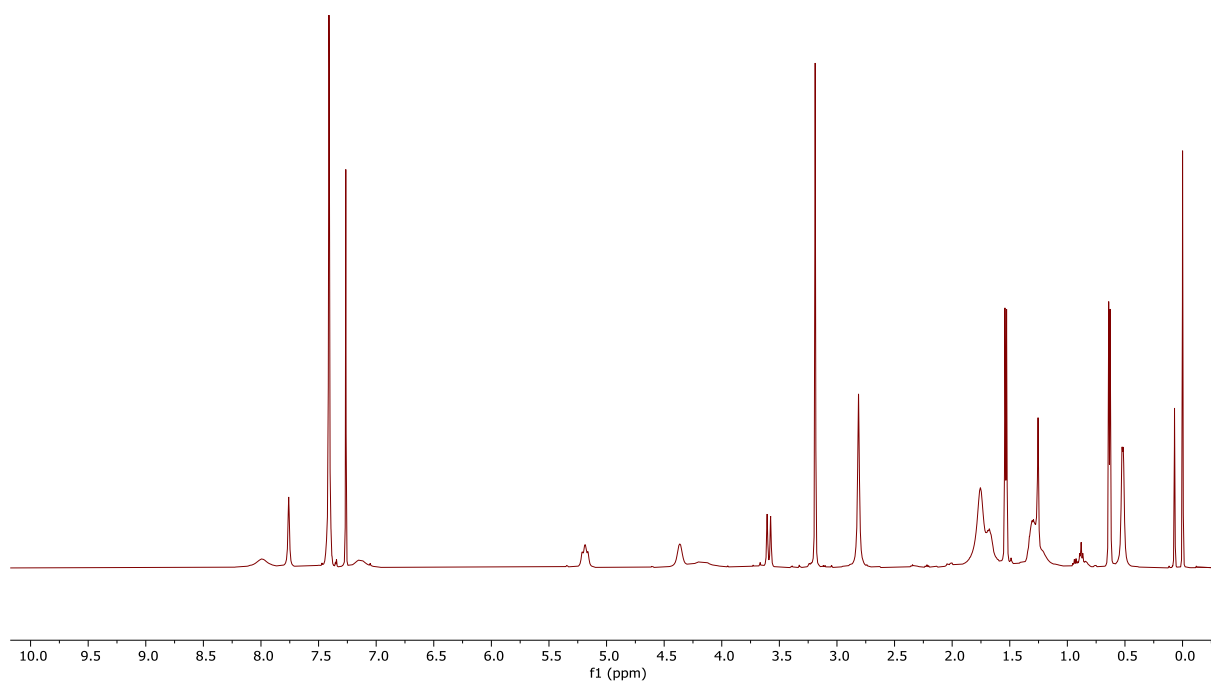


Figure 34: ¹H NMR spectrum (500 MHz, CDCl₃) of compound **5a** (Chapter 2, Tentoxin, synthesis via HWE-route).

GGX588.11.fid
GGX588/CDCl₃/1H
Fuchs 20221101_10
Proton_IPB CDCl₃ /opt/nmrdata/2020/GGX walkup 14

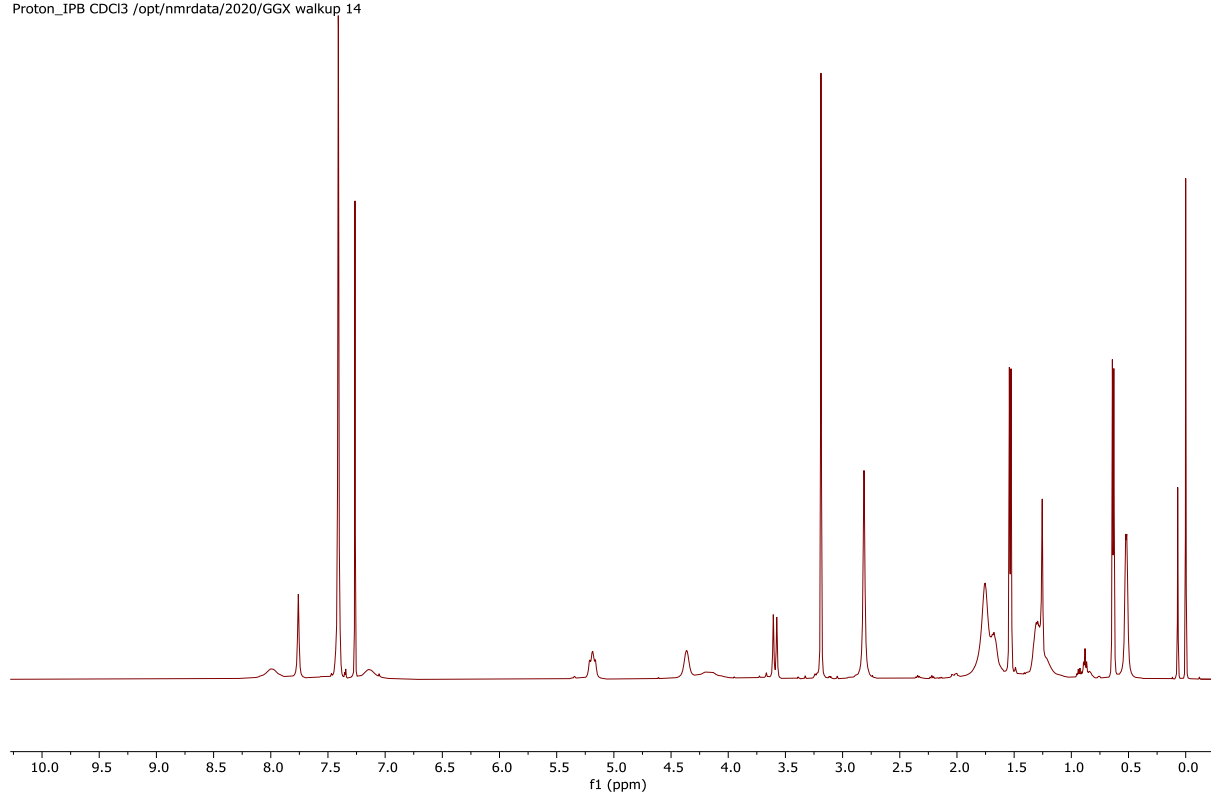


Figure 35: ¹³C NMR spectrum (126 MHz, CDCl₃) of compound **5a** (Chapter 2, Tentoxin, synthesis via HWE-route).

GGX208.11.fid
GGX208/CDCl₃/1H
Fuchs 20211029_02
Proton_IPB CDCl₃ /opt/nmrdata/2020/GGX walkup 11

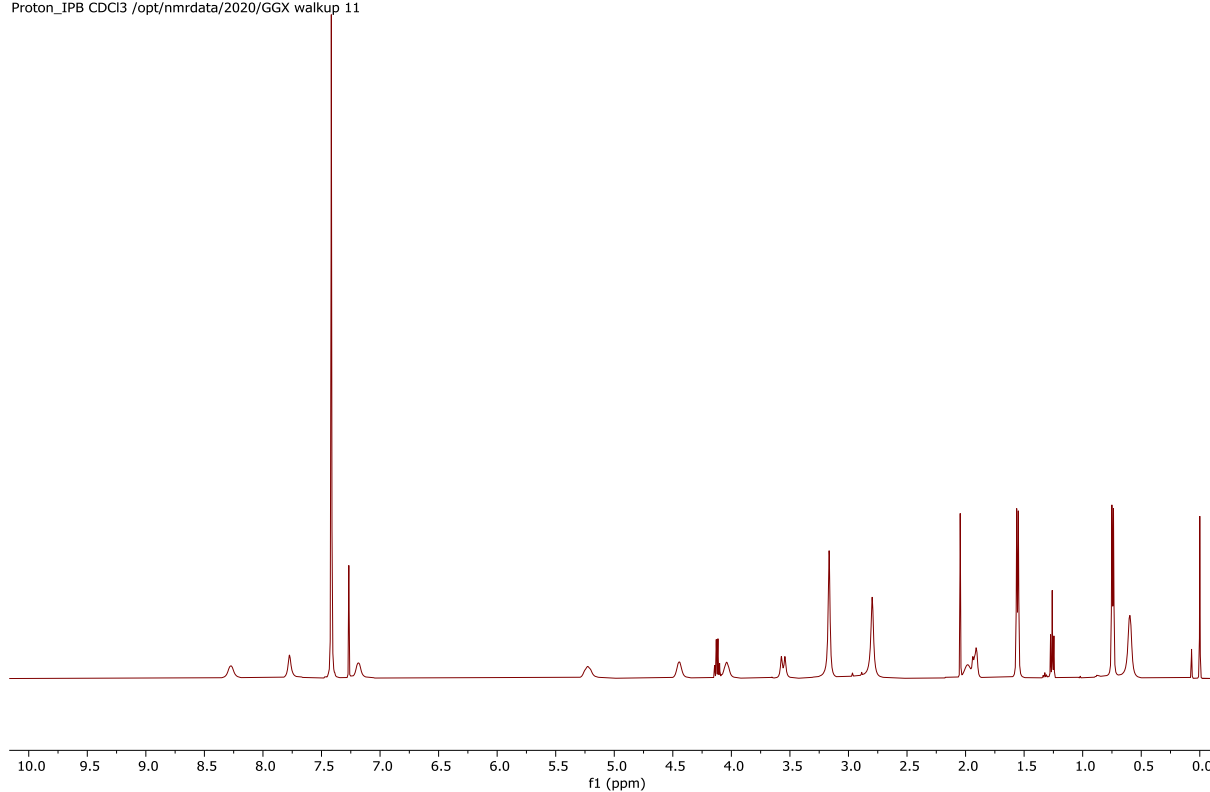


Figure 36: ¹H NMR spectrum of compound **5b** (Chapter 2)

GGX208.12.fid
GGX208/CDCl₃/13C
Fuchs 20211029_02
Carbon_dec_IPB CDCl₃ /opt/nmrdata/2020/GGX walkup 11

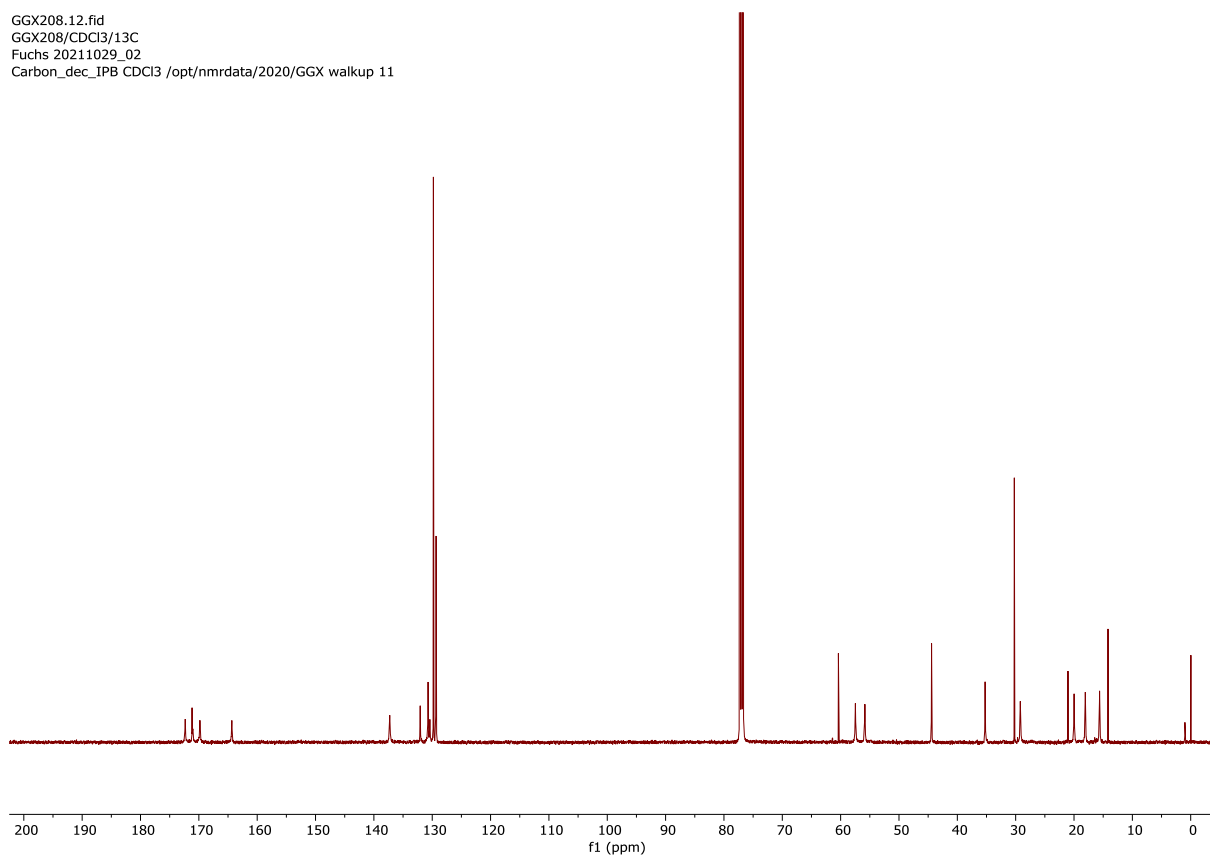


Figure 37: ¹³C NMR spectrum (126 MHz, CDCl₃) of compound **5b** (Chapter 2).

GGX224.11.fid
GGX224/CDCl₃/1H
Fuchs 20211102_05
Proton_IPB CDCl₃ /opt/nmrdata/2020 walkup 13

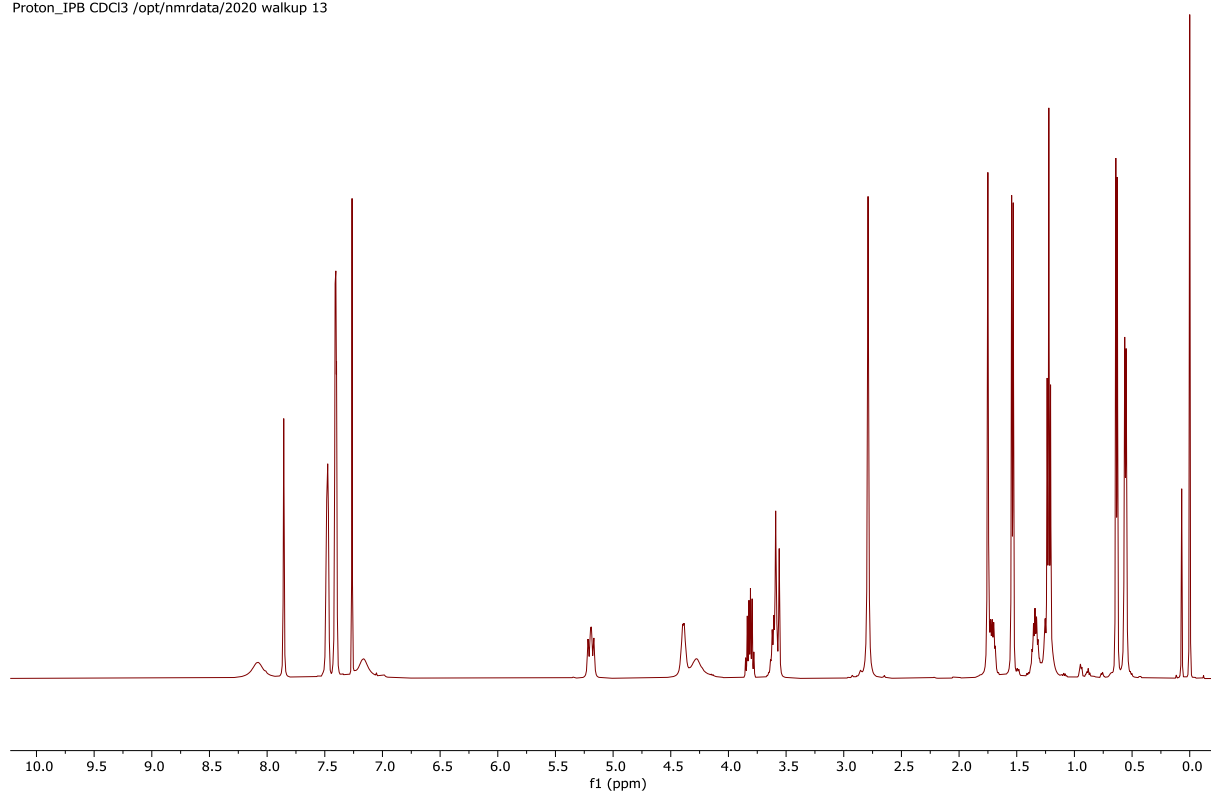


Figure 38: ¹H NMR spectrum (500 MHz, CDCl₃) of compound **5c** (Chapter 2).

GGX224.12.fid
GGX224/CDCl₃/13C
Fuchs 20211102_05
Carbon_dec_IPB CDCl₃ /opt/nmrdata/2020 walkup 13

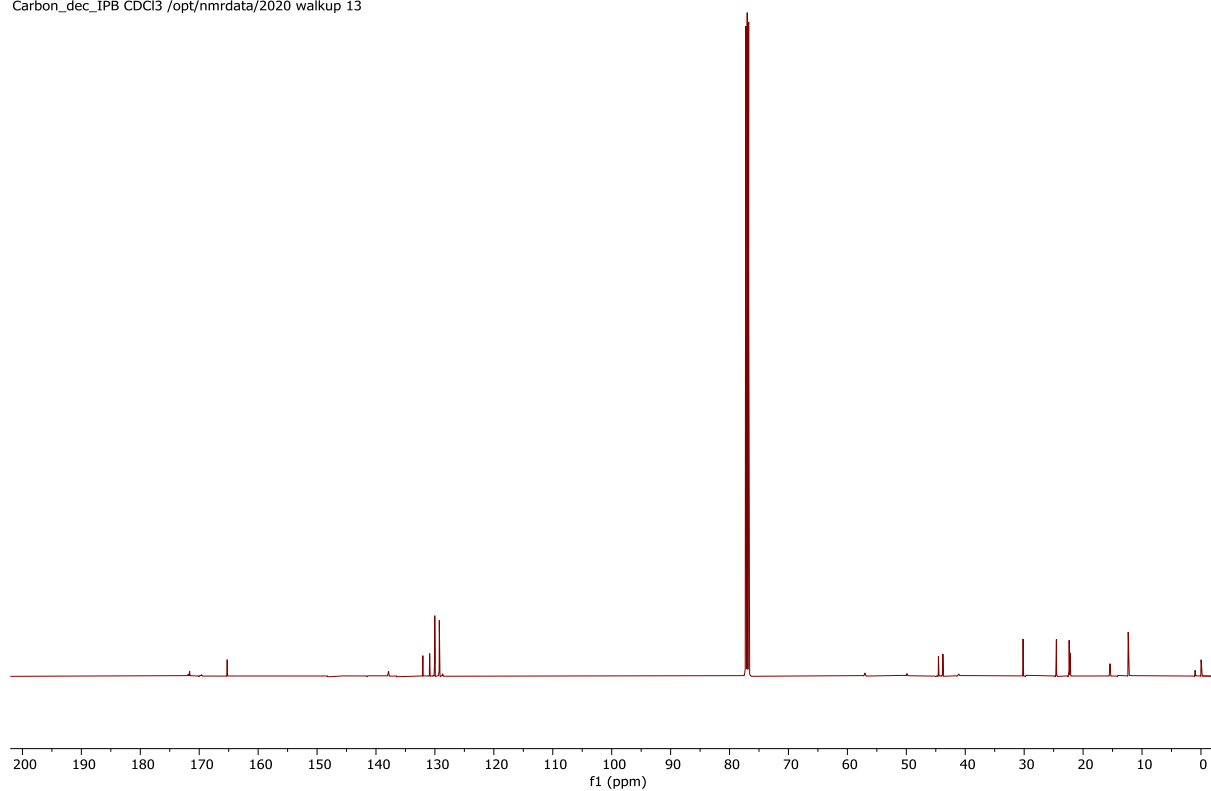


Figure 39: ¹³C NMR spectrum (126 MHz, CDCl₃) of compound **5c** (Chapter 2).

GGX258.11.fid
GGX258/CDCl₃/1H
Fuchs 20211112_04
Proton_IPB CDCl₃ /opt/nmrdata/2020/GGX walkup 19

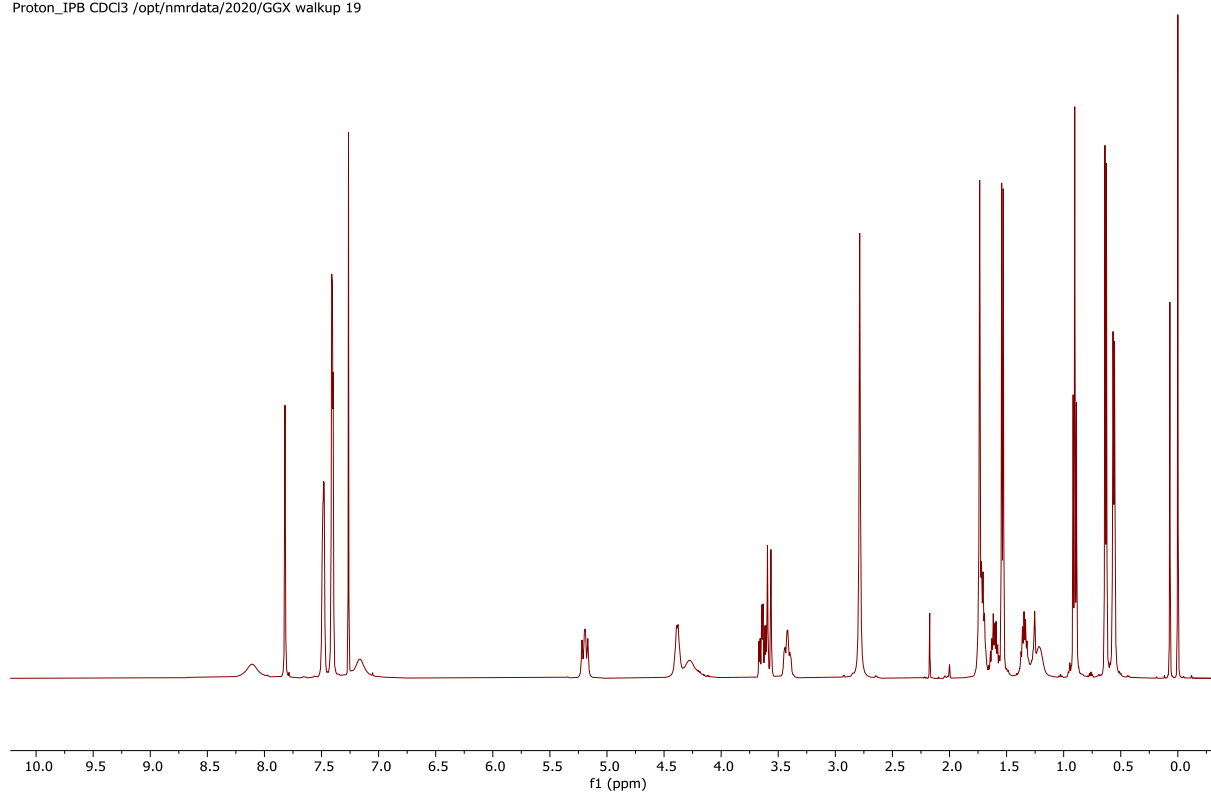


Figure 40: ¹H NMR spectrum (500 MHz, CDCl₃) of compound **5d** (Chapter 2).

GGX258.12.fid
GGX258/CDCl₃/13C
Fuchs 20211112_04
Carbon_dec_IPB CDCl₃ /opt/nmrdata/2020/GGX walkup 19

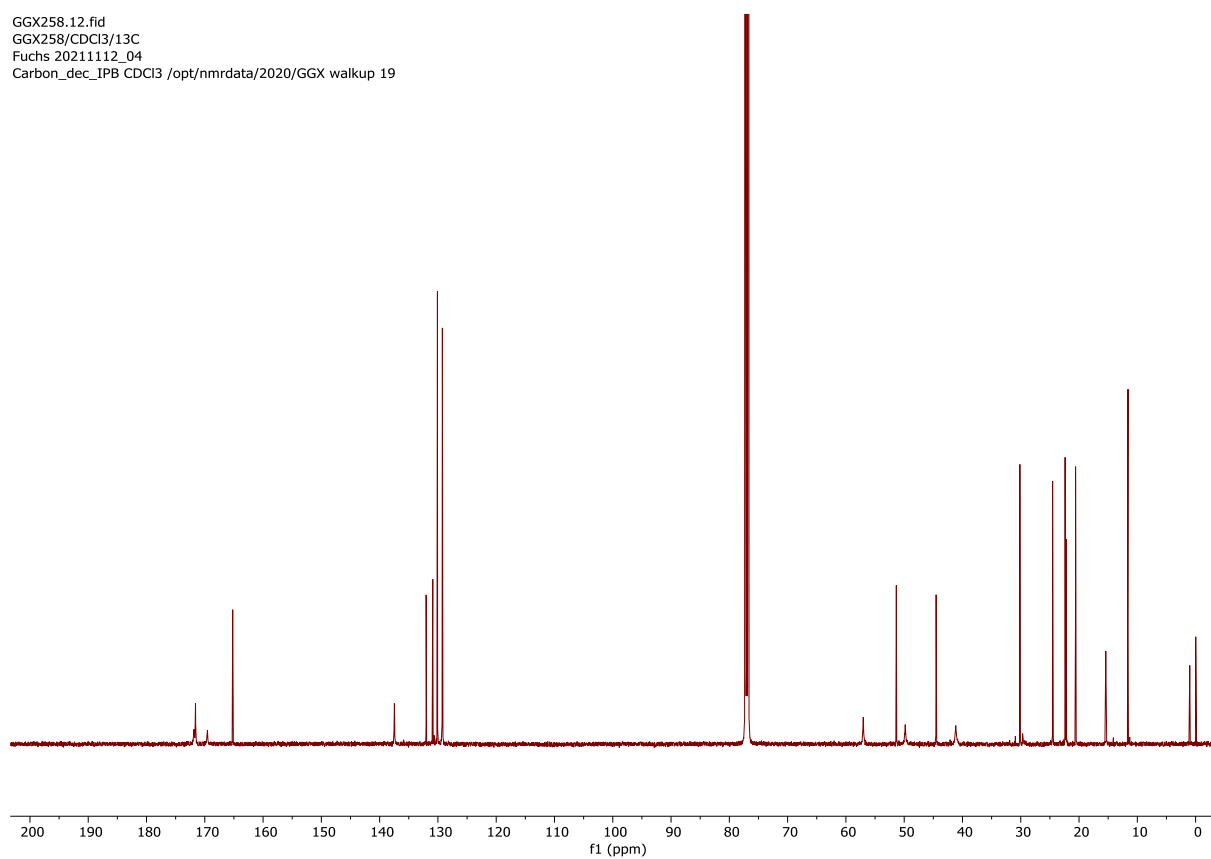


Figure 41: ¹³C NMR spectrum (126 MHz, CDCl₃) of compound **5d** (Chapter 2).

GGX256_PROTON_02
GGX256/CDCl₃

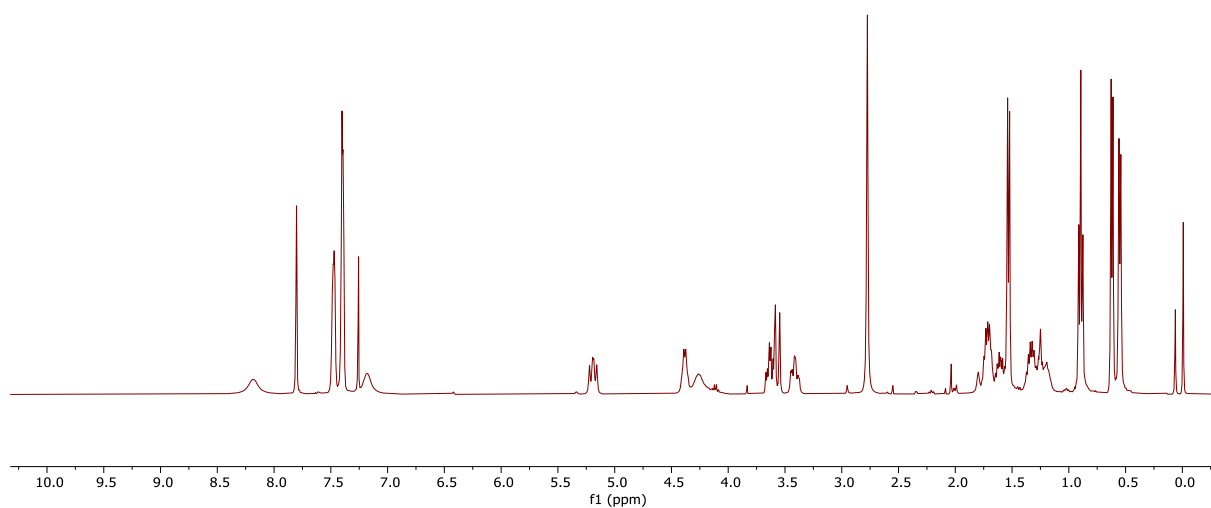


Figure 42: ¹H NMR spectrum (500 MHz, CDCl₃) of compound **5e** (Chapter 2).

GGX256_CARBON_01
GGX256/CDCl₃

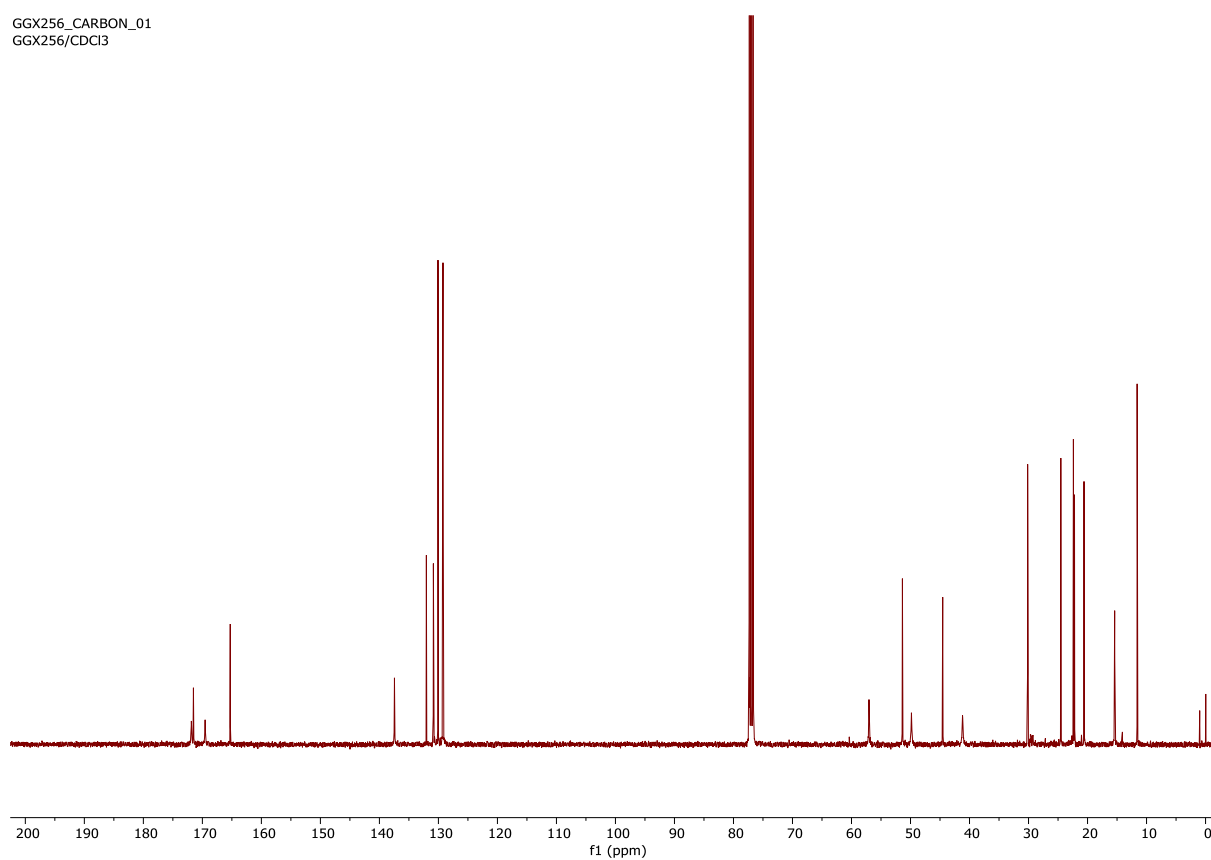


Figure 43: ¹³C NMR spectrum (126 MHz, CDCl₃) of compound **5e** (Chapter 2).

GGX247_II.11.fid
GGX247_II/CDCI3/1H
Fuchs 20211104_08
Proton_IPB CDCl3 /opt/nmrdata/2020/GGX walkup 14

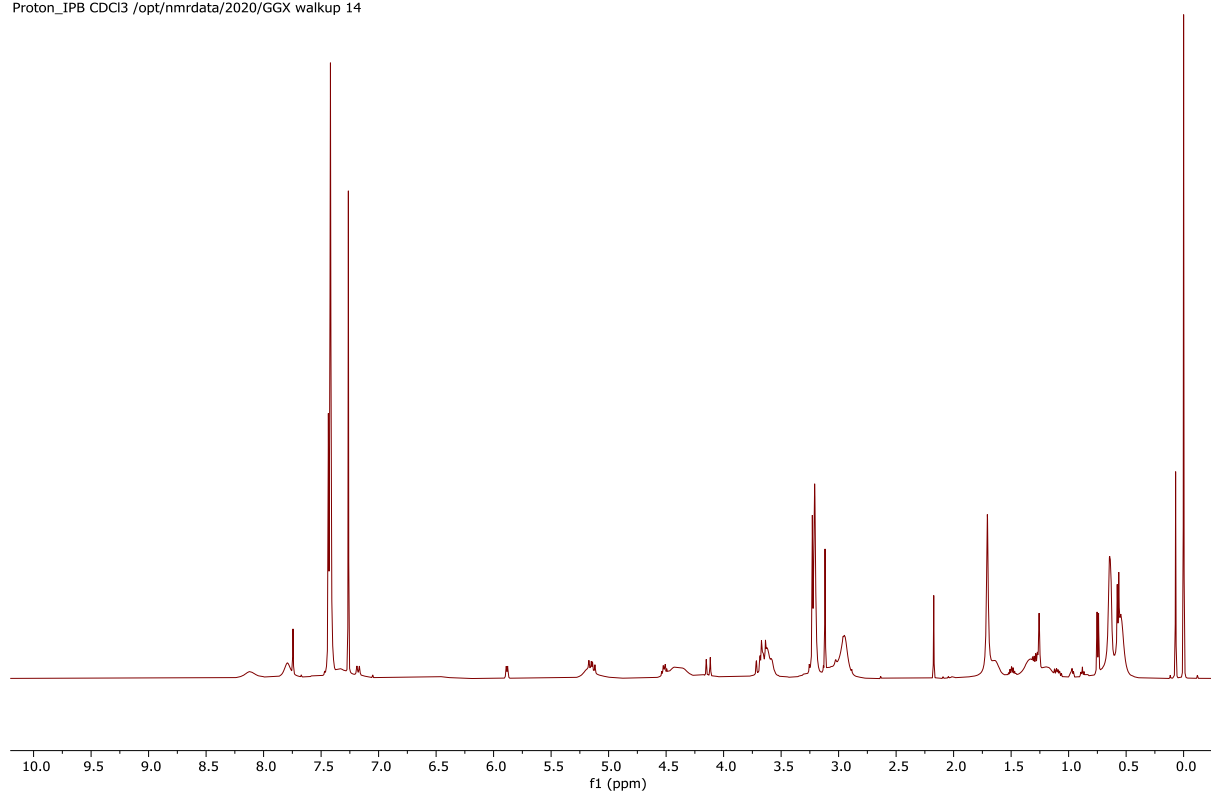


Figure 44: ¹H NMR spectrum (500 MHz, CDCl₃) of compound **5f** (Chapter 2).

GGX247_II.12.fid
GGX247_II/CDCI3/13C
Fuchs 20211104_08
Carbon_dec_IPB CDCl3 /opt/nmrdata/2020/GGX walkup 14

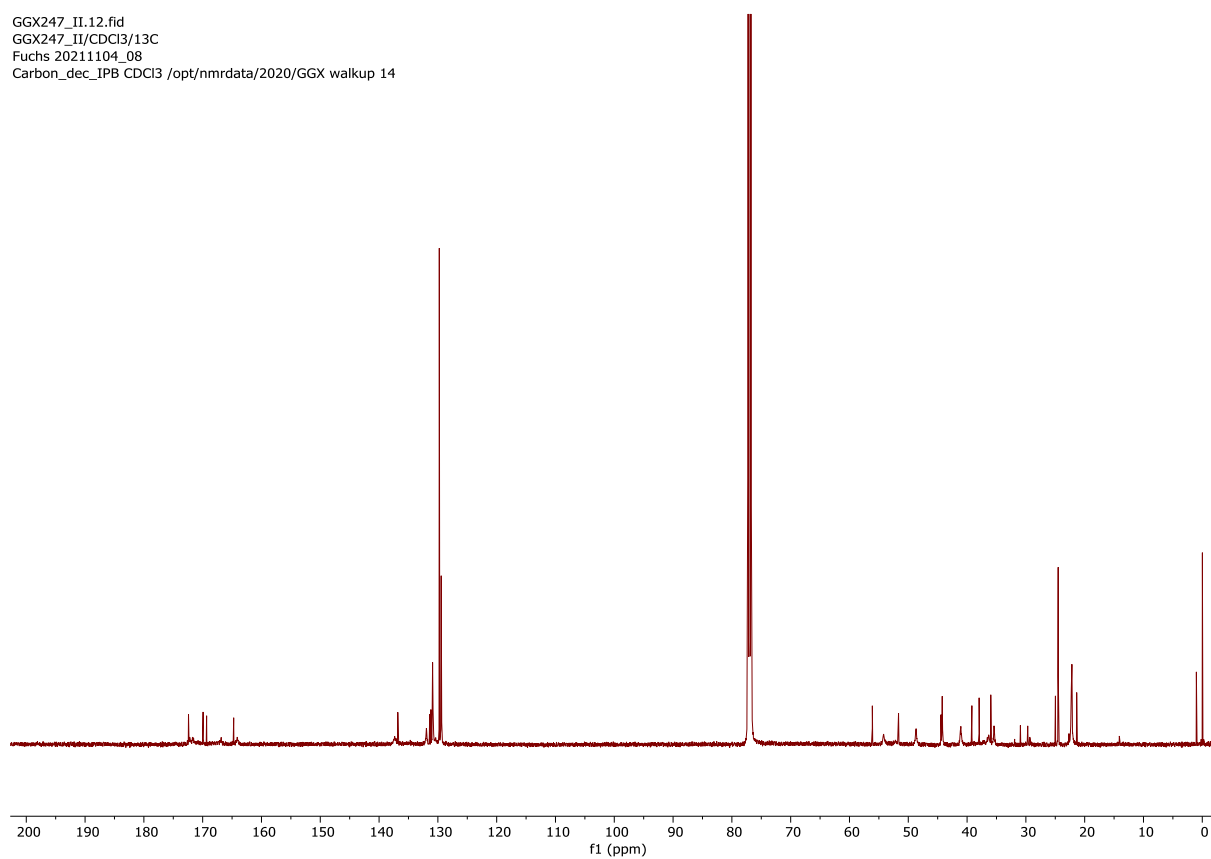


Figure 45: ¹³C NMR spectrum (126 MHz, CDCl₃) of compound **5f** (Chapter 2).

GGX602_PROTON_02
GGX602/CDCl₃/1H
Fuchs 20221220_01
Tue Dec 20 21:02 2022

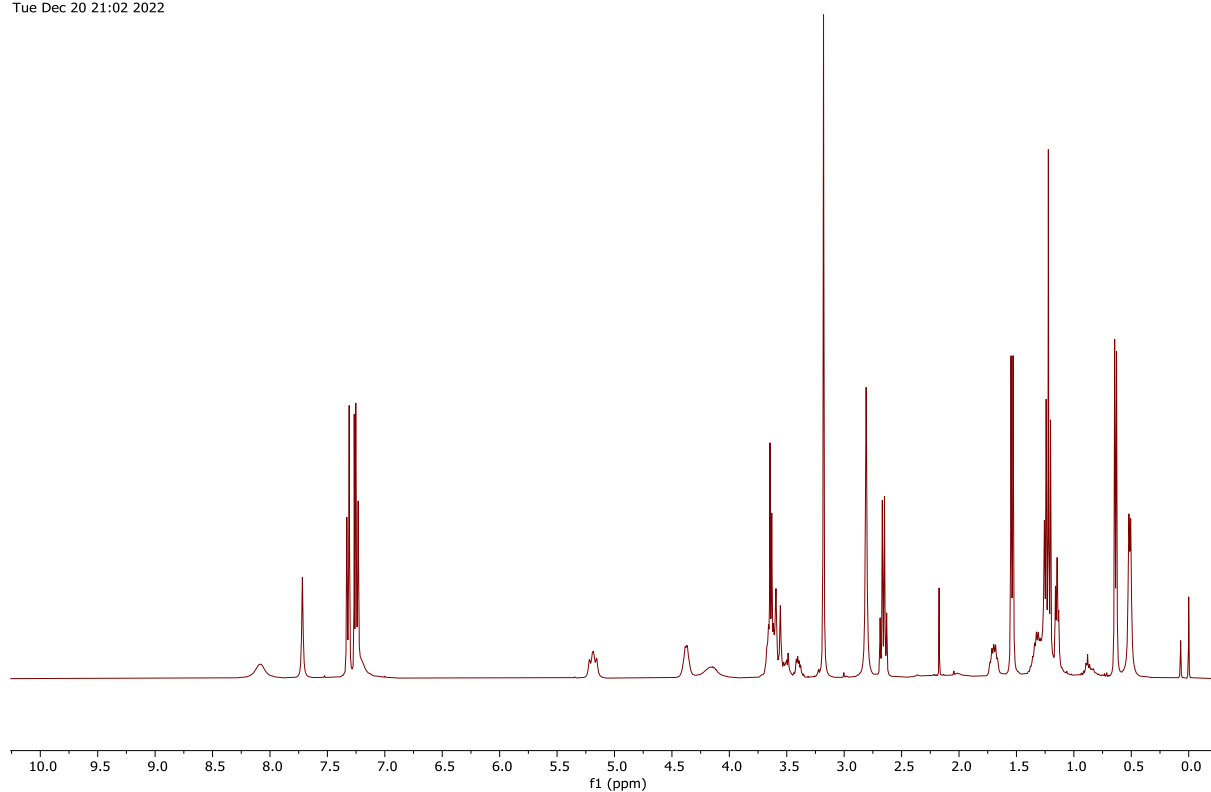


Figure 46: ¹H NMR spectrum (400 MHz, CDCl₃) of compound **5g** (Chapter 2).

GGX602_CARBON_01
GGX602/CDCl₃/13C
Fuchs 20221220_01
Wed Dec 21 00:37 2022

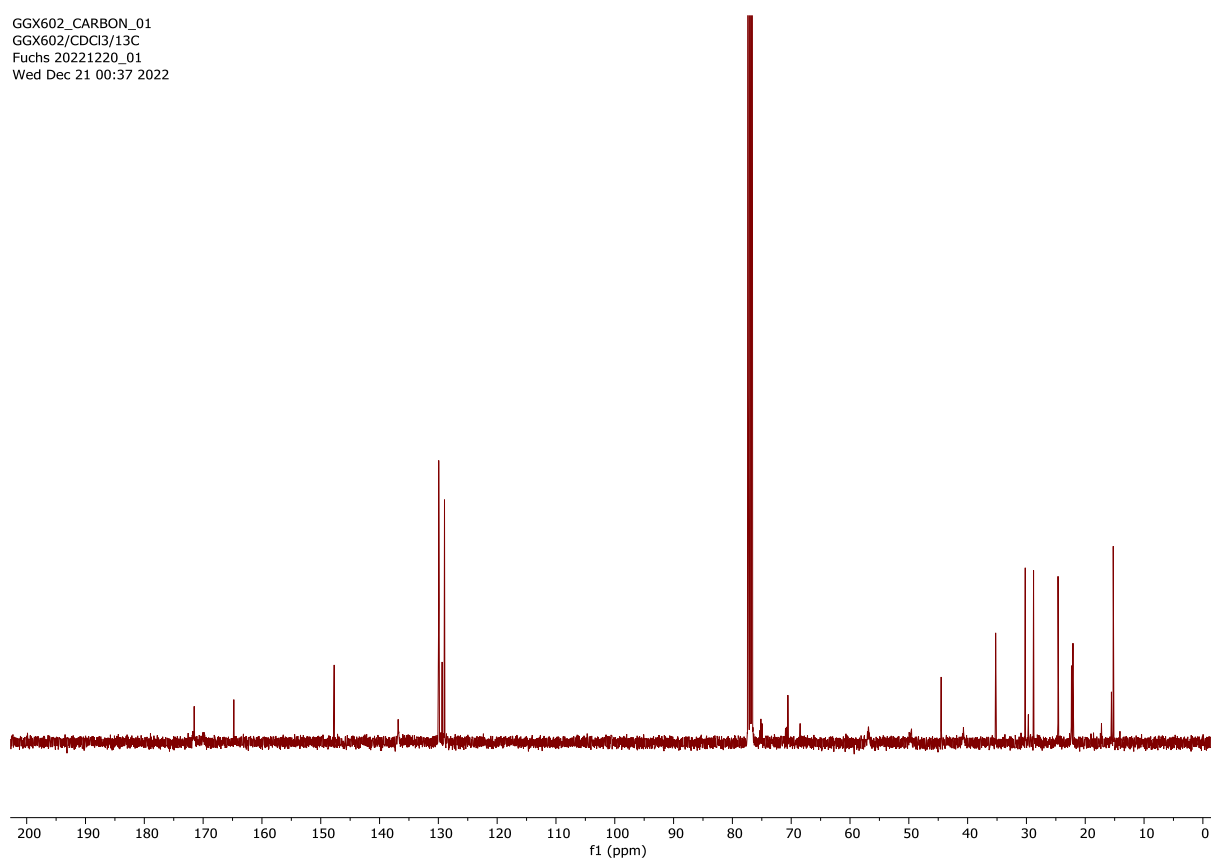


Figure 47: ¹³C NMR spectrum (101 MHz, CDCl₃) of compound **5g** (Chapter 2)

GGX628_PROTON_02
GGX628/CDCl₃/1H
Fuchs 20221220_06
Wed Dec 21 16:51 2022

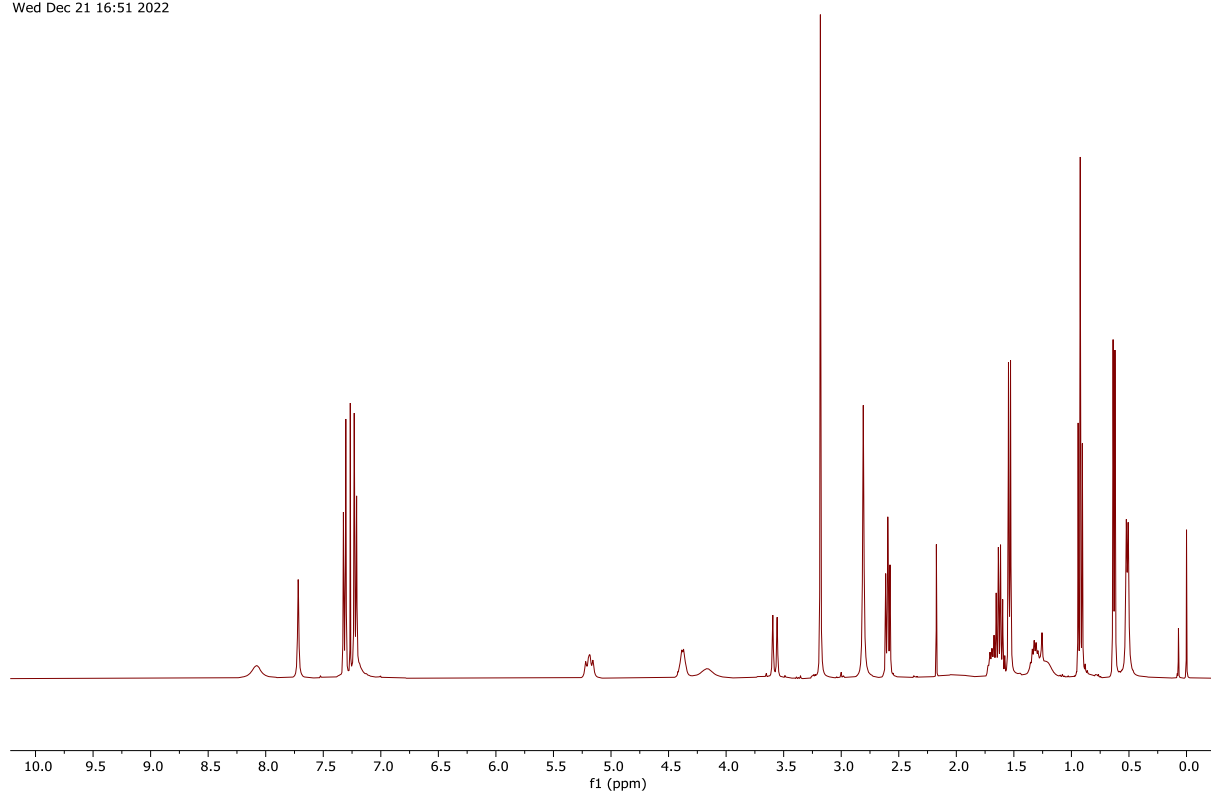


Figure 48: ¹H NMR spectrum (400 MHz, CDCl₃) of compound **5h** (Chapter 2).

GGX628_CARBON_01
GGX628/CDCl₃/13C
Fuchs 20221220_06
Wed Dec 21 22:13 2022

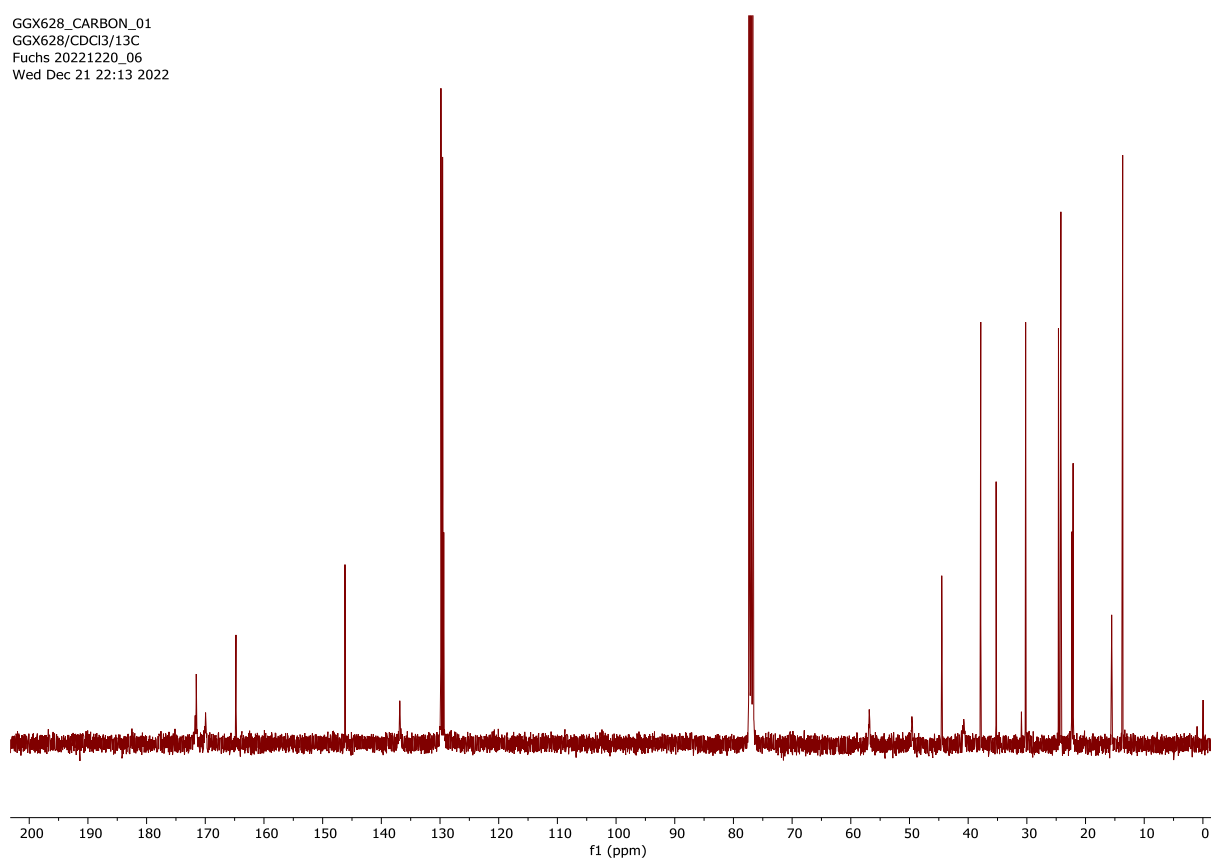


Figure 49: ¹³C NMR spectrum (101 MHz, CDCl₃) of compound **5h** (Chapter 2).

GGX608.11.fid
GGX608/CDCl₃/1H
Fuchs 20221220_03
Proton_IPB CDCl₃ /opt/nmrdata/2020/GGX walkup 15

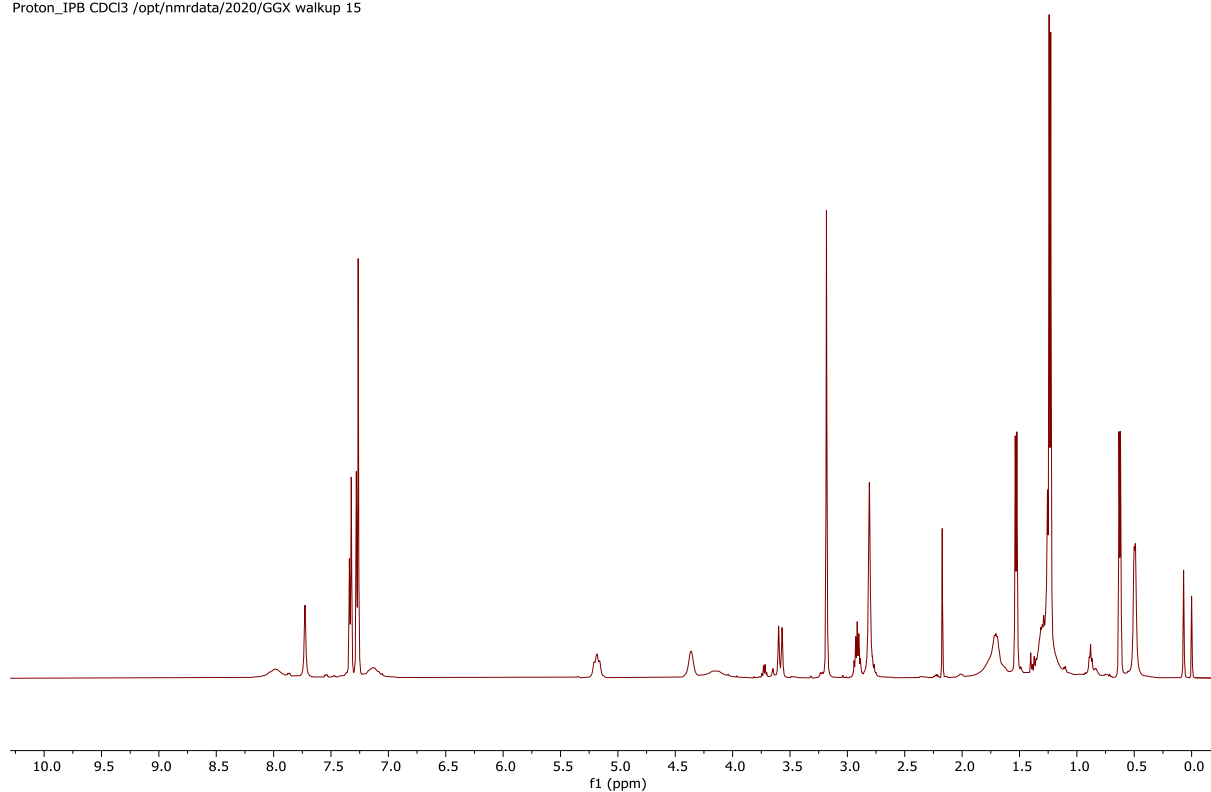


Figure 50: ¹H NMR spectrum (500 MHz, CDCl₃) of compound **5i** (Chapter 2).

GGX608.12.fid
GGX608/CDCl₃/13C
Fuchs 20221220_03
Carbon_dec_IPB CDCl₃ /opt/nmrdata/2020/GGX walkup 15

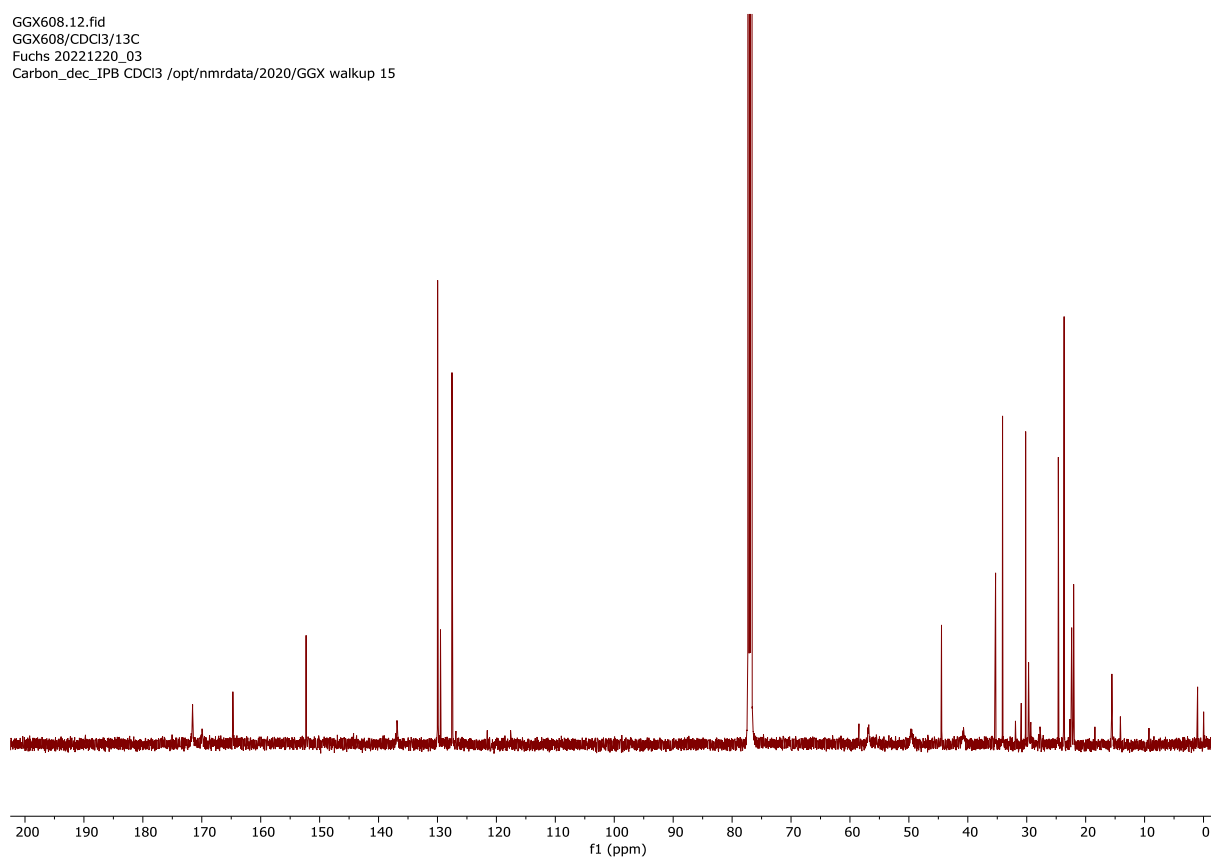


Figure 51: ¹³C NMR spectrum (126 MHz, CDCl₃) of compound **5i** (Chapter 2).

GGX626_PROTON_01
GGX626/CDCl₃/1H
Fuchs 20221220_05
Tue Dec 20 09:16 2022

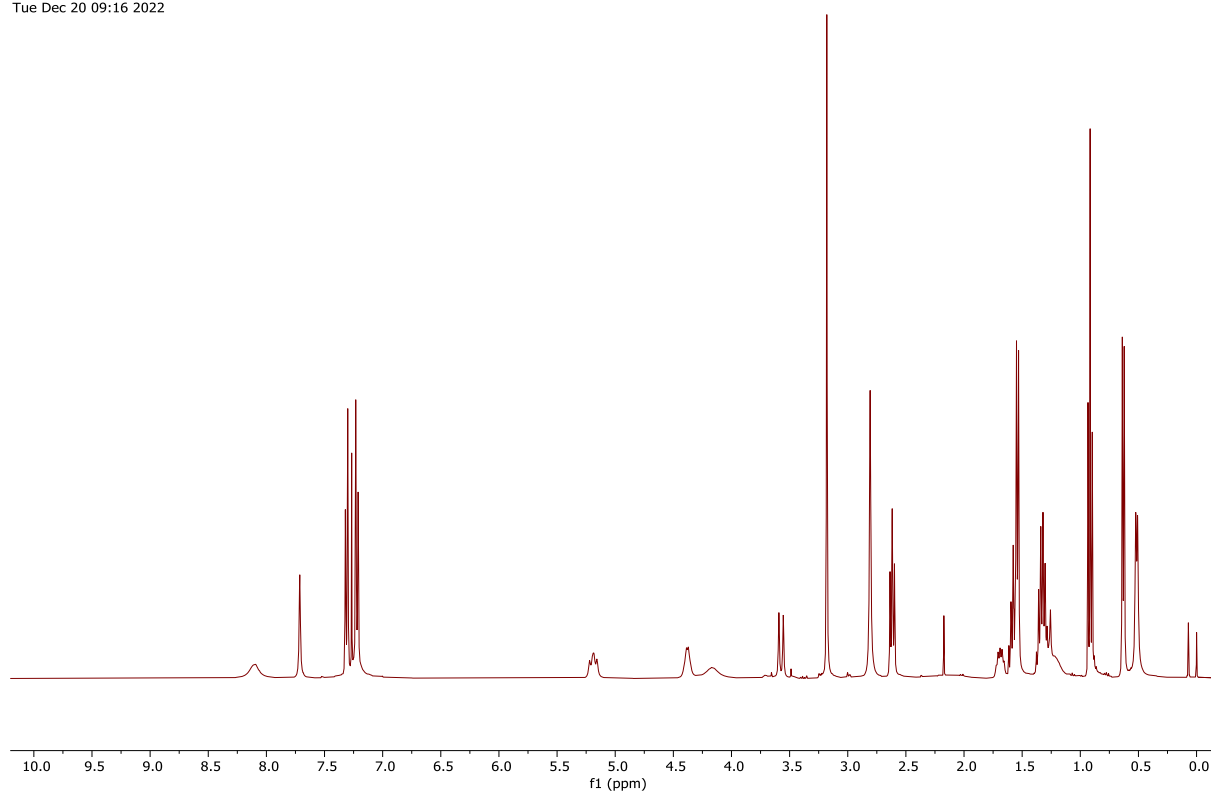


Figure 52: ¹H NMR spectrum (400 MHz, CDCl₃) of compound **5j** (Chapter 2).

GGX626_CARBON_01
GGX626/CDCl₃/13C
Fuchs 20221220_05
Wed Dec 21 05:56 2022

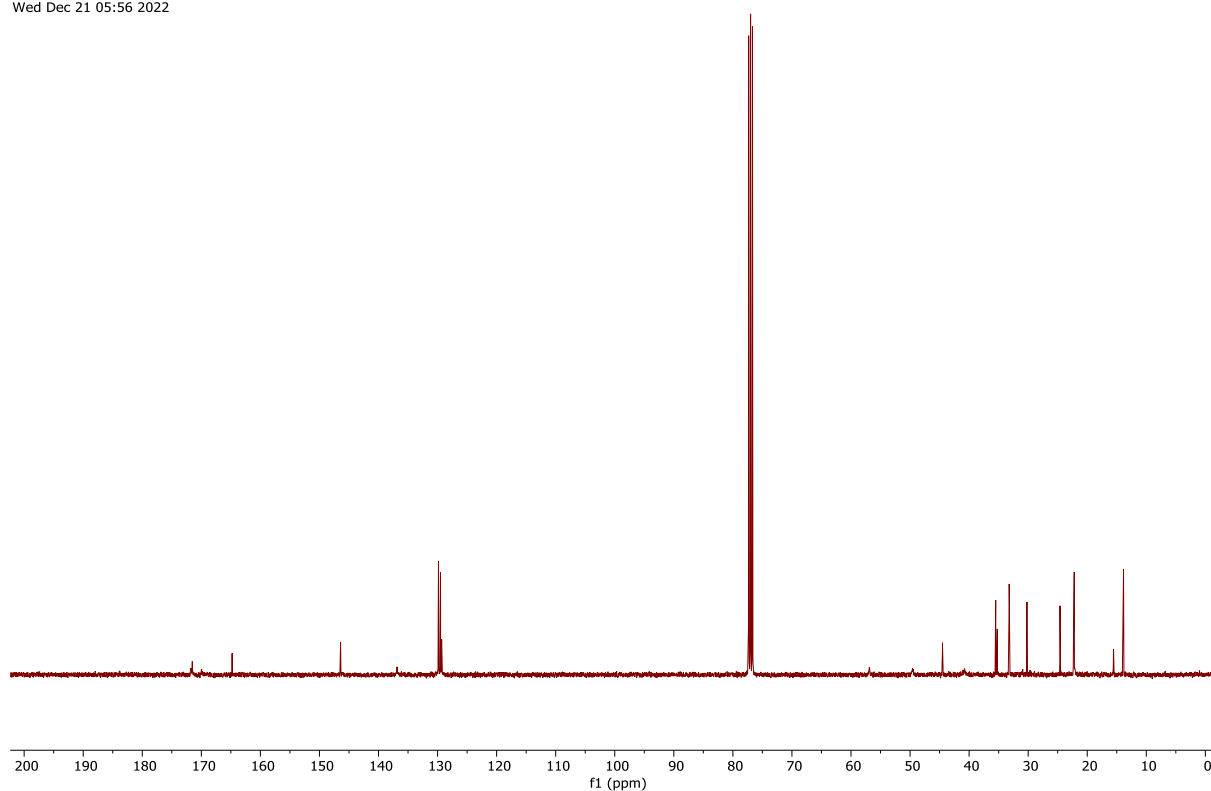


Figure 53: ¹³C NMR spectrum (101 MHz, CDCl₃) of compound **5j** (Chapter 2).

[illegible]

GGX633_CARBON_01
GGX633/CDCI3/13C
Fuchs 20221220_09
Wed Dec 21 07:43 2022

200 190 180 170 160 150 140 130 120 110 100 90 80 70 60 50 40 30 20 10 0

f1 (ppm)

XVIII

GGX593.11.fid
GGX593/CDCl₃/1H
Fuchs 20221219_07
Proton_IPB CDCl₃ /opt/nmrdata/2020/GGX walkup 13

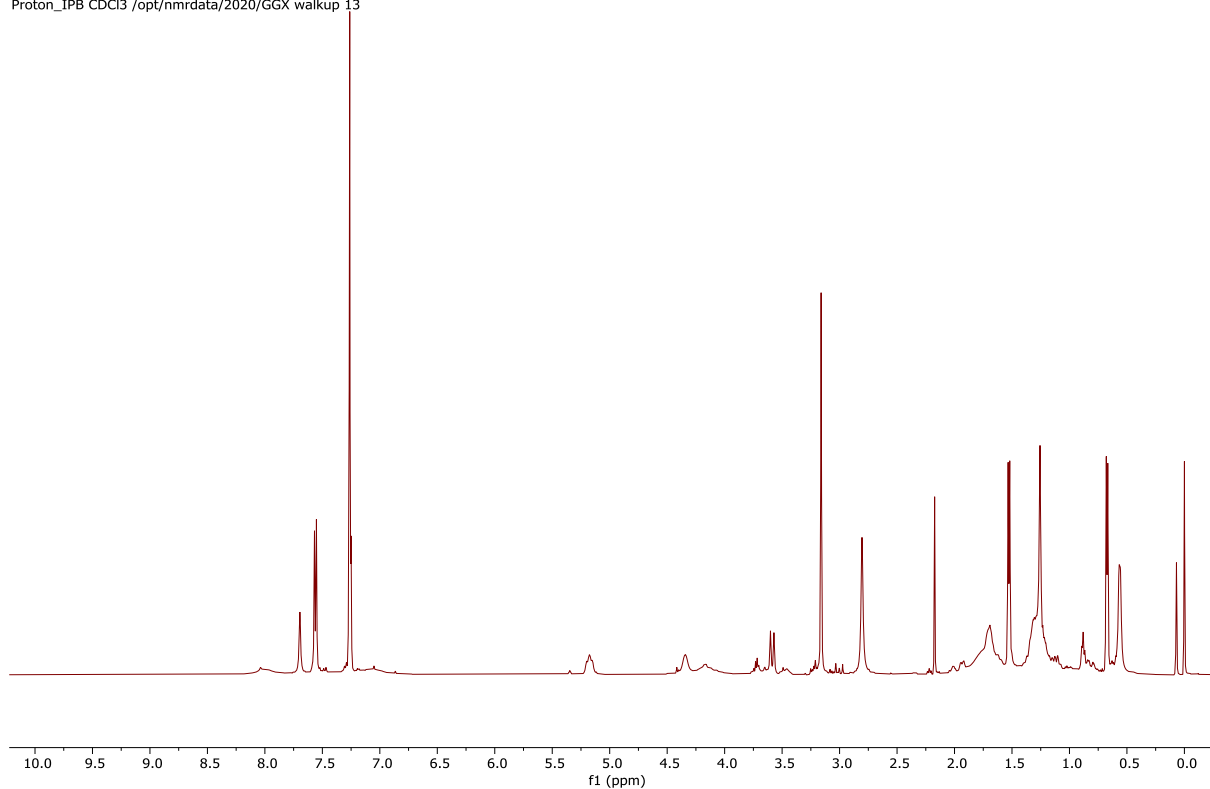


Figure 56: ¹H NMR spectrum (500 MHz, CDCl₃) of compound **5I** (Chapter 2).

GGX593.12.fid
GGX593/CDCl₃/13C
Fuchs 20221219_07
Carbon_dec_IPB CDCl₃ /opt/nmrdata/2020/GGX walkup 13

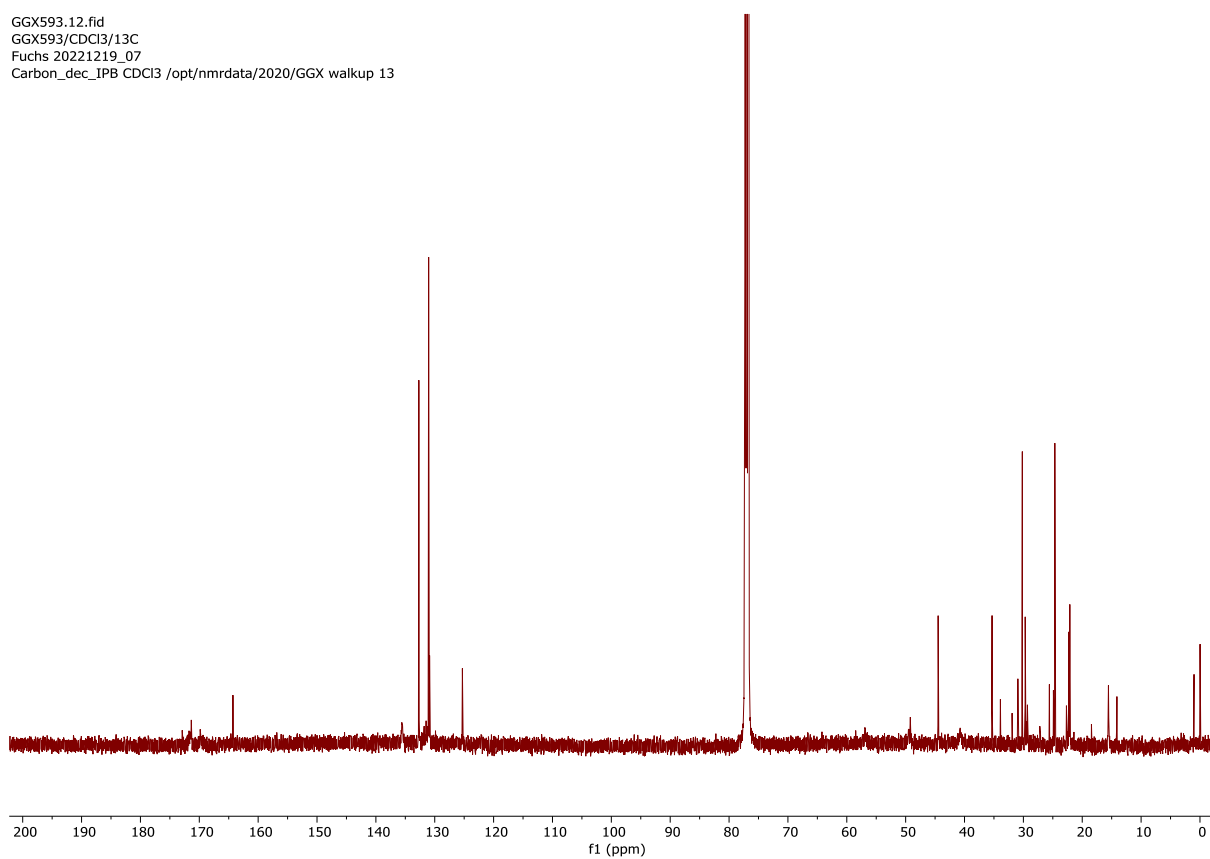


Figure 57: ¹³C NMR spectrum (126 MHz, CDCl₃) of compound **5I** (Chapter 2).

GGX591.11.fid
GGX591/CDCl₃/1H
Fuchs 20221219_05
Proton_IPB CDCl₃ /opt/nmrdata/2020/GGX walkup 11

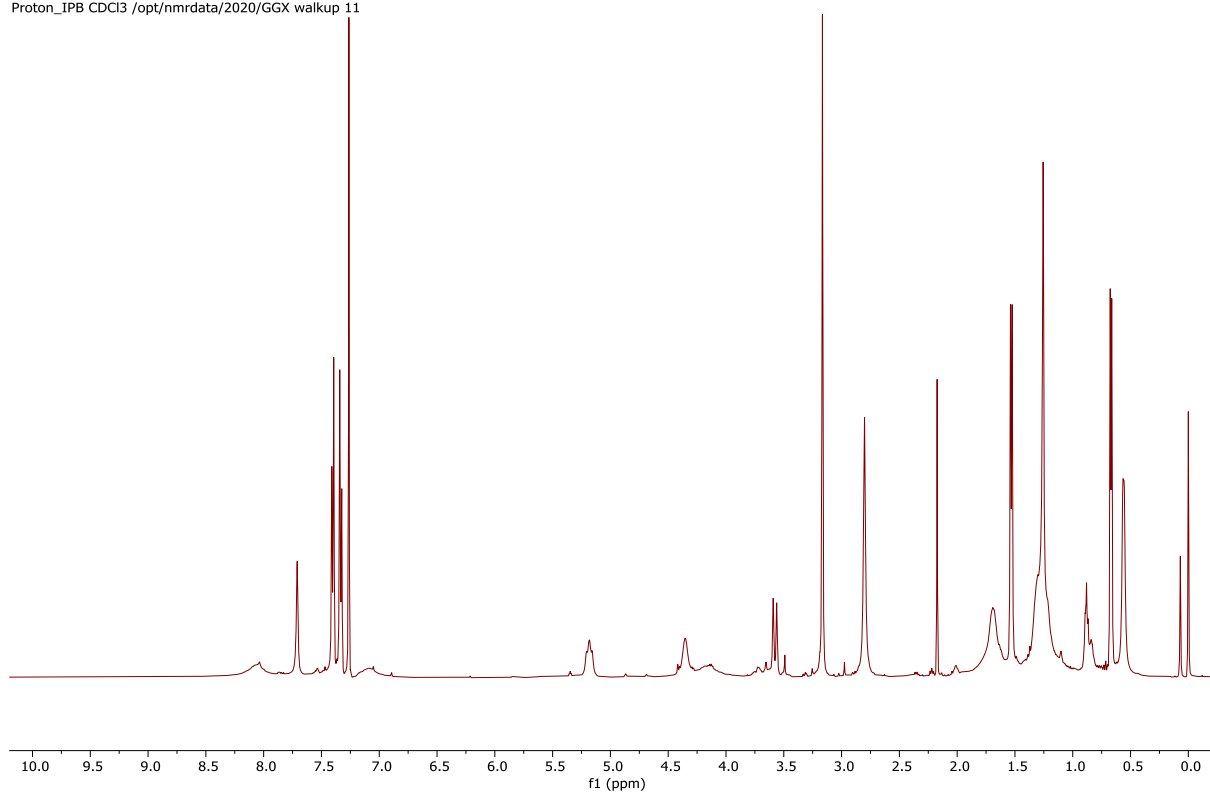


Figure 58: ¹H NMR spectrum (500 MHz, CDCl₃) of compound **5m** (Chapter 2).

GGX591.12.fid
GGX591/CDCl₃/13C
Fuchs 20221219_05
Carbon_dec_IPB CDCl₃ /opt/nmrdata/2020/GGX walkup 11

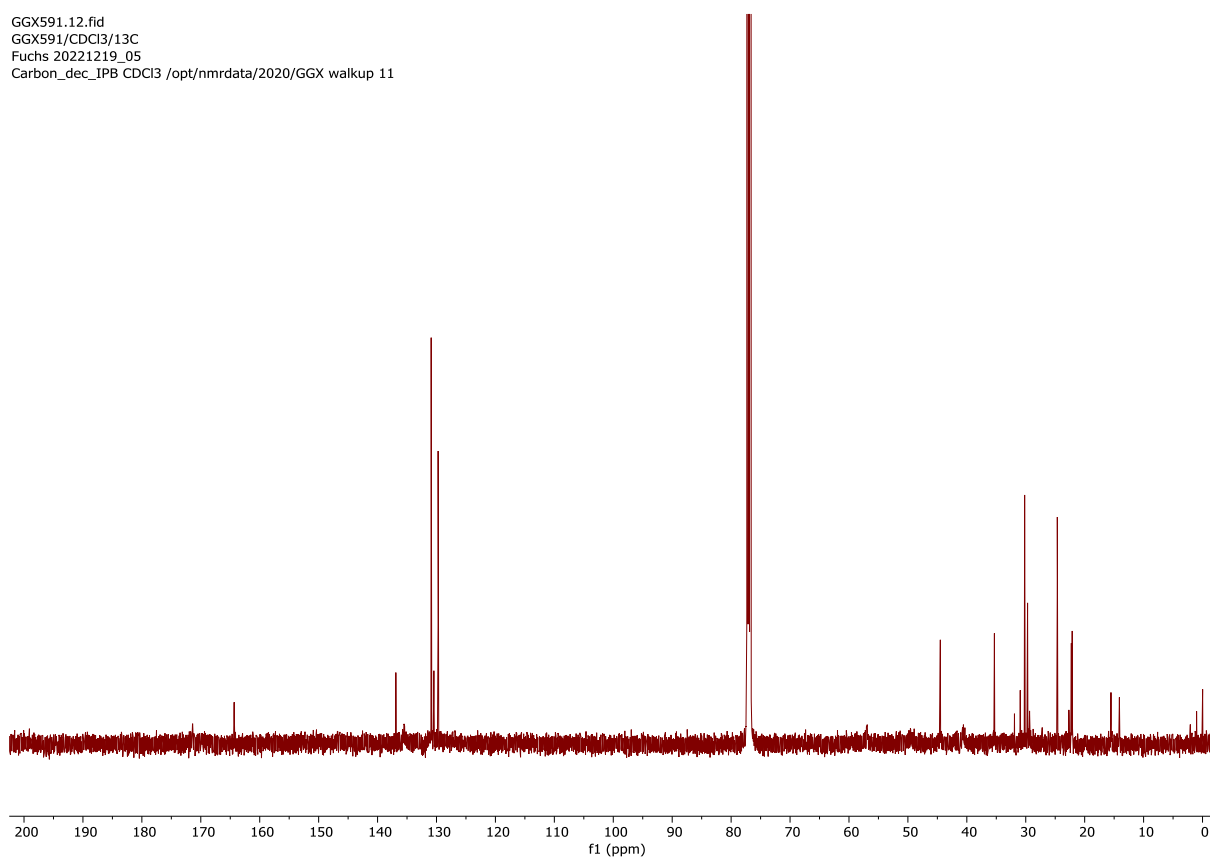


Figure 59: ¹³C NMR spectrum (126 MHz, CDCl₃) of compound **5m** (Chapter 2).

GGX592.11.fid
GGX592/CDCl₃/1H
Fuchs 20221219_06
Proton_IPB CDCl₃ /opt/nmrdata/2020/GGX walkup 12

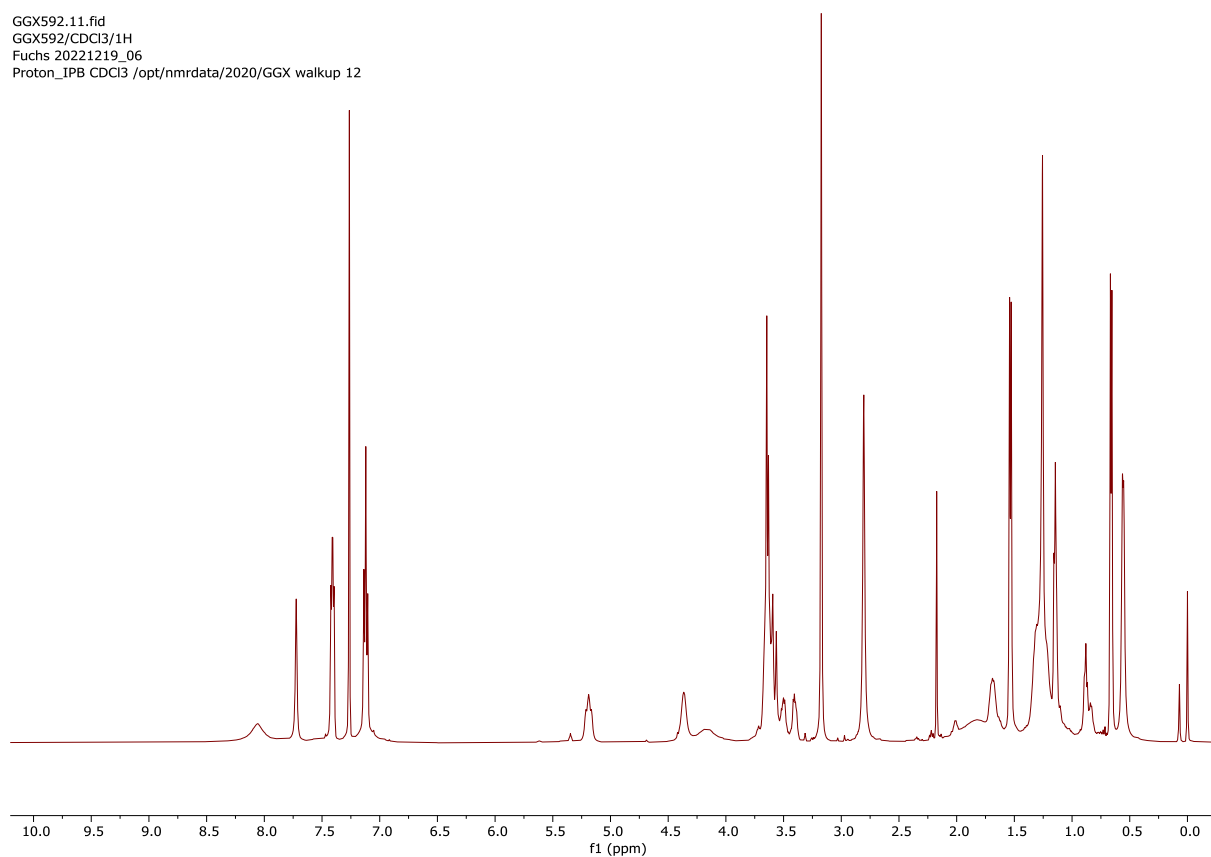


Figure 60: ¹H NMR spectrum (500 MHz, CDCl₃) of compound **5n** (Chapter 2).

GGX592.12.fid
GGX592/CDCl₃/13C
Fuchs 20221219_06
Carbon_dec_IPB CDCl₃ /opt/nmrdata/2020/GGX walkup 12

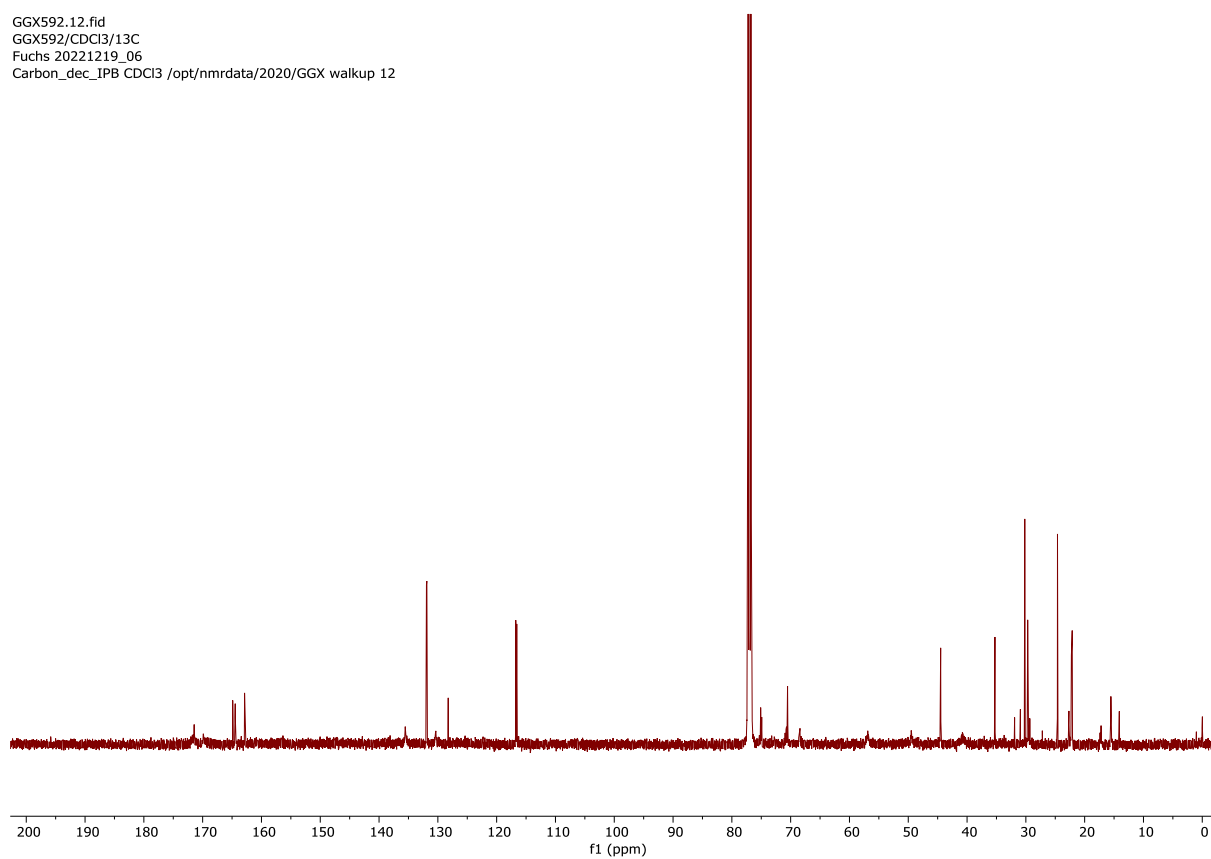


Figure 61: ¹³C NMR spectrum (126 MHz, CDCl₃) of compound **5n** (Chapter 2).

GGX599_PROTON_02
GGX599/CDCl₃/1H
Fuchs 20221219_09
Tue Dec 20 03:51 2022

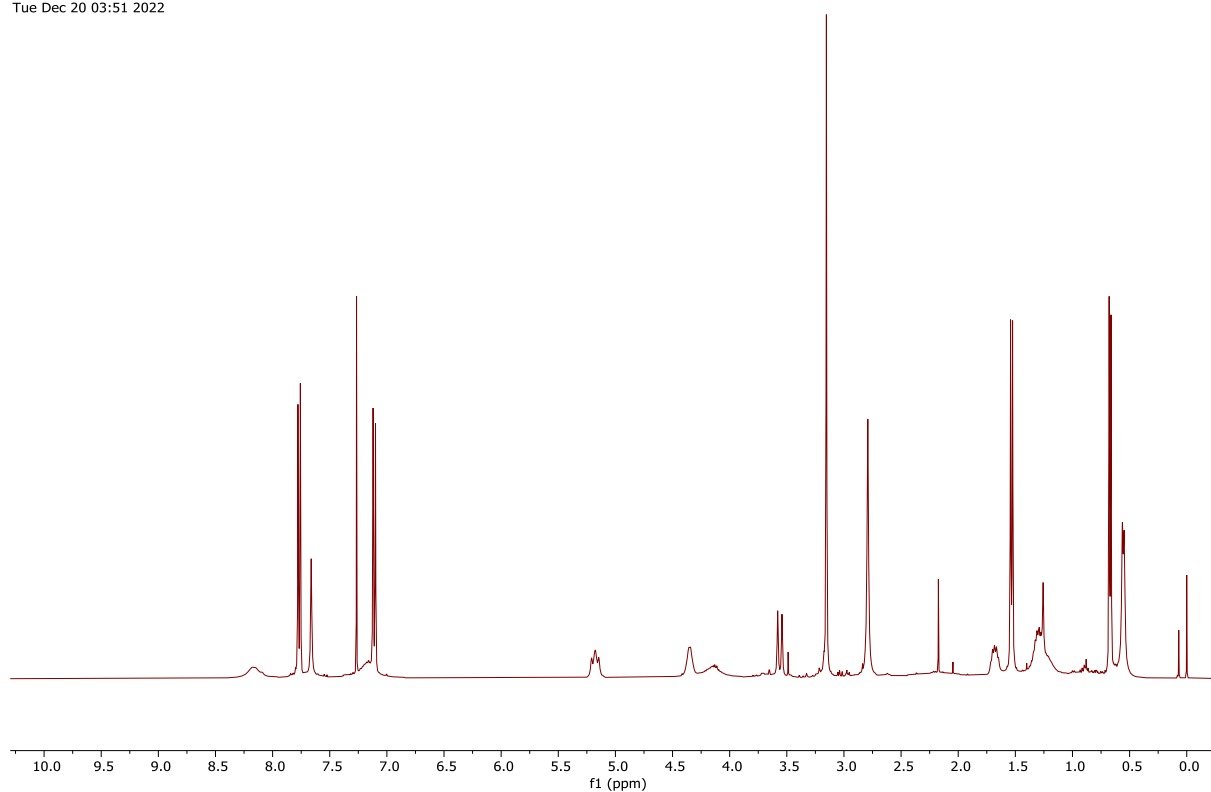


Figure 62: ¹H NMR spectrum (400 MHz, CDCl₃) of compound **5o** (Chapter 2).

GGX599_CARBON_01
GGX599/CDCl₃/13C
Fuchs 20221219_09
Tue Dec 20 03:54 2022

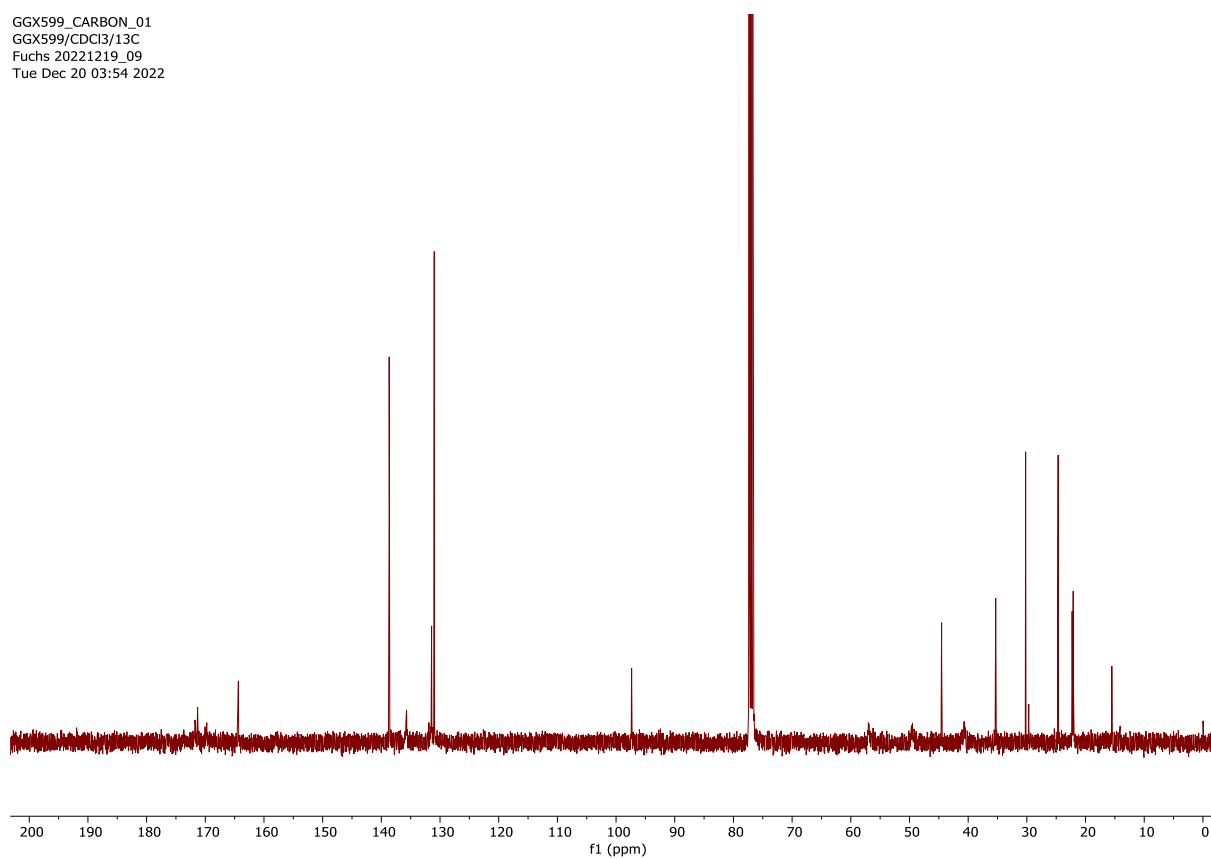


Figure 63: ¹³C NMR spectrum (101 MHz, CDCl₃) of compound **5o** (Chapter 2).

GGX605.11.fid
GGX605/CDCl₃/1H
Fuchs 20221220_02
Proton_IPB CDCl₃ /opt/nmrdata/2020/GGX walkup 14

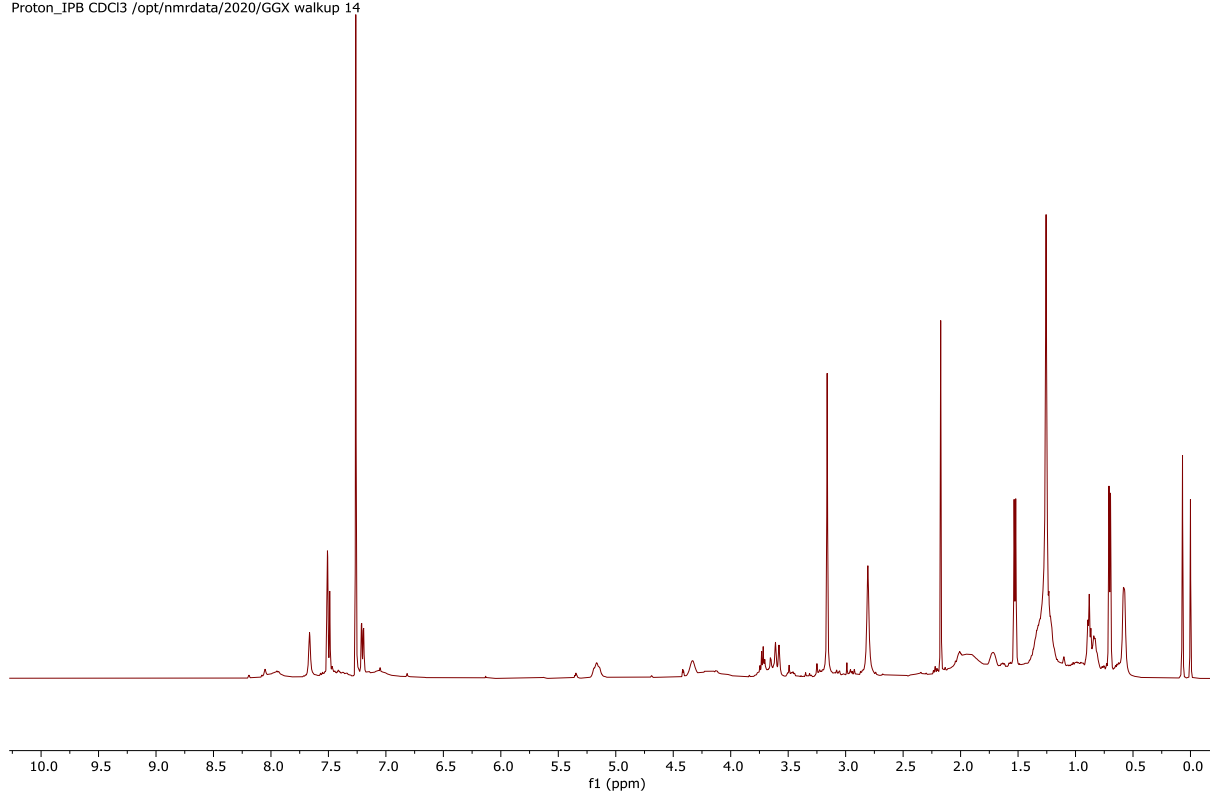


Figure 64: ¹H NMR spectrum (500 MHz, CDCl₃) of compound **5p** (Chapter 2).

GGX605.12.fid
GGX605/CDCl₃/13C
Fuchs 20221220_02
Carbon_dec_IPB CDCl₃ /opt/nmrdata/2020/GGX walkup 14

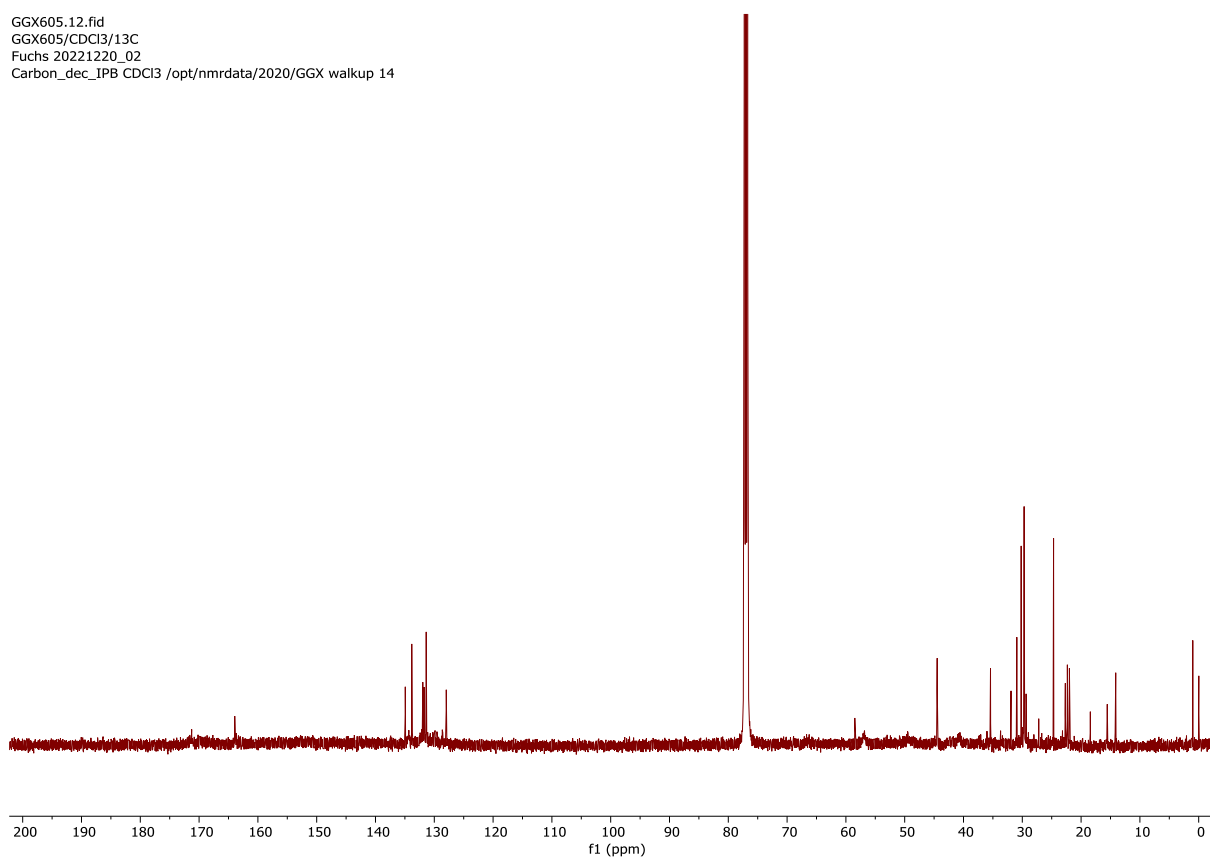


Figure 65: ¹³C NMR spectrum (126 MHz, CDCl₃) of compound **5p** (Chapter 2).

GGX611.11.fid
GGX611/CDCl₃/1H
Fuchs 20221220_04
Proton_IPB CDCl₃ /opt/nmrdata/2020/GGX walkup 16

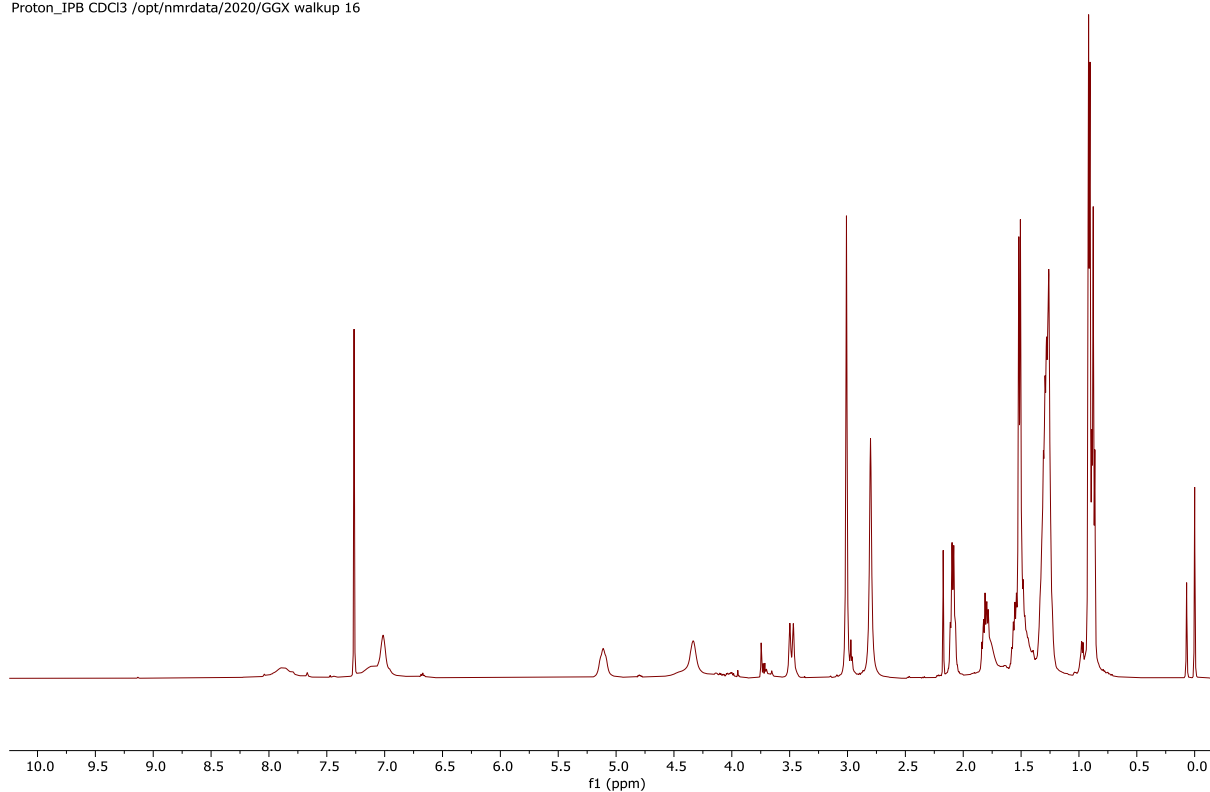


Figure 66: ¹H NMR spectrum (500 MHz, CDCl₃) of compound **5q** (Chapter 2).

GGX611.12.fid
GGX611/CDCl₃/13C
Fuchs 20221220_04
Carbon_dec_IPB CDCl₃ /opt/nmrdata/2020/GGX walkup 16

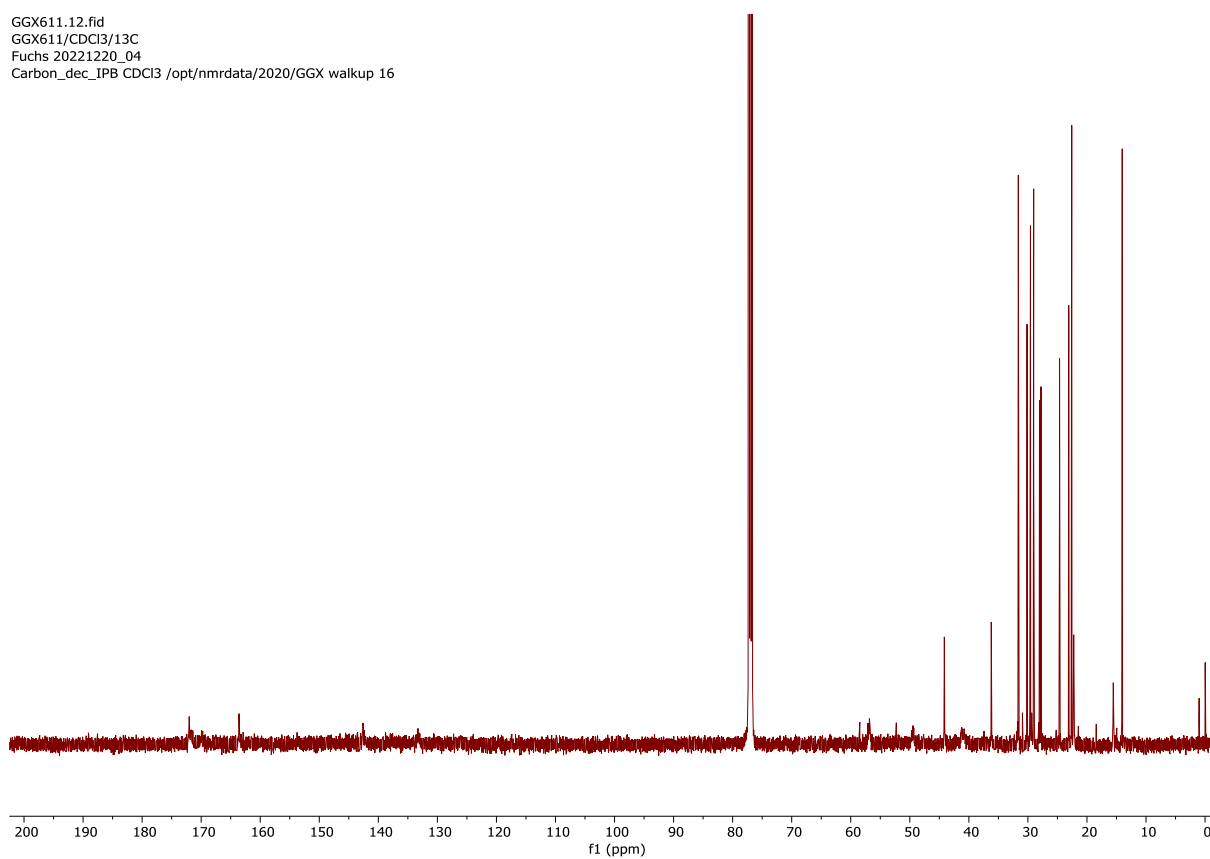


Figure 67: ¹³C NMR spectrum (126 MHz, CDCl₃) of compound **5q** (Chapter 2).

GGX629_PROTON_01
GGX629/CDCl₃/1H
Fuchs 20221220_07
Tue Dec 20 09:28 2022

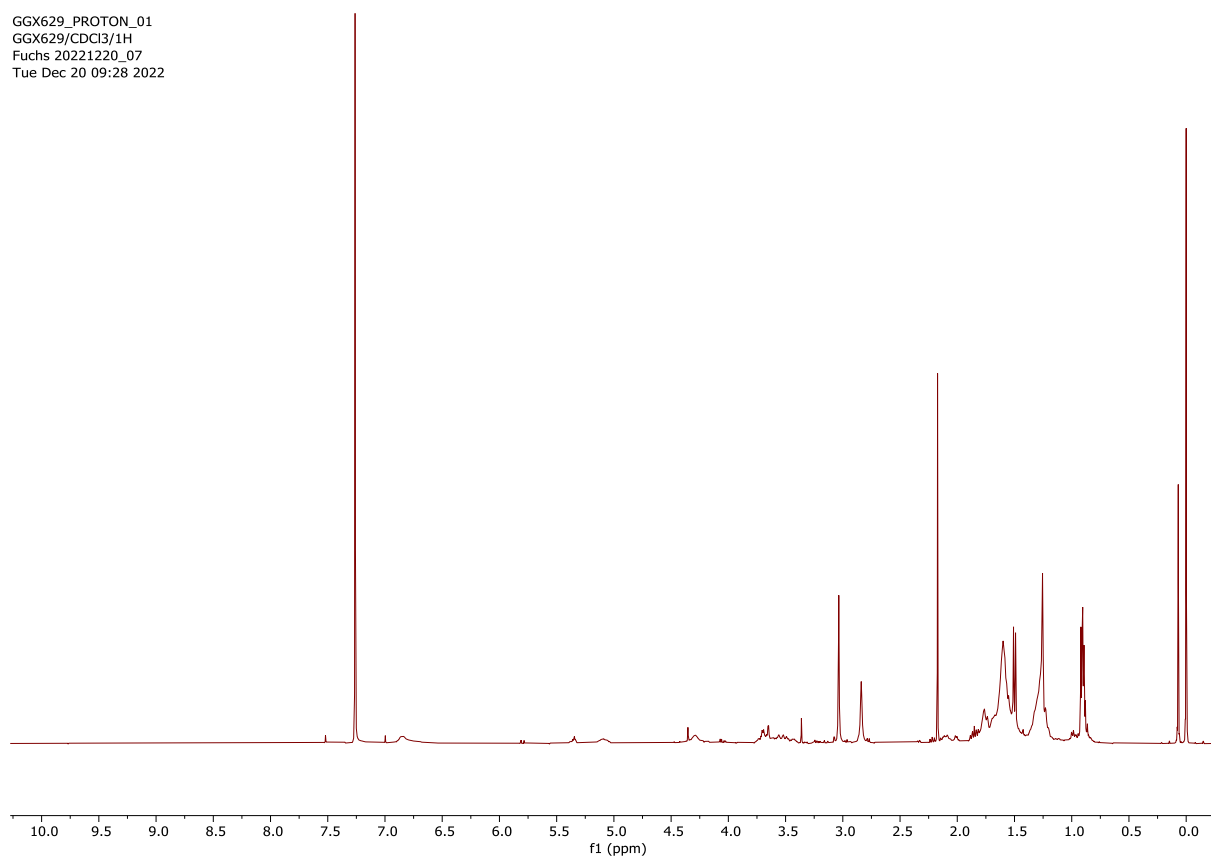


Figure 68: ¹H NMR spectrum (400 MHz, CDCl₃) of compound **5r** (Chapter 2).

GGX596_PROTON_02
GGX596/CDCl₃/1H
Fuchs 20221219_08
Mon Dec 19 17:26 2022

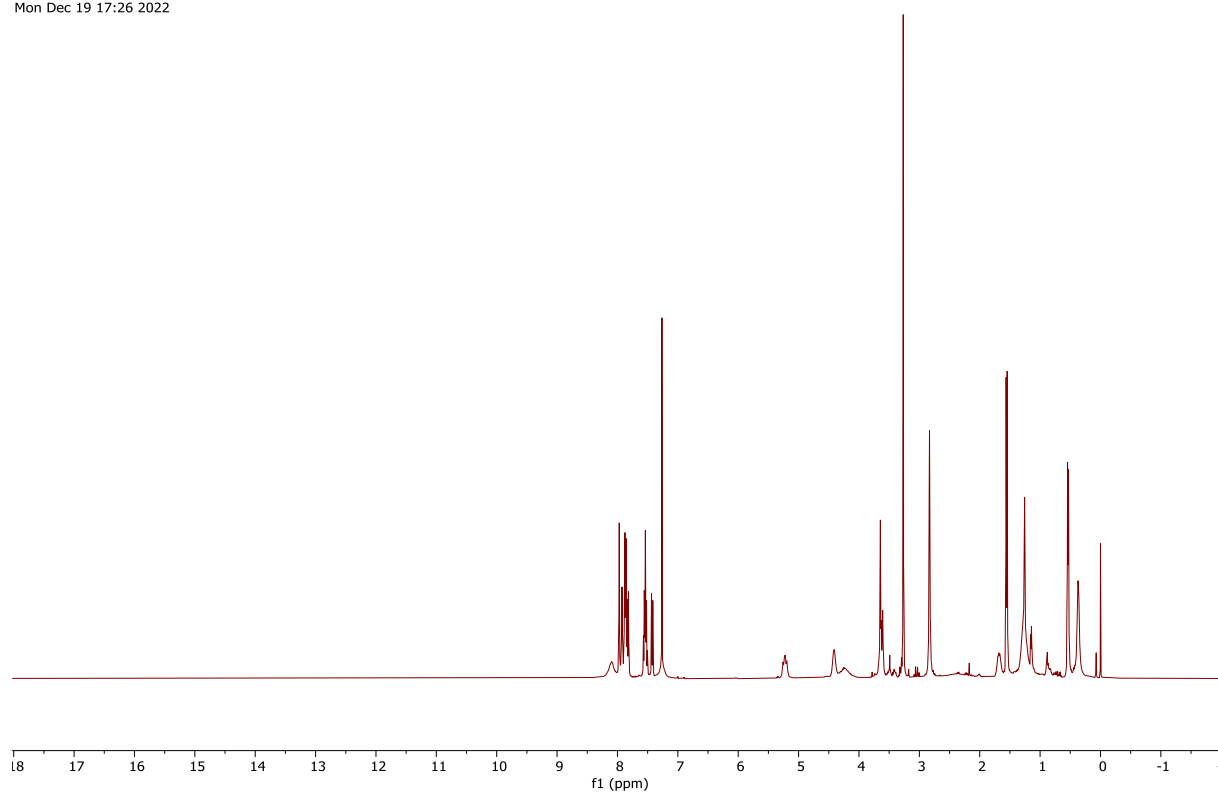


Figure 69: ¹H NMR spectrum (400 MHz, CDCl₃) of compound 5s (Chapter 2).

GGX596_CARBON_01
GGX596/CDCl₃/13C
Fuchs 20221219_08
Mon Dec 19 22:48 2022

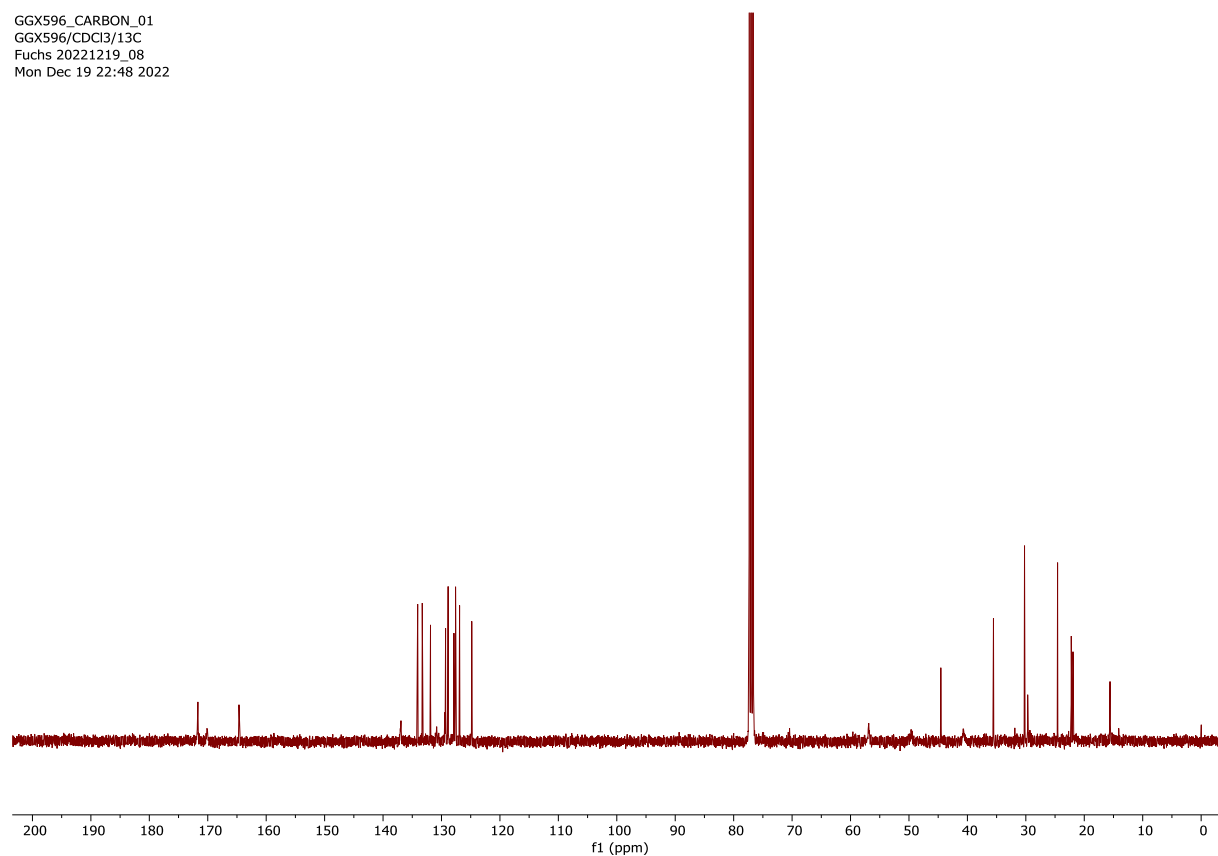


Figure 70: ¹³C NMR spectrum (101 MHz, CDCl₃) of compound 5s (Chapter 2).

630_Proton
GGX630/CDCl₃/1H
Kappen 20230901_01
Fri Sep 1 12:57 2023

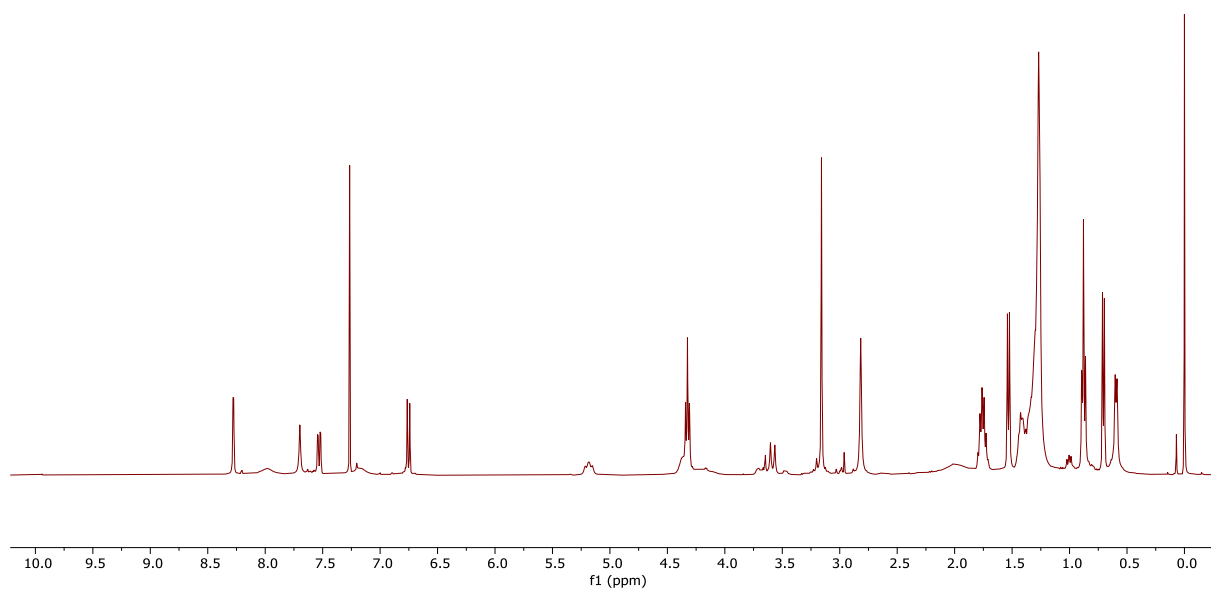


Figure 71: ¹H NMR spectrum (500 MHz, CDCl₃) of compound **5t** (Chapter 2).

630_Carbon
GGX630/CDCl₃/13C
Kappen 20230901_01
Fri Sep 1 20:11 2023

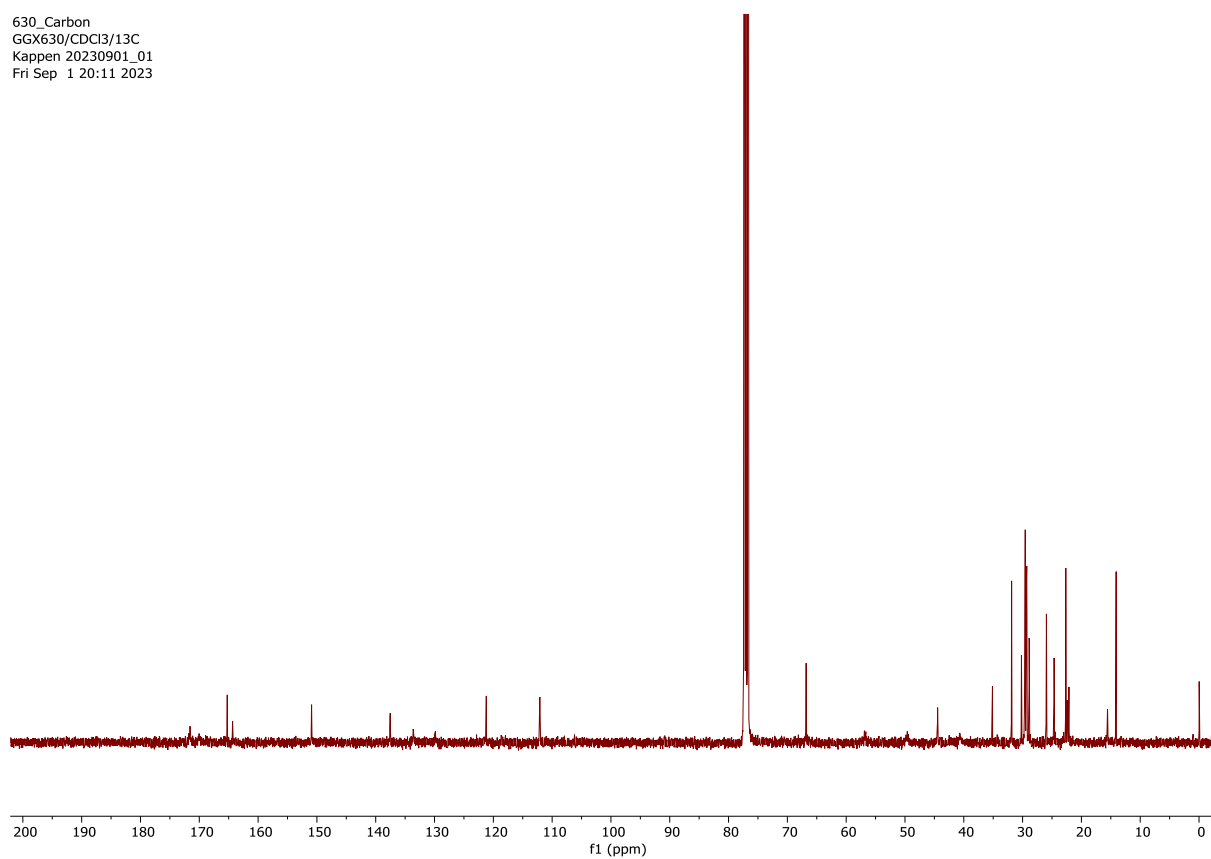


Figure 72: ¹³C NMR spectrum (126 MHz, CDCl₃) of compound **5t** (Chapter 2).

GGX402_PROTON_01
GGX402/DMSO-d6/1H
Fuchs 20201214_07
Mon Dec 14 16:19 2020

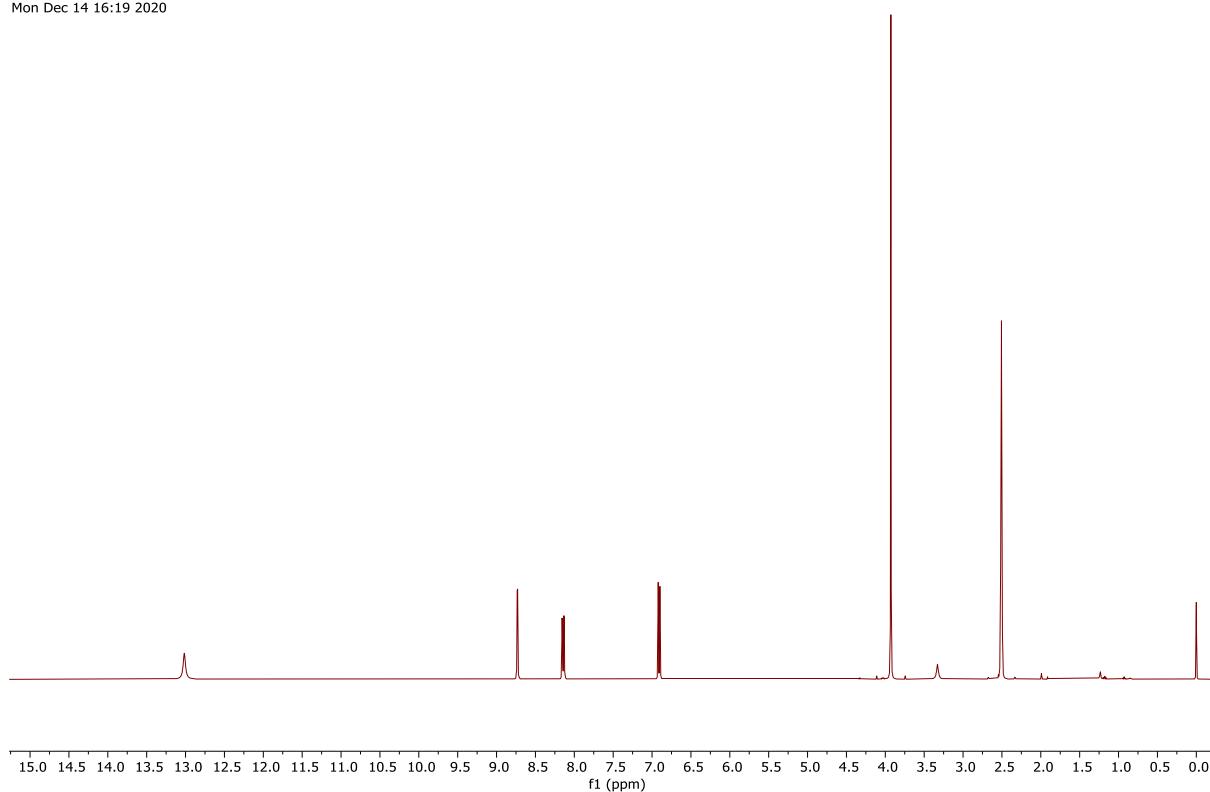


Figure 73: ¹H NMR spectrum (400 MHz, (CD₃)₂SO) of compound **1** (Chapter 3).

GGX402_CARBON_01
GGX402/DMSO-d6/13C
Fuchs 20201214_07
Tue Dec 15 13:41 2020

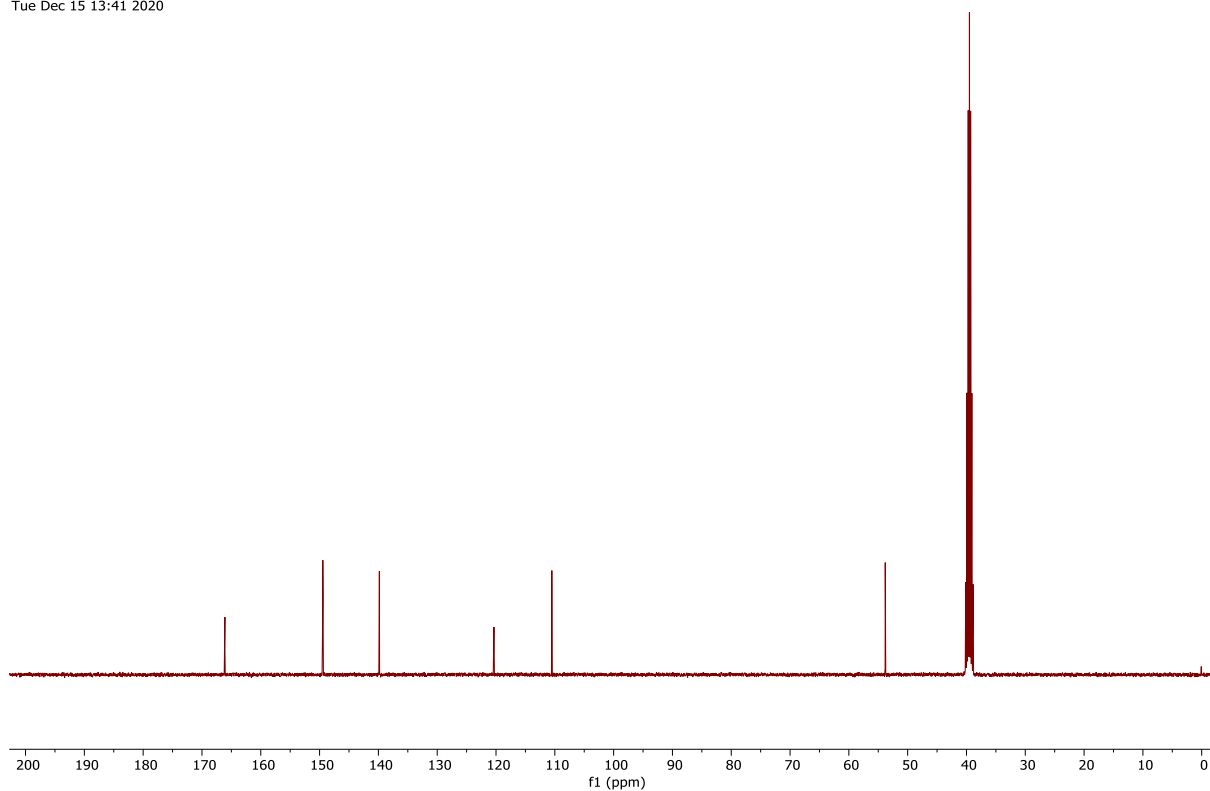


Figure 74: ¹³C NMR spectrum (101 MHz, (CD₃)₂SO) of compound **1** (Chapter 3).

GGX404_PROTON_01
GGX404/DMSO-d6/1H
Fuchs 20201215_06
Tue Dec 15 13:34 2020

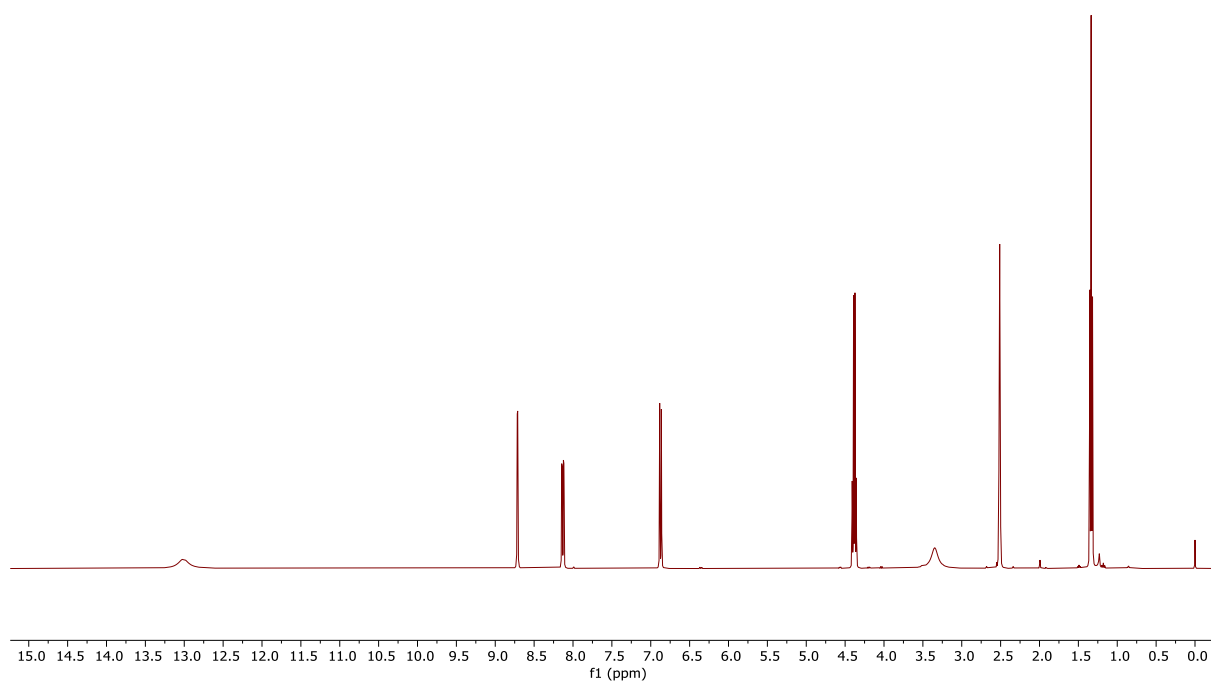


Figure 75: ¹H NMR spectrum (400 MHz, (CD₃)₂SO) of compound **2** (Chapter 3).

GGX404_CARBON_01
GGX404/DMSO-d6/13C
Fuchs 20201215_06
Tue Dec 15 15:34 2020

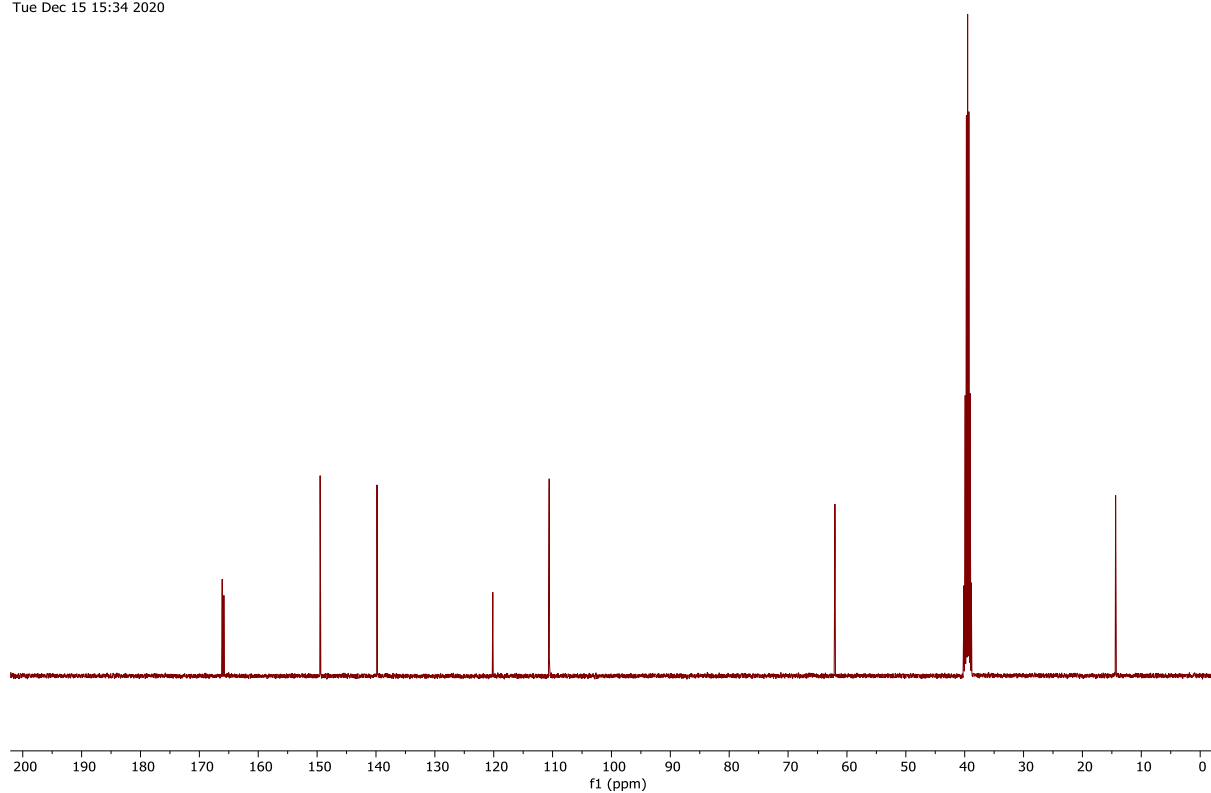


Figure 76: ¹³C NMR spectrum (101 MHz, (CD₃)₂SO) of compound **2** (Chapter 3).

GGX400_dmso_PROTON_01
GGX400_dmso/DMSO-d6/1H
Fuchs 20201211_05
Fri Dec 11 15:25 2020

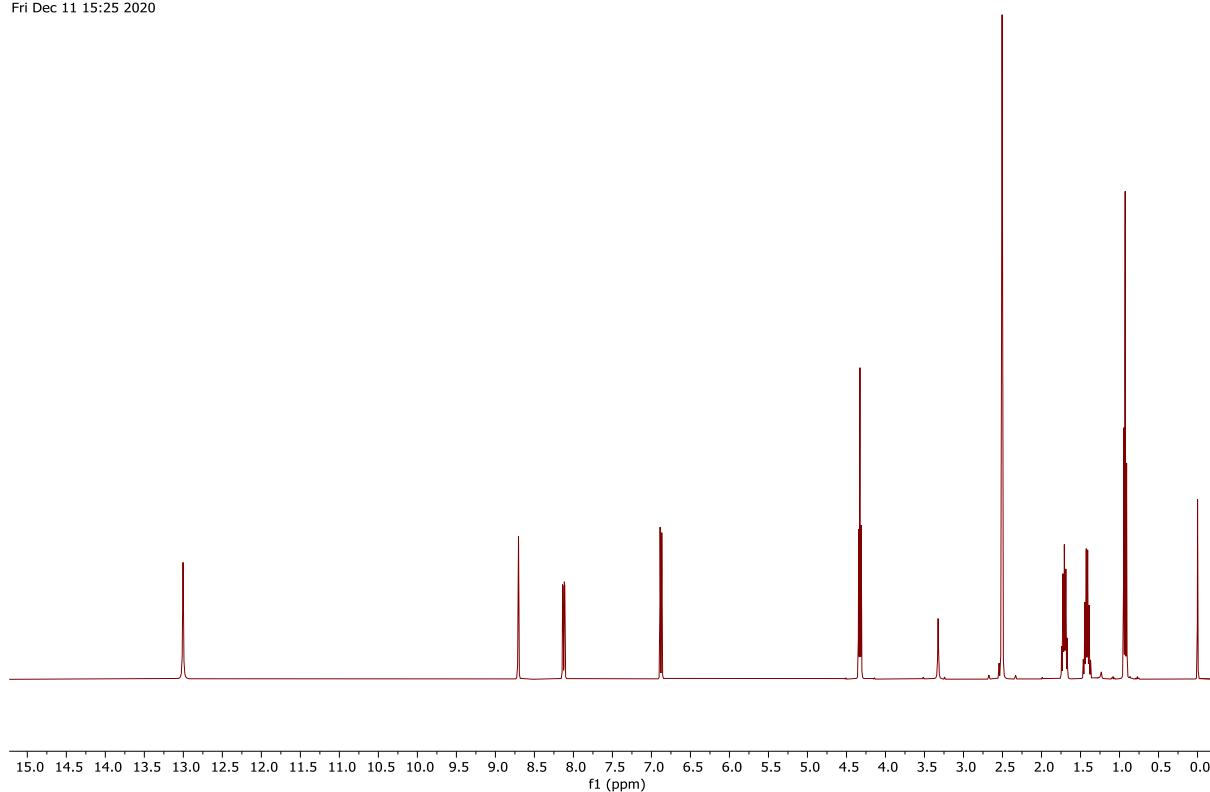


Figure 77: ¹H NMR spectrum (400 MHz, (CD₃)₂SO) of compound **3** (Chapter 3).

GGX400_dmso_CARBON_01
GGX400_dmso/DMSO-d6/13C
Fuchs 20201211_05
Fri Dec 11 17:21 2020

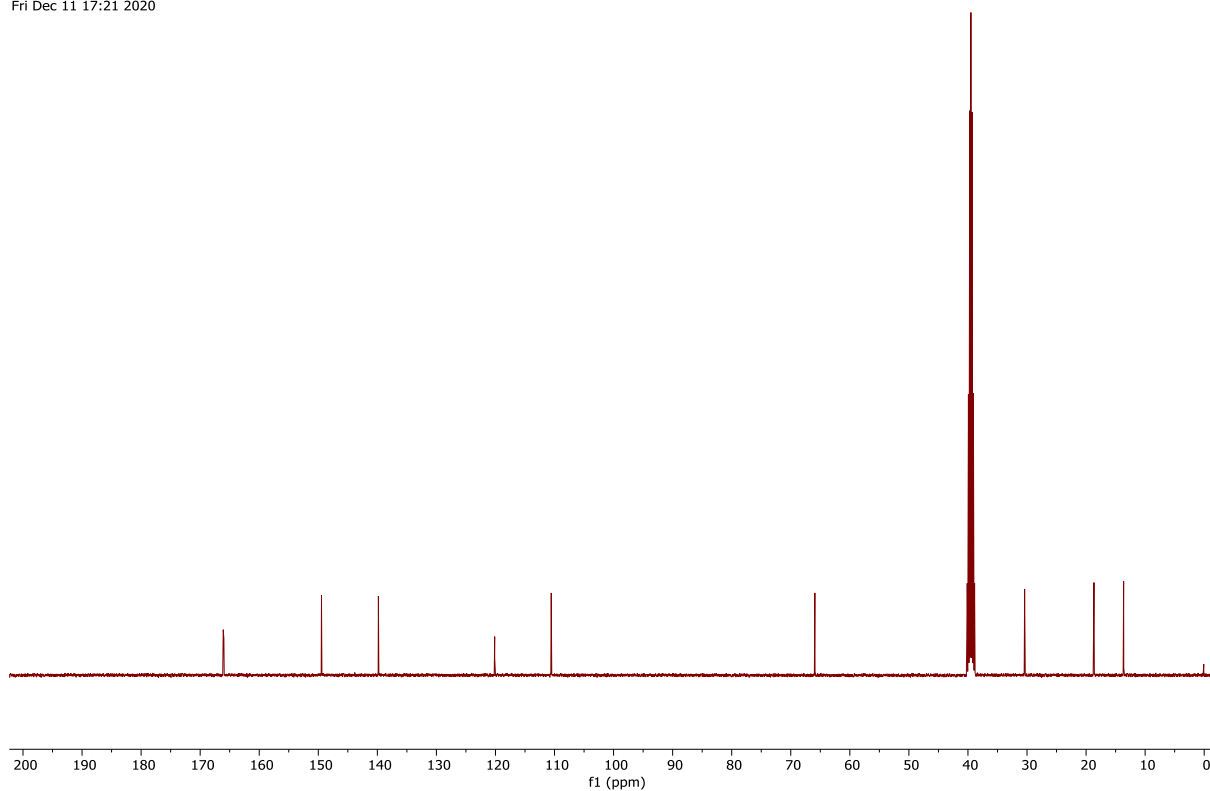


Figure 78: ¹³C NMR spectrum (101 MHz, (CD₃)₂SO) of compound **3** (Chapter 3).

GGX510_PROTON_01
GGX510/DMSO-d6/1H
Fuchs 20211111_02
Thu Nov 11 16:38 2021

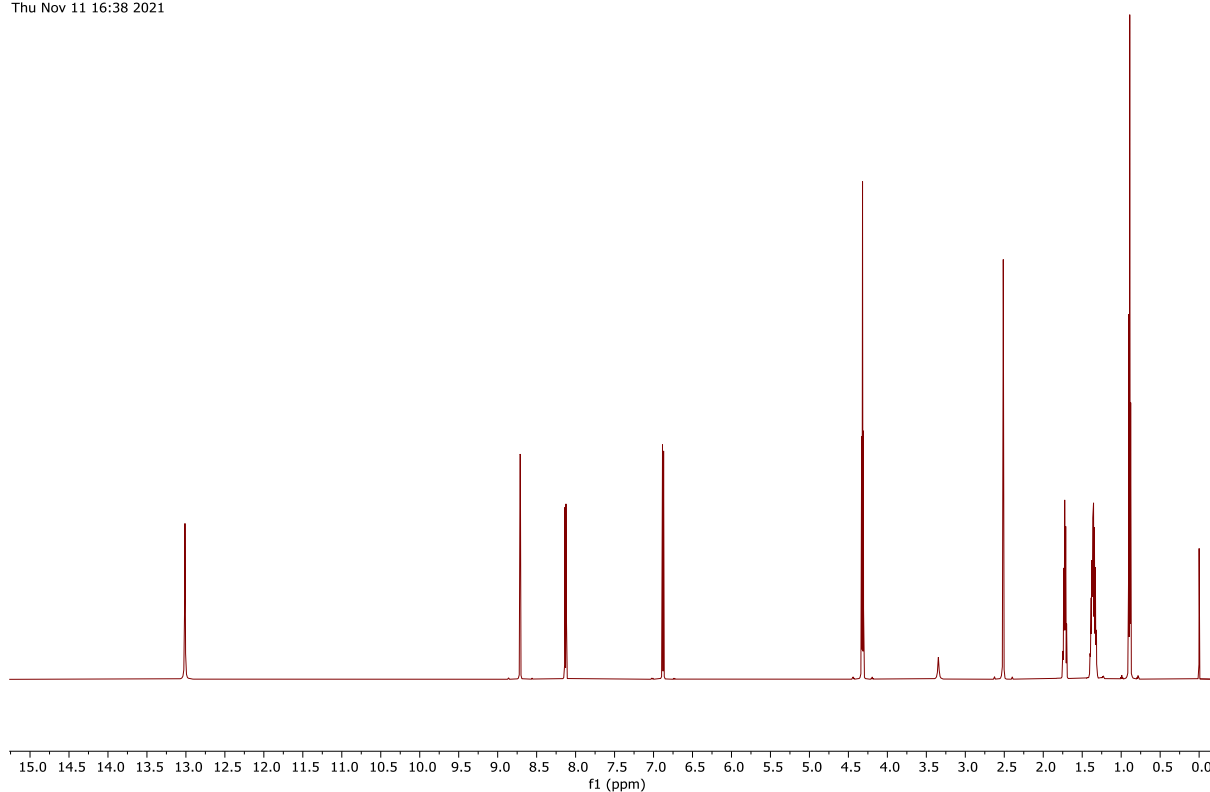


Figure 79: ¹H NMR spectrum (400 MHz, (CD₃)₂SO) of compound **4** (Chapter 3).

GGX510_CARBON_01
GGX510/DMSO-d6/13C
Fuchs 20211111_02
Thu Nov 11 16:42 2021

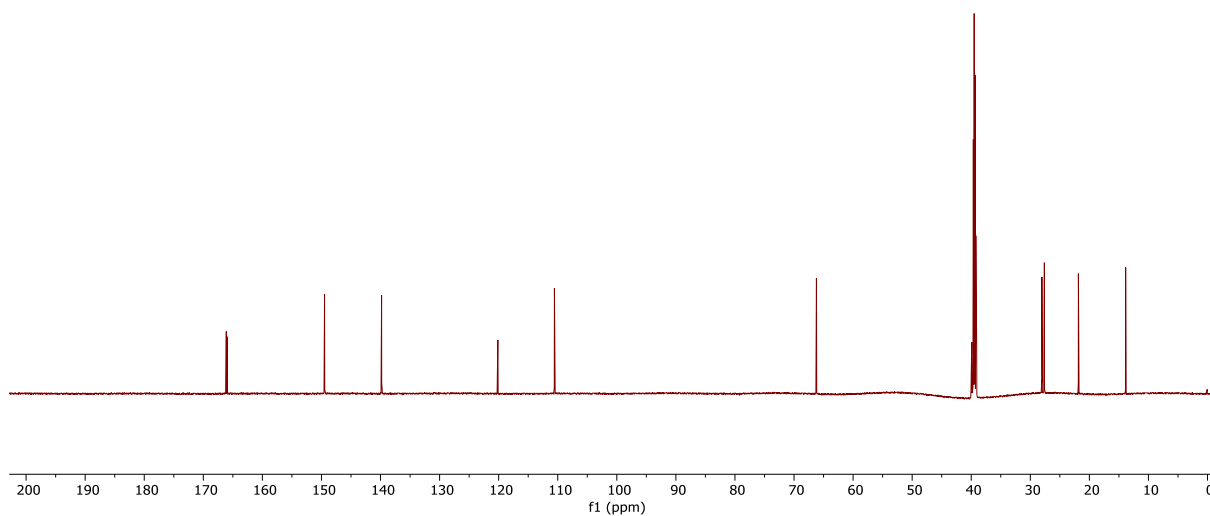


Figure 80: ¹³C NMR spectrum (101 MHz, (CD₃)₂SO) of compound **4** (Chapter 3).

GGX403_PROTON_01
GGX403/DMSO-d6/1H
Fuchs 20201214_04
Mon Dec 14 16:02 2020

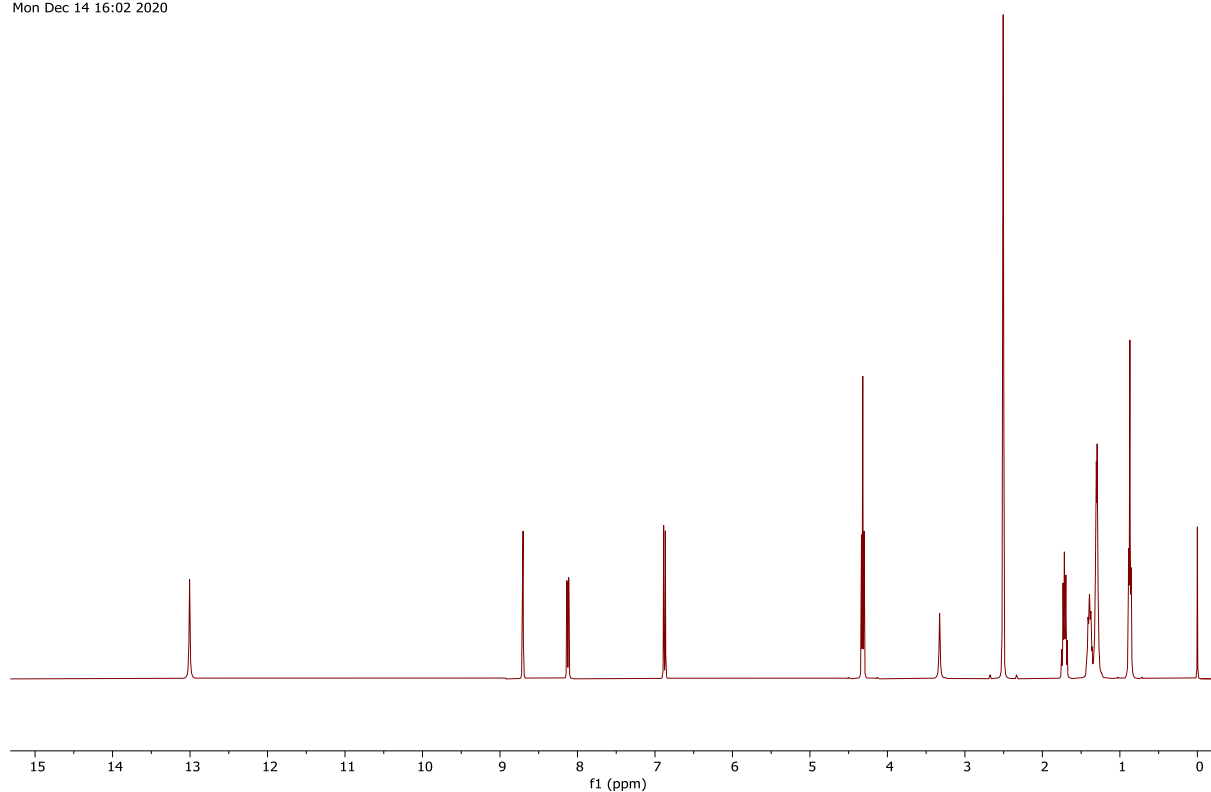


Figure 81: ¹H NMR spectrum (400 MHz, (CD₃)₂SO) of compound **5** (Chapter 3).

GGX403_CARBON_01
GGX403/DMSO-d6/13C
Fuchs 20201214_04
Tue Dec 15 11:43 2020

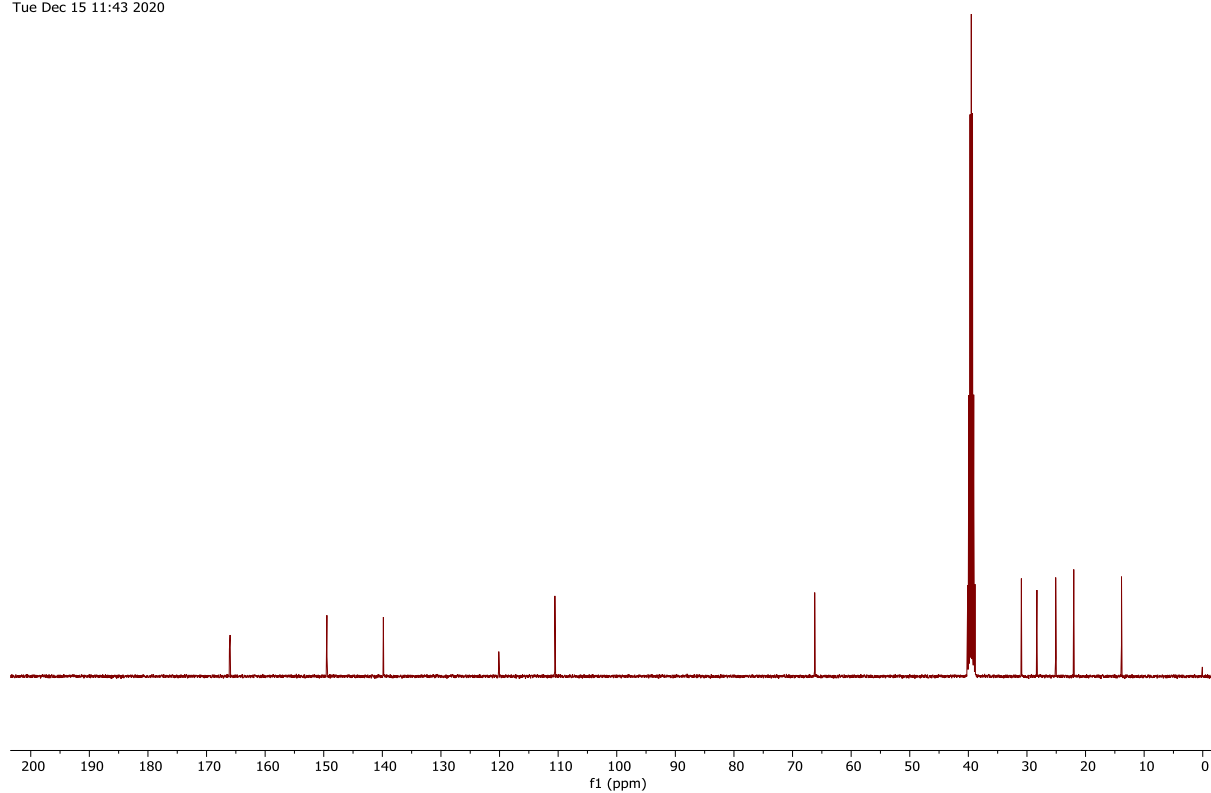


Figure 82: ¹³C NMR spectrum (101 MHz, (CD₃)₂SO) of compound **5** (Chapter 3).

GGX511_PROTON_01
GGX511/DMSO-d6/1H
Fuchs 20211112_03
Fri Nov 12 12:03 2021

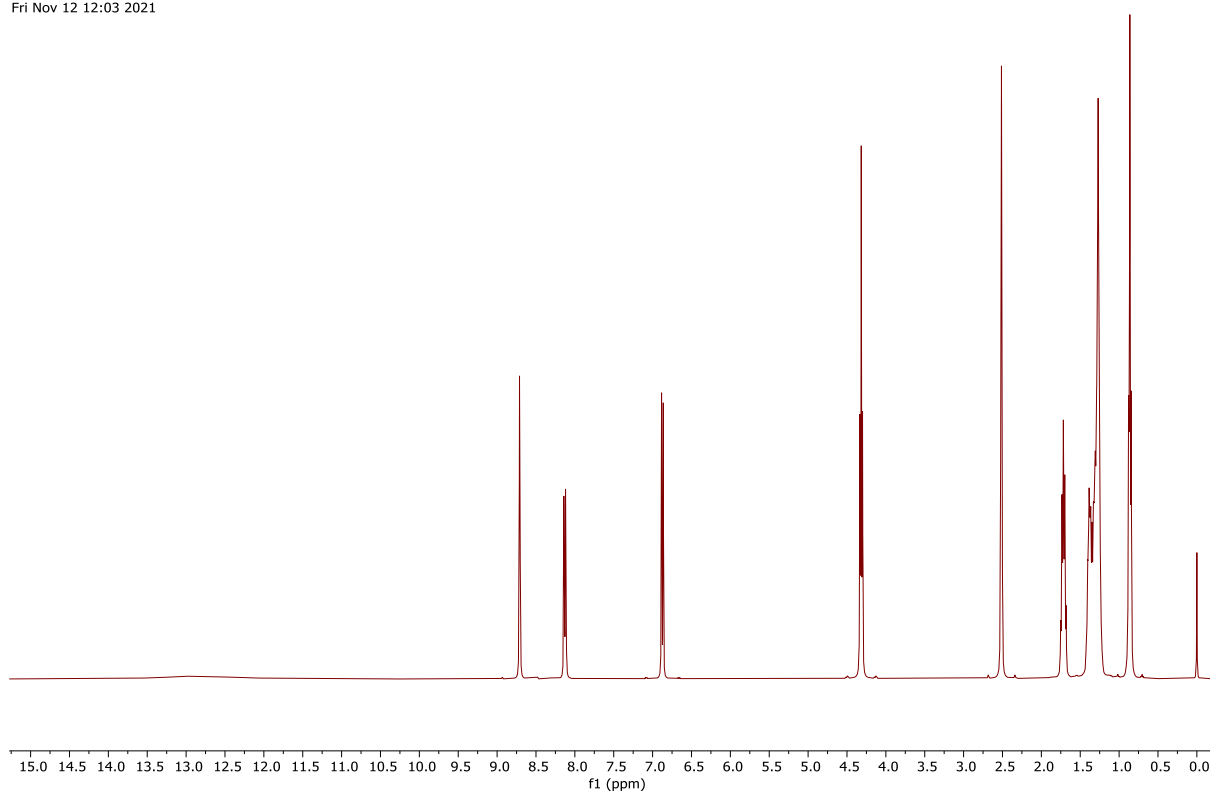


Figure 83: ¹H NMR spectrum (400 MHz, (CD₃)₂SO) of compound **6** (Chapter 3).

GGX511_CARBON_01
GGX511/DMSO-d6/13C
Fuchs 20211112_03
Fri Nov 12 12:06 2021

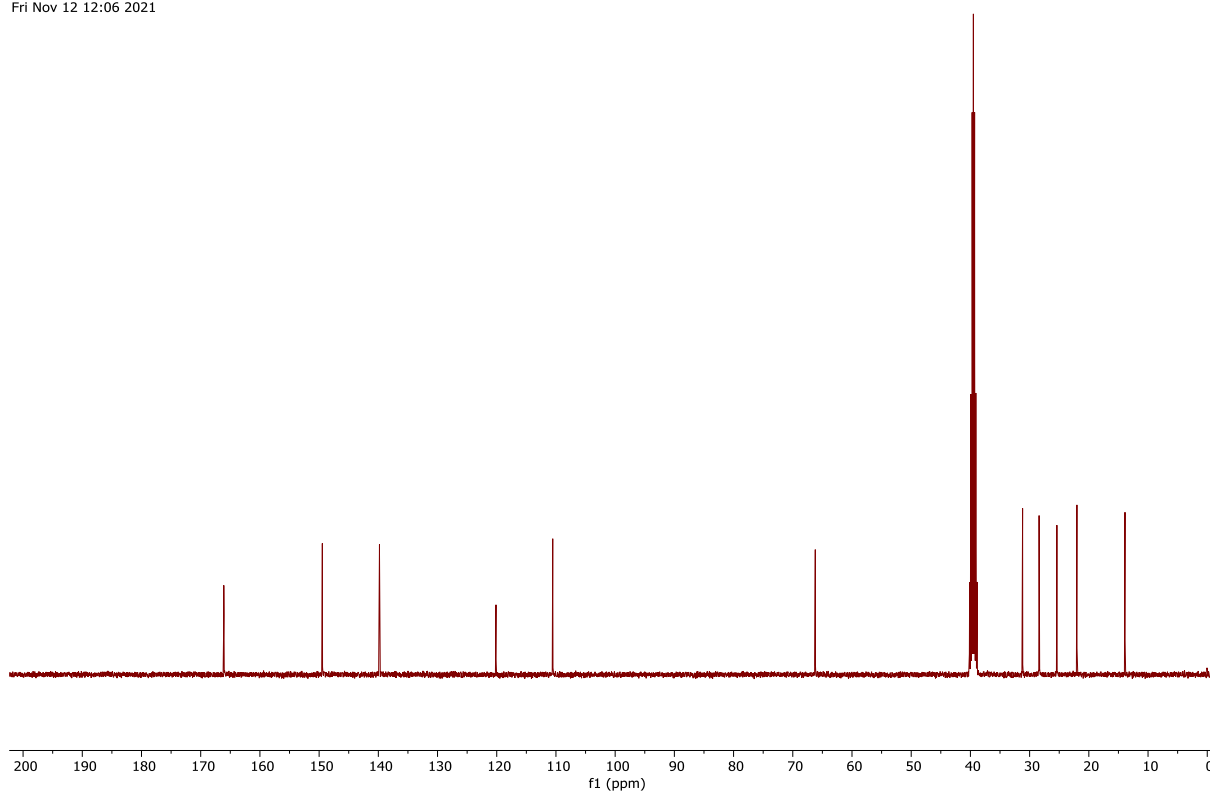


Figure 84: ¹³C NMR spectrum (101 MHz, (CD₃)₂SO) of compound **6** (Chapter 3).

GGX401_PROTON_01
GGX401/DMSO-d6/1H
Fuchs 20201211_04
Fri Dec 11 15:19 2020

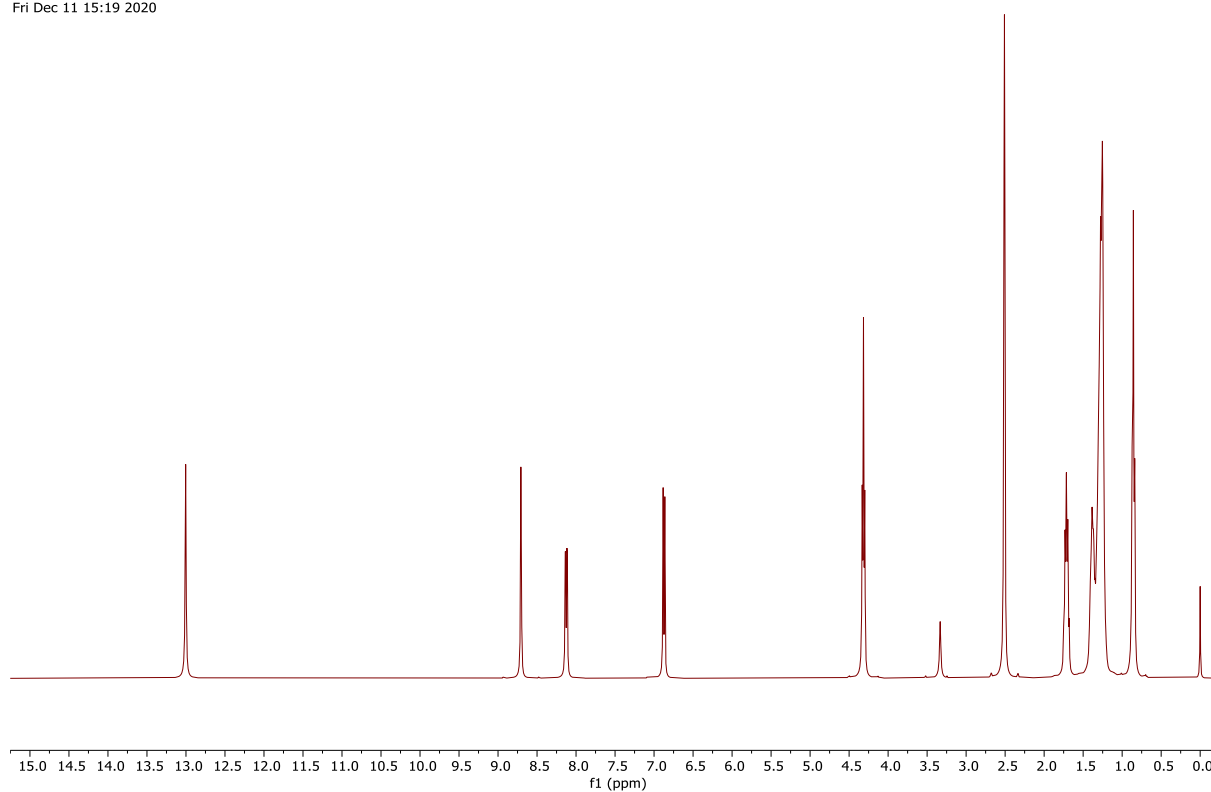


Figure 85: ¹H NMR spectrum (400 MHz, (CD₃)₂SO) of compound **7** (Chapter 3).

GGX401_CARBON_01
GGX401/DMSO-d6/13C
Fuchs 20201211_04
Fri Dec 11 15:37 2020

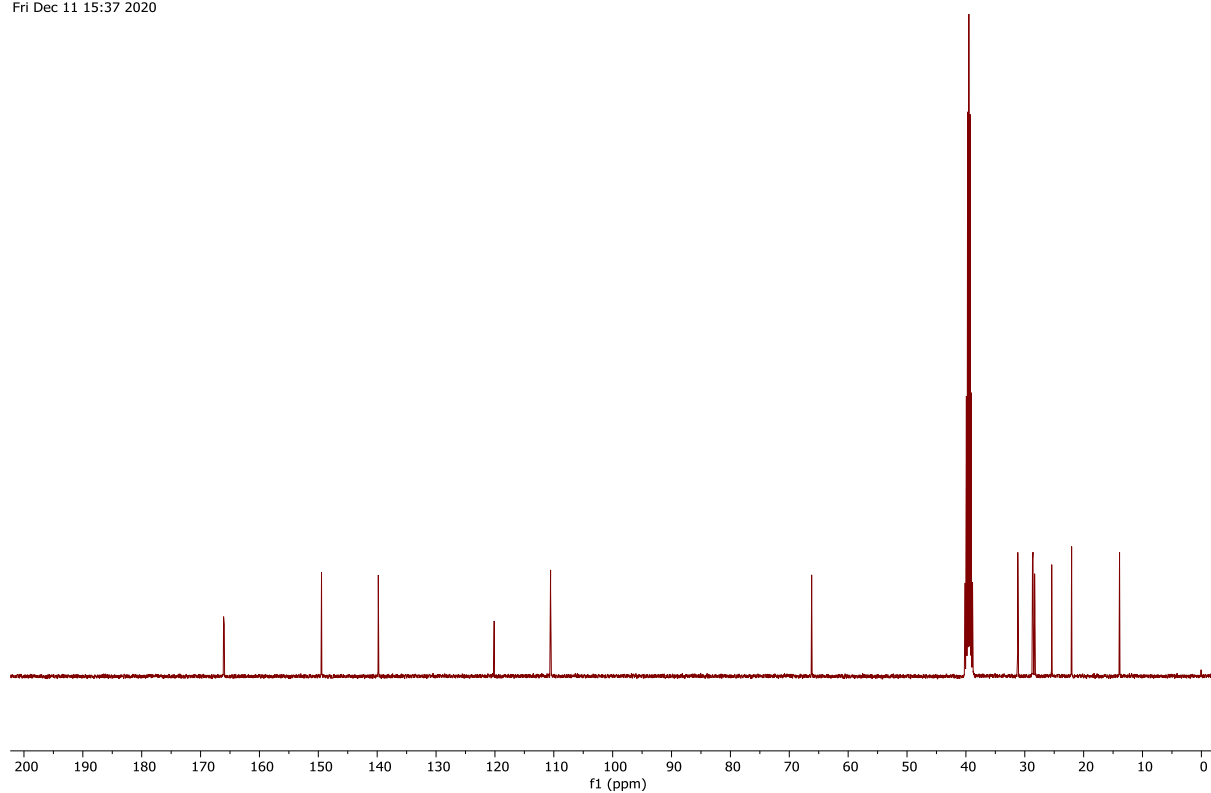


Figure 86: ¹³C NMR spectrum (101 MHz, (CD₃)₂SO) of compound **7** (Chapter 3).

GGX517_PROTON_01
GGX517/DMSO-d6/1H
Fuchs 20211201_03
Wed Dec 1 11:24 2021

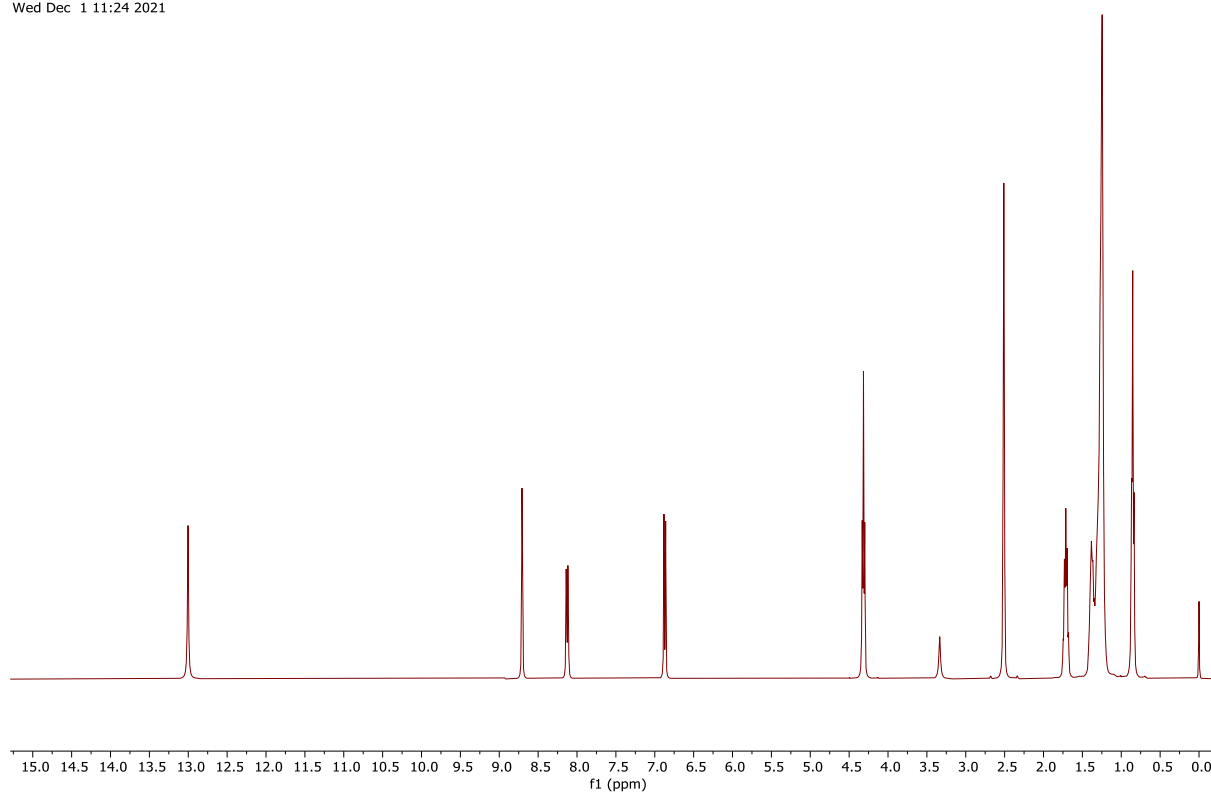


Figure 87: ¹H NMR spectrum (400 MHz, (CD₃)₂SO) of compound **8** (Chapter 3).

GGX517_CARBON_01
GGX517/DMSO-d6/13C
Fuchs 20211201_03
Wed Dec 1 12:15 2021

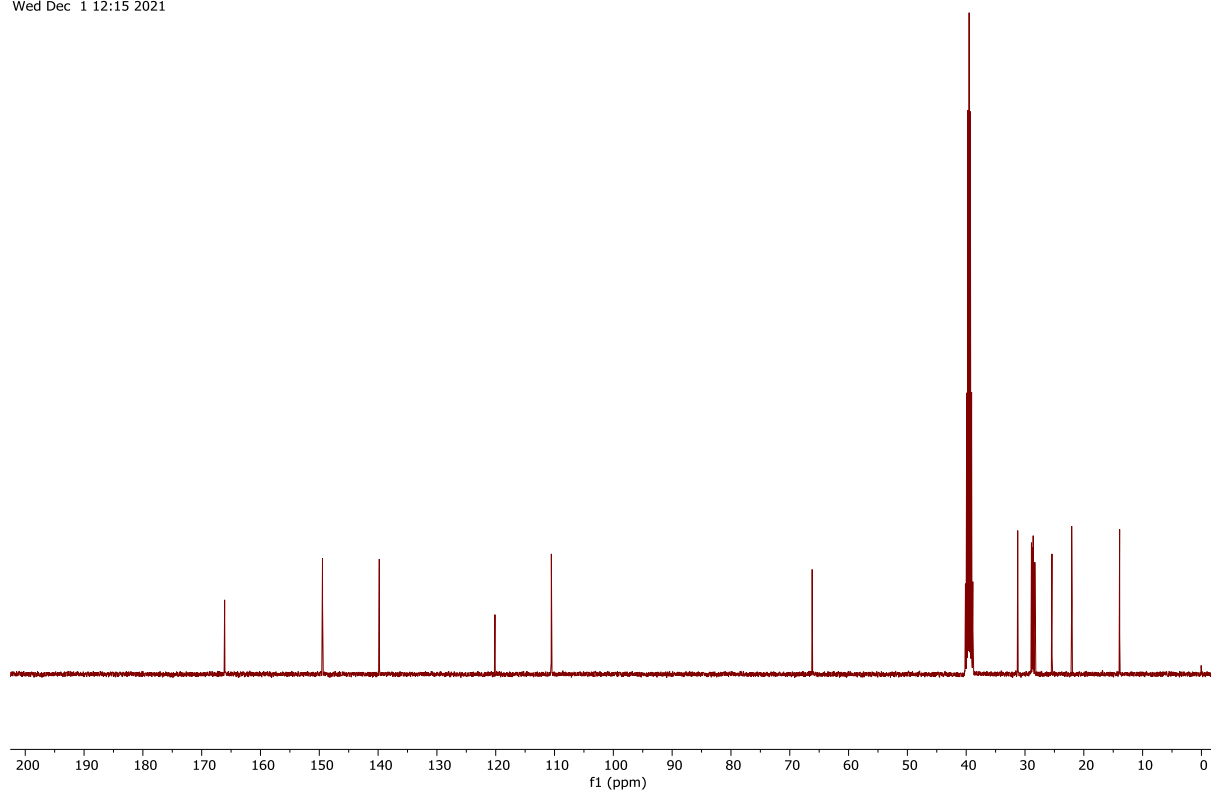


Figure 88: ¹³C NMR spectrum (101 MHz, (CD₃)₂SO) of compound **8** (Chapter 3).

GGX390_PROTON_01
GGX390/DMSO-d6/1H
Fuchs 20201119_08
Thu Nov 19 16:09 2020

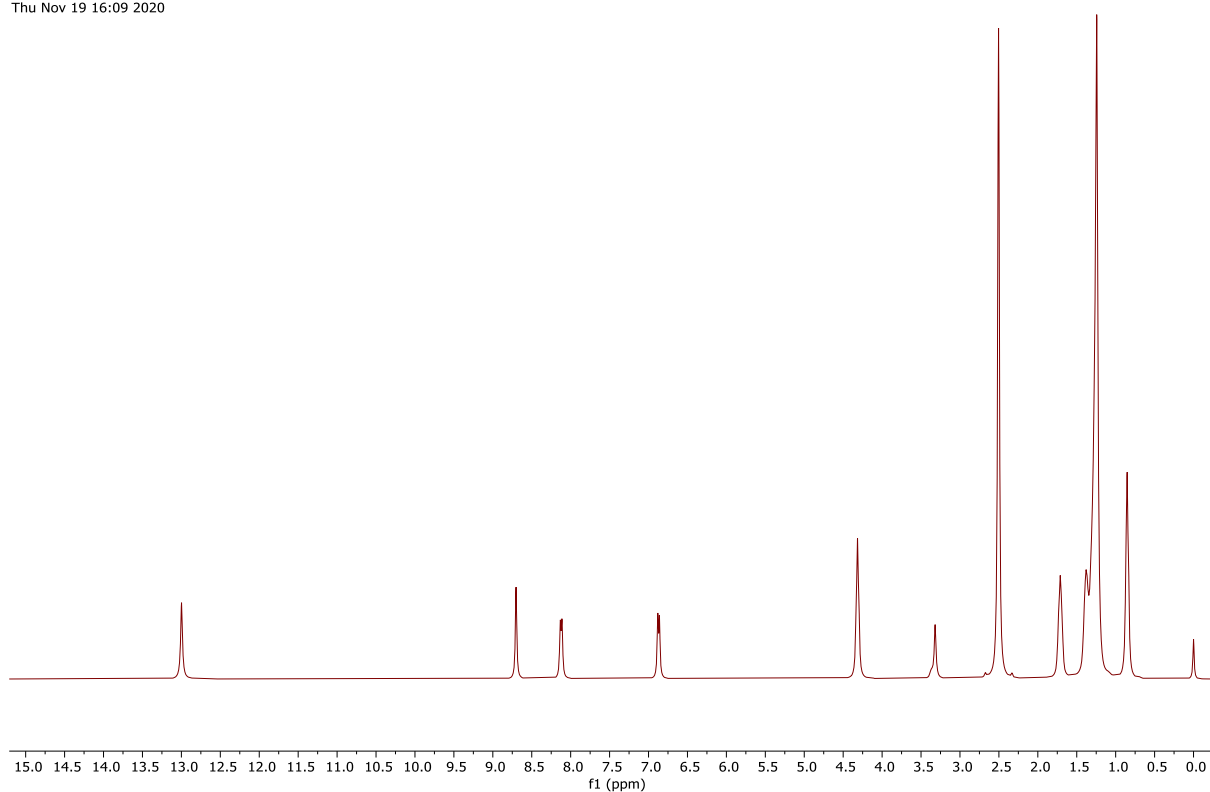


Figure 89: ¹H NMR spectrum (400 MHz, (CD₃)₂SO) of compound **9** (Chapter 3).

GGX390_CARBON_01
GGX390/DMSO-d6/13C
Fuchs 20201119_08
Fri Nov 20 02:52 2020

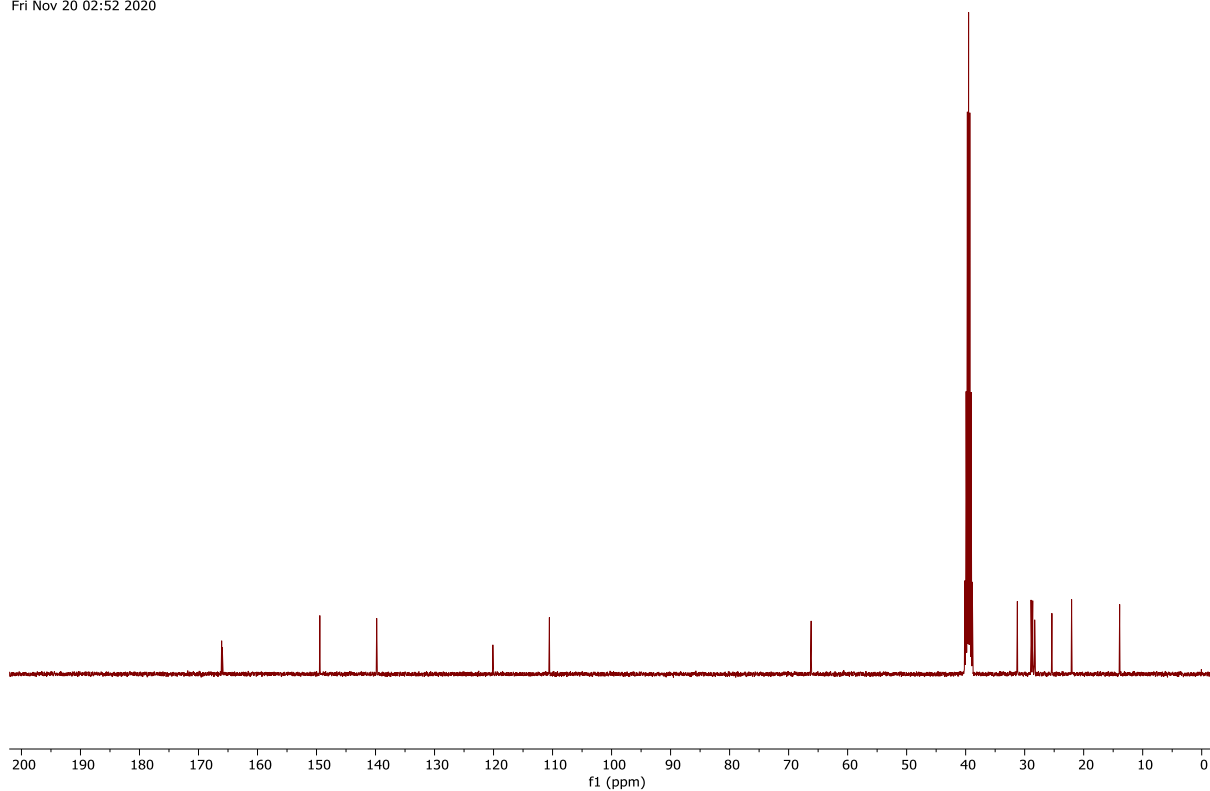


Figure 90: ¹³C NMR spectrum (101 MHz, (CD₃)₂SO) of compound **9** (Chapter 3).

GGX395_PROTON_01
GGX395/DMSO-d6/1H
Fuchs 20210505_01
Wed May 5 11:05 2021

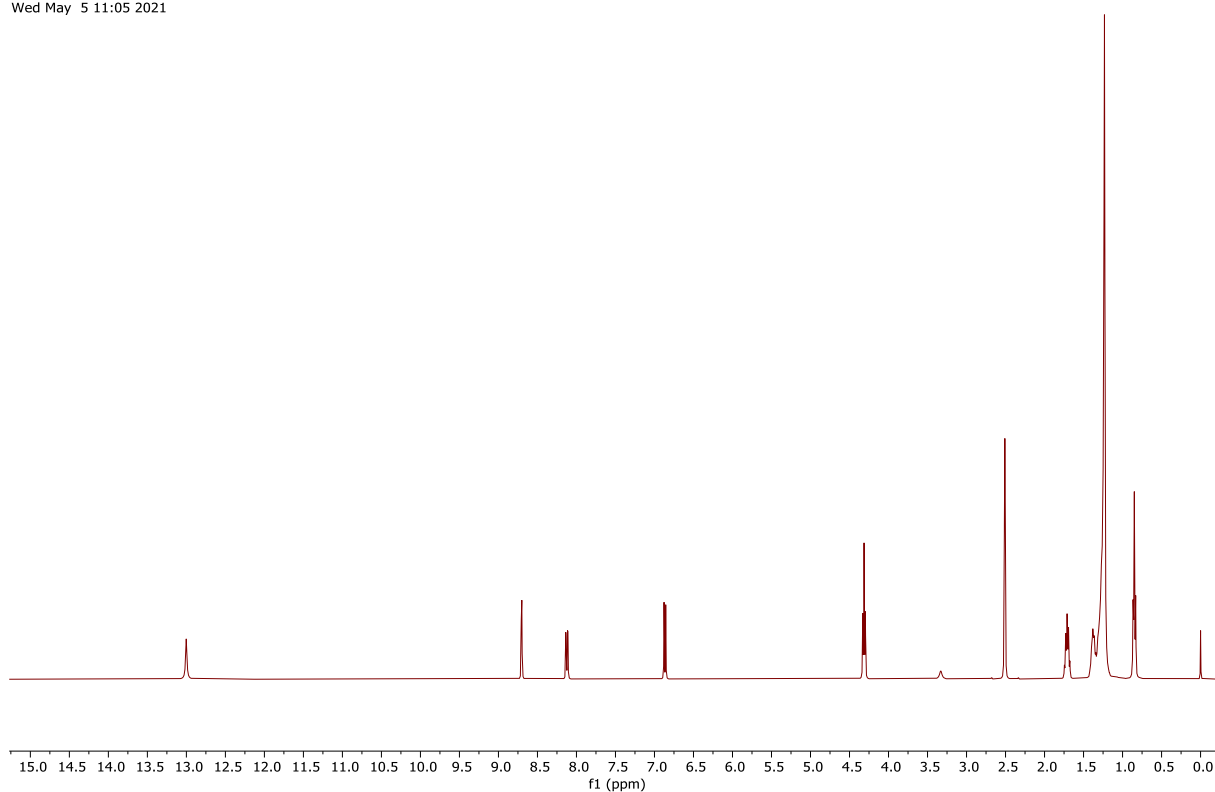


Figure 91: ¹H NMR spectrum (400 MHz, (CD₃)₂SO) of compound **10** (Chapter 3).

GGX395_CARBON_01
GGX395/DMSO-d6/13C
Fuchs 20210505_01
Wed May 5 16:31 2021

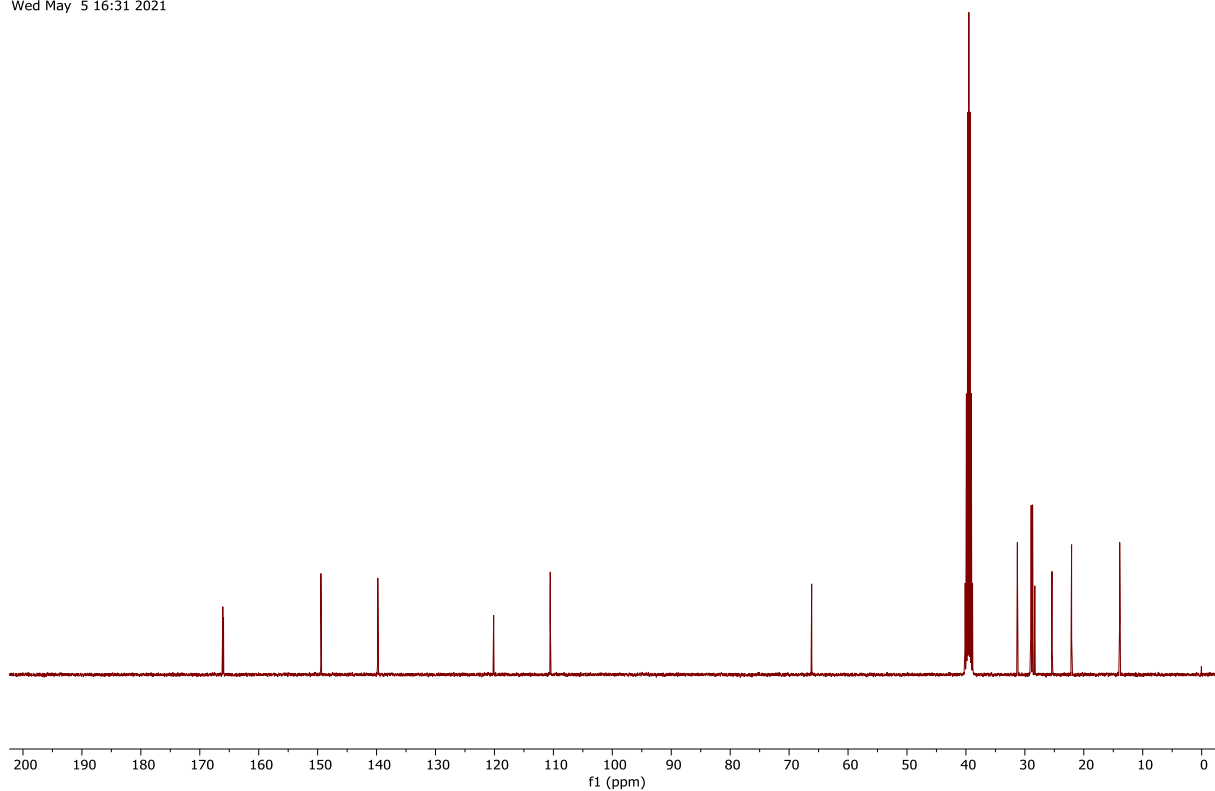


Figure 92: ¹³C NMR spectrum (101 MHz, (CD₃)₂SO) of compound **10** (Chapter 3).

GGX396_Fr2_PROTON_01
GGX396_Fr2/DMSO-d6/1H
Fuchs 20210504_02
Tue May 4 10:09 2021

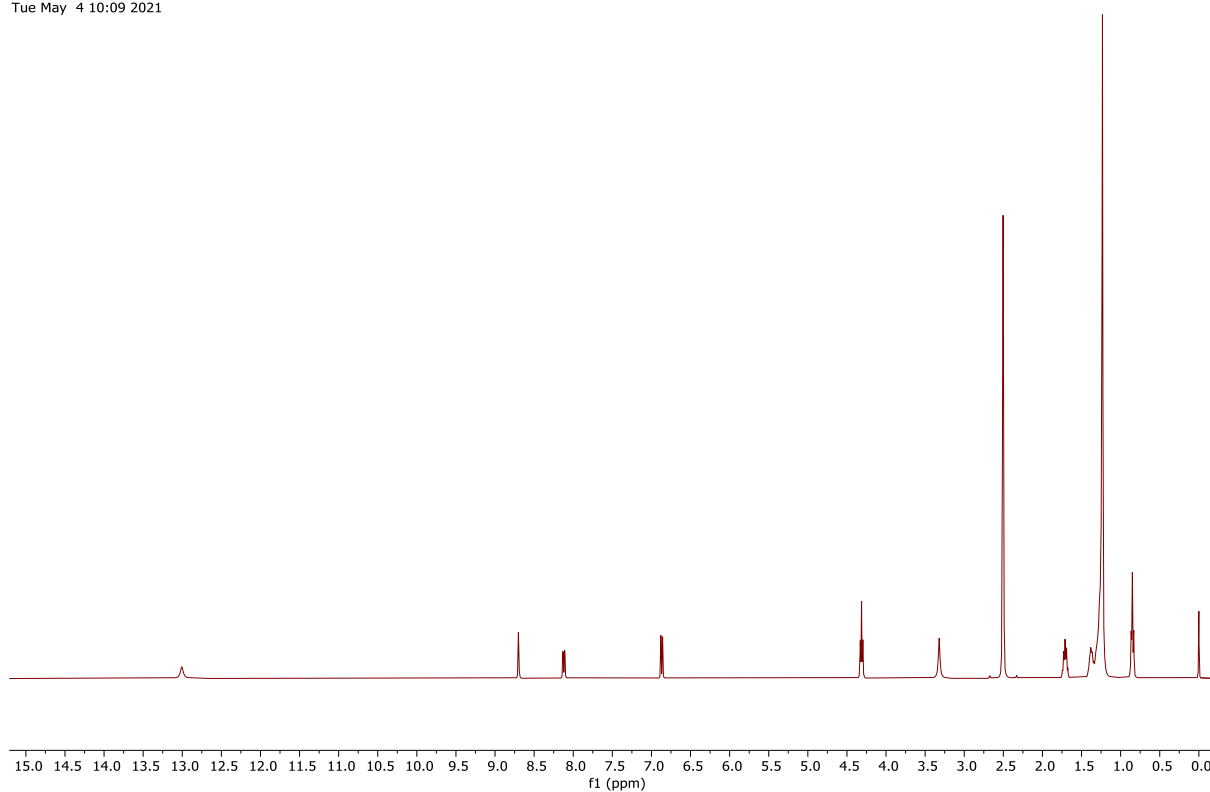


Figure 93: ¹H NMR spectrum (400 MHz, (CD₃)₂SO) of compound **11** (Chapter 3).

GGX396_Fr2_CARBON_01
GGX396_Fr2/DMSO-d6/13C
Fuchs 20210504_02
Tue May 4 17:39 2021

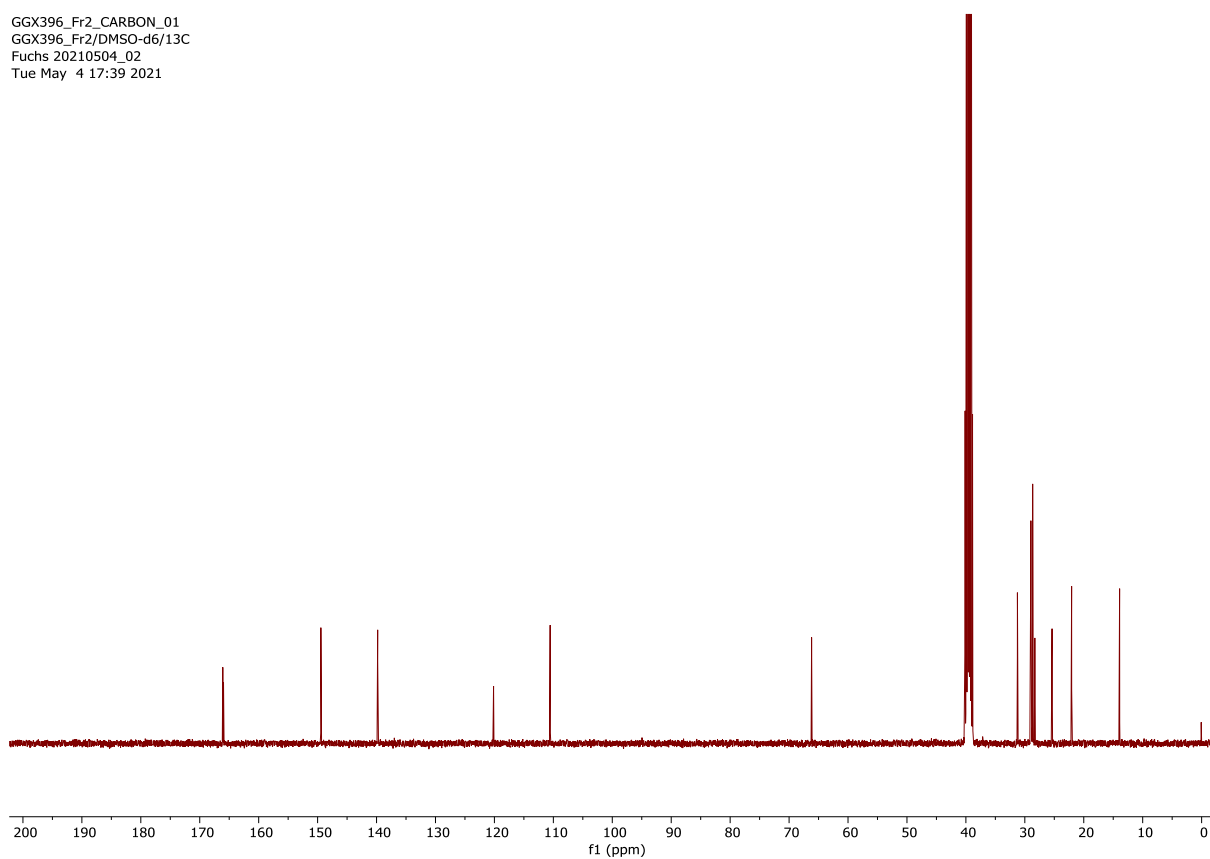


Figure 94: ¹³C NMR spectrum (101 MHz, (CD₃)₂SO) of compound **11** (Chapter 3).

GGX397_PROTON_01
GGX397/DMSO-d6/1H
Fuchs 20210505_02
Probe auf 40 grd C erwärmt
@ 25 grd C
Wed May 5 13:40 2021

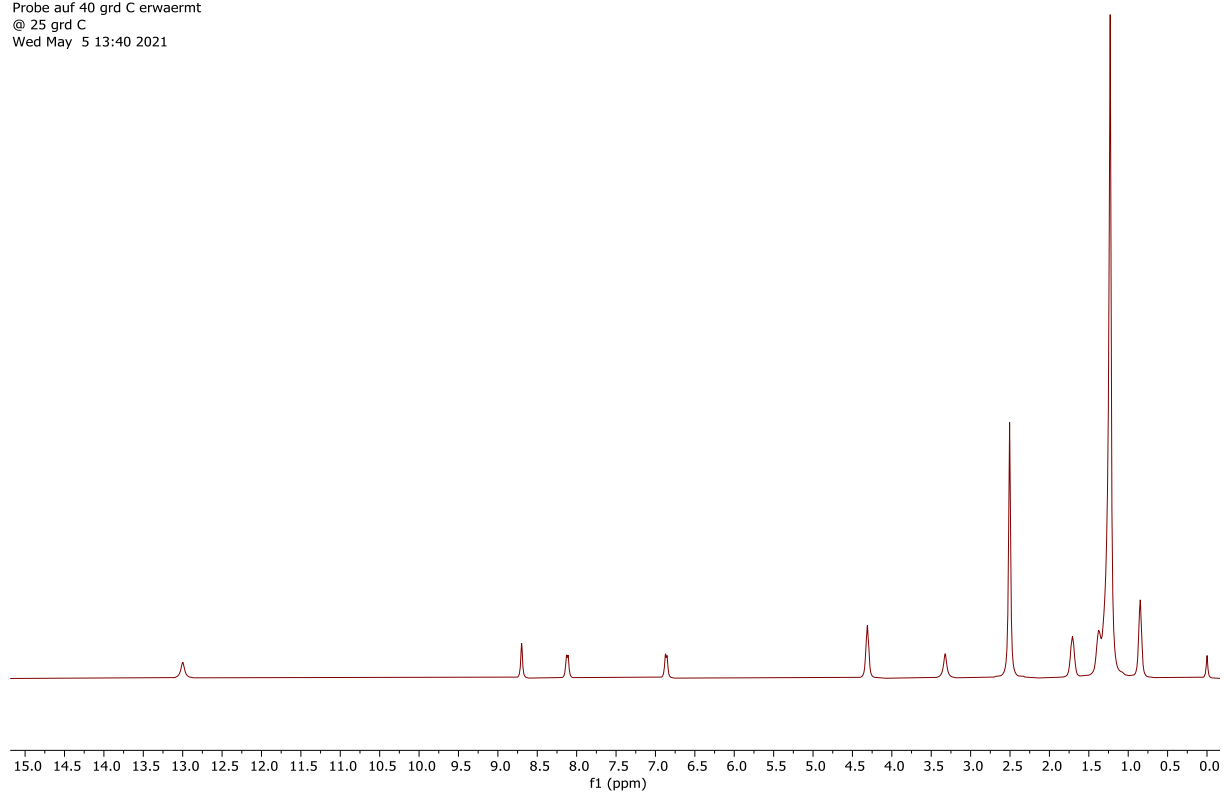


Figure 95: ¹H NMR spectrum (400 MHz, (CD₃)₂SO) of compound **12** (Chapter 3).

GGX397_CARBON_01
GGX397/DMSO-d4/13C
Fuchs 20210505_02
@ +40 grd C
Mon May 10 12:12 2021

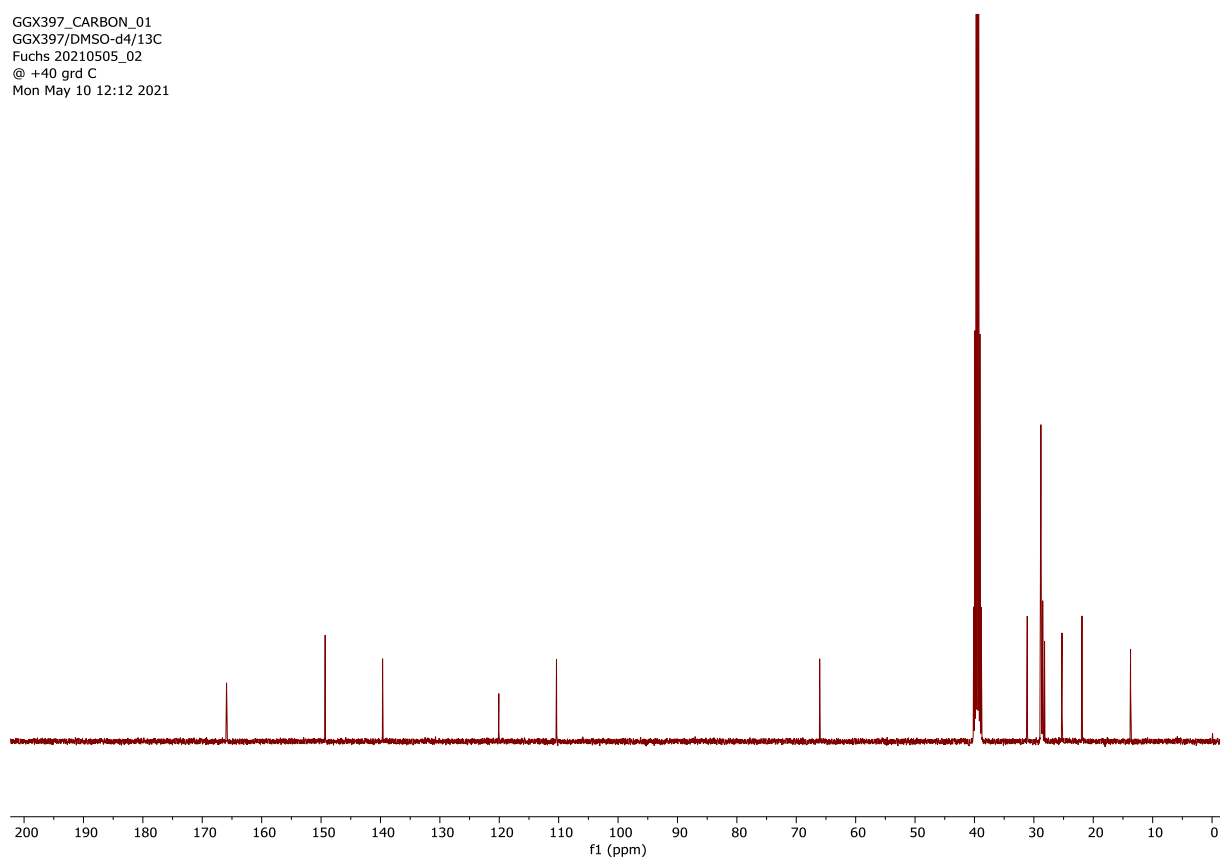


Figure 96: ¹³C NMR spectrum (101 MHz, (CD₃)₂SO) of compound **12** (Chapter 3).

GGX421.11.fid
GGX421/DMSO-d6/1H
Fuchs 20210203_04
Proton_IPB DMSO /opt/nmrdata/2020/GGX walkup 13

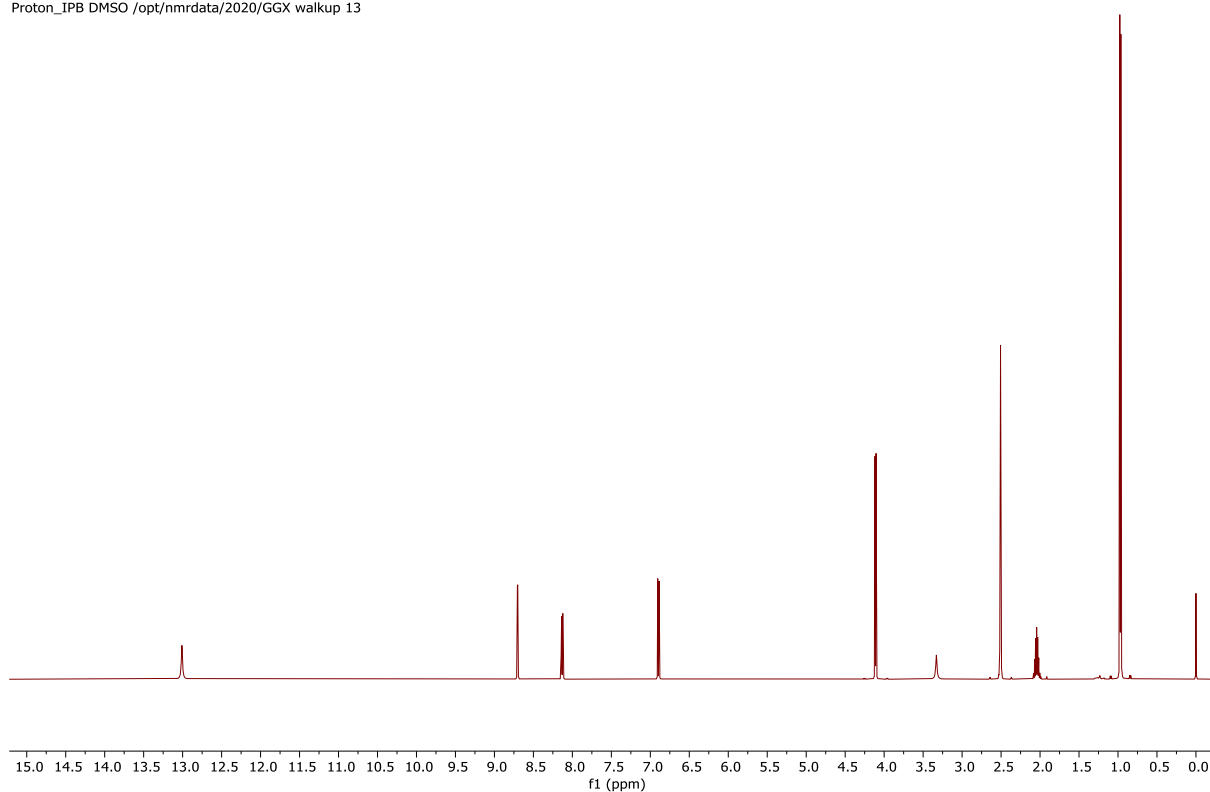


Figure 97: ¹H NMR spectrum (500 MHz, (CD₃)₂SO) of compound **13** (Chapter 3).

GGX421.12.fid
GGX421/DMSO-d6/13C
Fuchs 20210203_04
Carbon_dec_IPB DMSO /opt/nmrdata/2020/GGX walkup 13

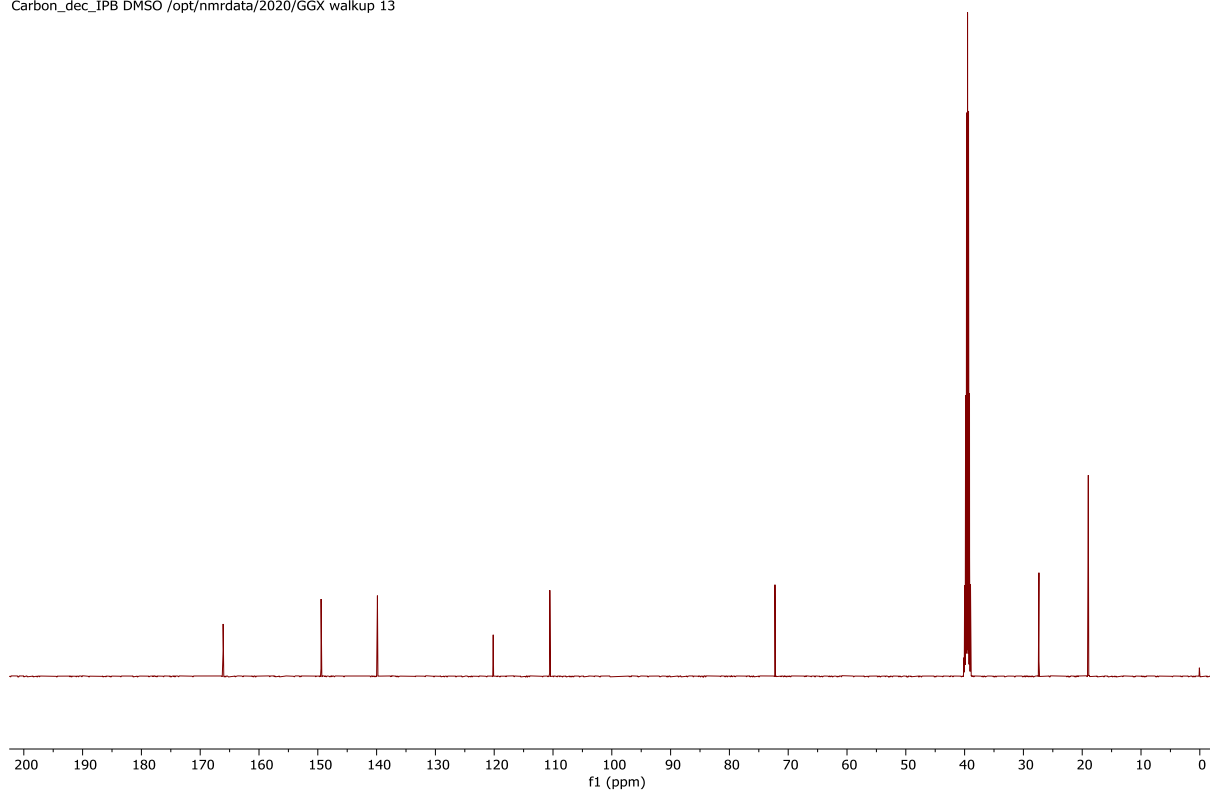


Figure 98: ¹³C NMR spectrum (126 MHz, (CD₃)₂SO) of compound **13** (Chapter 3).

GGX467_PROTON_01
GGX467/DMSO_d6/1H
Fuchs 20210628_05
Mon Jun 28 11:00 2021

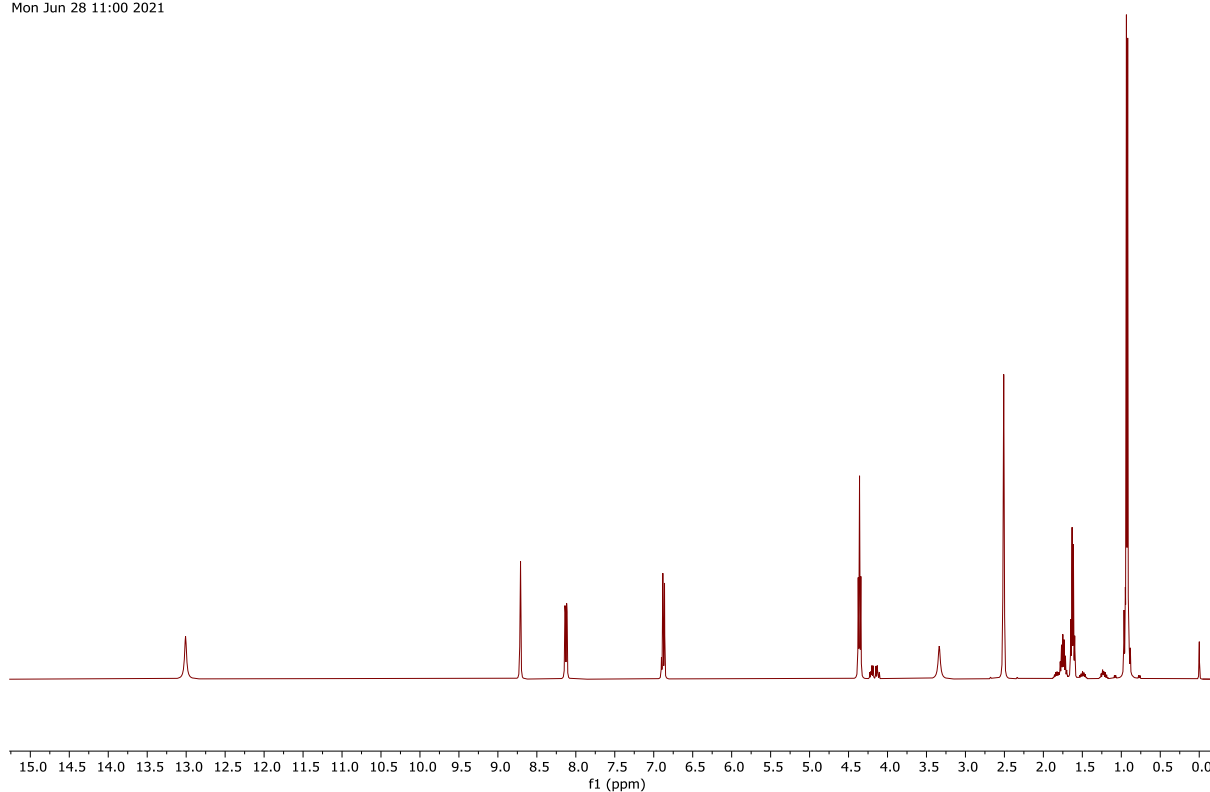


Figure 99: ¹H NMR spectrum (400 MHz, (CD₃)₂SO) of compound **14** (Chapter 3).

GGX467_CARBON_01
GGX467/DMSO_d6/13C
Fuchs 20210628_05
Mon Jun 28 11:03 2021

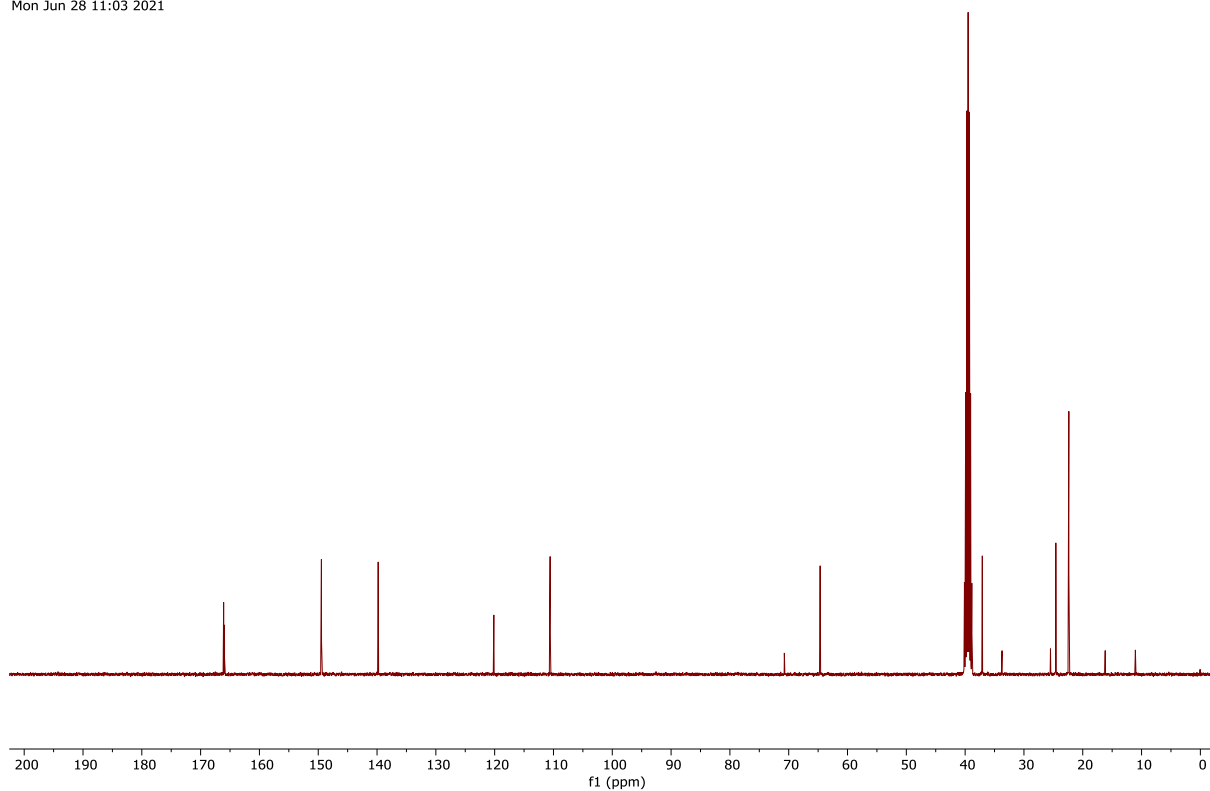


Figure 100: ¹³C NMR spectrum (101 MHz, (CD₃)₂SO) of compound **14** (Chapter 3).

GGX531_EE_PROTON_01
GGX531_EE/DMSO-d6/1H
Fuchs 20220419_01
Tue Apr 19 10:53 2022

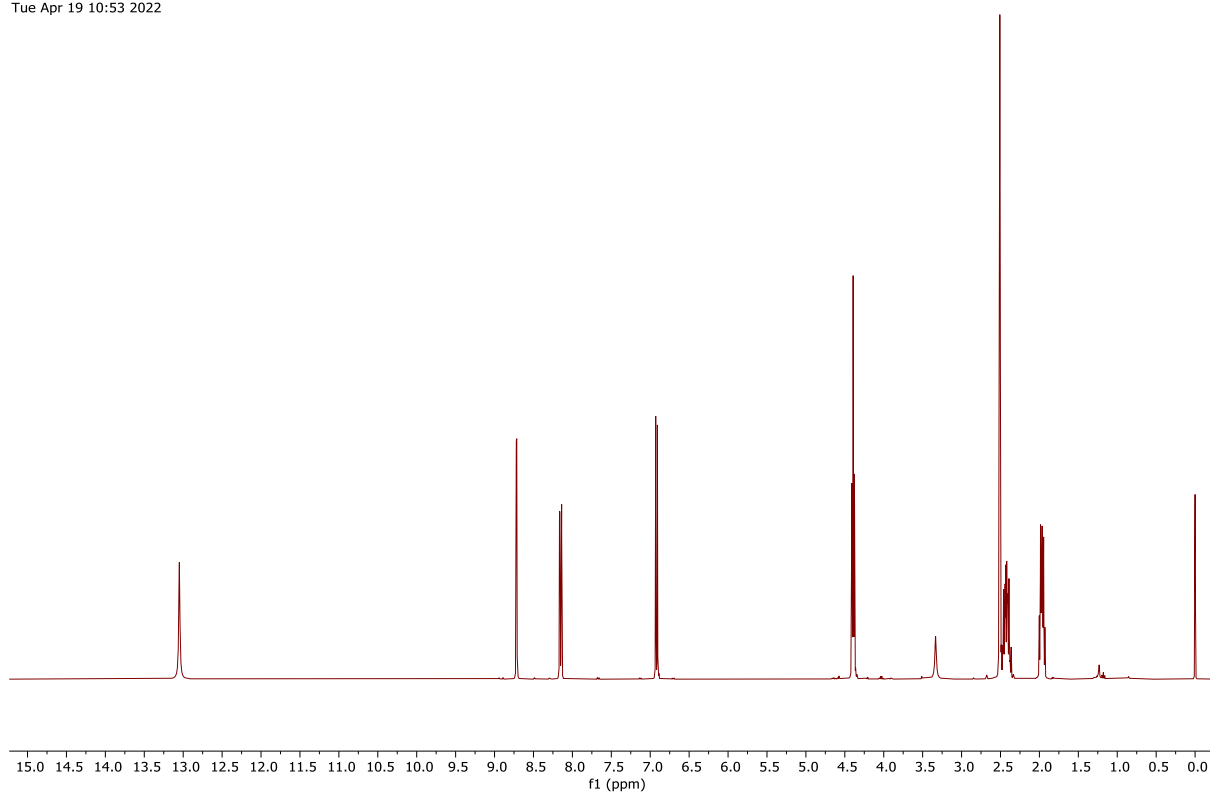


Figure 101: ¹H NMR spectrum (400 MHz, (CD₃)₂SO) of compound **15** (Chapter 3).

GGX531_EE_CARBON_01
GGX531_EE/DMSO-d6/13C
Fuchs 20220419_01
Tue Apr 19 11:10 2022

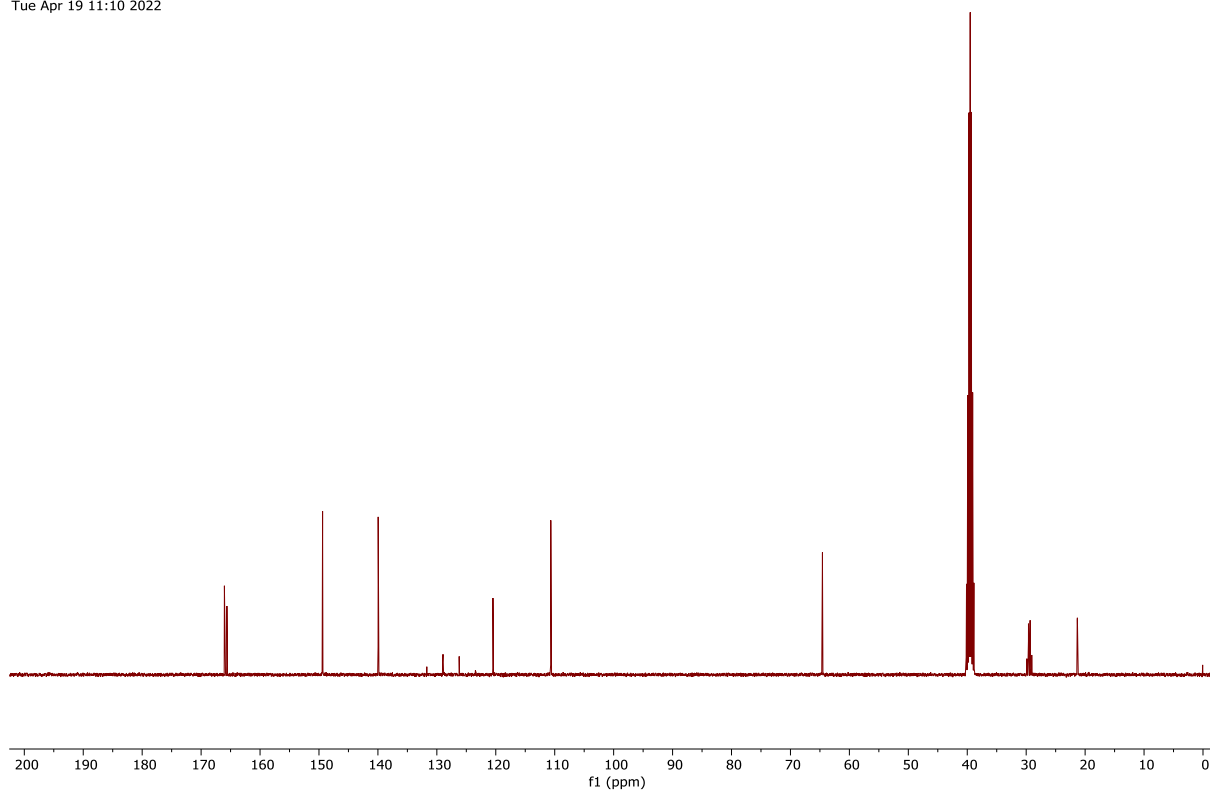


Figure 102: ¹³C NMR spectrum (101 MHz, (CD₃)₂SO) of compound **15** (Chapter 3).

GGX407_PROTON_01
GGX407/DMSO-d6/1H
Fuchs 20210112_01
Tue Jan 12 10:32 2021

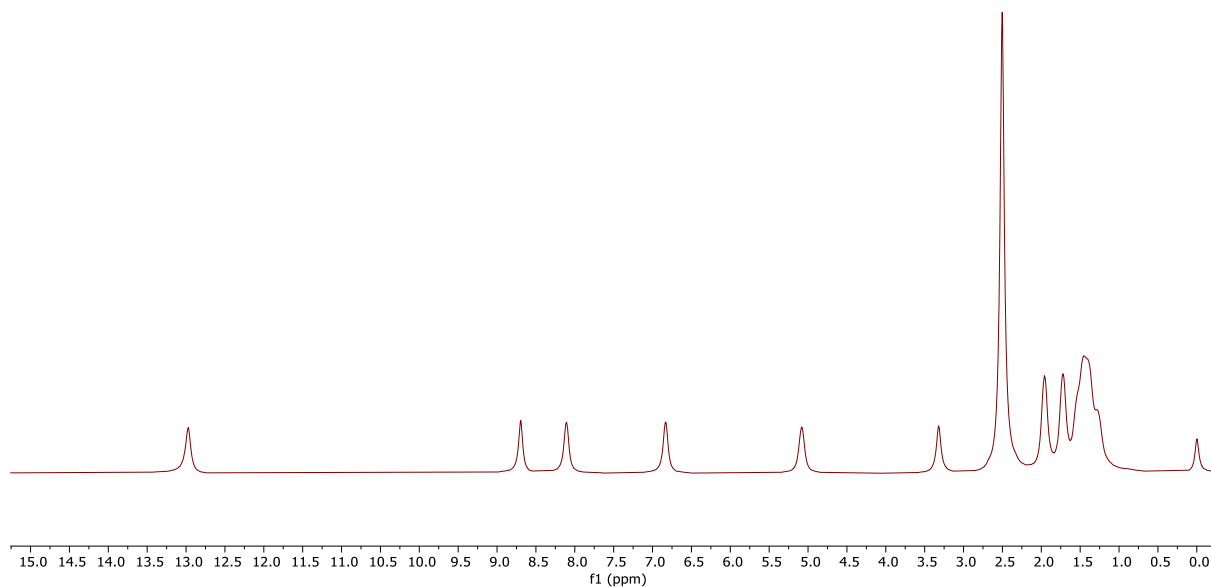


Figure 103: ¹H NMR spectrum (400 MHz, (CD₃)₂SO) of compound **16** (Chapter 3).

GGX407_CARBON_01
GGX407/DMSO-d6/13C
Fuchs 20210112_01
Tue Jan 12 16:27 2021

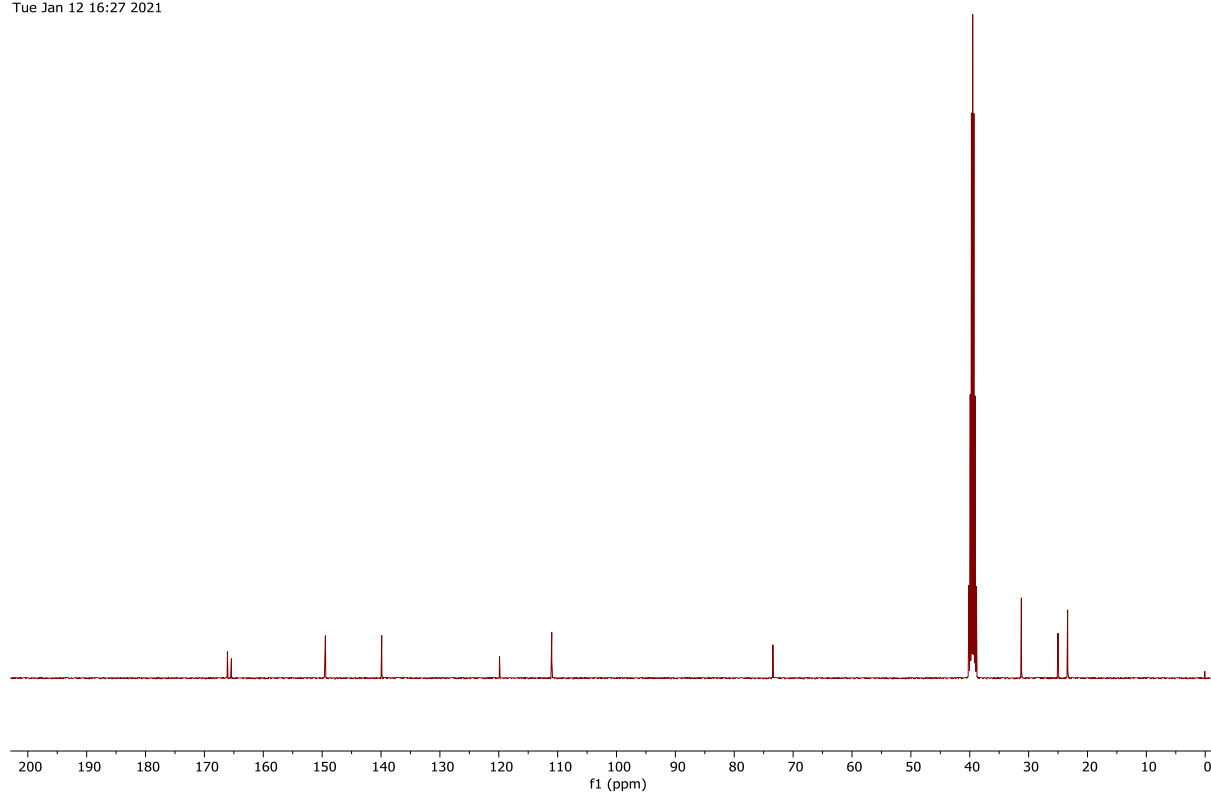


Figure 104: ¹³C NMR spectrum (101 MHz, (CD₃)₂SO) of compound **16** (Chapter 3).

GGX431_II_PROTON_01
GGX431_II/DMSO-d6/1H
Fuchs 20210325_01
Thu Mar 25 08:43 2021

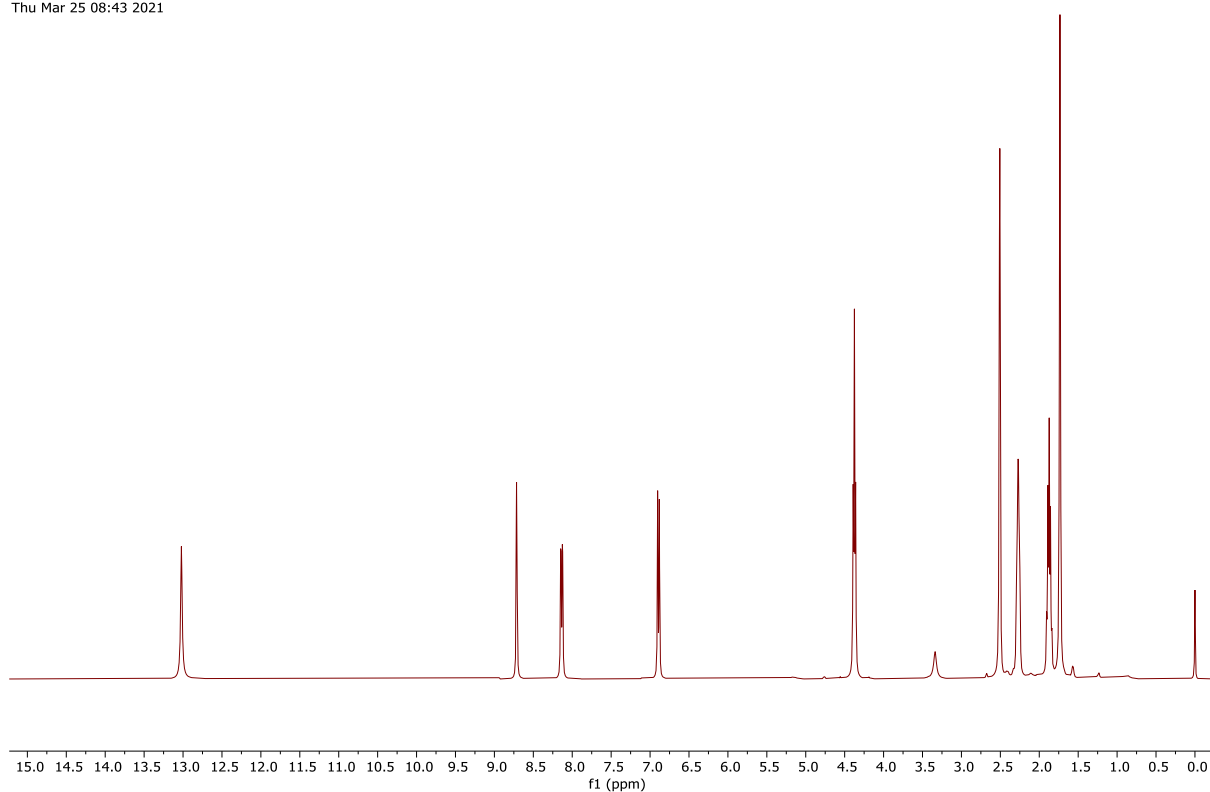


Figure 105: ¹H NMR spectrum (400 MHz, (CD₃)₂SO) of compound **17** (Chapter 3).

GGX431_II_CARBON_01
GGX431_II/DMSO-d6/13C
Fuchs 20210325_01
Thu Mar 25 20:05 2021

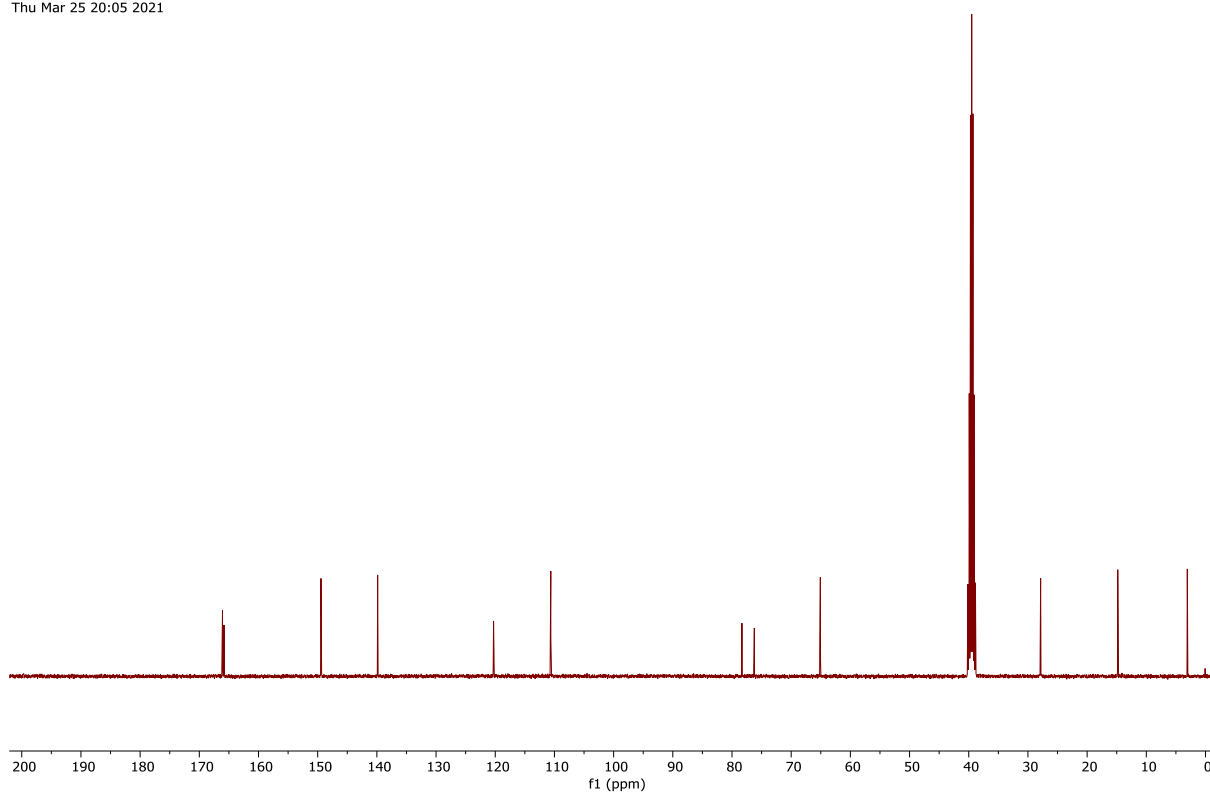


Figure 106: ¹³C NMR spectrum (101 MHz, (CD₃)₂SO) of compound **17** (Chapter 3).

GGX443_PROTON_01
GGX443/DMSO-d6/1H
Fuchs 20210510_03
Mon May 10 11:02 2021

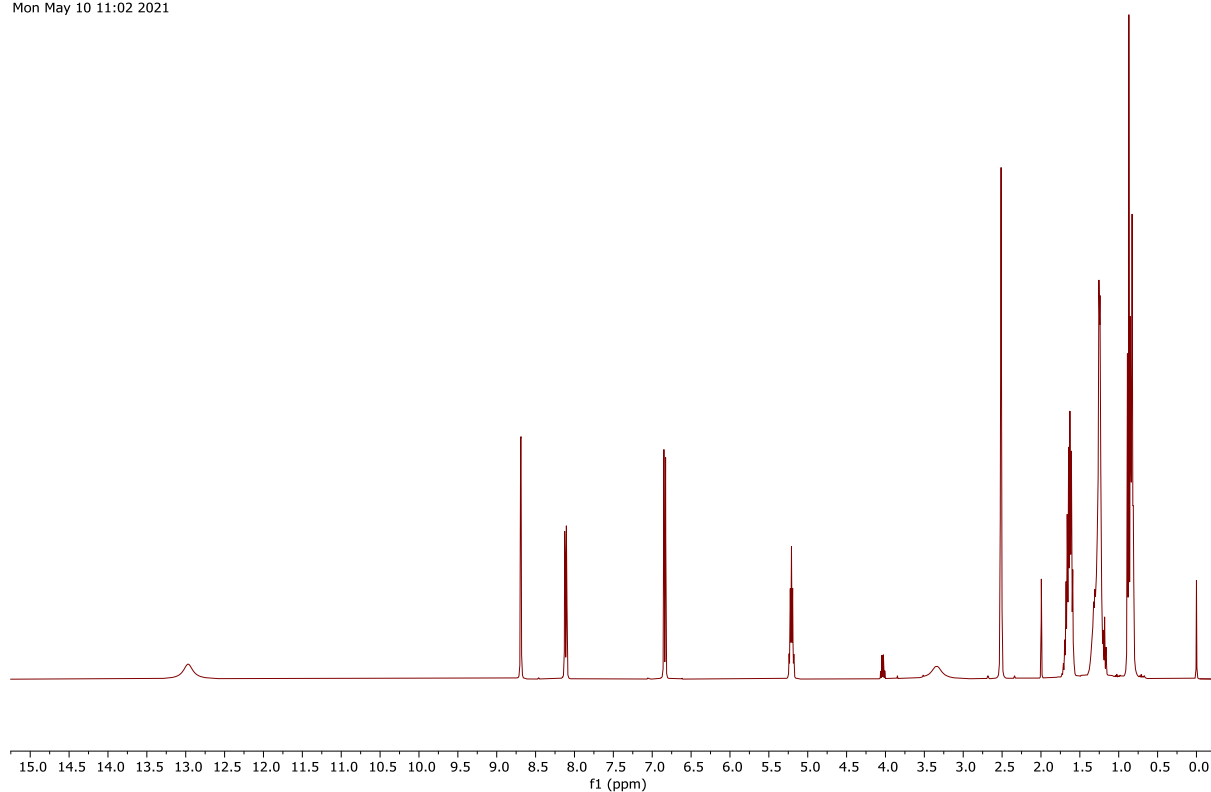


Figure 107: ¹H NMR spectrum (400 MHz, (CD₃)₂SO) of compound **18** (Chapter 3).

GGX443_CARBON_01
GGX443/DMSO-d6/13C
Fuchs 20210510_03
Mon May 10 16:23 2021

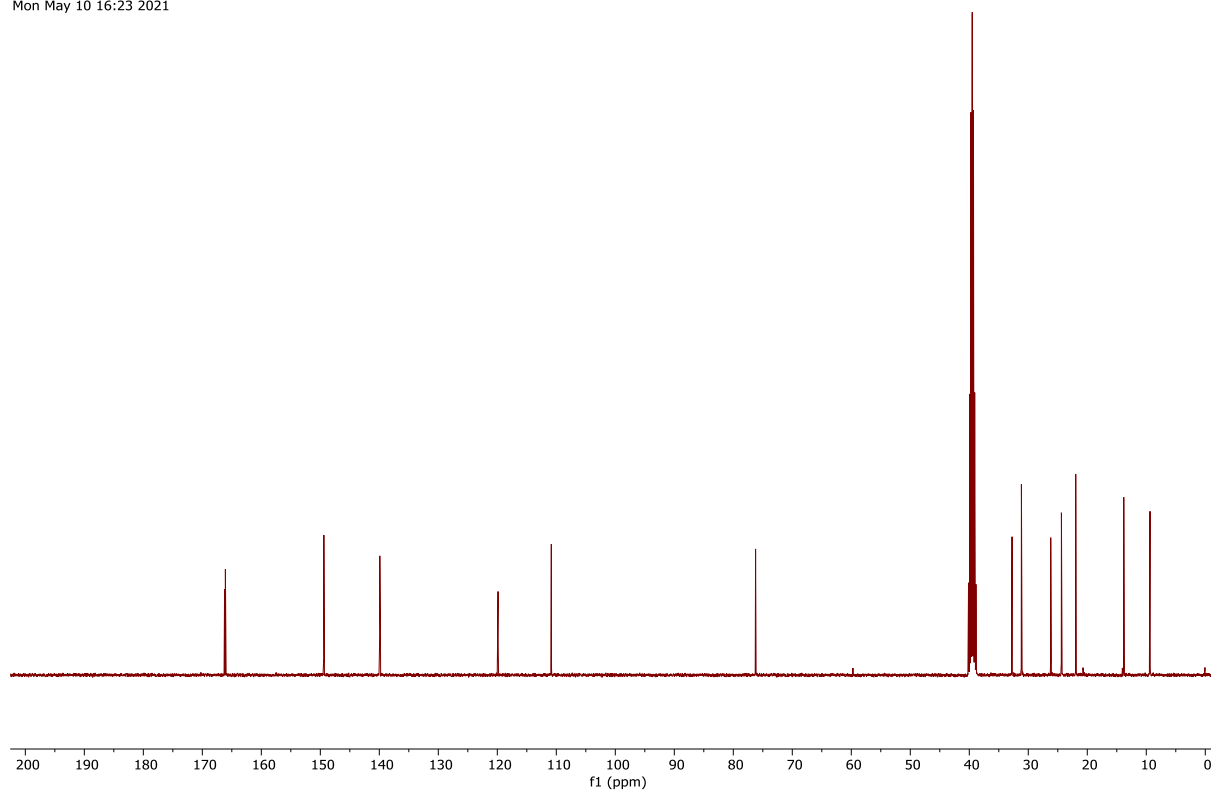


Figure 108: ¹³C NMR spectrum (101 MHz, (CD₃)₂SO) of compound **18** (Chapter 3).

GGX459_PROTON_01
GGX459/CDCl₃/1H
Fuchs 20210622_02
Tue Jun 22 09:18 2021

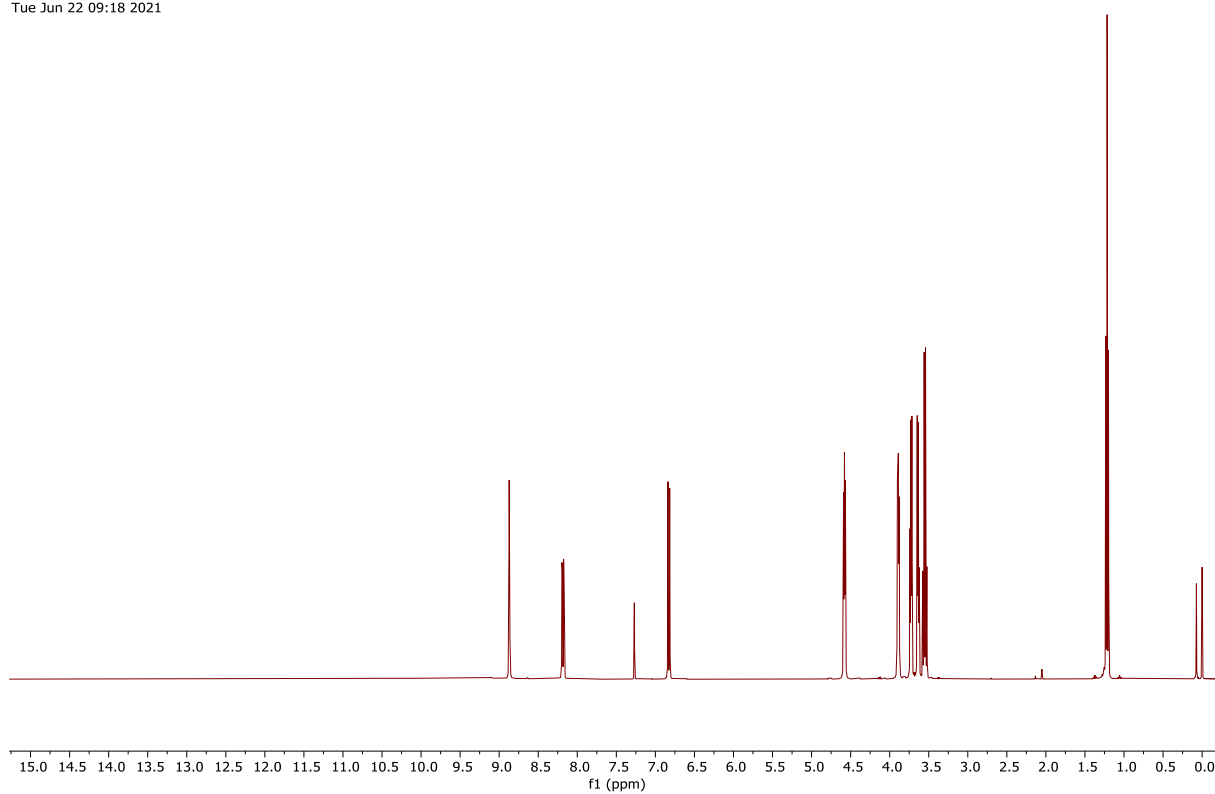


Figure 109: ¹H NMR spectrum (400 MHz, CDCl₃) of compound **19** (Chapter 3).

GGX459_CARBON_01
GGX459/CDCl₃/13C
Fuchs 20210622_02
Tue Jun 22 09:21 2021

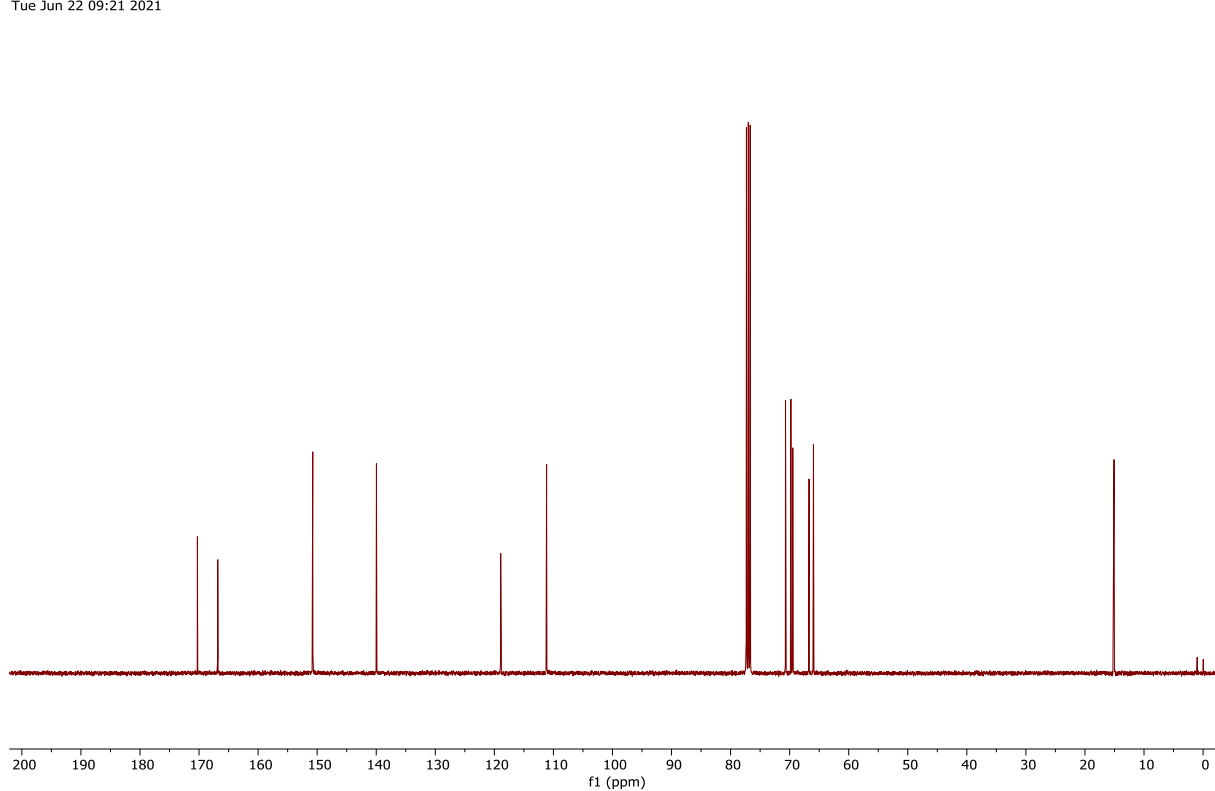


Figure 110: ¹³C NMR spectrum (101 MHz, CDCl₃) of compound **19** (Chapter 3).

GGX432_PROTON_01
GGX432/DMSO-d6/1H
Fuchs 20210323_05
Tue Mar 23 09:58 2021

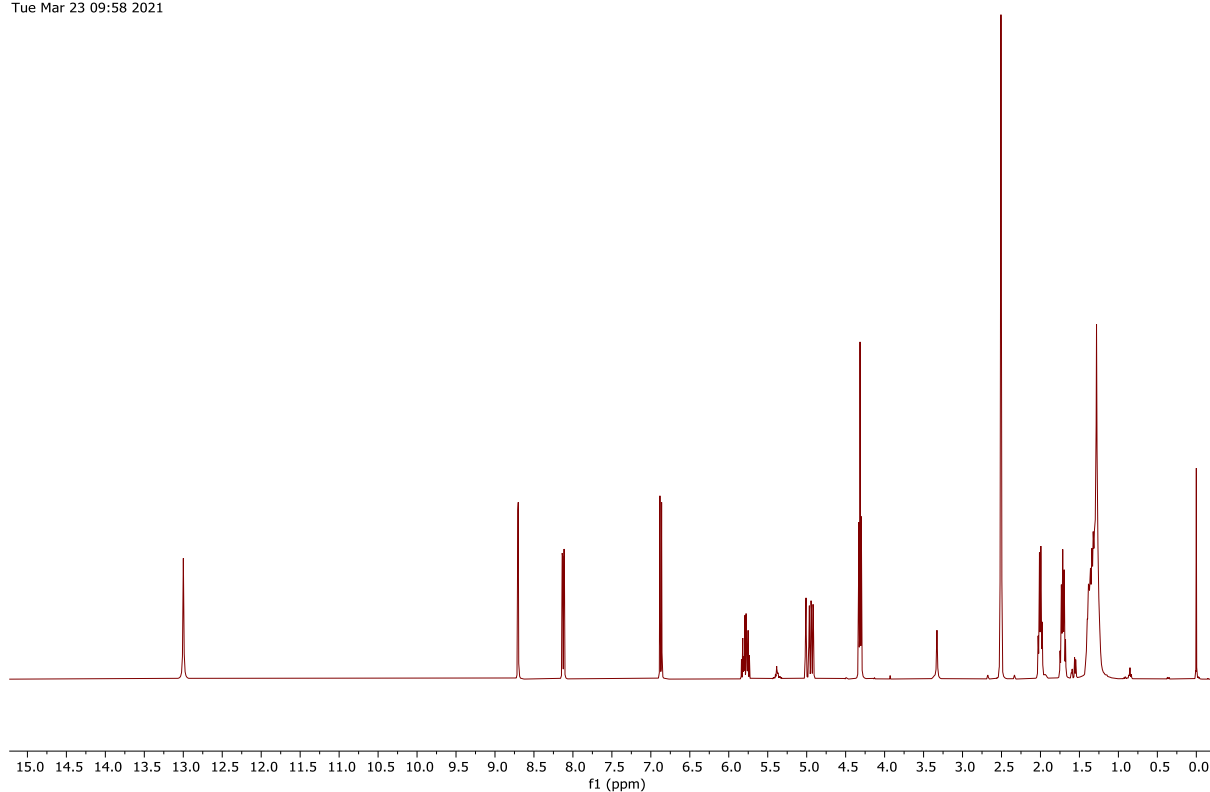


Figure 111: ¹H NMR spectrum (400 MHz, (CD₃)₂SO) of compound **20** (Chapter 3).

GGX432_CARBON_01
GGX432/DMSO-d6/13C
Fuchs 20210323_05
Tue Mar 23 12:38 2021

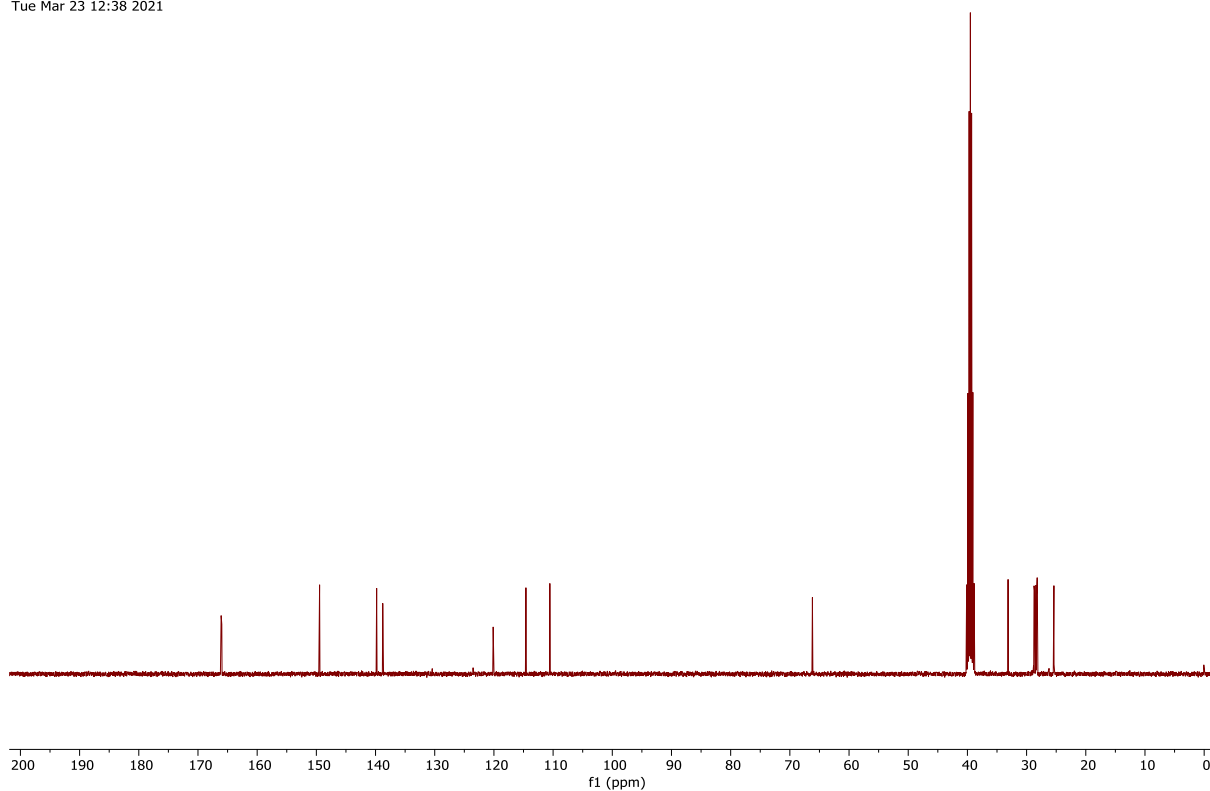


Figure 112: ¹³C NMR spectrum (101 MHz, (CD₃)₂SO) of compound **20** (Chapter 3).

GGX552_PROTON_01
GGX552/DMSO-d6/1H
Fuchs 20220720_03
Wed Jul 20 16:09 2022

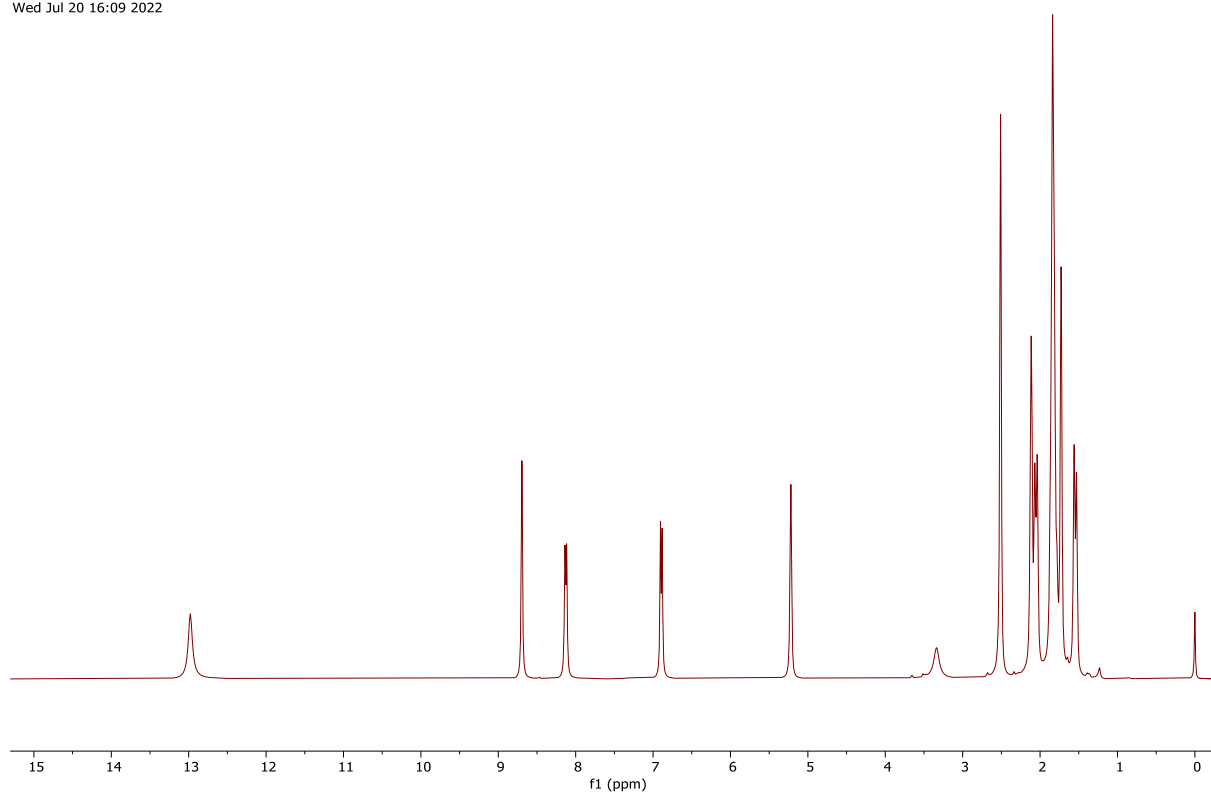


Figure 113: ¹H NMR spectrum (400 MHz, (CD₃)₂SO) of compound **21** (Chapter 3).

GGX552_CARBON_01
GGX552/DMSO-d6/13C
Fuchs 20220720_03
Wed Jul 20 16:12 2022

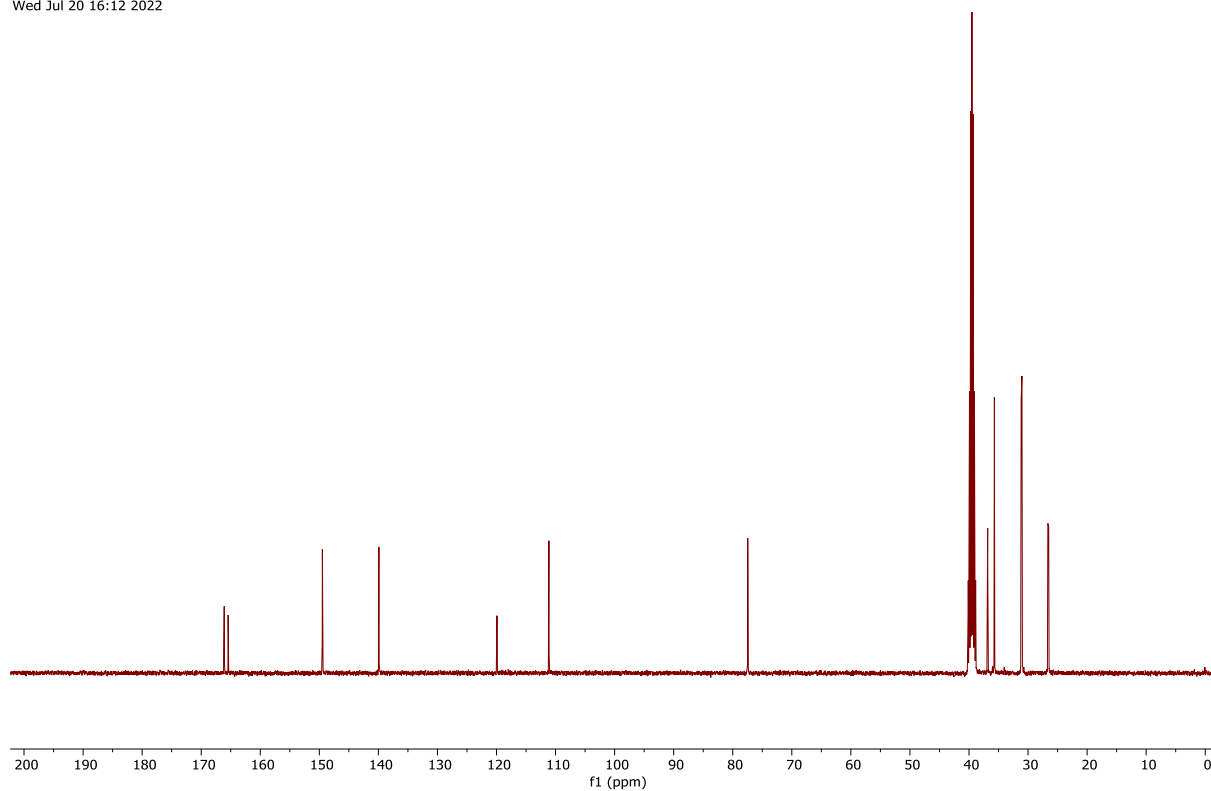


Figure 114: ¹³C NMR spectrum (101 MHz, (CD₃)₂SO) of compound **21** (Chapter 3).

GGX423_H2O_PROTON_01
GGX423_H2O/DMSO-d6/1H
Fuchs 20210203_03
Wed Feb 3 13:49 2021

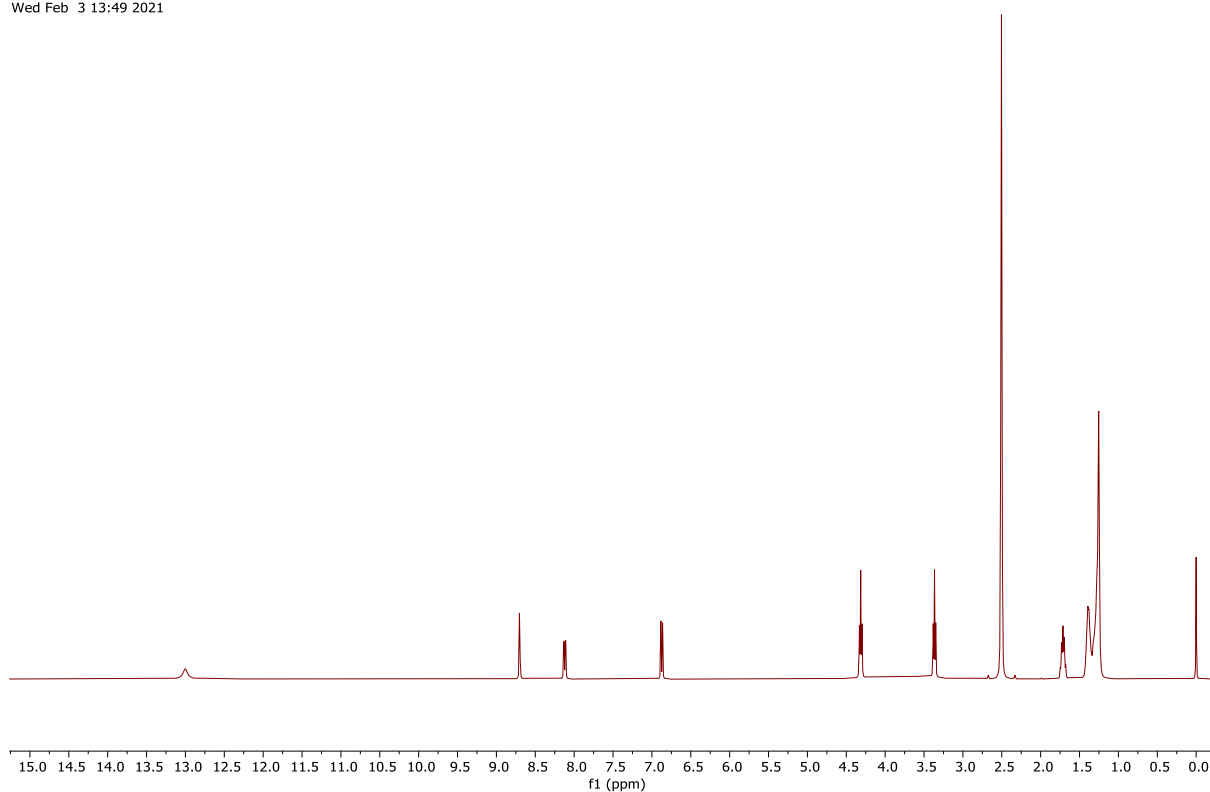


Figure 115: ¹H NMR spectrum (400 MHz, (CD₃)₂SO) of compound **22** (Chapter 3).

GGX423_H2O_CARBON_01
GGX423_H2O/DMSO-d6/13C
Fuchs 20210204_01
Thu Feb 4 10:41 2021

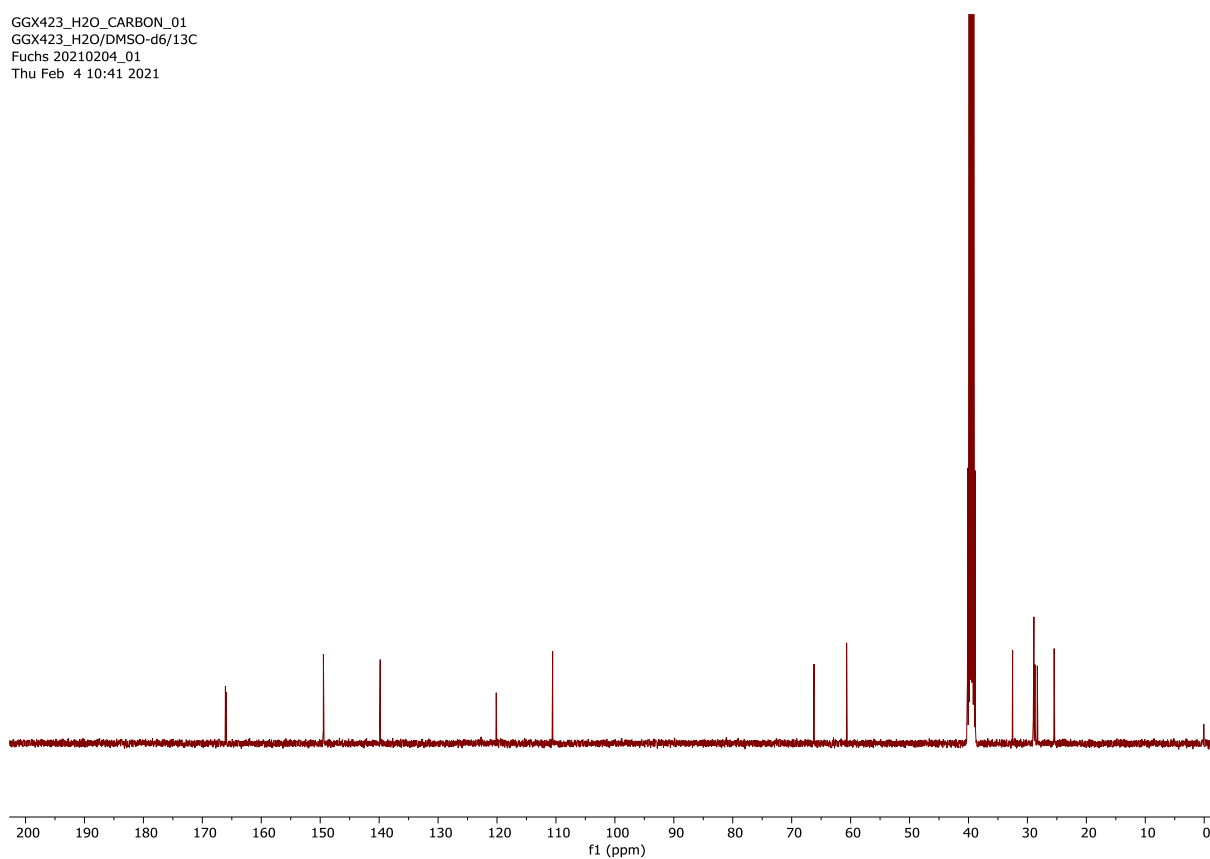


Figure 116: ¹³C NMR spectrum (101 MHz, (CD₃)₂SO) of compound **22** (Chapter 3).

GGX430_PROTON_01
GGX430/DMSO-d6/1H
Fuchs 20210305_03
Fri Mar 5 13:38 2021

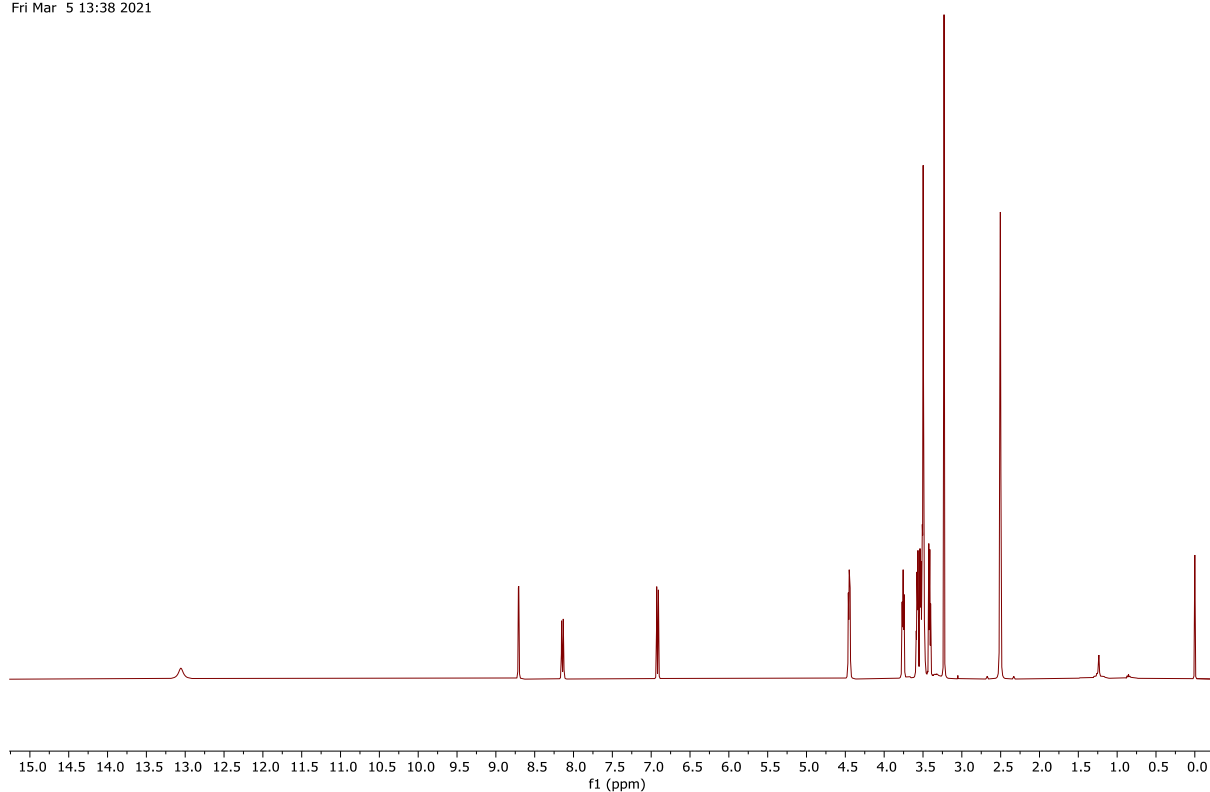


Figure 117: ¹H NMR spectrum (400 MHz, (CD₃)₂SO) of compound **23** (Chapter 3).

GGX430_CARBON_01
GGX430/DMSO-d6/13C
Fuchs 20210305_03
Fri Mar 5 14:12 2021

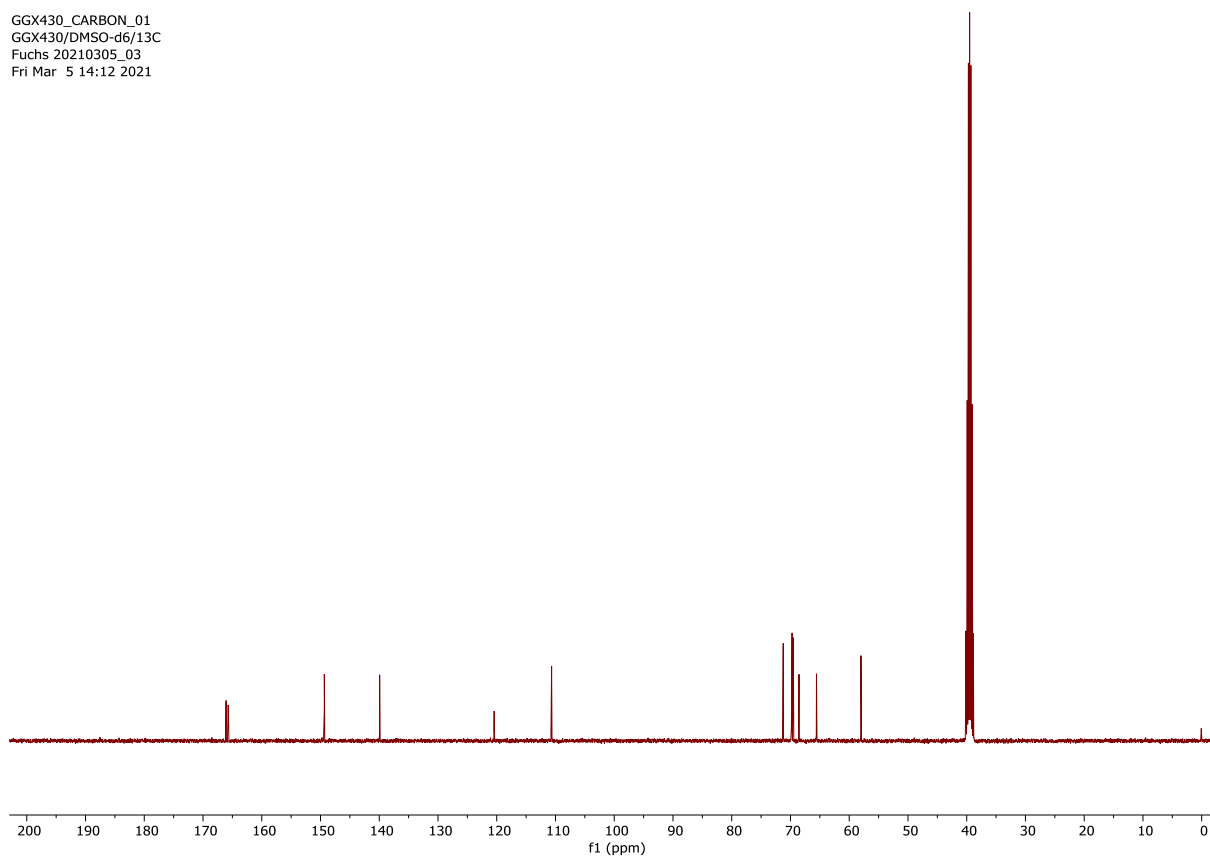


Figure 118: ¹³C NMR spectrum (101 MHz, (CD₃)₂SO) of compound **23** (Chapter 3).

GGX479_A_PROTON_01
GGX479_A/DMSO-d6/1H
Fuchs 20210714_01
Wed Jul 14 11:50 2021

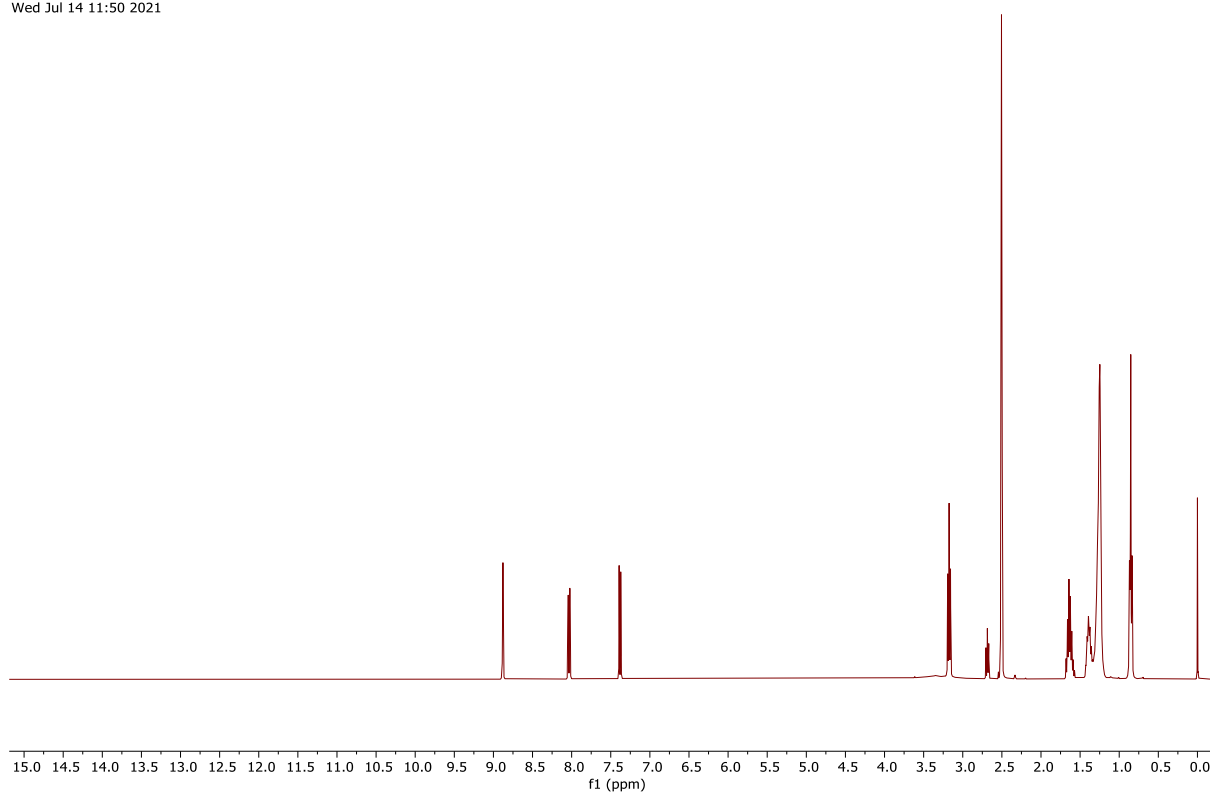


Figure 119: ¹H NMR spectrum (400 MHz, (CD₃)₂SO) of compound **24** (Chapter 3).

GGX479_A_CARBON_01
GGX479_A/DMSO-d6/13C
Fuchs 20210714_01
Wed Jul 14 16:18 2021

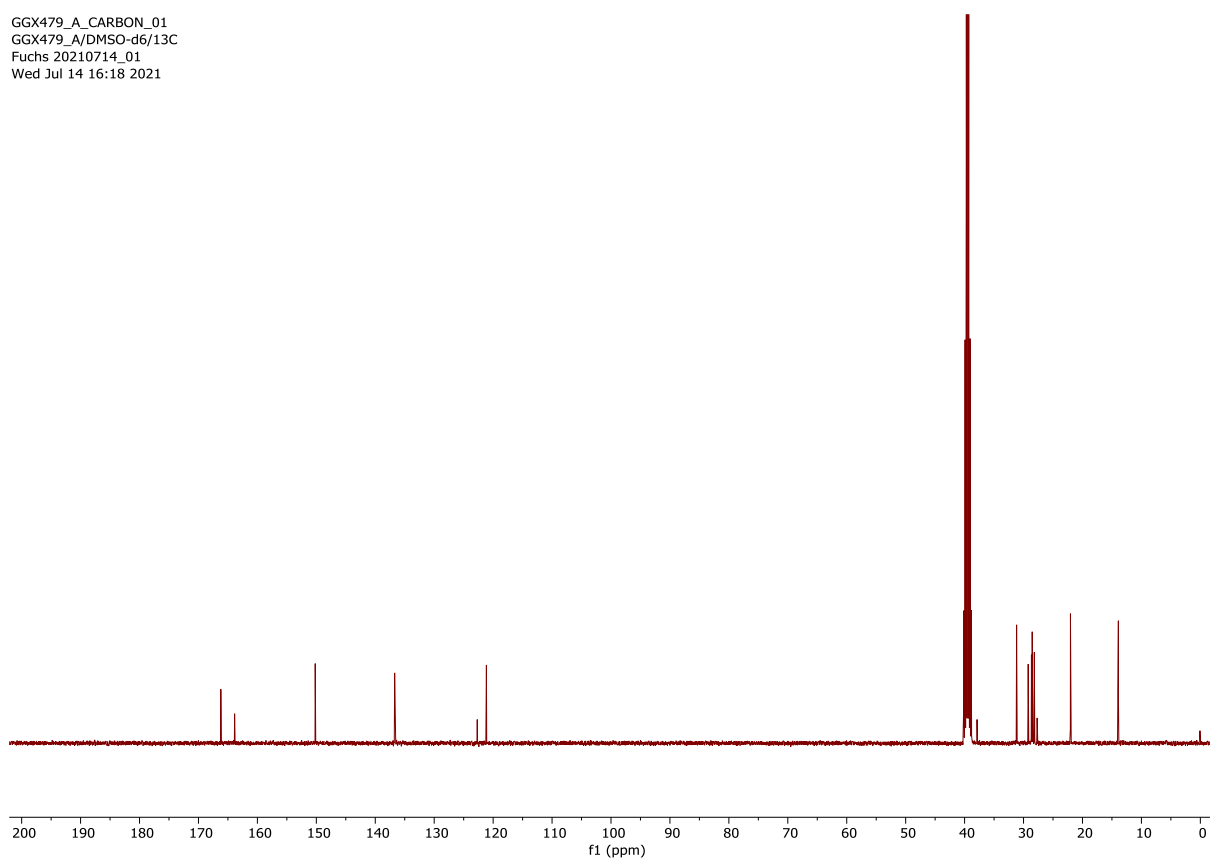


Figure 120: ¹³C NMR spectrum (101 MHz, (CD₃)₂SO) of compound **24** (Chapter 3).

GGX464_II.15.fid
GGX464_II/DMSO_d6/1H
Fuchs 20210625_02
Proton_IPB DMSO /opt/nmrdata/2020/GGX walkup 11

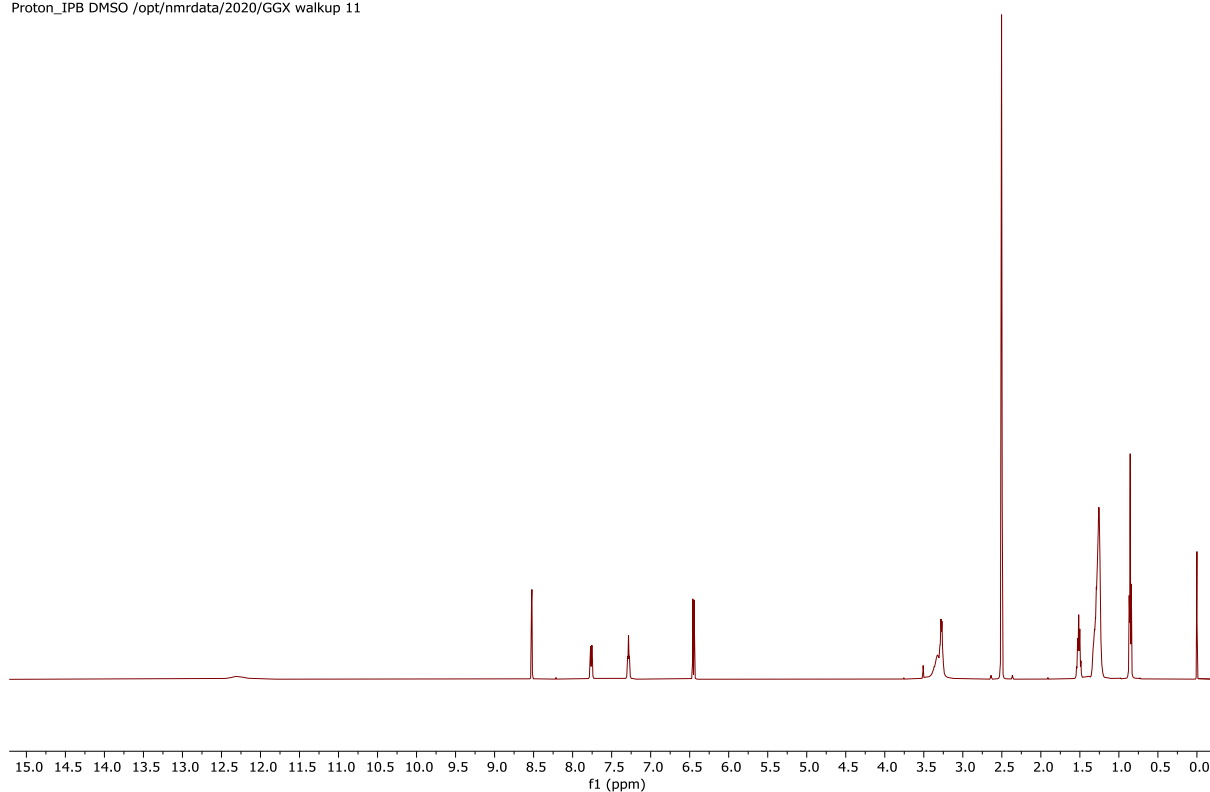


Figure 121: ¹H NMR spectrum (500 MHz, (CD₃)₂SO) of compound **25** (Chapter 3).

GGX464_II.12.fid
GGX464_II/DMSO_d6/13C
Fuchs 20210625_02
Carbon_dec_IPB DMSO /opt/nmrdata/2020/GGX walkup 11

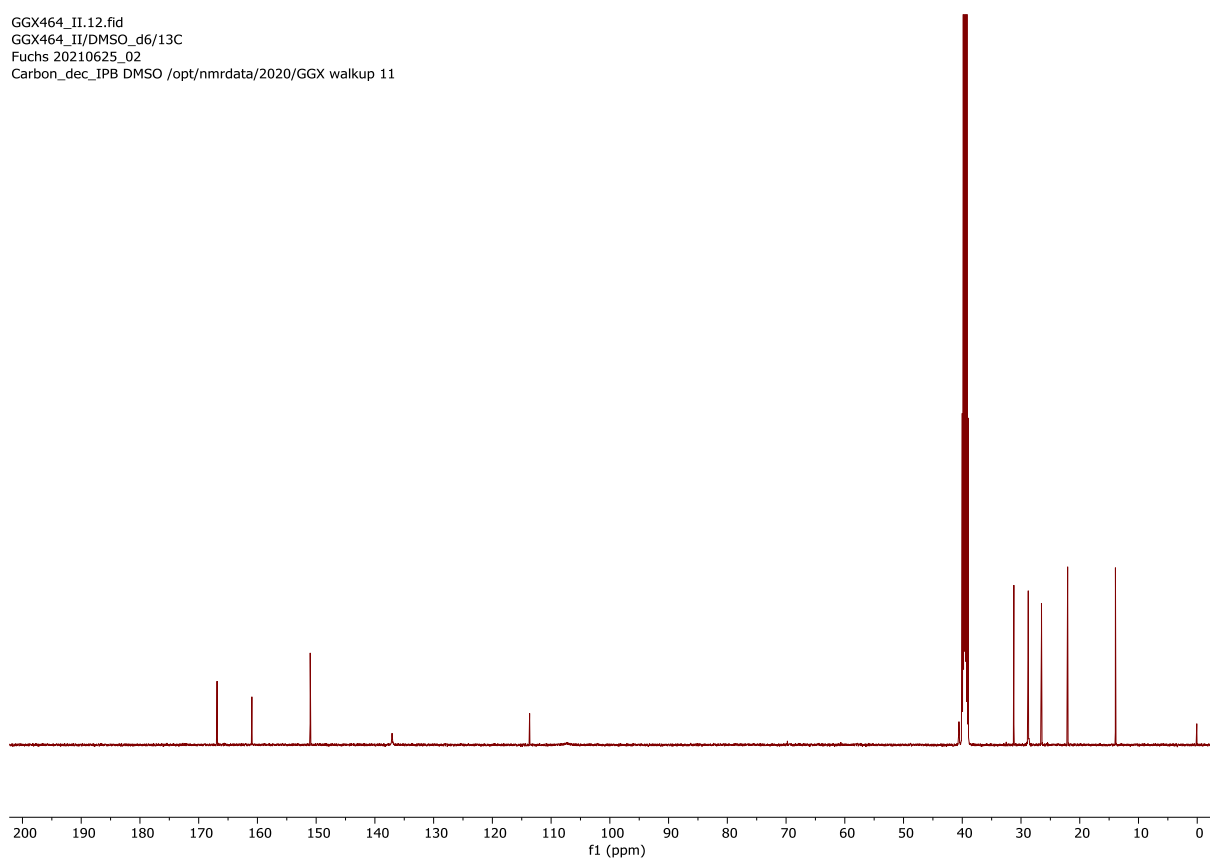


Figure 122: ¹³C NMR spectrum (126 MHz, (CD₃)₂SO) of compound **25** (Chapter 3).

GGX536_PROTON_01
GGX536/CDCl₃/1H
Fucha 20220627_05
Mon Jun 27 11:05 2022

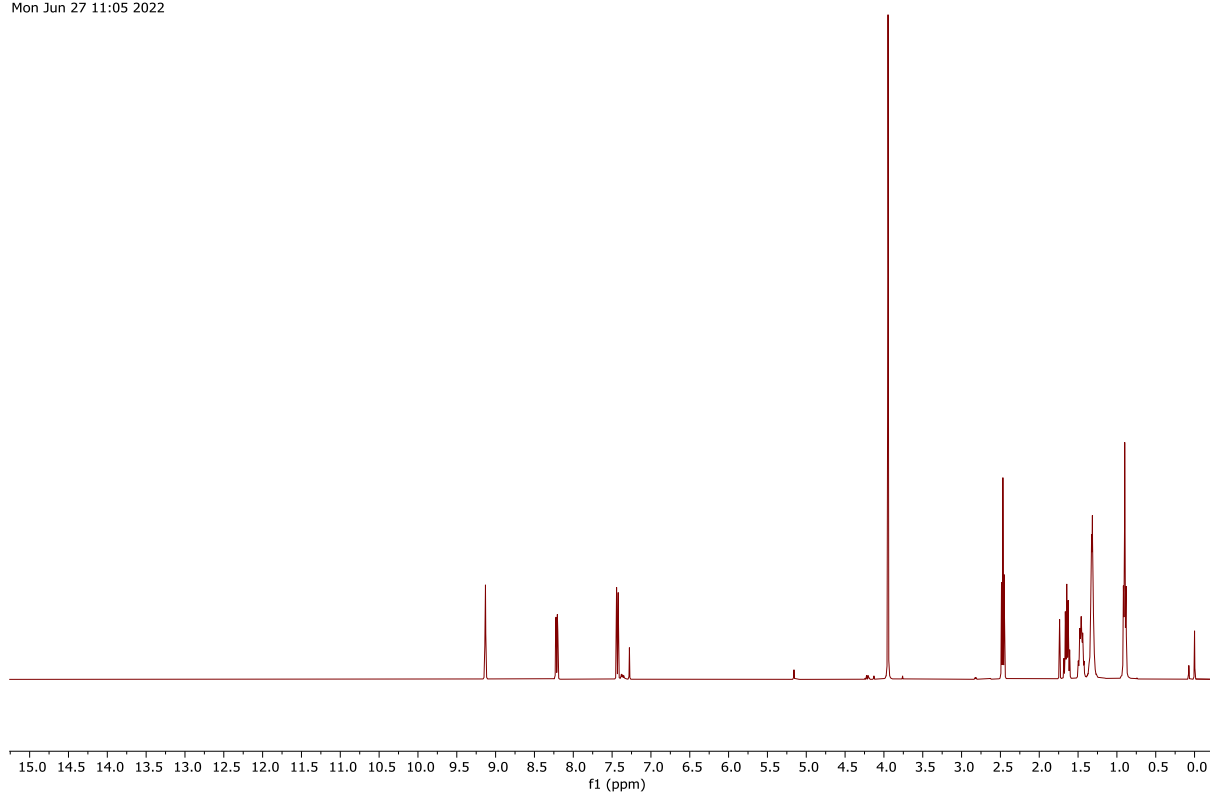


Figure 123: ¹H NMR spectrum (400 MHz, CDCl₃) of compound **26** (Chapter 3).

GGX536_CARBON_01
GGX536/CDCl₃/13C
Fucha 20220627_05
Tue Jun 28 10:27 2022

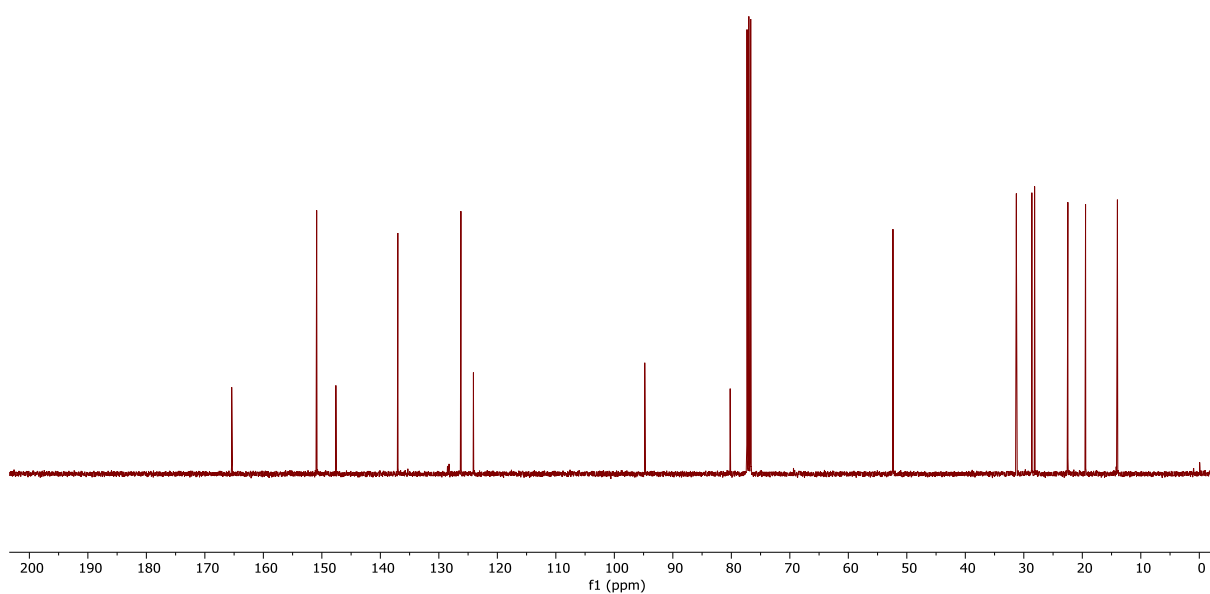


Figure 124: ¹³C NMR spectrum (101 MHz, CDCl₃) of compound **26** (Chapter 3).

GGX539_PROTON_01
GGX539/DMSO-d6/1H
Fuchs 20220629_09
Wed Jun 29 14:52 2022

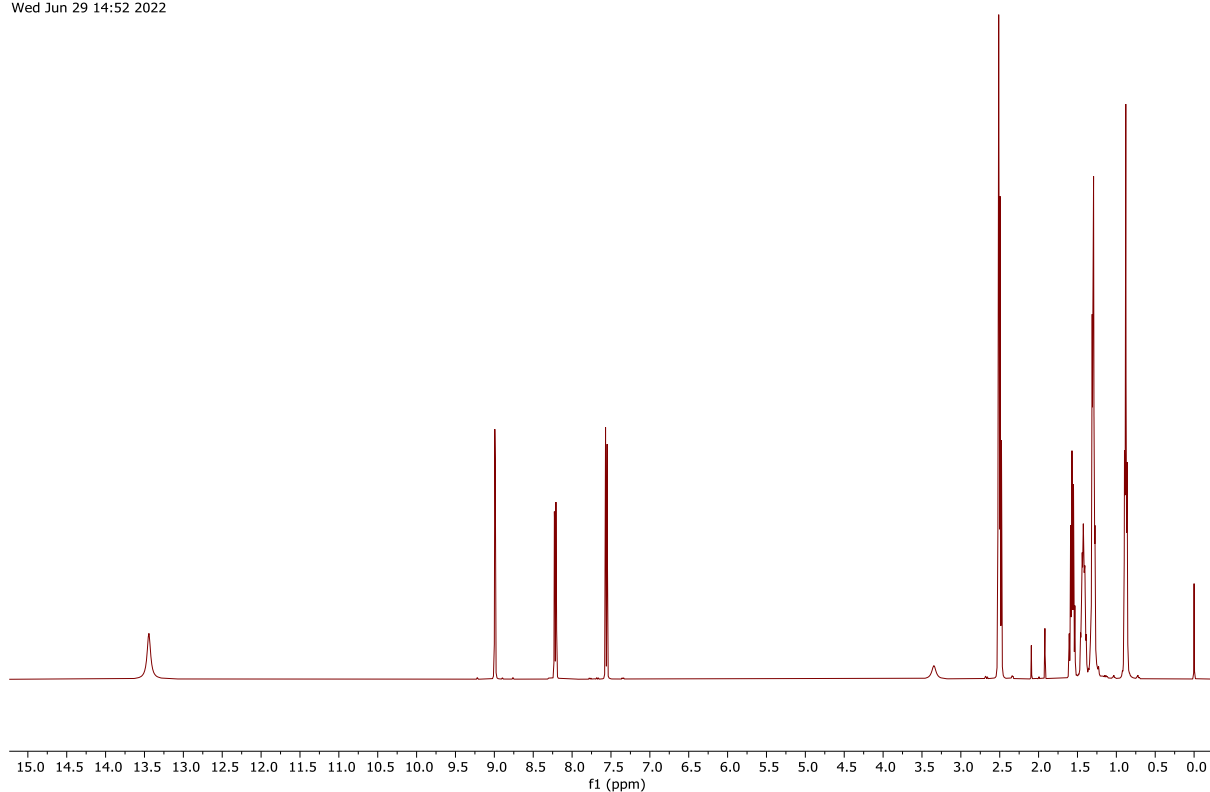


Figure 125: ¹H NMR spectrum (400 MHz, (CD₃)₂SO) of compound **27** (Chapter 3).

GGX539_CARBON_01
GGX539/DMSO-d6/13C
Fuchs 20220630_01
Thu Jun 30 11:57 2022

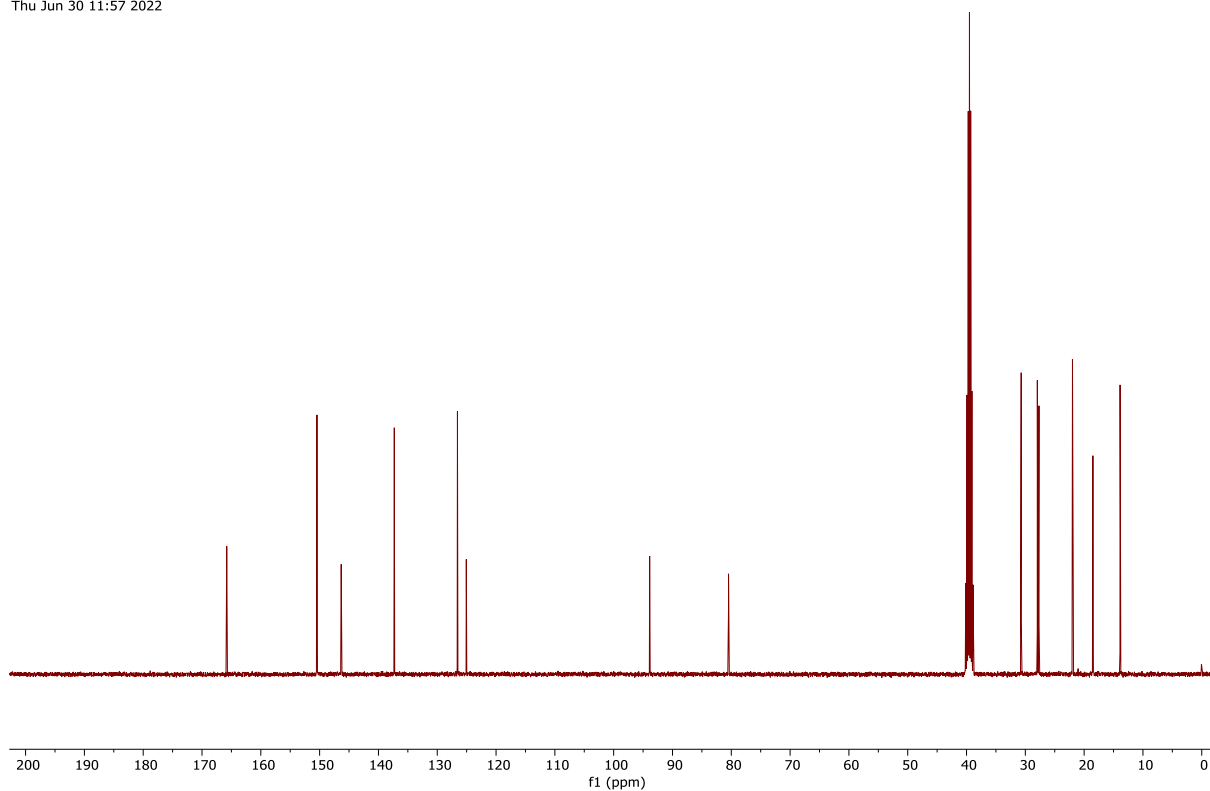


Figure 126: ¹³C NMR spectrum (101 MHz, (CD₃)₂SO) of compound **27** (Chapter 3).

GGX542_PROTON_01
GGX542_CDCI3

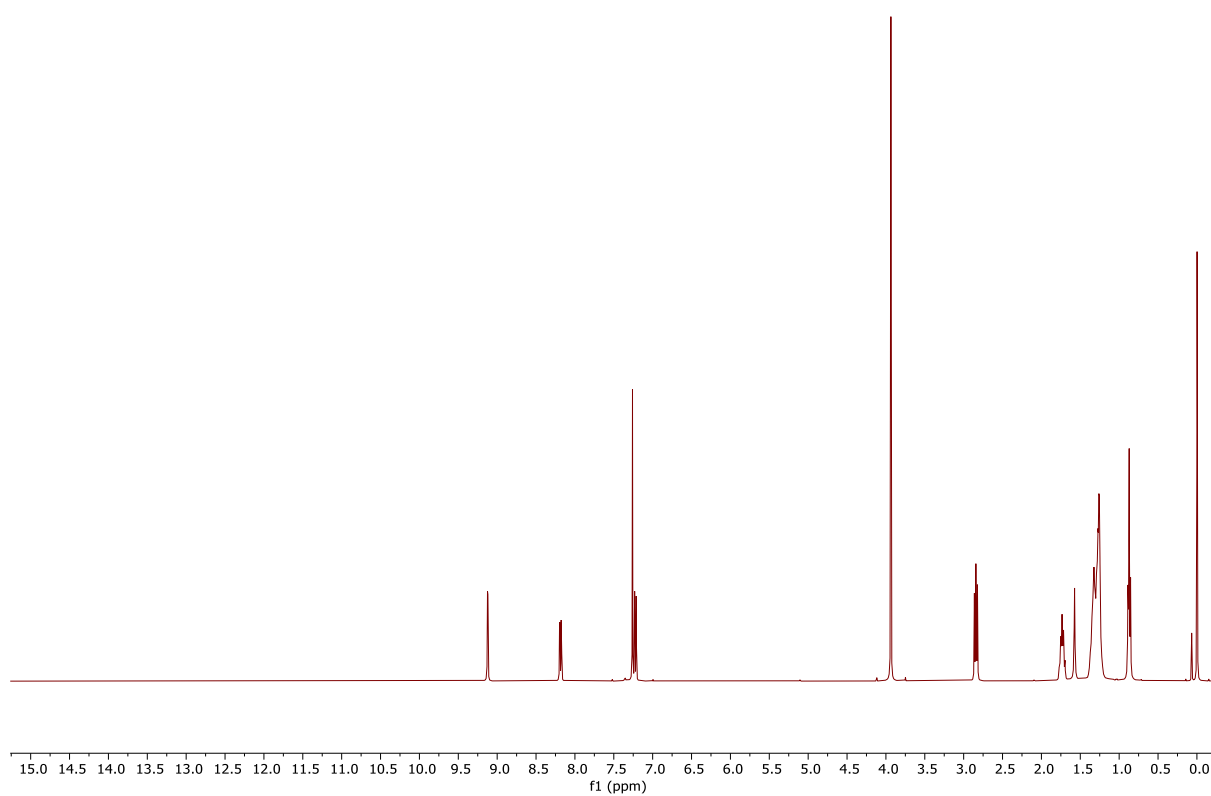


Figure 127: ¹H NMR spectrum (400 MHz, CDCl₃) of compound **28** (Chapter 3).

GGX542_CARBON_01
GGX542_CDCI3

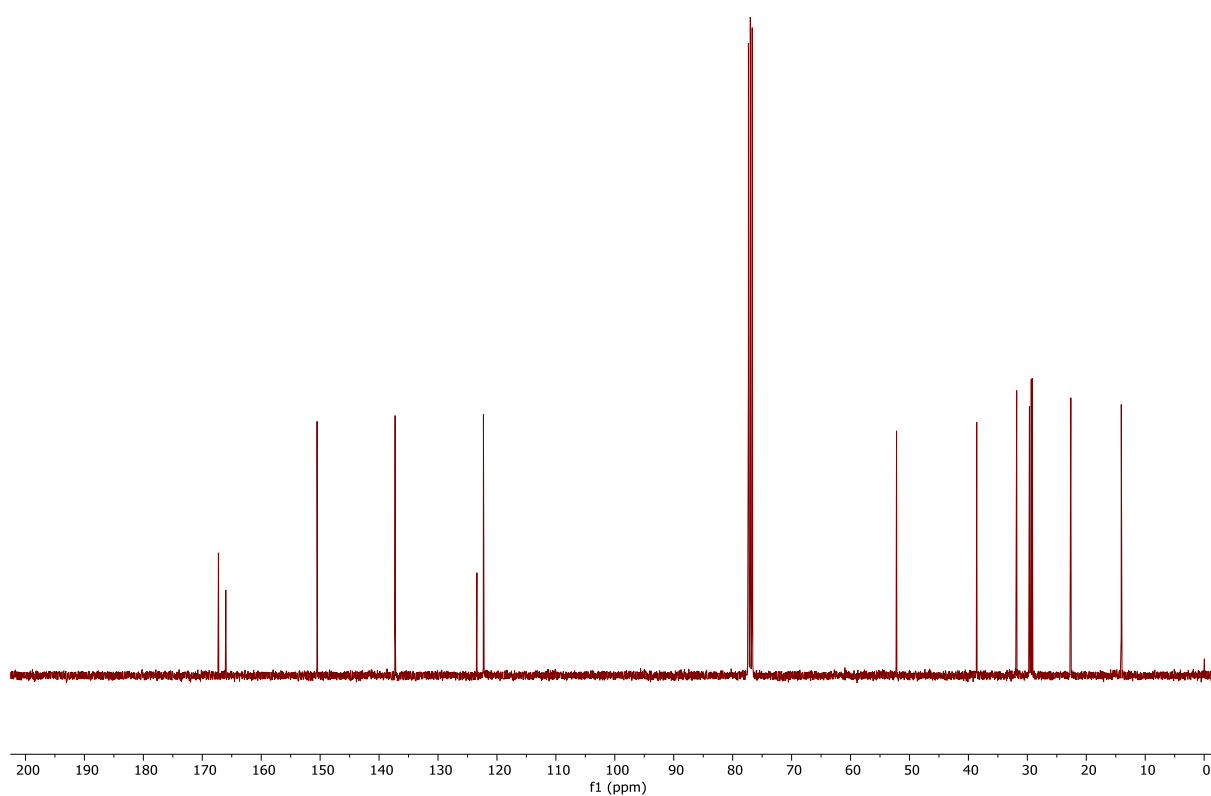


Figure 128: ¹³C NMR spectrum (101 MHz, CDCl₃) of compound **28** (Chapter 3).

GGX547_PROTON_01
GGX547/DMSO-d6/1H
Fuchs 20220714_05
Thu Jul 14 10:53 2022

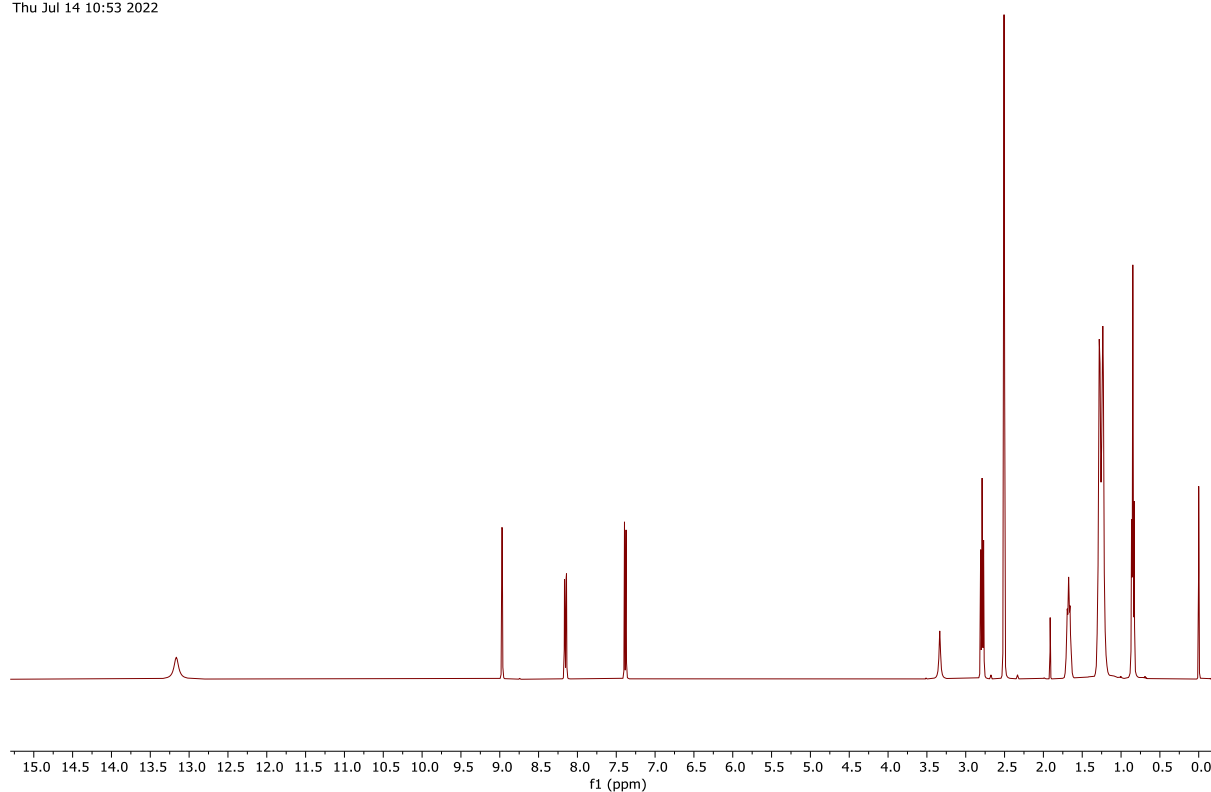


Figure 129: ¹H NMR spectrum (400 MHz, (CD₃)₂SO) of compound **29** (Chapter 3).

GGX547_CARBON_01
GGX547/DMSO-d6/13C
Fuchs 20220714_05
Thu Jul 14 11:21 2022

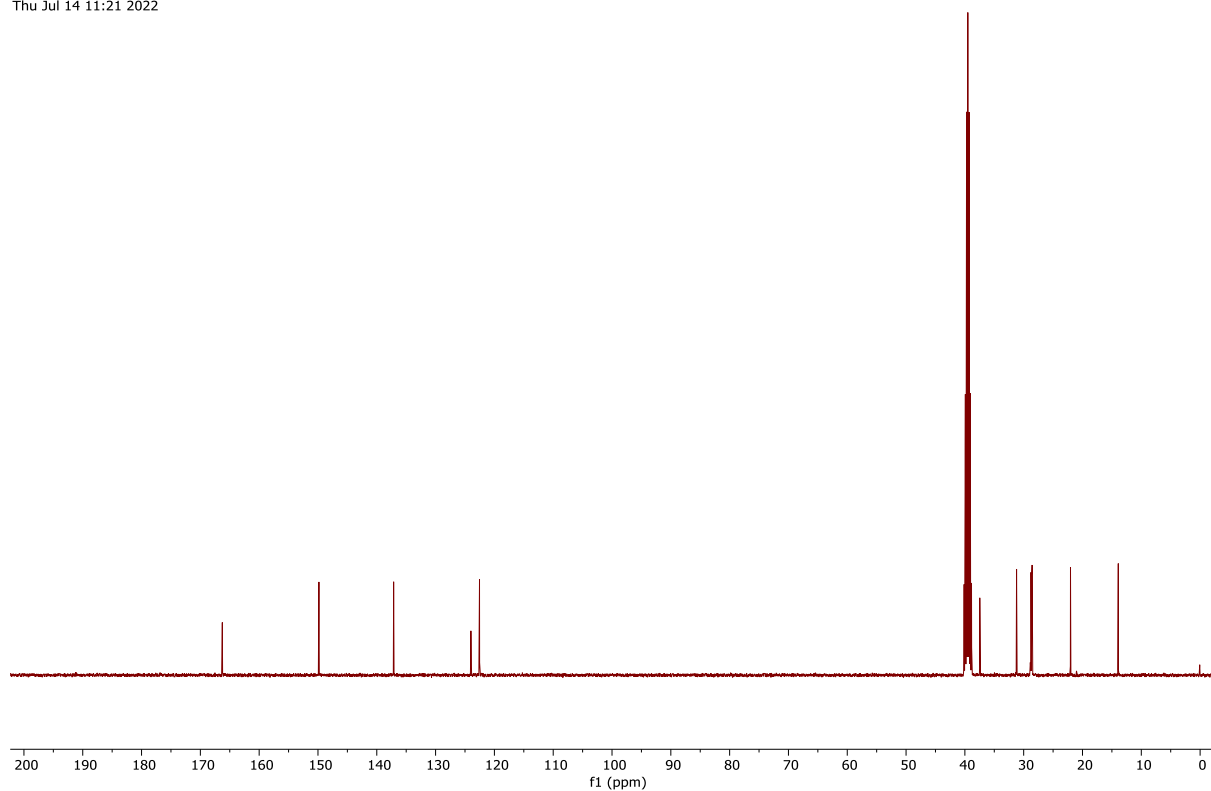


Figure 130: ¹³C NMR spectrum (101 MHz, (CD₃)₂SO) of compound **29** (Chapter 3).

GGX439_PROTON_01
GGX439/DMSO-d6/1H
Fuchs 20210401_03
Thu Apr 1 10:32 2021

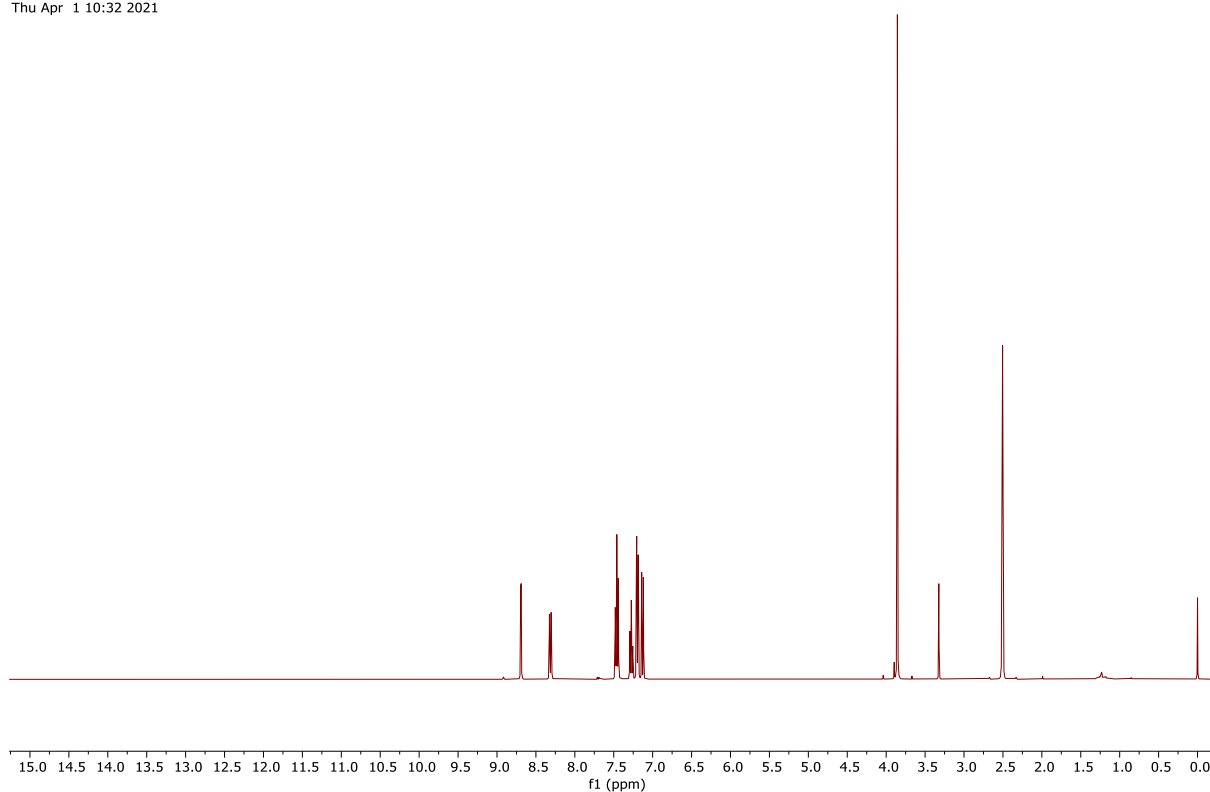


Figure 131: ¹H NMR spectrum (400 MHz, (CD₃)₂SO) of compound **30** (Chapter 3).

GGX439_CARBON_01
GGX439/DMSO-d6/13C
Fuchs 20210401_03
Thu Apr 1 19:13 2021

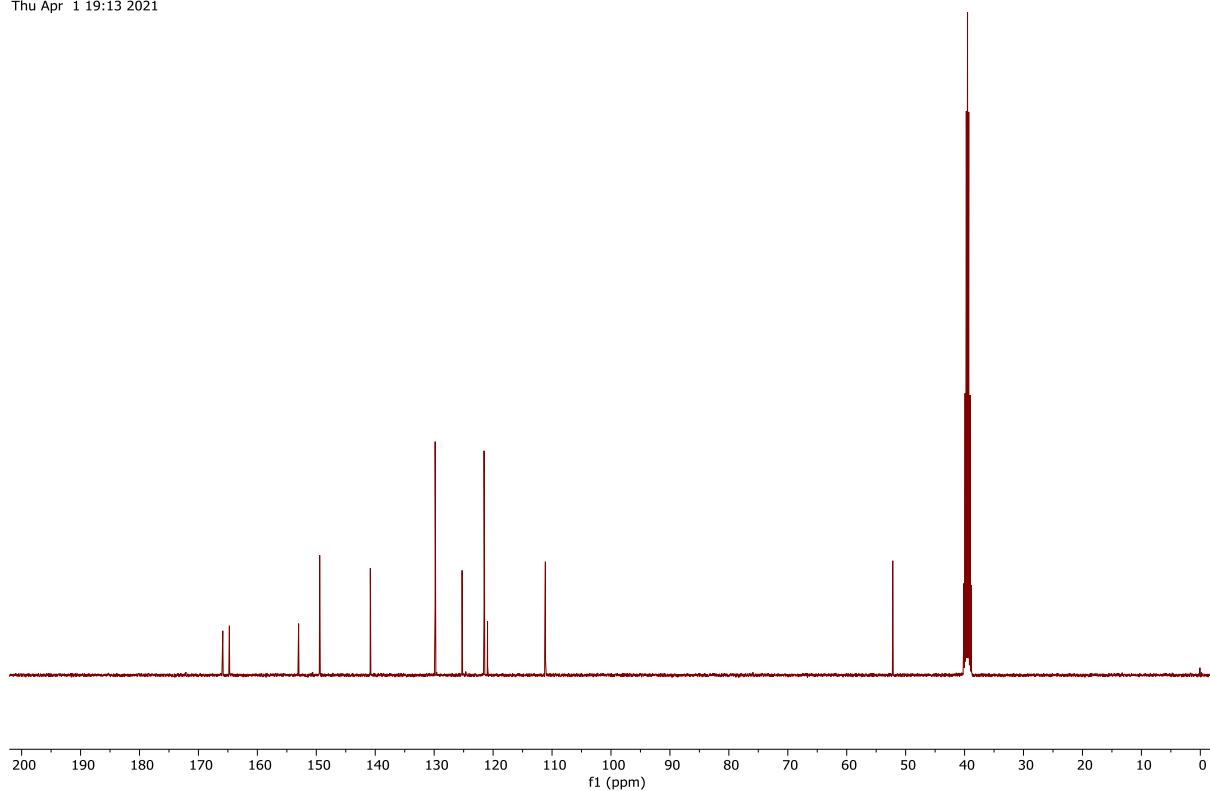


Figure 132: ¹³C NMR spectrum (101 MHz, (CD₃)₂SO) of compound **30** (Chapter 3).

GGX440_PROTON_01
GGX440/DMSO-d6/1H
Fuchs 20210401_04
Thu Apr 1 12:02 2021

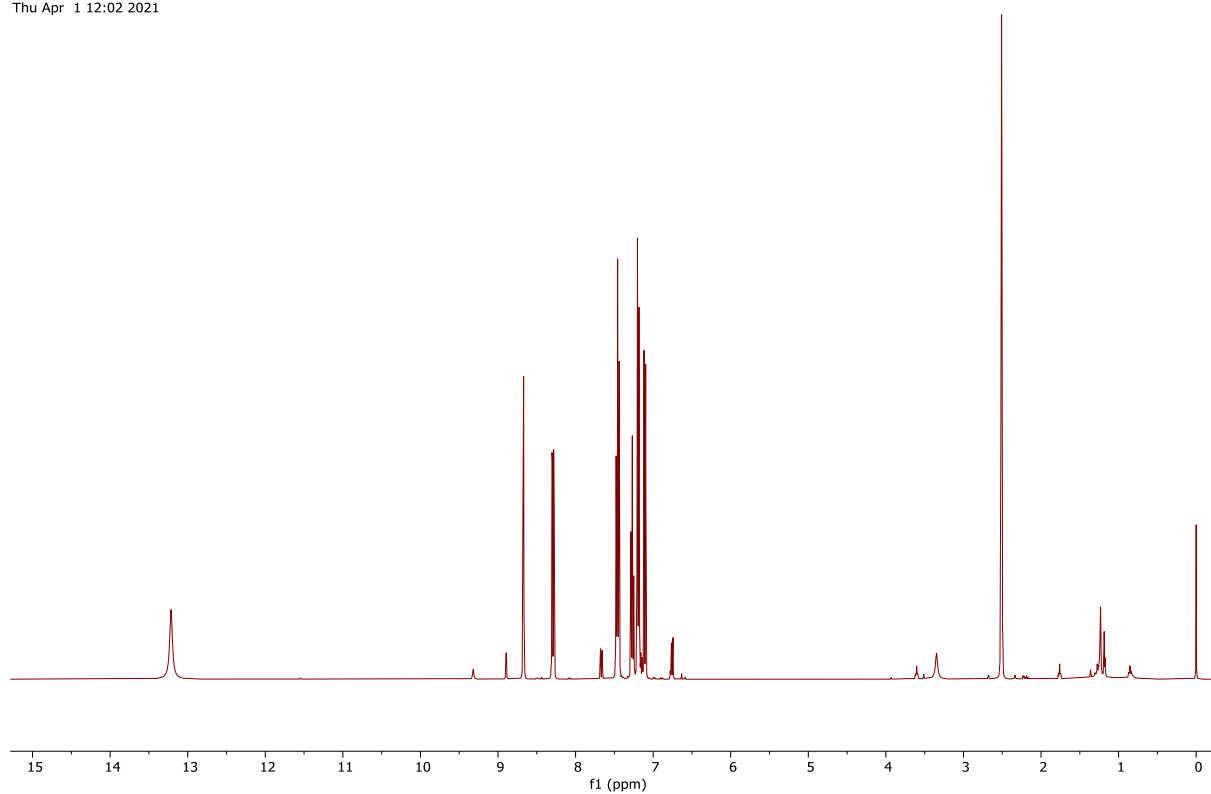


Figure 133: ¹H NMR spectrum (400 MHz, (CD₃)₂SO) of compound **31** (Chapter 3).

GGX440_CARBON_01
GGX440/DMSO-d6/13C
Fuchs 20210401_04
Thu Apr 1 20:58 2021

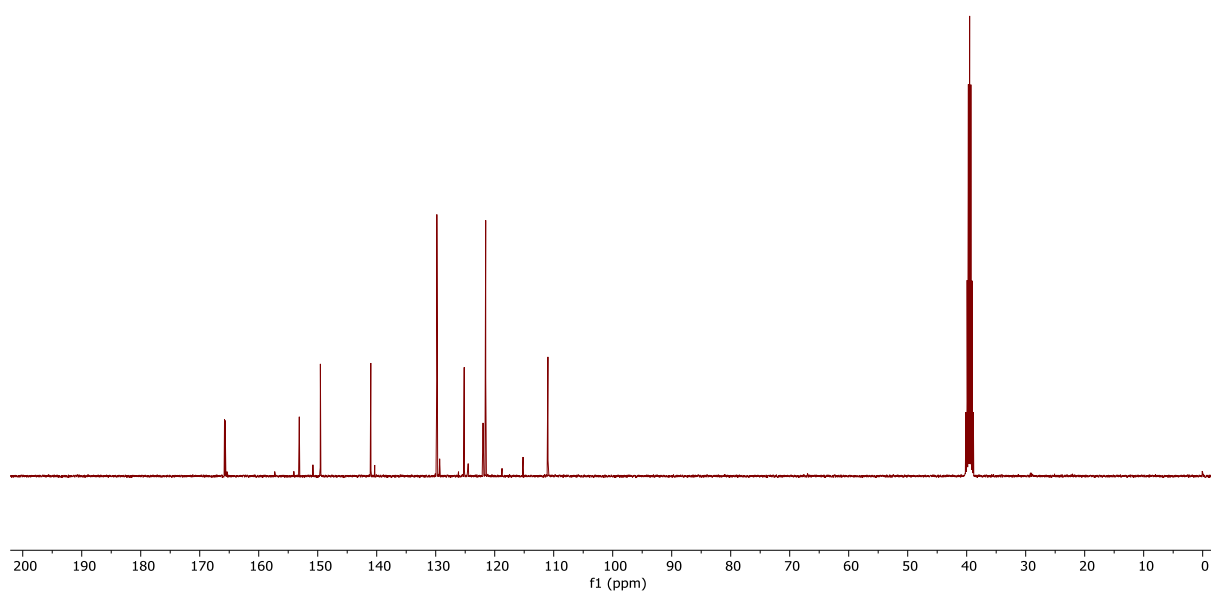


Figure 134: ¹³C NMR spectrum (101 MHz, (CD₃)₂SO) of compound **31** (Chapter 3).

GGX405_PROTON_01
GGX405/DMSO-d6/1H
Fuchs 20201216_01
Wed Dec 16 16:00 2020

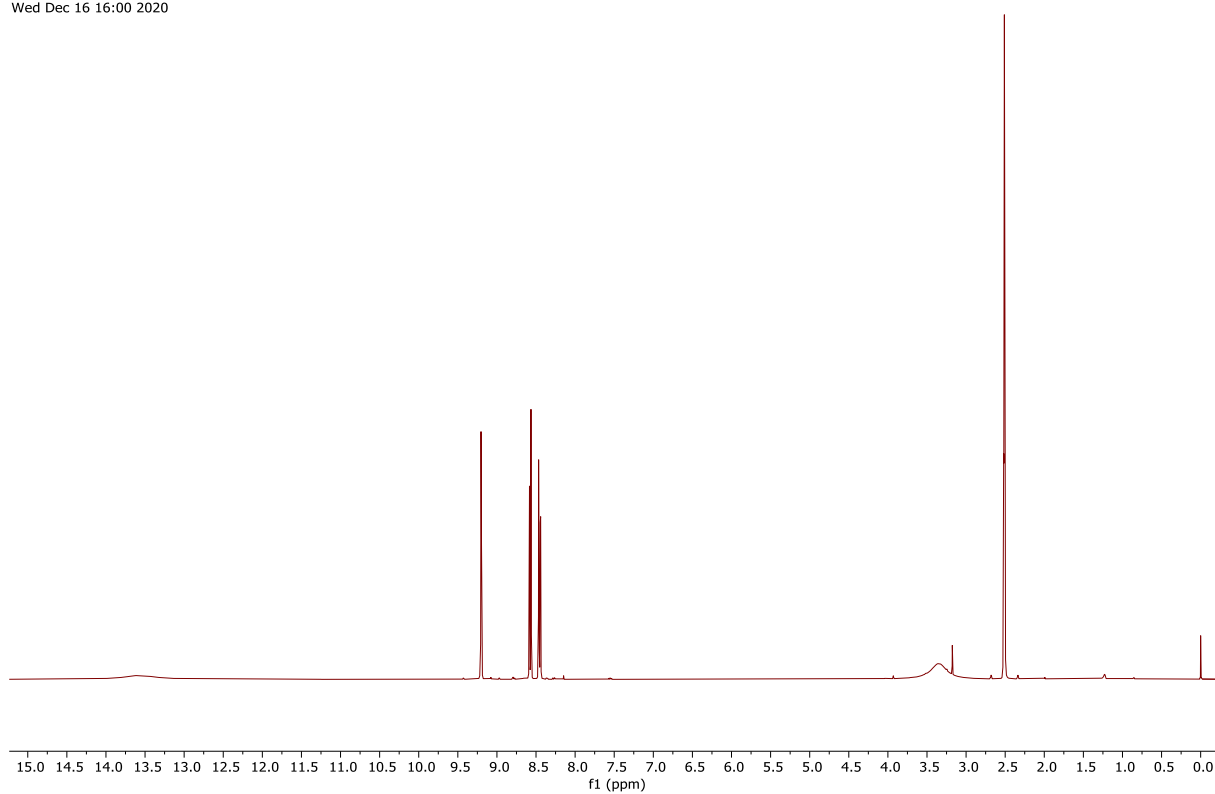


Figure 135: ¹H NMR spectrum (400 MHz, (CD₃)₂SO) of compound **32** (Chapter 3).

GGX405_CARBON_01
GGX405/DMSO-d6/13C
Fuchs 20201216_01
Thu Dec 17 02:33 2020

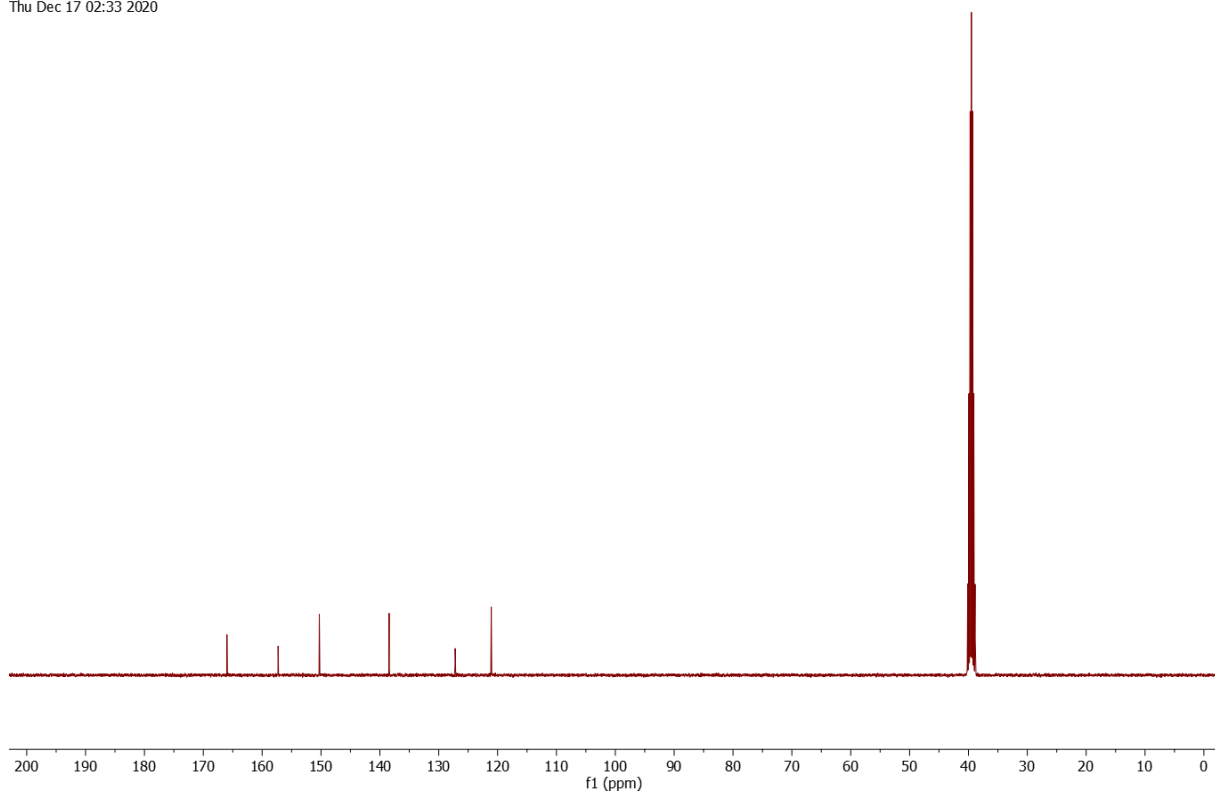


Figure 136: ¹³C NMR spectrum (101 MHz, (CD₃)₂SO) of compound **32** (Chapter 3).

GGX419_PROTON_01
GGX419/DMSO-d6/1H
Fuchs 20210129_01
Fri Jan 29 08:57 2021

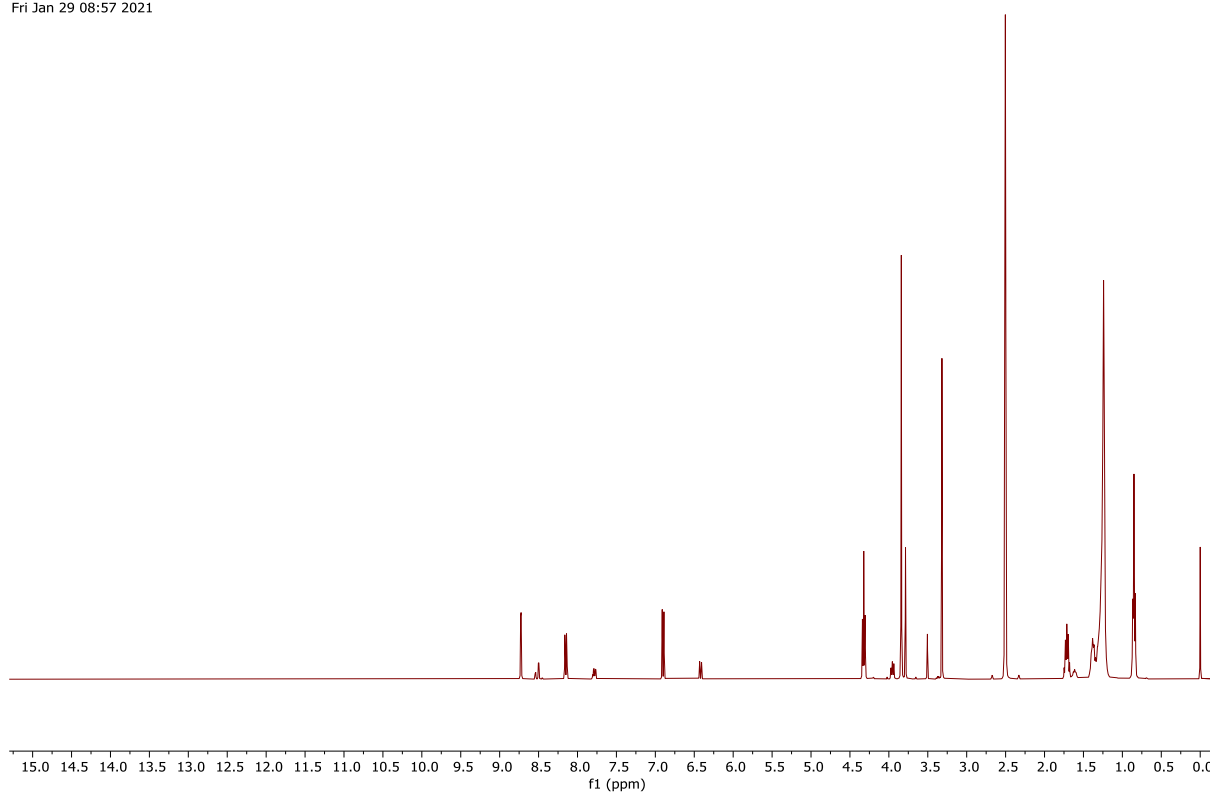


Figure 137: ¹H NMR spectrum (400 MHz, (CD₃)₂SO) of compound **33** (Chapter 3).

GGX419_CARBON_01
GGX419/DMSO-d6/13C
Fuchs 20210201_01
Mon Feb 1 19:12 2021

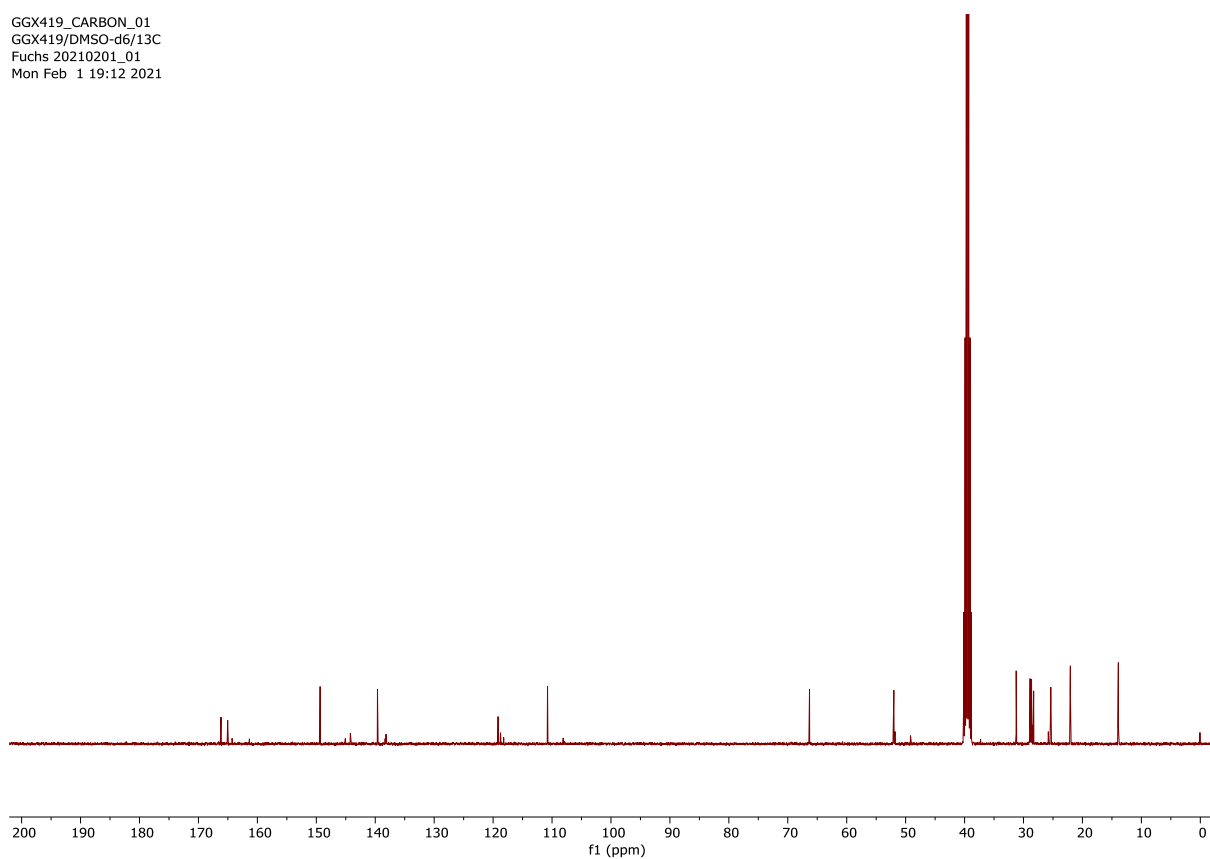


Figure 138: ¹³C NMR spectrum (101 MHz, (CD₃)₂SO) of compound **33** (Chapter 3).

GGX422_PROTON_01
GGX422/DMSO-d6/1H
Fuchs 20210202_10
Wed Feb 3 01:19 2021

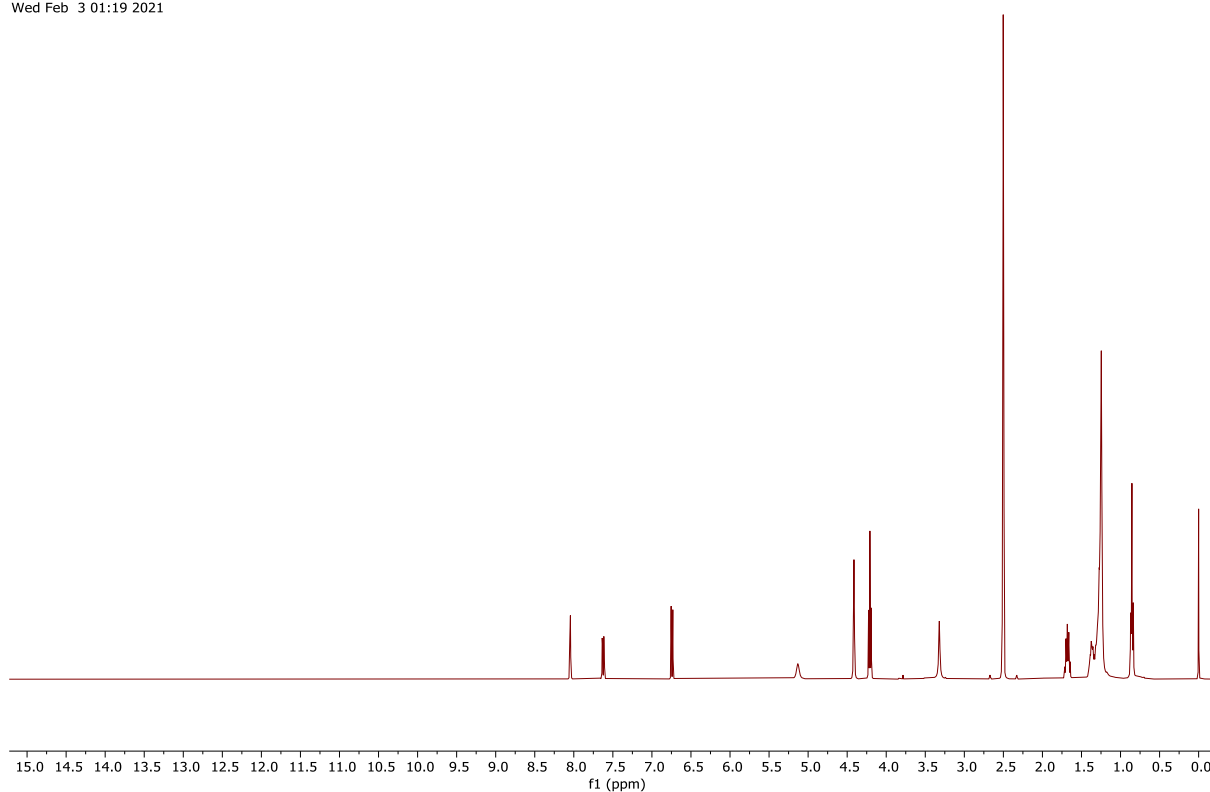


Figure 139: ¹H NMR spectrum (400 MHz, (CD₃)₂SO) of compound **34** (Chapter 3).

GGX422_CARBON_01
GGX422/DMSO-d6/1H
Fuchs 20210202_10
Wed Feb 3 01:22 2021

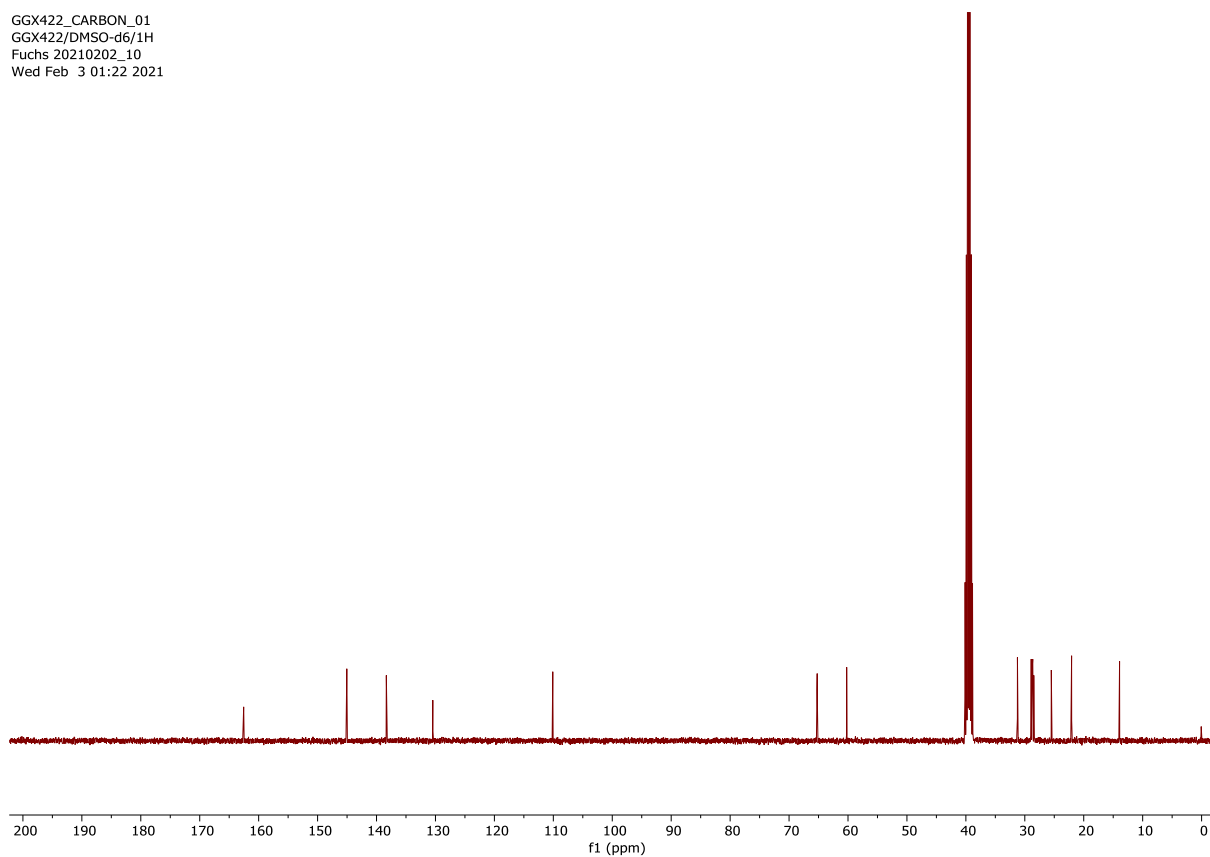


Figure 140: ¹³C NMR spectrum (101 MHz, (CD₃)₂SO) of compound **34** (Chapter 3).

GGX418_PROTON_01
GGX418/DMSO-d6/1H
Fuchs 20210128_02
Thu Jan 28 10:40 2021

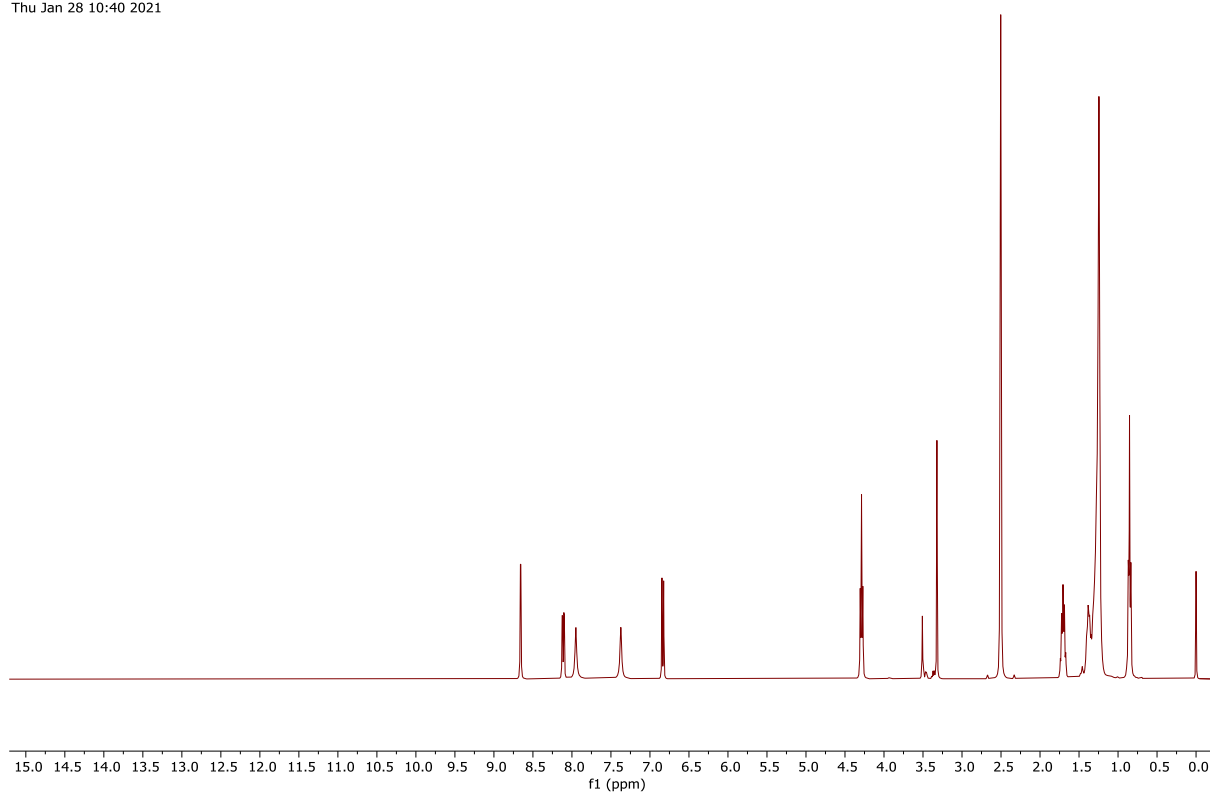


Figure 141: ¹H NMR spectrum (400 MHz, (CD₃)₂SO) of compound **35** (Chapter 3).

GGX418_CARBON_01
GGX418/DMSO-d6/13C
Fuchs 20210128_02
Thu Jan 28 16:29 2021

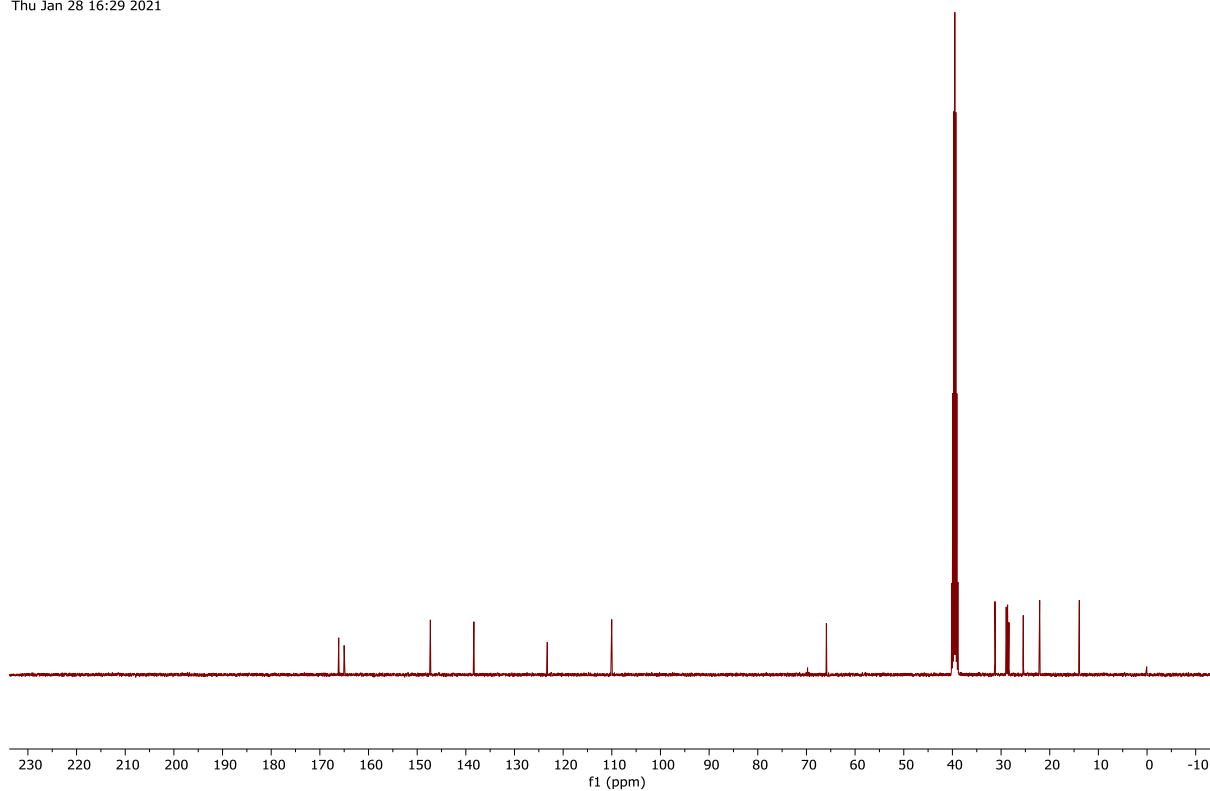


Figure 142: ¹³C NMR spectrum (101 MHz, (CD₃)₂SO) of compound **35** (Chapter 3).

GGX442_PROTON_01
GGX442/DMSO-d6/1H
Fuchs 20210413_05
Tue Apr 13 16:03 2021

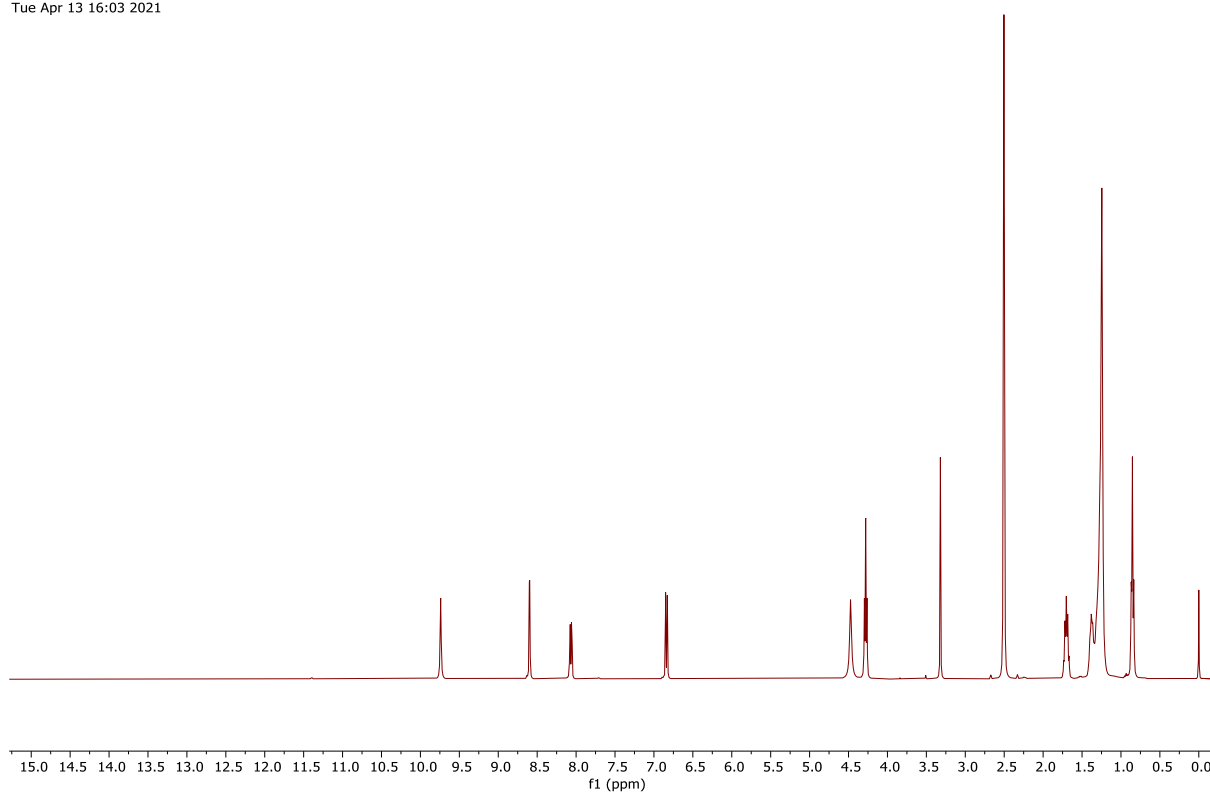


Figure 143: ¹H NMR spectrum (400 MHz, (CD₃)₂SO) of compound **36** (Chapter 3).

GGX442_CARBON_01
GGX442/DMSO-d6/13C
Fuchs 20210413_05
Tue Apr 13 16:05 2021

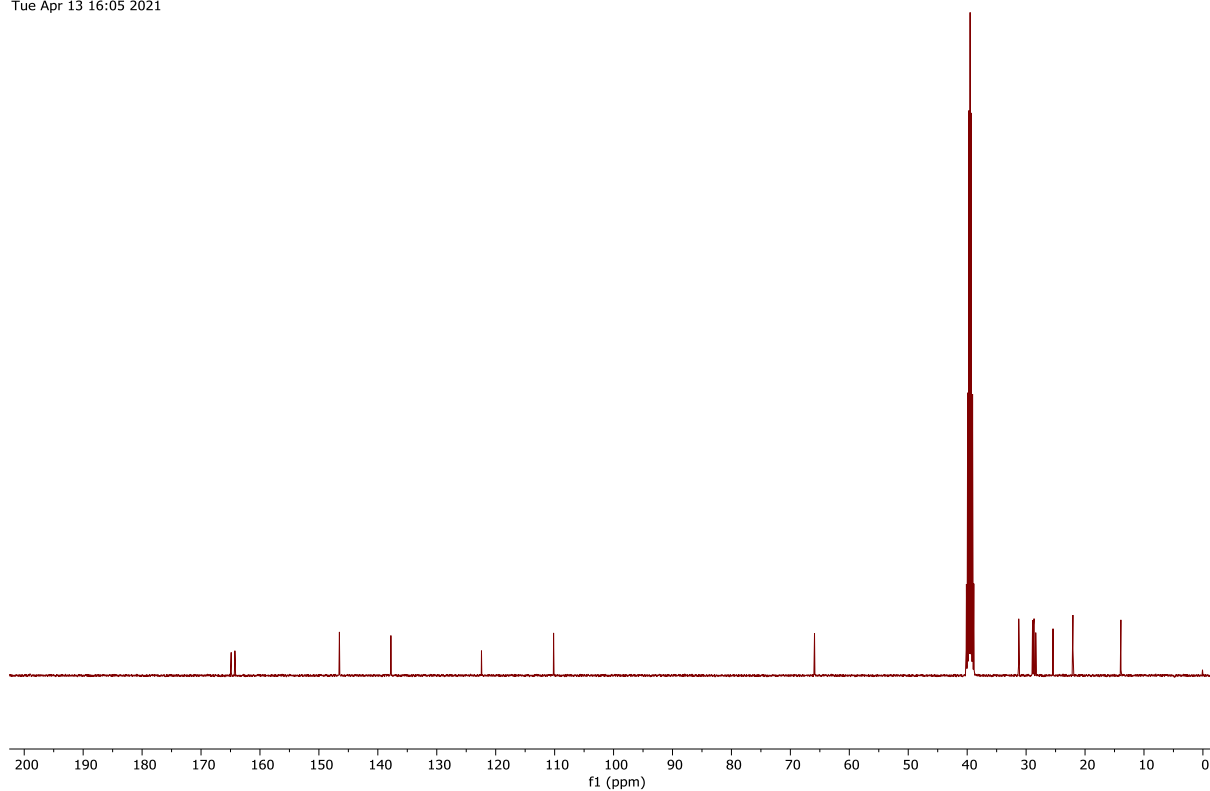


Figure 144: ¹³C NMR spectrum (101 MHz, (CD₃)₂SO) of compound **36** (Chapter 3).

GGX420_PROTON_01
GGX420/DMSO-d6/1H
Fuchs 20210129_02
Fri Jan 29 09:42 2021

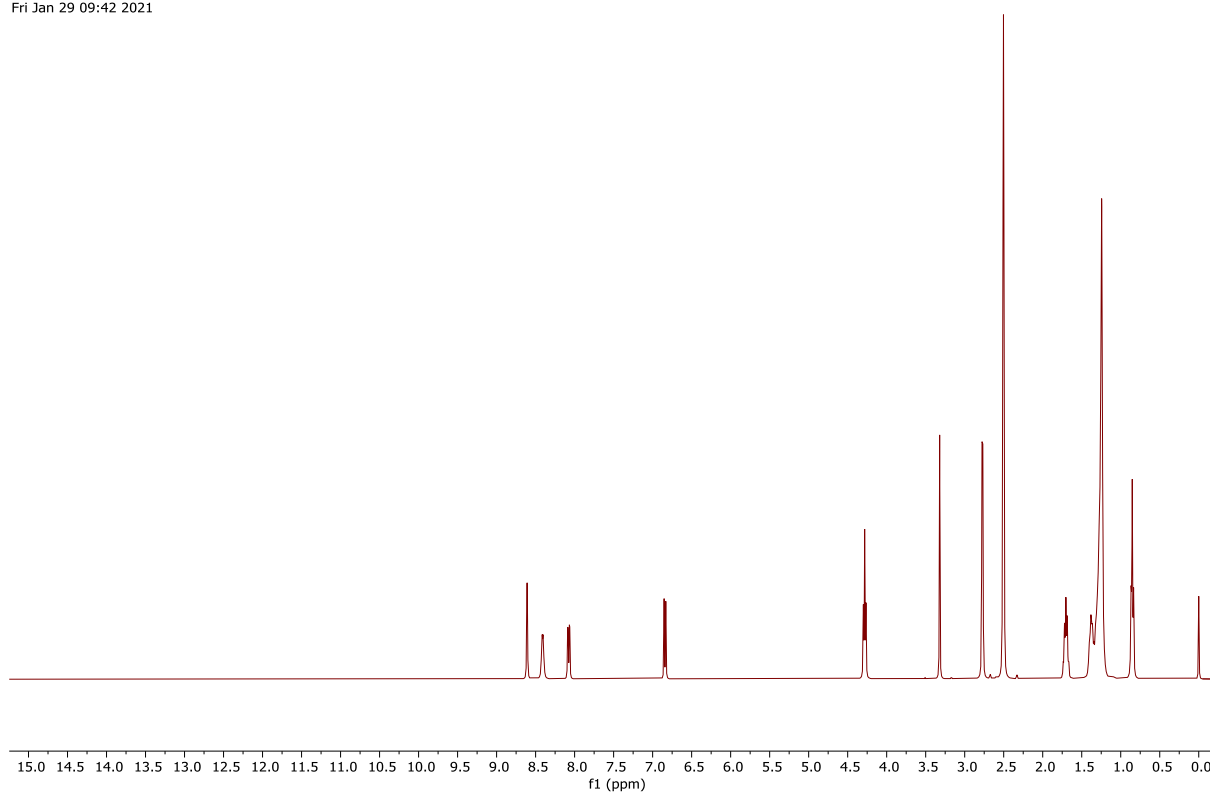


Figure 145: ¹H NMR spectrum (400 MHz, (CD₃)₂SO) of compound **37** (Chapter 3).

GGX420_CARBON_01
GGX420/DMSO-d6/13C
Fuchs 20210201_02
Mon Feb 1 23:29 2021

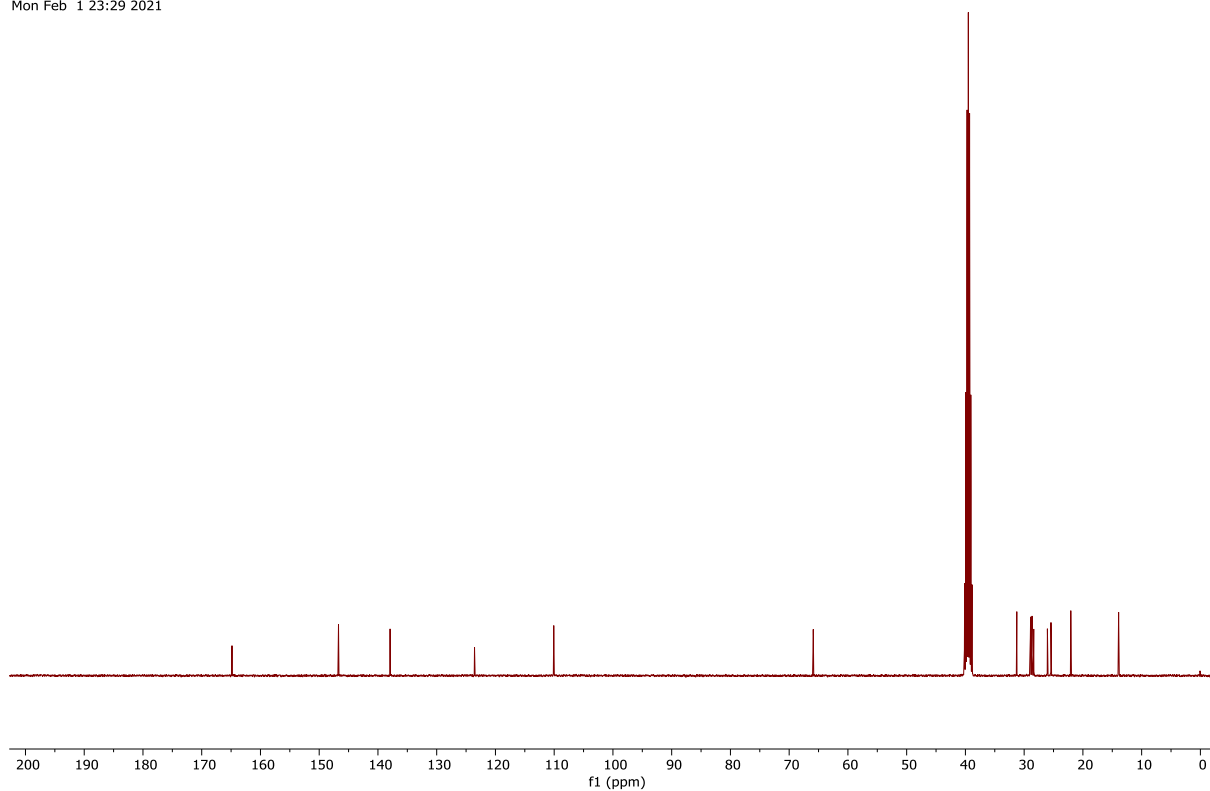


Figure 146: ¹³C NMR spectrum (101 MHz, (CD₃)₂SO) of compound **37** (Chapter 3).

GGX411_PROTON_01
GGX411/CDCl₃/1H
Fuchs 20210120_02
Wed Jan 20 14:02 2021

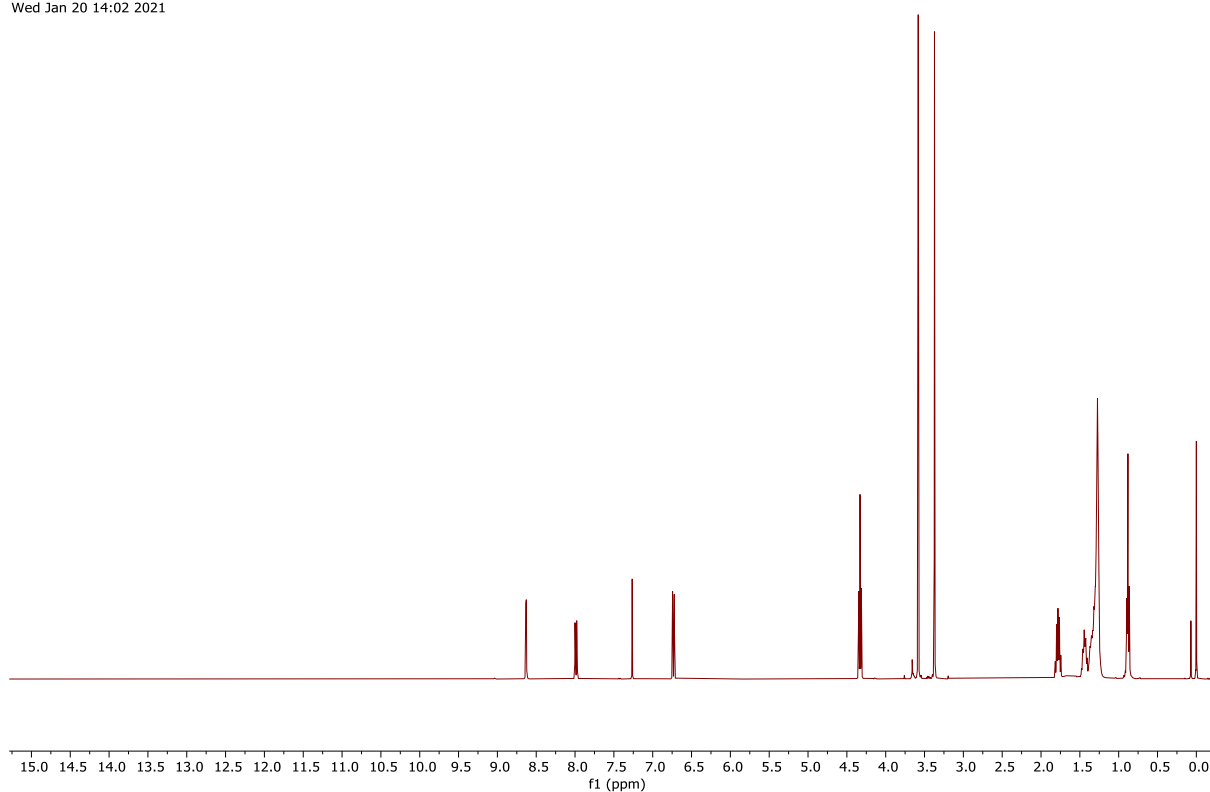


Figure 147: ¹H NMR spectrum (400 MHz, CDCl₃) of compound **38** (Chapter 3).

GGX411_CARBON_01
GGX411/CDCl₃/13C
Fuchs 20210120_02
Wed Jan 20 15:54 2021

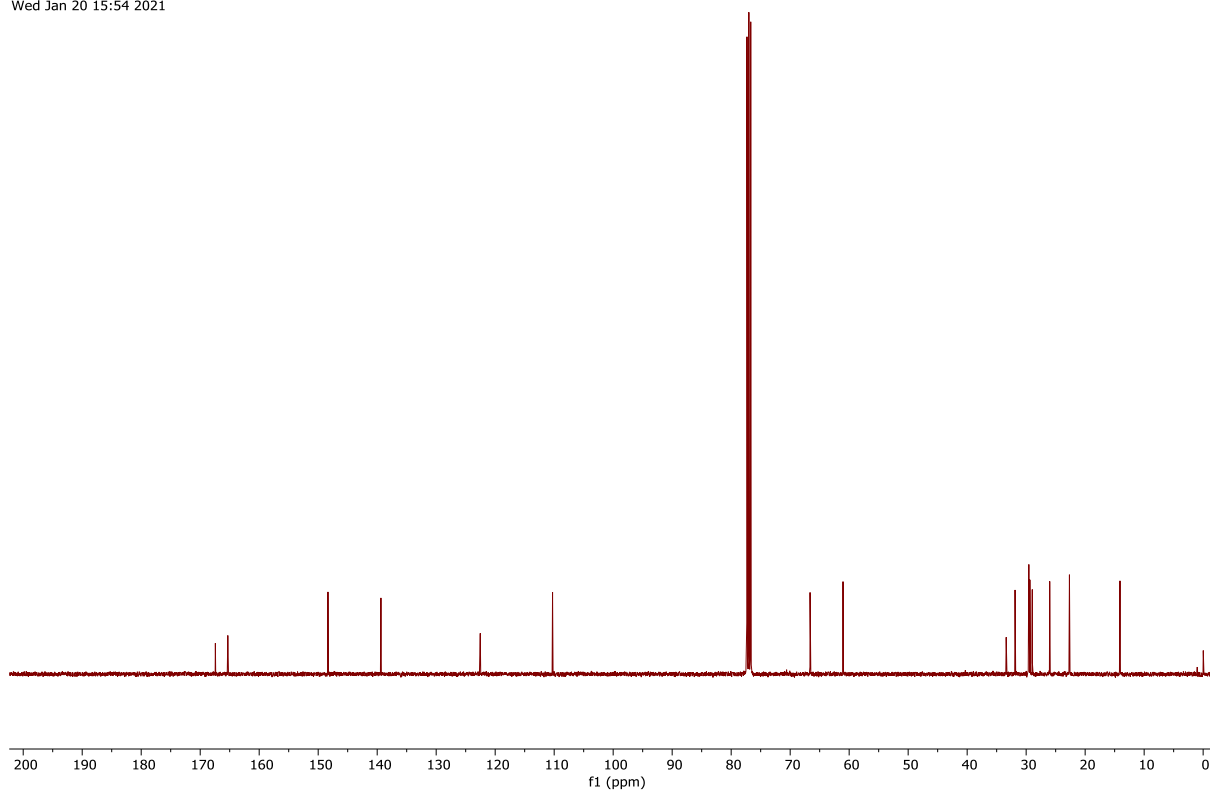


Figure 148: ¹³C NMR spectrum (101 MHz, CDCl₃) of compound **38** (Chapter 3).

GGX617_PROTON_01
GGX617/CDCl₃/1H
Fuchs 20221114_06
Mon Nov 14 09:35 2022

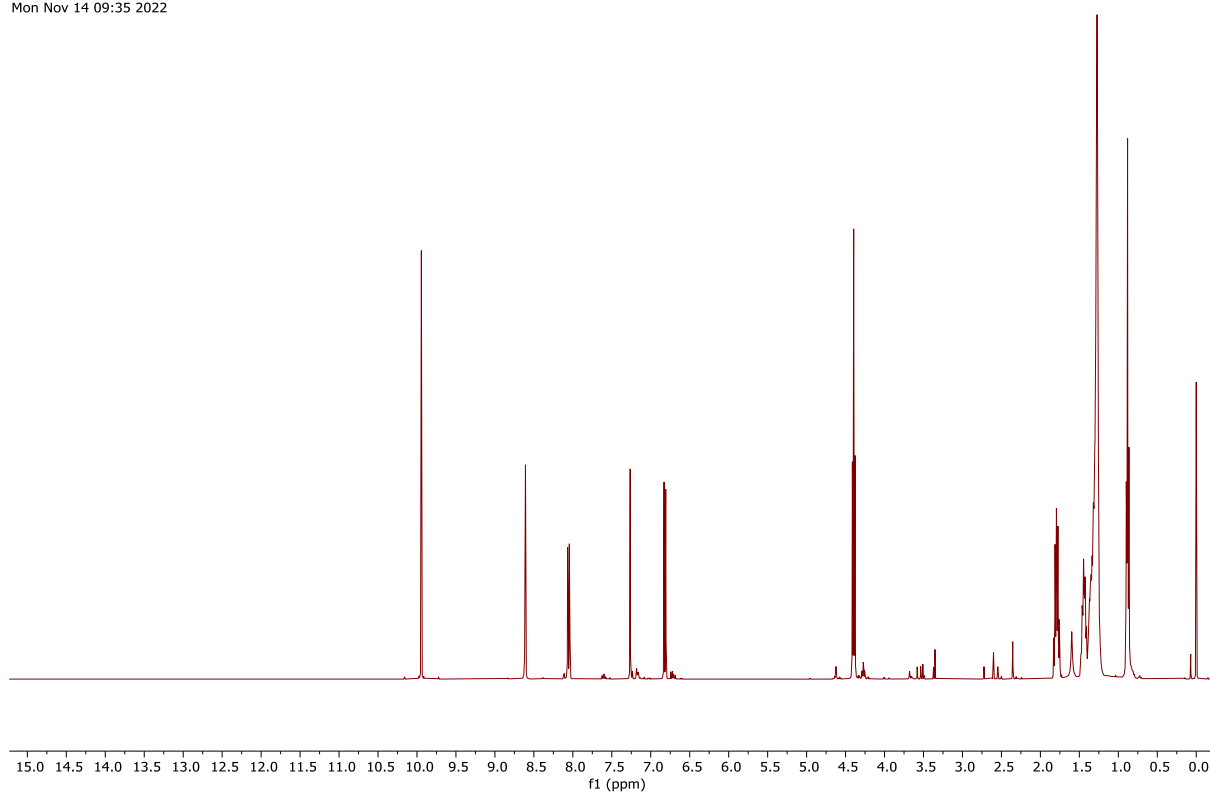


Figure 149: ¹H NMR spectrum (400 MHz, CDCl₃) of compound **39** (Chapter 3).

GGX617_CARBON_01
GGX617/CDCl₃/13C
Fuchs 20221114_06
Mon Nov 14 16:10 2022

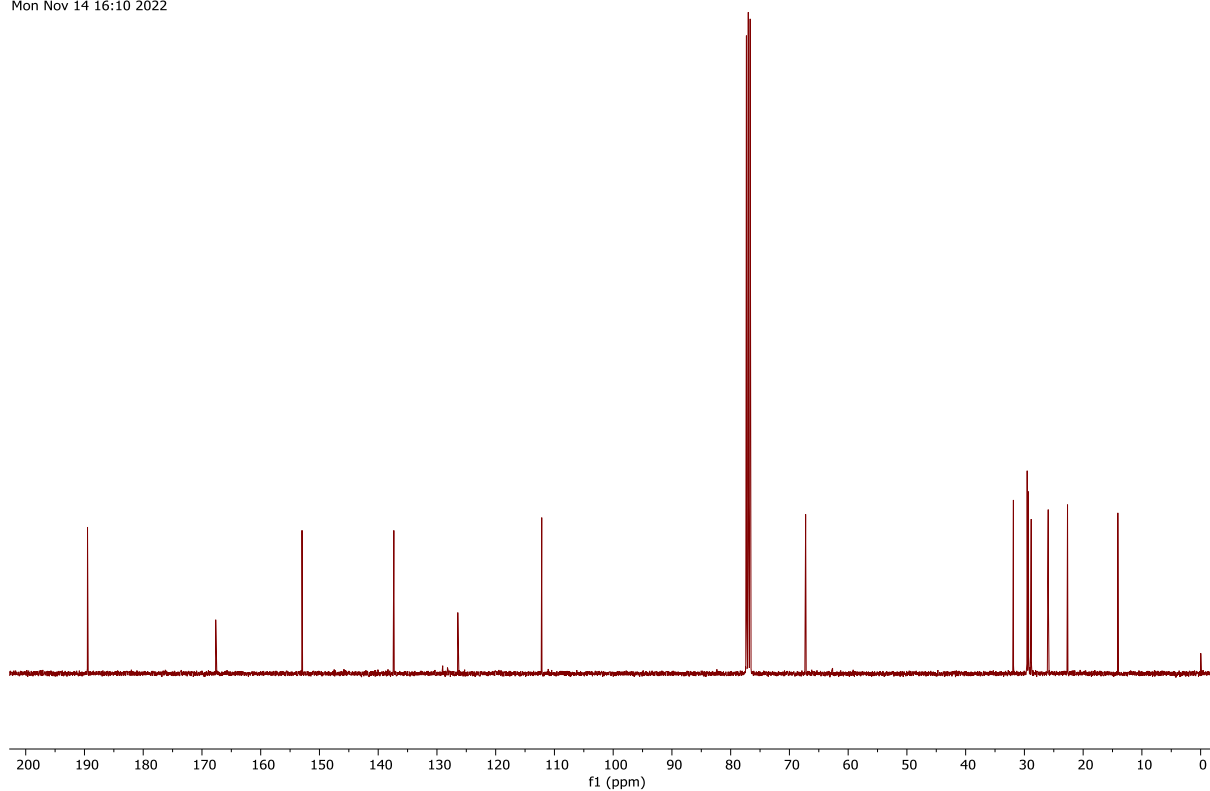


Figure 150: ¹³C NMR spectrum (101 MHz, CDCl₃) of compound **39** (Chapter 3).

GGX523_PROTON_01
GGX523/CDCl₃/1H
Fuchs 20220405_01
Tue Apr 5 15:35 2022

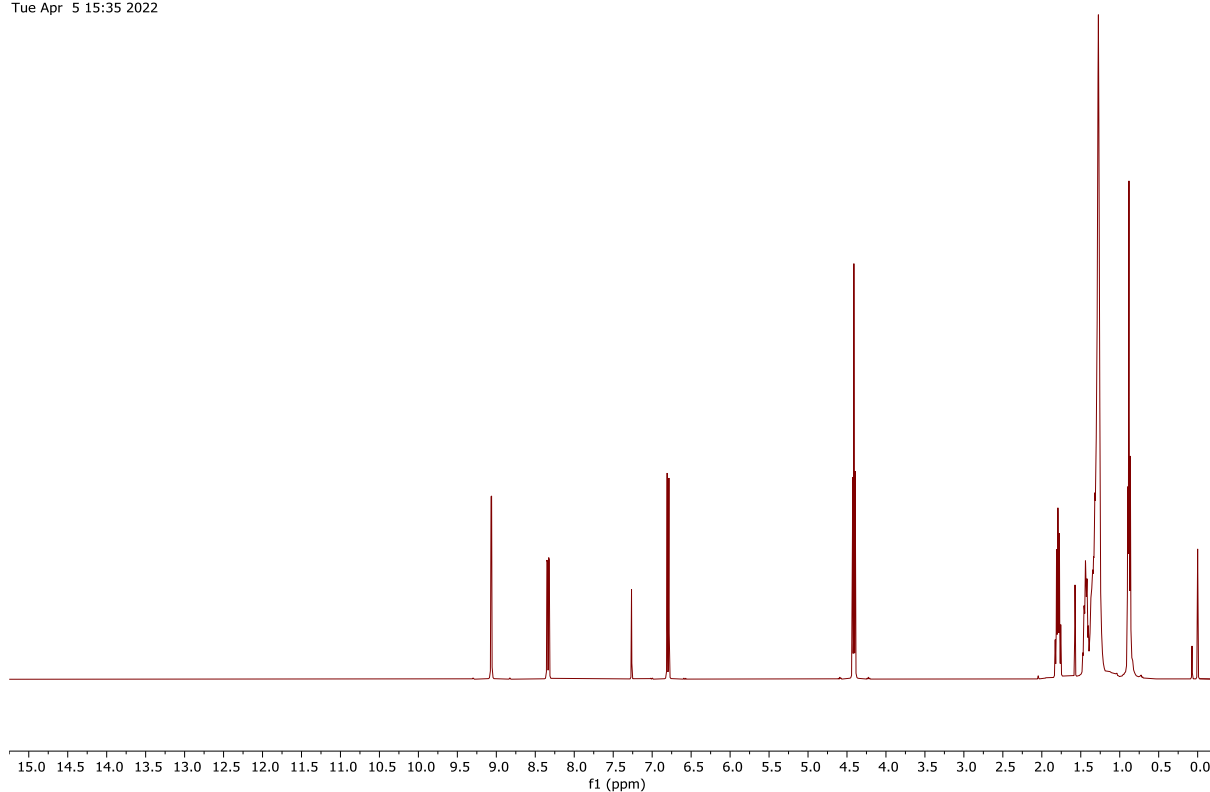


Figure 151: ¹H NMR spectrum (400 MHz, CDCl₃) of compound **40** (Chapter 3).

GGX523_CARBON_01
GGX523/CDCl₃/13C
Fuchs 20220405_01
Tue Apr 5 15:54 2022

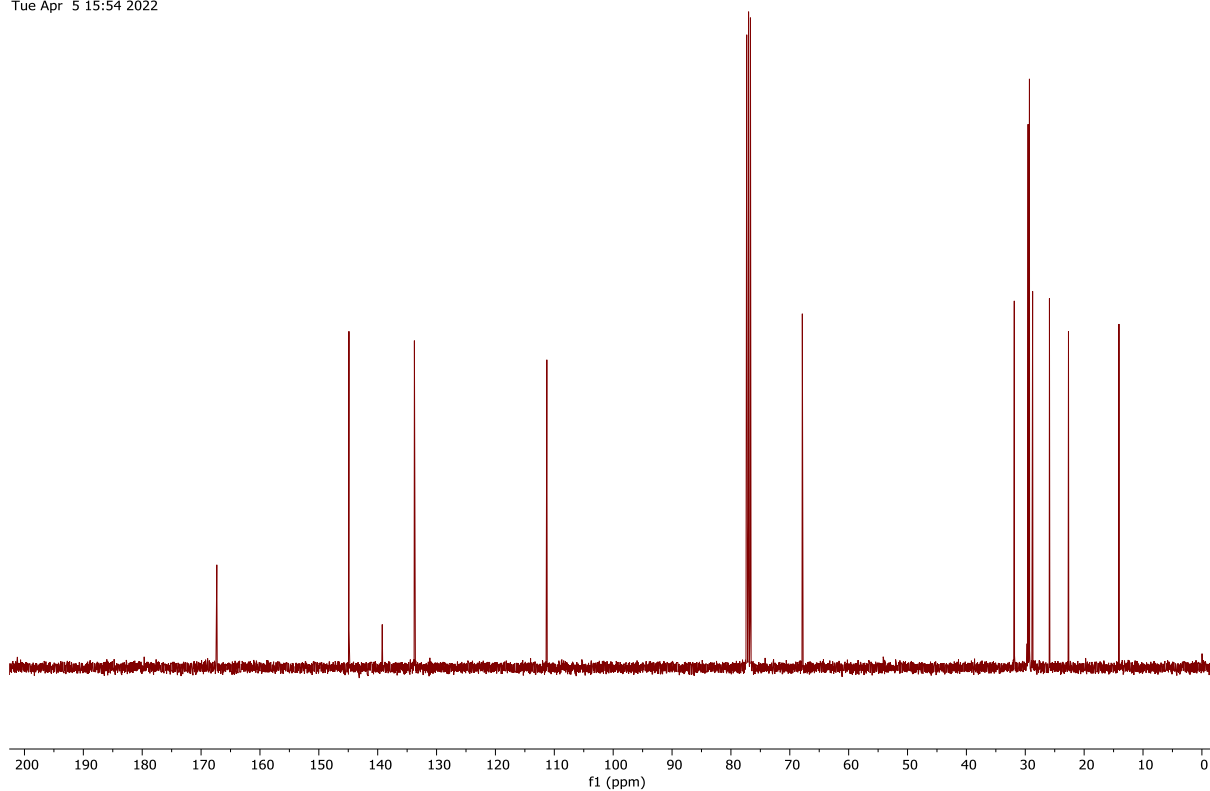


Figure 152: ¹³C NMR spectrum (101 MHz, CDCl₃) of compound **40** (Chapter 3).

GGX527_PROTON_01
GGX527/CDCl₃/1H
Fuchs 20220407_01
Thu Apr 7 08:26 2022

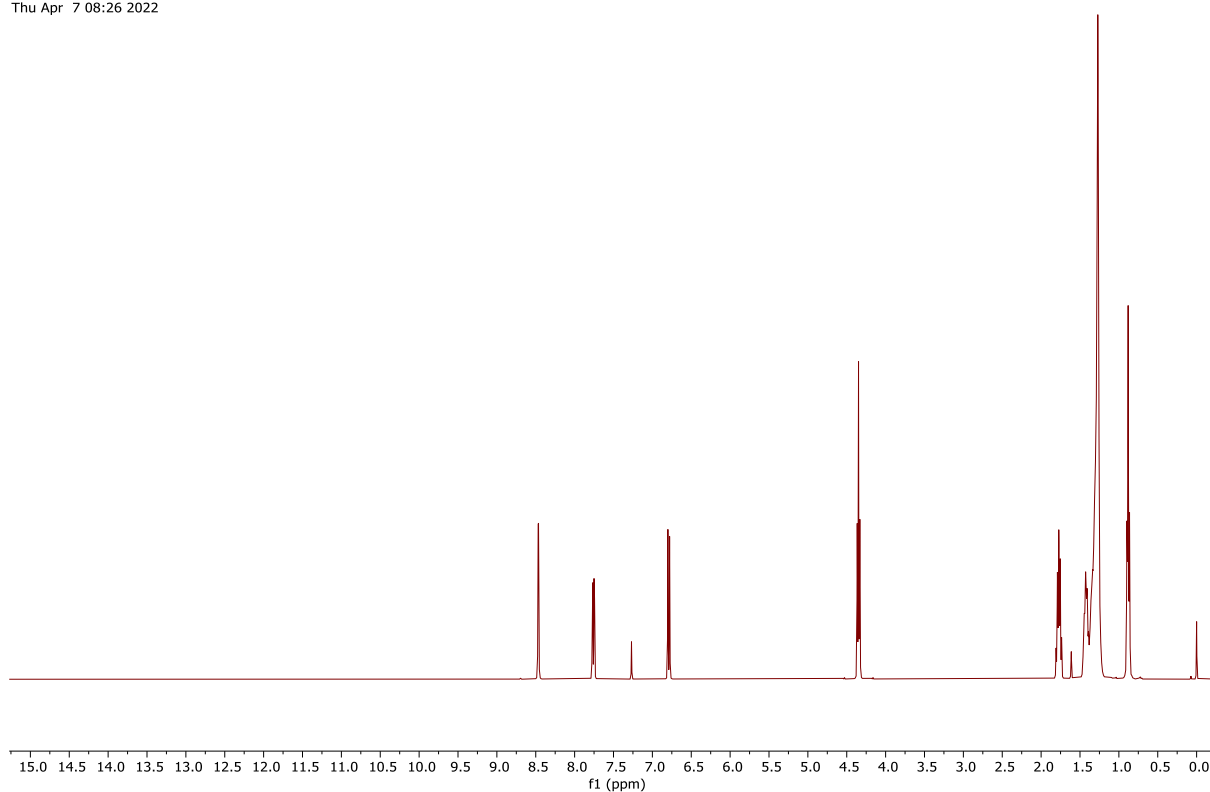


Figure 153: ¹H NMR spectrum (400 MHz, CDCl₃) of compound **41** (Chapter 3).

GGX527_CARBON_01
GGX527/CDCl₃/13C
Fuchs 20220407_01
Thu Apr 7 09:10 2022

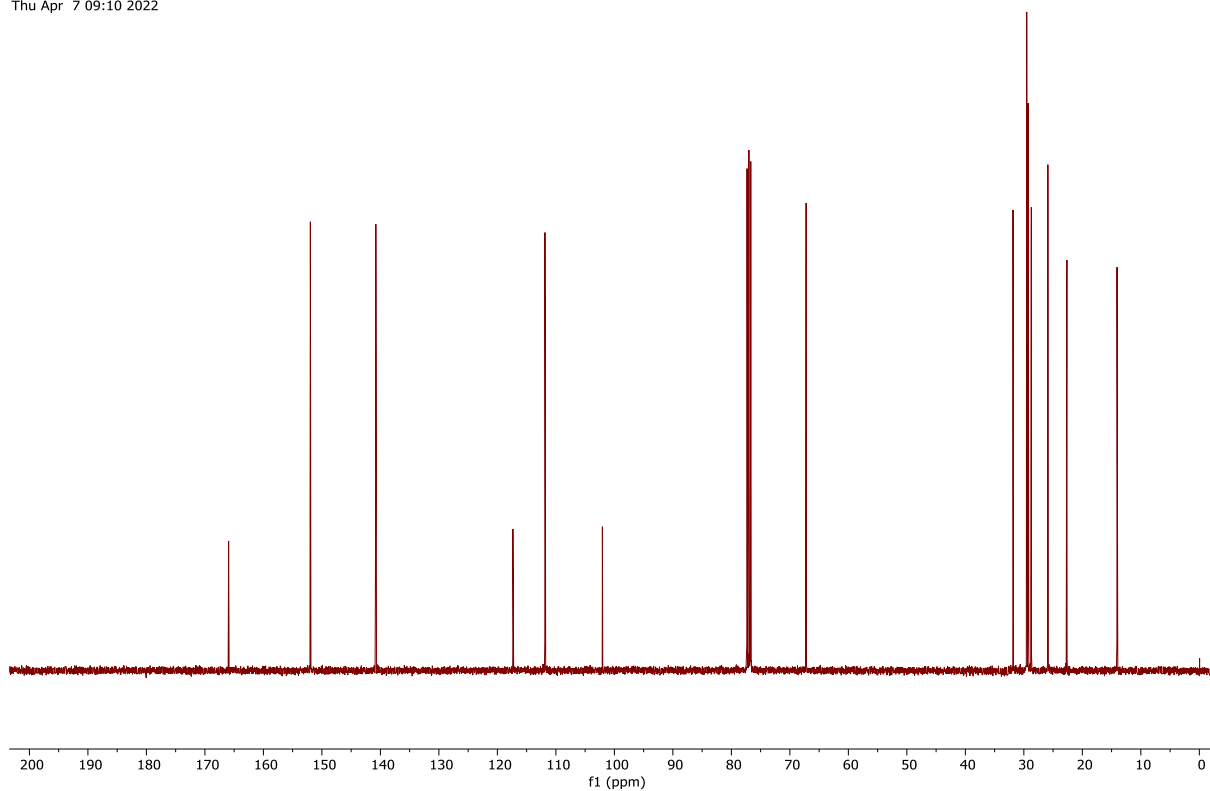


Figure 154: ¹³C NMR spectrum (101 MHz, CDCl₃) of compound **41** (Chapter 3).

GGX528_PROTON_01
GGX528/DMSO-d6/1H
Fuchs 20220408_01
Fri Apr 8 12:34 2022

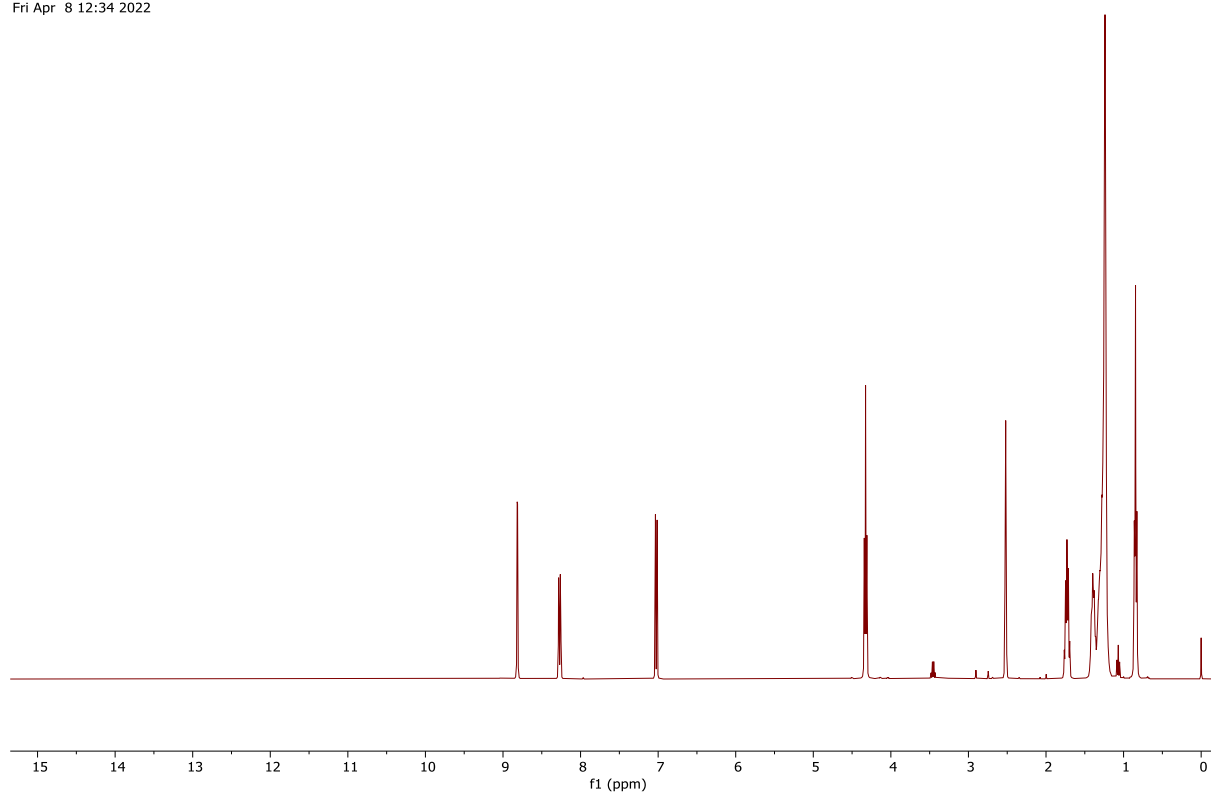


Figure 155: ¹H NMR spectrum (400 MHz, (CD₃)₂SO) of compound **42** (Chapter 3).

GGX528_CARBON_01
GGX528/DMSO-d6/1H
Fuchs 20220408_01

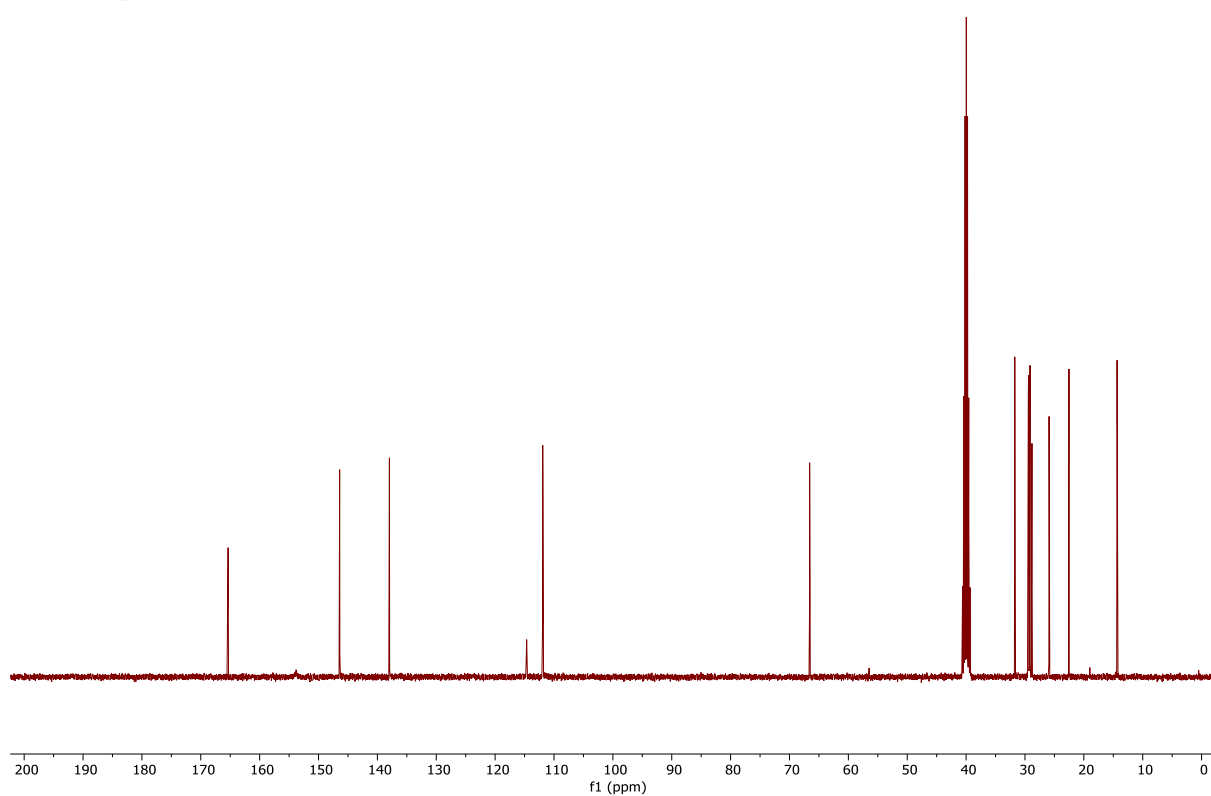


Figure 156: ¹³C NMR spectrum (101 MHz, (CD₃)₂SO) of compound **42** (Chapter 3).

GGX514_PROTON_01
GGX514/CDCl₃/1H
Fuchs 20211124_04
Wed Nov 24 17:27 2021

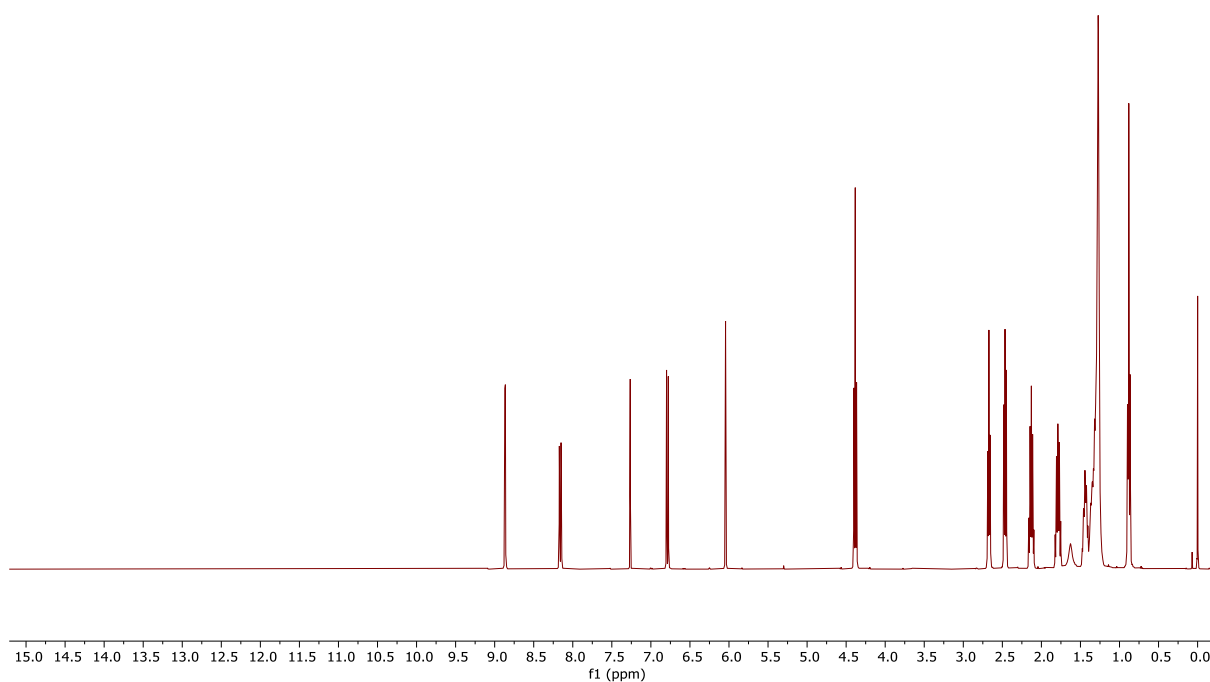


Figure 157: ¹H NMR spectrum (400 MHz, CDCl₃) of compound **43** (Chapter 3).

GGX514_CARBON_01
GGX514/CDCl₃/13C
Fuchs 20211124_04
Wed Nov 24 17:30 2021

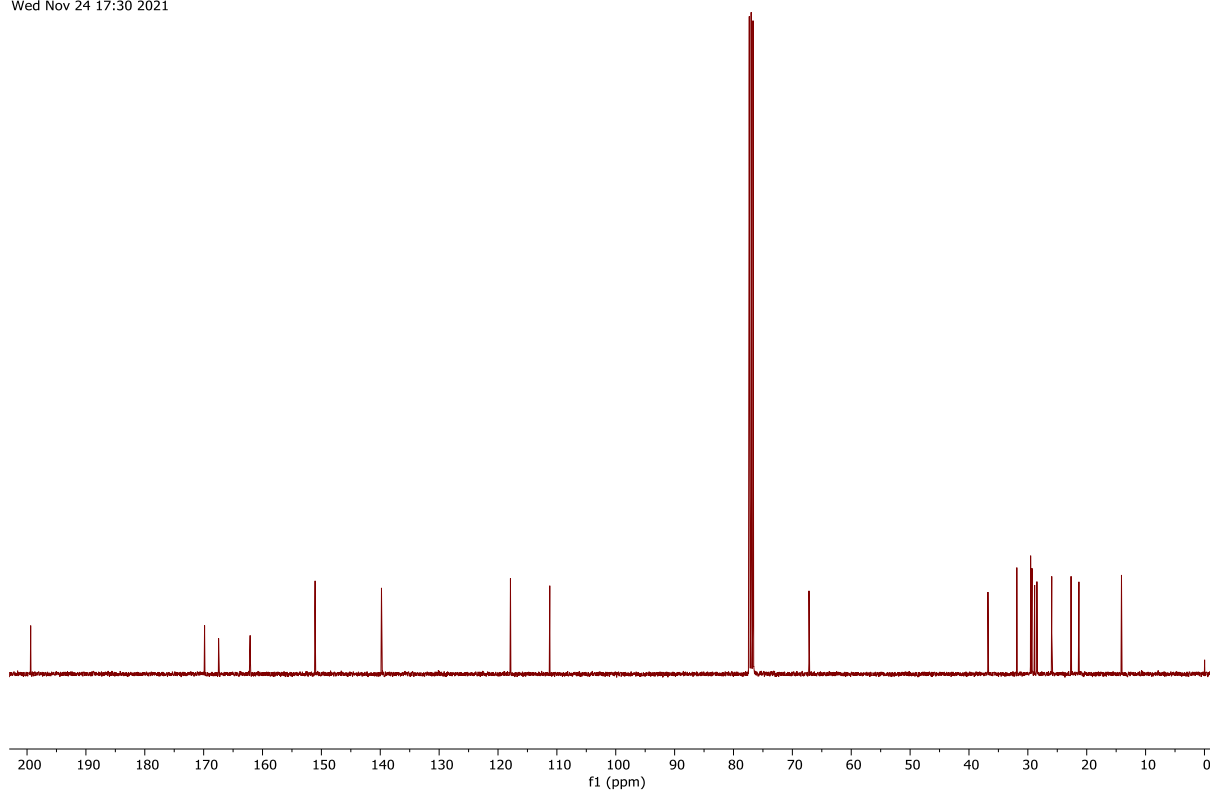


Figure 158: ¹³C NMR spectrum (101 MHz, CDCl₃) of compound **43** (Chapter 3).

GGX515_PROTON_01
GGX515/CDCl₃/1H
Fuchs 20211220_03
Mon Dec 20 16:26 2021

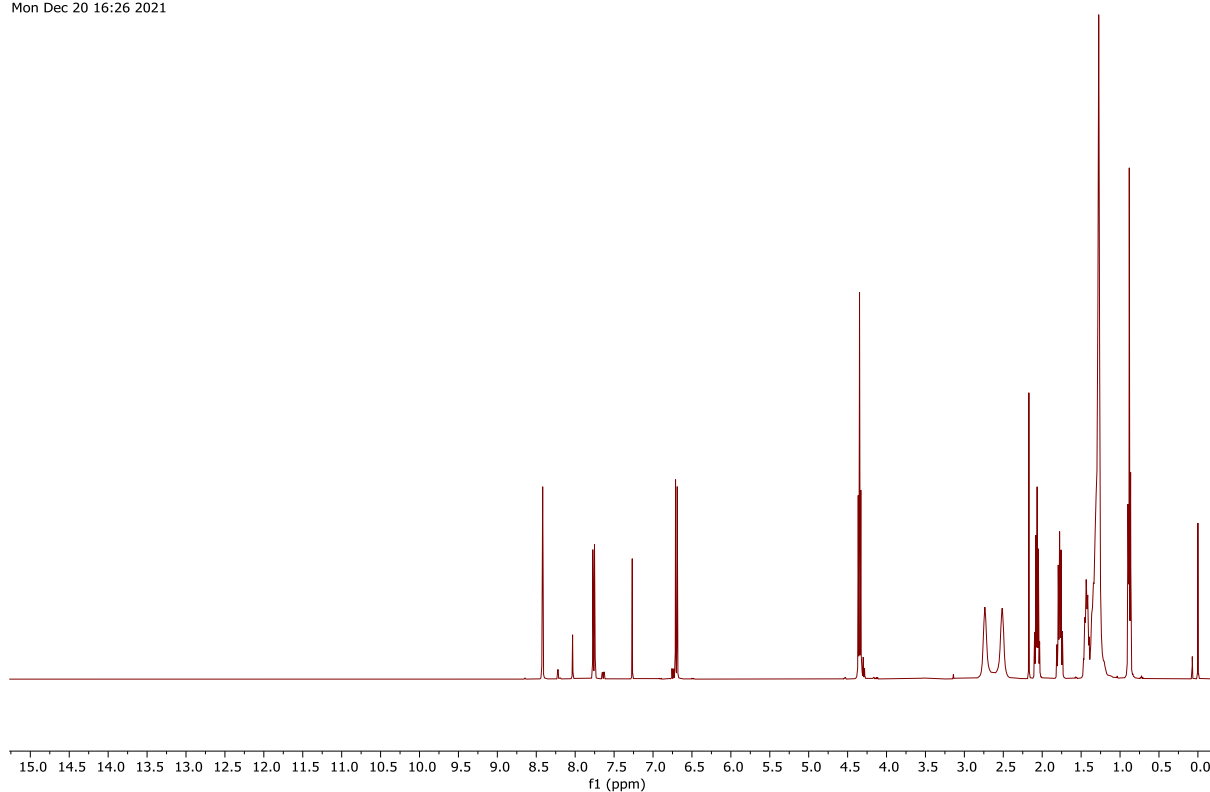


Figure 159: ¹H NMR spectrum (400 MHz, CDCl₃) of compound **44** (Chapter 3).

GGX515_CARBON_01
GGX515/CDCl₃/13C
Fuchs 20211220_03
Mon Dec 20 16:48 2021

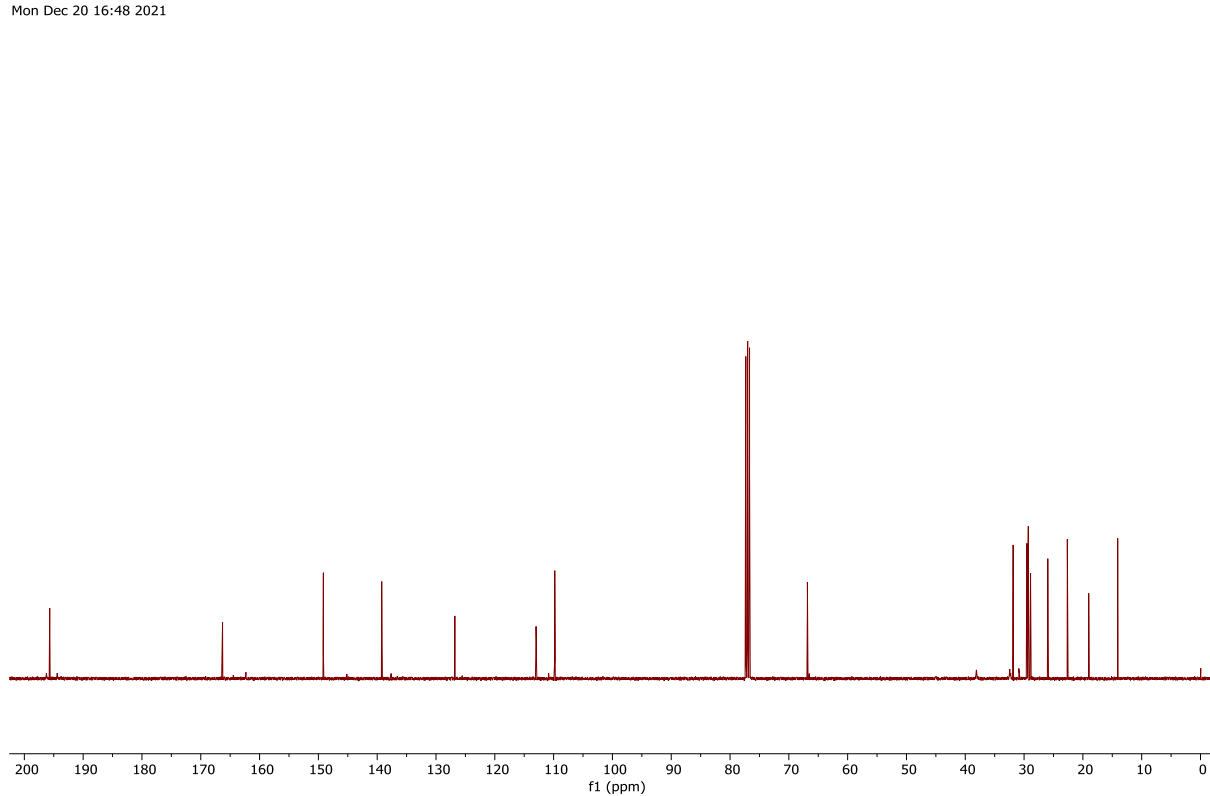


Figure 160: ¹³C NMR spectrum (101 MHz, CDCl₃) of compound **44** (Chapter 3).

GGX470_PROTON_01
GGX470/DMSO-d5/1H
Fuchs 20210701_02
Thu Jul 1 11:23 2021

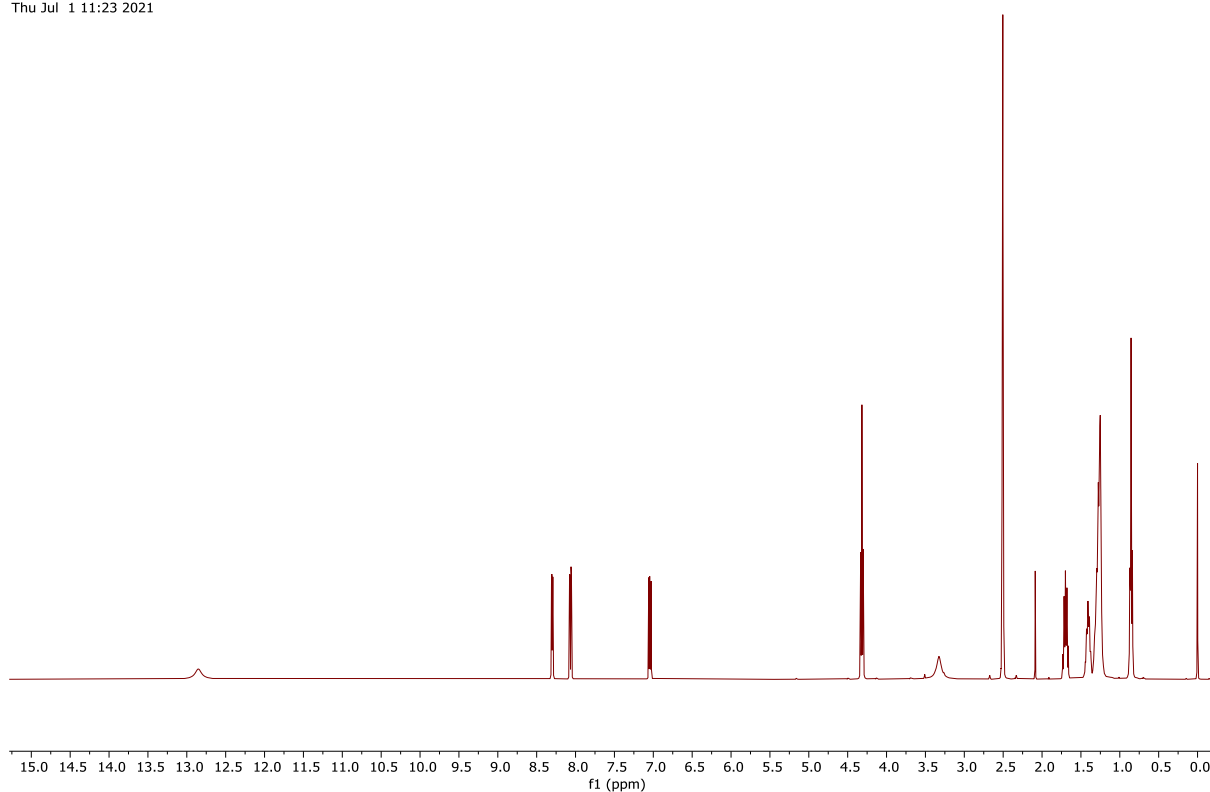


Figure 161: ¹H NMR spectrum (400 MHz, (CD₃)₂SO) of compound **45** (Chapter 3).

GGX470_CARBON_01
GGX470/DMSO-d5/13C
Fuchs 20210701_02
Thu Jul 1 12:10 2021

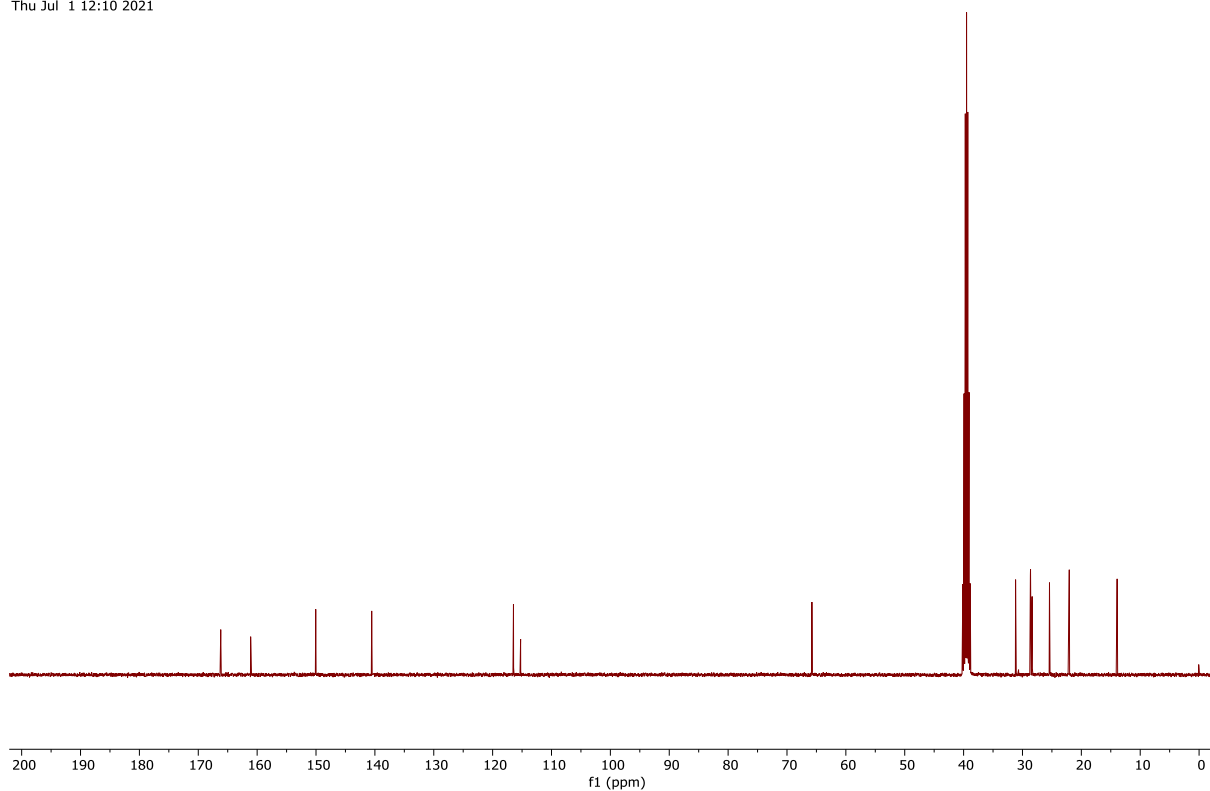


Figure 162: ¹³C NMR spectrum (101 MHz, (CD₃)₂SO) of compound **45** (Chapter 3).

GGX466_Fr1_PROTON_01
GGX466_Fr1/DMSO_d6/1H
Fuchs 20210625_09
Fri Jun 25 12:44 2021

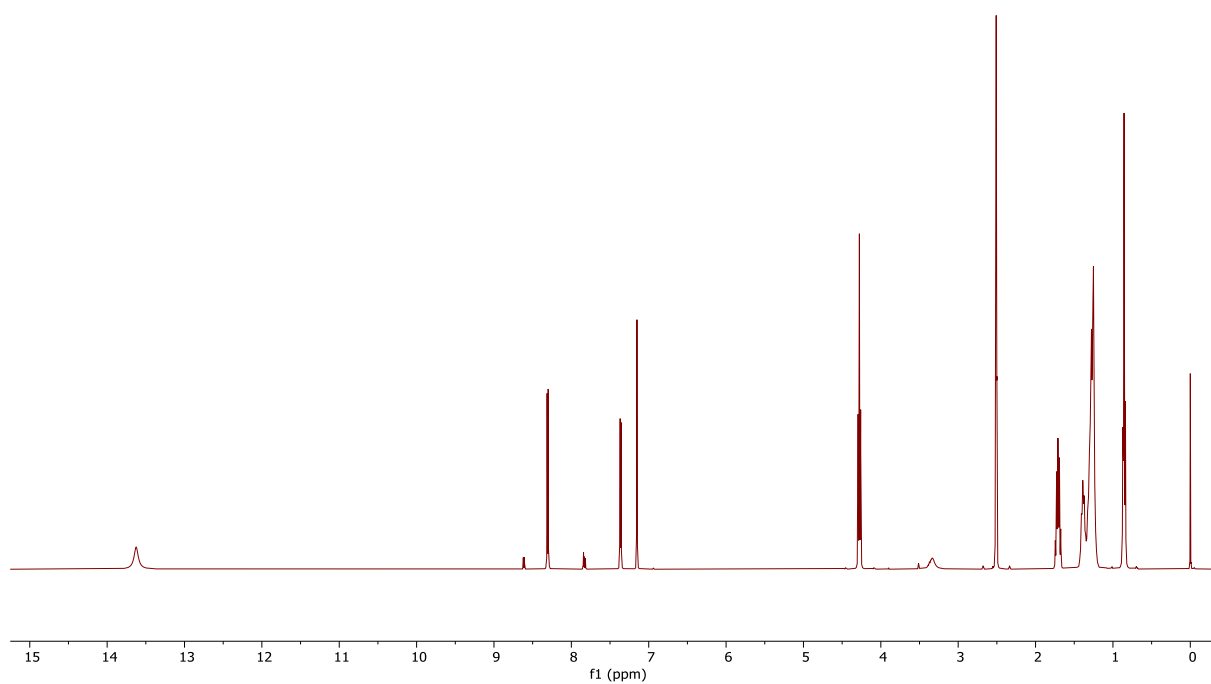


Figure 163: ¹H NMR spectrum (400 MHz, (CD₃)₂SO) of compound **46** (Chapter 3).

GGX466_Fr1_CARBON_01
GGX466_Fr1/DMSO_d6/13C
Fuchs 20210625_09
Fri Jun 25 12:46 2021

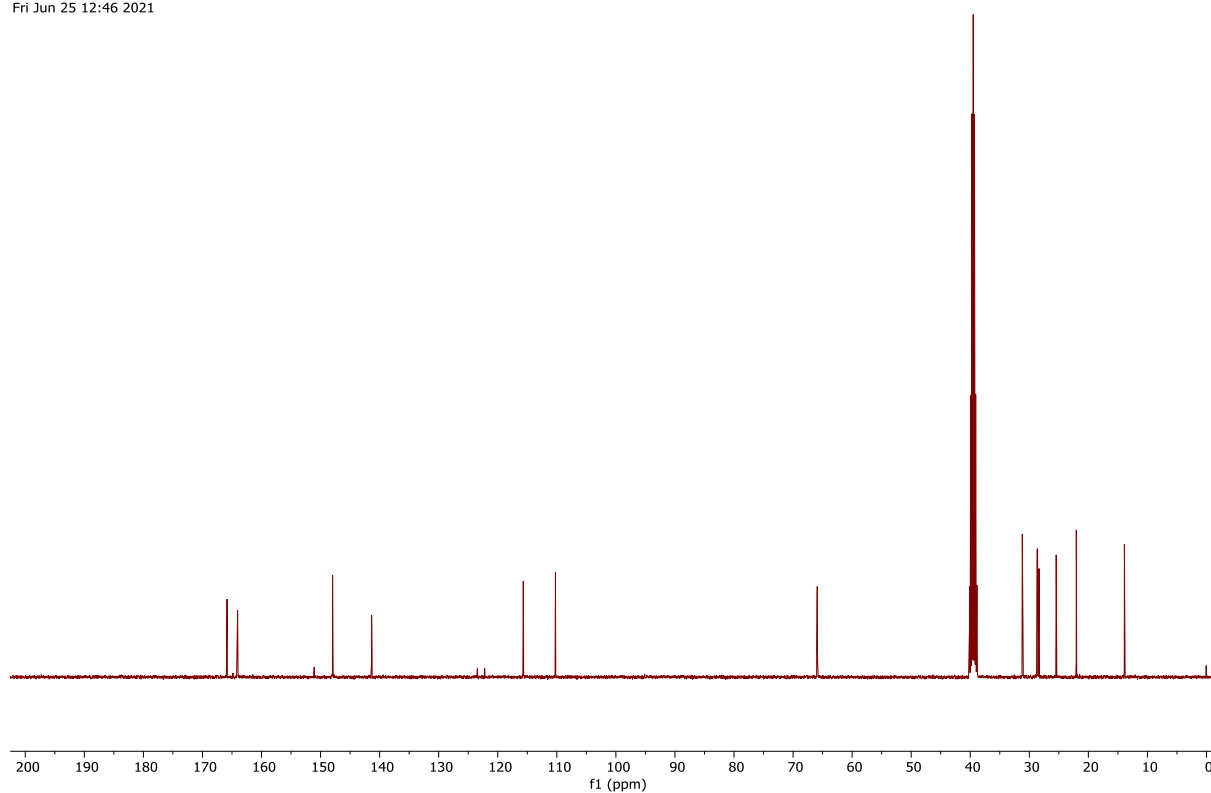


Figure 164: ¹³C NMR spectrum (101 MHz, (CD₃)₂SO) of compound **46** (Chapter 3).

GGX488_PROTON_01
GGX488/DMSO-d6/1H
Fuchs 20210729_02
Thu Jul 29 11:50 2021

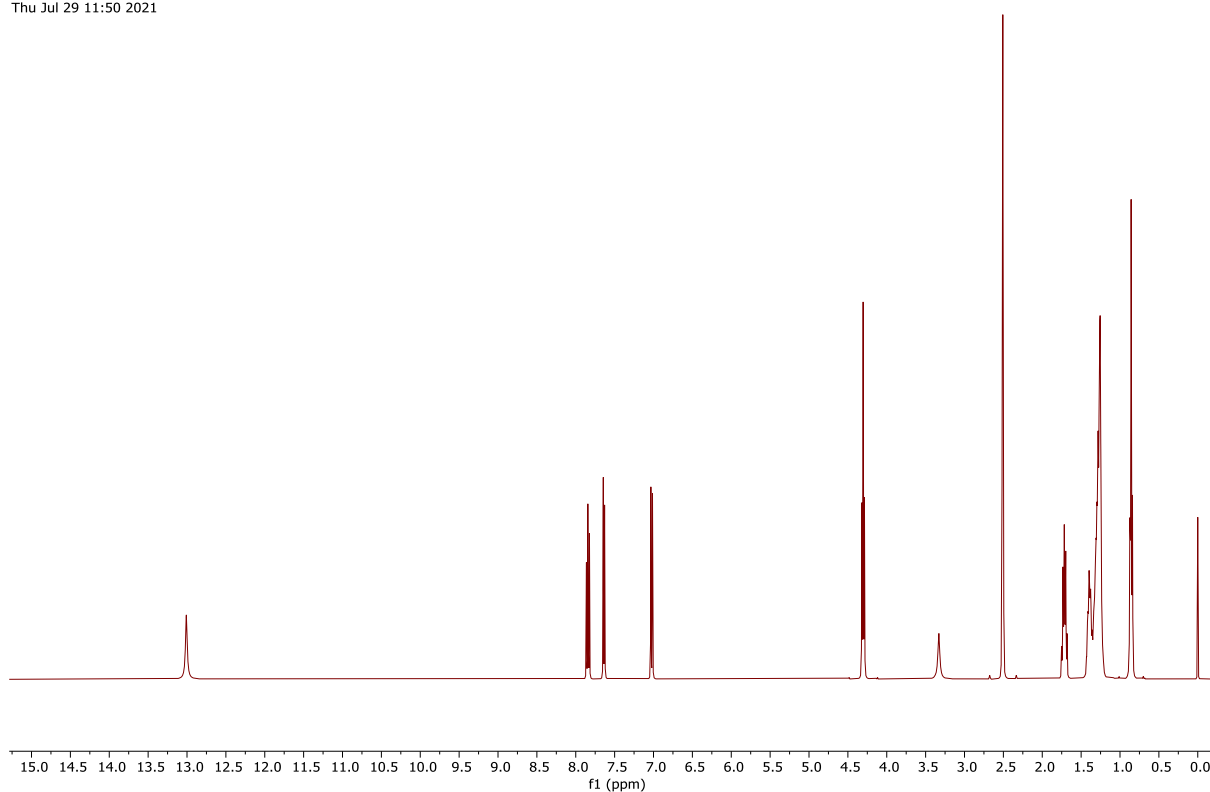


Figure 165: ¹H NMR spectrum (400 MHz, (CD₃)₂SO) of compound **47** (Chapter 3).

GGX488_CARBON_01
GGX488/DMSO-d6/13C
Fuchs 20210729_02
Thu Jul 29 14:48 2021

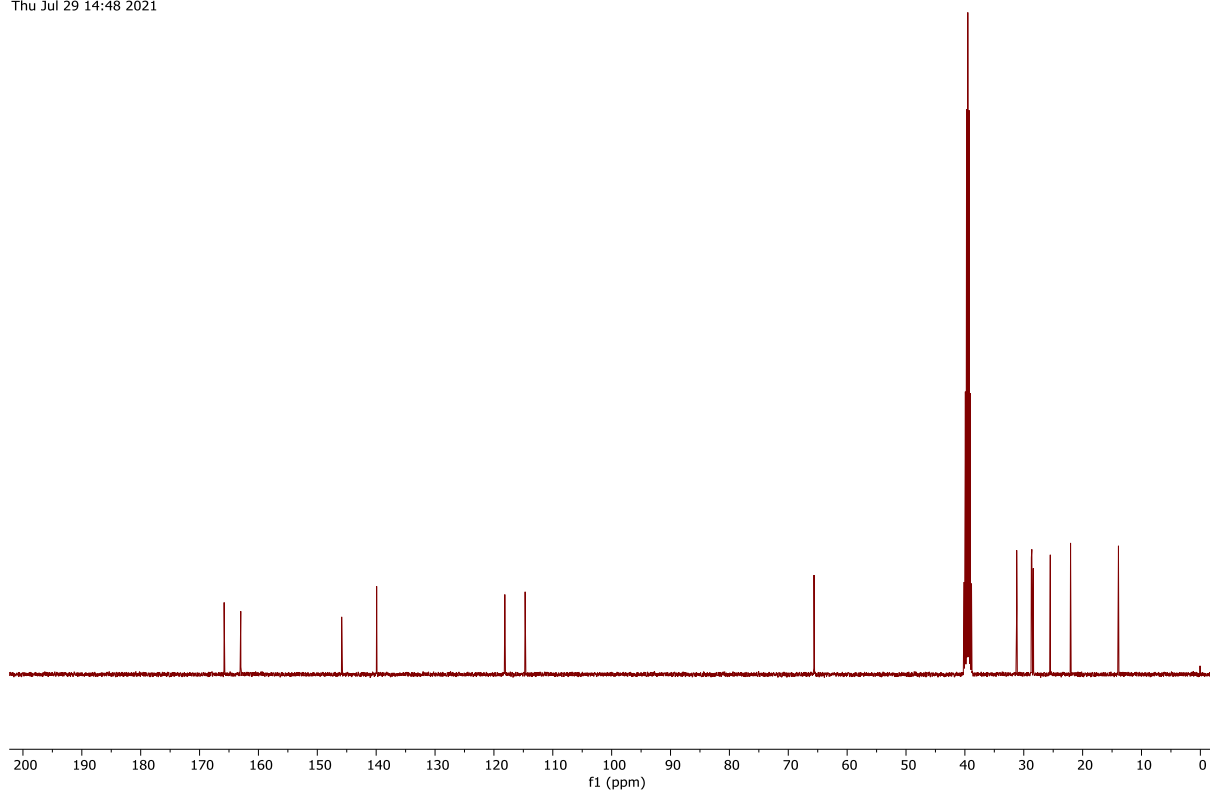


Figure 166: ¹³C NMR spectrum (101 MHz, (CD₃)₂SO) of compound **47** (Chapter 3).

GGX494_PROTON_01
GGX494/DMSO-d6/1H
Fuchs 20210921_12
Tue Sep 21 15:22 2021

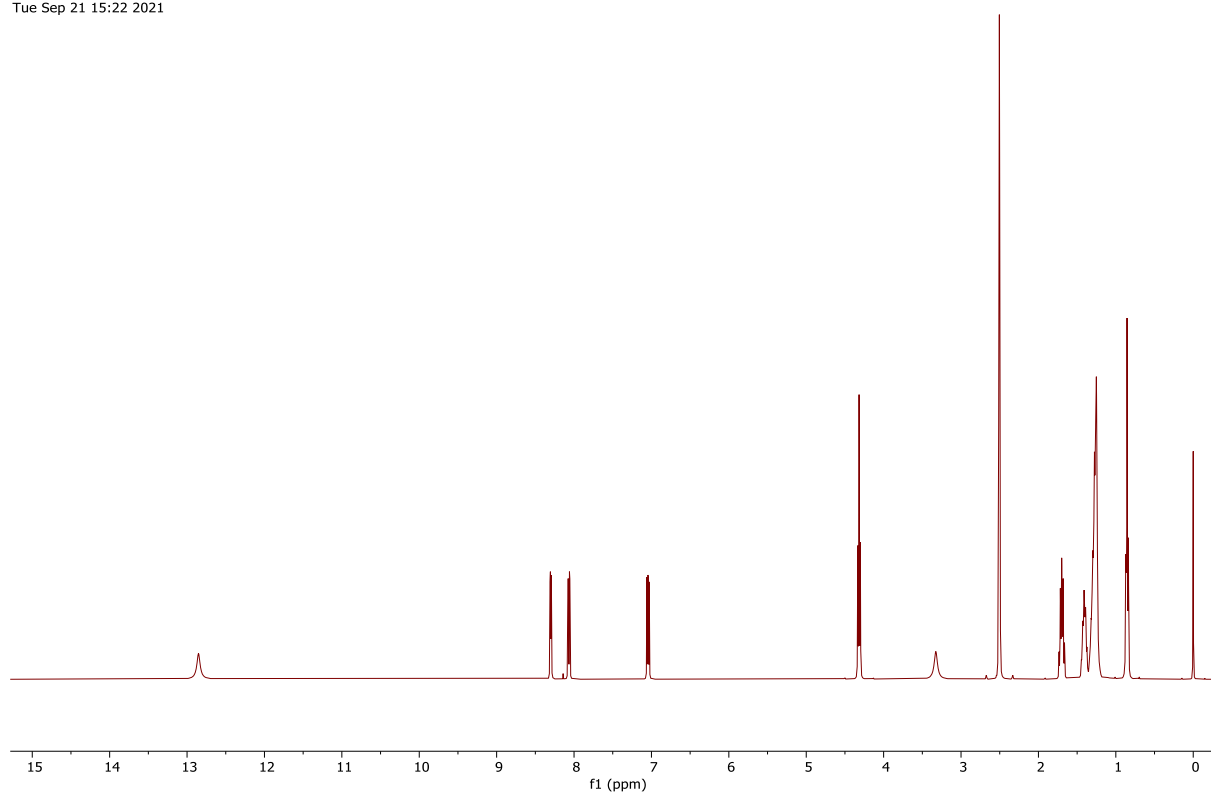


Figure 167: ¹H NMR spectrum (400 MHz, (CD₃)₂SO) of compound **48** (Chapter 3).

GGX494_CARBON_01
GGX494/DMSO-d6/13C
Fuchs 20210921_12
Tue Sep 21 16:18 2021

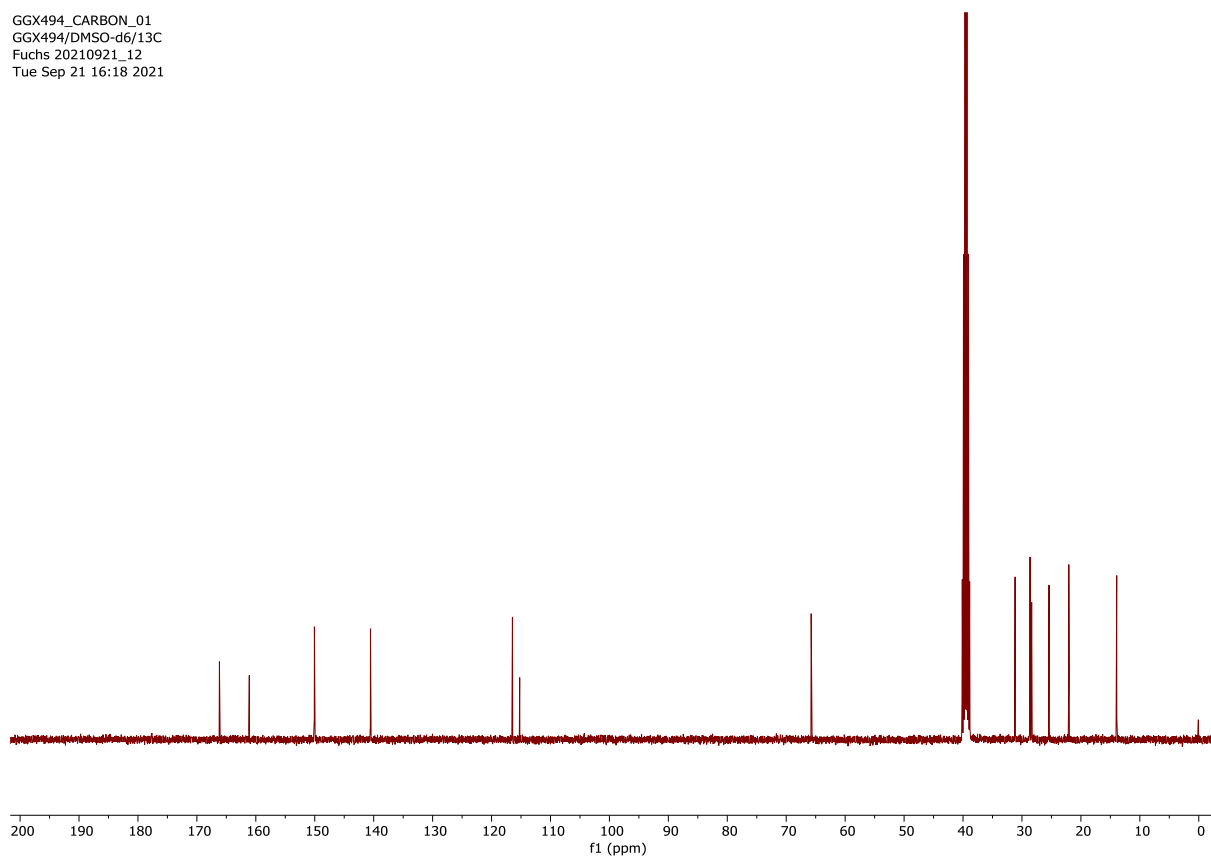


Figure 168: ¹³C NMR spectrum (101 MHz, (CD₃)₂SO) of compound **48** (Chapter 3).

GGX495_PROTON_01
GGX495/DMSO-d6/1H
Fuchs 20210922_05
Wed Sep 22 15:05 2021

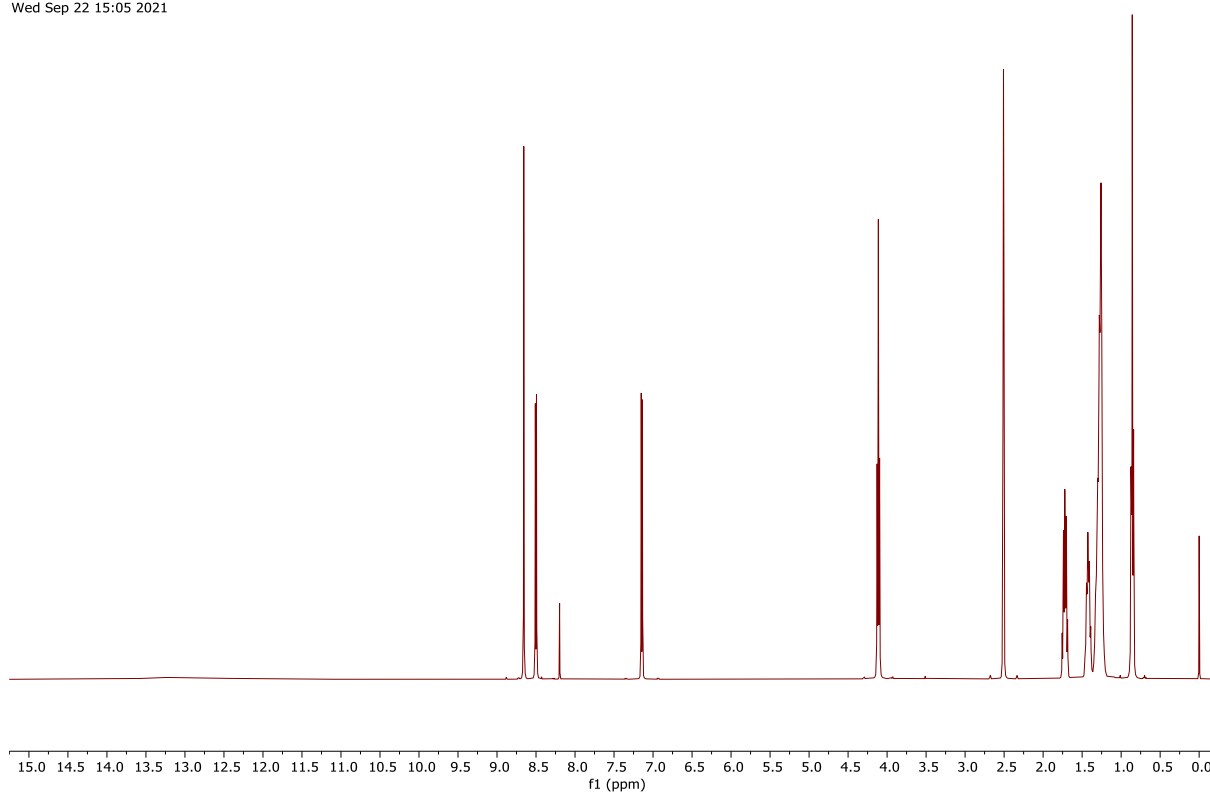


Figure 169: ¹H NMR spectrum (400 MHz, (CD₃)₂SO) of compound **49** (Chapter 3).

GGX495_CARBON_01
GGX495/DMSO-d6/13C
Fuchs 20210922_05
Wed Sep 22 15:08 2021

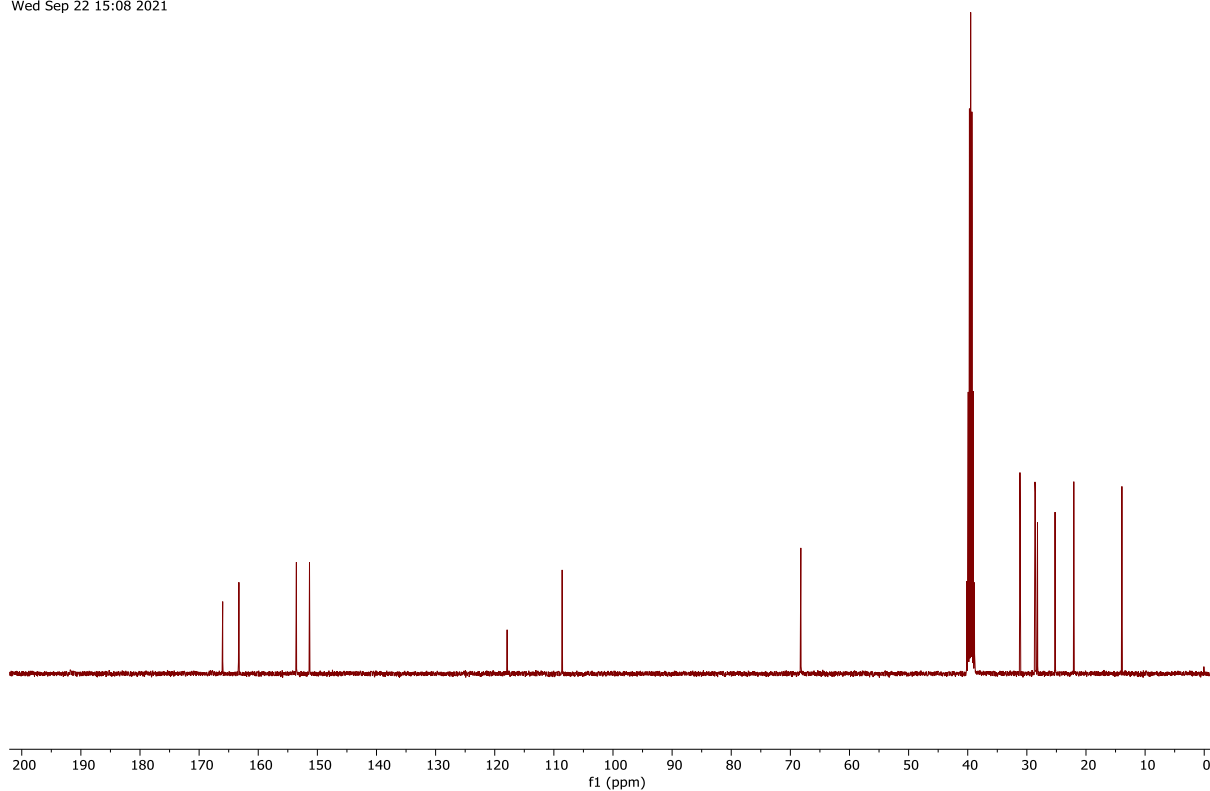


Figure 170: ¹³C NMR spectrum (101 MHz, (CD₃)₂SO) of compound **49** (Chapter 3).

GGX496_PROTON_02
GGX496/DMSO-d6/1H
Fuchs 20210927_01
Mon Sep 27 09:03 2021

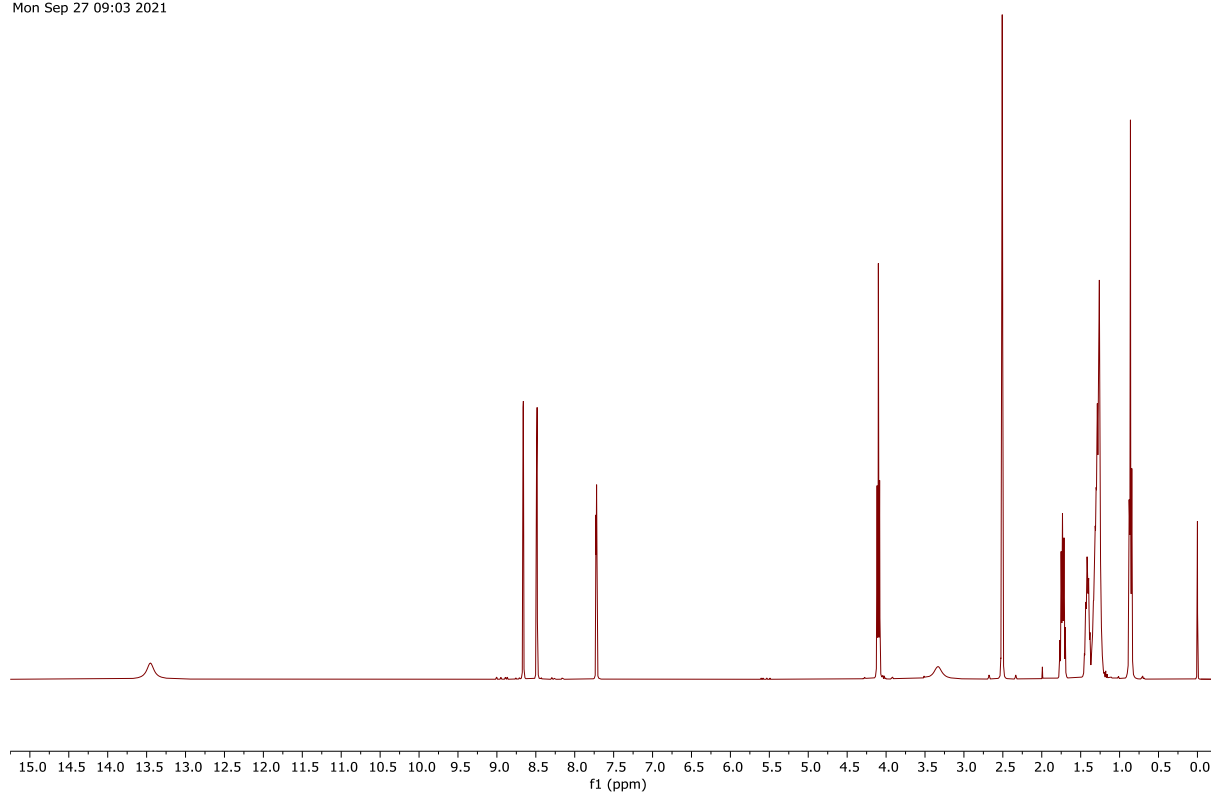


Figure 171: ¹H NMR spectrum (400 MHz, (CD₃)₂SO) of compound **50** (Chapter 3).

GGX496_CARBON_01
GGX496/DMSO-d6/13C
Fuchs 20210927_01
Mon Sep 27 09:58 2021

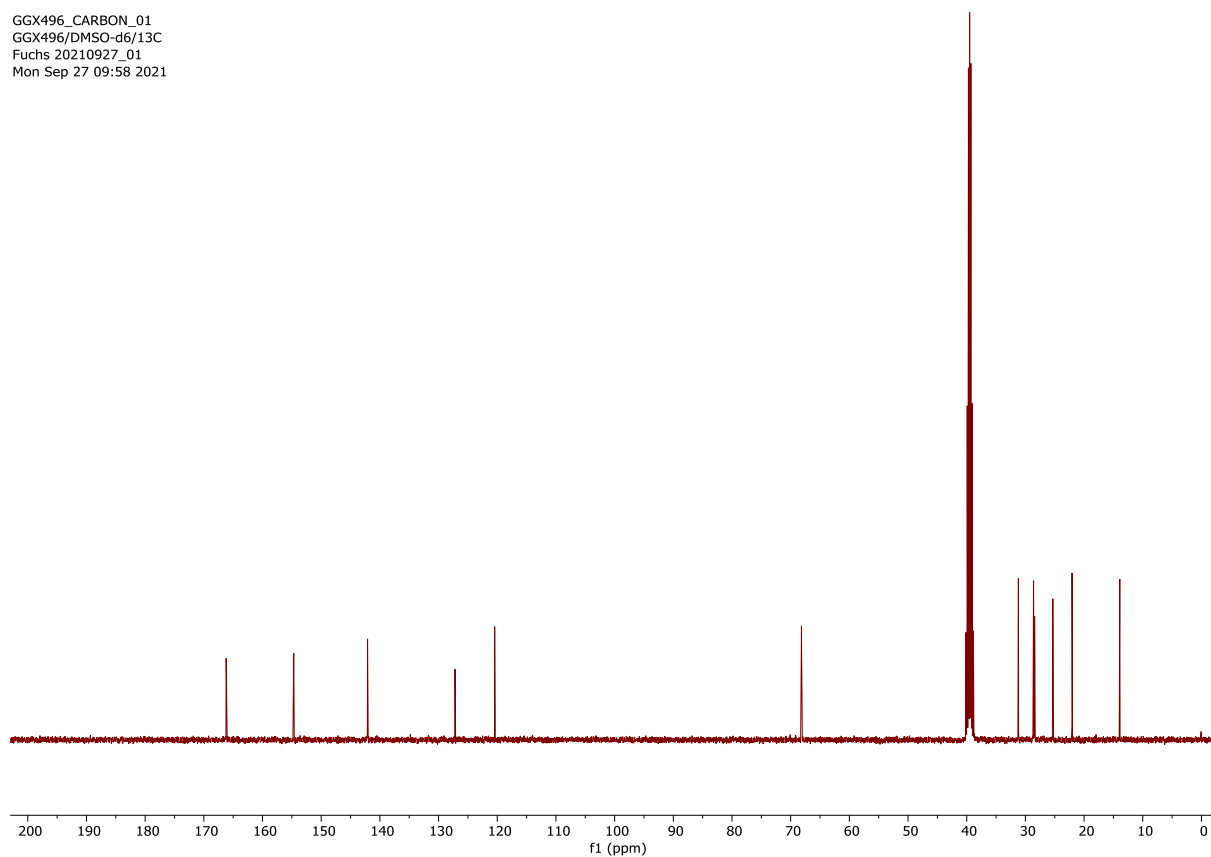


Figure 172: ¹³C NMR spectrum (101 MHz, (CD₃)₂SO) of compound **50** (Chapter 3).

GGX497_PROTON_01
GGX497/DMSO-d6/1H
Fuchs 20210924_03
Fri Sep 24 10:43 2021

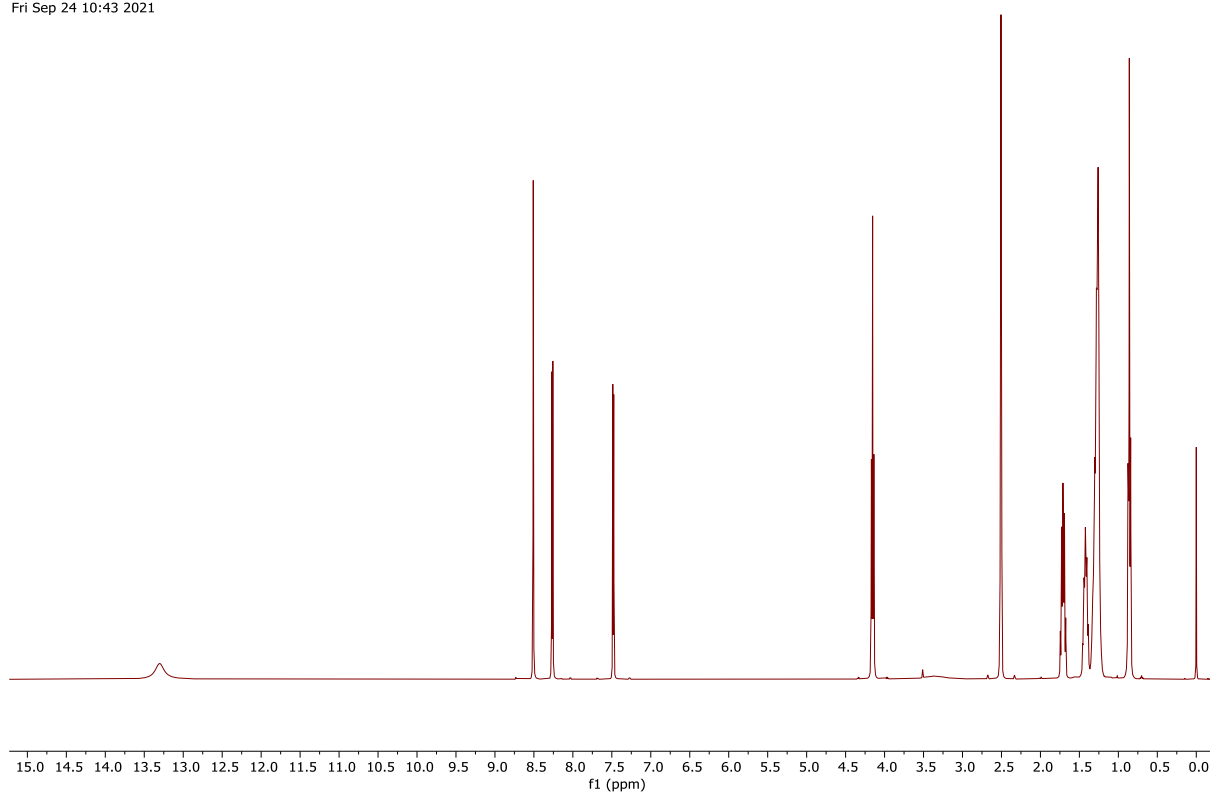


Figure 173: ¹H NMR spectrum (400 MHz, (CD₃)₂SO) of compound **51** (Chapter 3).

GGX497_CARBON_01
GGX497/DMSO-d6/13C
Fuchs 20210924_03
Fri Sep 24 10:45 2021

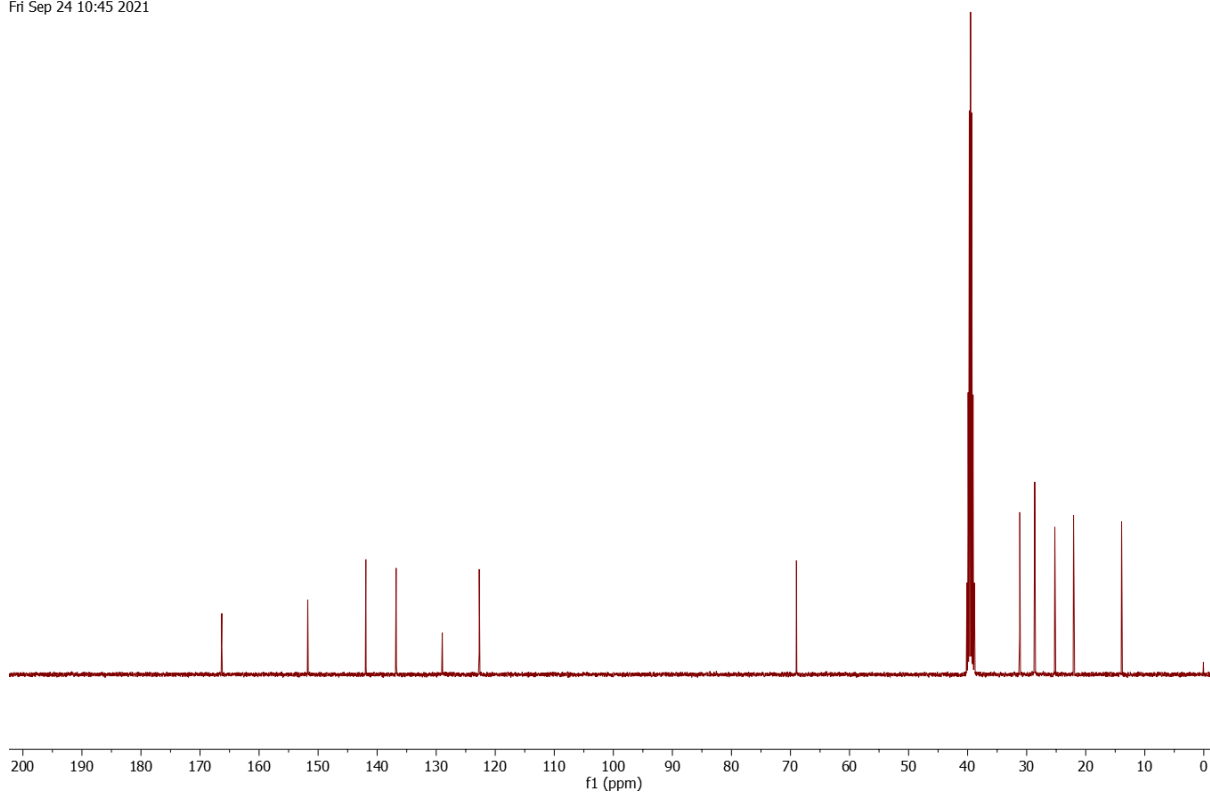


Figure 174: ¹³C NMR spectrum (101 MHz, (CD₃)₂SO) of compound **51** (Chapter 3).

GGX499_PROTON_01
GGX499/DMSO-d6/1H
Fuchs 20210930_01

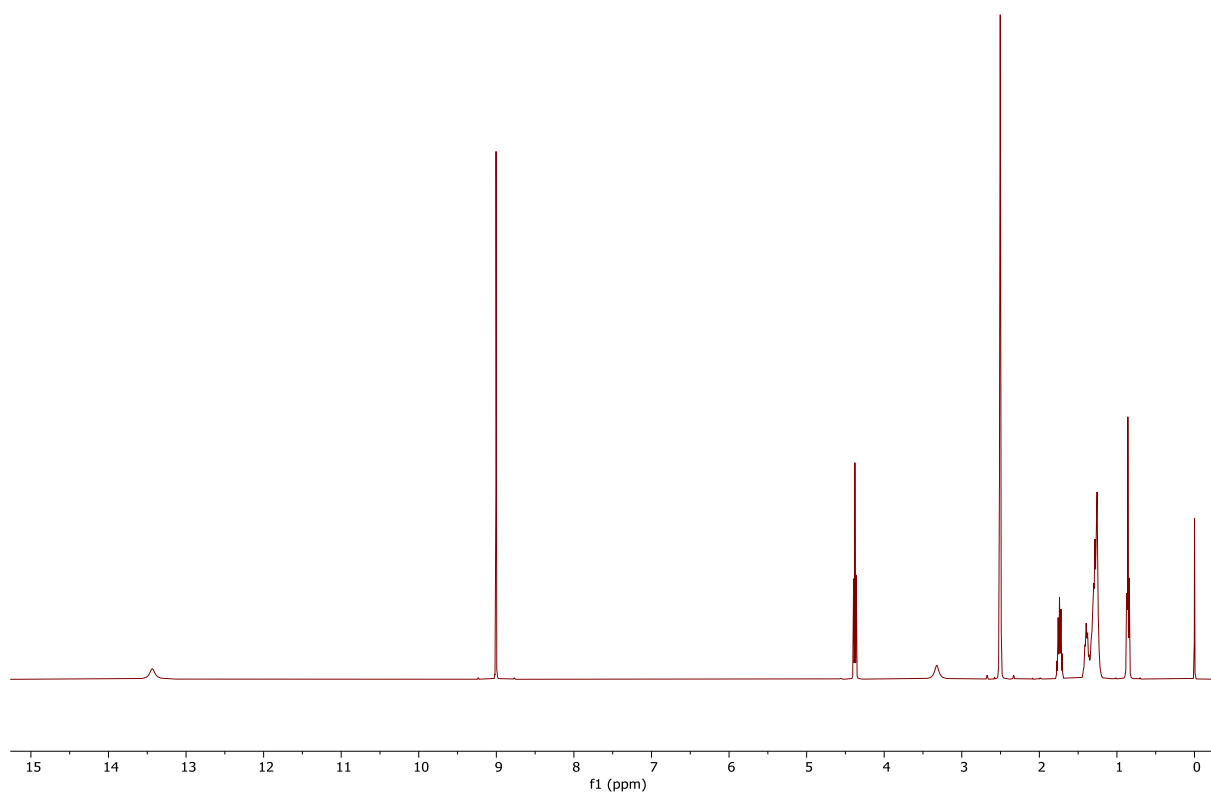


Figure 175: ¹H NMR spectrum (400 MHz, (CD₃)₂SO) of compound **52** (Chapter 3).

GGX499_CARBON_01
GGX499/DMSO-d6/1H
Fuchs 20210930_01
Thu Sep 30 08:25 2021

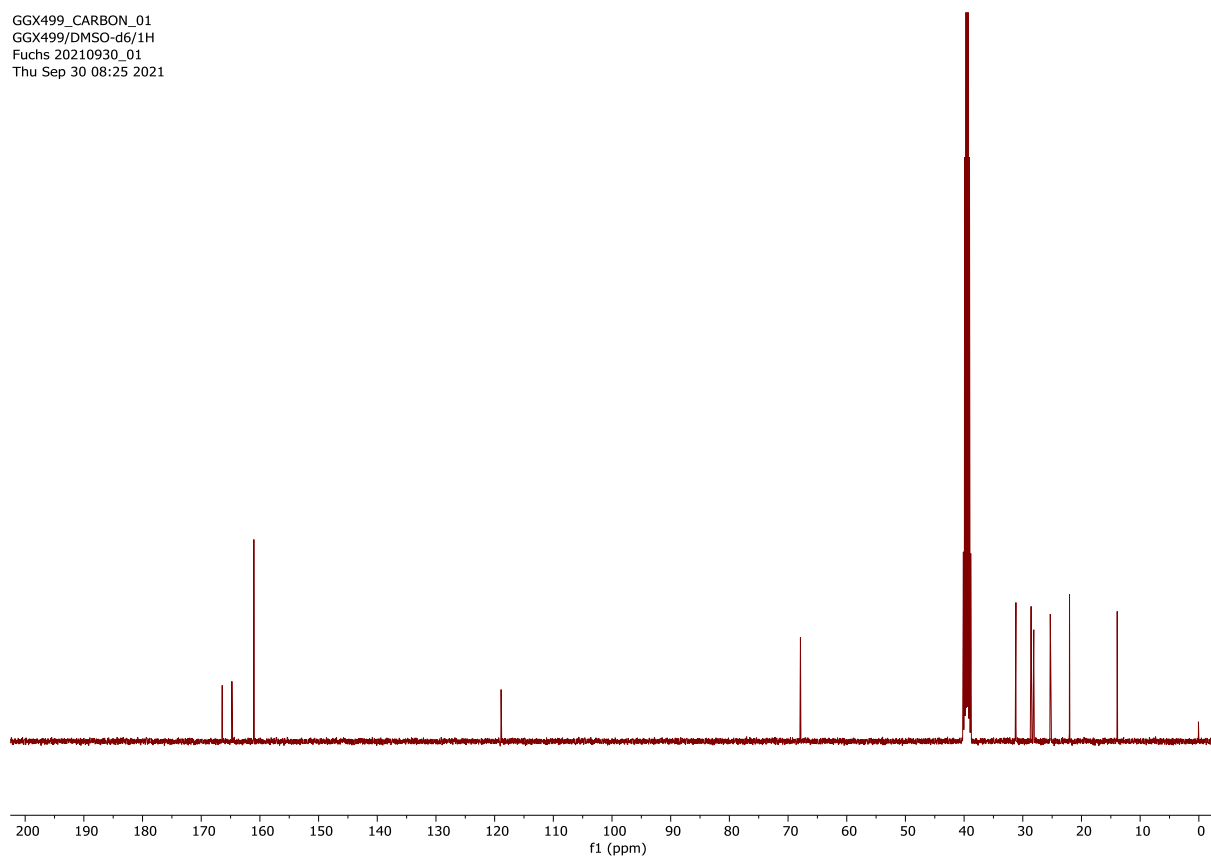


Figure 176: ¹³C NMR spectrum (101 MHz, (CD₃)₂SO) of compound **52** (Chapter 3).

GGX530_PROTON_01
GGX530/DMSO-d6/1H
Fuchs 20220412_04
Tue Apr 12 10:26 2022

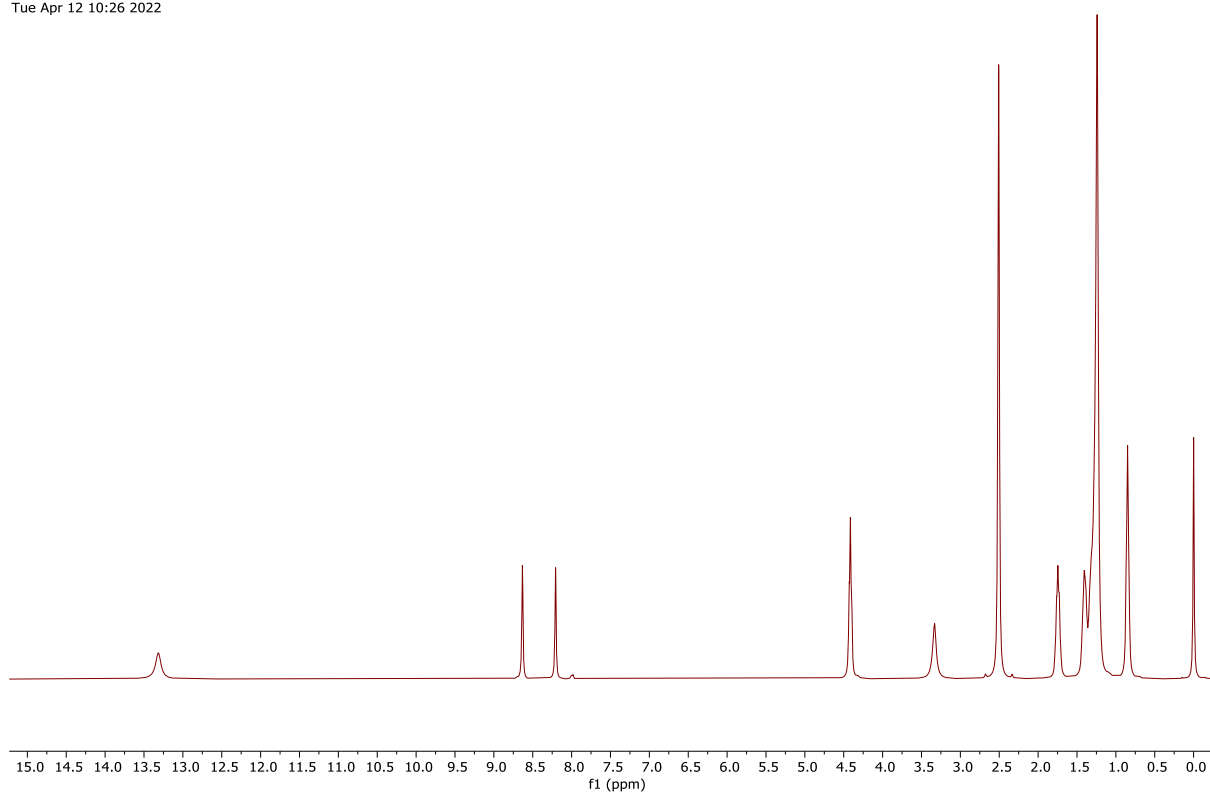


Figure 177: ¹H NMR spectrum (400 MHz, (CD₃)₂SO) of compound **53** (Chapter 3).

GGX530_CARBON_01
GGX530/DMSO-d6/13C
Fuchs 20220412_04
Tue Apr 12 12:12 2022

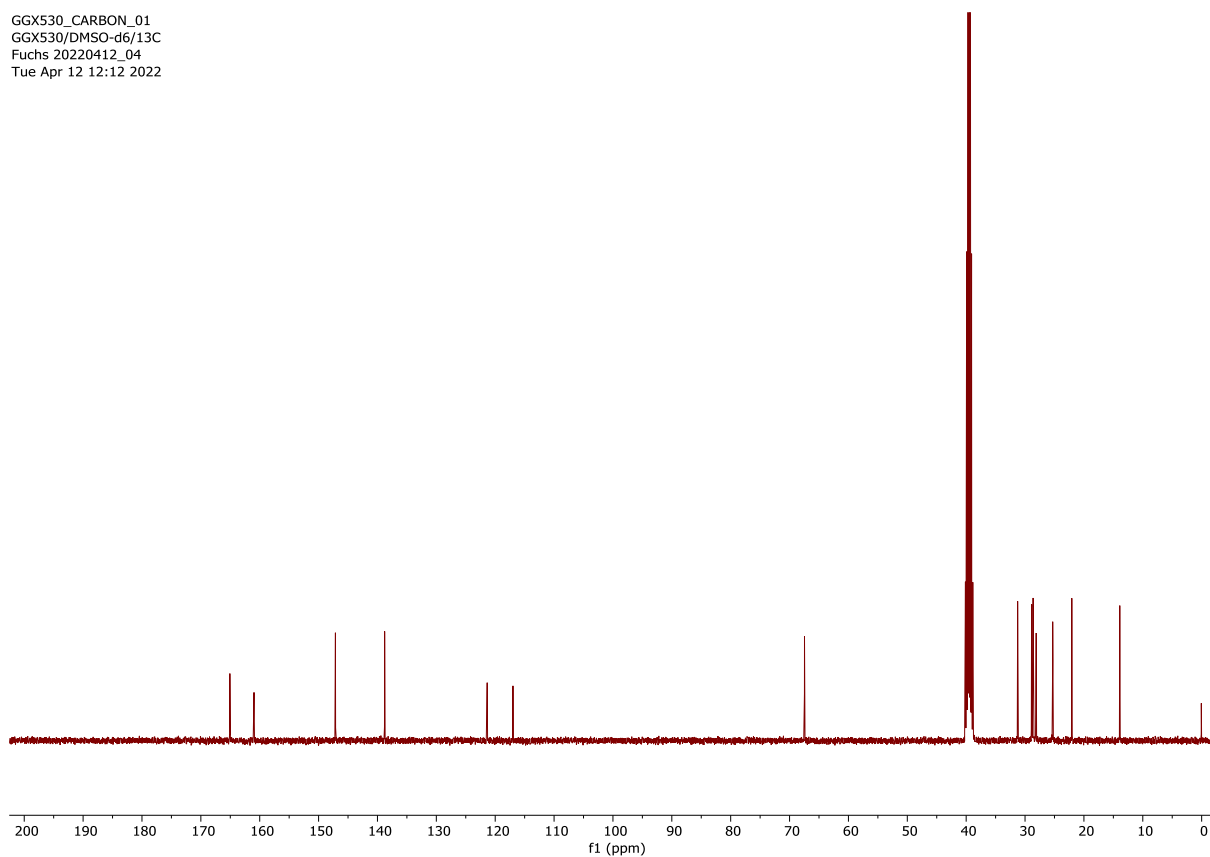


Figure 178: ¹³C NMR spectrum (101 MHz, (CD₃)₂SO) of compound **53** (Chapter 3).

GGX524_PROTON_01
GGX524/CDCl₃/1H
Fuchs 20220331_02
Fri Apr 1 09:05 2022

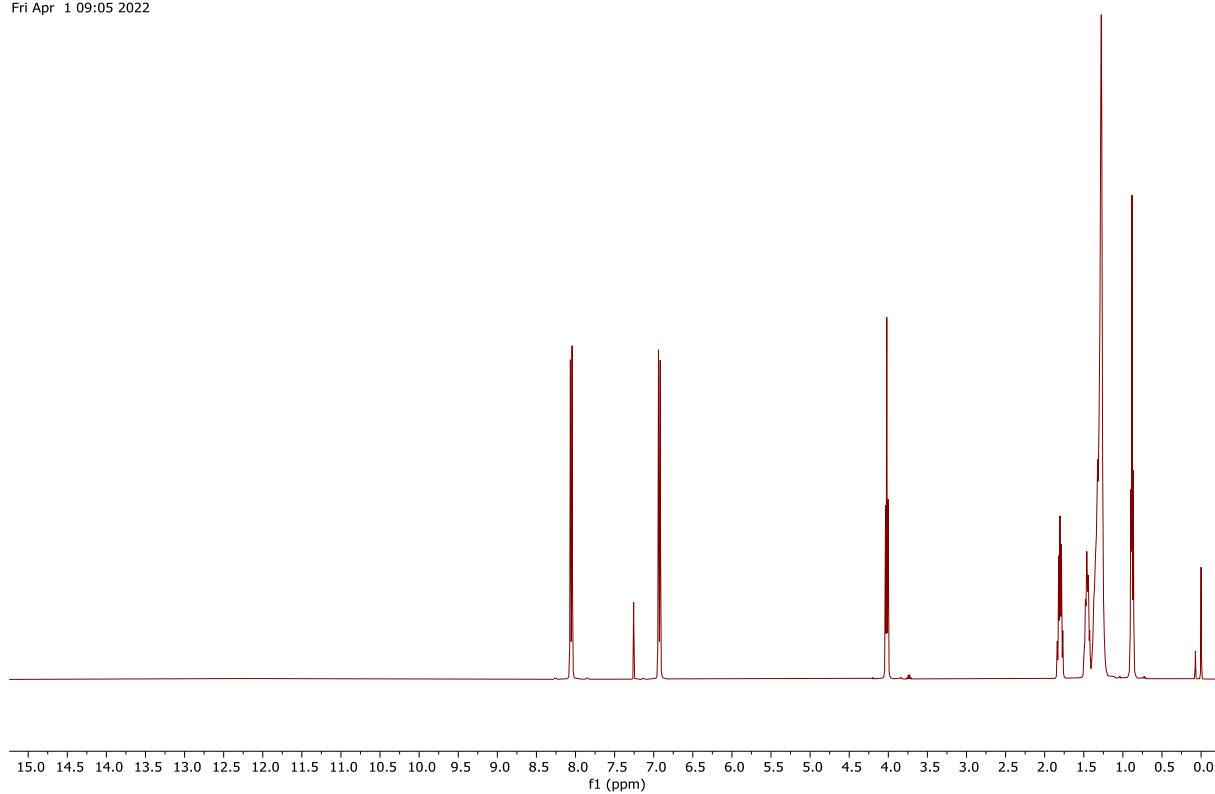


Figure 179: ¹H NMR spectrum (400 MHz, CDCl₃) of compound **54** (Chapter 3).

GGX524_CARBON_01
GGX524/CDCl₃/13C
Fuchs 20220331_02
Fri Apr 1 09:22 2022

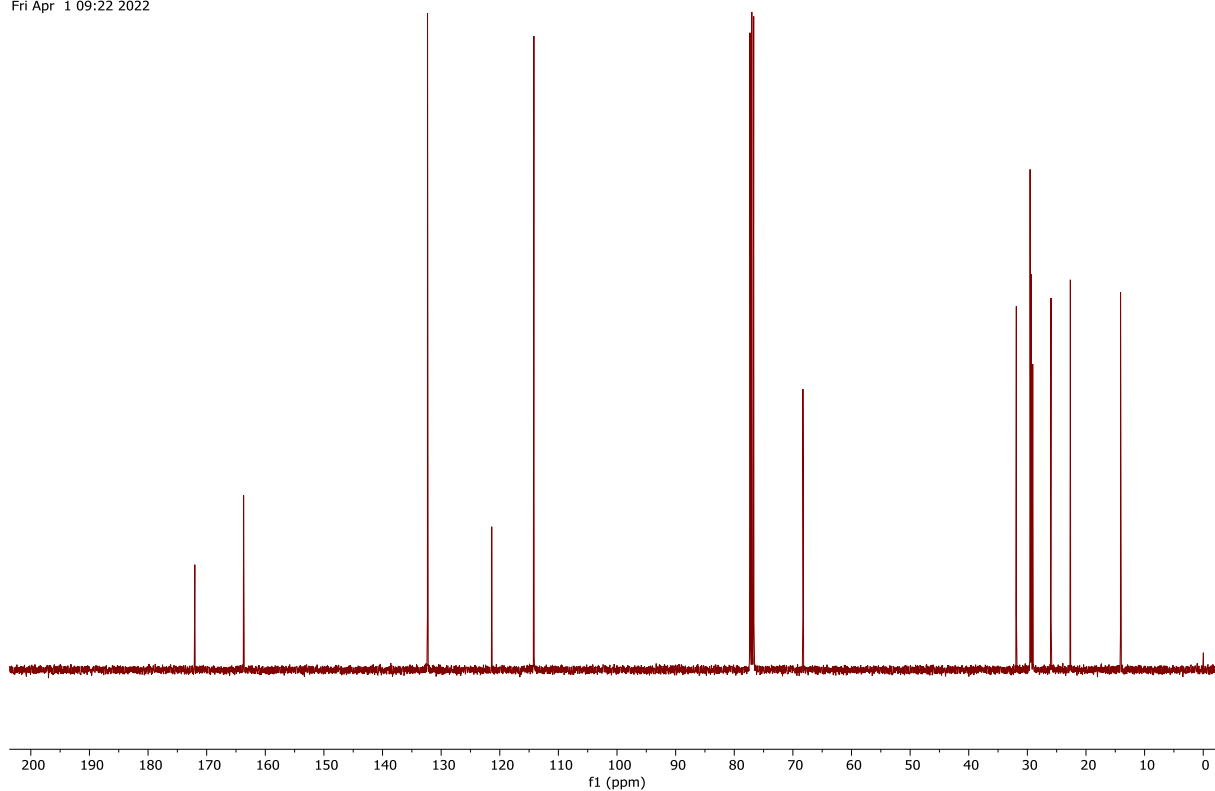


Figure 180: ¹³C NMR spectrum (101 MHz, CDCl₃) of compound **54** (Chapter 3).

GGX333.11.fid
GGX333/CDCl₃/1H
Fuchs 20200728_05
Proton_IPB CDCl₃ /opt/nmrdata/2020/GGX walkup 13

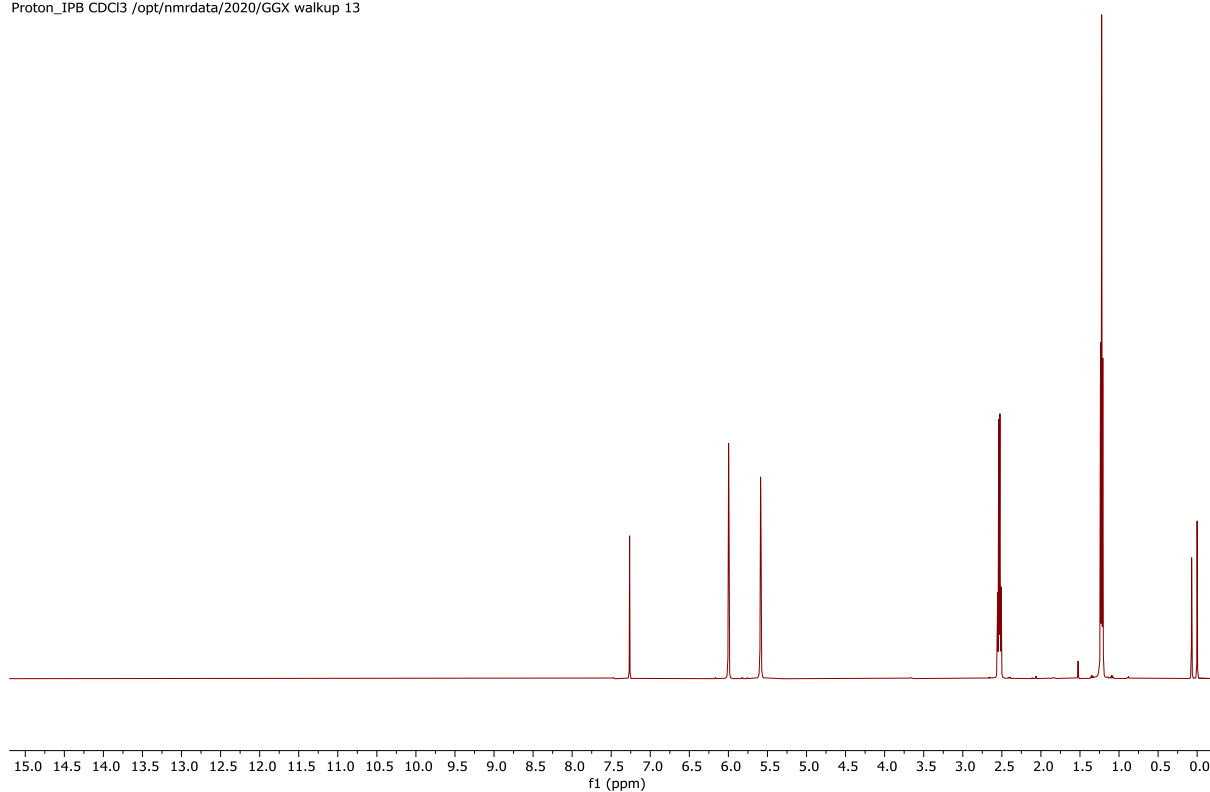


Figure 181: ¹H NMR spectrum (500 MHz, CDCl₃) of compound **1** (Chapter 4).

GGX333.12.fid
GGX333/CDCl₃/13C
Fuchs 20200728_05
Carbon_dec_IPB CDCl₃ /opt/nmrdata/2020/GGX walkup 13

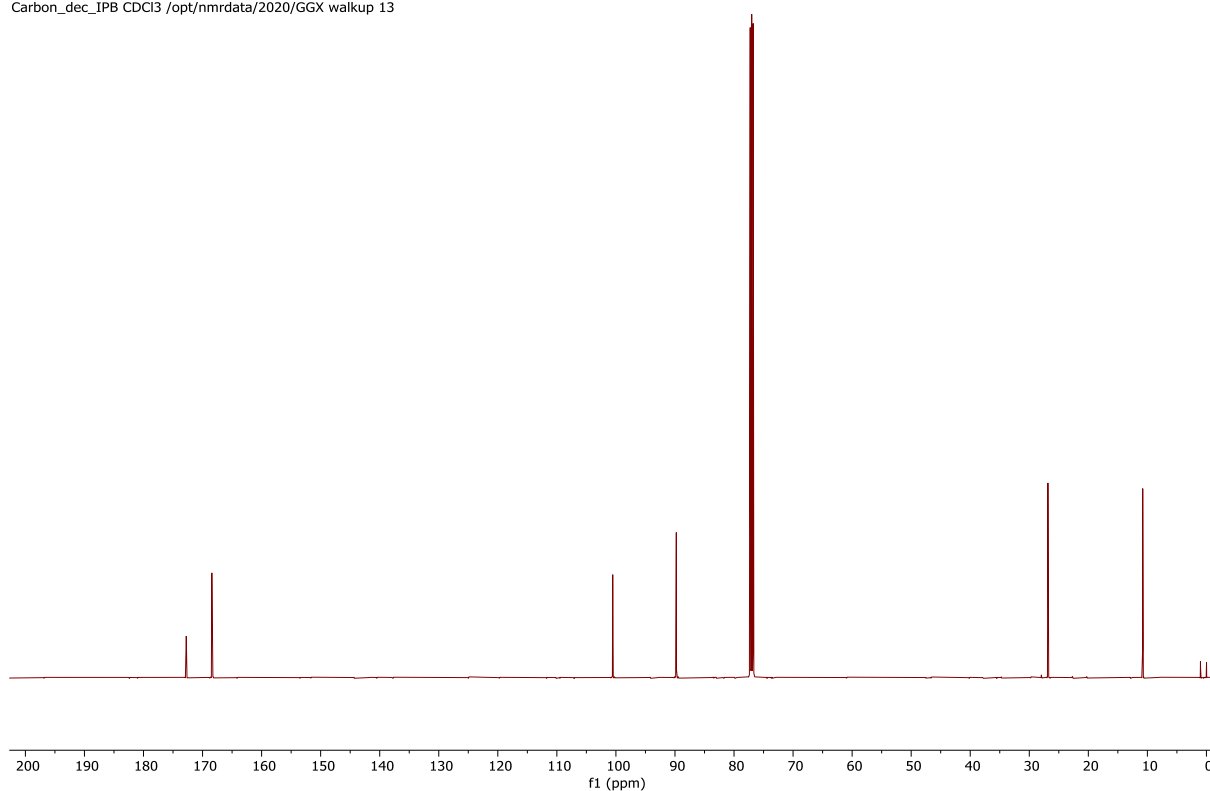


Figure 182: ¹³C NMR spectrum (126 MHz, CDCl₃) of compound **1** (Chapter 4).

GGX334.11.fid
GGX334/CDCl₃/1H
Fuchs 20200728_06
Proton_IPB CDCl₃ /opt/nmrdata/2020/GGX walkup 14

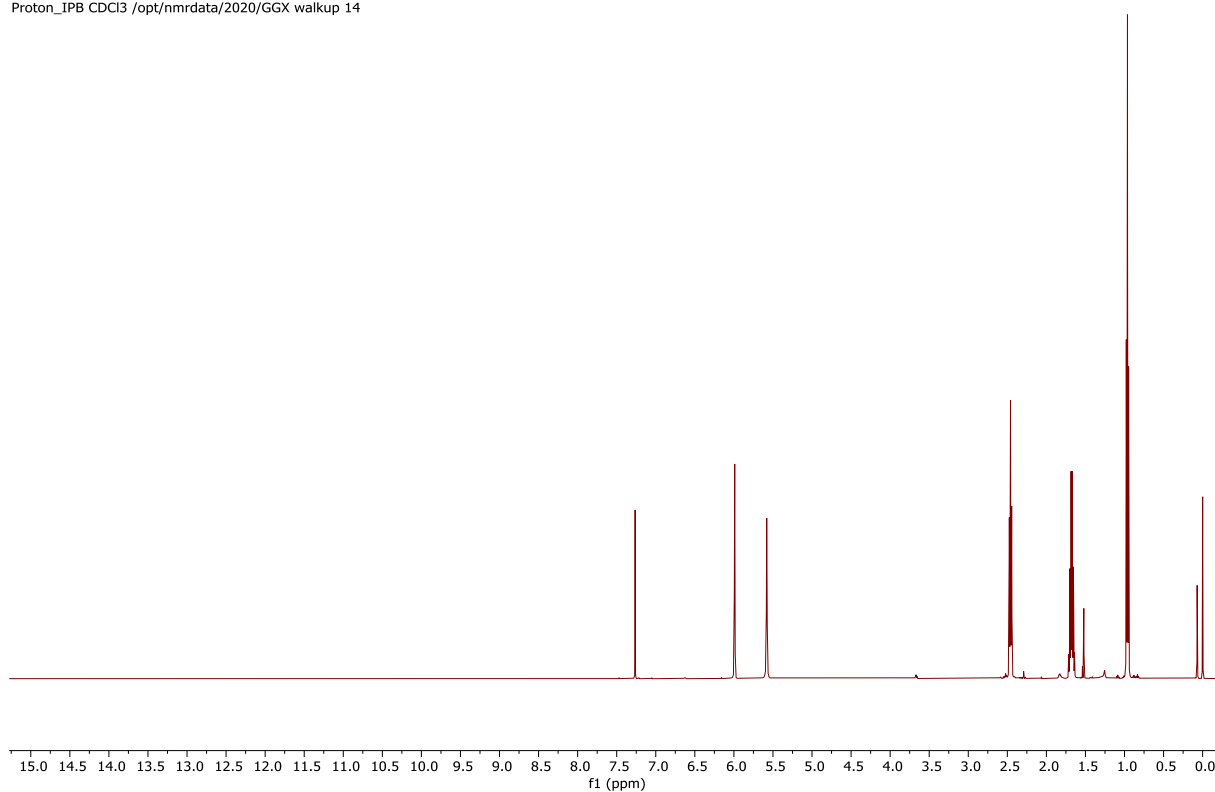


Figure 183: ¹H NMR spectrum (500 MHz, CDCl₃) of compound **2** (Chapter 4).

GGX334.12.fid
GGX334/CDCl₃/13C
Fuchs 20200728_06
Carbon_dec_IPB CDCl₃ /opt/nmrdata/2020/GGX walkup 14

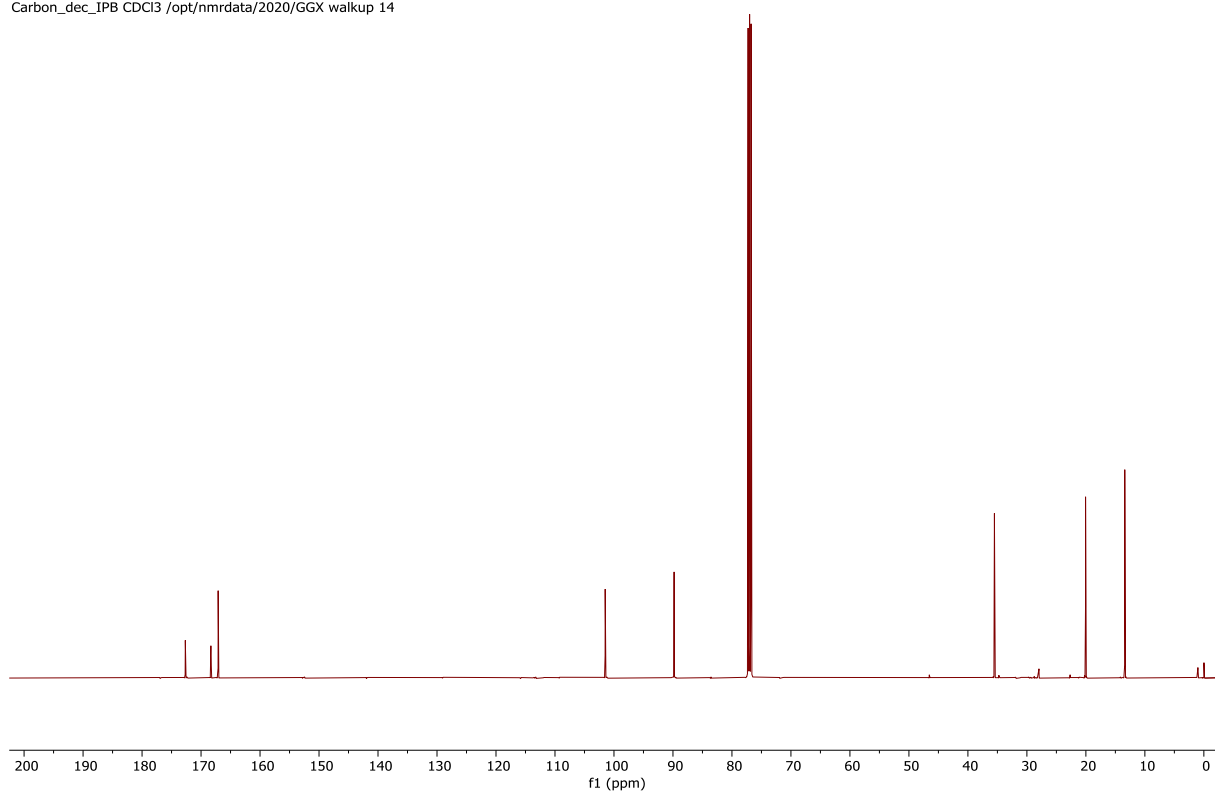


Figure 184: ¹³C NMR spectrum (126 MHz, CDCl₃) of compound **2** (Chapter 4).

GGX325_F2.11.fid
GGX325_F2/CDCl3/1H
Fuchs 20200625_02
Proton_IPB CDCl3 /opt/nmrdata/2020/GGX walkup 11

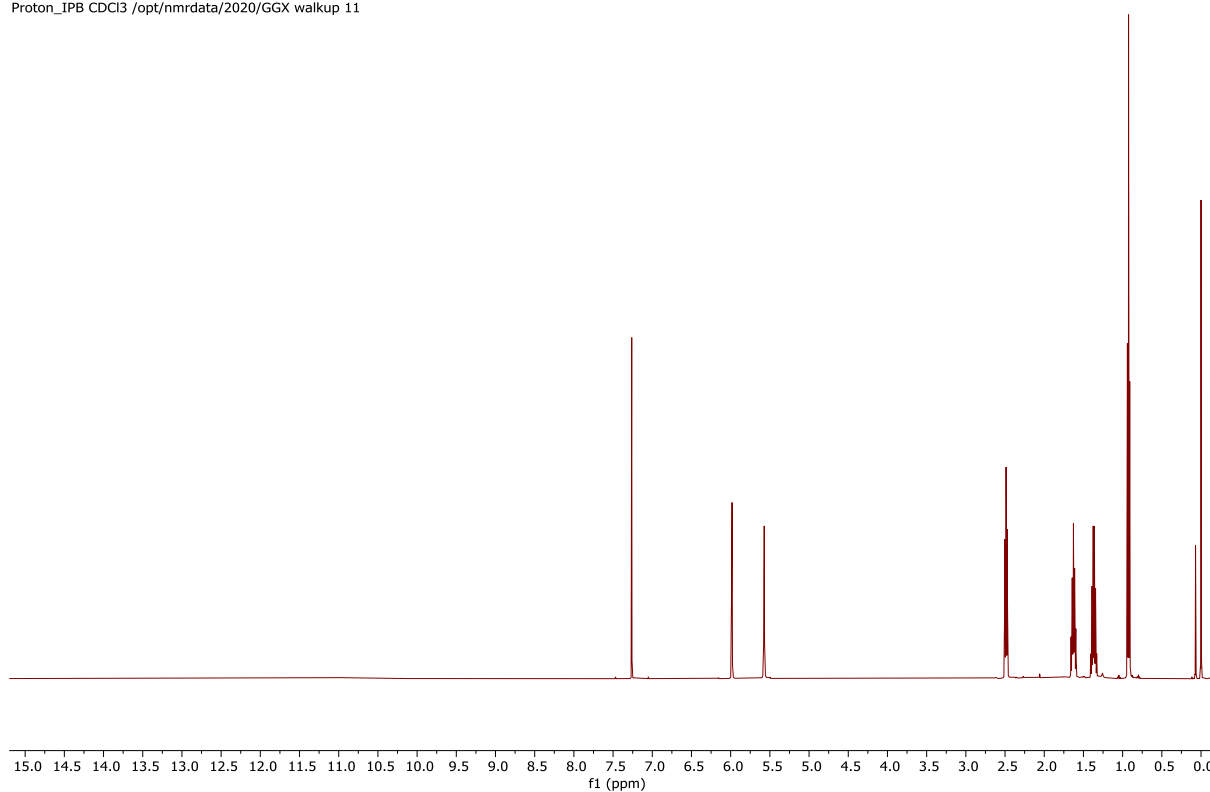


Figure 185: ¹H NMR spectrum (500 MHz, CDCl₃) of compound **3** (Chapter 4).

GGX325_F2.12.fid
GGX325_F2/CDCl3/13C
Fuchs 20200625_02
Carbon_dec_IPB CDCl3 /opt/nmrdata/2020/GGX walkup 11

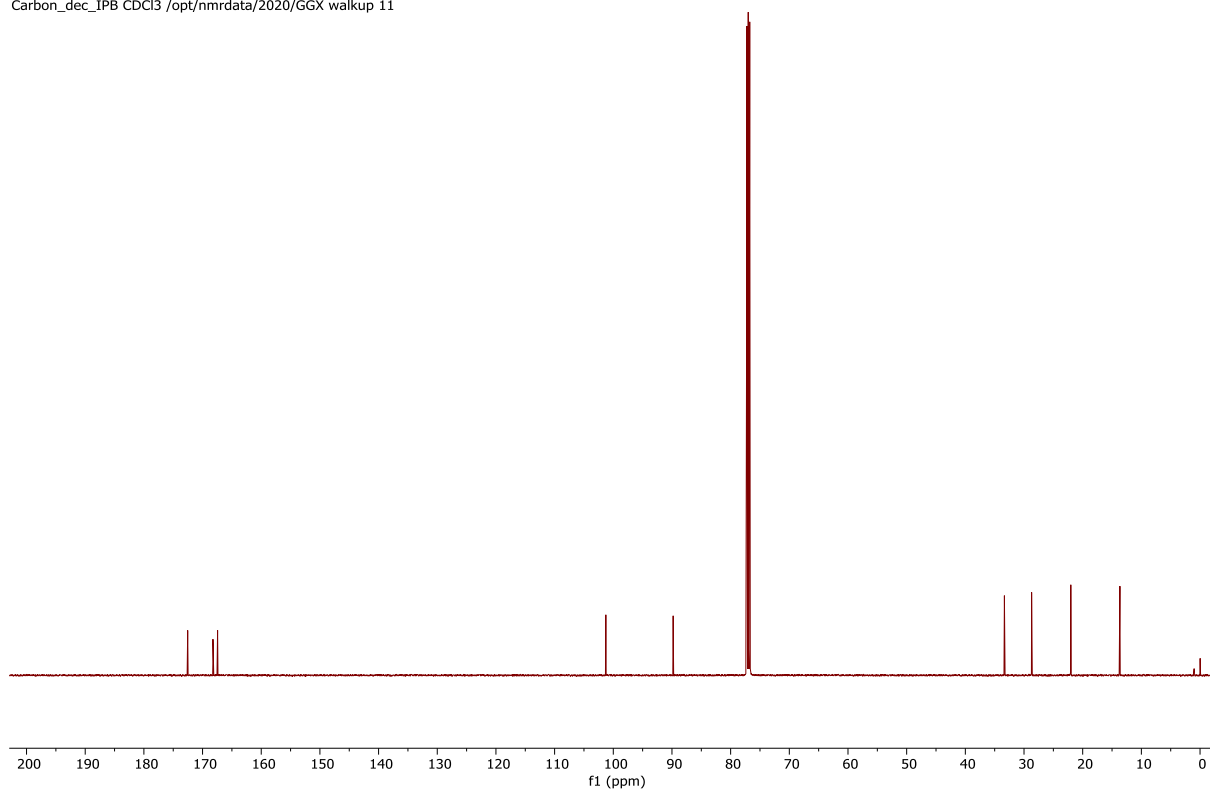


Figure 186: ¹³C NMR spectrum (126 MHz, CDCl₃) of compound **3** (Chapter 4).

GGX324_F1_PROTON_01
GGX324_F1/CDCl₃/1H
Fuchs 20200625_10
Thu Jun 25 16:22 2020

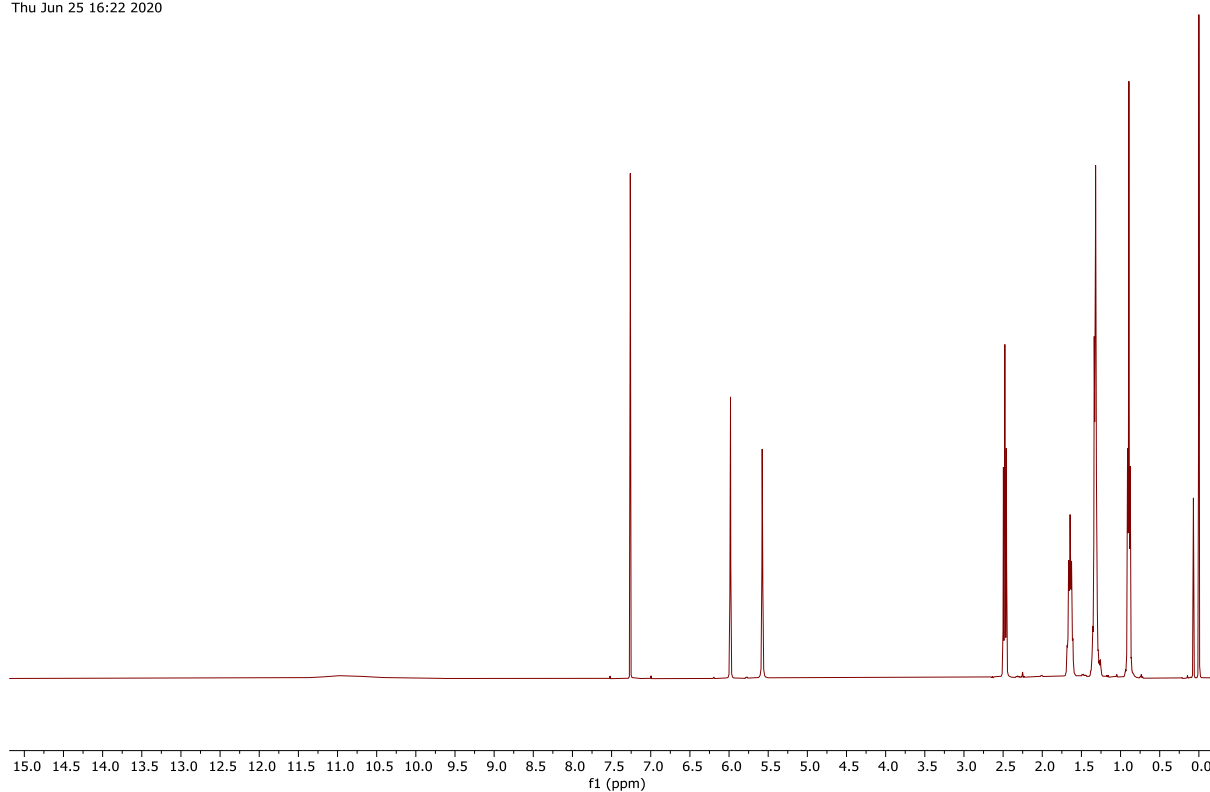


Figure 187: ¹H NMR spectrum (500 MHz, CDCl₃) of compound **4** (Chapter 4).

GGX324_F1_CARBON_01
GGX324_F1/CDCl₃/13C
Fuchs 20200625_10
Fri Jun 26 10:04 2020

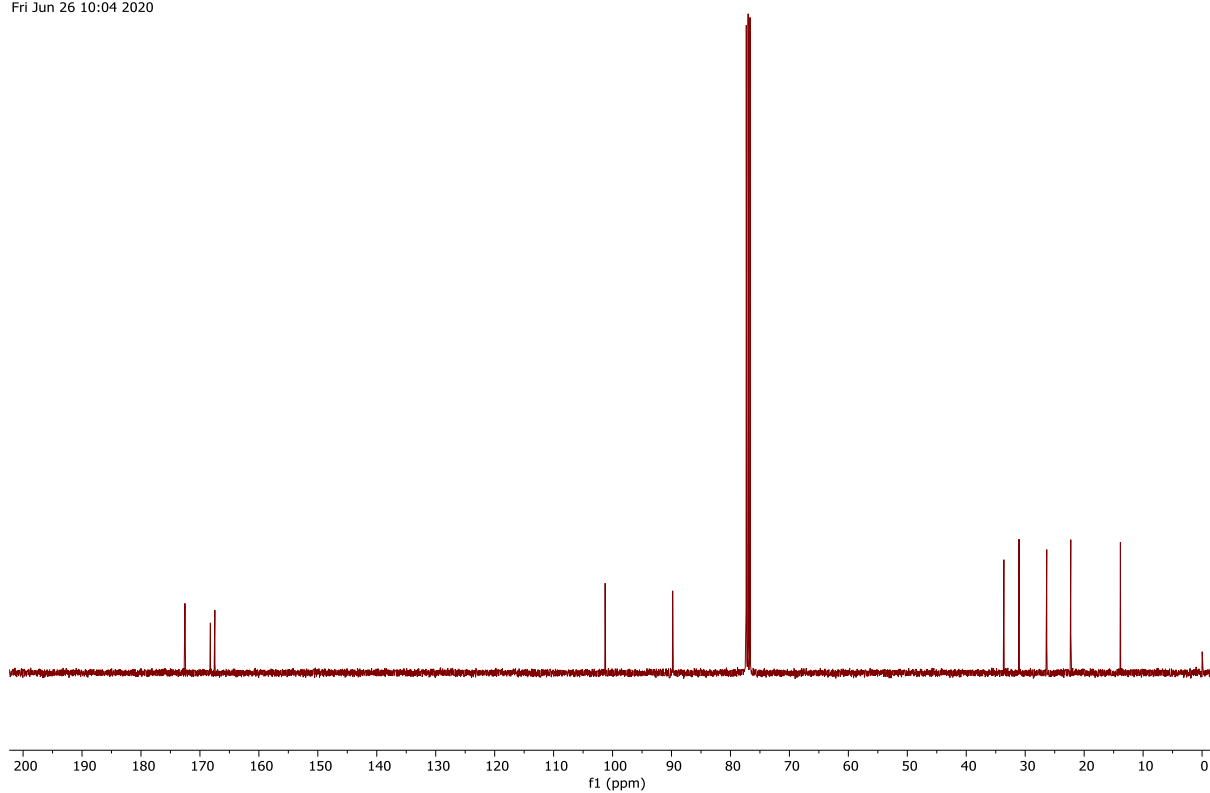


Figure 188: ¹³C NMR spectrum (126 MHz, CDCl₃) of compound **4** (Chapter 4).

GGX433_PROTON_01
GGX433/CDCl₃/1H
Fuchs 20210318_05
Thu Mar 18 10:49 2021

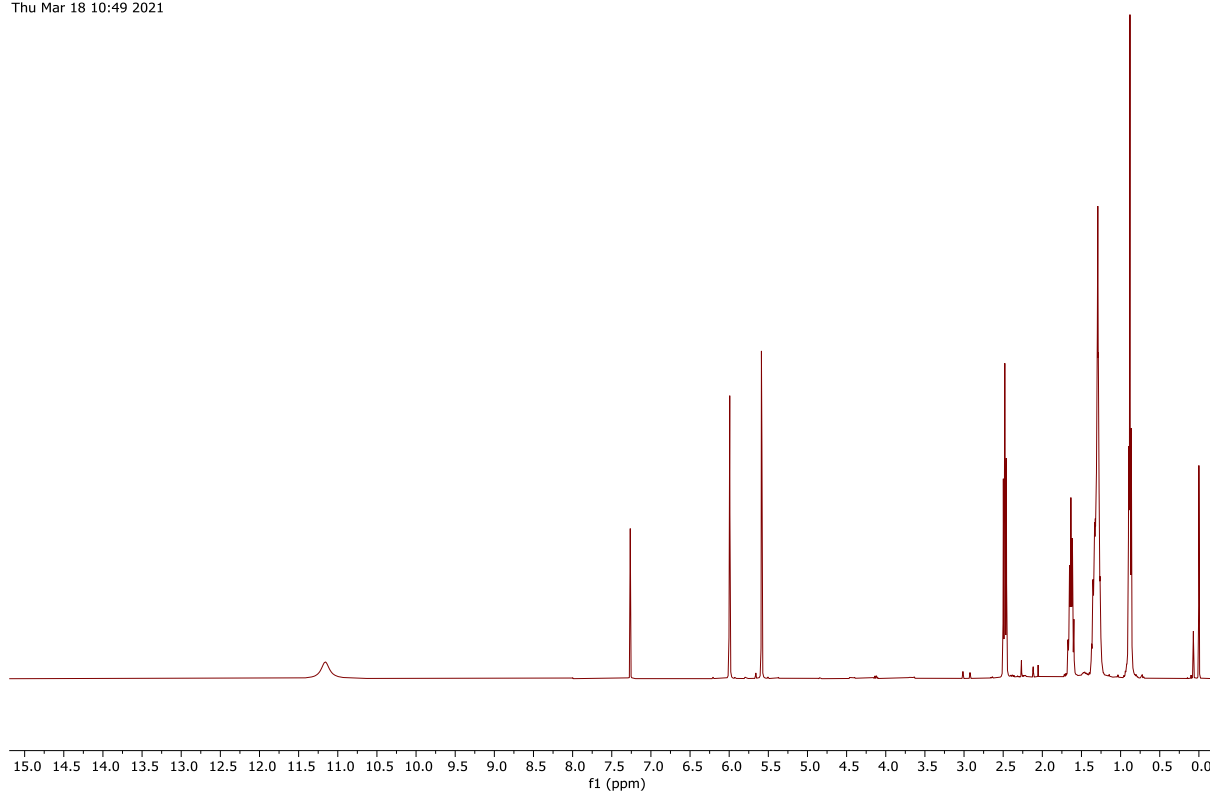


Figure 189: ¹H NMR spectrum (400 MHz, CDCl₃) of compound **5** (Chapter 4).

GGX433_CARBON_01
GGX433/CDCl₃/13C
Fuchs 20210318_05
Thu Mar 18 21:23 2021

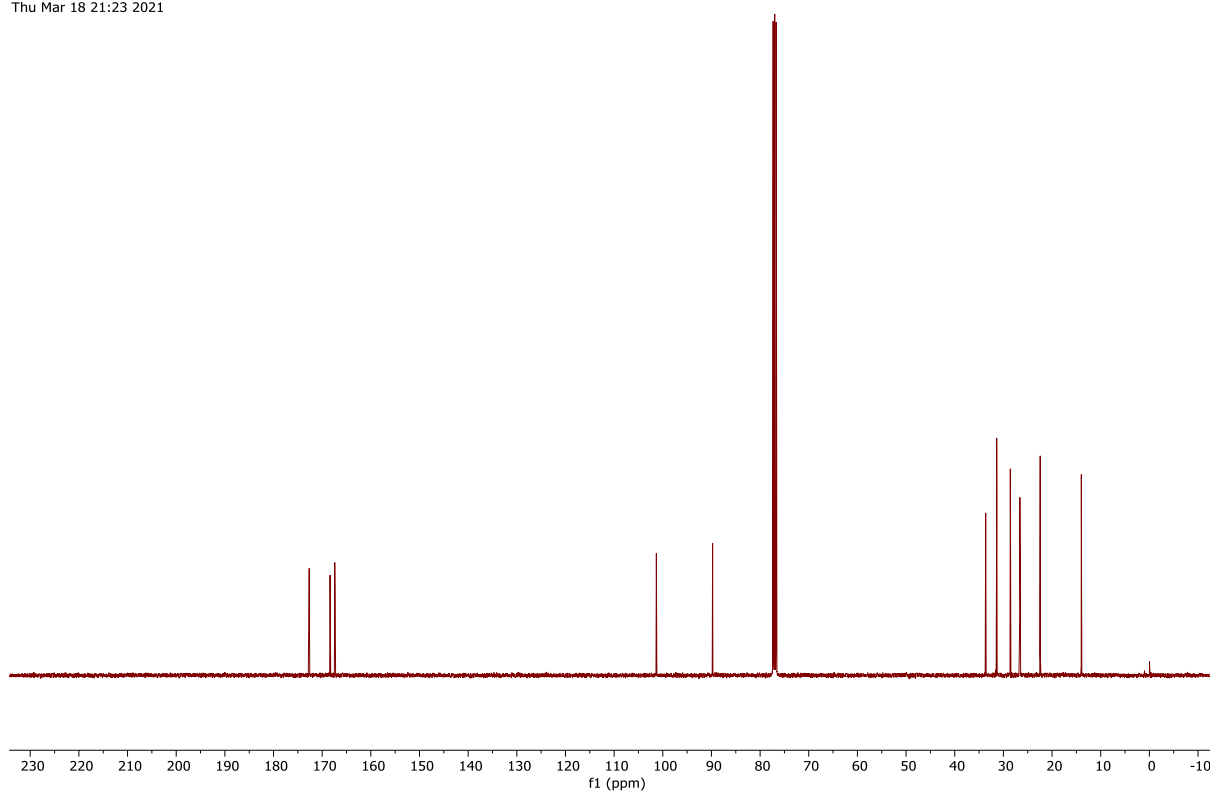


Figure 190: ¹³C NMR spectrum (101 MHz, CDCl₃) of compound **5** (Chapter 4).

GGX434_PROTON_02
GGX434/CDCl₃/1H
Fuchs 20210329_02
Mon Mar 29 09:21 2021

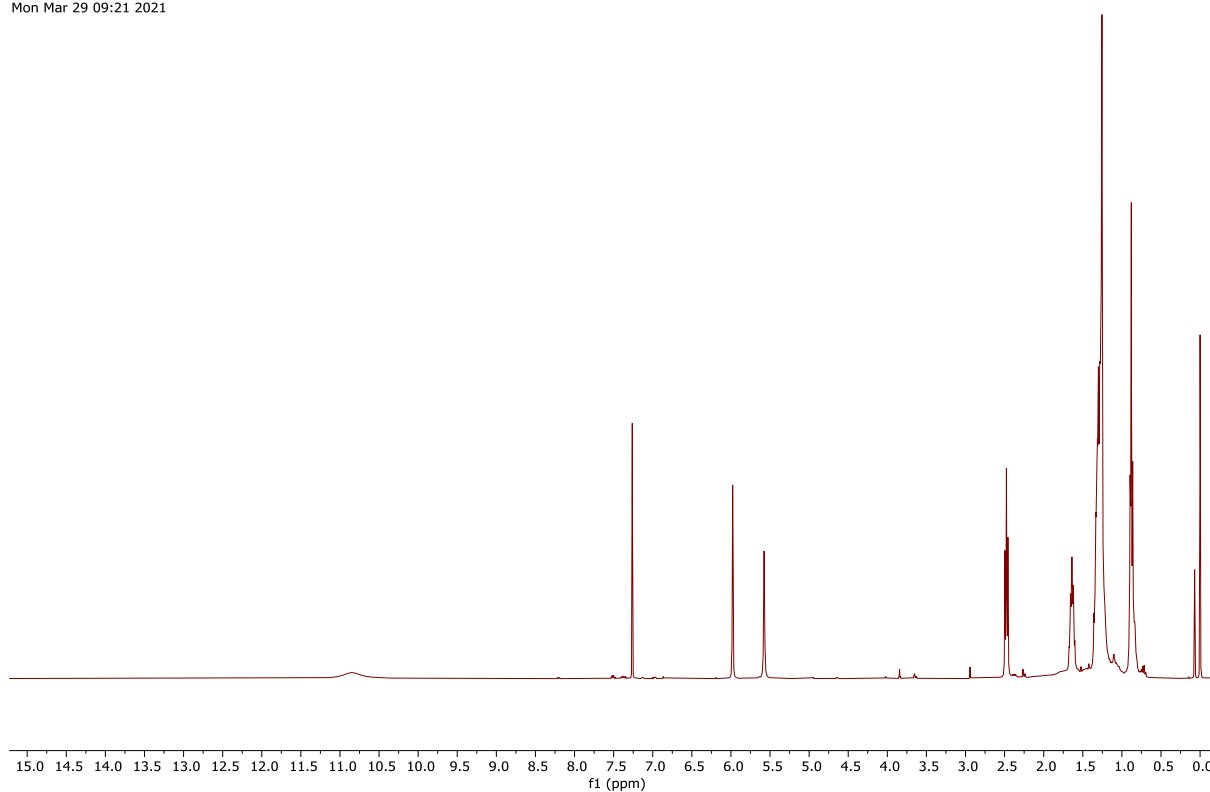


Figure 191: ¹H NMR spectrum (400 MHz, CDCl₃) of compound **6** (Chapter 4).

GGX434_CARBON_01
GGX434/CDCl₃/13C
Fuchs 20210329_02
Mon Mar 29 16:53 2021

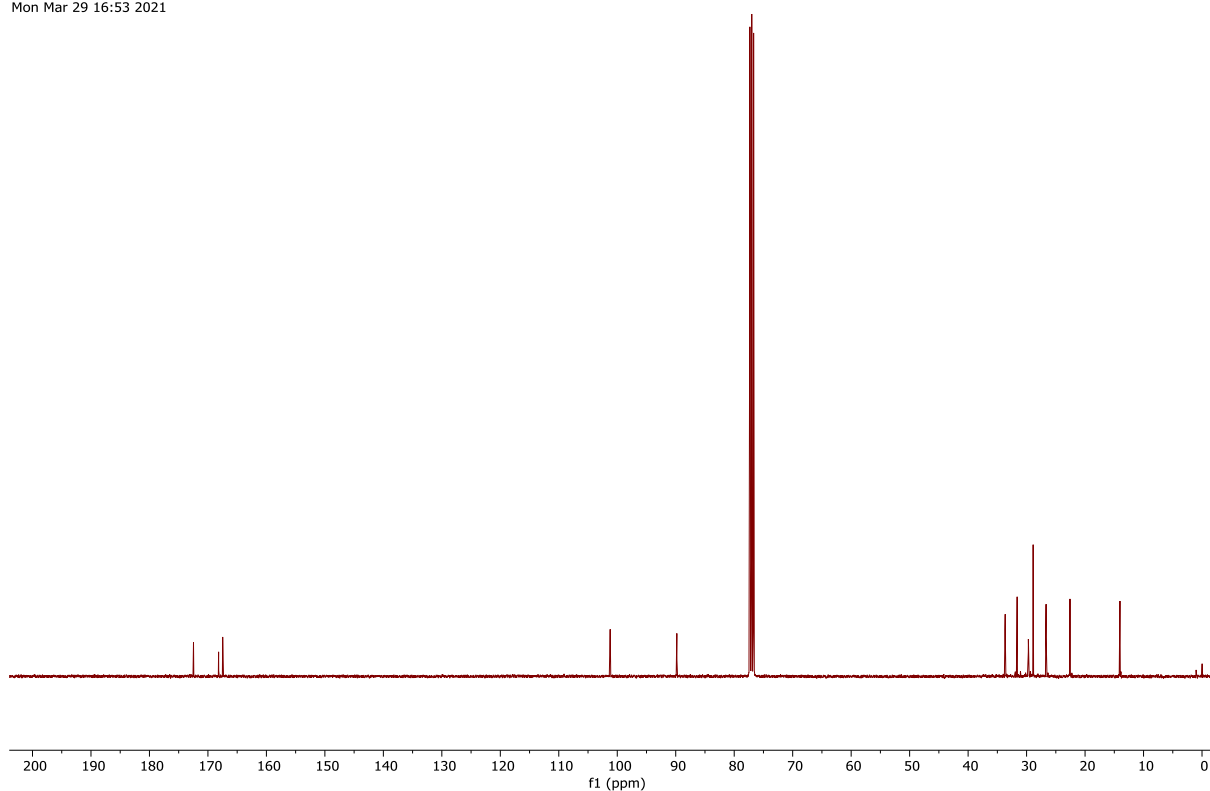


Figure 192: ¹³C NMR spectrum (101 MHz, CDCl₃) of compound **6** (Chapter 4).

GGX381_PROTON_01
GGX381/CDCl₃/1H
Fuchs 20201119_05
Thu Nov 19 13:58 2020

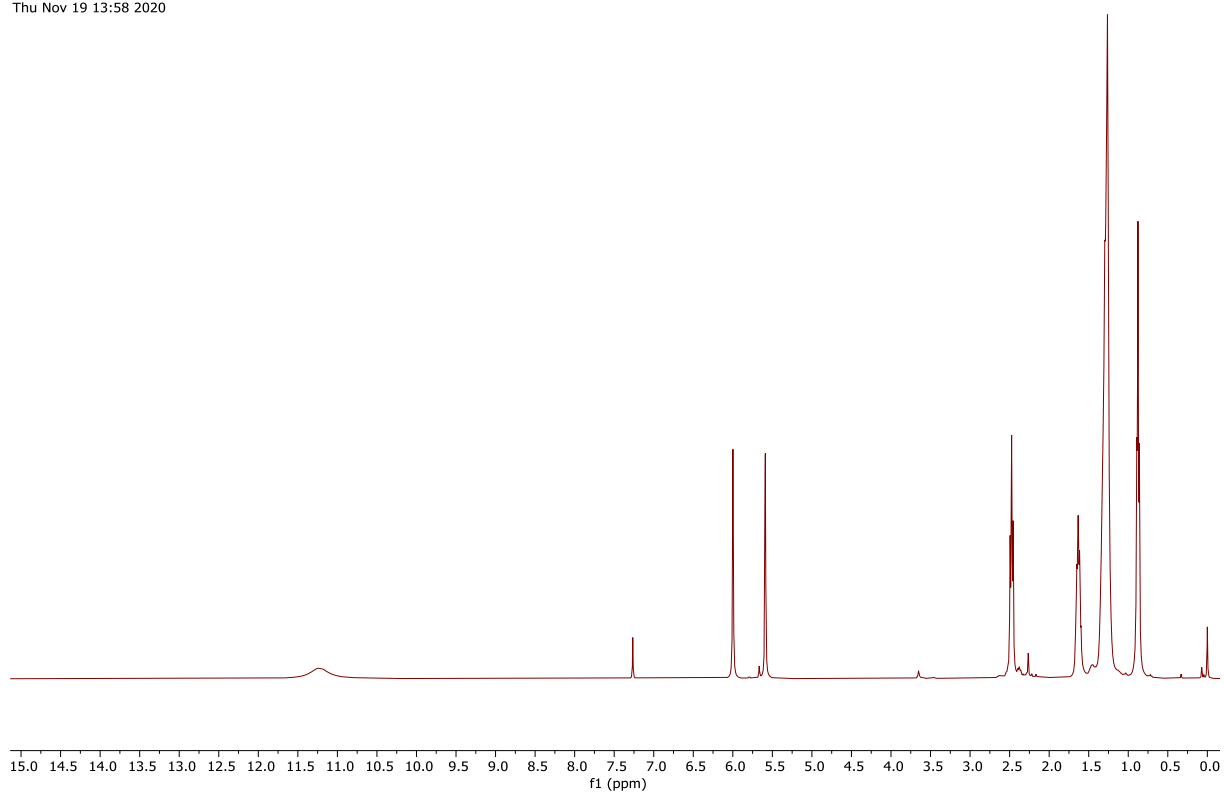


Figure 193: ¹H NMR spectrum (400 MHz, CDCl₃) of compound **7** (Chapter 4).

GGX381_CARBON_01
GGX381/CDCl₃/13C
Fuchs 20201119_05
Thu Nov 19 15:25 2020

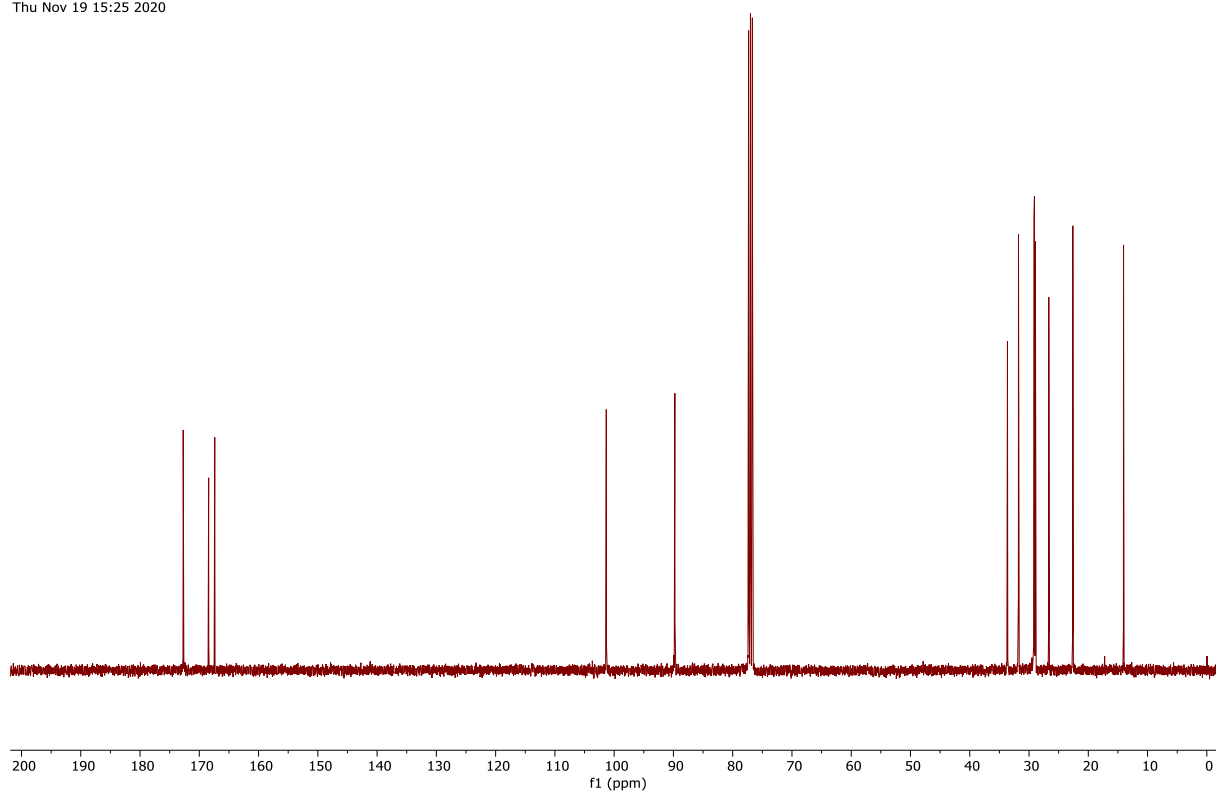


Figure 194: ¹³C NMR spectrum (101 MHz, CDCl₃) of compound **7** (Chapter 4).

GGX435_PROTON_03
GGX435/CDCl₃/1H
Fuchs 20210315_17
Tue Mar 16 05:01 2021

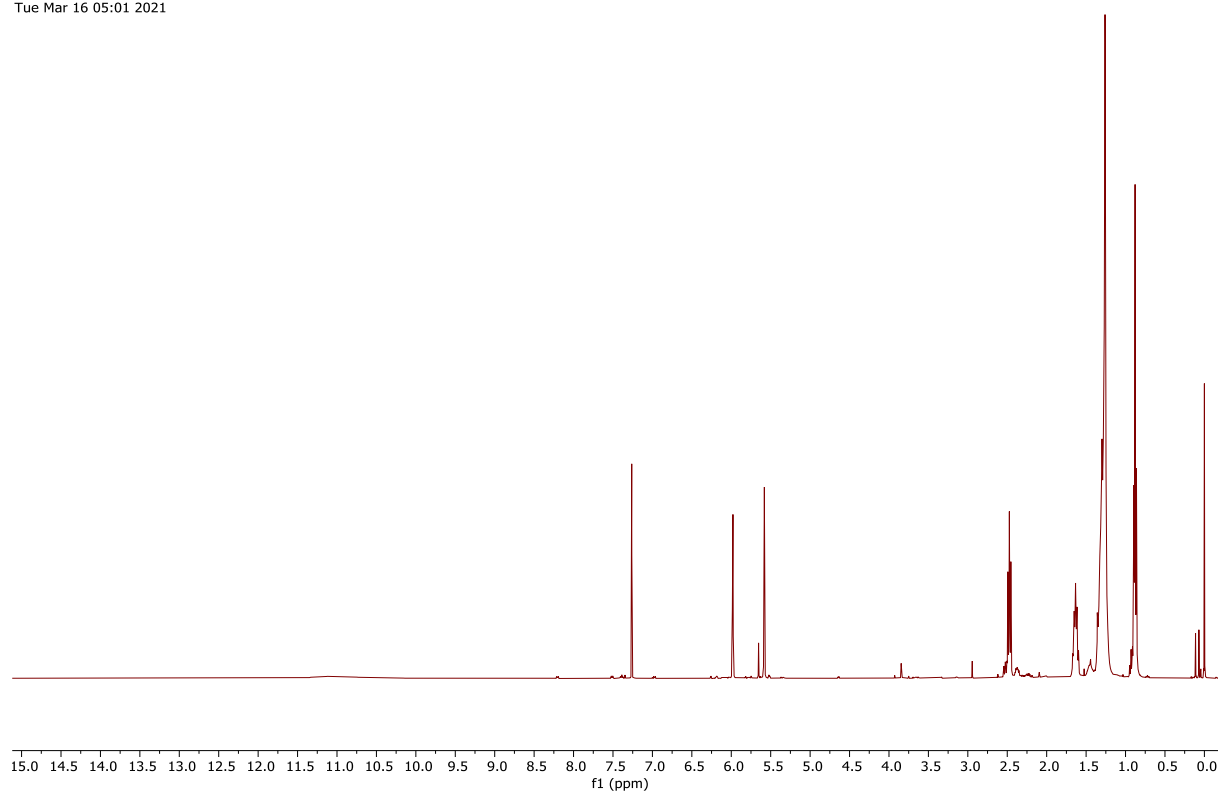


Figure 195: ¹H NMR spectrum (400 MHz, CDCl₃) of compound **8** (Chapter 4).

GGX435_CARBON_01
GGX435/CDCl₃/13C
Fuchs 20210315_17
Tue Mar 16 05:02 2021

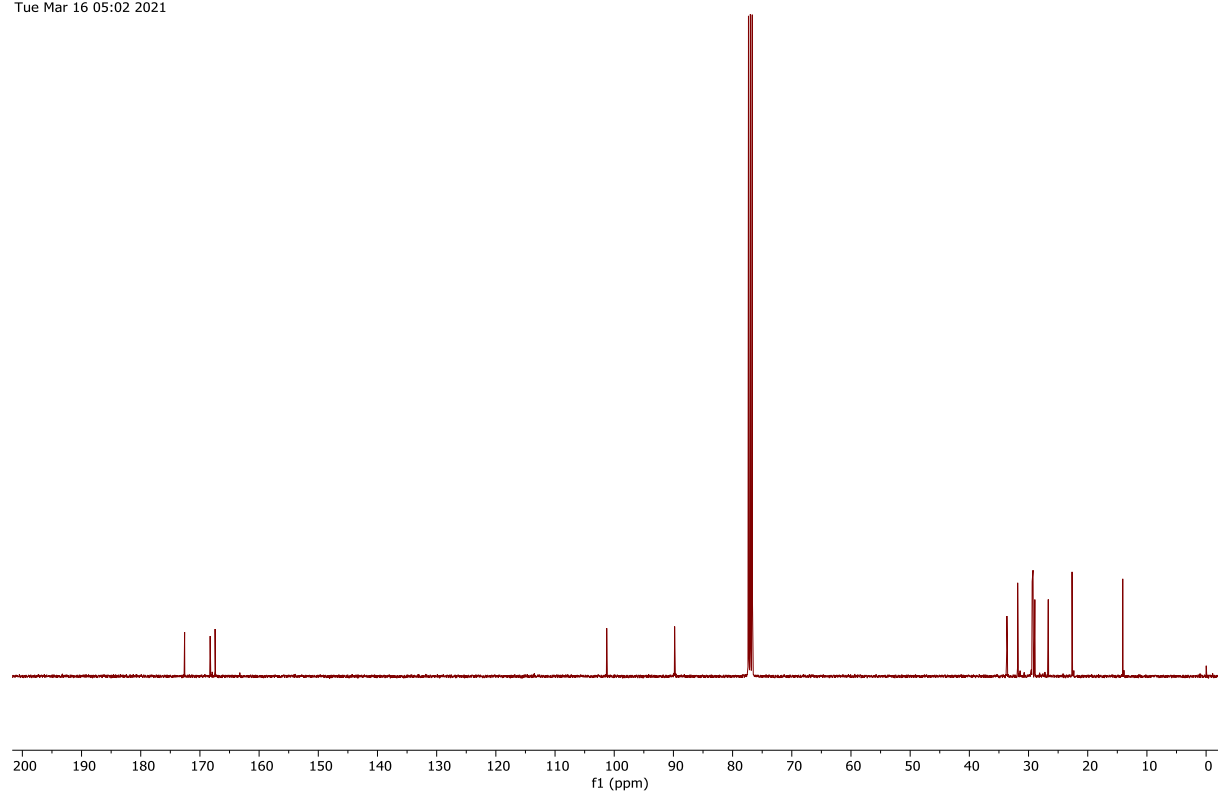


Figure 196: ¹³C NMR spectrum (101 MHz, CDCl₃) of compound **8** (Chapter 4).

GGX389_PROTON_02
GGX389/CDCl₃/1H
Fuchs 20210111_03
Mon Jan 11 14:21 2021

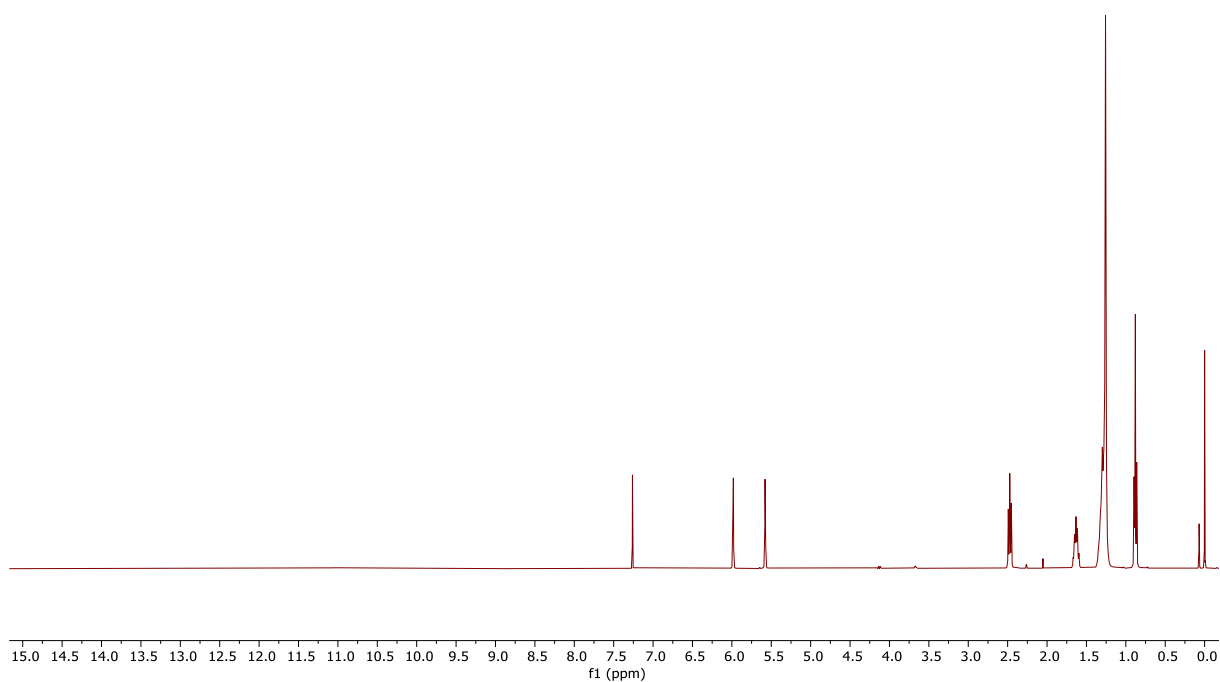


Figure 197: ¹H NMR spectrum (400 MHz, CDCl₃) of compound **9** (Chapter 4).

GGX389_CARBON_01
GGX389/CDCl₃/13C
Fuchs 20210111_03
Mon Jan 11 14:22 2021

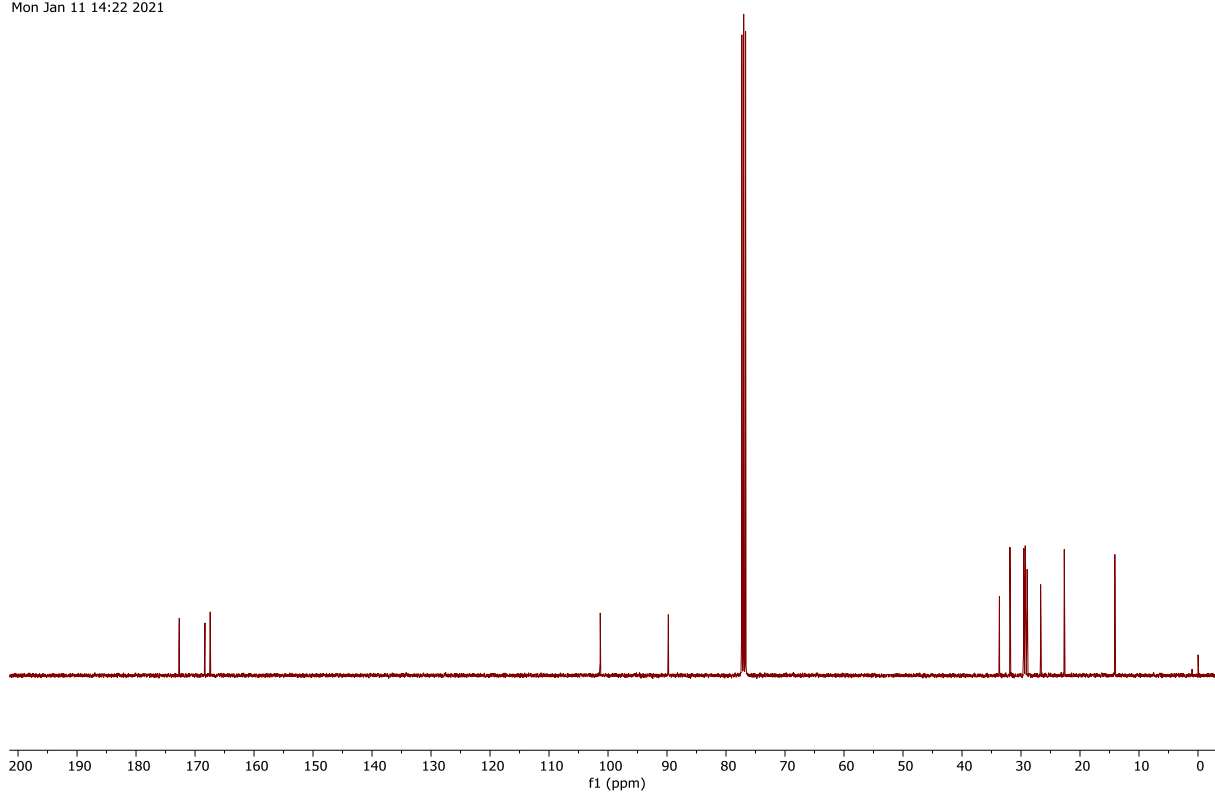


Figure 198: ¹³C NMR spectrum (101 MHz, CDCl₃) of compound **9** (Chapter 4).

GGX436.11.fid
GGX436/CDCl₃/1H
Fuchs 20210426_01
Proton_IPB CDCl₃ /opt/nmrdata/2020/GGX walkup 11

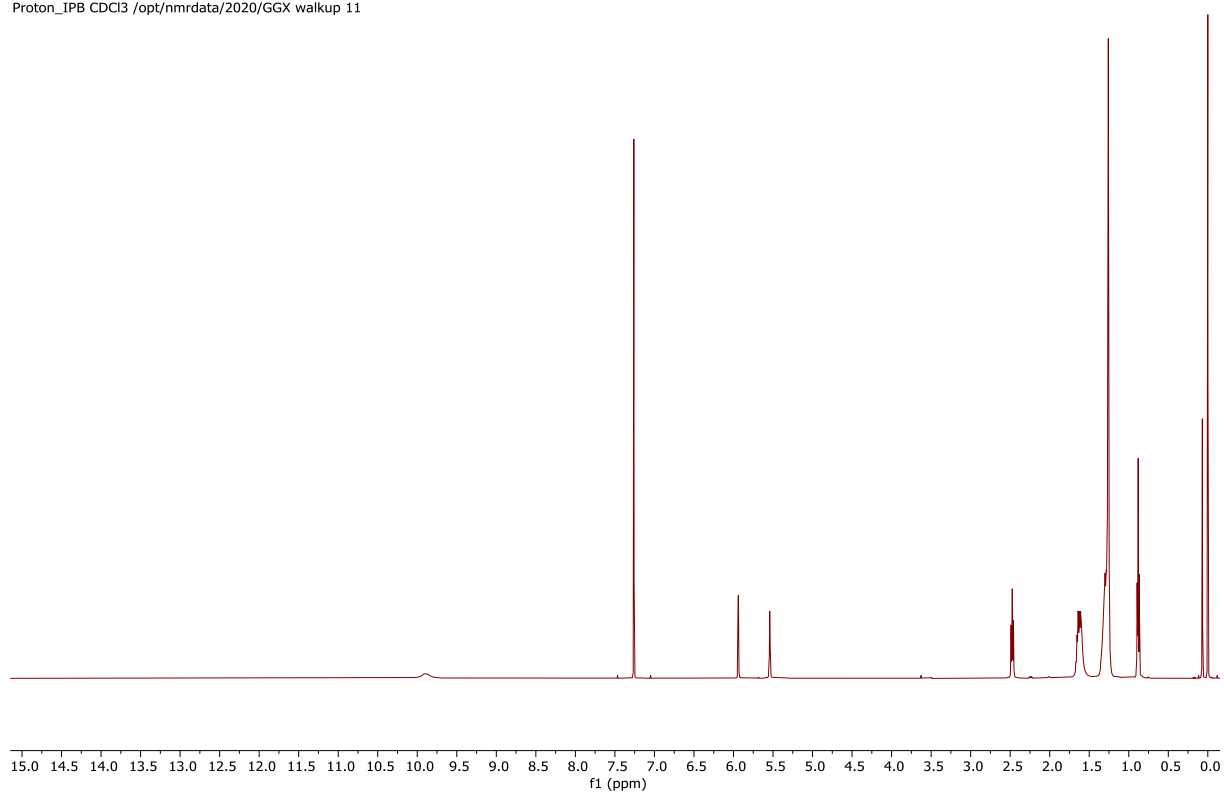


Figure 199: ¹H NMR spectrum (500 MHz, CDCl₃) of compound **10** (Chapter 4).

GGX436.12.fid
GGX436/CDCl₃/13C
Fuchs 20210426_01
Carbon_dec_IPB CDCl₃ /opt/nmrdata/2020/GGX walkup 11

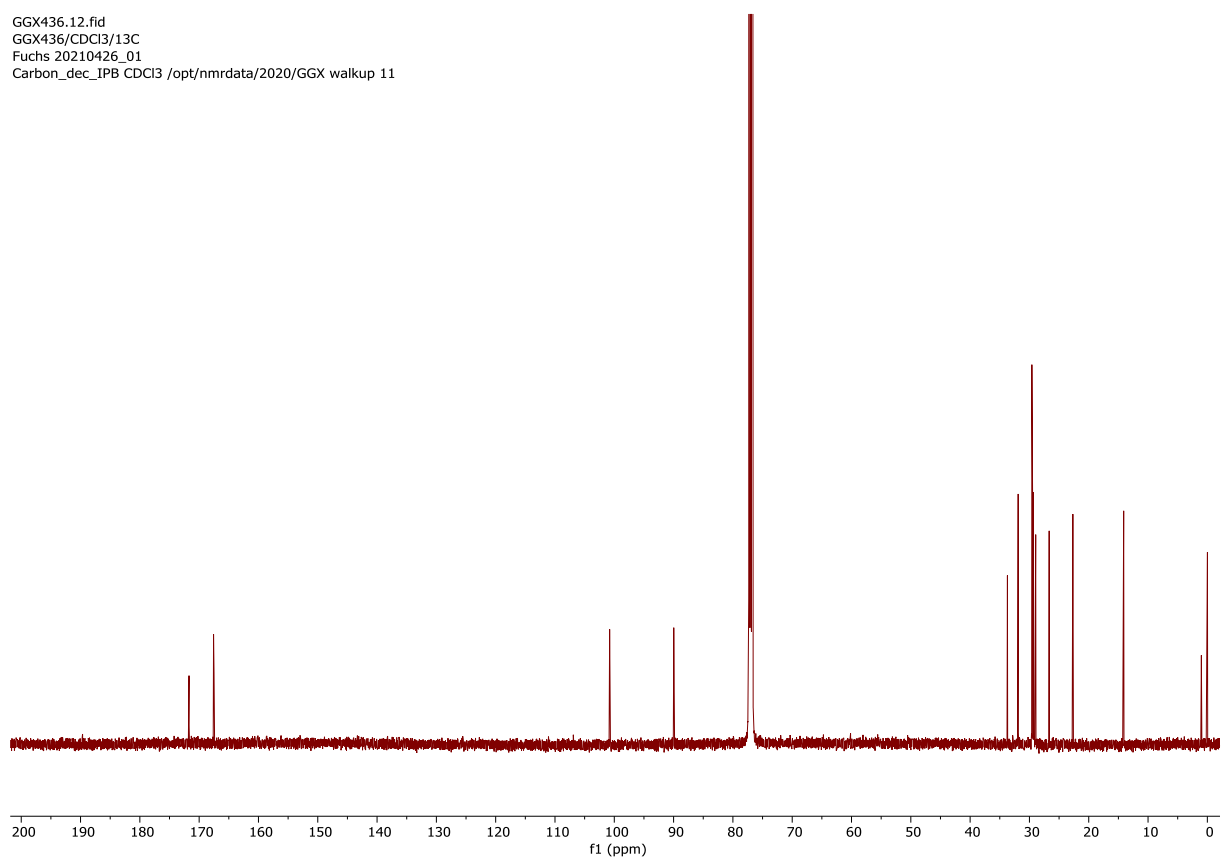


Figure 200: ¹³C NMR spectrum (126 MHz, CDCl₃) of compound **10** (Chapter 4).

GGX382_D_PROTON_02
GGX382_D/CDCI3/1H
Fuchs 20201118_02
Wed Nov 18 16:45 2020

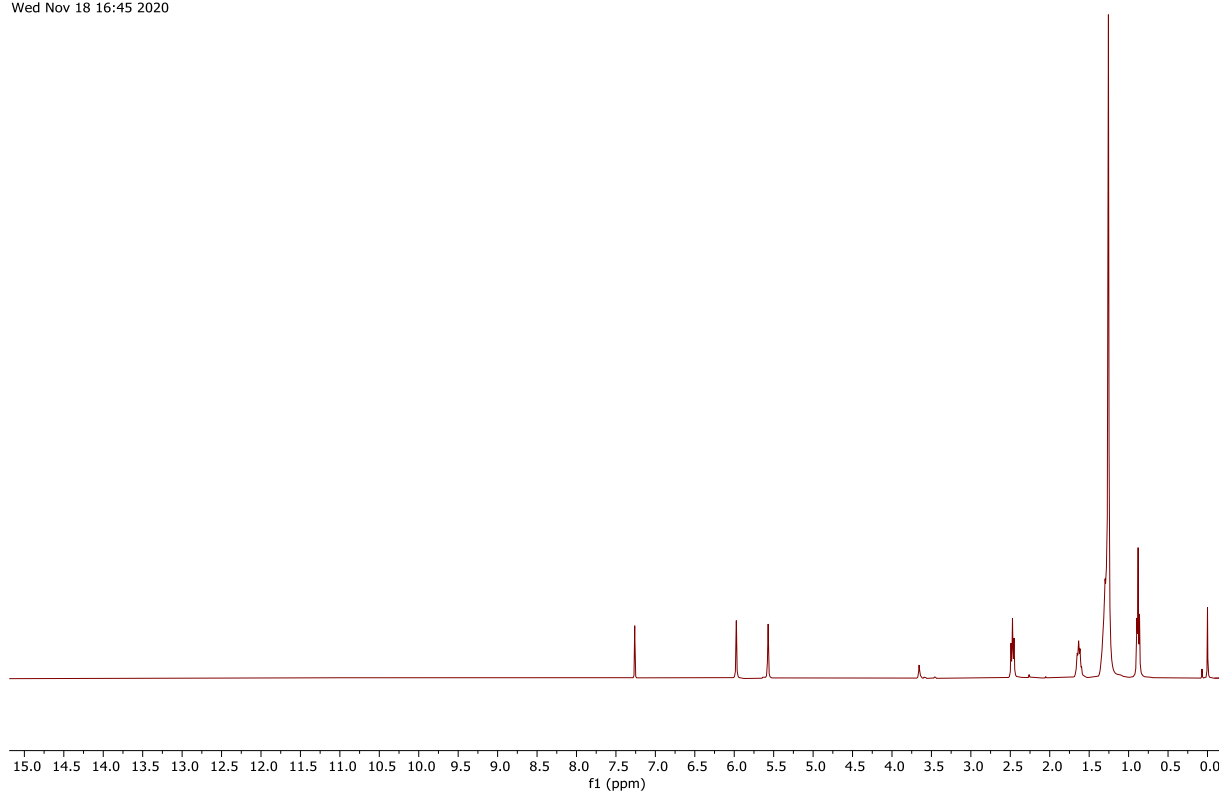


Figure 201: ¹H NMR spectrum (400 MHz, CDCl₃) of compound **11** (Chapter 4).

GGX382_D_CARBON_01
GGX382_D/CDCI3/13C
Fuchs 20201118_02
Wed Nov 18 16:46 2020

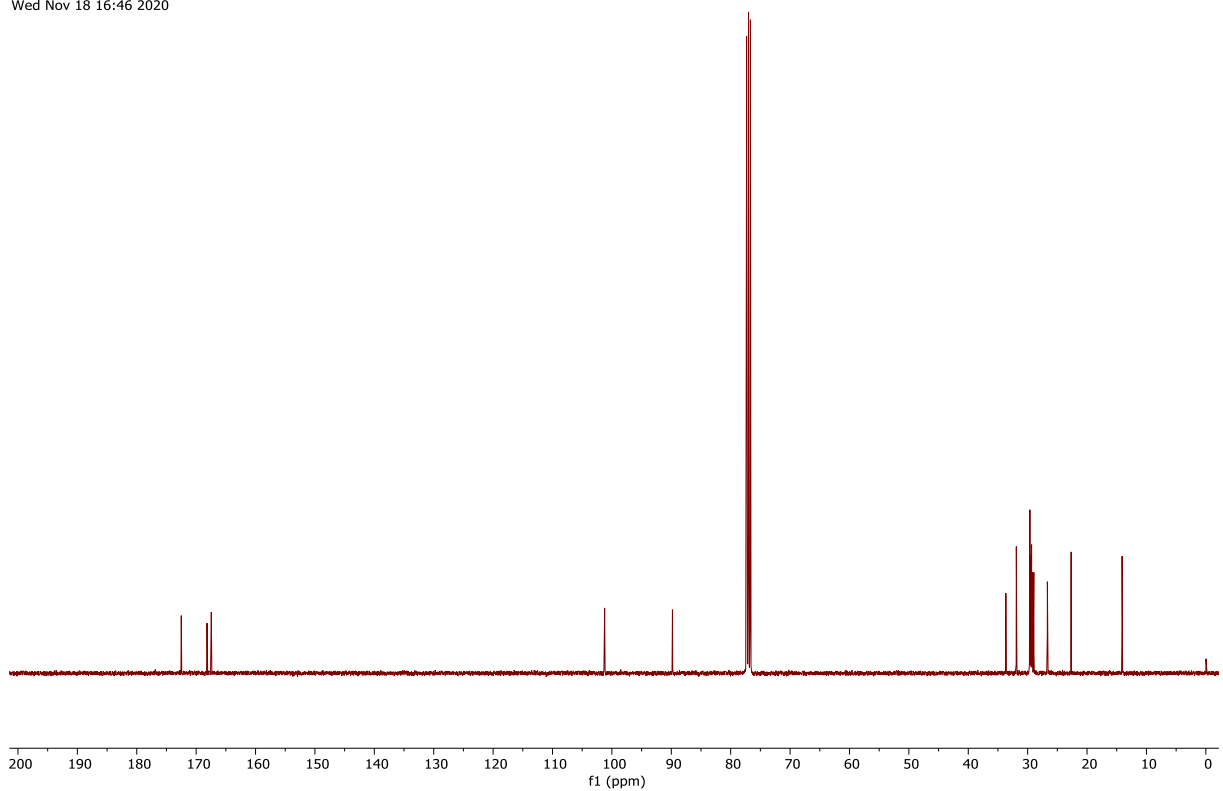


Figure 202: ¹³C NMR spectrum (101 MHz, CDCl₃) of compound **11** (Chapter 4).

GGX392_P_PROTON_01
GGX392_P/CDCl₃/1H
Fuchs 20201130_09
Mon Nov 30 12:03 2020

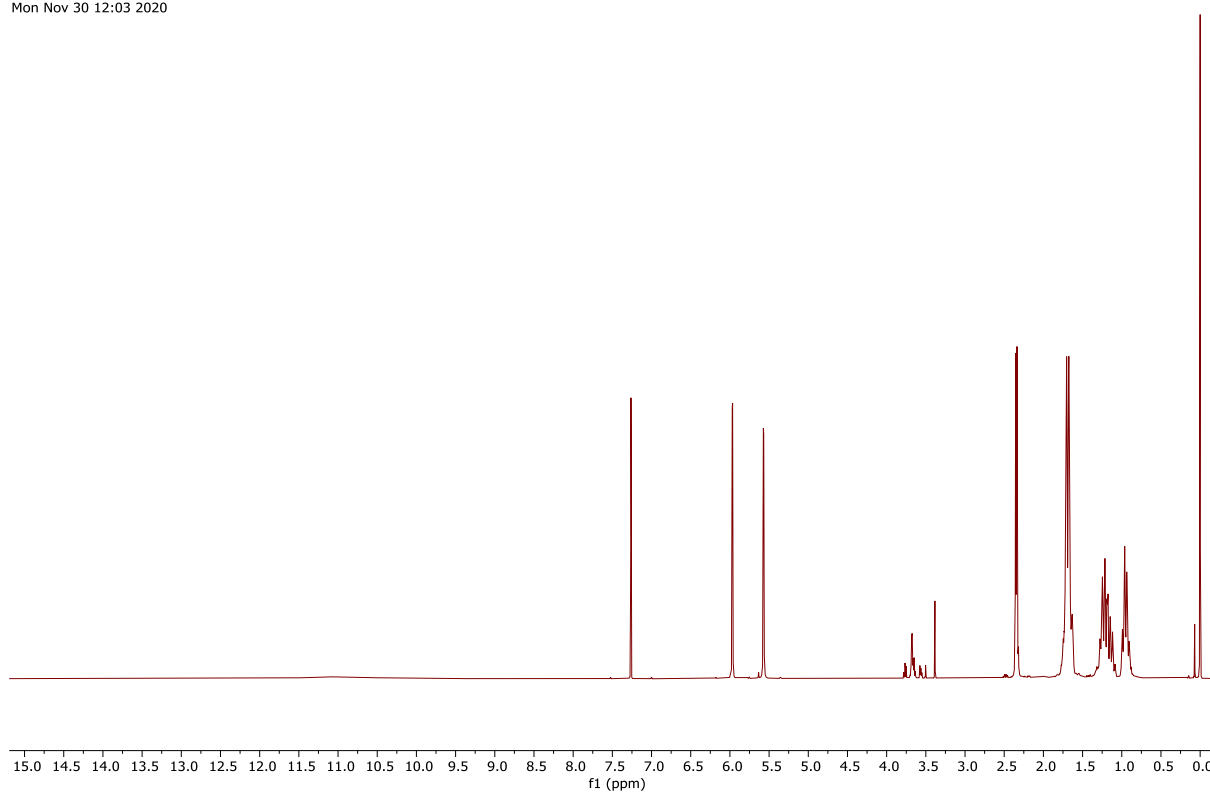


Figure 203: ¹H NMR spectrum (400 MHz, CDCl₃) of compound **12** (Chapter 4).

GGX392_P_CARBON_01
GGX392_P/CDCl₃/13C
Fuchs 20201130_09
Mon Nov 30 19:26 2020

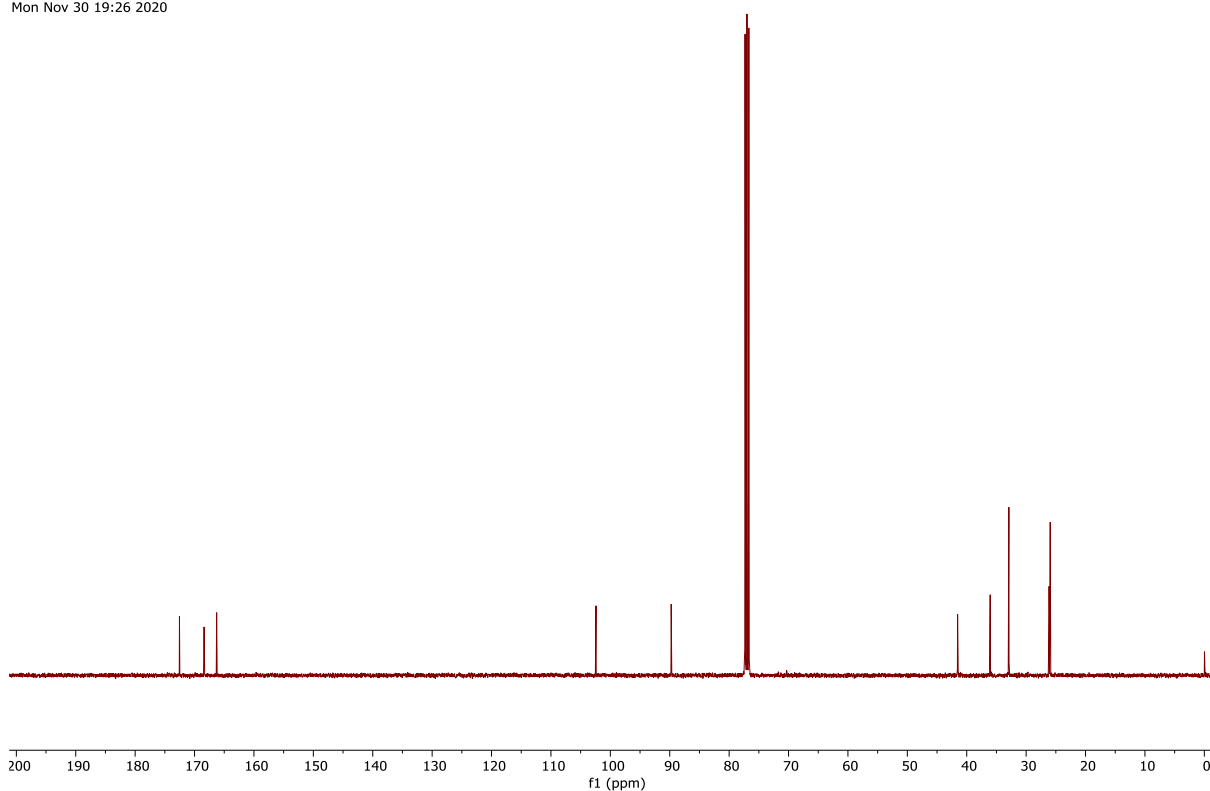


Figure 204: ¹³C NMR spectrum (101 MHz, CDCl₃) of compound **12** (Chapter 4).

GGX357_P_PROTON_02
GGX357_P/CDCl₃/1H
Fuchs 20200907_01
Sat Sep 5 10:47 2020

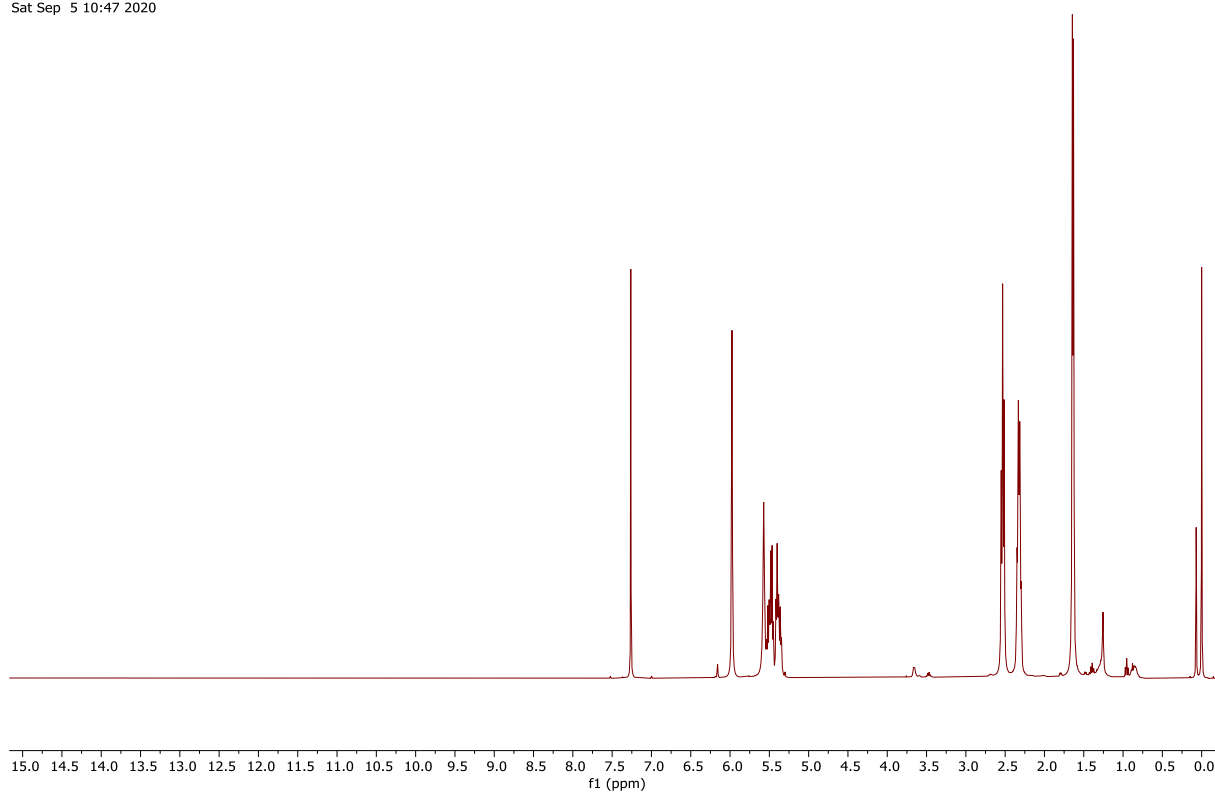


Figure 205: ¹H NMR spectrum (400 MHz, CDCl₃) of compound **13** (Chapter 4).

GGX357_P_CARBON_01
GGX357_P/CDCl₃/13C
Fuchs 20200907_01
Sat Sep 5 14:28 2020

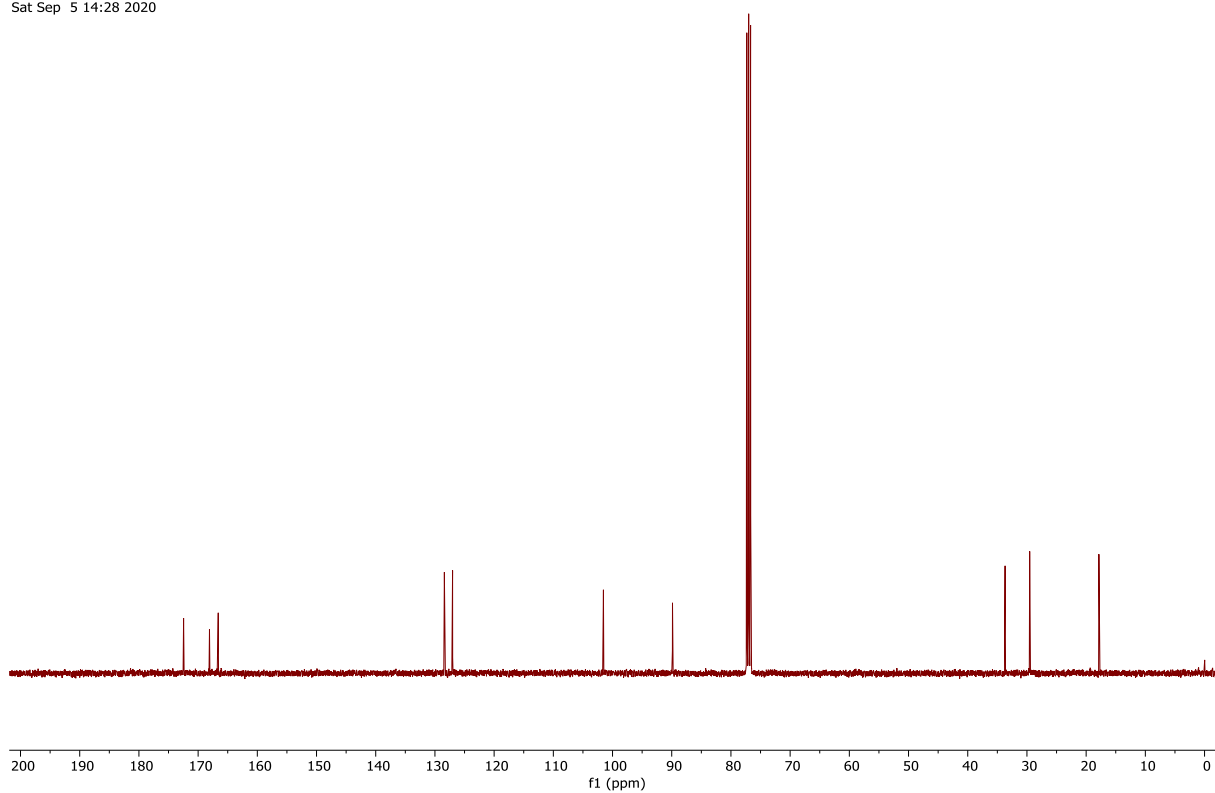


Figure 206: ¹³C NMR spectrum (101 MHz, CDCl₃) of compound **13** (Chapter 4).

GGX335_PROTON_01
GGX335/CDCl₃/1H
Fuchs 20200803_09
Mon Aug 3 16:35 2020

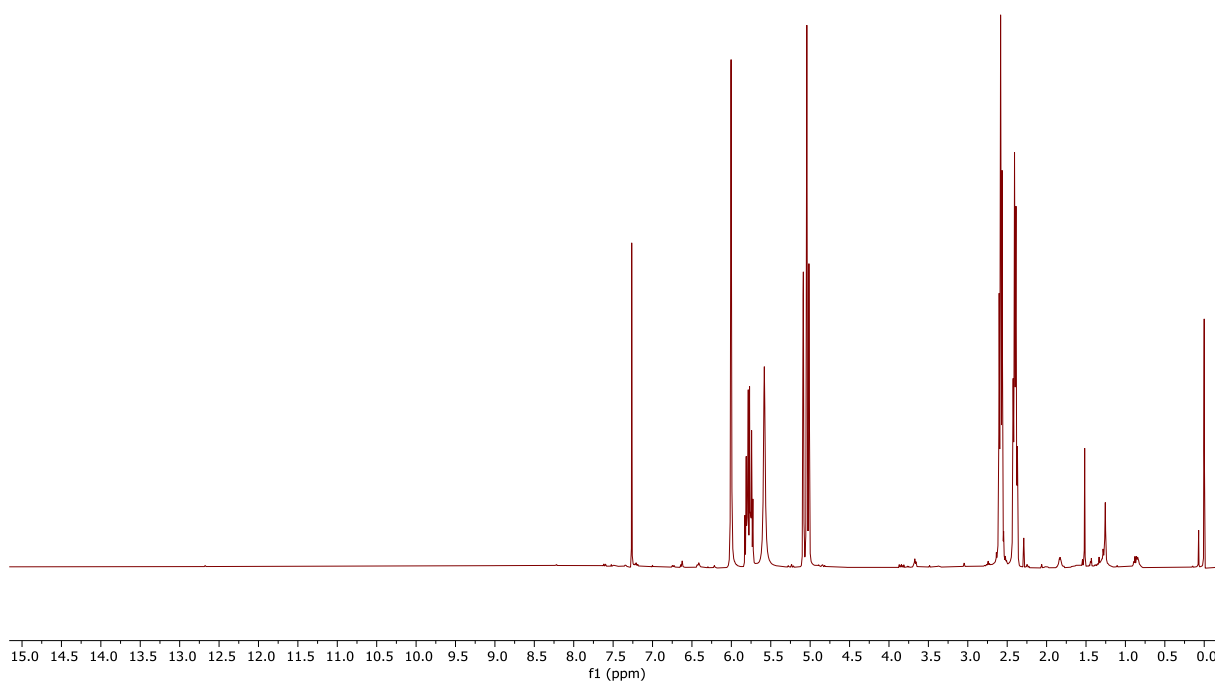


Figure 207: ¹H NMR spectrum (400 MHz, CDCl₃) of compound **14** (Chapter 4).

GGX335_CARBON_01
GGX335/CDCl₃/13C
Fuchs 20200803_09
Tue Aug 4 06:09 2020

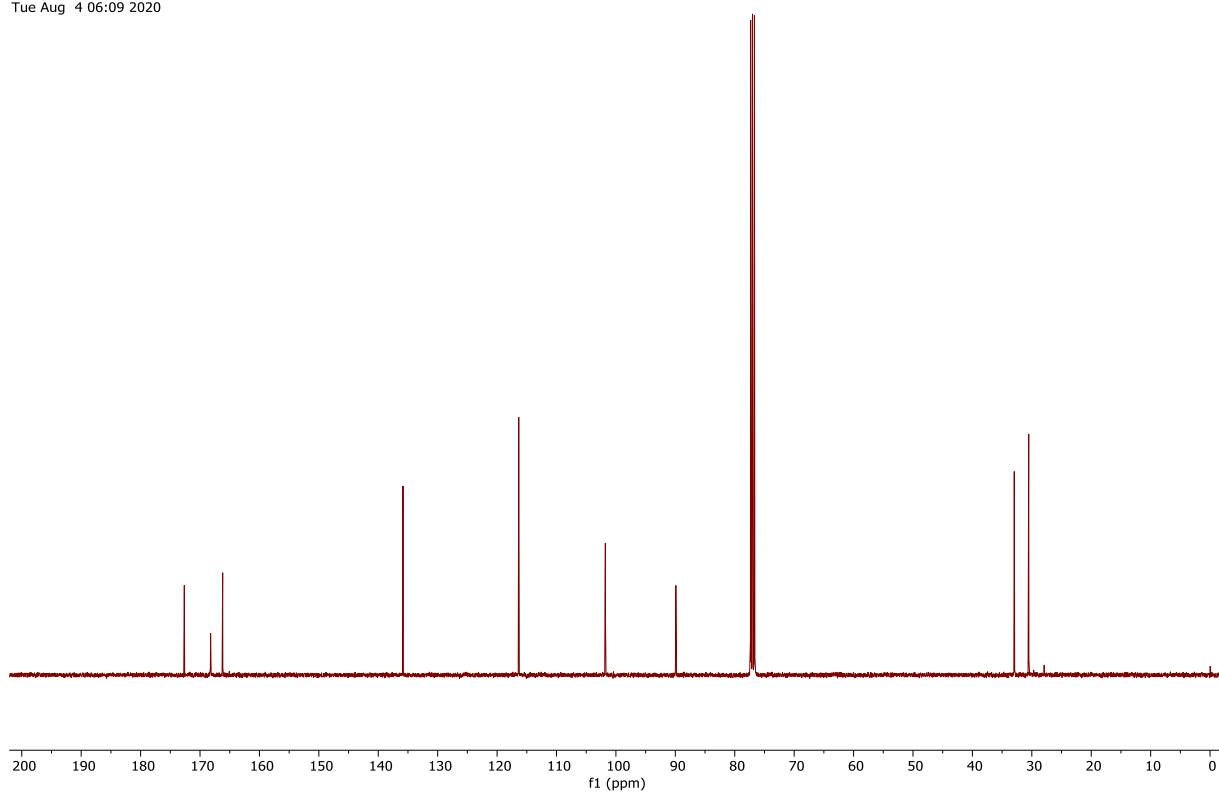


Figure 208: ¹³C NMR spectrum (101 MHz, CDCl₃) of compound **14** (Chapter 4).

GGX336_A_PROTON_02
GGX336_A/CDCl₃/1H
Fuchs 20200811_02
Tue Aug 11 12:01 2020

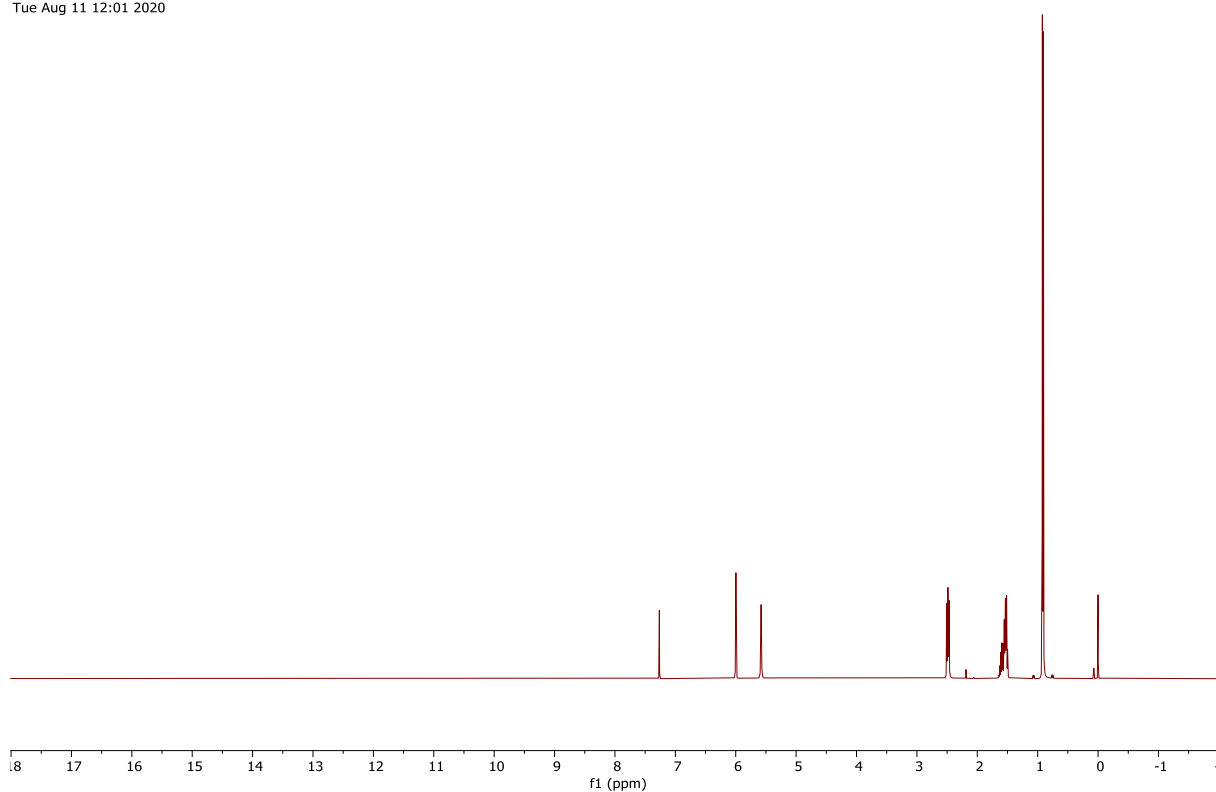


Figure 209: ¹H NMR spectrum (400 MHz, CDCl₃) of compound **15** (Fistupyrene, Chapter 4).

GGX336_A_CARBON_01
GGX336_A/CDCl₃/13C
Fuchs 20200811_02
Tue Aug 11 12:02 2020

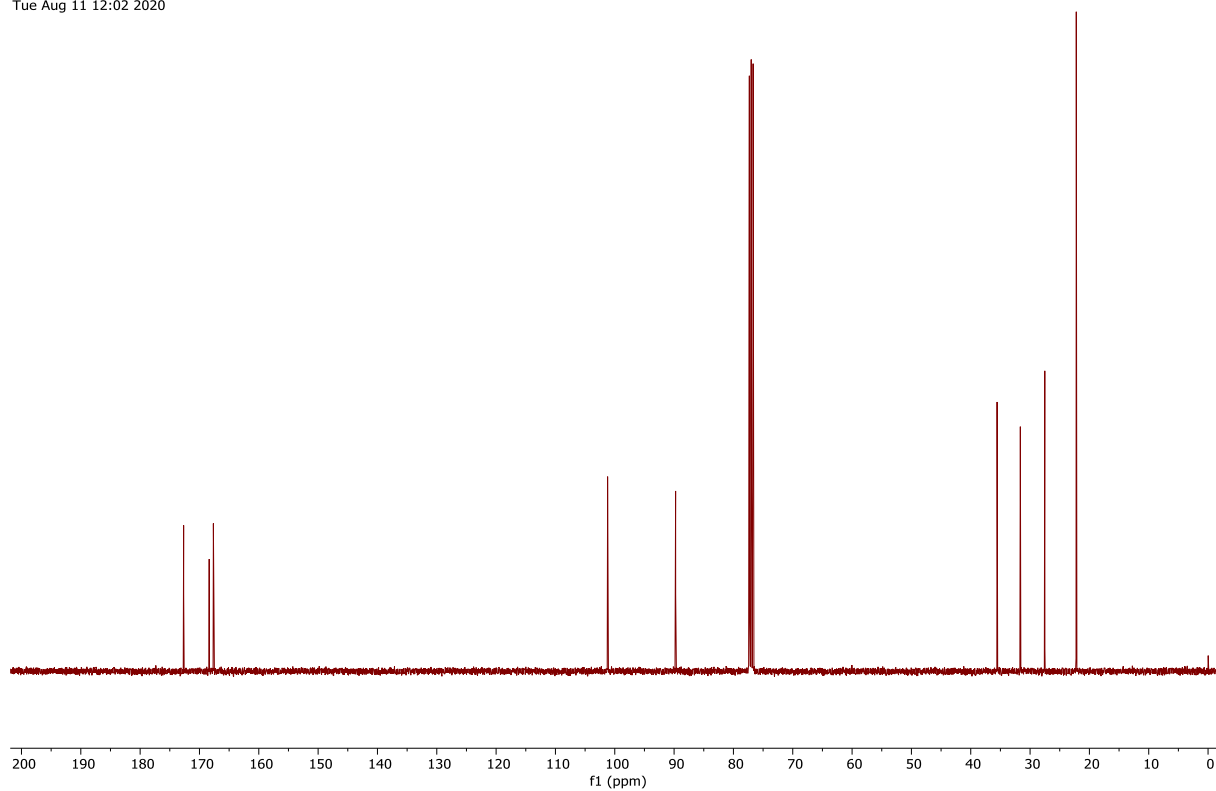


Figure 210: ¹³C NMR spectrum (101 MHz, CDCl₃) of compound **15** (Fistupyrene, Chapter 4).

GGX391_Fr14_PROTON_02
GGX391_Fr14/CDCl₃/1H
Fuchs 20201125_02
Wed Nov 25 16:21 2020

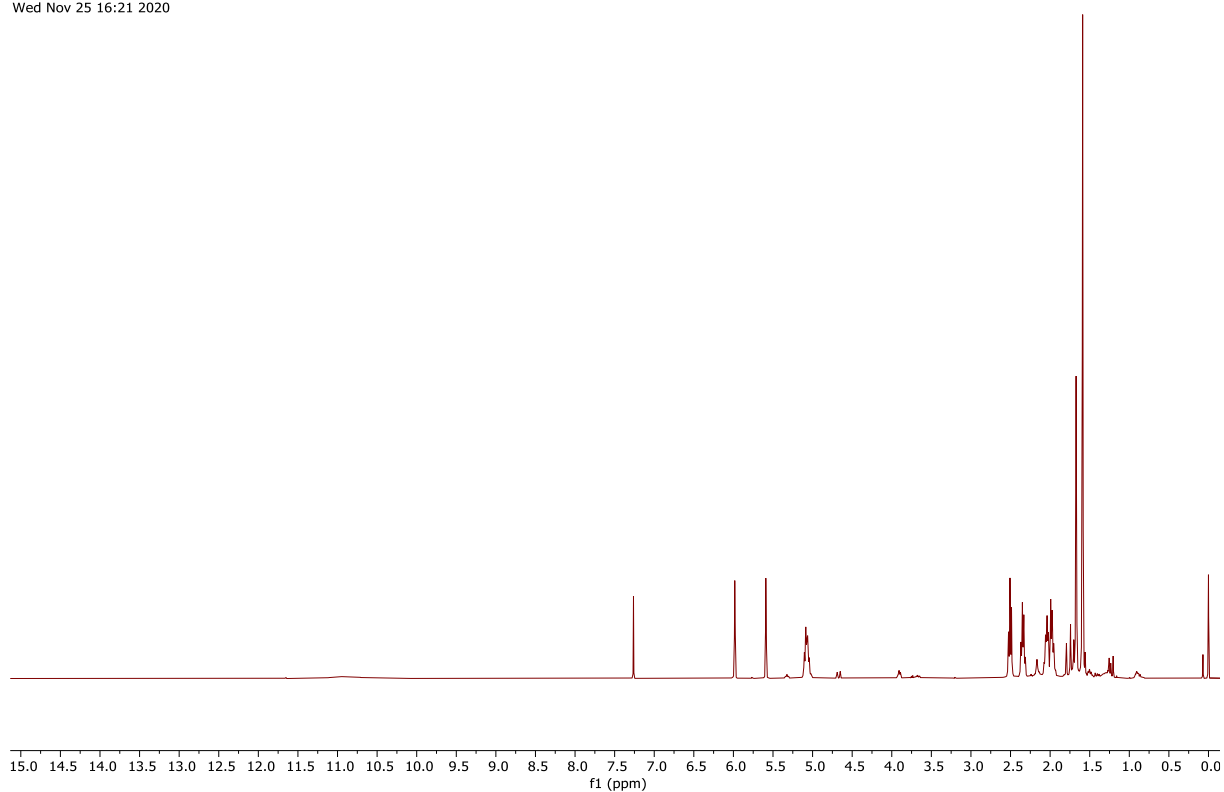


Figure 211: ¹H NMR spectrum (400 MHz, CDCl₃) of compound **16** (Chapter 4).

GGX391_Fr14_CARBON_01
GGX391_Fr14/CDCl₃/13C
Fuchs 20201125_02
Wed Nov 25 16:21 2020

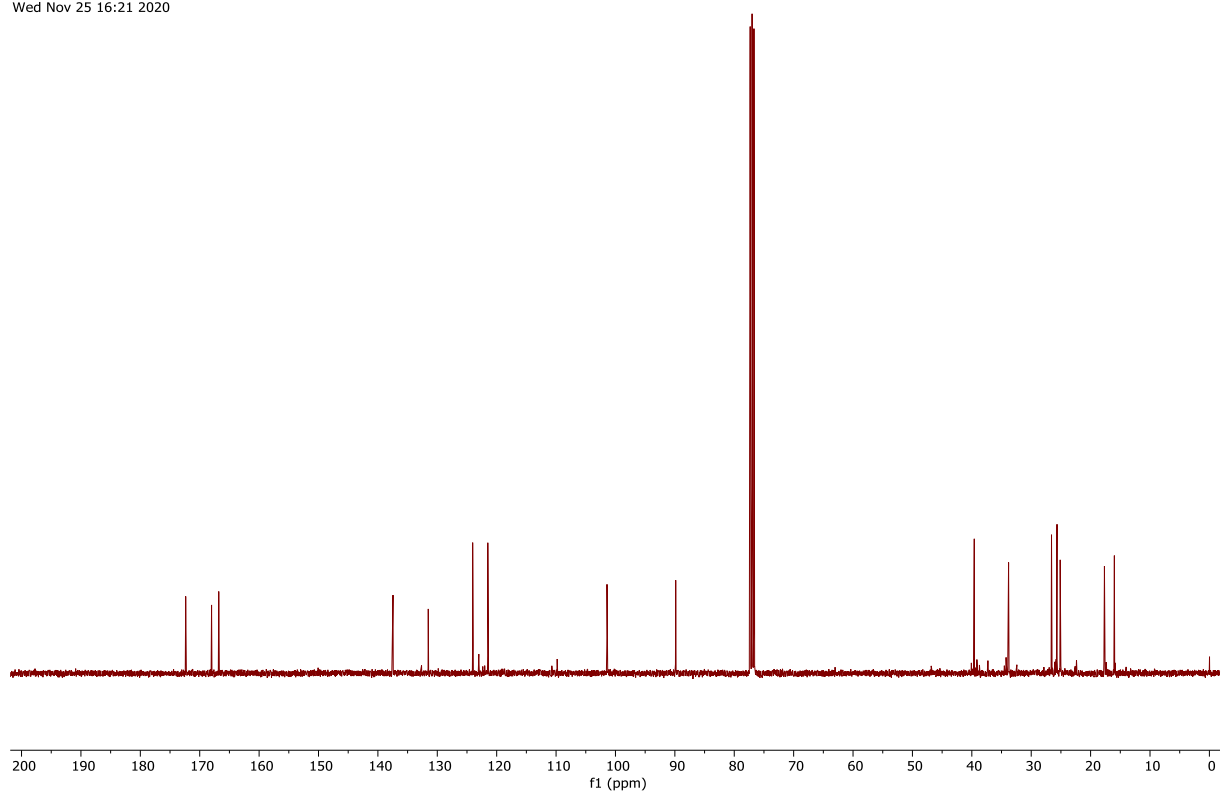


Figure 212: ¹³C NMR spectrum (101 MHz, CDCl₃) of compound **16** (Chapter 4).

GGX534_PROTON_01
GGX534/CDCl₃/1H
Fuchs 20220517_01
Tue May 17 09:04 2022

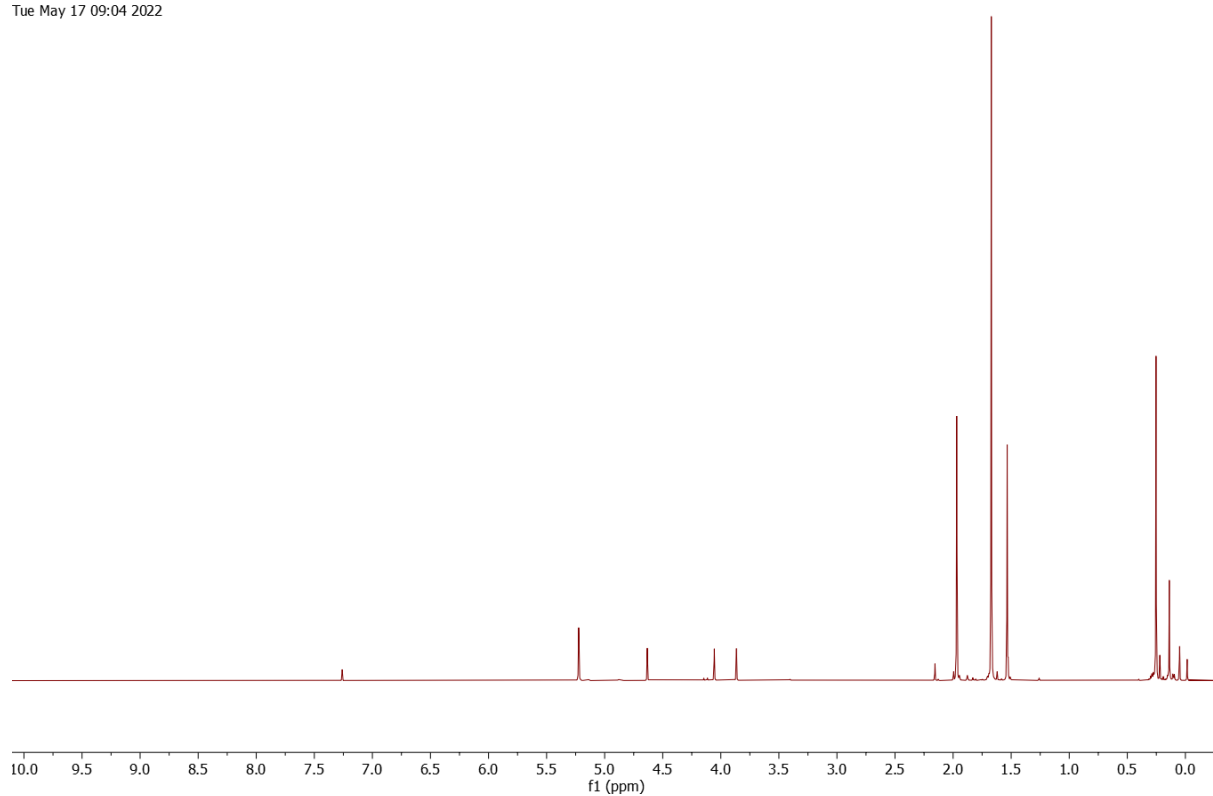


Figure 213: ¹H NMR spectrum (400 MHz, CDCl₃) of compound **17** (Chapter 4).

GGX535_PROTON_01
GGX535/CDCl₃/1H
Fuchs 20220525_01
Wed May 25 10:55 2022

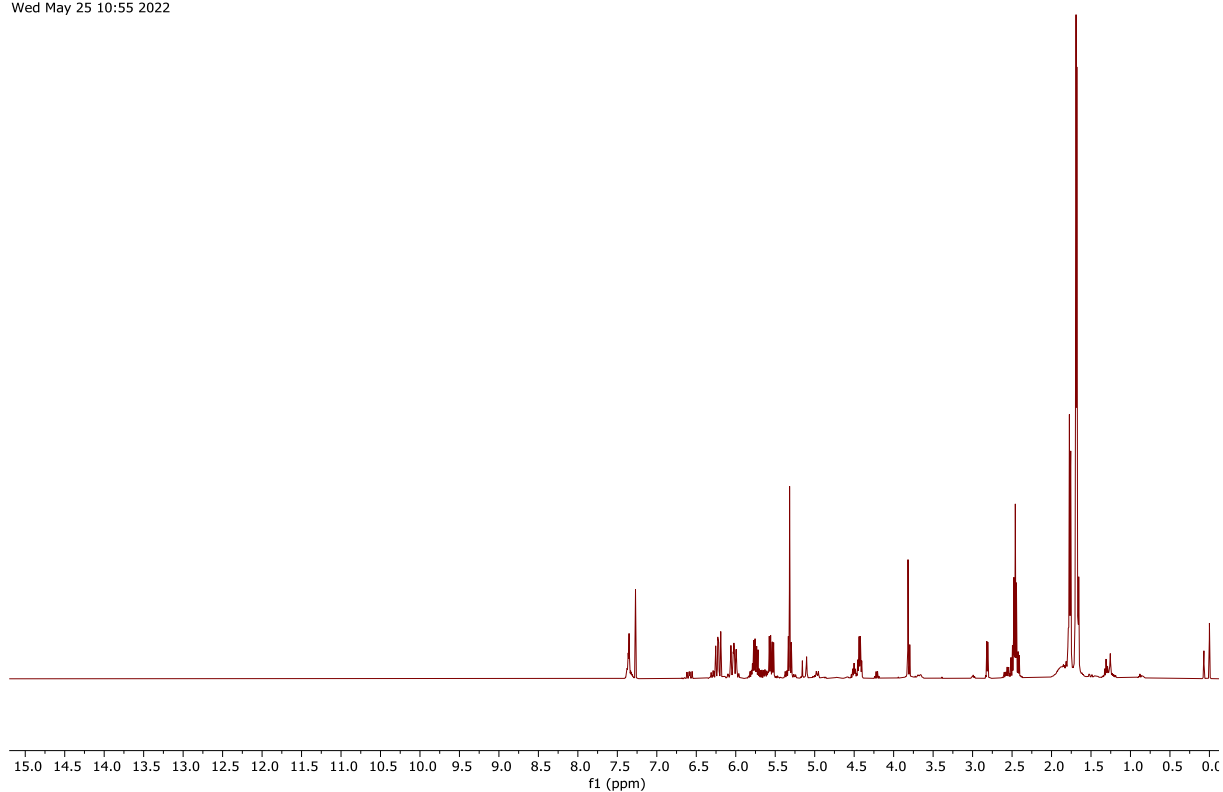


Figure 214: ¹H NMR spectrum (400 MHz, CDCl₃) of compound **18** (Chapter 4).

GGX535_CARBON_01
GGX535/CDCl₃/13C
Fuchs 20220525_01
Wed May 25 11:14 2022

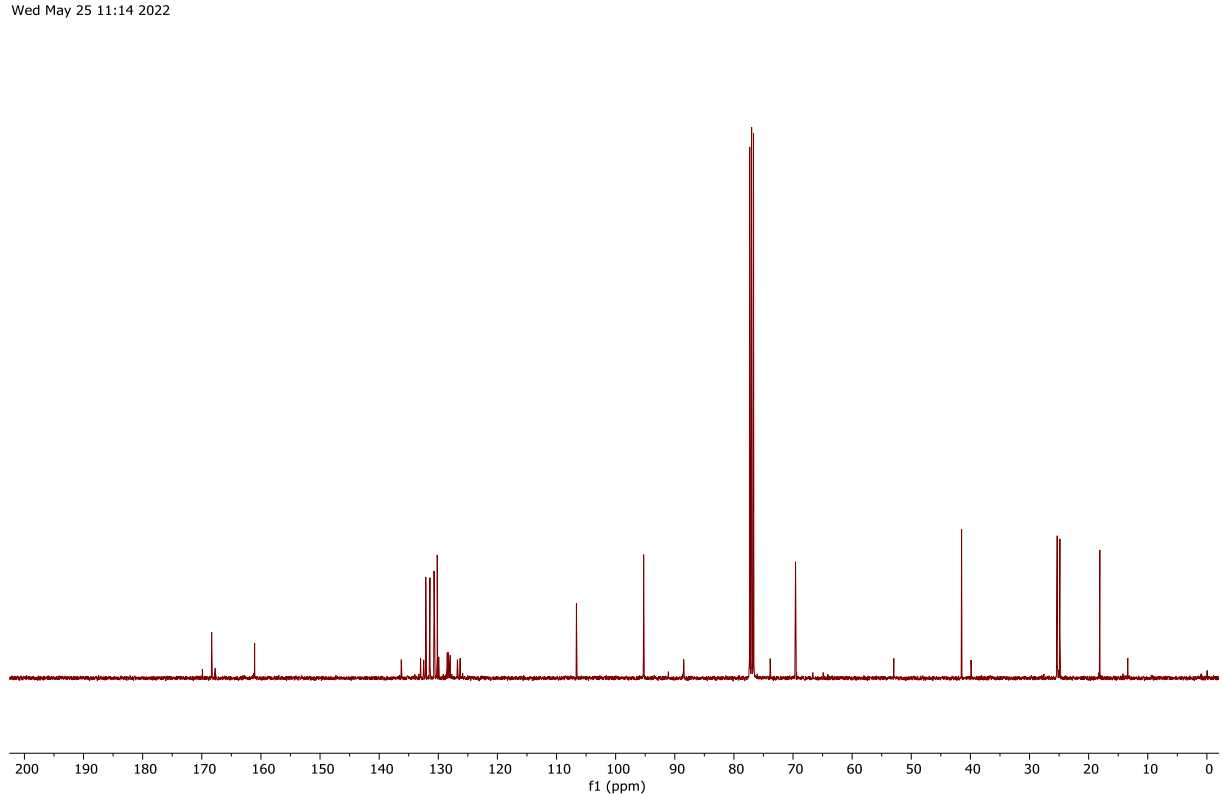


Figure 215: ¹³C NMR spectrum (101 MHz, CDCl₃) of compound **18** (Chapter 4).

GGX546_F2_PROTON_01
GGX546_F2/CDCl3/1H
Fuchs 20220718_03
Mon Jul 18 10:19 2022

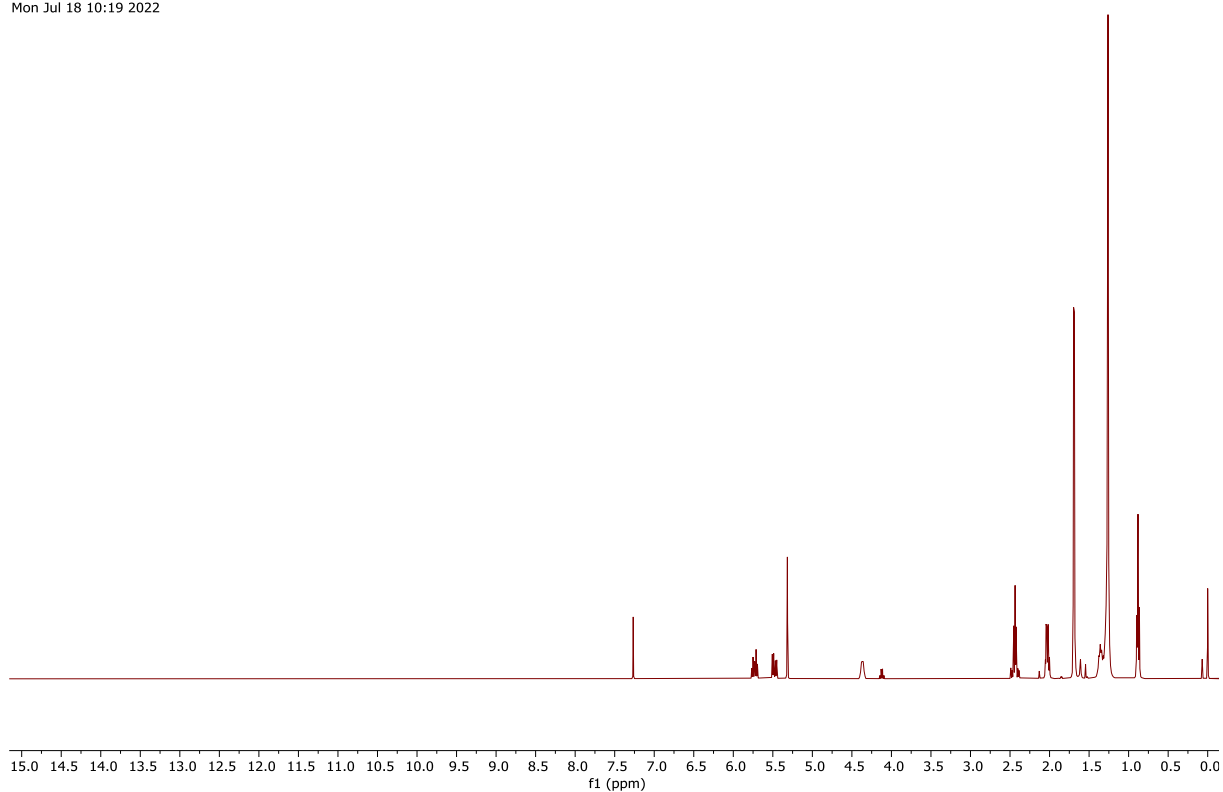


Figure 216: ¹H NMR spectrum (400 MHz, CDCl₃) of compound **19** (Chapter 4).

GGX546_F2_CARBON_01
GGX546_F2/CDCl3/13C
Fuchs 20220719_01
Tue Jul 19 05:38 2022

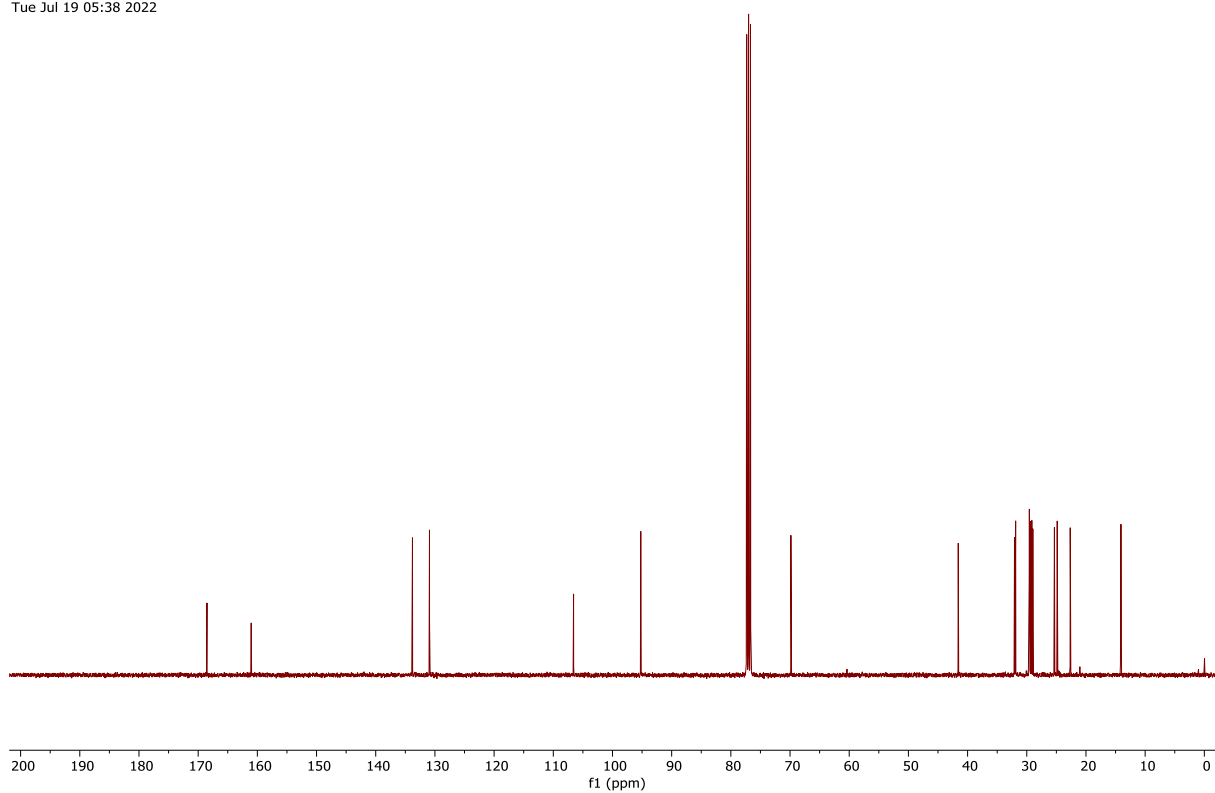


Figure 217: ¹³C NMR spectrum (101 MHz, CDCl₃) of compound **19** (Chapter 4).

GGX363_P_PROTON_01
GGX363_P/CDCl₃/1H
Fuchs 20200831_19
Mon Aug 31 16:37 2020

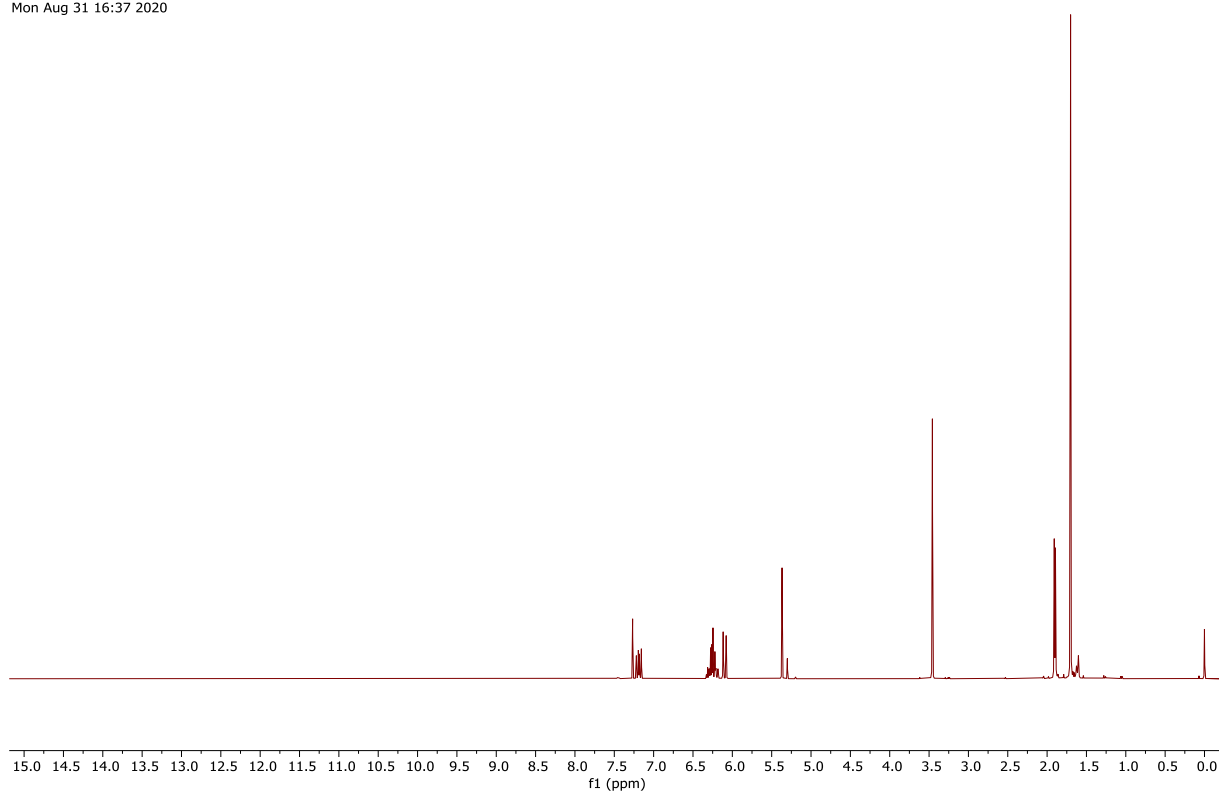


Figure 218: ¹H NMR spectrum (400 MHz, CDCl₃) of compound **20** (Chapter 4).

GGX363_P_CARBON_01
GGX363_P/CDCl₃/13C
Fuchs 20200831_19
Tue Sep 1 15:59 2020

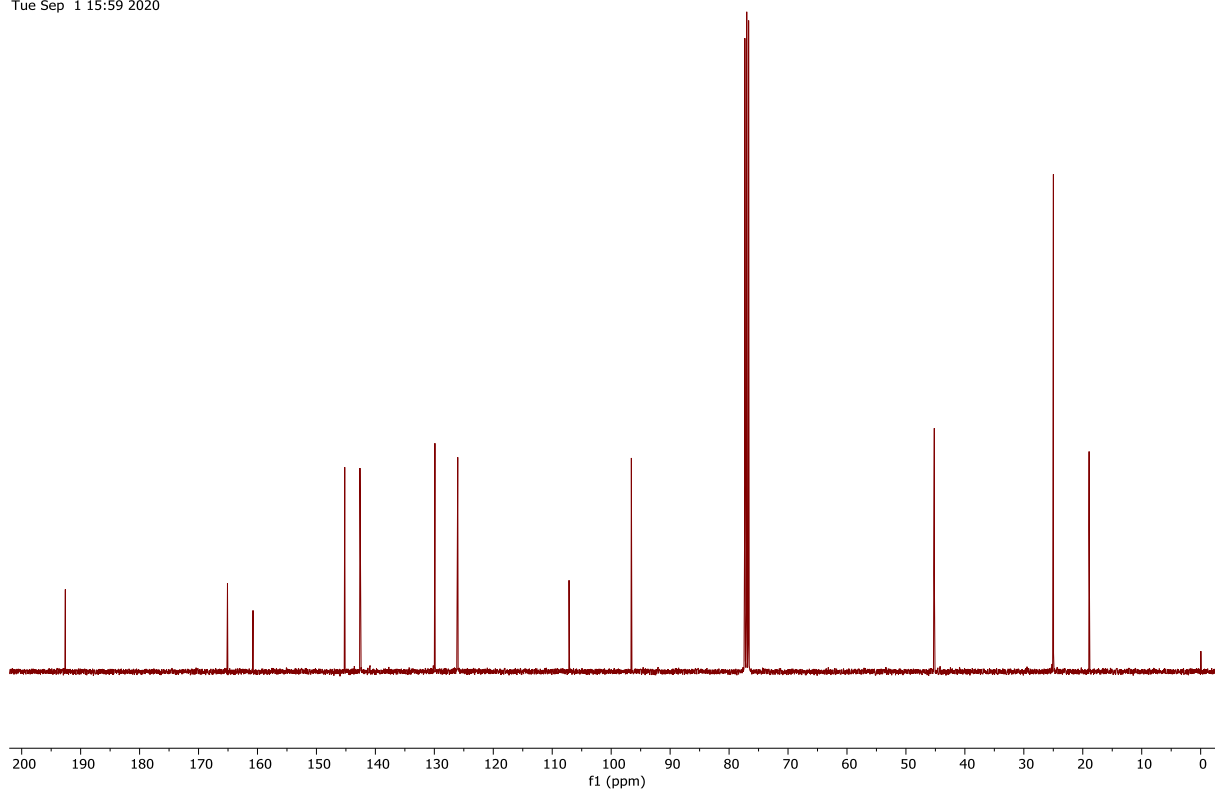


Figure 219: ¹³C NMR spectrum (101 MHz, CDCl₃) of compound **20** (Chapter 4).

GGX549_PROTON_01
GGX549/CDCl₃/1H
Wolf 20231009_03
Mon Oct 9 13:50 2023

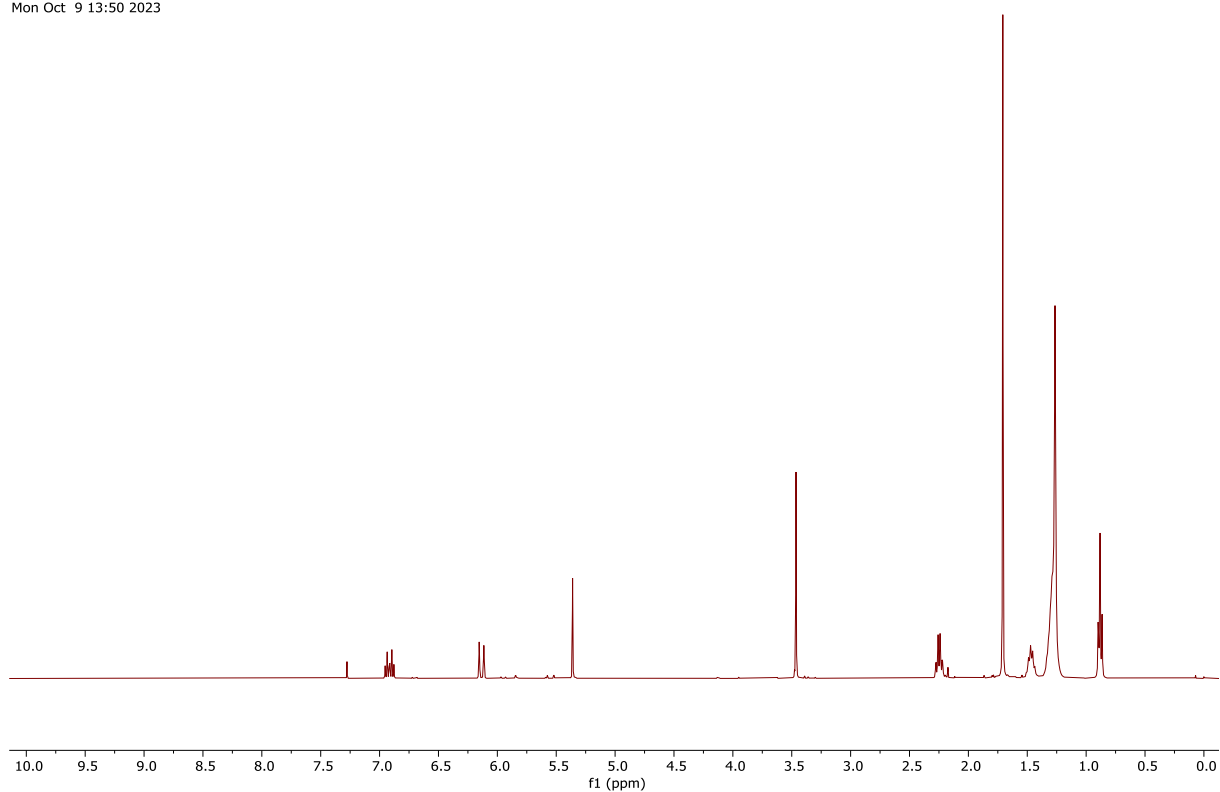


Figure 220: ¹H NMR spectrum (400 MHz, CDCl₃) of compound **21** (Chapter 4).

GGX549_CARBON_01
GGX549/CDCl₃/13C
Wolf 20231009_03
Mon Oct 9 15:23 2023

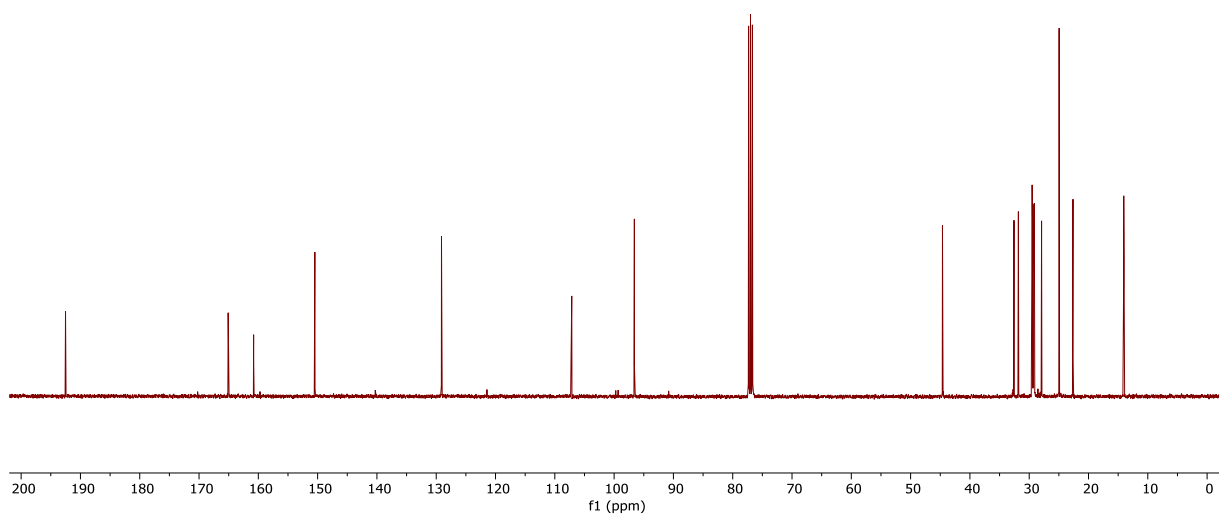


Figure 221: ¹³C NMR spectrum (101 MHz, CDCl₃) of compound **21** (Chapter 4).

GGX365_PROTON_02
GGX365/DMSO-d6/1H
Fuchs 20200903_02
Thu Sep 3 16:31 2020

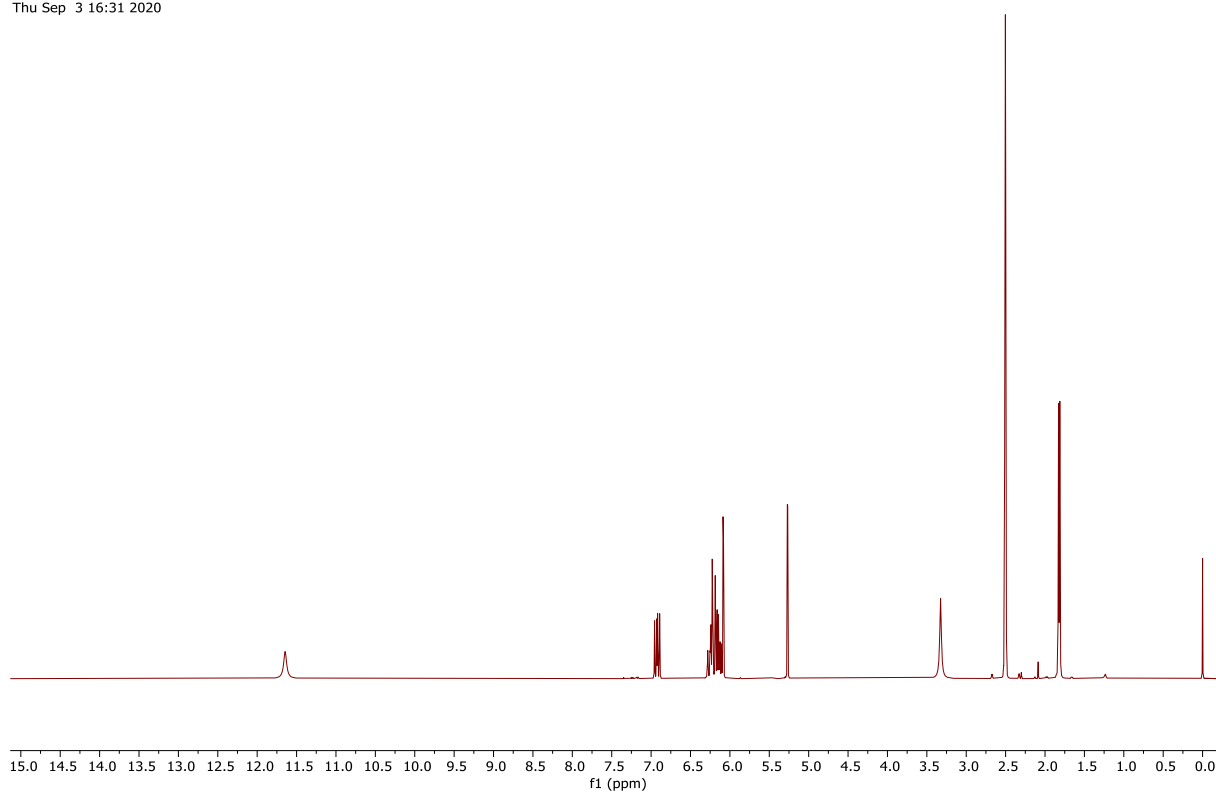


Figure 222: ¹H NMR spectrum (400 MHz, CDCl₃) of compound **22** (Chapter 4).

GGX365_CARBON_01
GGX365/DMSO-d6/13C
Fuchs 20200903_02
Thu Sep 3 16:33 2020

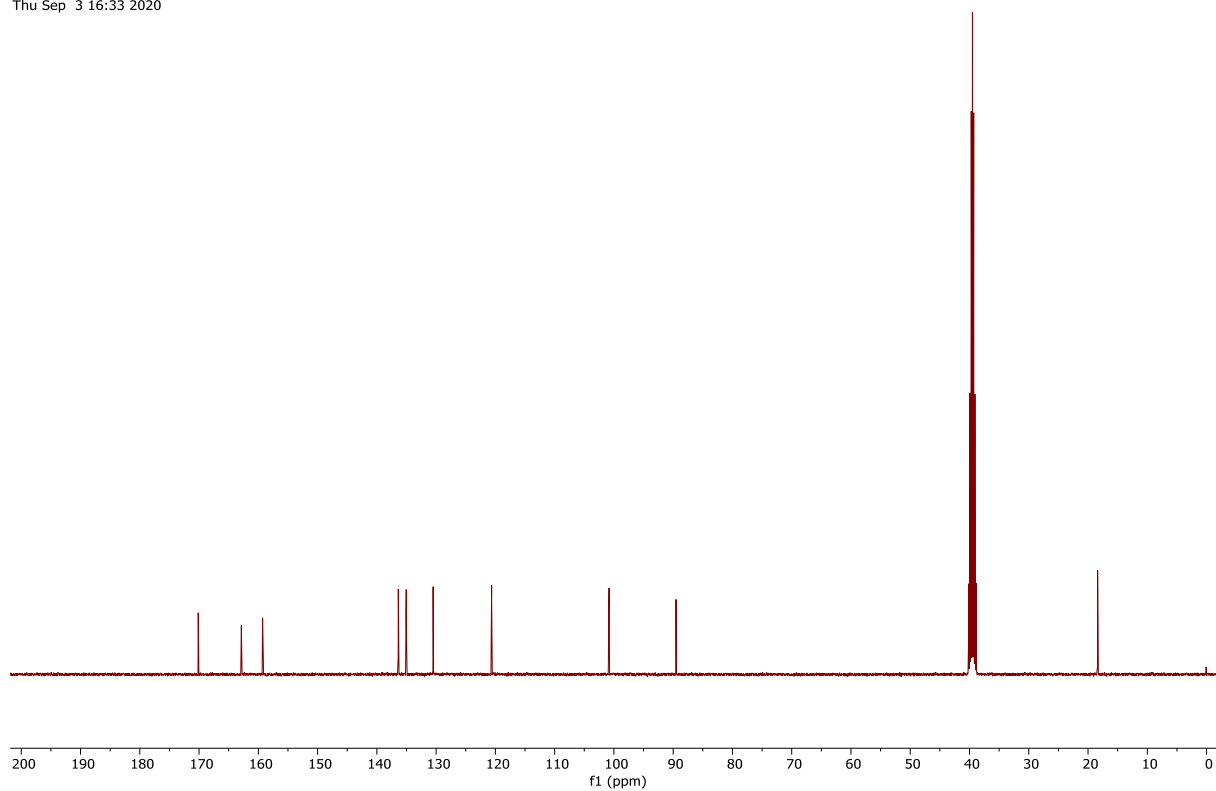


Figure 223: ¹³C NMR spectrum (101 MHz, CDCl₃) of compound **22** (Chapter 4).

GGX553_PROTON_01
GGX553/DMSO-d6/1H
Fuchs 20220728_01
Thu Jul 28 08:50 2022

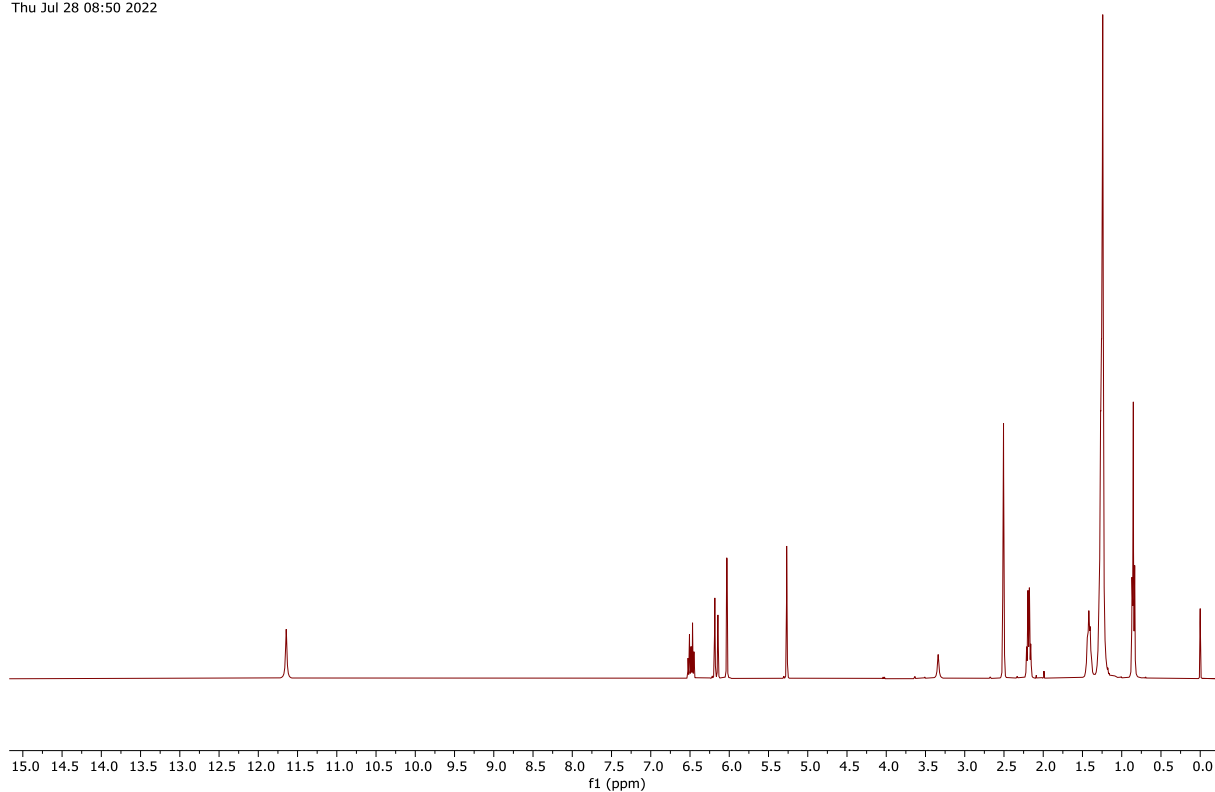


Figure 224: ¹H NMR spectrum (400 MHz, CDCl₃) of compound **23** (Chapter 4).

GGX553_CARBON_01
GGX553/DMSO-d6/13C
Fuchs 20220728_01
Thu Jul 28 09:15 2022

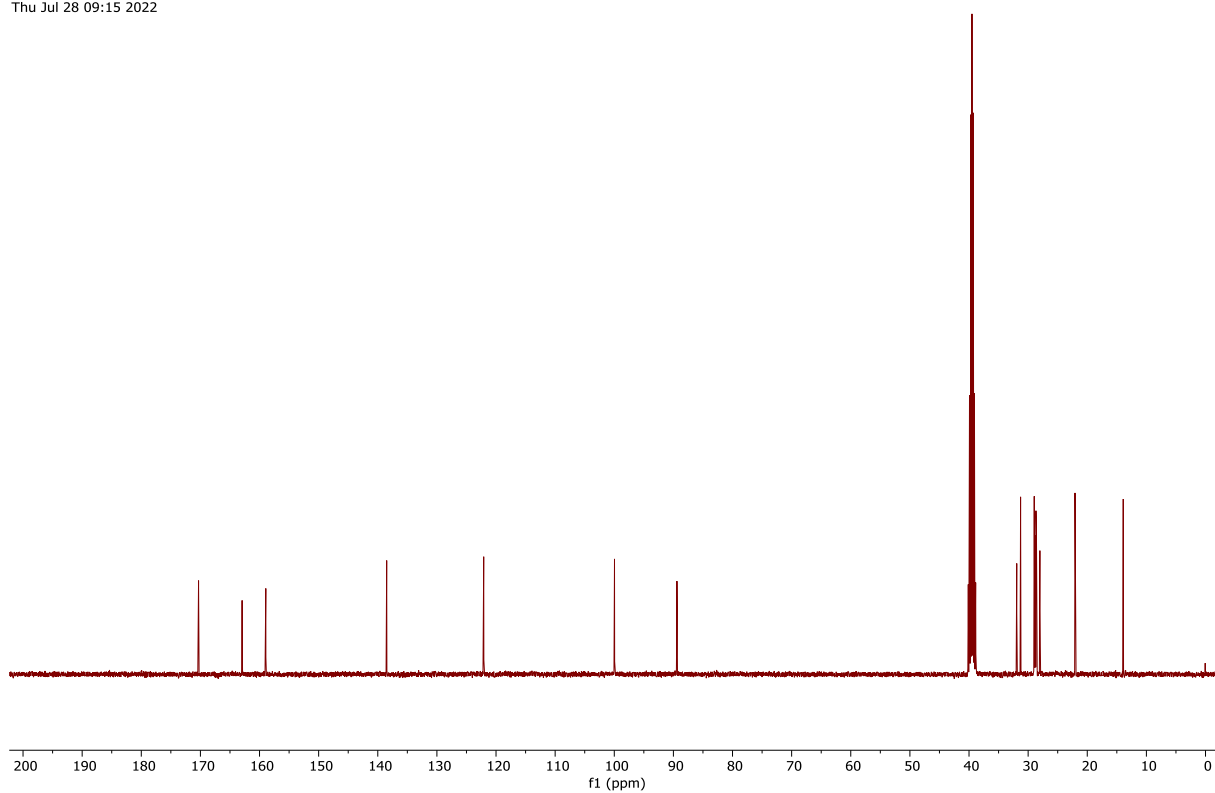


Figure 225: ¹³C NMR spectrum (101 MHz, CDCl₃) of compound **23** (Chapter 4).

GGX370_PROTON_02
GGX370/CDCl₃/1H
Fuchs 20201001_01
Thu Oct 1 09:18 2020

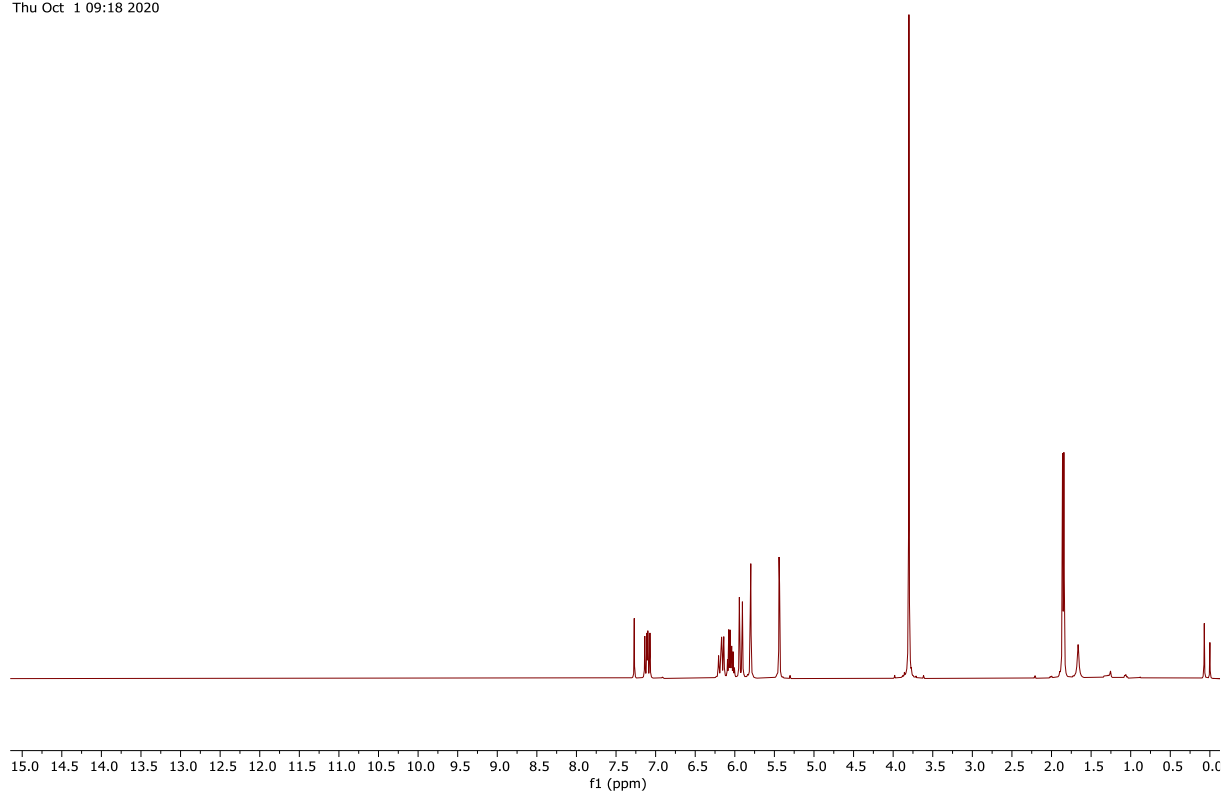


Figure 226: ¹H NMR spectrum (400 MHz, CDCl₃) of compound **24** (Chapter 4).

GGX370_CARBON_01
GGX370/CDCl₃/13C
Fuchs 20201001_01
Thu Oct 1 09:19 2020

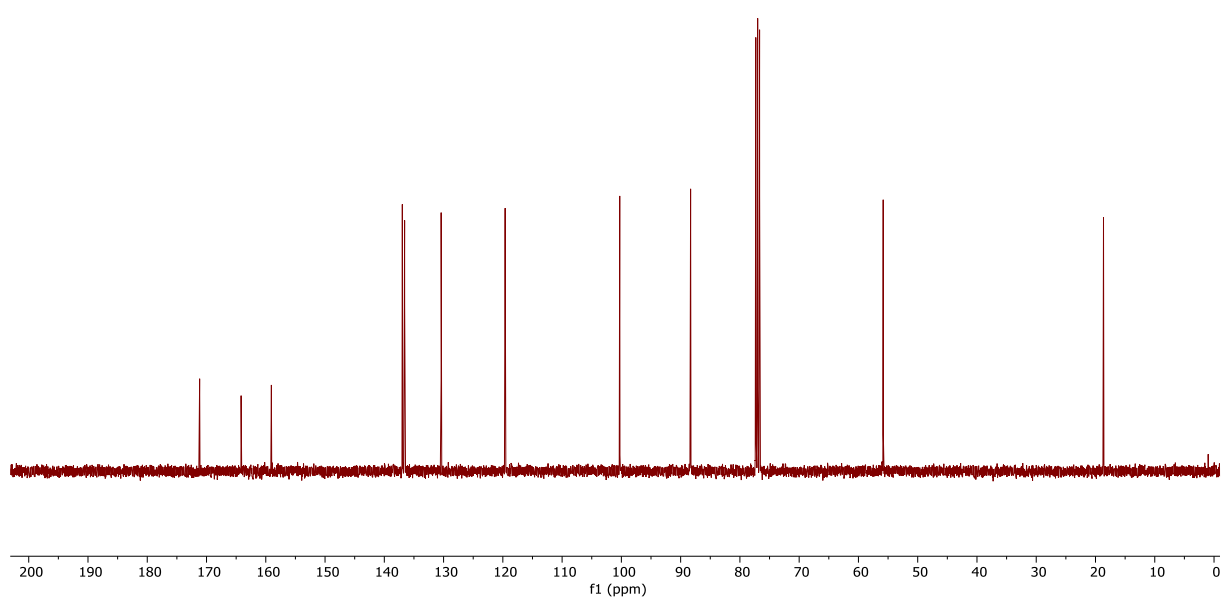


Figure 227: ¹³C NMR spectrum (101 MHz, CDCl₃) of compound **24** (Chapter 4).

GGX350.11.fid
GGX350/CDCl₃/1H
Fuchs 20200730_08
Proton_IPB CDCl₃ /opt/nmrdata/2020/GGX walkup 17

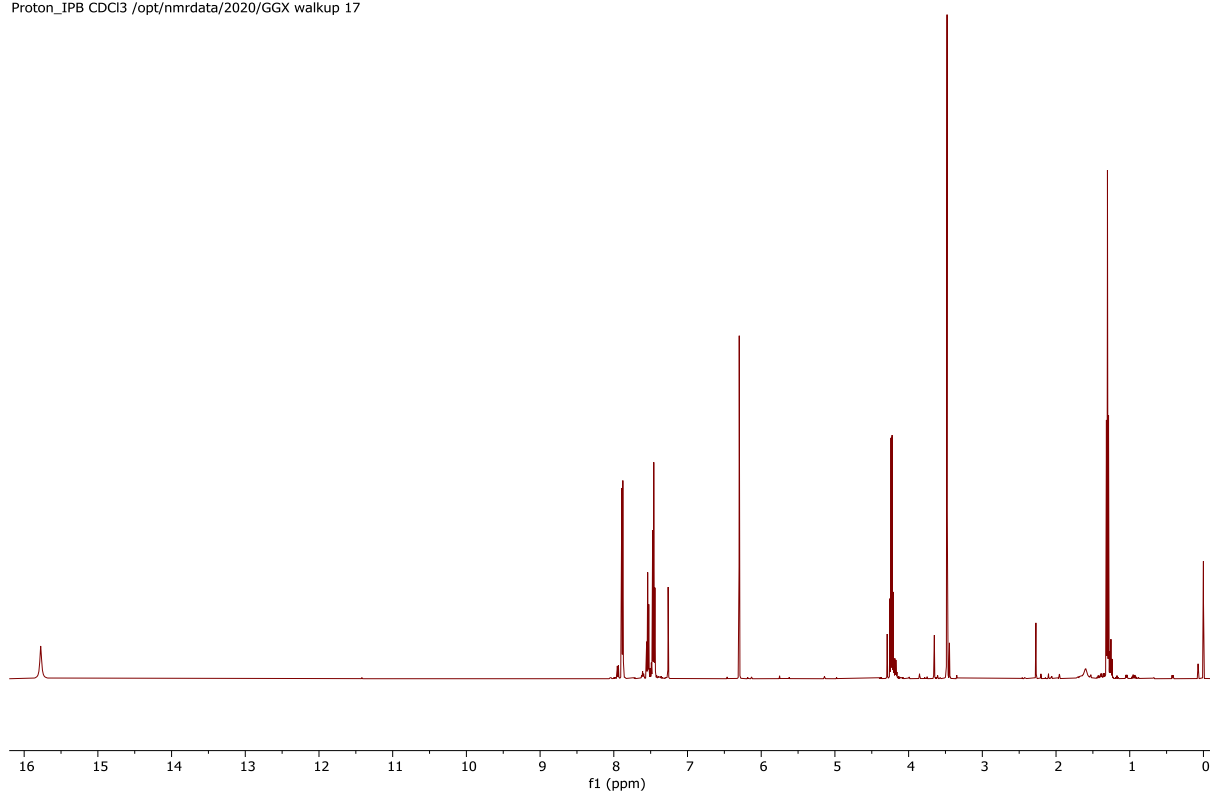


Figure 228: ¹H NMR spectrum (500 MHz, CDCl₃) of compound **25** (Chapter 4).

GGX350.12.fid
GGX350/CDCl₃/13C
Fuchs 20200730_08
Carbon_dec_IPB CDCl₃ /opt/nmrdata/2020/GGX walkup 17

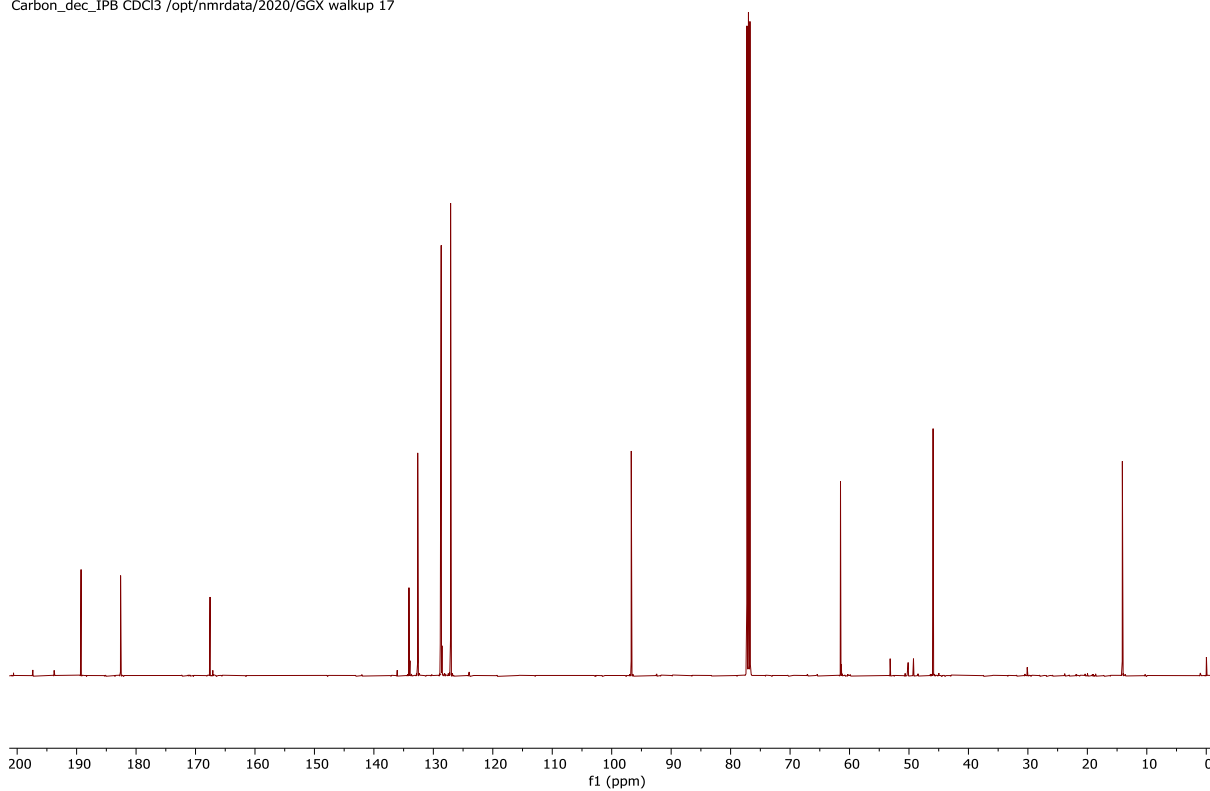


Figure 229: ¹³C NMR spectrum (126 MHz, CDCl₃) of compound **25** (Chapter 4).

GGX358_A_PROTON_02
GGX358_A/CDCl₃/1H
Fuchs 20200813_06
Thu Aug 13 16:40 2020

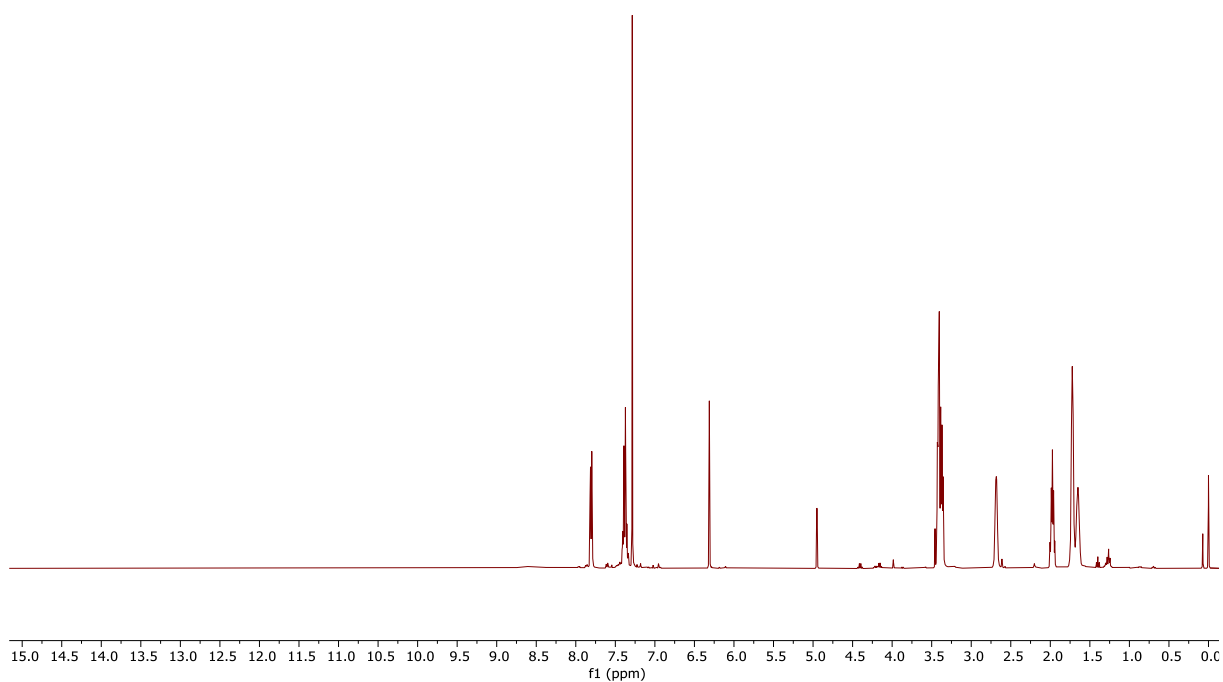


Figure 230: ¹H NMR spectrum (400 MHz, CDCl₃) of compound **26** (Chapter 4).

GGX358_A_CARBON_01
GGX358_A/CDCl₃/13C
Fuchs 20200813_06
Thu Aug 13 16:41 2020

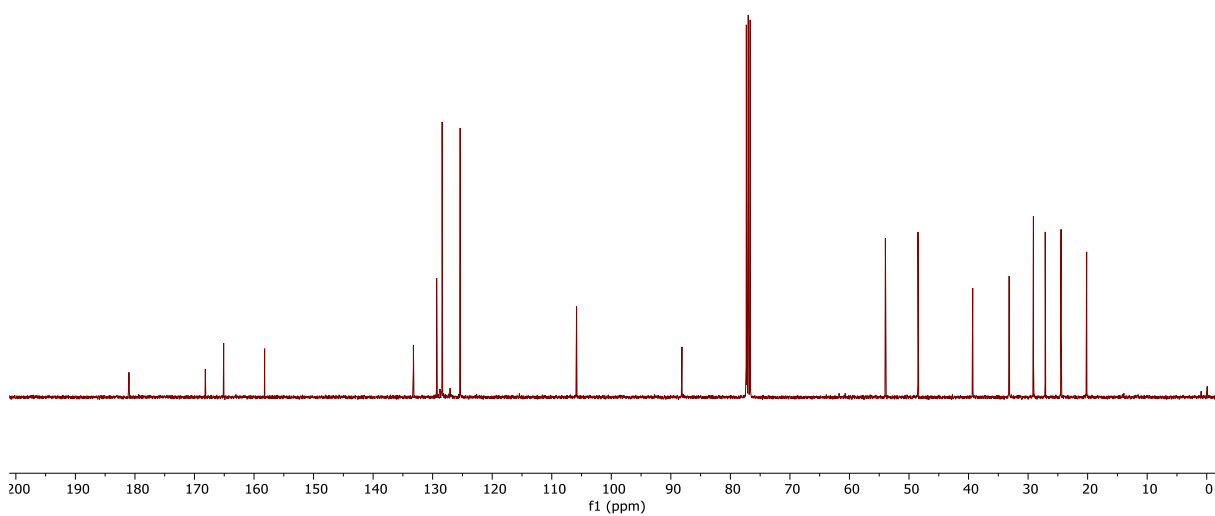


Figure 231: ¹³C NMR spectrum (101 MHz, CDCl₃) of compound **26** (Chapter 4).

GGX412_20210113_01.1H
GGX412/Acetone-d6/1H
Fuchs 20210113_01
Thu Jan 13 10:47 2021

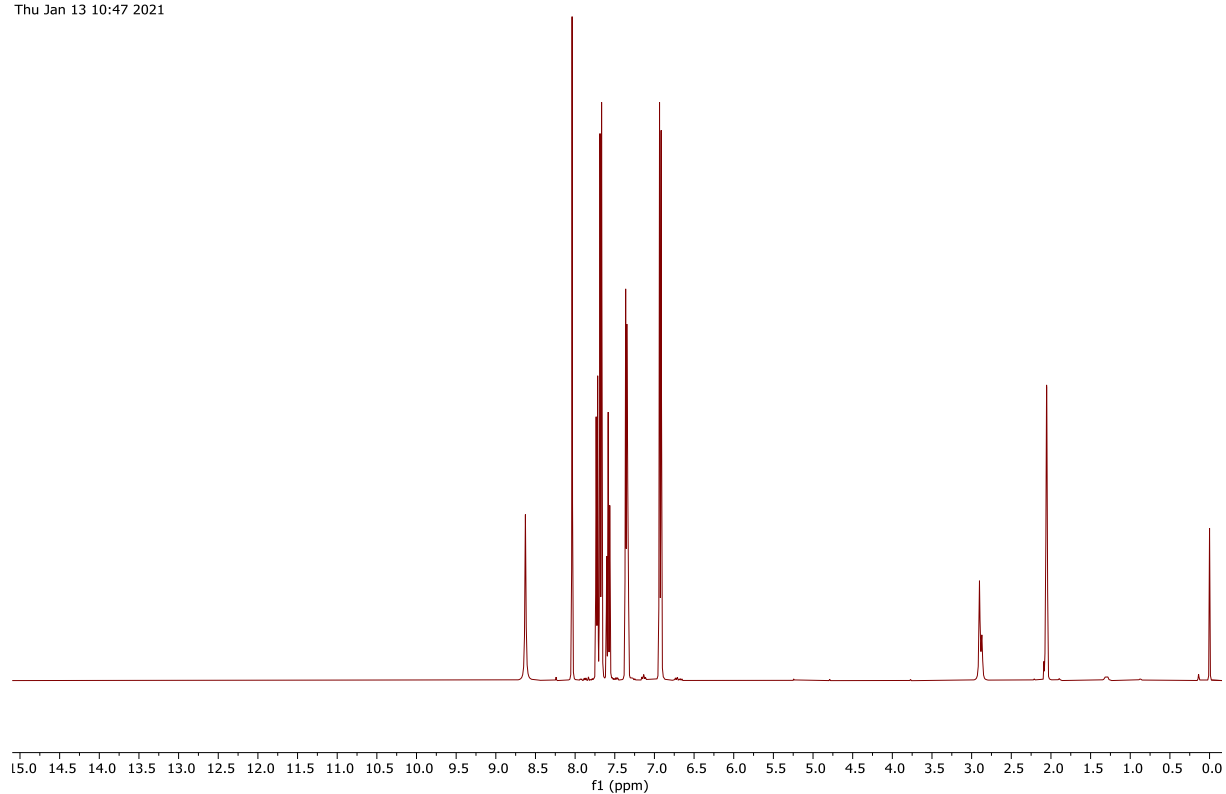


Figure 232: ¹H NMR spectrum (400 MHz, (CD₃)₂CO) of compound **27** (Chapter 4).

GGX412_20210113_01.13C
GGX412/Acetone-d6/13C
Fuchs 20210113_01
Thu Jan 13 10:52 2021

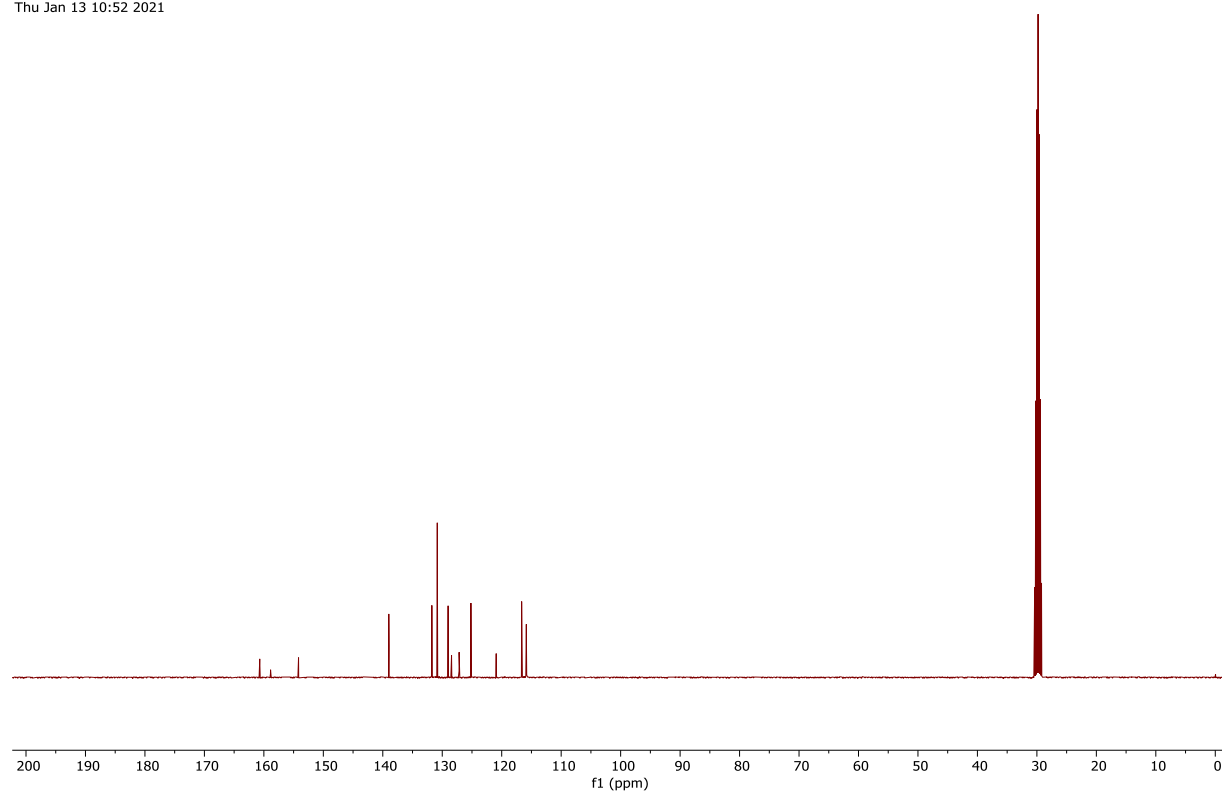


Figure 233: ¹³C NMR spectrum (101 MHz, (CD₃)₂CO) of compound **27** (Chapter 4).

GGX413_20210113_01.1H
GGX413/Acetone-d6/13C
Fuchs 20210113_01
Thu Jan 13 12:16 2021

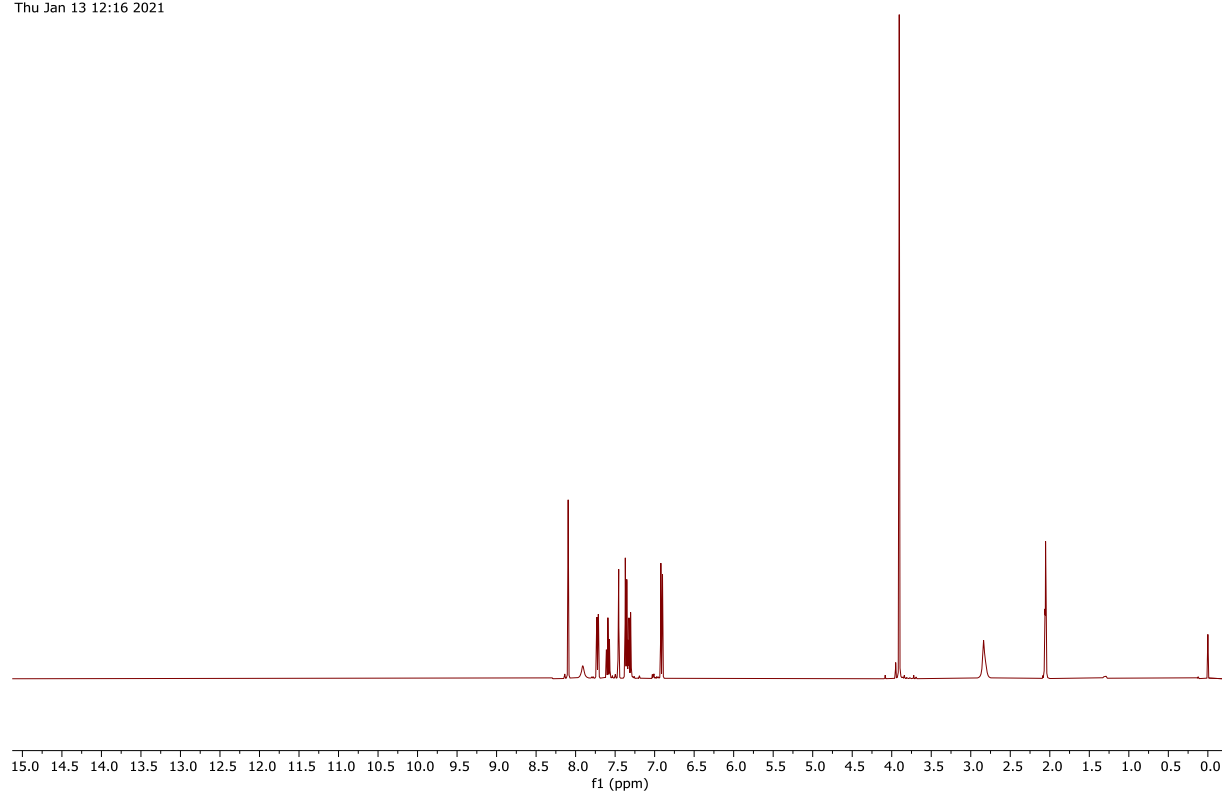


Figure 234: ¹H NMR spectrum (400 MHz, (CD₃)₂CO) of compound **28** (Chapter 4).

GGX413_20210113_01.13C
GGX413/Acetone-d6/1H
Fuchs 20210113_01
Thu Jan 13 12:19 2021

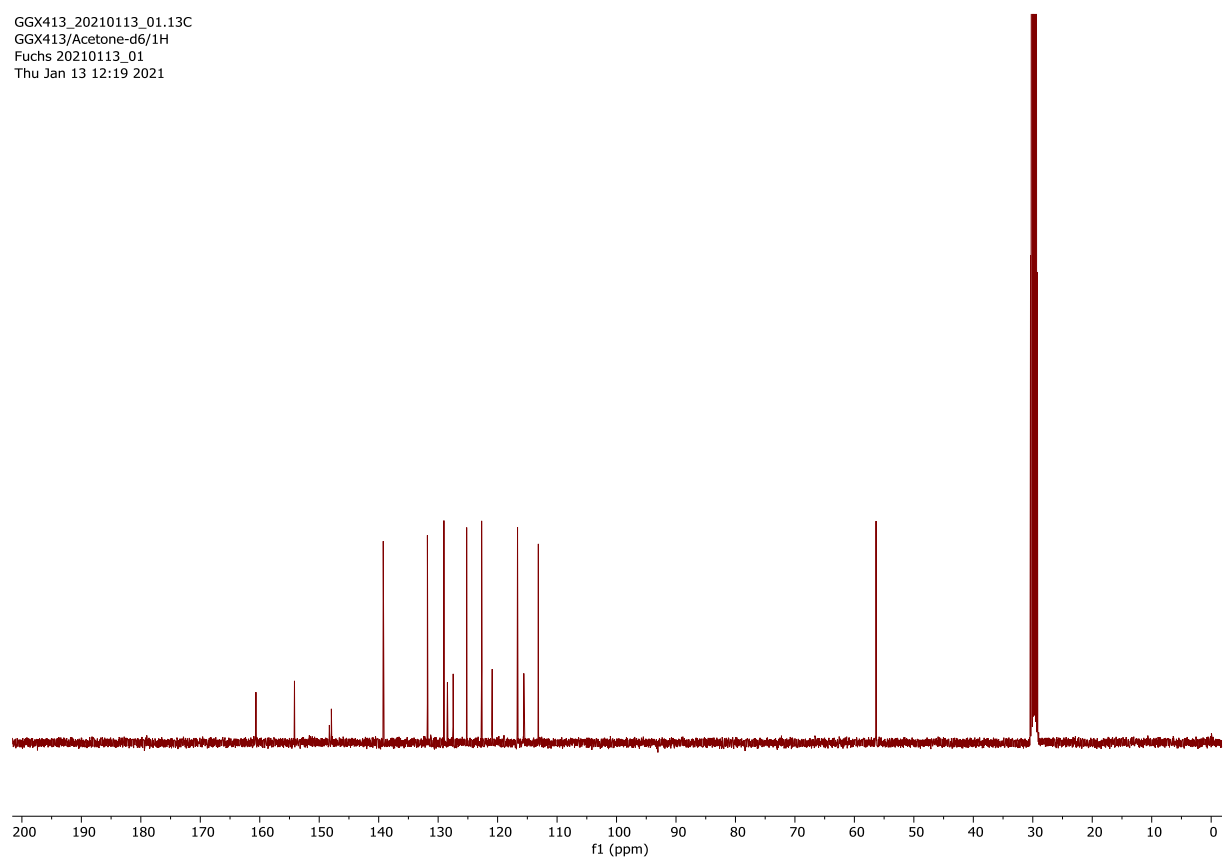


Figure 235: ¹³C NMR spectrum (101 MHz, (CD₃)₂CO) of compound **28** (Chapter 4).

GGX414_20210113_01.1H
GGX414/Acetone-d6/1H
Fuchs 20210113_01
Thu Jan 13 14:30 2021

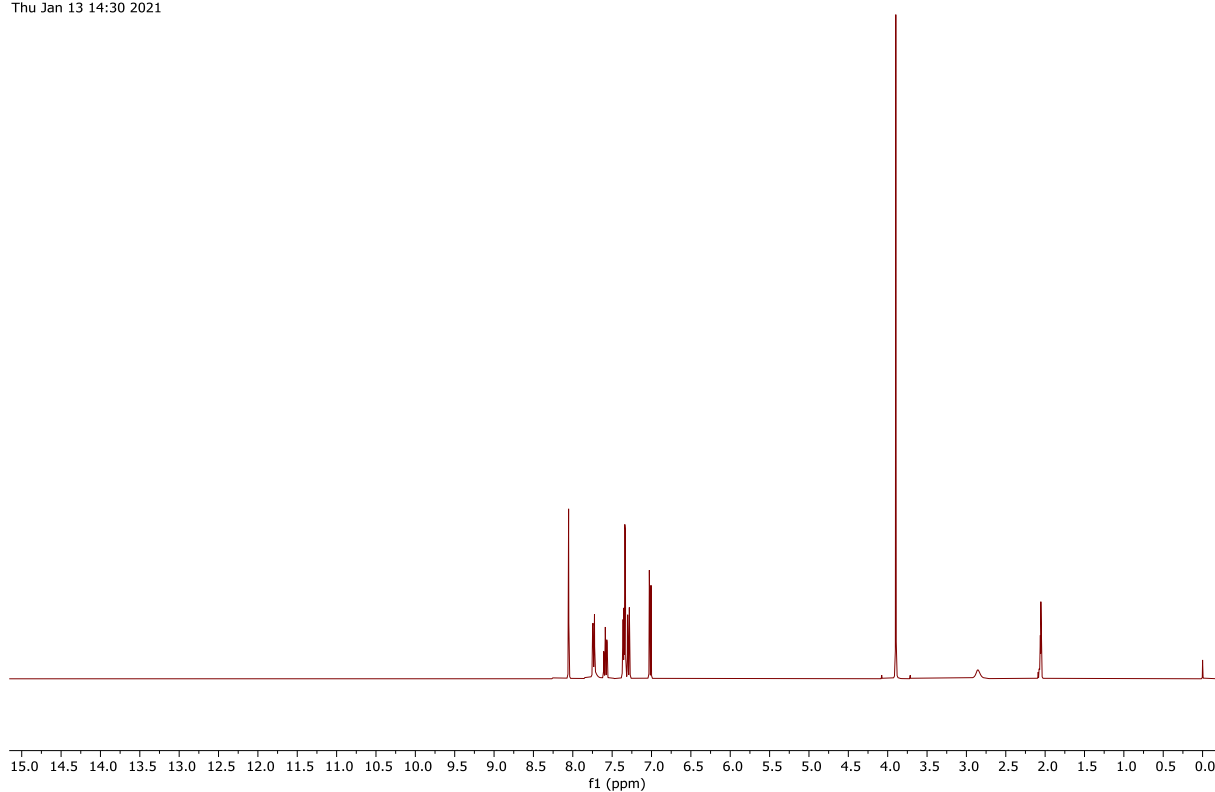


Figure 236: ¹H NMR spectrum (400 MHz, (CD₃)₂CO) of compound **29** (Chapter 4).

GGX414_20210113_01.13C
GGX414/Acetone-d6/13C
Fuchs 20210113_01
Thu Jan 13 14:34 2021

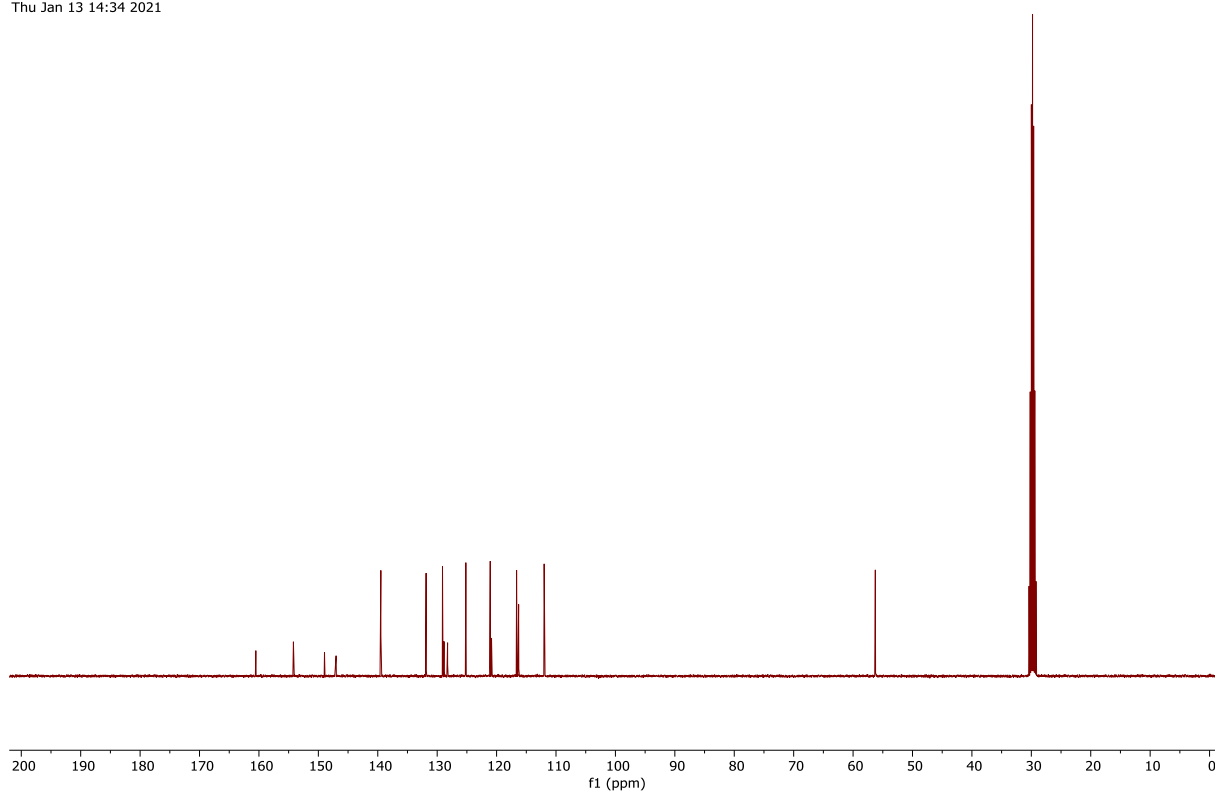


Figure 237: ¹³C NMR spectrum (101 MHz, (CD₃)₂CO) of compound **29** (Chapter 4).

GGX408_PROTON_02
GGX408/CDCl₃/1H
Fuchs 20200113_01
Thu Jan 14 09:50 2021

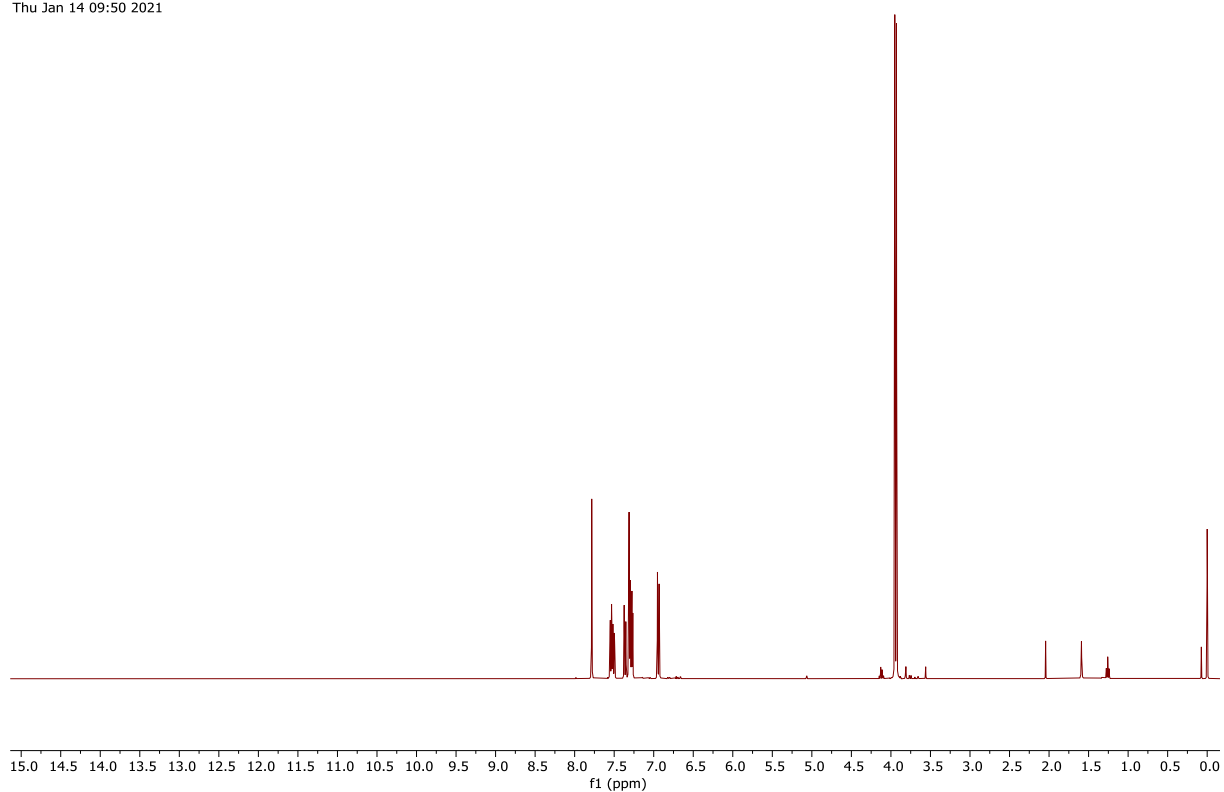


Figure 238: ¹H NMR spectrum (400 MHz, CDCl₃) of compound **30** (Chapter 4).

GGX408_CARBON_01
GGX408/CDCl₃/13C
Fuchs 20200113_01
Thu Jan 14 09:51 2021

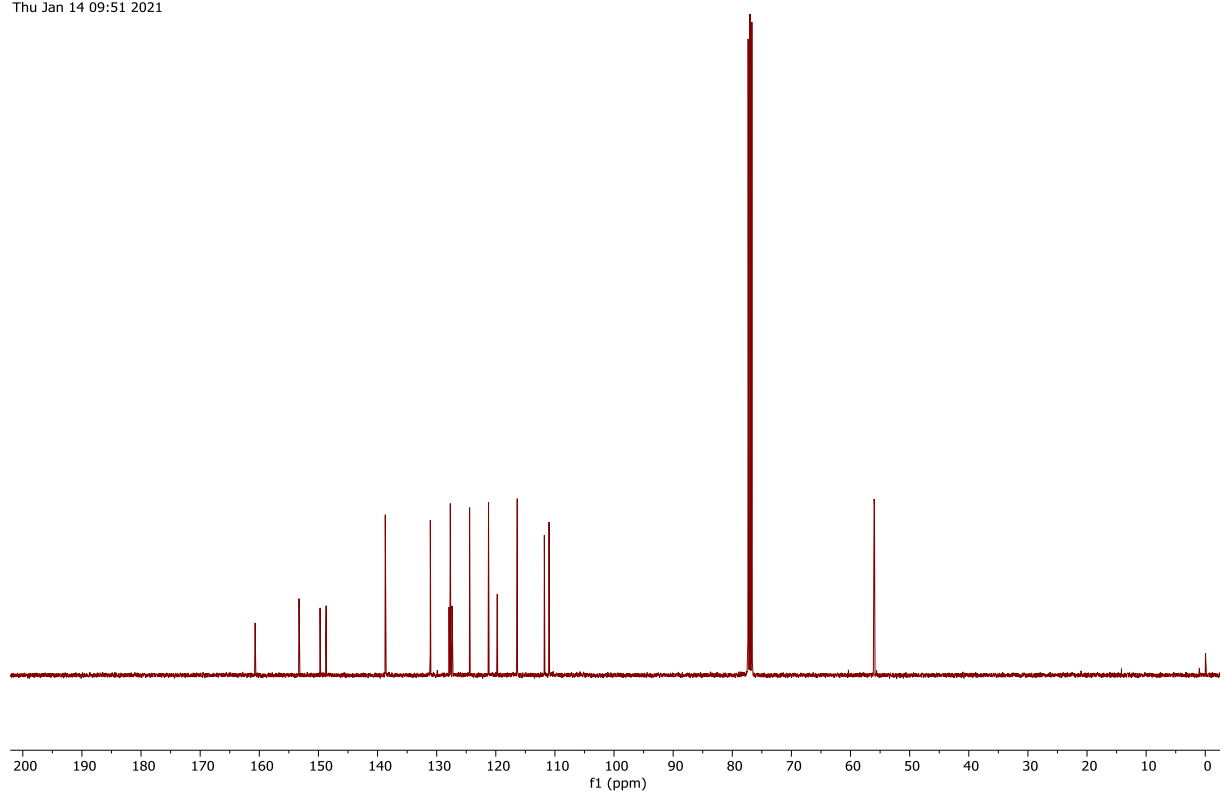


Figure 239: ¹³C NMR spectrum (101 MHz, CDCl₃) of compound **30** (Chapter 4).

GGX415_20210113_01.1H
GGX415/CDCl₃/1H
Fuchs 20210113_01
Thu Jan 13 15:49 2021

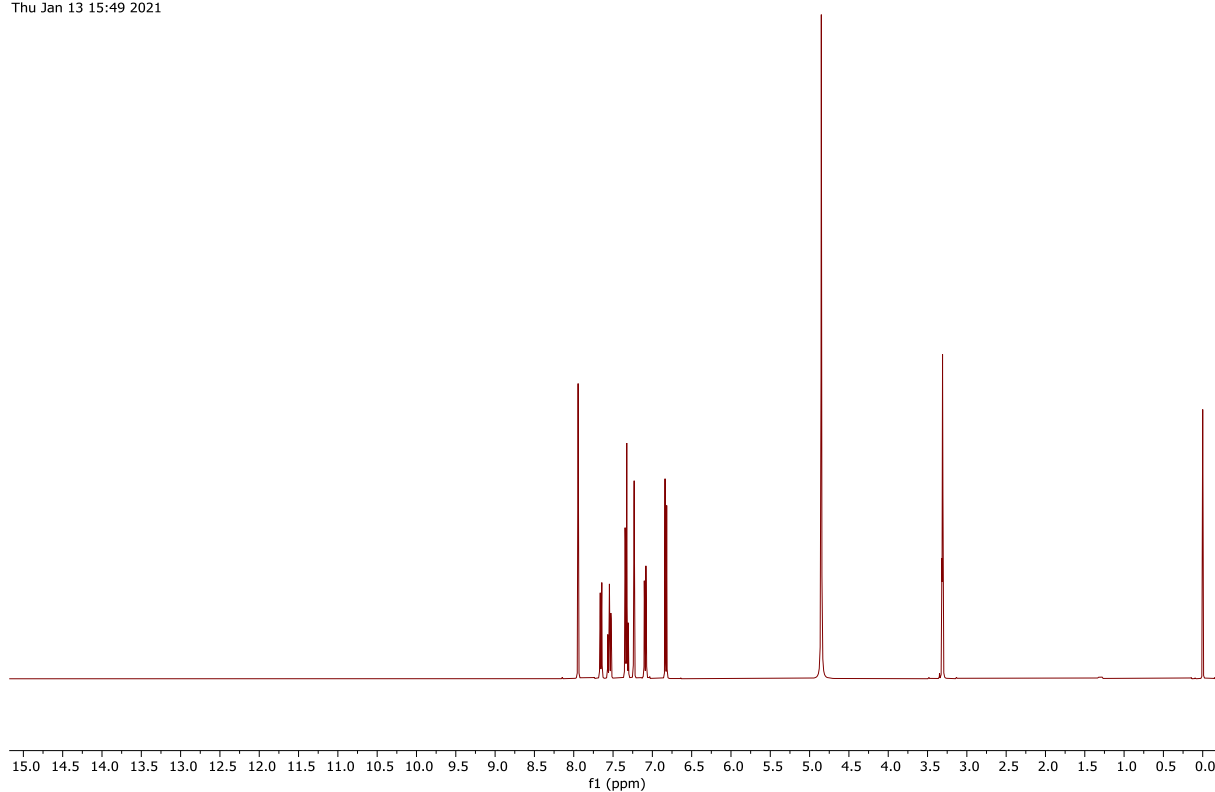


Figure 240: ¹H NMR spectrum (400 MHz, CDCl₃) of compound **31** (Chapter 4).

GGX415_20210113_01.13C
GGX415/CDCl₃/13C
Fuchs 20210113_01
Thu Jan 13 15:54 2021

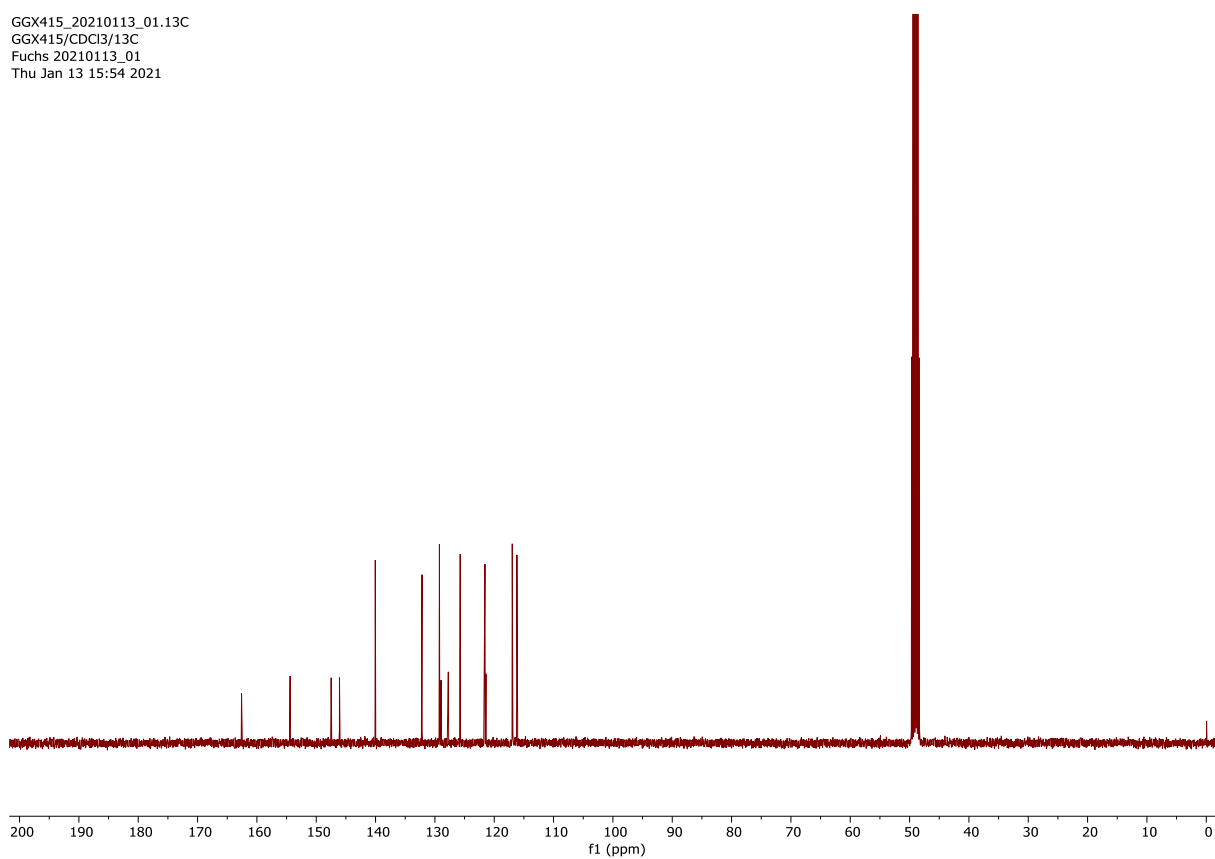


Figure 241: ¹³C NMR spectrum (101 MHz, CDCl₃) of compound **31** (Chapter 4).

GGX416_20210113_02.1H
GGX416/Acetone-d6/1H
Fuchs 20210113_01
Thu Jan 13 17:01 2021

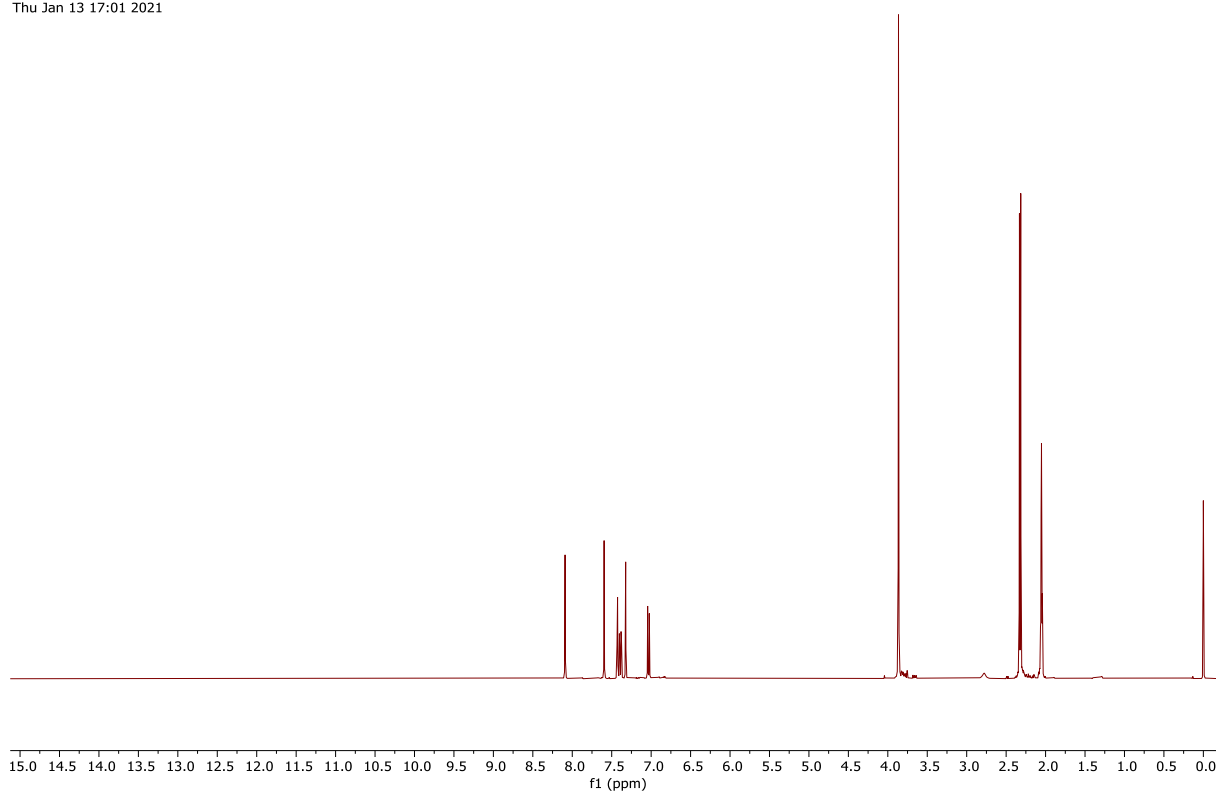


Figure 242: ¹H NMR spectrum (400 MHz, (CD₃)₂CO) of compound **32** (Chapter 4).

GGX416_20210113_02.13C
GGX416/Acetone-d6/13C
Fuchs 20210113_01
Thu Jan 13 17:06 2021

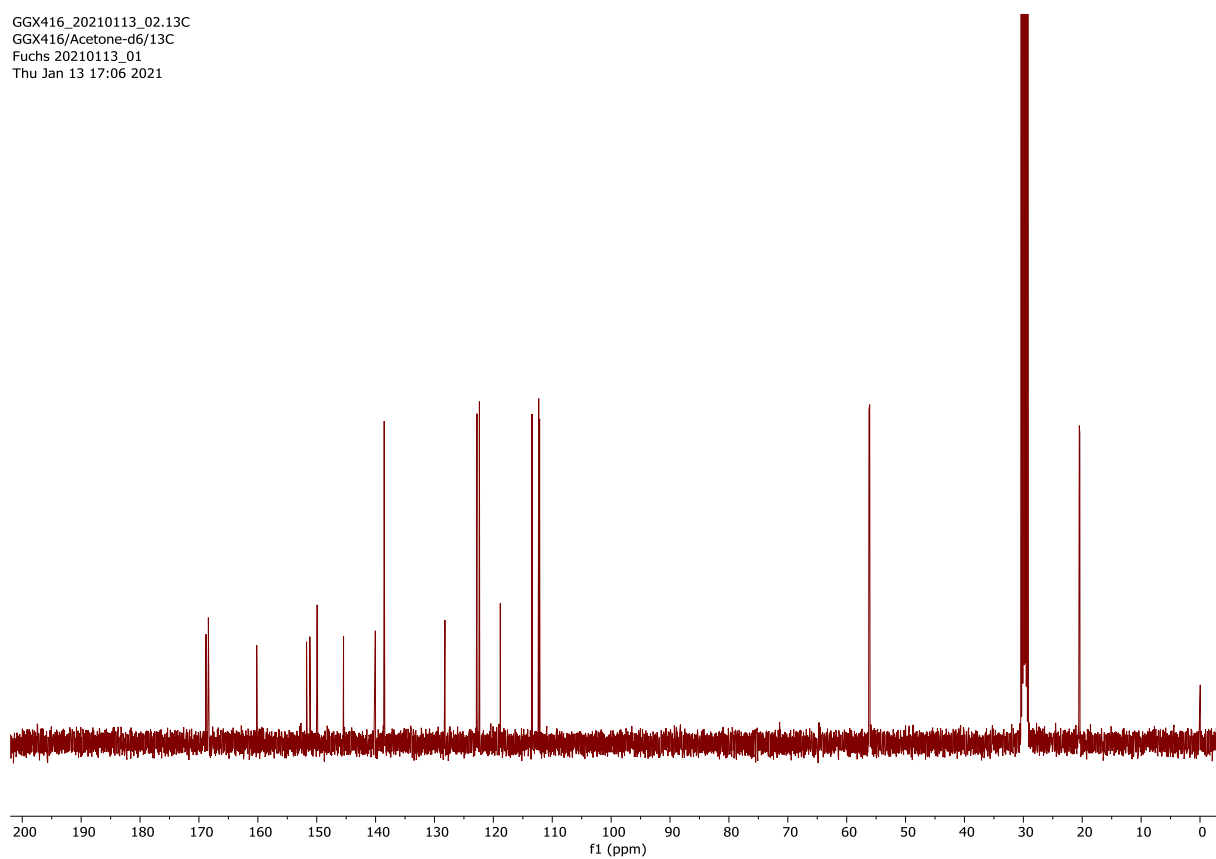


Figure 243: ¹³C NMR spectrum (101 MHz, (CD₃)₂CO) of compound **32** (Chapter 4).

GGX417_20210113_01.1H
GGX417/Acetone-d6/1H
Fuchs 20210113_01
Thu Jan 13 19:30 2021

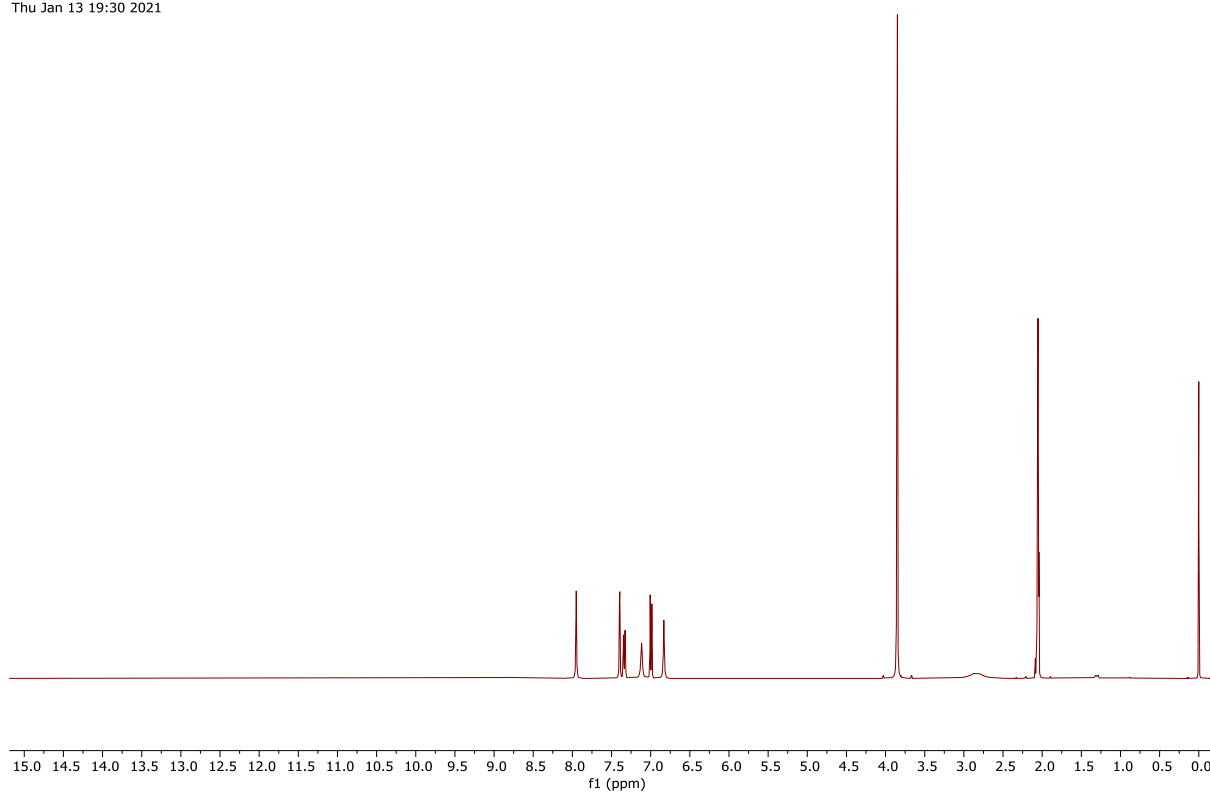


Figure 244: ¹H NMR spectrum (400 MHz, (CD₃)₂CO) of compound **33** (Chapter 4).

GGX417_20210113_01.13C
GGX417/Acetone-d6/13C
Fuchs 20210113_01
Thu Jan 13 19:34 2021

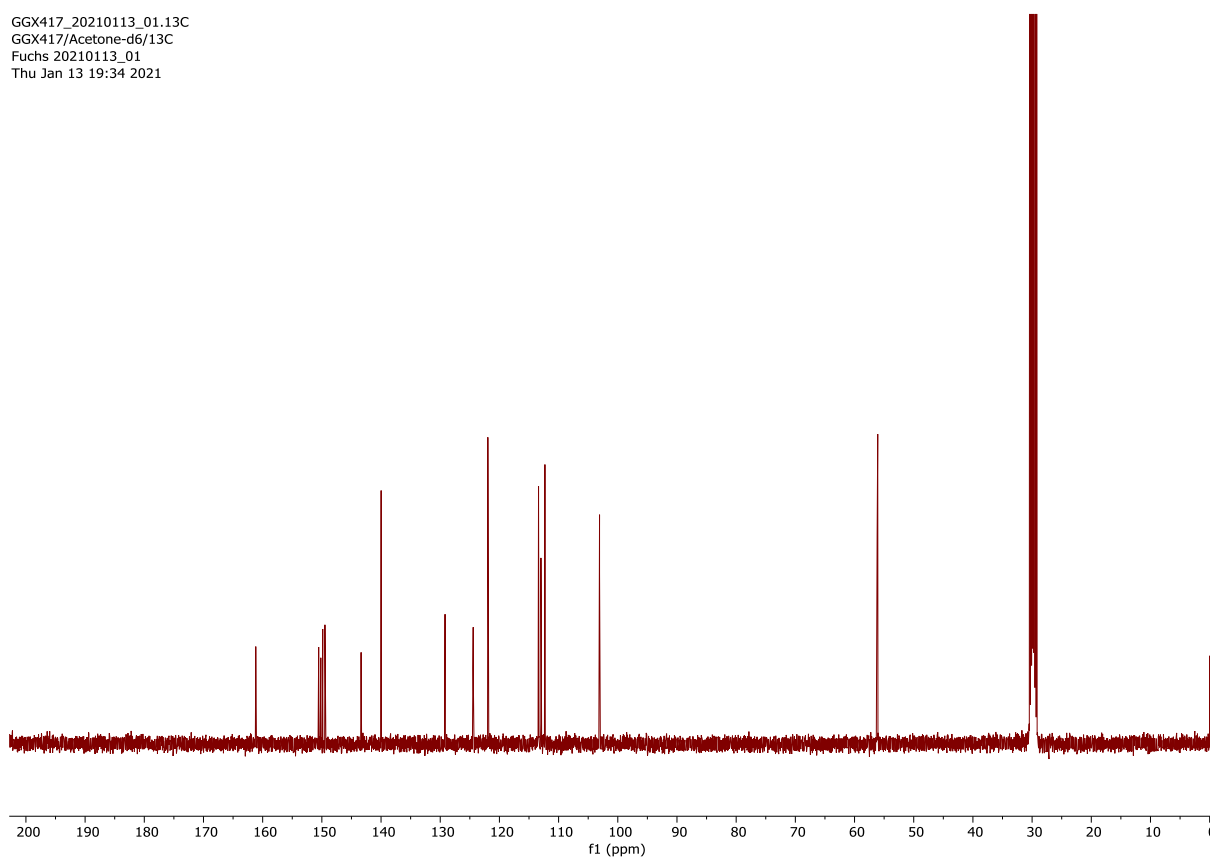


Figure 245: ¹³C NMR spectrum (101 MHz, (CD₃)₂CO) of compound **33** (Chapter 4).

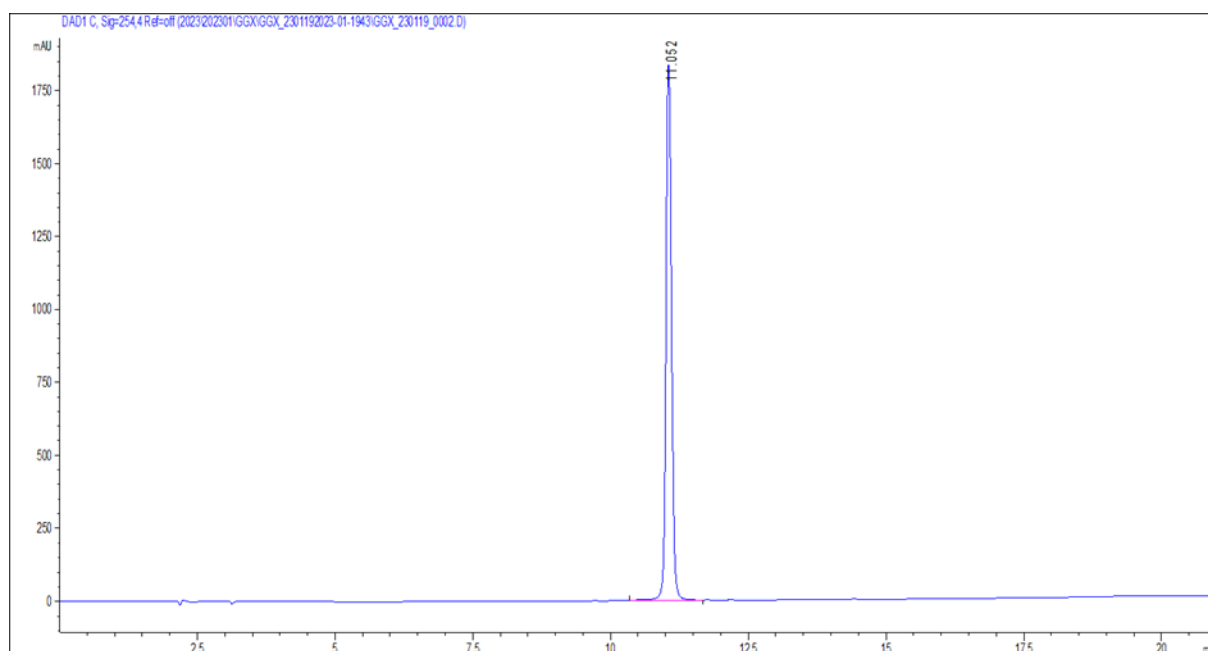


Figure 246: HPLC chromatogram of compound **5a** (Chapter 2, Tentoxin, synthesis via Ugi-route), absorbance detection at 254 nm.

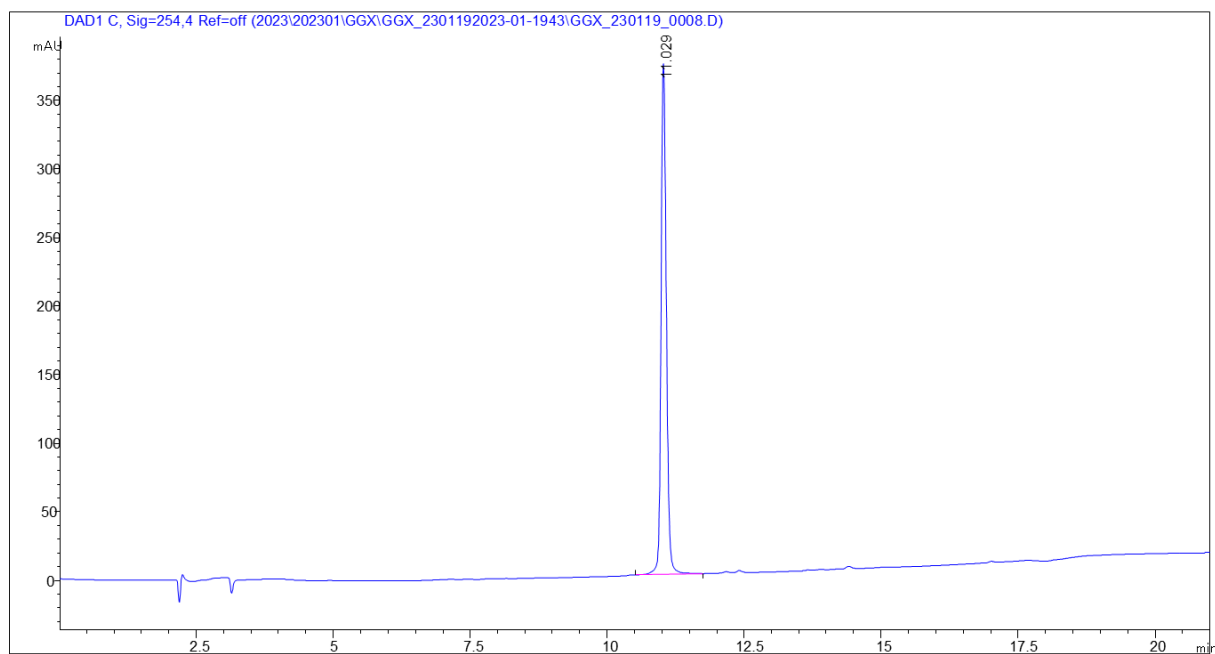


Figure 247: HPLC chromatogram of compound **5a** (Chapter 2, Tentoxin, synthesis via HWE-route), absorbance detection at 254 nm.

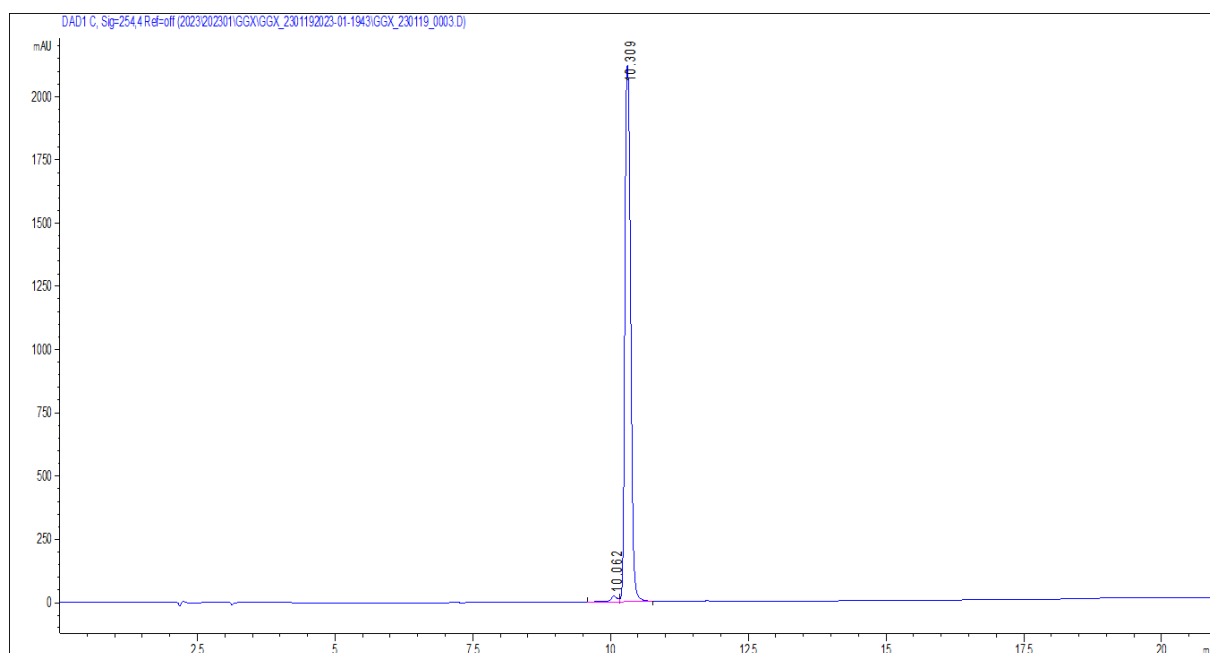


Figure 248: HPLC chromatogram of compound **5b** (Chapter 2), absorbance detection at 254 nm.

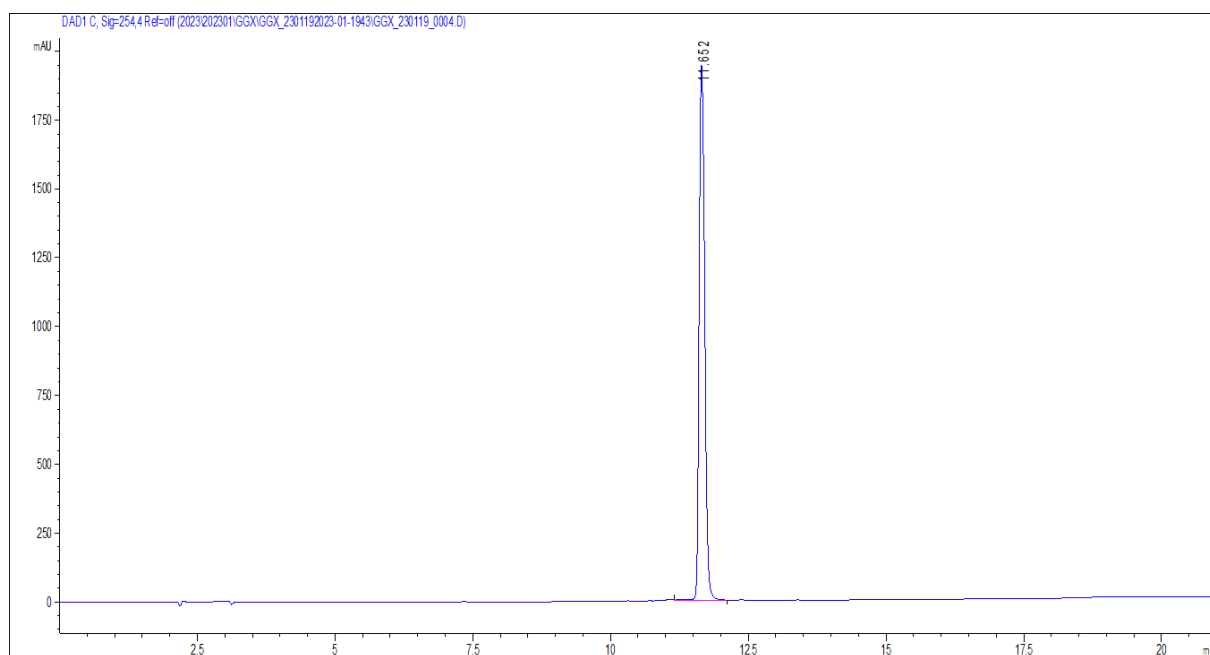


Figure 249: HPLC chromatogram of compound **5c** (Chapter 2), absorbance detection at 254 nm.

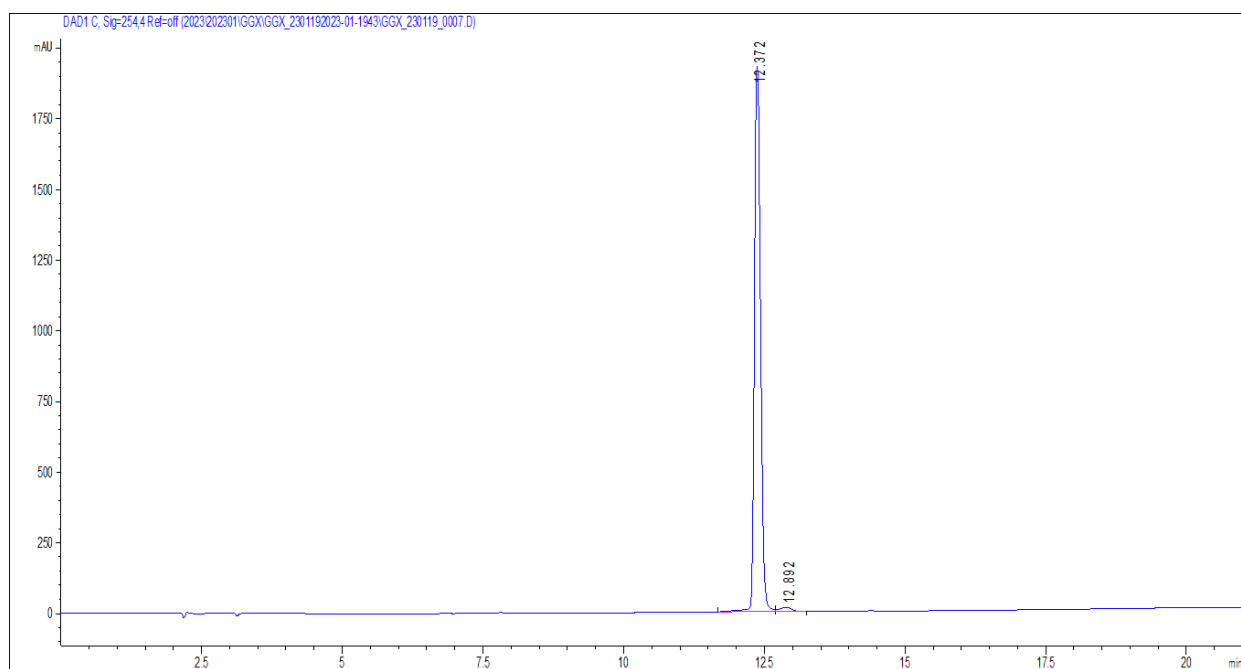


Figure 250: HPLC chromatogram of compound **5d** (Chapter 2), absorbance detection at 254 nm.

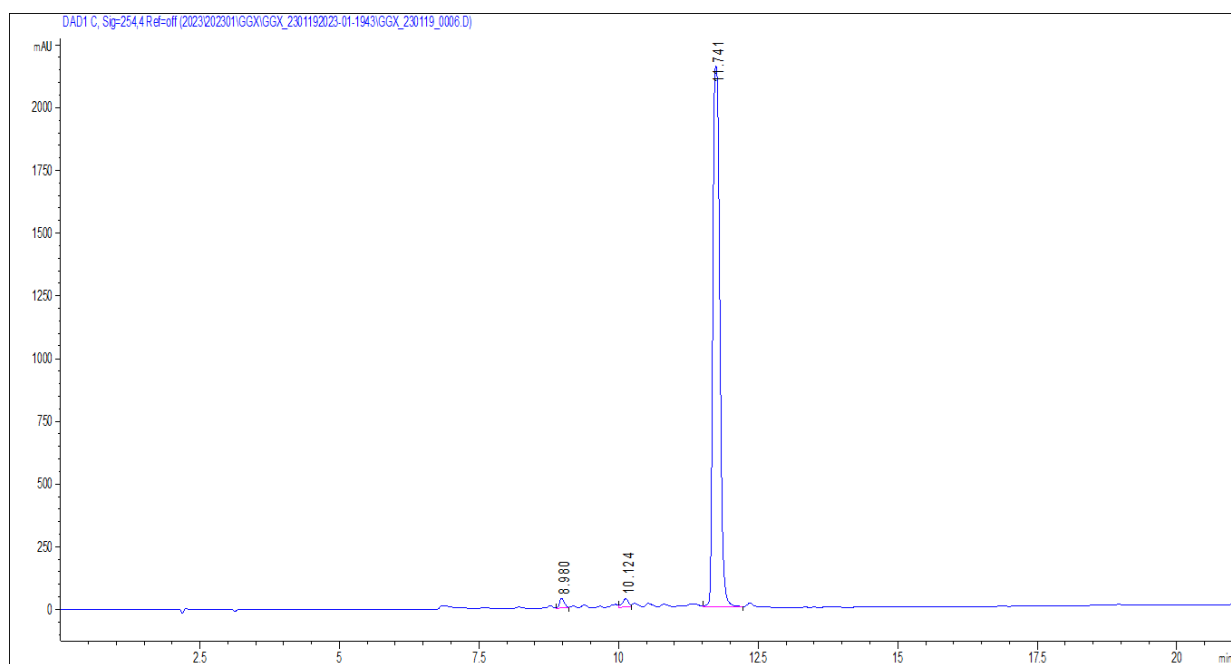


Figure 251: HPLC chromatogram of compound **5e** (Chapter 2), absorbance detection at 254 nm.

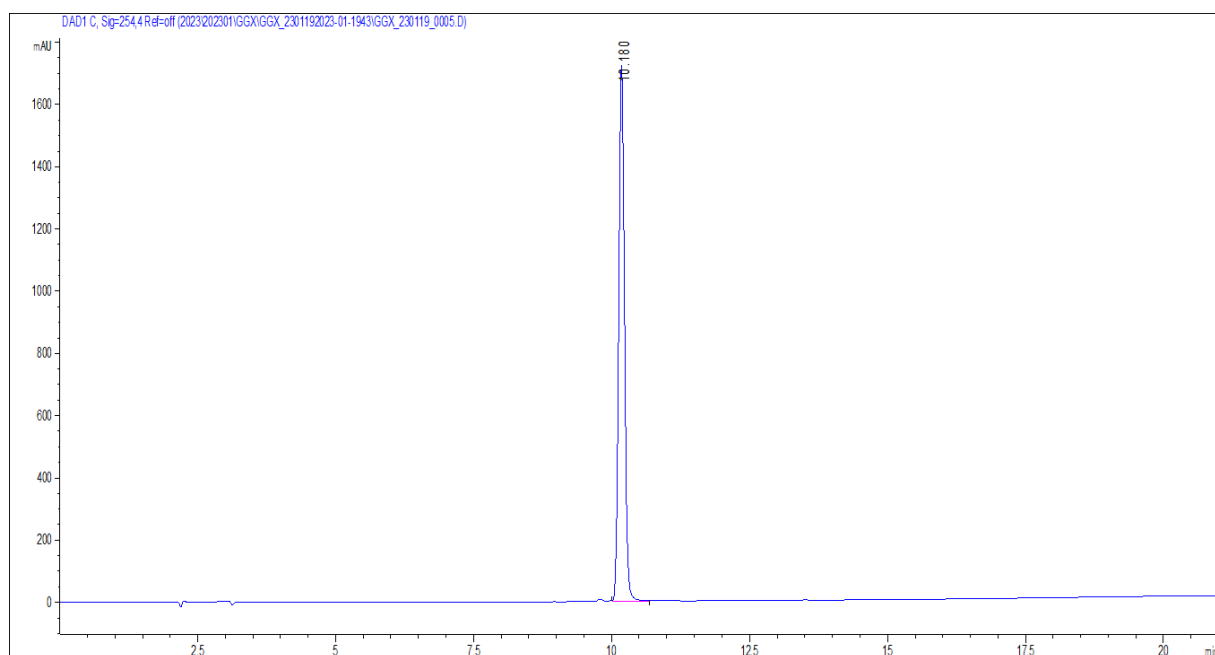


Figure 252: HPLC chromatogram of compound **5f** (Chapter 2), absorbance detection at 254 nm.

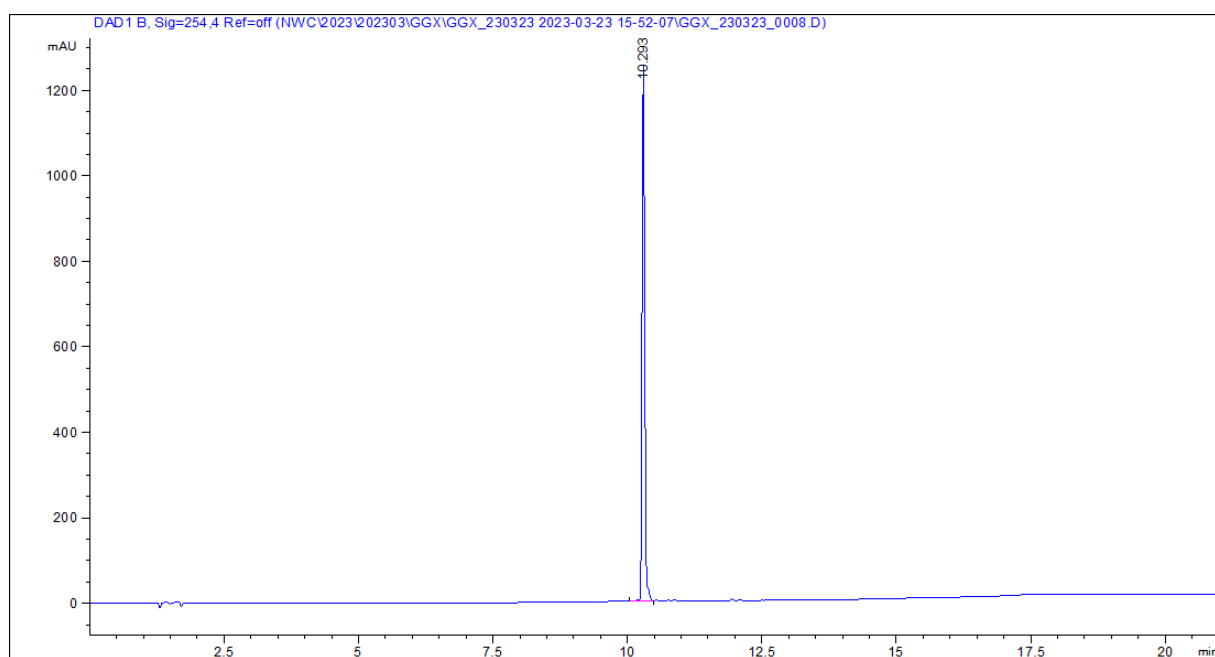


Figure 253: HPLC chromatogram of compound **5g** (Chapter 2), absorbance detection at 254 nm.

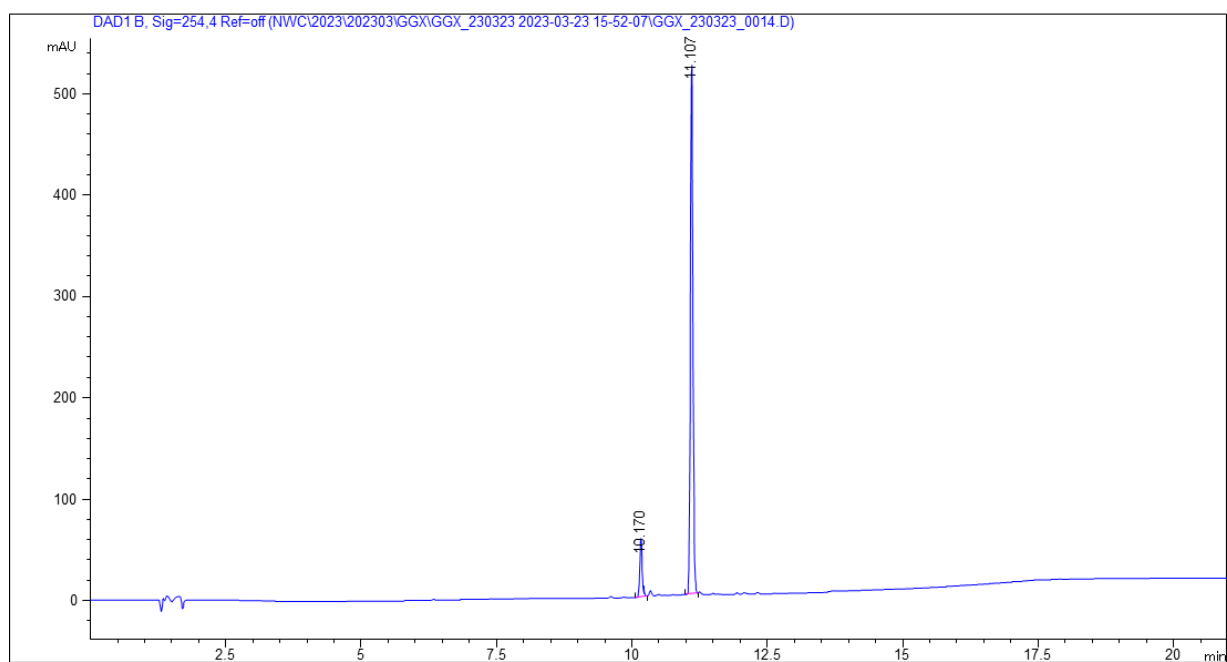


Figure 254: HPLC chromatogram of compound **5h** (Chapter 2), absorbance detection at 254 nm.

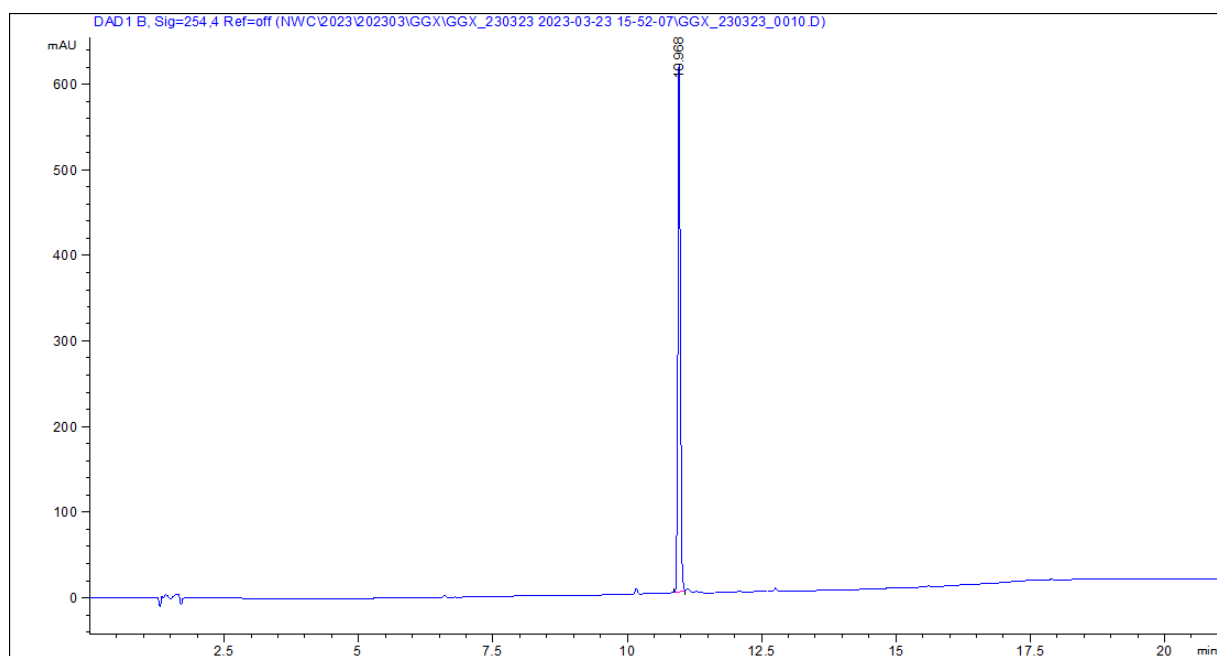


Figure 255: HPLC chromatogram of compound **5i** (Chapter 2), absorbance detection at 254 nm.

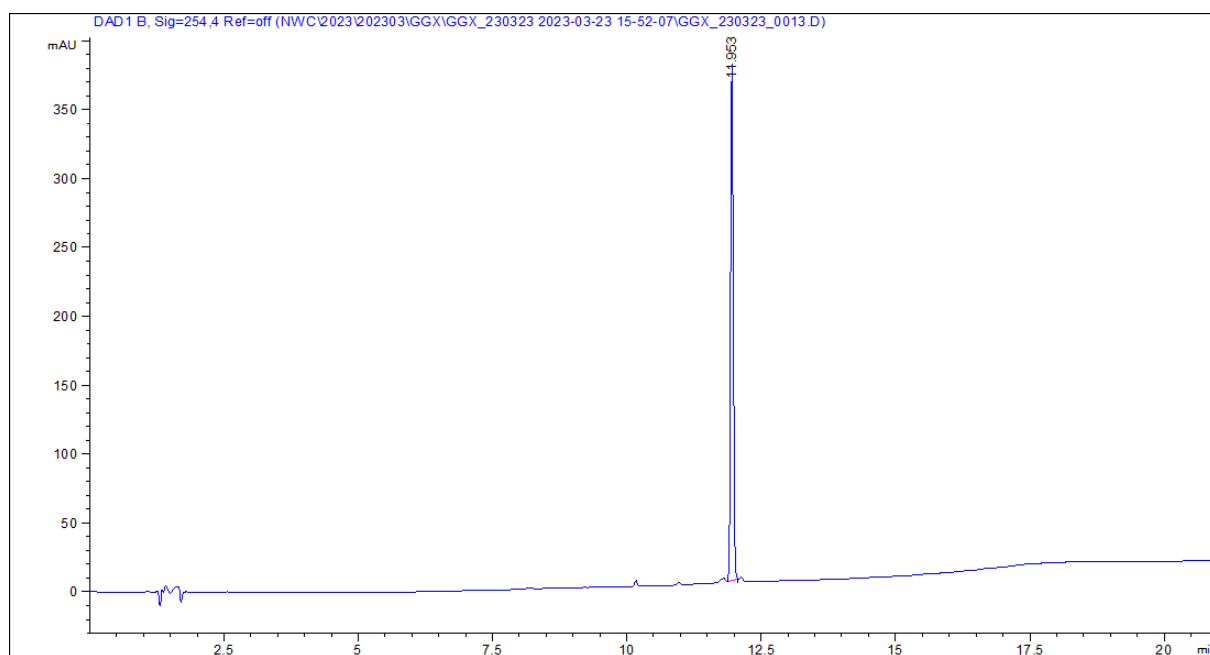


Figure 256: HPLC chromatogram of compound **5j** (Chapter 2), absorbance detection at 254 nm.

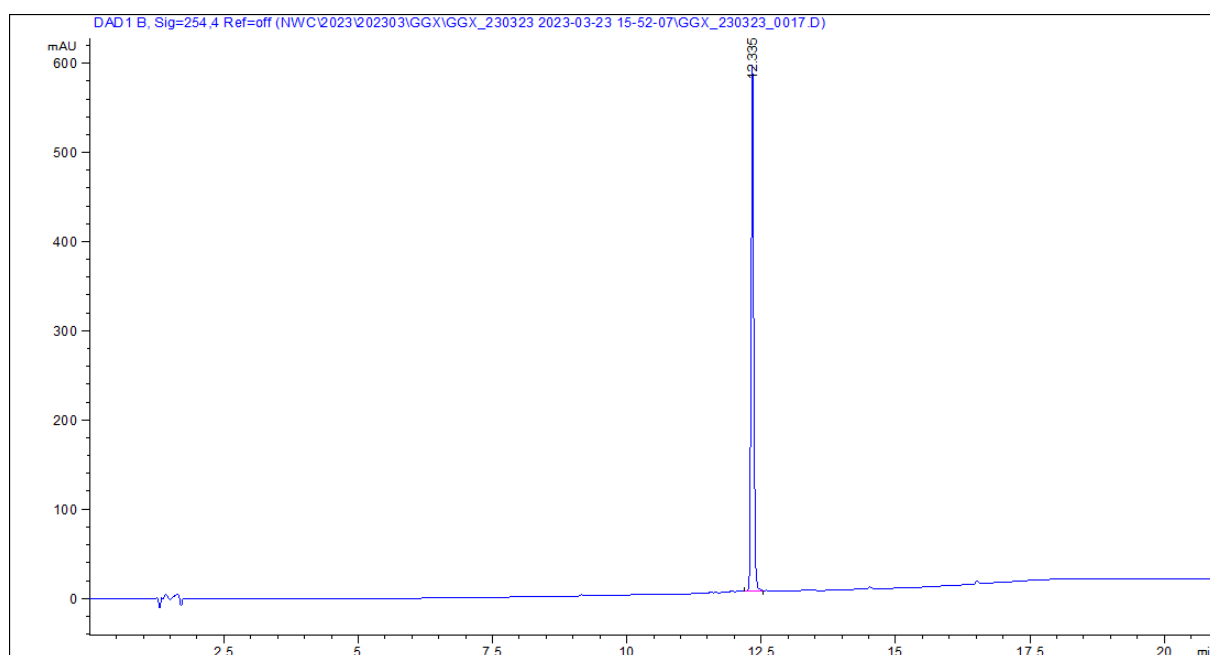


Figure 257: HPLC chromatogram of compound **5k** (Chapter 2), absorbance detection at 254 nm.

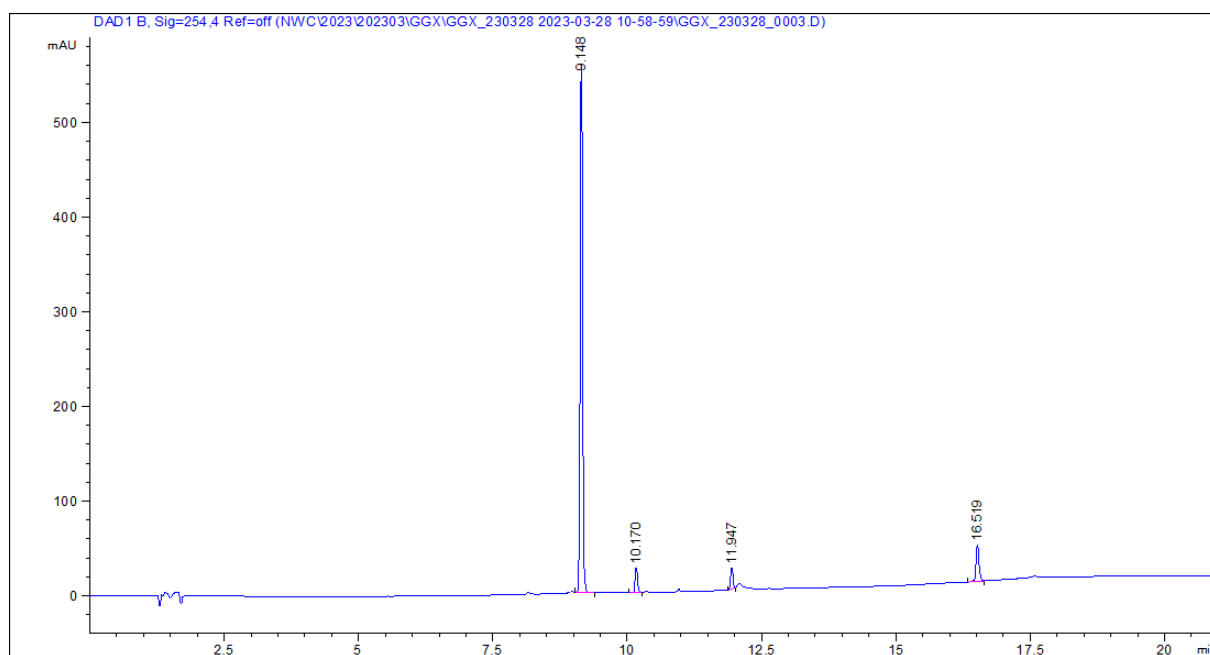


Figure 258: HPLC chromatogram of compound **5l** (Chapter 2), absorbance detection at 254 nm.

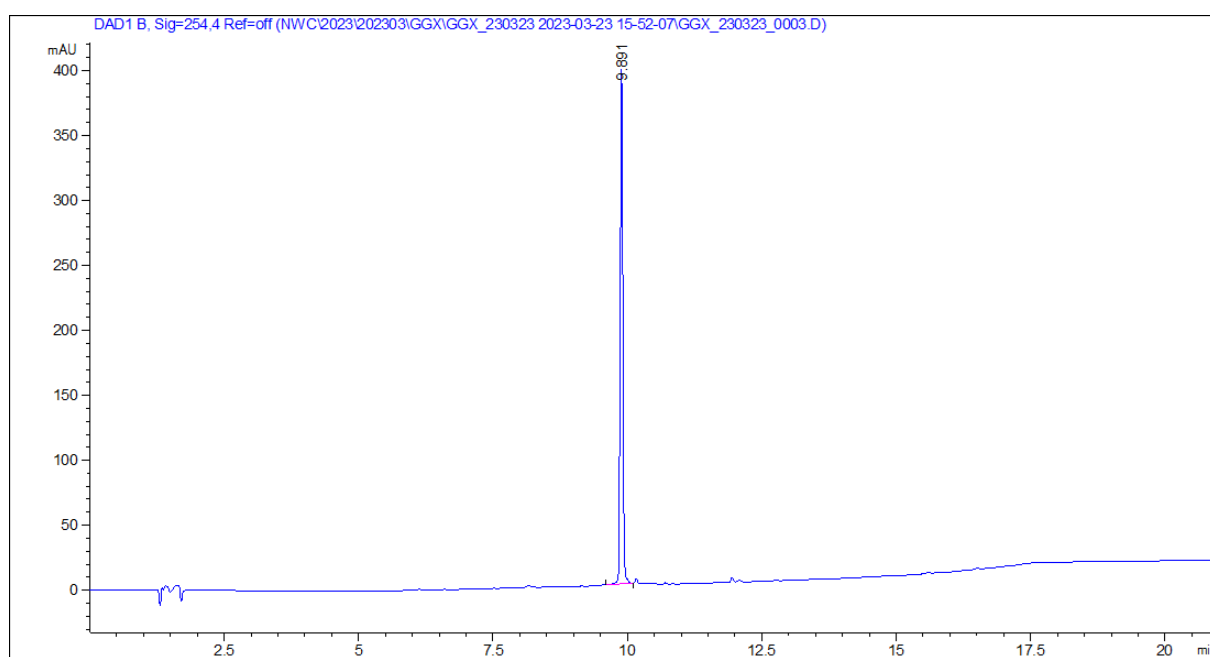


Figure 259: HPLC chromatogram of compound **5m** (Chapter 2), absorbance detection at 254 nm.

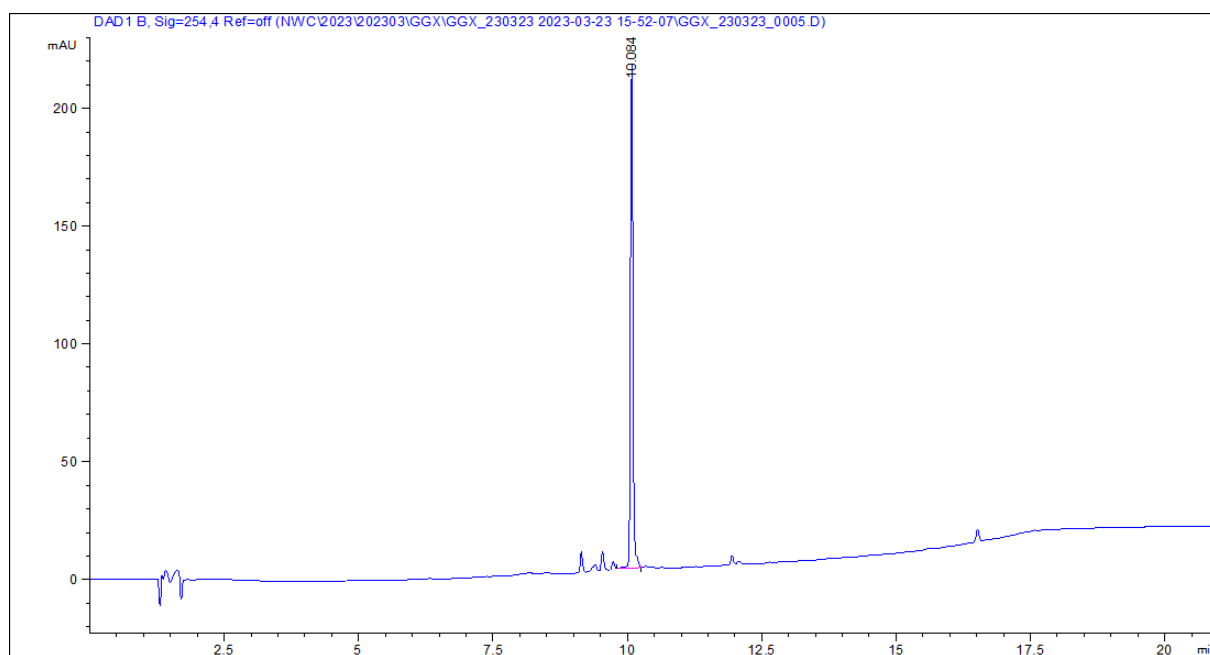


Figure 260: HPLC chromatogram of compound **5n** (Chapter 2), absorbance detection at 254 nm.

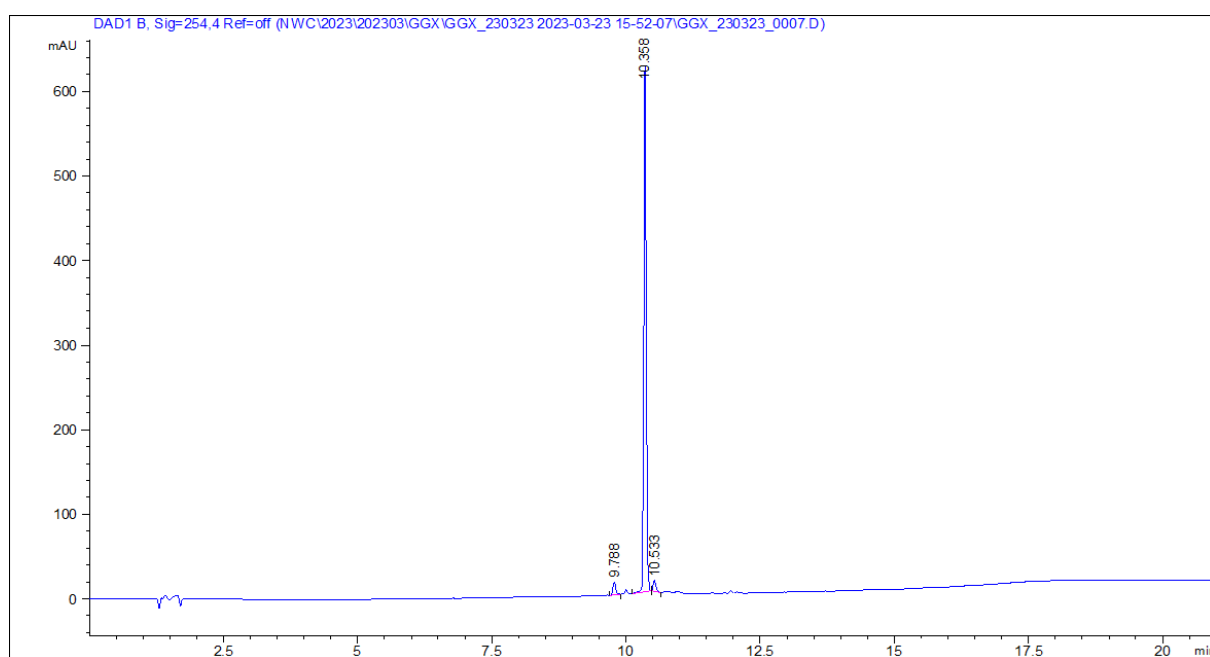


Figure 261: HPLC chromatogram of compound **5o** (Chapter 2), absorbance detection at 254 nm.

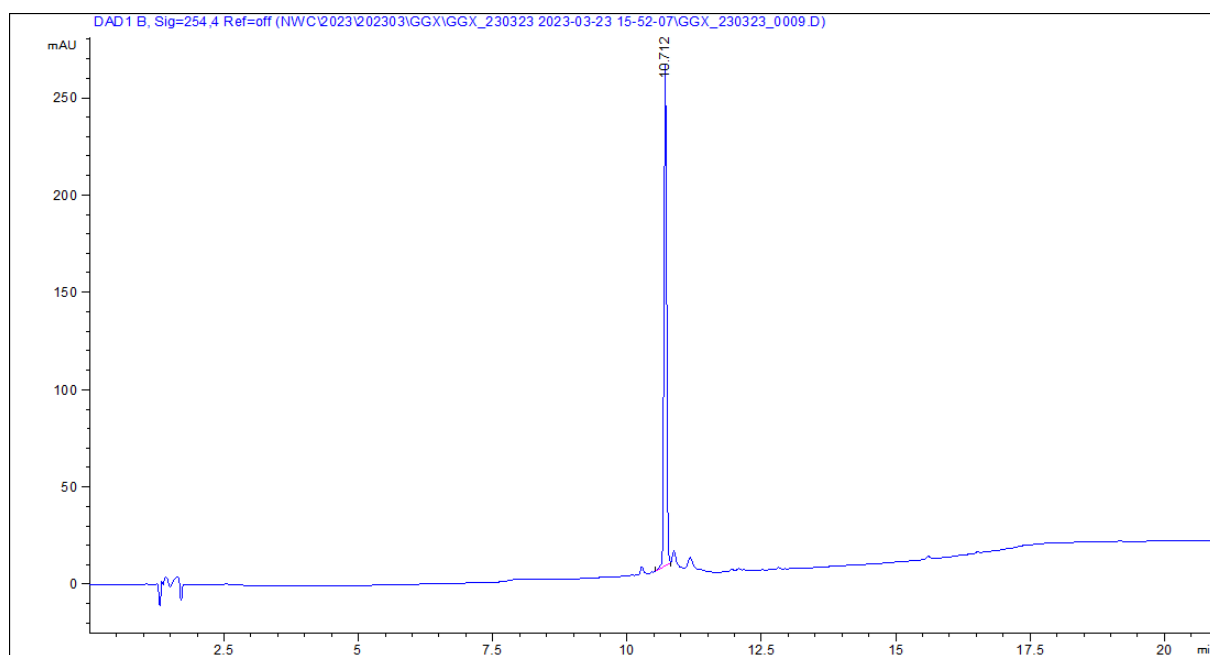


Figure 262: HPLC chromatogram of compound **5p** (Chapter 2), absorbance detection at 254 nm.

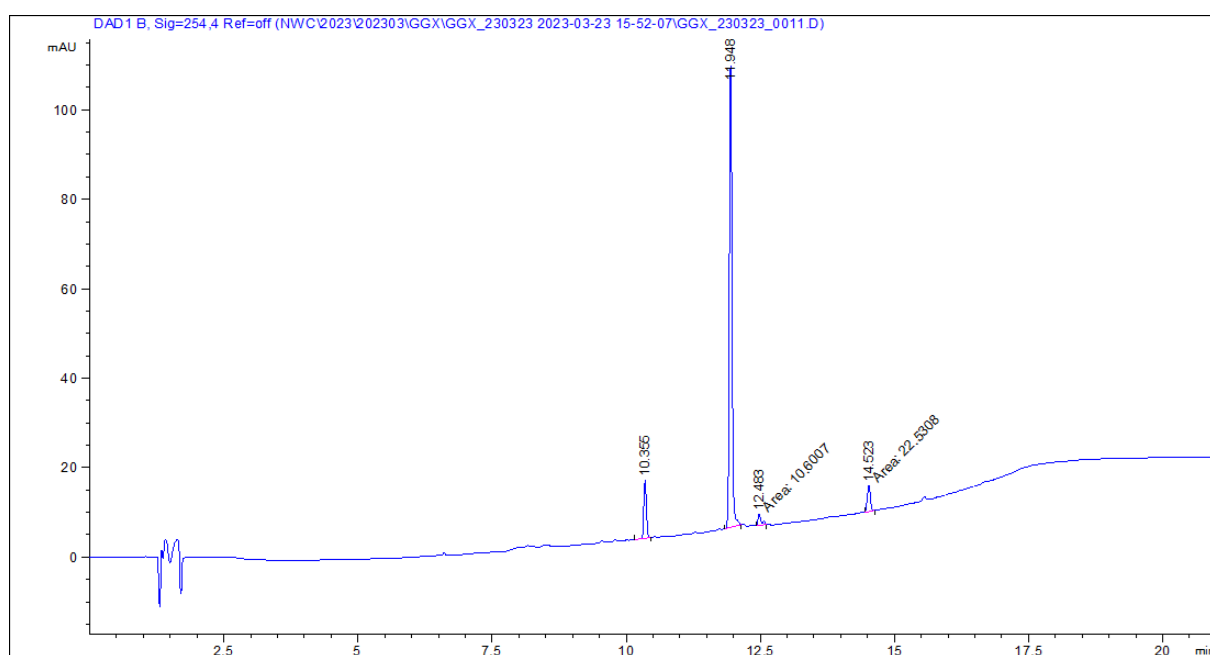


Figure 263: HPLC chromatogram of compound **5q** (Chapter 2), absorbance detection at 254 nm.

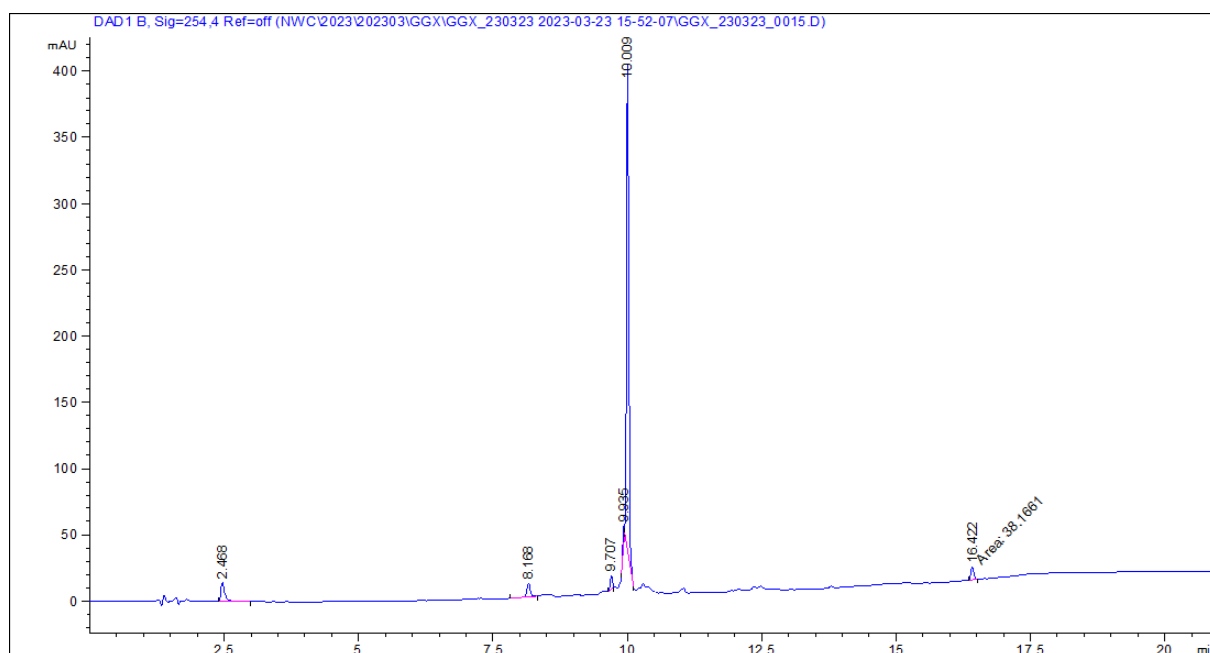


Figure 264: HPLC chromatogram of compound **5r** (Chapter 2), absorbance detection at 254 nm.

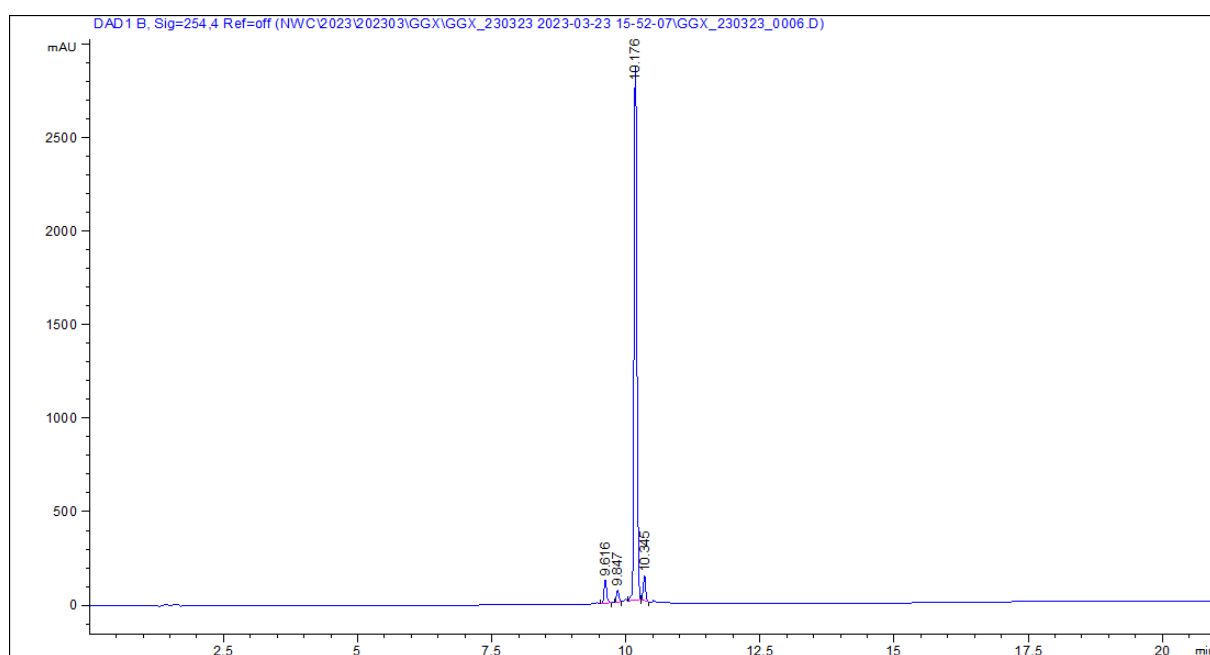


Figure 265: HPLC chromatogram of compound **5s** (Chapter 2), absorbance detection at 254 nm.

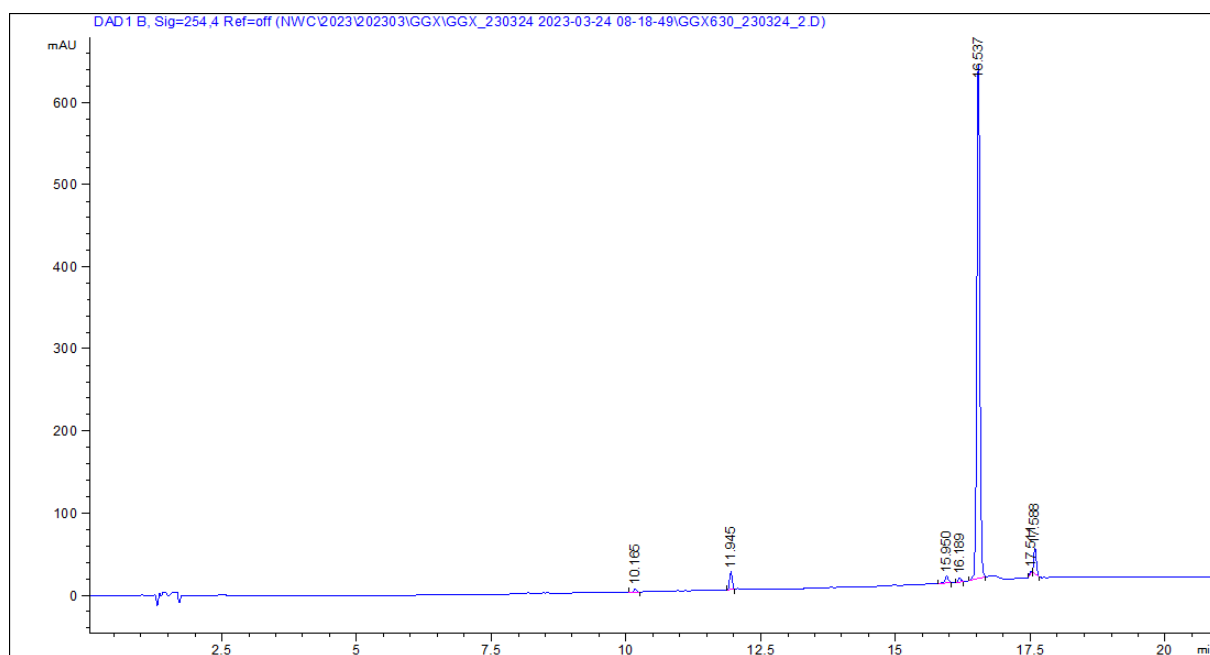


Figure 266: HPLC chromatogram of compound **5t** (Chapter 2), absorbance detection at 254 nm.

Docking schemes of Tentoxin and derivatives in the alpha and beta subunits of the ATPase

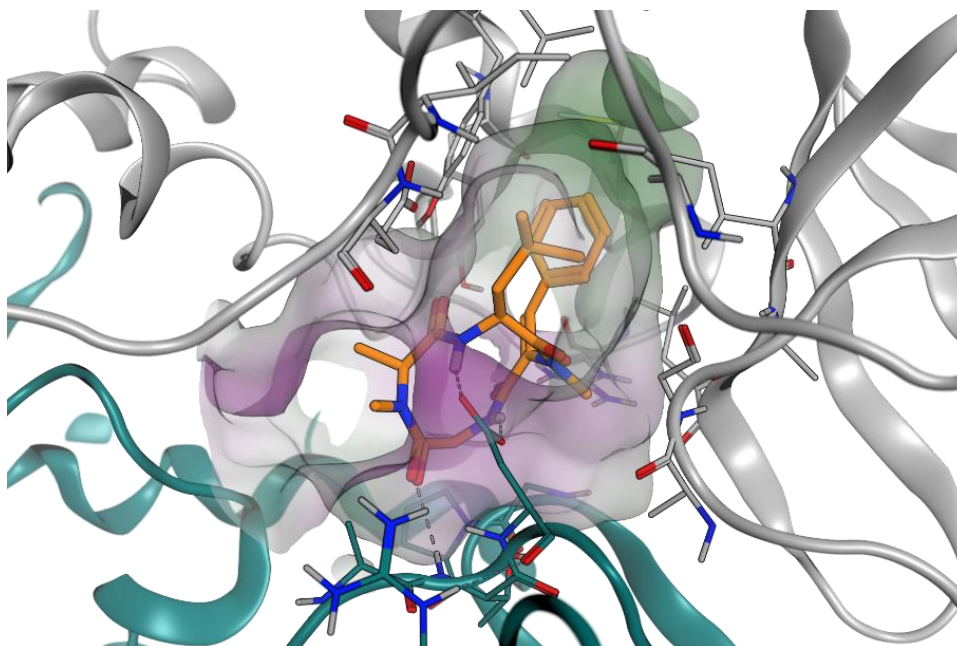


Figure 267: Docking of tentoxin **5a** (Chapter 2) in the alpha (grey) and beta (cyan) subunit of the ATPase. Green: lipophile, purple: hydrophile, white: neutral.

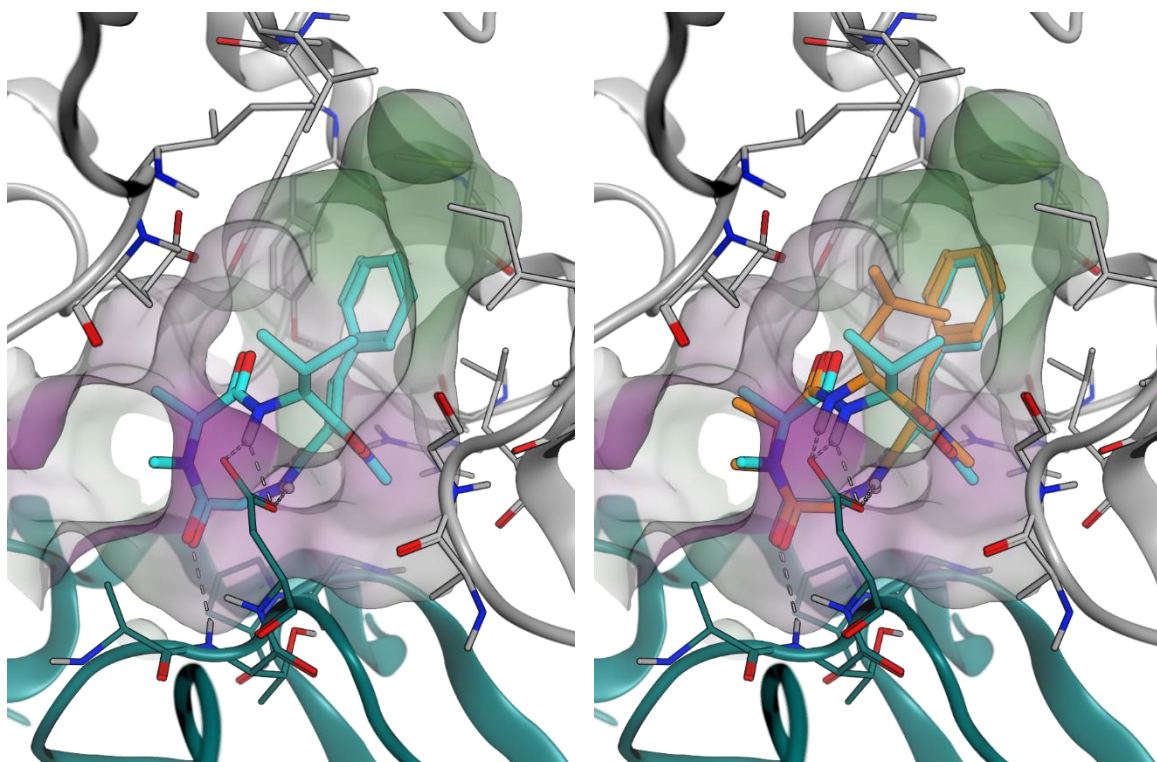


Figure 268: Docking of compound **5b** (Chapter 2, cyan, left figure) and tentoxin **5a** (Chapter 2, orange, right figure) in the alpha (grey) and beta (cyan) subunit of the ATPase. Green: lipophile, purple: hydrophile, white: neutral.

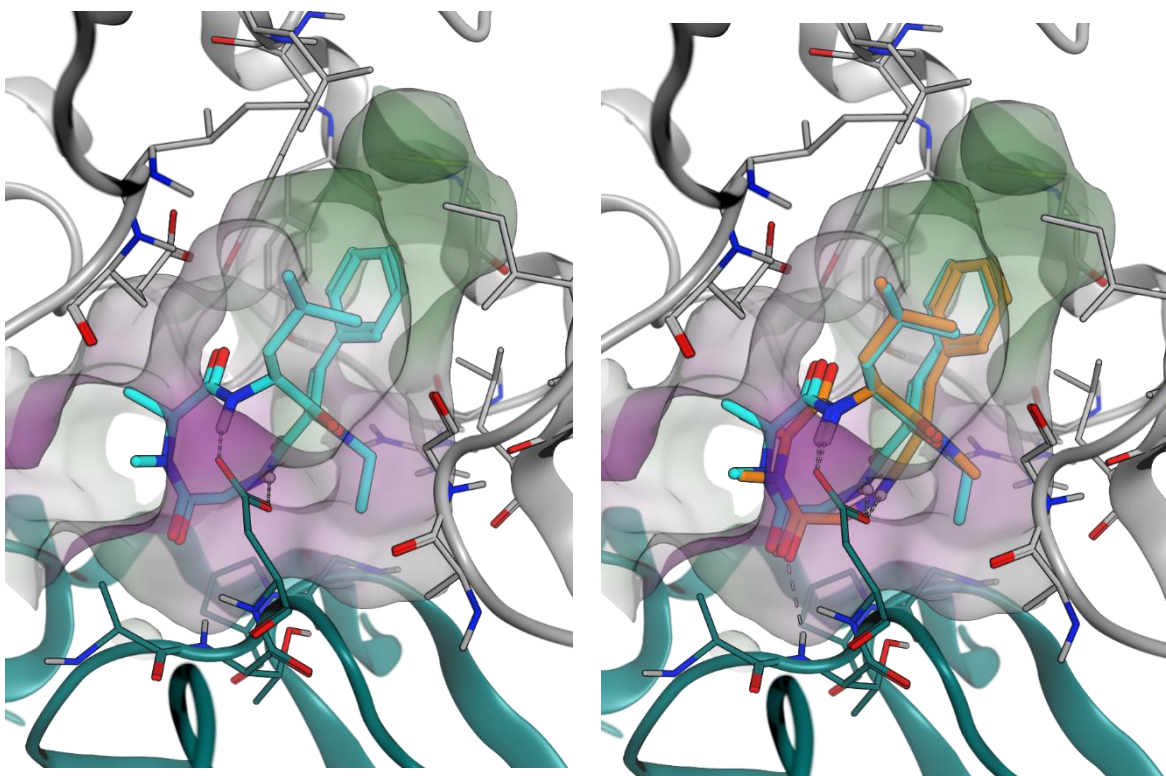


Figure 269: Docking of compound **5c** (Chapter 2, cyan, left figure) and tentoxin **5a** (Chapter 2, orange, right figure) in the alpha (grey) and beta (cyan) subunit of the ATPase. Green: lipophile, purple: hydrophile, white: neutral.

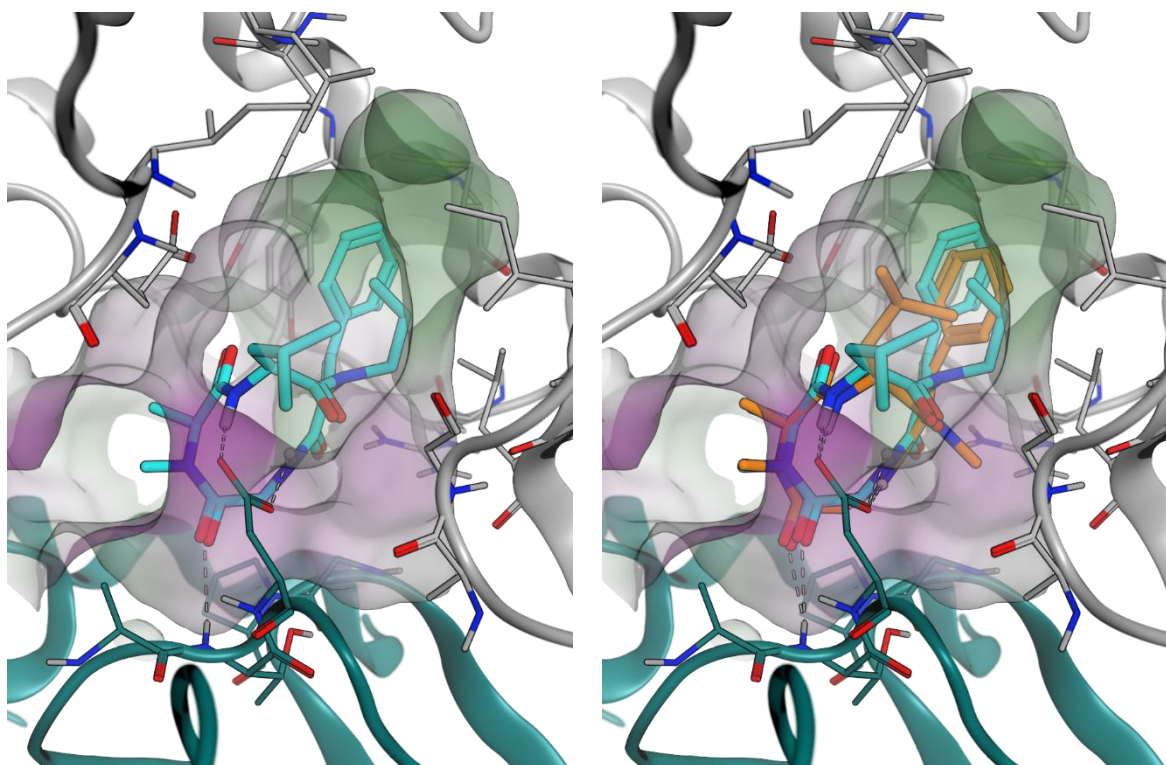


Figure 270: Docking of compound **5d** (Chapter 2, cyan, left figure) and tentoxin **5a** (Chapter 2, orange, right figure) in the alpha (grey) and beta (cyan) subunit of the ATPase. Green: lipophile, purple: hydrophile, white: neutral.

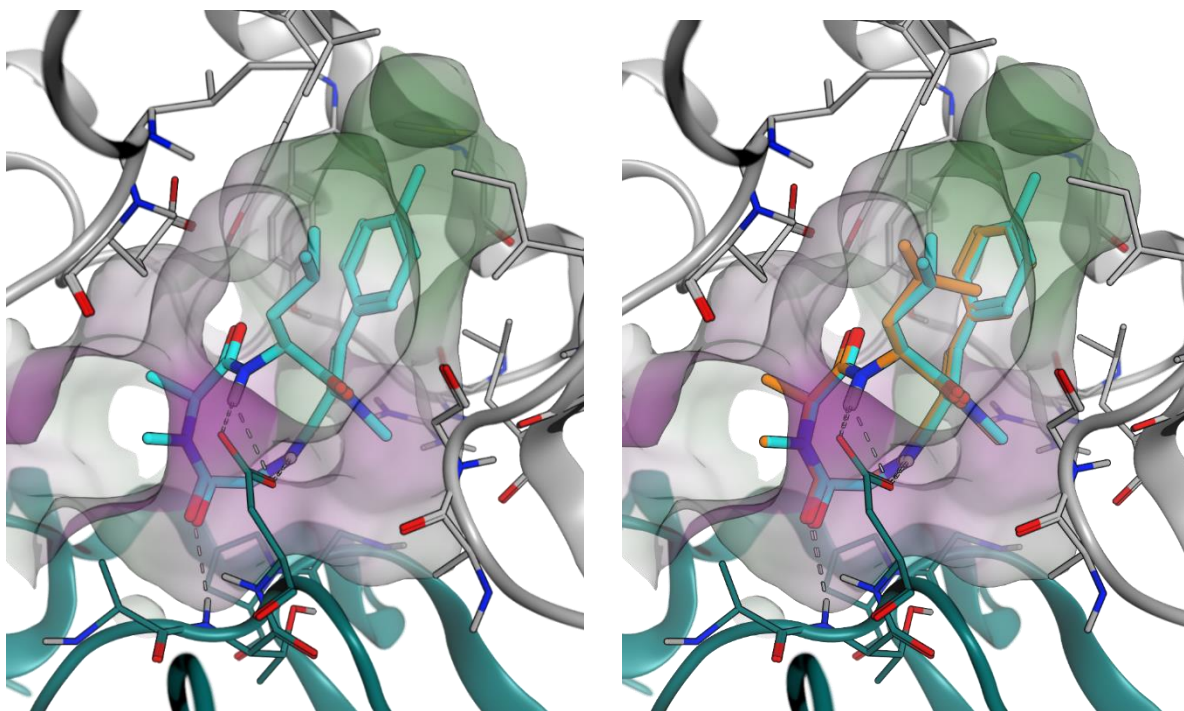


Figure 271: Docking of compound **5e** (Chapter 2, cyan, left figure) and tentoxin **5a** (Chapter 2, orange, right figure) in the alpha (grey) and beta (cyan) subunit of the ATPase. Green: lipophile, purple: hydrophile, white: neutral.

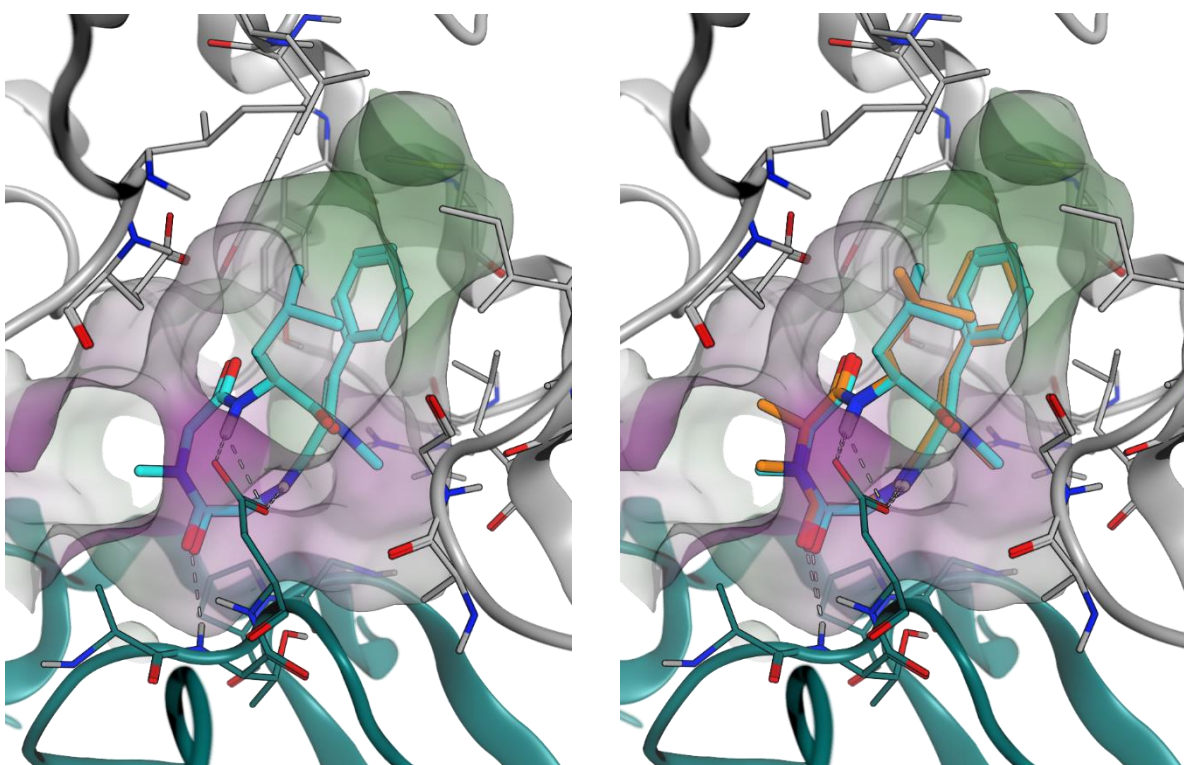


Figure 272: Docking of compound **5f** (Chapter 2, cyan, left figure) and tentoxin **5a** (Chapter 2, orange, right figure) in the alpha (grey) and beta (cyan) subunit of the ATPase. Green: lipophile, purple: hydrophile, white: neutral.

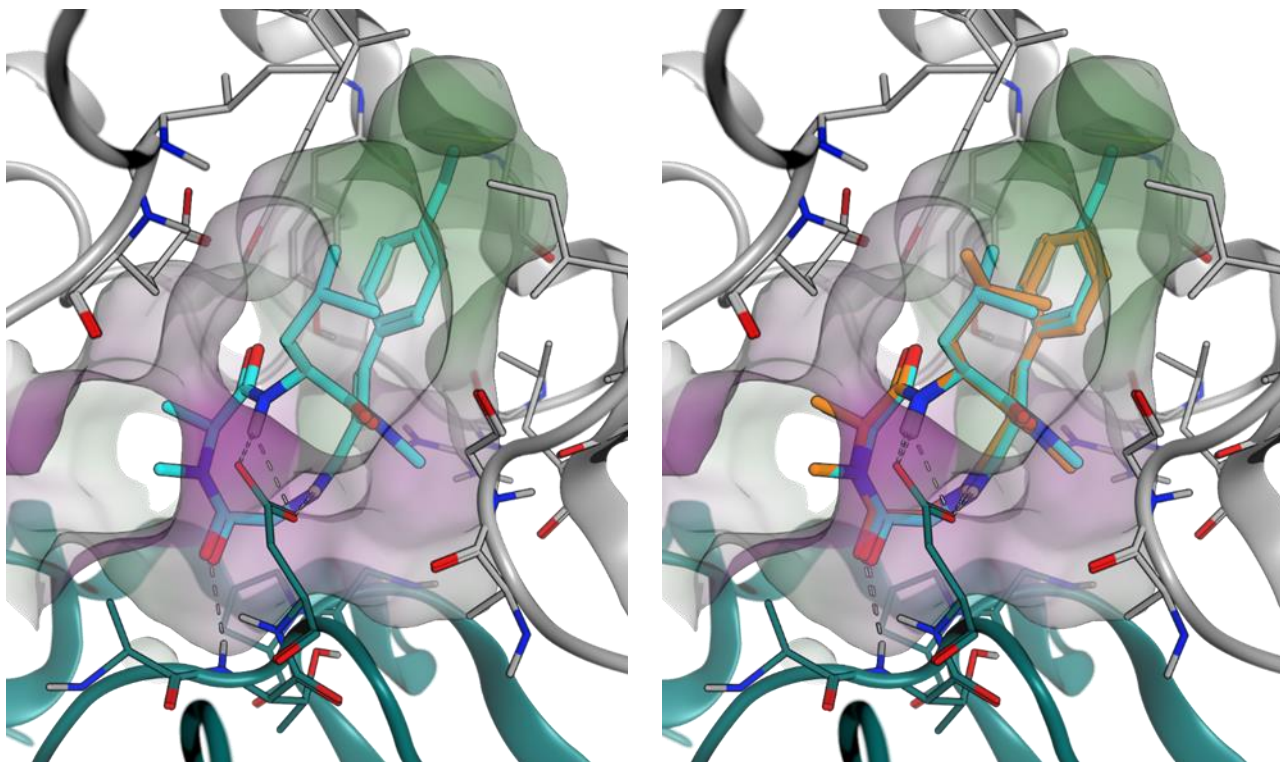


Figure 273: Docking of compound **5g** (Chapter 2, cyan, left figure) and tentoxin **5a** (Chapter 2, orange, right figure) in the alpha (grey) and beta (cyan) subunit of the ATPase. Green: lipophile, purple: hydrophile, white: neutral.

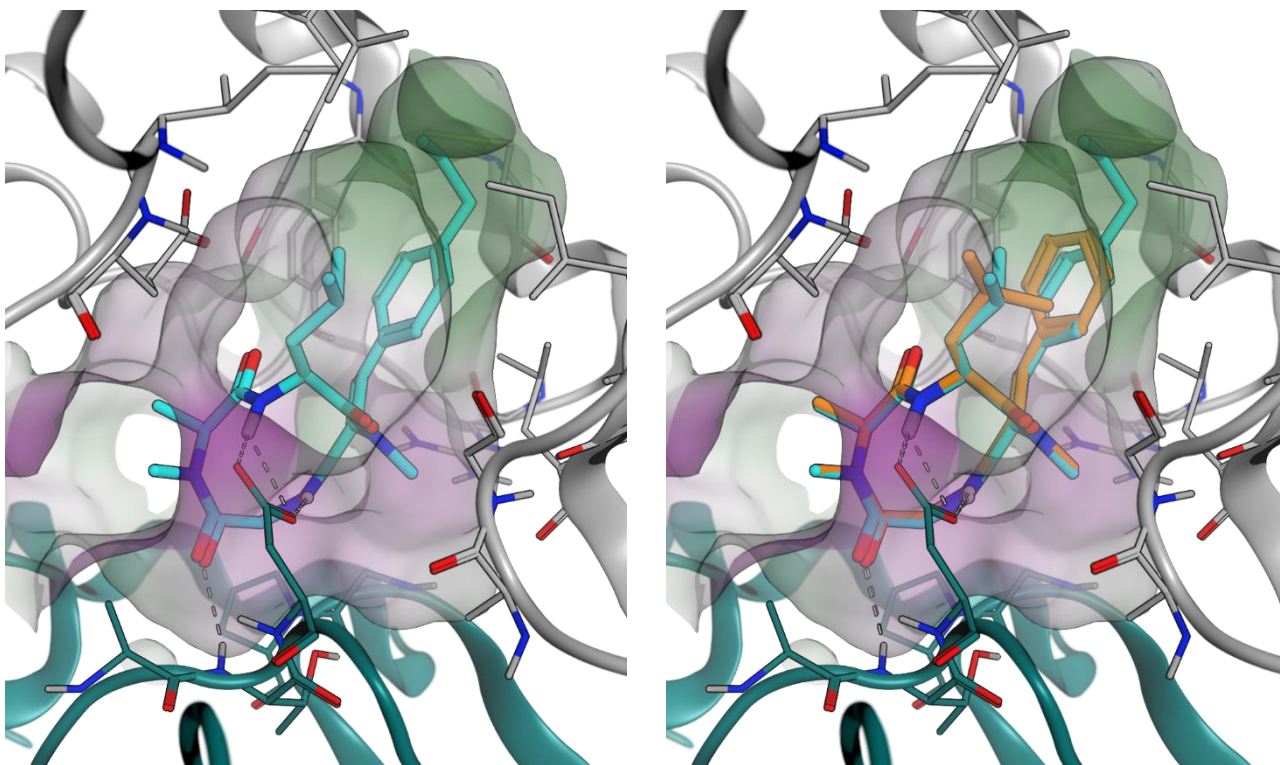


Figure 274: Docking of compound **5h** (Chapter 2, cyan, left figure) and tentoxin **5a** (Chapter 2, orange, right figure) in the alpha (grey) and beta (cyan) subunit of the ATPase. Green: lipophile, purple: hydrophile, white: neutral.

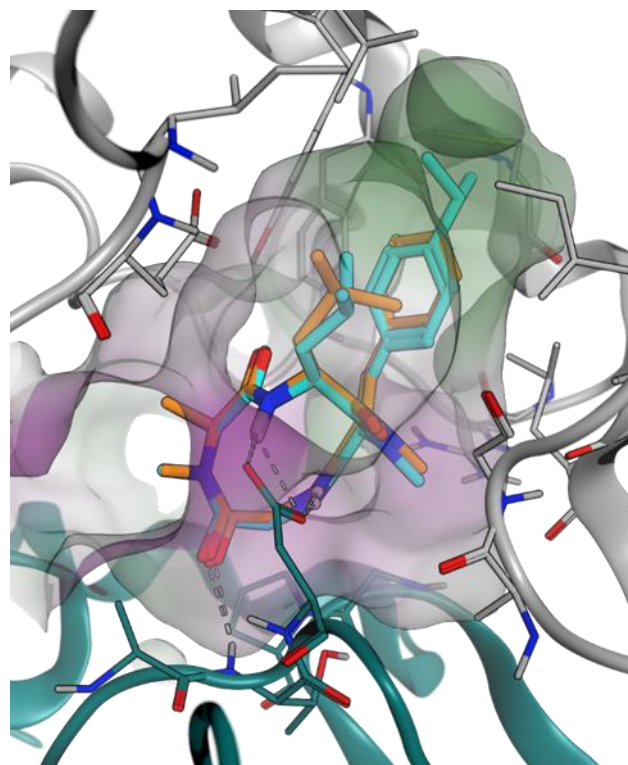
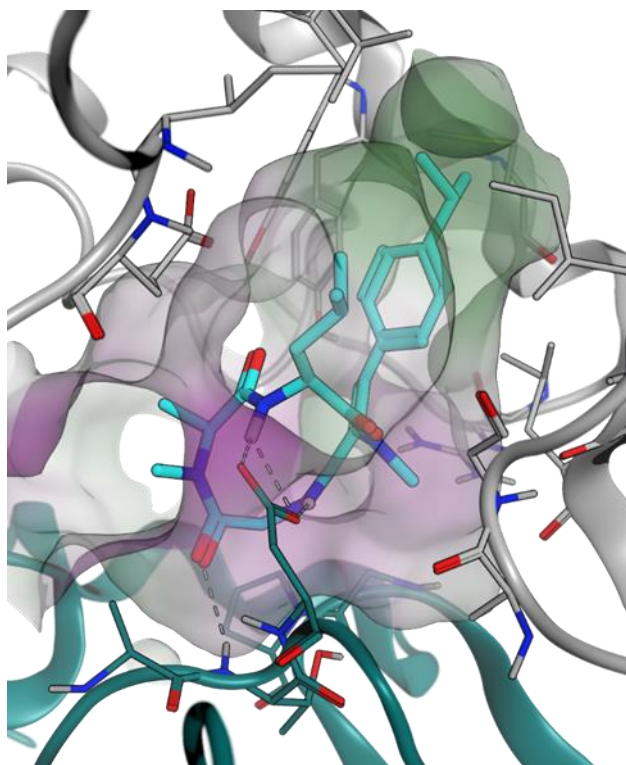


Figure 275: Docking of compound **5i** (Chapter 2, cyan, left figure) and tentoxin **5a** (Chapter 2, orange, right figure) in the alpha (grey) and beta (cyan) subunit of the ATPase. Green: lipophile, purple: hydrophile, white: neutral.

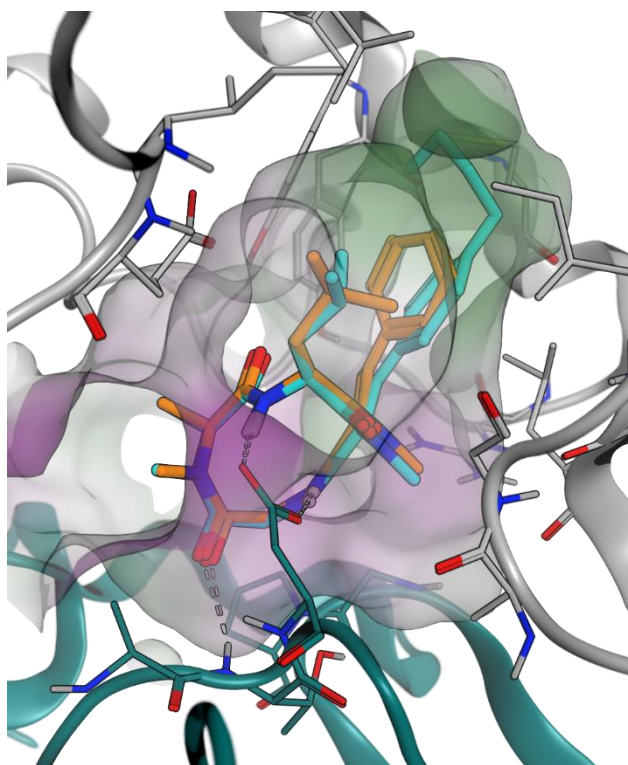
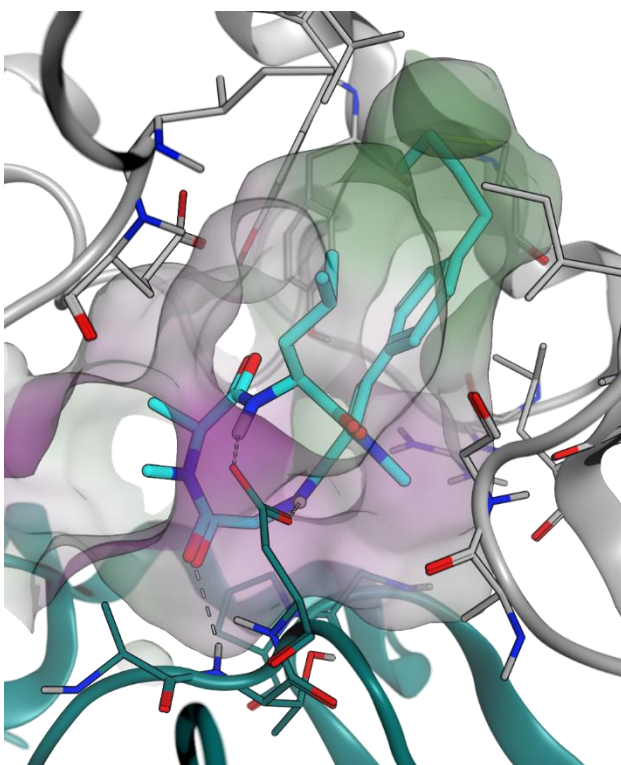


Figure 276: Docking of compound **5j** (Chapter 2, cyan, left figure) and tentoxin **5a** (Chapter 2, orange, right figure) in the alpha (grey) and beta (cyan) subunit of the ATPase. Green: lipophile, purple: hydrophile, white: neutral.

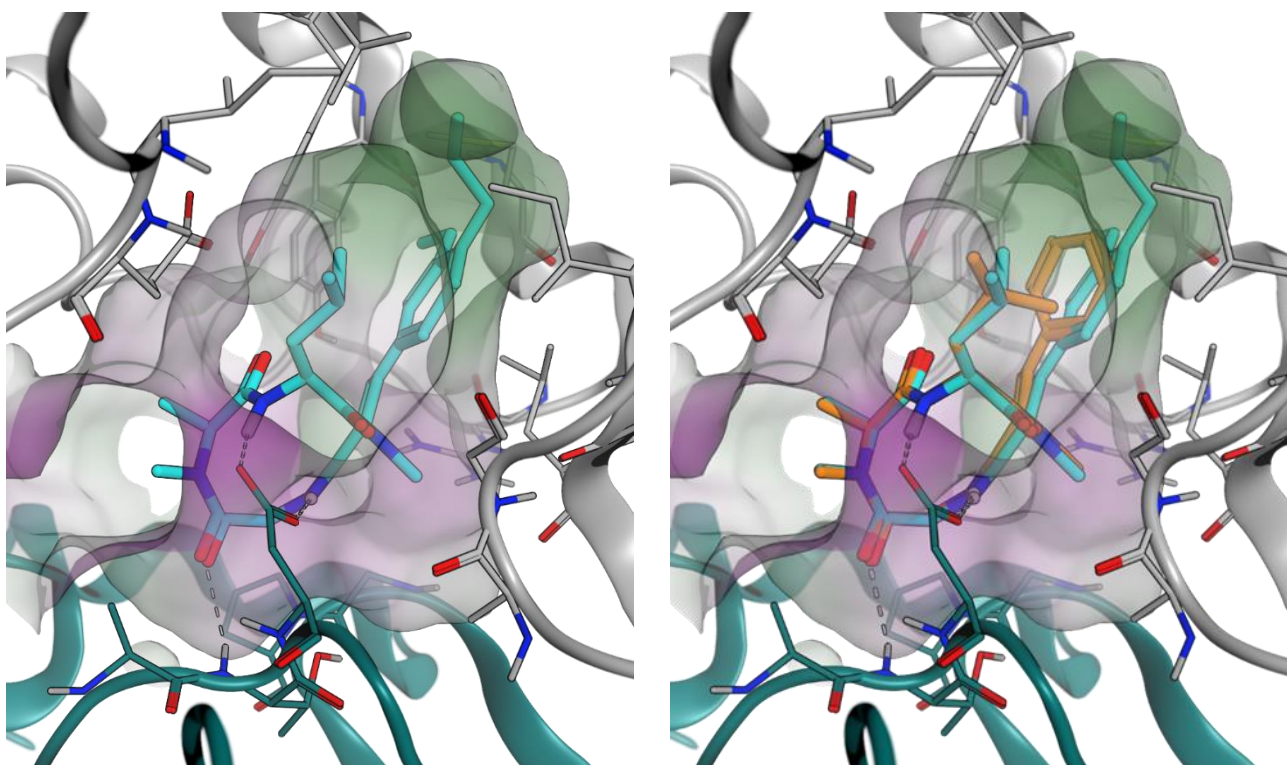


Figure 277: Docking of compound **5k** (Chapter 2, cyan, left figure) and tentoxin **5a** (Chapter 2, orange, right figure) in the alpha (grey) and beta (cyan) subunit of the ATPase. Green: lipophile, purple: hydrophile, white: neutral.

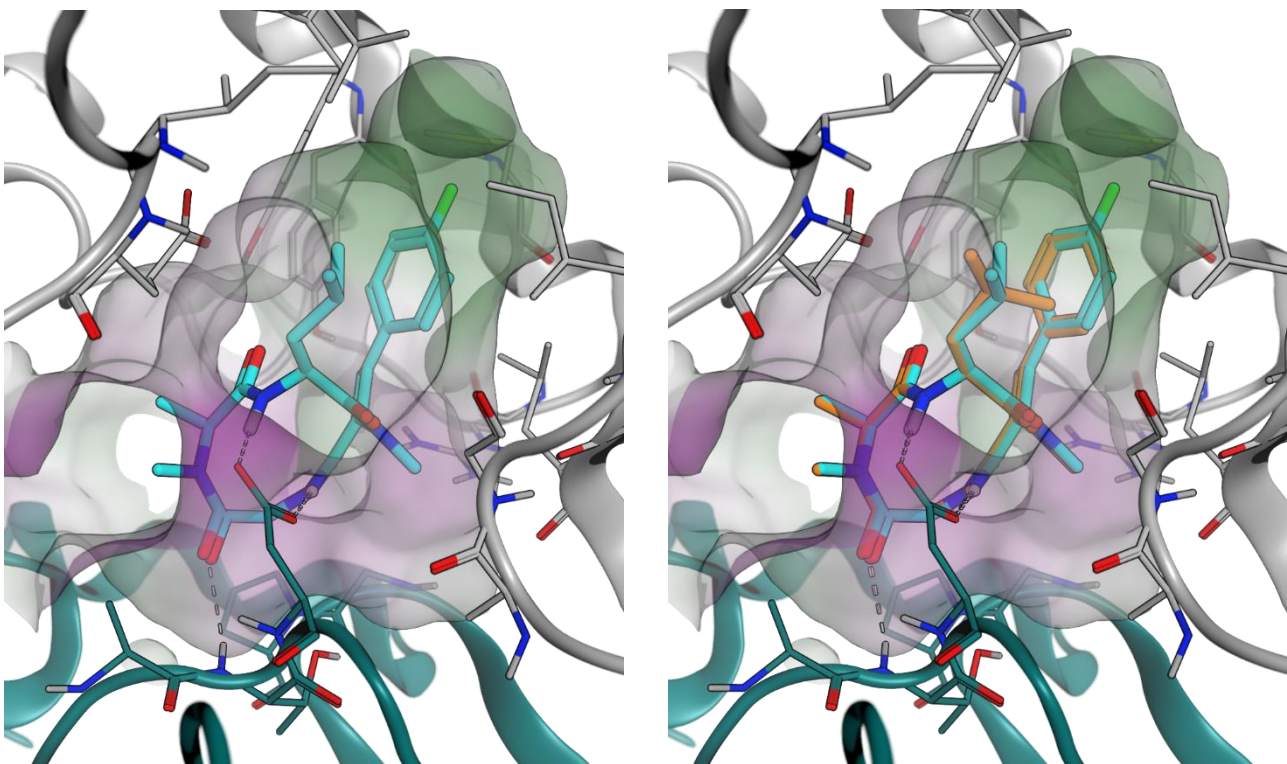


Figure 278: Docking of compound **5l** (Chapter 2, cyan, left figure) and tentoxin **5a** (Chapter 2, orange, right figure) in the alpha (grey) and beta (cyan) subunit of the ATPase. Green: lipophile, purple: hydrophile, white: neutral.

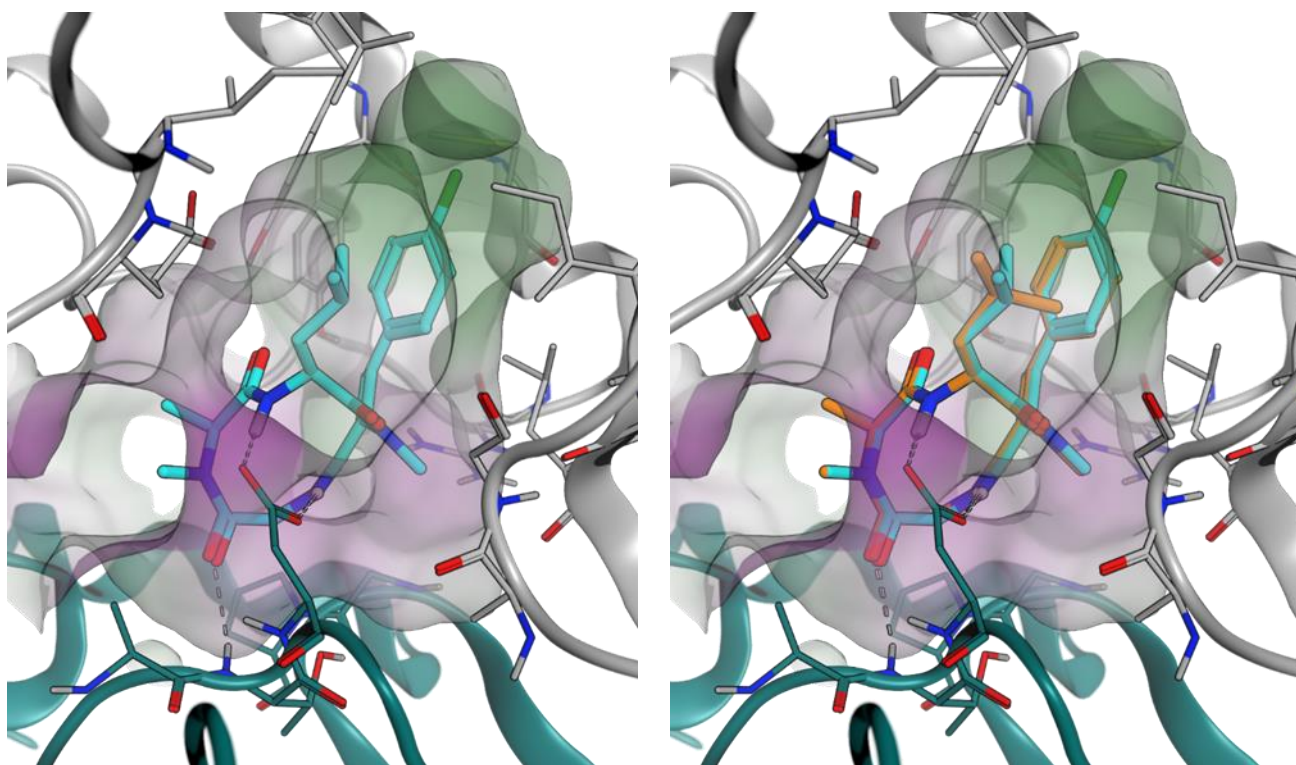


Figure 279: Docking of compound **5m** (Chapter 2, cyan, left figure) and tentoxin **5a** (Chapter 2, orange, right figure) in the alpha (grey) and beta (cyan) subunit of the ATPase. Green: lipophile, purple: hydrophile, white: neutral.

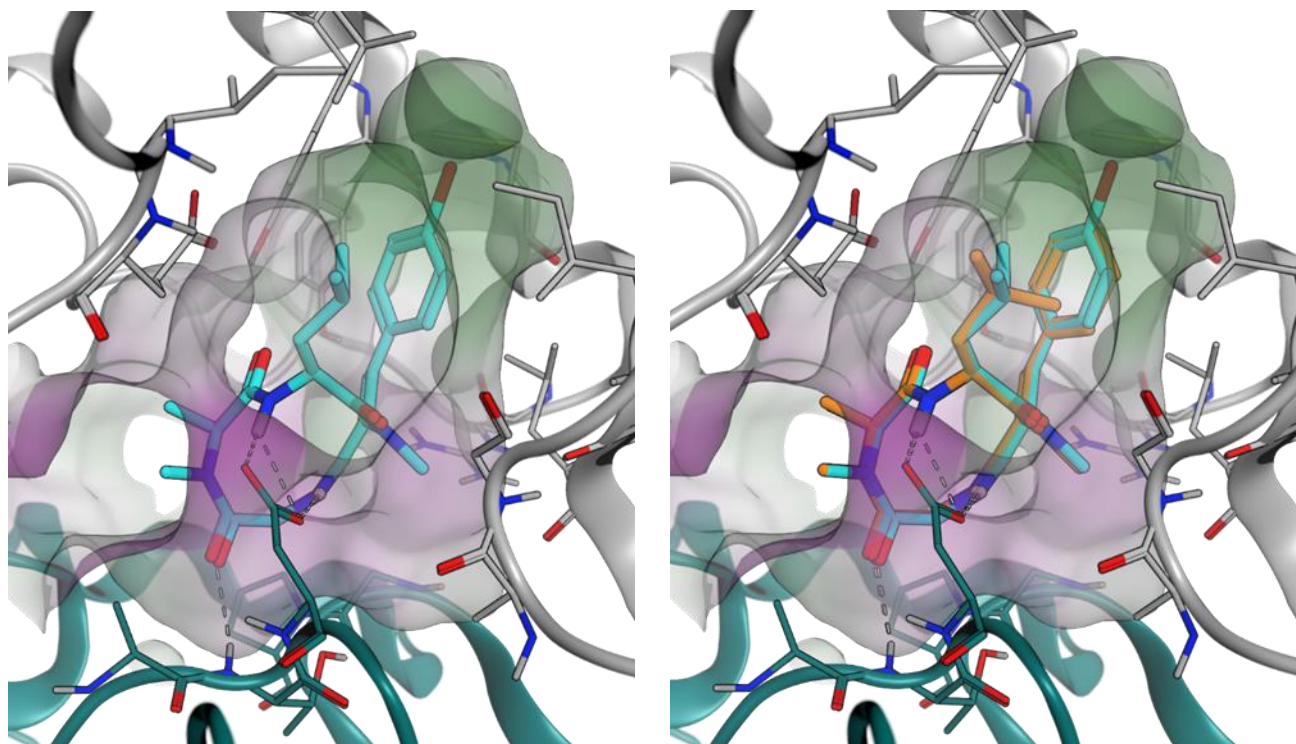


Figure 280: Docking of compound **5n** (Chapter 2, cyan, left figure) and tentoxin **5a** (Chapter 2, orange, right figure) in the alpha (grey) and beta (cyan) subunit of the ATPase. Green: lipophile, purple: hydrophile, white: neutral.

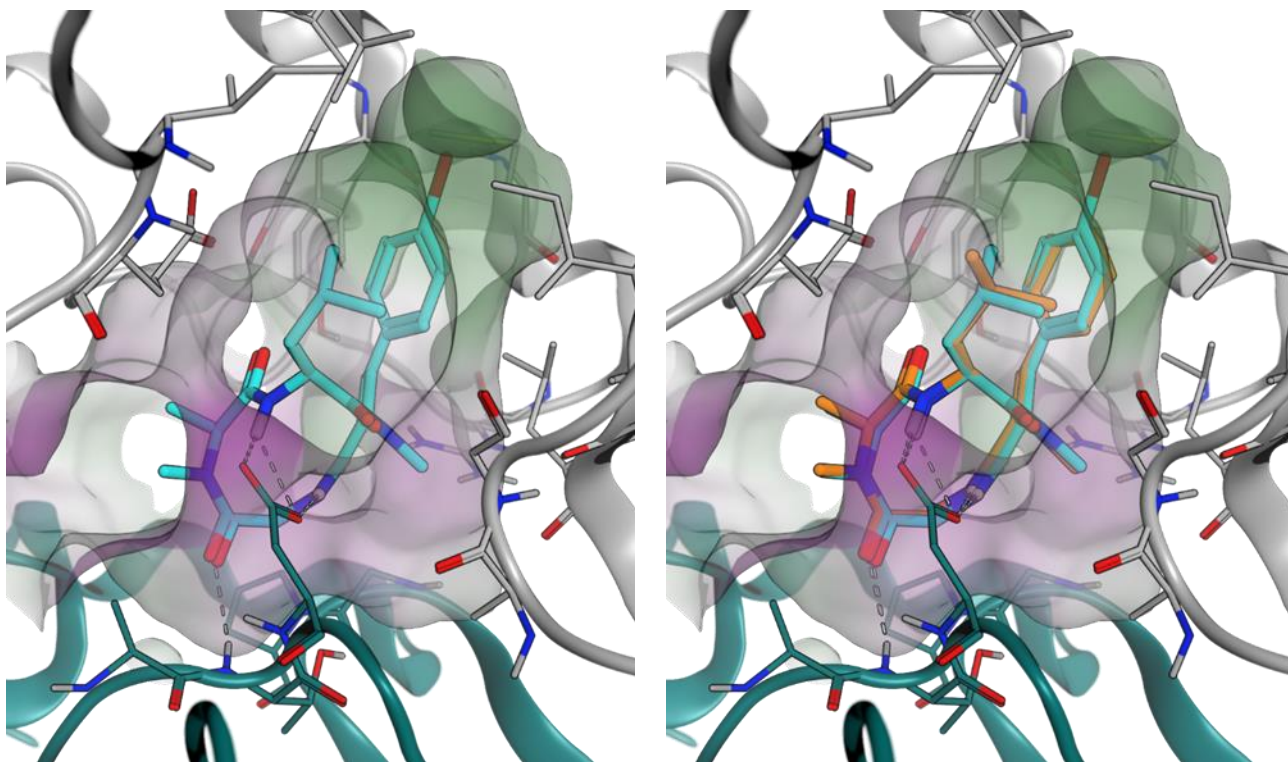


Figure 281: Docking of compound **5o** (Chapter 2, cyan, left figure) and tentoxin **5a** (Chapter 2, orange, right figure) in the alpha (grey) and beta (cyan) subunit of the ATPase. Green: lipophile, purple: hydrophile, white: neutral.

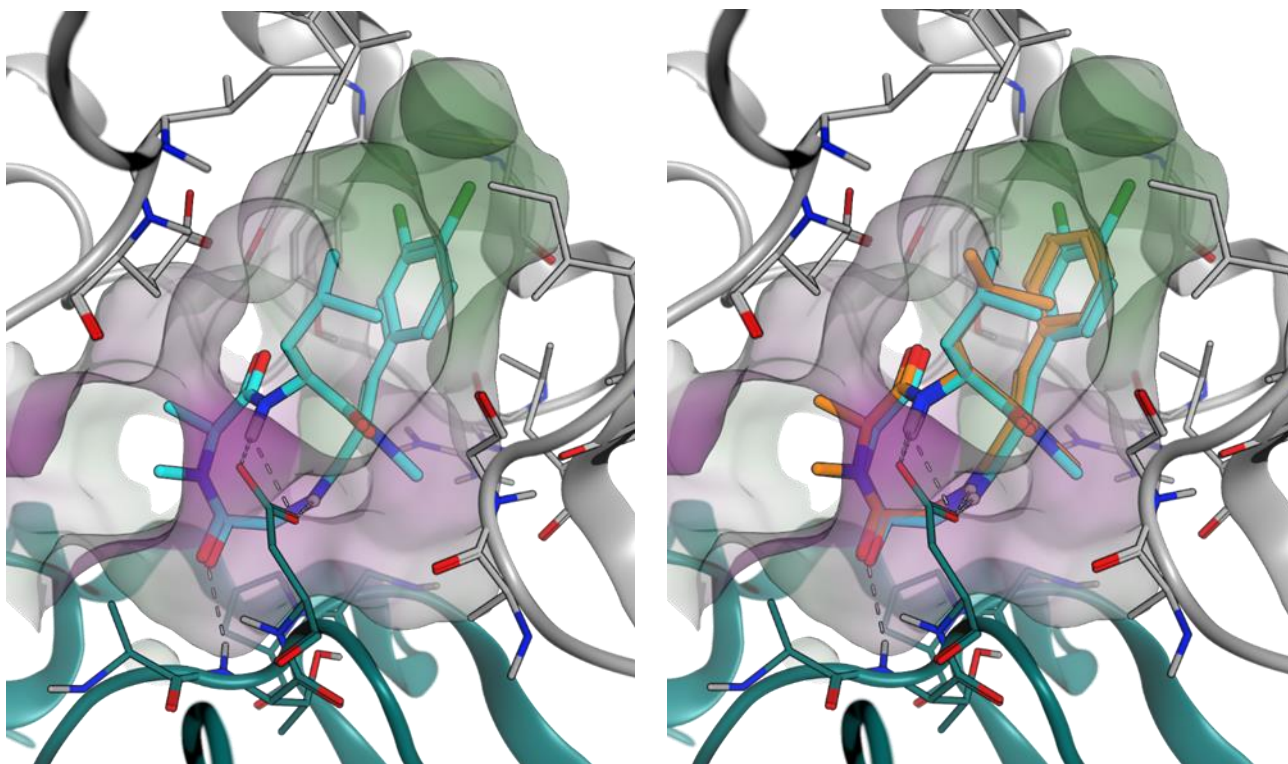


Figure 282: Docking of compound **5p** (Chapter 2, cyan, left figure) and tentoxin **5a** (Chapter 2, orange, right figure) in the alpha (grey) and beta (cyan) subunit of the ATPase. Green: lipophile, purple: hydrophile, white: neutral.

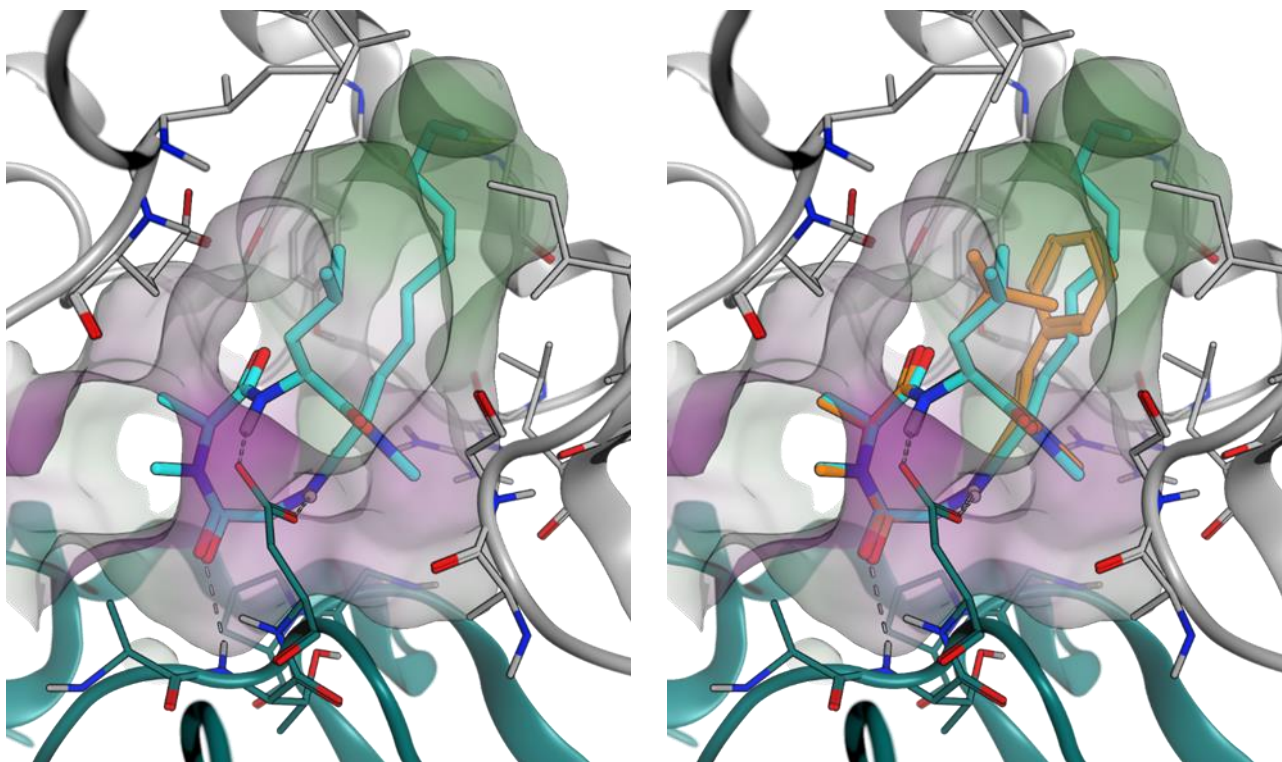


Figure 283: Docking of compound **5q** (Chapter 2, cyan, left figure) and tentoxin **5a** (Chapter 2, orange, right figure) in the alpha (grey) and beta (cyan) subunit of the ATPase. Green: lipophile, purple: hydrophile, white: neutral.

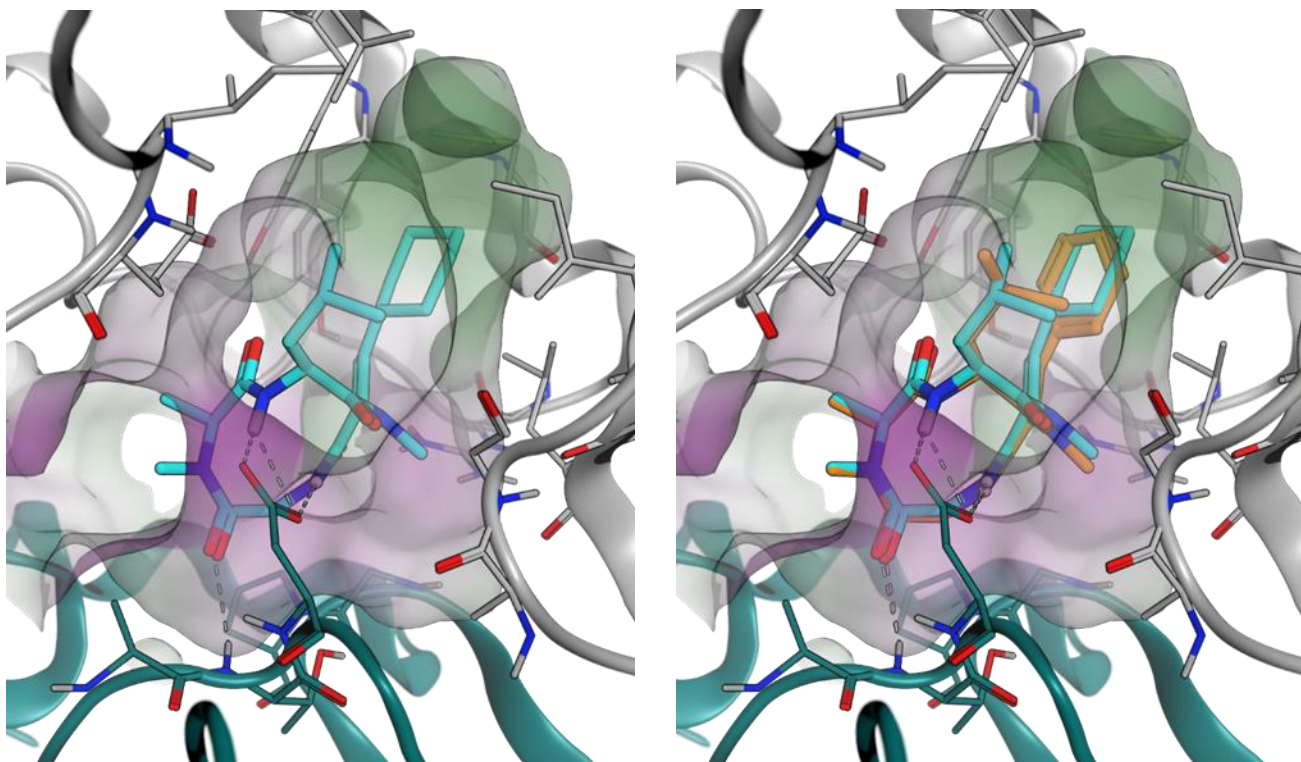


Figure 284: Docking of compound **5r** (Chapter 2, cyan, left figure) and tentoxin **5a** (Chapter 2, orange, right figure) in the alpha (grey) and beta (cyan) subunit of the ATPase. Green: lipophile, purple: hydrophile, white: neutral.

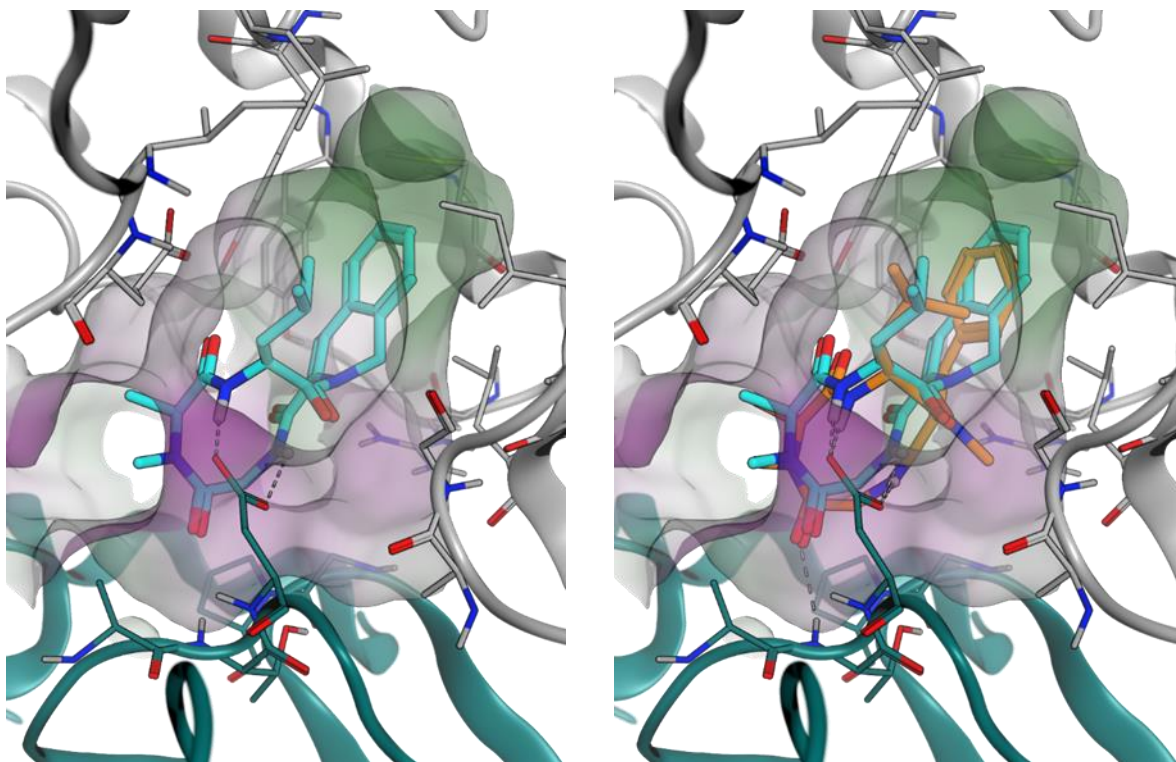


Figure 285: Docking of compound **5s** (Chapter 2, cyan, left figure) and tentoxin **5a** (Chapter 2, orange, right figure) in the alpha (grey) and beta (cyan) subunit of the ATPase. Green: lipophile, purple: hydrophile, white: neutral.

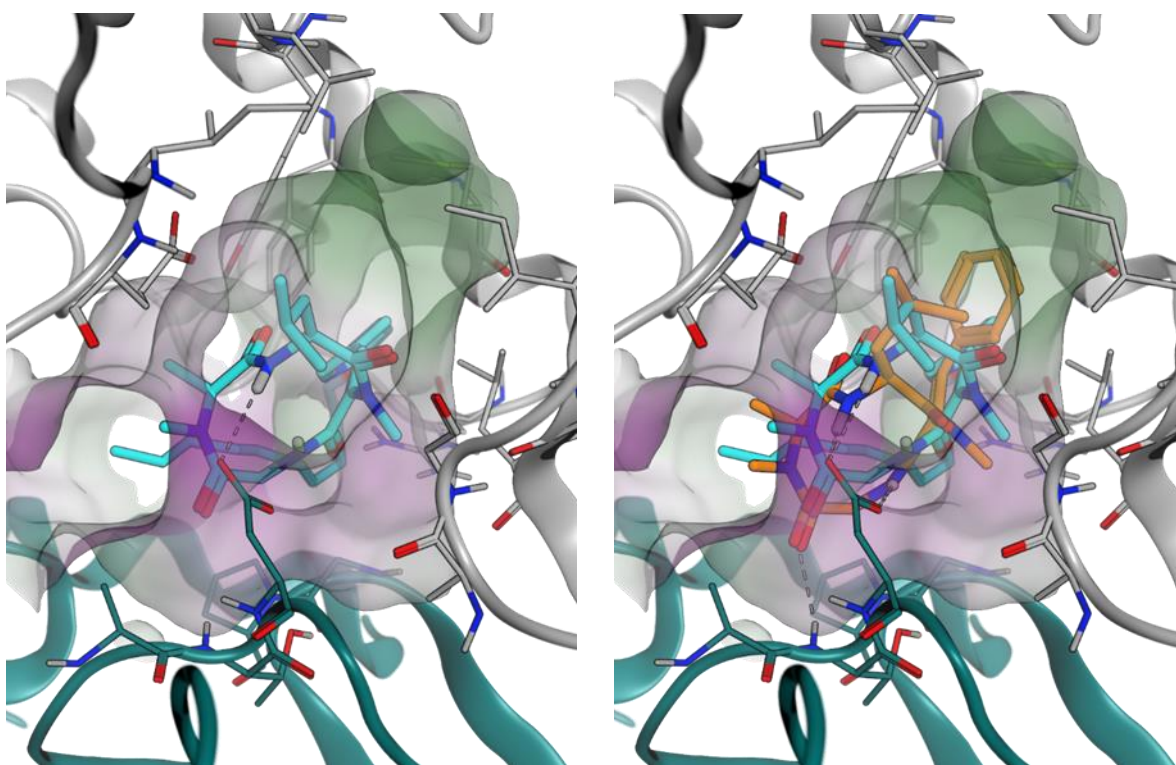


Figure 286: Docking of compound **5t** (Chapter 2, cyan, left figure) and tentoxin **5a** (Chapter 2, orange, right figure) in the alpha (grey) and beta (cyan) subunit of the ATPase. Green: lipophile, purple: hydrophile, white: neutral.

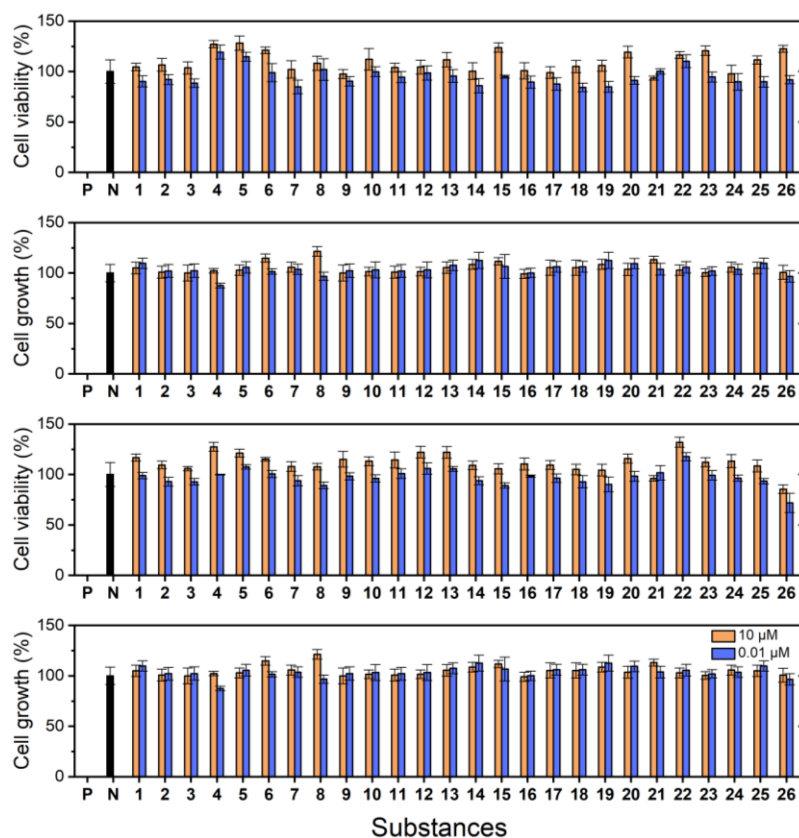


Figure 287: Antiproliferative and cytotoxic activities of compounds **1 - 26** (Chapter 3) against colorectal (HT-29, top two graphs) and human prostate (PC-3, bottom two graphs) cancer cell lines.

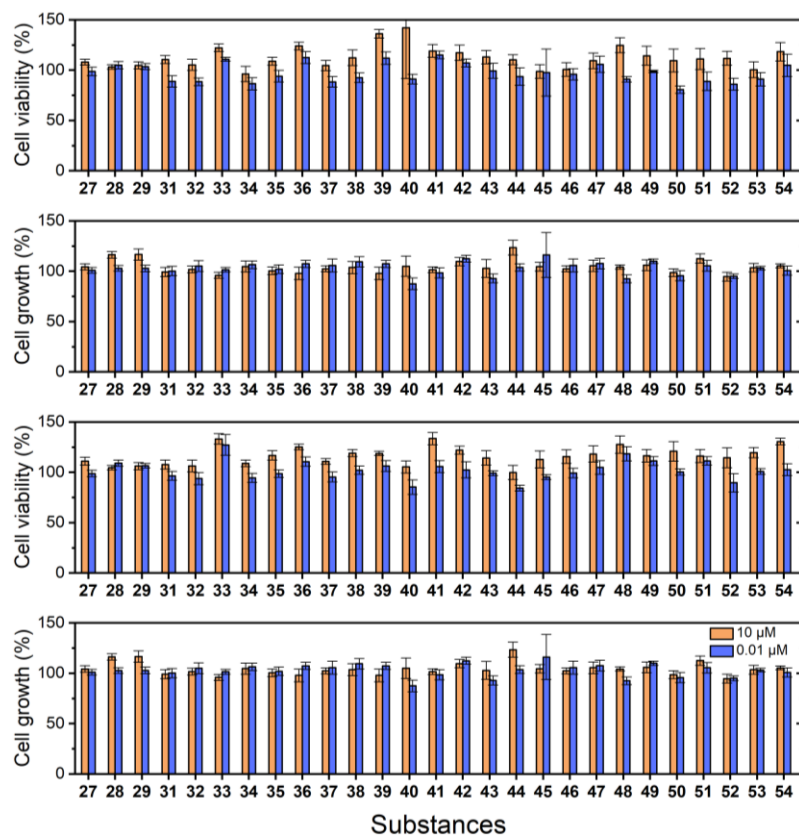


Figure 288: Antiproliferative and cytotoxic activities of compounds **27 - 54** (Chapter 3) against colorectal (HT-29, top two graphs) and human prostate (PC-3, bottom two graphs) cancer cell lines.

Register of internal IPB codes (3LC) of compounds

Table 8: Compound numbers and corresponding IPB 3LC (Chapter 2).

Chapter 2

Compound	IPB 3LC	Compound	IPB 3LC
1a	GGX194	5d	GGX258
1b	GGX197	5e	GGX256
1c	GGX209	5f	GGX247
1d	GGX246	5g	GGX602
1e	GGX250	5h	GGX628
2a	GGX198	5i	GGX608
2b	GGX200	5j	GGX626
2c	GGX210	5k	GGX633
2d	GGX248	5l	GGX593
2e	GGX251	5m	GGX591
3a	GGX199	5n	GGX592
3b	GGC201	5o	GGX599
3c	GGX211	5p	GGX605
3d	GGX253	5q	GGX611
3e	GGX252	5r	GGX629
4a (Ugi)	GGX203	5s	GGX596
4a (HWE)	GGX583	5t	GGX630
4b	GGC207	6	GGX569
4c	GGX221	7	GGX570
4d	GGX255	8	GGX579
4e	GGX254	9	GGX565
4f	GGX235	10	GGX580
4g	GGX601	11a	GGX581
4h	GGX625	11g	GGX600
4i	GGX607	11h	GGX612
4j	GGX623	11i	GGX606
4k	GGX632	11j	GGX621
4l	GGX590	11k	GGX631
4m	GGX587	11l	GGX586
4n	GGX589	11m	GGX584
4o	GGX598	11n	GGX585
4p	GGX604	11o	GGX597
4q	GGX610	11p	GGX603
4r	GGX622	11q	GGX609
4s	GGX595	11r	GGX620
4t	GGX627	11s	GGX594
5a (Ugi)	GGX204	11t	GGX624
5a (HWE)	GGX588	12	GGX614
5b	GGX208	13	GGX615
5c	GGX224		

Table 9: Table 8: Compound numbers and corresponding IPB 3LC (Chapter 3 and 4).

Chapter 3

Compound	IPB 3LC
1	GGX402
2	GGX404
3	GGX400
4	GGX510
5	GGX403
6	GGX511
7	GGX401
8	GGX517
9	GGX390
10	GGX395
11	GGX396
12	GGX397
13	GGX421
14	GGX467
15	GGX531
16	GGX407
17	GGX431
18	GGX443
19	GGX459
20	GGX432
21	GGX552
22	GGX423
23	GGX430
24	GGX479
25	GGX464
26	GGX536
27	GGX539

Compound	IPB 3LC
28	GGX542
29	GGX547
30	GGX439
31	GGX440
32	GGX405
33	GGX419
34	GGX422
35	GGX418
36	GGX442
37	GGX420
38	GGX411
39	GGX617
40	GGX523
41	GGX527
42	GGX528
43	GGX514
44	GGX515
45	GGX470
46	GGX466
47	GGX488
48	GGX494
49	GGX495
50	GGX496
51	GGX497
52	GGX499
53	GGX530
54	GGX524

Chapter 4

Compound	IPB 3LC
1	GGX333
2	GGX334
3	GGX325
4	GGX324
5	GGX433
6	GGX434
7	GGX381
8	GGX435
9	GGX389
10	GGX436
11	GGX382
12	GGX392
13	GGX357
14	GGX335
15	GGX336
16	GGX391
17	GGX534
18	GGX535
19	GGX546
20	GGX363
21	GGX549
22	GGX365
23	GGX553
24	GGX370
25	GGX350
26	GGX358
27	GGX412
28	GGX413
29	GGX414
30	GGX408
31	GGX415
32	GGX416
33	GGX417

Curriculum vitae

Personal details

Name Tristan Fuchs
Nationality German

Education

11/2018 – 12/2022 PhD candidate (Dr. rer. nat.) at Leibniz Institute of Plant Biochemistry, Department of Bioorganic Chemistry, IPB, Halle (Saale)
Title: Design, synthesis, and biological activity of nature-derived herbicides

10/2018 – 09/2020 Postgraduate Studies in Analytics and Spectroscopy at the University of Leipzig

10/2015 – 09/2018 Master of Science at Martin Luther University Halle-Wittenberg
Specialization in Organic Chemistry
Thesis: Novel approach for the synthesis of organic diphosphates using trichloroacetimidates

10/2012 – 07/2015 Bachelor of Science at Martin Luther University Halle-Wittenberg
Thesis: Synthesis of phenylpropanoids and their enzymatic application

Work experience

Since 2023 R&D Project Manager at Mylva SA (Spain)

04/2017 – 09/2017 Industry Internship at Syft Technologies Christchurch (New Zealand)

08/2017 – 09/2017 Research Internship at University Niš (Serbia)

08/2014 – 09/2014 Research Internship at Al-Farabi University Almaty (Kazakhstan)

Publications

Manoilenko, S., Dippe, M., Fuchs, T., Eisenschmidt-Bönn, D., Ziegler, J., Bauer, A-K., Wessjohann, LA. Enzymatic one-step synthesis of natural 2-pyrones and new-to-nature derivatives from coenzyme A esters, *Journal of Biotechnology*, **2024**, 388, 72-82, doi.org/10.1016/j.jbiotec.2024.04.006

Kappen, J., Manurung, J., Fuchs, T., Vemulapalli, SPB., Schmitz, LM., Frolov, A., Agusta, A., Muellner-Riehl, AN., Griesinger, C., Franke, K., Wessjohann, LA. Challenging Structure Elucidation of Lumnitzerolactone, an Ellagic Acid Derivative from the Mangrove *Lumnitzera racemosa*. *Marine Drugs*, **2023**, 21(4), 242, doi.org/10.3390/md21040242

Patents

Fuchs, T., Berger, R., Wessjohann, LA. Niacin derivatives, isonicotinic acid derivatives, and picolinic acid derivatives, as phytoeffectors and plant protectants. European patent application (pending).

Eidesstattliche Erklärung

Hiermit erkläre ich an Eides statt, dass ich die vorliegende Arbeit selbstständig und nur unter der Verwendung der angegebenen Quellen und Hilfsmittel angefertigt habe. Zitate und andere Anlehnungen hinsichtlich Aussagen und Konzepten sind als solche gekennzeichnet. Die vorliegende Arbeit wurde in gleicher oder ähnlicher Form noch keiner Prüfungsbehörde zur Begutachtung vorgelegt.

Halle (Saale), den 14. August 2024

Tristan Fuchs